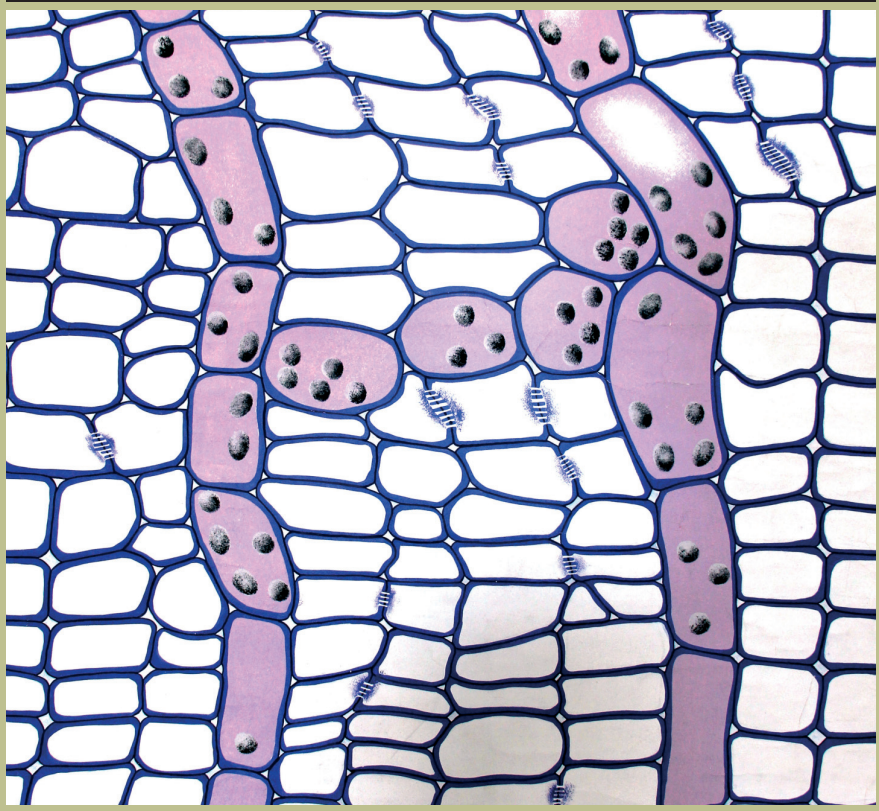

МОСКОВСКИЙ ГОСУДАРСТВЕННЫЙ УНИВЕРСИТЕТ
ИМЕНИ М.В. ЛОМОНОСОВА
БИОЛОГИЧЕСКИЙ ФАКУЛЬТЕТ

PLANT ANATOMY: TRADITIONS AND PERSPECTIVES

АНАТОМИЯ РАСТЕНИЙ: ТРАДИЦИИ И ПЕРСПЕКТИВЫ

Международный симпозиум, посвященный 90-летию профессора Людмилы Ивановны Лотовой

ЧАСТЬ 1

МОСКОВСКИЙ ГОСУДАРСТВЕННЫЙ УНИВЕРСИТЕТ имени М. В. ЛОМОНОСОВА
Биологический факультет

АНАТОМИЯ РАСТЕНИЙ:
ТРАДИЦИИ И ПЕРСПЕКТИВЫ

Материалы Международного симпозиума,
посвященного 90-летию профессора
ЛЮДМИЛЫ ИВАНОВНЫ ЛОТОВОЙ
16–22 сентября 2019 г.
В двух частях

Часть 1
МАТЕРИАЛЫ НА АНГЛИЙСКОМ ЯЗЫКЕ

PLANT ANATOMY:
TRADITIONS AND PERSPECTIVES

Materials of the International Symposium
dedicated to the 90th anniversary
of Prof. **LUDMILA IVANOVNA LOTOVA**
September 16–22, Moscow
In two parts

Part 1
CONTRIBUTIONS IN ENGLISH

МАКС ПРЕСС
Москва – 2019

УДК 58
ББК 28.56
А64

DOI 10.29003/m664.conf-lotova2019_part1

Издание осуществлено при финансовой поддержке
Российского фонда фундаментальных исследований по проекту 19-04-20097

Анатомия растений: традиции и перспективы. Материалы Международного
А64 симпозиума, посвященного 90-летию профессора Людмилы Ивановны Лотовой. 16–22 сентября 2019 г. В двух частях. – Москва : МАКС Пресс, 2019.
ISBN 978-5-317-06198-2

Часть 1. Материалы на английском языке / Ред.: А. К. Тимонин, Д. Д. Соколов. – 308 с.

ISBN 978-5-317-06174-6

УДК 58
ББК 28.56

Plant anatomy: traditions and perspectives. Materials of the International Symposium dedicated to the 90th anniversary of Prof. Ludmila Ivanovna Lotova. September 16–22, 2019. In two parts. – Moscow : MAKS Press, 2019.
ISBN 978-5-317-06198-2

Part 1. Contributions in English / Ed. by A. C. Timonin, D. D. Sokoloff. – 308 p.

ISBN 978-5-317-06174-6

Издание доступно на ресурсе E-library

ISBN 978-5-317-06198-2
ISBN 978-5-317-06174-6 (Часть 1)

BASIC PRINCIPLES OF THE CONDUCTIVE APPARATUS STRUCTURE IN WOODY PLANTS[1]

L.I. LOTOVA †

Prof. Sergey I. Vanin used to define the wood science as a science about the wood consumer properties and methods to study them. Vanin's definition means that technological issues are the base for the wood science as determined by great economic importance of this tissue. However, I do believe that the principal aspect of the wood science is biological one, and wood investigations are just a constituent part of the complex morphological and anatomical research of woody plants. Such a research should primarily involve studies of wood development, wood structure and aging, correlations of its physical and mechanical features with the forest type, environments etc.

Every plant is a very complex integrated structural and functional system, whose all the organs and tissues are closely interrelated. The cambium governs the rate of wood formation and wood structural features which were fixed during the evolution. The wood and the bast jointly constitute the complete conductive apparatus to transport mineral and organic aqueous solutes through the plant body. The bast is a principal component of the bark. Therefore, I believe that modern wood science should not deal with only the wood. This science should cover the bark as well, especially since the latter is also quite usable. However, the bark is usually just a waste of the wood industry because of our squandering. It is almost never used in economics despite of some elaborated valuable technologies of bark processing.

A need for bark investigations was emphasized by Karl Mercklin, the first Russian researcher of the bark. In his "Anatomy of the stem bark and wood of forest trees and shrubs of Russia" published in 1857 he wrote that "the wood alone is insufficient for distinguishing similar genera of trees and even less for distinguishing between their species… Not only the bark but the very elementary bodies, i.e. cells and vessels should be examined under the potent microscope to comprehend completely the inner structure and properties of the stems of forest trees".

When summarizing his scientific and educational activity, illustrious Prof. Ivan P. Borodin who taught botanical disciplines in full their entirety at the St. Petersburg Forestry Institute for many years, said that he could not vouch that progressing specialization in science would not cause the wood structure and the bark structure to be taught by different professors in 21st century.

However, we are in opposite position by the end of 20th century. There is the wood that has grabbed all attention of plant anatomists, while the bark has still

[1] A talk delivered at Ivanov Readings on late 1980s. Unpublished Russian manuscript translated by A.C. Timonin.

been ignored. Only a few Russian botanists are interested in exploring bark. The situation is quite the same abroad.

But why is bark investigation necessary within the framework of wood science? The main reason is that the bark greatly influences the wood development, but it also affects the wood structure. The bark is understood as a heterogeneous complex of tissues outside the cambium.

Plant physiology data show that the inner bark accumulates hormones of auxin group in autumn to stimulate cambium activity next spring. Everton, Kozlowski & Davis conducted an interesting experiment in 1972. They made girdling of the trunks of maple trees and other tree species without damaging the cambium. Debarked areas of the trunks were waxed. The wood was then periodically sampled from both injured and intact areas of the trunks. If the girdling was made in winter when the cambium was dormant, it prevented spring resumption of cambium activity in 50% debarked areas of the trunks, though rare tangential divisions of the cambium fusiform initials were noted. The cambium functioned normally in the intact areas of the same trunks.

If the girdling was made in summer in July and August when the conductive tissues were differentiating in the trunk, the wood cells were prevented from developing their secondary cell walls whereas the cambium fusiform initials were provoked to divide tangentially. Both results caused increased parenchymatization of the wood, i.e. significant changing of wood structure and consequently wood properties.

Thus, the bark or rather its bast indirectly affects the wood structure through influencing cambium activity.

Close physiological connection between the bark and the wood is caused not only by the hormones but also by the presence of radial communications in the stem in the form of the radial rays.

The bark and the wood are rather similar in their topographic differentiation into functional zones. The bast zone adjacent to the cambium which corresponds to one growth ring is termed ‘conducting’. The sapwood is its counterpart in the wood. It is also adjacent to the cambium but usually includes several growth rings. The sapwood rarely consists of only one growth ring. The non-conducting bast zone is outside the conducting one and corresponds either to the heartwood or to the ripe wood, the latter one being less hydrated than the sapwood.

My speculations on analogy of the topographic patterns of bark and wood could be considered superficial, especially as there are woody species that have neither heartwood nor ripe wood. However, this analogizing of the bark and wood topographies seems quite acceptable as it shows general principles of age changes of both tissues associated with loss of their conductivity. But such changes are amplified outwards in the bark and terminate with the rhytidome formation.

The bark is more complex functionally than the wood. It maintains the descending transport and also accumulates waste metabolites and removes them out

of the plant body due to shedding off outer layers of the rhytidome. The bark is the first to react to the mechanical damages and pathogen invasions. The plant blocks damager intruding by means of additional cork development in the bark or in some other ways including bark cell sclerification and resin production (in conifers).

Histological compositions of the bark and wood are quite similar as composed by 2 systems. The vertical (axial) system is represented by prosenchymatous cells; the transverse (radial) system is represented by the bast and wood rays. The components of the axial system originate from the cambium fusiform initials and those of the transverse system derive from the cambium ray initials.

Constituents of the bast and wood are combined not only topographically but also functionally as they compose 3 systems.

The conductive system of the wood includes solitary cells termed 'tracheids' and/or uniseriate longitudinal files of end-perforated cells termed 'tracheas' or 'vessels'. The conductive system of the bast consists either of the sieve-cells, e.g. in conifers, or of the sieve-tubes; the former resemble the tracheids, and the latter are comparable with the vessels in the structure of the end walls of their segments.

The supporting system of the coniferous woods consists of the late-wood (summer wood) tracheids, which are narrower and less-pitted than the early-wood (spring wood) tracheids. The most advanced supporting system is inherent in the hardwood species which have fiber tracheids and specific wood fibers also reported to as libriform fibers. There are also bast fibers, but only in some species. The sclereids very often develop in the bast; some of them look like the bast fibers, e.g. fiber sclereids of larch bast, but they differ from the genuine bast fibers in their origin. The bast fibers directly differentiate from the cambium derivatives and have few-layered walls, whereas the sclereids develop from the bast parenchyma cells *via* sclerification; they are varied in shape and have multilayered pitted walls.

The woody species comprise three groups according to the type of supporting system of their bast, viz. 1) those with only bast fibers (e.g. linden, chestnut), 2) those with both bast fibers and sclereids (e.g. ash, maple, coniferous *Metasequoia*, yew) and 3) those with only sclereids (e.g. birch, alder, spruce, fir etc.). There are also woody species that have no supporting system in their basts; these are pine, currant and euonymus among others.

The third functional system of the plant conductive apparatus is alive, parenchymal. It is constituted by the cells of both ray and axial parenchyma. Both ray and axial parenchyma cells of the bast are similar with their counterparts of the wood; all are usually multifunctional. The wood parenchyma cells are involved in salt metabolism by accumulating mineral ions; they are more often storage cells just as the cells of the bast parenchyma. Many parenchyma cells, especially those in the bast, contain tannins, mucilage, oils, calcium oxalate crystals; the parenchyma cells can also participate in formation of specialized secretory system. The latter one is represented by the resin ducts in conifers. Similar structures can also be in the hardwood species, e.g. in Araliaceae.

Quantitative relations between the listed histological components of the wood and bast differ in different woody species. These relations largely determine the strength properties of the concerned tissues, those of the wood being best studied. For example, the libriform-rich wood of tropical lignum vitae (*Guajacum officinale*) is the hardest, densest and heaviest one; its specific gravity is 1.42. The specific gravity of solid wood of the ebony (one of *Diospyros* species) is 1.17. Parenchymatous balsa wood (*Ochroma lagopus*) of thin-walled elements is lighter than the cork; its specific gravity is 0.12. This explains the high buoyancy of this wood. The specific gravity and the hardness of the bast also depend on the proportion of mechanical elements therein.

The wood and the bast arose as purely conductive tissues; they acquired additional functions only in the course of subsequent evolution.

The wood must conduct the water not only longitudinally but also radially and tangentially, i.e. throughout the annual ring. Some features of the wood, namely the specificity of the contacts between its constituents are associated with this 3D conduction. The conifers have woods of tracheid-leveled organization. The radial conduction of the water through such woods is possible due to that the tracheids are not rectangular but polygonal in cross-section and bear bordered pits in their oblique radial walls. Thanks to this structure, each vertical tracheid is communicated with 2–3 neighboring ones to enable radial water flow, albeit tortuous. The arcuate endings of the vertical tracheids of different levels overlap in such a way that the number of communicated tracheids increases to contribute additionally to the radial water flow. Pine, larch and spruce have additional structures, namely the ray tracheids to conduct water radially, what is more, each ray tracheid is pit-connected with several vertical tracheids.

Such a wood of tracheid-leveled organization has paratracheal axial parenchyma which is scattered among vertical tracheids. I have already said that the late-wood tracheids perform the supporting function. Their very last layer is characterized by the pits in the tangential walls, just as the very early tracheids of the next annual ring.

The tracheids have evolutionary diverged into the vessel segments and specialized supporting cells. The wood conductivity has enhanced by the tracheid-to-vessel substitution, because the vessel segments were communicated through perforations. But when the vessels are scanty and practically unconnected, then the tracheids become the links. This is the tracheid-vascular level of the wood organization. In such a wood, there are libfriform fibers inter the water-conducting areas of various shapes and sizes. The axial parenchyma in this wood is usually apotracheal, viz. either diffuse or metatracheal, located among the tracheids. However, it can partially be paratracheal, associated with scanty vessels. These are the woods of oak, buckthorn etc.

The consecutive annual rings are intercommunicated through the tracheids in the tracheid-vascular woods.

The conductive tracheids are absent, if only the vessels are numerous, tortuous and contacting each other to be interconnected through the intervessel pitting. In such a wood of vascular level of organization, the libriform fibers take the intervessel space, while the axial parenchyma constitutes partial or complete sheaths of the vessels, i.e. the axial parenchyma is paratracheal. The paratracheal parenchyma enables rapid sugar translocation into the vessels in spring to be transported to the opening buds. Dr. Kedrov, the employee of the Dept. of Higher Plants, MSU has experimentally shown that the parenchymal sheath of vessel is important for strengthening vessel walls when it is under progress. One-leveled transverse walls of the parenchyma cells of vessel sheath function like the annular wall thickenings of the protoxylem vessels, though they are not inside but outside the vessel, like the tightening hoops.

Only two levels of the bast organization could be distinguished as opposed to three ones of the wood organization. The first bast level organization is characteristic of the gymnosperms whose conductive structures are the sieve-cells. The second level is inherent in angiosperms which have the sieve-tubes as conductive structures. There is no intermediary bast organization. There are no plant revealed that would have both sieve-cells and sieve-tubes. The first level of the bast organization certainly corresponds to the tracheidal level of wood organization and the second one corresponds to the vascular level of wood organization.

The bast always contains more parenchyma cells than the wood; and it is not by the chance. It is specific developmental pathway of the sieve elements associated with degradation of their protoplasts including nucleus that causes numerous parenchyma cells to form in the bast and some of them to connect directly with the sieve elements. Since conducting of substances through the bast is associated with energy-consuming redox reactions which require certain enzymes, then the numerous parenchyma cells are necessary as the enzyme and ‘fuel’ suppliers. In gymnosperms, any cell of the axial or ray parenchyma can become such a supplier (so-called Strasburger cells). In angiosperms, the suppliers are only the companion cells related by their origin to the sieve-tube segments. These cells are comparable to the paratracheal parenchyma of the wood.

The structure of the bast conductive system does not correlate with the arrangement of bast constituents.

Both abundance and arrangement of the axial parenchyma determine the tangential growth pattern of the bast caused by the trunk thickening. This tangential growth of the bast is termed ‘dilation’.

When abundant, there is the axial parenchyma that performs the bast dilation along with its other functions. When the axial parenchyma is scant, there are the bast rays that highly dilate. Two fundamentally different architectural types of the bast can be recognized according to the amount and arrangement of its axial parenchyma. The open type is characterized by the abundant axial parenchyma and diffuse dilation. The closed type is characterized by scanty axial parenchyma whose

dilation is prevented by numerous clustered supporting constituents of the bast, as in the linden, juniper.

The conductive and supporting systems are substantial in the wood. The latter system conditions the wood hardness and makes optimal spatial arrangement of the trunk and branches.

In contrast, the conductive system of the bast is more optimally coordinated with the parenchymal system. This is largely determined by peripheral location of the bast which unavoidably causes its dilation and cell production for generating the phellogen, the latter one preceding cork formation.

Thus, general structural principles of the wood and bast do not exclude substantial differences between them. Therefore, the research approaches to these two tissues which combined constitute the conductive apparatus of a plant, must be different.

SCIENTIFIC HERITAGE OF L.I. LOTOVA

Andrey G. DEVYATOV, Irina M. KALINICHENKO, Alexander C. TIMONIN

Lomonosov Moscow State University, Moscow, Russia

adeviatov@yandex.ru

Plant anatomy is a traditional scientific and educational specialization at the Department of Higher Plants of Moscow State University. Ludmila Ivanovna Lotova (1929–2017) was a principal contributor to this area in the second half of the 20th and in the beginning 21th centuries.

Her scientific heritage consists of more than 150 publications on plant anatomy and morphology, application of morphological and anatomical data in plant phylogenetics. Lotova's first publications and PhD dissertation dealt with applied plant anatomy. This field of botany took essential part of her scientific activity later on. Dr. Lotova elaborated keys to identify frost-resistant apple trees by the bud scale anatomy (1964, 1967) and to identify Russian trees and shrubs by their bark anatomy (1982, 1997, 1998), etc. She supervised the development of methods for using plant anatomy data in forensic examination in the 1980s.

As to fundamental science, Dr. Lotova was a founder and long-term leader of Russian taxonomic plant anatomy. She was successively studying bark anatomy in conifers, *Ginkgo*, Betulaceae, Fagaceae, Caprifoliaceae, Oleaceae, Rosaceae, Fabaceae since the middle 1960s. Her Doctor of Science dissertation (1983) completely covered the diversity of bark anatomy of the coniferous plants and was reshaped into the monograph (1987) which is still the most comprehensive contribution to the theme. Taxonomic fruit anatomy was another field Dr. Lotova consistently elaborated especially the fruit anatomy of Leguminosae (1967, 1989, 1991,

2006), Rosaceae (1997, 2014), Brassicaceae (1999) etc. She also dealt with leptom organization in tracheophytes, diversity and classification of the meristems, phloem–xylem comparative evolution. Her principal ideas are still actual and inspiring.

Dr. Lotova was an outstanding teacher and methodologist. She published more than 30 manuals for practical works on plant cytology, plant anatomy and field botany. Her major "Botany" (2000) has become the most sought-after Russian textbook, which has annually been reprinted so far. Dr. Lotova developed personally or in collaborations a number of training standards for Moscow University and other Russian universities for teaching botany. Her manuals are distinguished by thorough selection, consistency and clarity of presentation of the material and by great literary style. They are thereof a kind of benchmark for Russian-language educational literature.

Dr. Ludmila Lotova was working at the Faculty of Biology, Moscow State University over 60 years. She published either original paper(s), or monograph every year and regularly presented her results at symposia. Dynamics of Lotova's publication activity is presented in the Table.

Table. Numbers of publications per periods of Lotova's employment.

Years	1957–1960	1961–1965	1966–1970	1971–1975	1976–1980	1981–1985
Number of publications per period	8	7	15	10	14	16
Years	1986–1990	1991–1995	1996–2000	2001–2005	2006–2010	2011–2018
Number of publications per period	30	7	29	19	6	5

Most of these publications describe in detail anatomical structures of various plants with high-quality illustrations. They are comprehensive and highly illustrated. Many (52) articles were prepared in collaboration with her students. These works covered comparative anatomy of rather many plant taxa, the evolution of tracheophyte conductive system and taxonomic bearing of the bark traits. Dr. Lotova revised and improved the terminology in use in Russian plant anatomy. Her "Dictionary of phyto-anatomical terms" (2007) became the acme of this work. Dr. Lotova also published essays in the "Great Soviet Encyclopedia" and in "Biological encyclopedic dictionary".

Dr. Lotova's published results have been cited many times and remain relevant so far. However, they are becoming less accessible every year. Yandex and Google give short information about 129 of 166 her published works. Neither full texts nor abstracts are usually accessible. Lotova's long ago published works are now in the process of being digitized to increase the accessibility of Lotova's concepts and ideas. Her 22 digitized manuals and monographs are accessible in the

websites http://bookre.org, http://www.studmed.ru and http://docplayer.ru, but her articles mostly remain inaccessible. To fill this gap we have selected and digitized 50 most revealing Lotova's articles which are now accessible in full in the website https://msu-botany.ru.

We are indebted to Dr. Maya V. Nilova for assistance in selecting articles to be digitized and to Dr. Nikolay A. Vyslobokov for placing digitized papers into the https://msu-botany.ru website.

This work was supported by Goverment order for the Lomonosov Moscow State University (project No. AAAA-A16-116021660045-2).

DIVERSITY AND EVOLUTION OF MICROSPOROGENESIS IN ANGIOSPERMS

Beatrice ALBERT, Sophie NADOT

AgroParisTech, CNRS, Université Paris-Sud, Université Paris-Saclay, Orsay, France
sophie.nadot@u-psud.fr

Pollen grains, the male gametophytes of angiosperms (and more generally of extant seed plants), are particular organisms that are liberated from mature anthers and have to be passively transported to the female organs by biotic or abiotic vectors. They have to survive through the dispersion phase before landing on a compatible stigma and further germinate. They are surrounded by an extremely resistant multi-layered wall whose properties largely condition their survival capacity. The outer pollen wall is essentially composed of sporopollenin, which presents more or less complex patterns of ornamentation that are loosely linked to the pollination syndrome. In most species, the wall is interrupted in places by apertures, revealing the inner wall. The apertures play a key role in pollen survival and germination, and a wide range of variation in aperture pattern (shape, number and position of apertures on the pollen surface) is observed throughout angiosperms. Variation may occur at any taxonomic level, even down to the intra-individual level, even though large categories can be recognized within angiosperms according to the predominant aperture type. Basal angiosperms and monocots have inherited the ancestral monosulcate type, while eudicots, the largest clade of angiosperms, tend to produce tricolpate pollen grains, their main morphological synapomorphy.

In most cases, apertures are already visible at the end of meiosis, before microspores are released from the tetrad, indicating that aperture pattern is determined during microsporogenesis, the earliest step in pollen ontogeny. During this process, callose walls are formed among the four microspores, either simultaneously after both meiotic divisions, or successively after each meiotic division, resulting

in a variety of tetrad shapes. In some cases, callose thickenings (hereafter callose deposits) are observed at particular places of the intersporal walls. During the last decade, we have revealed the existence of a correlation between the location of apertures, and patterns of additional callose deposits in a variety of angiosperm species belonging to monocots, eudicots, and early diverging angiosperms. We have also shown that when no additional callose deposits were detectable, the apertures are formed at the last points of contact among the microspores.

We will review here the anatomical features of microsporogenesis in species presenting additional callose deposits in light of the phylogenetic distribution of these species, and discuss how selection and developmental constraints have interacted during the course of evolution to produce the observed diversity of pollen morphology.

STUDY PROSPECTS ON THE COMPLEXITY OF STRUCTURE, DEVELOPMENT AND EVOLUTION OF SIMAROUBACEAE FLOWERS

***Gisele Gomes Nogueira ALVES*, Diego DEMARCO, José R. PIRANI**

University of São Paulo, São Paulo, Brazil

gisele.biology@gmail.com

The Simaroubaceae family is a group of eudicots – rosids – malvids (APG-IV, 2016). With an essentially pantropical distribution, it is a monophyletic and morphologically diverse group (Clayton, 2011). There are two comprehensive monographs of Simaroubaceae, provided by Engler (1931) and Clayton (2011), but there is still much to be explored on the group. The flowers of their representatives exhibit wide morphological diversity, occuring either dialisepaly and gamosepaly, bisexuality and unisexuality, diplostemony, obdiplostemony or haplostemony, apocarpy and several degrees of syncarpy, besides the floral merism which can be tetramerous to hexamerous (e.g. Nairl, Joshi, 1958). These variations or their degrees of occurrence are not commonly found in groups of angiosperms and may be a result of a recent diversification, even though the age of the group dates back to the Late Cretaceous (Clayton et al., 2009), offering a wide array of questions on the structural evolution and history of the family.

In order to improve the knowledge about the floral features of Simaroubaceae in detail, our study intend to develop a comparative analysis of the floral structure of selected representatives of its main lineages, searching for patterns among them, and mapping the floral characters upon the most recent molecular phylogeny available for the group. To evaluate the evolution of the floral characteristics found

under a phylogenetic context, we intend to establish its implications in the group's systematics and to foresight its possible role in the biology and reproductive success of these plants throughout their history and diversification. In addition, a floral ontogenetic study will be carried out with at least three species of distinct genera, aiming to elucidate some evolutionary steps of contrasting floral forms, which may be better understood when data on structural development are available.

The wide floral diversity in Simaroubaceae and the existence of scarce studies on this group instigate a detailed investigation of the floral characteristics of its representatives. Recent findings regarding anatomical study of the flowers of *Simaba*, developed during my Master's degree (partially published – Alves et al., 2017), revealed the need for expansion and deepening of structural studies in the family. The variations and intermediate states found between two of the sections previously recognized in *Simaba* also raised questions about the degree of similarity and relations between flowers of these groups and of other genera, and the phylogenetic work carried out by Devecchi et al. (2018) culminated with the segregation of the group in two genera (*Simaba* and *Homalolepis*), indicating that new data may still provide valuable insights on the relationships among them and other groups in the family. For instance, flowers of *Simaba*, *Homalolepis* and *Quassia* share bisexual flowers provided with a conspicuous gynophore, while *Simarouba* presents unisexual flowers with a nectariferous disk. However, in my Master's dissertation I found evidence that some *Simaba* and *Homalolepis* species may be functionally unisexual (Alves et al., 2017). This shows the need for careful analysis of the development of structures, to allow a confident codification of states of characters for the evolutionary studies.

The detailed comparative study of the floral structure of Simaroubaceae species can also provide additional evidence to improve the taxonomy of the group, besides assisting in floral and evolutionary biology studies, by providing new data of the floral structure of members of the Sapindales order. Until the present moment, we observed 32 morphological and anatomical characters of the flowers of the following genera: *Simaba*, *Homalolepis*, *Simarouba*, *Quassia*, *Picrolemma*, *Picrasma* and *Ailanthus*. Features as unisexual functionality, fusion degrees of the floral organs, ovule and carpel numbers and the presence of pistillodes and stylodia show that the analysis of the reconstruction of these characters may lead us to a greater perspective of how floral evolution in this group occurred. Our preliminary results allow us to observe an interesting range of variations in these floral structural patterns, enabling us to trace the best way to analyze the representatives of these genera and help to elucidate how their floral evolution may occurred, as well as revising their position on the Sapindales phylogeny (Muellner-Riehl et al., 2016).

References

Alves G.G.N., El Ottra J., Devecchi M.F., Demarco D., Pirani J.R. 2017. Structure of the flower of *Simaba* (Simaroubaceae) and its anatomical novelties. *Bot. J. Linn. Soc.* **183**: 162–176.

APG IV. 2016. An update of the Angiosperm Phylogeny Group classification for the orders and families of flowering plants: APG IV. *Bot. J. Linn. Soc.* **181**: 1–20.

Bukatsch F. 1972. Bermerkungen zur Doppelfärbung Astrablau-Safranin. *Mikrokosmos* **61**: 255.

Clayton J.W. 2011. Simaroubaceae. In: K. Kubitzki (ed.): *The families and genera of vascular plants*. Heildelberg: Springer. V. **10**. P. 408–423.

Clayton J.W., Soltis P.S., Soltis D.E. 2009. Recent long-distance dispersal overshadows ancient biogeographical patterns in a pantropical angiosperm family (Simaroubaceae, Sapindales). *Syst. Biol.* **58**: 395–410.

Devecchi M.F., Thomas W.W., Plunkett G.M., Pirani J.R. 2018. Testing the monophyly of *Simaba* (Simaroubaceae): Evidence from five molecular regions and morphology. *Mol. Phyl. Evol*. **120**: 63–82.

Engler A. 1931. Simaroubaceae. In: Engler A., Prantl K. (Hrsg.): *Die natürlichen Pflanzenfamilien*. 2. Aufl. Leipzig: Engelmann. Bd. **19a**. S. 359–405.

Gerrits P.O. 1991. *The application of glycol methacrylate in histotechnology; some fundamental principles.* Groningen: Department of Anatomy and Embryology, State University Groningen.

Johansen D.A. 1940. *Plant Microtechnique*. New York: McGraw-Hill Book Company.

Kraus J., Arduin M. 1997. *Manual básico de métodos em morfologia vegetal.* Rio de Janeiro: EDUR, Seropédica.

Maddison W.P., Maddison D.R. 2014. *Mesquite: a modular system for evolutionary analysis.* Version 3.02. http://mesquoteproject.org

Muellner-Riehl A.N., Weeks A., Clayton J.W., Buerki S., Nauheimer L., Chiang Y.C., Cody S., Pell S.K. 2016. Molecular phylogenetics and molecular clock dating of Sapindales based on plastid *rbc*L, *atp*B and *trn*L-*trn*F DNA sequences. *Taxon* **65**: 1019–1036.

Nair N.C., Joshi R.K. 1958. Floral morphology of some members of the Simaroubaceae. *Bot. Gaz*. **120**: 88–99.

Silveira M. 1989. Preparação de amostras biológicas para microscopia eletrônica de varredura. In: Souza W. (ed.): *Manual sobre técnicas básicas em microscopia eletrônica*. São Paulo: USP. P. 71–79.

ANATOMY OF EXTRAFLORAL NECTARIES IN *LEUCADENDRON MUIRII* PHILLIPS AND *MIMETES CUCULLATUS* R. BR. (PROTEACEAE)

Maxim I. ANTIPIN, Vladimir V. CHOOB

Lomonosov Moscow State University, Moscow, Russia

sagefool@rambler.ru

Leaf margin characters are taxa specific and may serve as an important tool in systematics, including identification of fossil records (Hickey, Wolfe, 1975; Hickey, 1979). Shapes of lamina and leaf margin in Proteaceae in general are quite diverse, but Proteaceae of Cape Floristic region are more uniform regarding leaf margin characters, having either an entire leaf edge or just a few teeth at the lamina apex. Both entire and dentate leaves often terminate with special structure, generally referred to as mucro (Rebelo, 2001). Its shape may range from needle-

or awn-shaped to rounded/hemispherical. It differs from the rest of the lamina by its indumentum features (it is usually glabrous but in some cases it has trichomes that are arranged in a specific way), by shape, size and colour of epidermal cells and underlying mesophyll cells (often brightly colored with anthocyanins) and by smoother cuticle.

The rounded 'mucrones' inherent in several genera of Cape Proteaceae of so called Cape Clade (Weston, Barker, 2002) may be classified among salicoid teeth ("a dark, but not opaque, nondeciduous spherical callosity fused to the tooth apex") according to the classification of Hickey &Wolfe (1975). Teeth of this type in Salicaceae (including some genera of former Flacourtiaceae) are often secretory (see Wilkinson, 2007), appearing to be resin glands or foliar nectaries. Rebelo (2001) prefers to call such mucrones in *Mimetes* and *Leucospermum* the 'glandular teeth', but he refers to them simply as 'glands' in *Leucadendron*, the genus whose leaf margin is entire in all species and only some species have leaf apices terminating with structures of this type.

Brightly coloured rounded leaf glands, or salicoid teeth, of many species of *Mimetes*, *Leucospermum* and *Leucadendron* are documented to attract insects and referred to as extrafloral nectaries (Midgley, 1987; Rebelo, 1995; Zachariades, Midgley, 1999). Although ant-attracting nectaries are usually considered an adaptation that reduces herbivory due to attracted ants preying on herbivorous insects, experiments had shown that excluding ants from nectary-bearing plants of extant Cape Proteaceae does not increase herbivory levels (Zachariades, Midgley, 1999). Lawton & Heads (1984) suppose that nectaries in such cases may be 'ghosts of predation past', meaning that insect phytophages avoid visiting plants with nectaries (and ants), thus the exclusion of ants has no noticeable effect on herbivory. Midgley (1987) suggests that nectaries in extant Cape Proteaceae represent an atavistic defence mechanism that eventually became less and less needed with leaves were becoming smaller, more terete and sclerophyllous in responce to recent climate aridification in the Cape. Existing works on leaf morphology of Cape Proteaceae did not attribute any functions to these organs, just mentioning them as 'teeth' (Rourke, 1984) or 'apical callus' (Williams, 1972). No works on anatomy of these structures or on leaf dentition and distribution of substances they produce have been published yet.

This work aimed to describe the anatomy features of a typical 'rounded mucro' (salicoid tooth, apical foliar nectary) in species of *Mimetes* and *Leucadendron*, to test the structures for mono- and disaccharide occurrence and spatial distribution using *in vivo* methods of hystochemical testing, and to compare them with morphologically similar secretory structures of Salicaceae/Flacourtiaceae.

Live shoots of *Mimetes cucullatus* R.Br. were collected near Fernkloof, South Africa, in June 2017. Those of *Leucadendron muirii* Phillips were taken from plants grown in Botanical garden of Lomonosov Moscow State University from seeds collected in the wild in the vicinity of Struisbaai, South Africa.

Live leaves of both species were longitudinally sectioned with hand razor and mounted on slides. Molisch test was immediately performed on some of the sections (alpha-naphthol alcohol solution and concentrated sulphuric acid). Both stained and control leaf sections were observed and photographed using light microscope with digital camera (Olympus CX41).

Fully developed leaves of *Mimetes cucullatus* vegetative shoots usually terminate with three rounded teeth (some smaller leaves only have a single tooth). The teeth are somewhat swollen structures thicker than the leaf blade, they are brightly coloured with anthocyanins, covered with a thick and smooth cuticle, and glabrous. The rest of the blade is covered with abundant trichomes and its cuticle is rough.

The leaf blade of *Leucadendron muirii* acropetally narrows and terminates with single brightly coloured salicoid tooth with distinctly more smooth cuticle. Its apical area is somewhat flattened or concave.

Molisch test revealed sugars in vascular bundles reaching the tooth in *Mimetes cucullatus*. The tooth part of the section is wider than the blade *per se*; its epidermal and subepidermal cells are red of anthocyanin. Sugar is also noted in large polygonal mesophyll cells situating abaxially in relation to the vascular bundle and almost lacking the chlorophyll. It is detected in loose round parenchyma cells between these polygonal cells and the abaxial epidermis. Cells of tooth epidermis are square or elongated (palisade-like *sensu* Wilkinson, 2007), noticeably longer radially than flatter epidermal cells of the blade; they are longest on the abaxial side of the tooth. Mesophyll cells and intercellular spaces underlying the epidermis are most stained in the proximal part of the tooth at its abaxial side. This seems to be an area where exudates reach the gland surface through epidermis.

In *Leucadendron muirii* leaf sections, the borderline between the gland and the rest of the lamina is clearly seen in the most apical narrowing part of the leaf. Epidermal cells of the gland are only slightly elongated compared to the blade epidermal cells, but mesophyll cells underlying them are quite distinct as they are bright purple-red and contain no chloroplasts. The most apical, flattened part of the gland is characterized by the longest, square epidermal cells. Parenchyma cells in the flattened apical part of the gland are large and polygonal and lack both chlorophyll and anthocyanins. There is a small space between these large parenchyma cells and the epidermal layer of the flattened apex of the gland, which stains orange with Molisch reagent.

In genera of Salicaceae s. str. and former Flacourtiaceae, the secretory epidermis of the glandular salicoid teeth consists of elongated, palisade-like cells perpendicular to the leaf surface (Wilkinson, 2007). Subepidermal mesophyll consists of rounded or polygonal cells lacking chloroplasts. It is supplied by one to several veins and more or less modified for nectar or resin production; some authors refer to it as ‘nectariferous parenchyma’ (Thadeo et al., 2008). Nectar or other excretes

may concentrate either in a cavity between the outer epidermal walls and the cuticle (*Prockia*, Thadeo et al., 2008), or between the loose spongy cells of partly disintegrated mesophyll under palisade-like epidermis (*Polyothyrsis, Idesia*, Wilkinson, 2007). Secretory teeth of *Idesia* and *Populus* are glabrous, while the rest of the leaf is covered with trichomes (Wilkinson, 2007). The same pattern of indumentum distribution is observed in apical leaf glands of Proteaceae.

Teeth of *Leucadendron muirii* and *Mimetes cucullatus* strickingly liken *Idesia* foliar nectaries in their morphology and anatomy. In spite of that, the epidermal cells on Proteaceae salicoid teeth are less elongated radially than the typical palisade-like epidermal cells of secretory glands of Salicaceae/Flacourtiaceae, these cells seem to have changed their shape due to their secretory function. As the secretory teeth usually actually produce nectar only at certain stages of leaf developmetn, it is worth to perform a detailed study of the changes these structures experience in the course of leaf development. The genus *Leucadendron* is characterized by a wide adaptive radiation. Therefore, studies to cover the whole range of mucro forms within the genus could shed some light on evolutionary history of foliar nectaries as a highly specialized structure of great ecological importance.

References

Hickey L.J. 1979. A revised classification of the architecture of dicotyledonous leaves. In: Metcalfe C.R., Chalk L. (eds.): *Anatomy of the dicotyledons*. 2nd ed. Oxford: Clarendon Press. V. **1**. P. 25–39.

Hickey L.J., Wolfe J.A. 1975. The bases of angiosperm phylogeny: vegetative morphology. *Ann. Mo. Bot. Gard.* **62**: 538–589.

Lawton J., Heads P. 1984. Bracken, ants and extrafloral nectaries. I. The components of the system. *J. Animal Ecol.* **53**: 995–1014.

Midgley J.J. 1987. *Aspects of the evolutionary biology of the Proteaceae, with emphasis on the genus* Leucadendron *and its phylogeny*. Ph.D. Thesis. University of Cape Town.

Rebelo A.G. 1995. *A field guide to the proteas of Southern Africa*. Vlaeberg: Fernwood Press.

Rebelo A.G. 2001. *A field guide to the proteas of Southern Africa*. 2nd ed. Vlaeberg: Fernwood Press.

Rourke J.P. 1984. A revision of the genus *Mimetes* Salisb. (Proteaceae). *J. S. Afr. Bot.* **50**: 171–236.

Thadeo M., Cassino M.F., Vitarelli N.C., Azevedo A.A., Araújo J.M., Valente V.M., Meira R.M. 2008. Anatomical and histochemical characterization of extrafloral nectaries of *Prockia crucis* (Salicaceae). *Am. J. Bot.* **95**: 1515–1522.

Weston P.H., Barker N.P. 2006. A new suprageneric classification of the Proteaceae, with an annotated checklist of genera. *Telopea* **11**: 314–44.

Wilkinson H.P. 2007. Leaf teeth in certain Salicaceae and 'Flacourtiaceae'. *Bot. J. Linn. Soc*. **155**: 241–256.

Williams I.J.M. 1972. A revision of the genus *Leucadendron* (Proteaceae). *Contr. Bol. Herb.* **3**: 1–425.

Zachariades C., Midgley J.J. 1999. Extrafloral nectaries of South African Proteaceae attract insects but do not reduce herbivory. *Afr. Entomol.* **7**: 67–76.

TRANSFUSION TISSUE AND WATER RELATIONS IN THE LEAVES OF PODOCARPACEAE SPECIES OF THE TEMPERATE RAINFOREST OF SOUTH-CENTRAL CHILE

Alisa I. ARBICHEVA[1]***, Anatoly A. PAUTOV***[1]***, Alfredo SALDAÑA***[2]

[1] Komarov Botanical Institute of Russian Academy of Sciences, Saint Petersburg, Russia
[2] Universidad de Concepcion, Concepcion, Chile
alisaads@rambler.ru

Podocarpaceae Endl. is the second largest extant conifer family in terms of the number of genera and exhibits the greatest amount of morphological diversity (Taylor et al., 2009). Leaves of most podocarps are univeined, and it is a major limitation on overall leaf size and shape (Hill, Brodribb, 1999). In such leaves, water conduction occurs through the so-called transfusion tissue (TT). It is common for many species of gymnosperms (Frank, 1864; Esau, 1977; Hu, Yao, 1981). This adaptation in Podocarpaceae, along with shoot flattening, enables them to compete successfully with angiosperms in the tropics and temperate zones (Hill, Brodribb, 1999; Brodribb, 2011). Podocarpaceae of the temperate zone of south-central Chile include five species (Veblen et al., 2005), four of which possess leaves comparable in size with angiosperms. They are of interest for comparative analysis of water-conducting tissue architecture and water relations in leaves. The aim of the study is to identify water use strategies in the leaves of endemic Podocarpaceae of south-central Chilean temperate rainforest. Plant specimens were collected in Puyehue National Park and Nahuelbuta National Park. The methods used in the study are light and transmission electron microscopy.

The water conducting system in the leaves of *Podocarpus salignus* D. Don. includes the main vein, conspicuous transfusion tissue and accessory transfusion tissue (ATT). TT cells lie on both sides of the midvein and have an irregular isodiametric shape, sometimes elongate. They bear scalariform thickenings or circular bordered pits. Pit apertures are circular or slitlike. The border is pronounced. One may describe the TT tracheids in *P. salignus* leaves as specialized. They differ from wood tracheids in the disordered pit arrangement that cannot be classified as either alternate or opposite. Primary cell walls of transfusion tracheids are loose. Accessory transfusion tissue is composed of long tracheids, which extend perpendicularly to the main vein and almost reach the edge of leaf lamina. They have conspicuous cavities and slitlike bordered pits. Primary cell walls of ATT tracheids are dense. There are many prismatic or irregular crystals on the cell surface and in the primary cell wall. Parenchyma cells between ATT and mesophyll also bear numerous crystals on the walls contacting with intercellular spaces.

The water conducting system in the leaves of *Prumnopitys andina* (Poepp. ex Endl.) de Laub. includes the main vein with transfusion tissue located on both sides of it. TT consists of circular-elongated tracheids with reticulated thickenings, some of them with a prominent border. Primary cell walls of transfusion tracheids are loose. In the TT sheath cells there are occasional large prismatic crystals in the middle lamella. Sometimes they can be found on the cell walls contacting with intercellular spaces. Mesophyll is multilayered and isolateral.

The water conducting system in the leaves of *Podocarpus nubigenus* Lindl. includes the main vein with scarce transfusion tissue located on both sides of it. TT includes isodiametric tracheids of irregular shape bearing scalariform and reticulate thickenings, which are occasionally located in the same cell. Primary cell wall in the TT tracheids is heterogeneous: there are areas of loose and dense structure. A significant part of the mesophyll volume in this species is taken up by water-storage tissue (water-storing parenchyma). Its cells are less specialized and similar in shape and size to spongy mesophyll cells.

The water conducting system in the leaves of *Saxegothaea conspicua* Lindl. includes the main vein with extremely scarce transfusion tissue located on both sides of it. TT consists of isodiametric tracheids of irregular shape with reticulate cell wall thickening. The border is not prominent. Primary cell walls of transfusion tracheids are heterogeneous. A significant part of the mesophyll volume is taken up by water-storage tissue, which consists of large cells with chloroplasts indistinguishable in the light microscope.

Accessory transfusion tissue, which is characteristic of the *P. salignus* leaves, was described in broadleaf podocarps (Griffith, 1957; Brodribb et al., 2007; Locosselli, Ceccantini, 2012). ATT is considered to be an adaptation designed to enhance hydraulic conductance (K_{leaf}) through leaf lamina in the regions remote from the main vein (Brodribb, Holbrook, 2005; Brodribb et al., 2007). ATT cell function is analogous to regular xylem tracheids. The efficiency of this adaptation is quite obvious in that it enables single-vein leaves to achieve leaf widths that are orders of magnitude wider than predicted if they possessed unmodified mesophyll (Brodribb et al., 2007). ATT is an alternative to the dense venation system common in most angiosperms and Gnetaceae. It enables *P. salignus* to produce leaves with area more than 3 times larger than in podocarps lacking ATT. Pronounced transfusion tissue with loose primary cell walls permeable by water also reflects the specialization of this species in water conduction through leaf. *Podocarpus salignus* has a tendency to occur in gravelly riversides and moist canyons (Debreczy, Rácz, 2012), where it is not necessary to save water. *Podocarpus andina* leaves do not possess accessory transfusion tissue, because of which their size is significantly restricted. However, Brodribb et al. (2014) revealed that *P. andina* K_{leaf} is about 4 mmol/(m^2sMPa). This value exceeds the *P. salignus* hydraulic conductance (2.3 mmol/(m^2sMPa) measured in the same study. Multilayered isolateral mesophyll in *P. andina* leaves apparently greatly increases its conductivity to water.

We assumed that *P. andina* leaves have a capacity to conduct water apoplastically through the mesophyll, which is sufficient given the small leaf size. Primary cell walls in transfusion tracheids in *P. andina* leaves are loose, allowing unimpeded water movement. Crystals in the *P. andina* and *P. salignus* leaves are likely to be calcium oxalate and are the result of the elevated water flux through the leaves.

Saxegothaea conspicua and *P. nubigenus* possess another strategy, which is based on the accumulation, conservation and economical use of the water. It is realized through water-storage tissue (hydrenchyma) well-developed in both species. Water-storing cells in *S. conspicua* leaves are larger in size compared with chlorenchyma cells. They contain poorly developed chloroplasts and are simplastically isolated from spongy mesophyll cells. Water-storage tissue takes up the entire central part of the leaf in both species. This tissue in the *P. nubigenus* leaves is less specialized and contains well-developed chloroplasts. Water-storing cells are similar to spongy mesophyll cells and are connected with them by numerous plasmodesmatal connections. Transfusion tissue is poorly developed in both species. It is represented by single cells. At the same time, primary cell walls in transfusion tracheids contain dense areas, which may potentially impair their water permeability. *Saxegothaea conspicua* leaf hydraulic conductance varies from 1.6 mmol/(m^2sMPa) (Brodribb et al., 2005) to 2.5 mmol/(m^2sMPa) (Brodribb et al., 2014). *Podocarpus nubigenus* leaves have not yet been studied for this parameter, but it is reasonable to assume that it is within a similar range.

We have identified two water relation strategies in the podocarpaceous leaves of the studied community. The first is based on the intensification of water movement through the leaf. It manifests itself in the presence of specialized transfusion tissue tracheids and tracheids of accessory transfusion tissue (*P. salignus*) or in the tight placement of mesophyll cells, creating conditions for a continuous water path through apoplast (*P. andina*). The second strategy aims to accumulate water and use it sparingly. It is characteristic of species with water-storage tissue and poorly developed transfusion tissue tracheids (*P. nubigenus* and *S. conspicua*).

The authors are grateful to the Core Centre ‘Cell and Molecular Technology in the Plant Science’ at the Komarov Botanical Institute and the Resource Center for Molecular and Cell Technologies and Resource Center ‘Chromas’ of SPBU Research park. This study was supported by the RFBR (grant No. 17-04-01213A to AAP) and government assignment of the Komarov Botanical Institute No. AAAA-A18-118031690084-9 “Structural-functional basis of higher plants development and adaptation”.

References

Brodribb T.J. 2011. A functional analysis of podocarp ecology. In: Turner B.L., Cernusak L.A. (eds.): *Ecology of the Podocarpaceae in tropical forests*. Washington: Smithsonian Institution Scholarly Press. P. 165–173.

Brodribb T.J., Feild T.S., Jordan G.J. 2007. Leaf maximum photosynthetic rate and venation are linked by hydraulics. *Plant Physiol.* **144**: 1890–1898.

Brodribb T.J., Holbrook N.M. 2005. Water stress deforms tracheids peripheral to the leaf vein of a tropical conifer. *Plant Physiol.* **137**: 1139–1146.

Brodribb T.J., Holbrook N.M., Zwieniecki M.A., Palma B. 2005. Leaf hydraulic capacity in ferns, conifers and angiosperms: impacts on photosynthetic maxima. *New Phytol.* **165**: 839–846.

Brodribb T.J., McAdam S.A.M., Jordan G.J., Martins S.C.V. 2014. Conifer species adapt to low-rainfall climates by following one of two divergent pathways. *Proc. Natl. Acad. Sci. USA*. **111**: 14489–14493.

Debreczy Z., Rácz I. 2012. *Conifers around the world: conifers of the temperate zones and adjacent regions*. Budapest: DendroPress Ltd.

Esau K. 1977. *Anatomy of the seed plants*. New York: John Wiley & Sons.

Frank A.B. 1864. Beiträge zur Kenntnis der Gefässbündel. *Bot. Zeit.* **22**: 167–169.

Griffith M.M. 1957. Foliar ontogeny in *Podocarpus macrophyllus*, with special reference to transfusion tissue. *Am. J. Bot.* **44**: 705–715.

Hill R.S., Brodribb T.J. 1999. Turner Review No. 2 – Southern conifers in time and space. *Aust. J. Bot.* **47**: 639–696.

Hu Y.-S., Yao B.-J. 1981. Transfusion tissue in gymnosperm leaves. *Bot. J. Linn. Soc.* **83**: 263–272.

Locosselli G.M., Ceccantini G. 2012. Plasticity of stomatal distribution pattern and stem tracheid dimensions in *Podocarpus lambertii*: an ecological study. *Ann. Bot.* **110**: 1057–1066.

Taylor E.L., Taylor T.N., Krings M. 2009. *Paleobotany: the biology and evolution of fossil plants*. New York: Elsevier Science Publ.

Veblen T.T., Armesto J.J., Burns B.R., Kitzberger T., Lara A., León B., Young K.R. 2005. The coniferous forests of South America. In Andersson F. (ed.): *Coniferous forests*. Amsterdam: Elsevier. P. 293–317.

ANTHER DEVELOPMENT AND MICROSPOROGENESIS IN *HELIANTHUS CILIARIS* DC. AND *H. MAXIMILIANI* SCHRAD. (ASTERACEAE)

Anastasiya A. BABRO, Maria K. RYASANOVA, Olga N. VORONOVA

Komarov Botanical Institute of Russian Academy of Sciences,
Saint Petersburg, Russia
o_voronova@binran.ru

Sunflower is a very important agricultural plant in Russia. Plant breeders use interspecific hybridization of cultivated annual sunflower with wild perennials in order to improve the cultivars. Meanwhile, embryology of the most perennial *Helianthus* is not studied or studied insufficiently.

The wild perennial sunflowers *Helianthus ciliaris* DC. and *H. maximiliani* Schrad. studied here belong to *Ciliares* and *Divaricati* sections of the genus *Helianthus*, respectively (Schilling, Heiser, 1981). They differ in habit, flowering time and chromosome number, *H. ciliaris* being a tetraploid with chromosome number $2n = 68$, and *H. maximiliani* being a diploid with $2n = 34$.

The material was collected at Kuban experimental station of Vavilov Research Institute of Plant Industry. Whole flower heads at different developmental stages were picked up and fixed in FAA. The material was treated according to the classical method (Barykina et al., 2000). Permanent preparations for light microscopy were stained with: Toluidine Blue, Ehrlich's Hematoxyline with Eosine or Alcyan Blue, Heidenhain's Hematoxyline with Alcyan Blue (Zhinkina, Voronova, 2000), 'triple staining' (Kamelina et al., 1992) and Feulgen's Schiff reagent with Alcyan Blue ('triple staining' without Erlich's Hematoxyline).

The disk florets of *H. ciliaris* and *H. maximiliani* are similar in structure and development. They demonstrate characters typical of many Asteraceae (Babro, Voronova, 2018; Voronova, Babro, 2018). The parts of the flower differentiate centripetally (Fig. 1 *1, 2a, 3a*).

The anthers are tetrasporangiate and dithecous. Anther shape and microsporangia arrangement are similar in both species (Fig. 1 *2b, 3c;* 2 *2b*). The anthers are introrse, i.e. microsporangia on the adaxial (inner) side of anther are somewhat smaller, than the abaxial ones (Fig. 1 *5;* 2 *2b*). The anthers have long apical sterile appendage (Fig. 2 *2a*) which takes part in pollen releasing. There is an epidermal layer and more or less uniform cells inside it at the beginning of anther development. The archesporium initiation starts on the abaxial anther side when pistil is already formed (Fig. 1 *3b*). The more advanced stage of microsporangium wall development can be seen on the abaxial side (Fig. 1 *4, 5*).

Anther wall in both species develops centrifugally (Fig. 1 *3b, 4, 5, 6*) according to dicotyledonous type (Davis, 1966).

Completely differentiated anther wall in both species is four-layered and consists of epidermis, endothecium, middle layer and tapetum (Fig. 1 *6*). The middle layer is ephemeral, at the beginning of meiosis it usually undergoes degeneration and cannot be seen further on. At the stage of meiosis, the anther wall consists of three layers: epidermis, endothecium and tapetum (Fig. 2 *1a–c*).

Shift of the cytoplasm to the cell walls from the middle layer side is sometimes observed in the entire tapetal layer. This can be caused either by their functional state or by the effect of fixing solution. Shrinkage is observed only in the tapetal cells, while other anther tissues are fixed without such effects. So, this may indicate the onset of structural changes in the tapetum cells.

At the end of the meiosis II, the first signs of reorganization to false periplasmodium (syncitium) can be seen in tapetal cells of *H. ciliaris* (Fig. 2 *1c*). These cells begin to protrude into the locule, but they have cell walls at this stage; the entire reorganization occurs in postmeiotic period. In *H. maximiliani* such transformations can be observed earlier, during the first meiotic division.

In postmeiotic period, walls of tapetal cells disintegrate and 2–4-nucleate protoplasts migrate gradually inwards the locule (Fig. 2 *2c*).

In both species, some rather large tapetal patches remain at the periphery of anther locules at the stage of microspore releasing from tetrads. They persist dur-

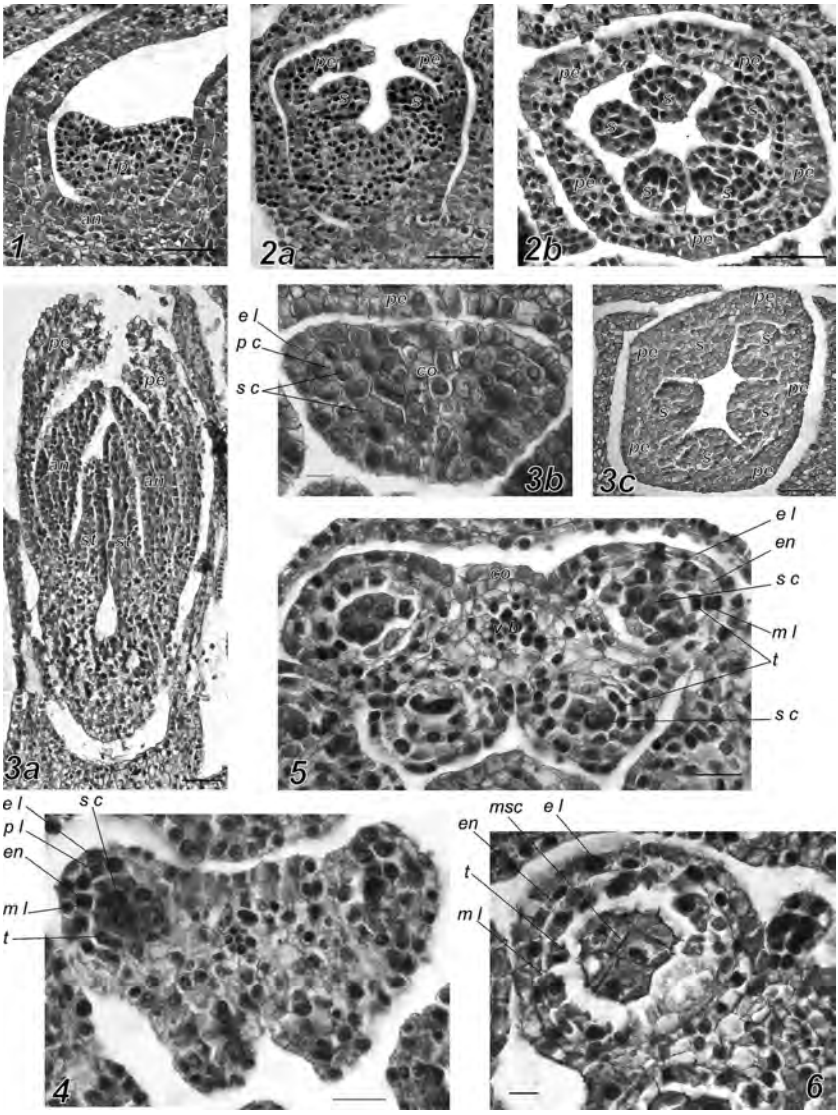

Fig. 1. Tubular flower initiation, androecium development and earlier stages of anther formation in *Helianthus ciliaris*.

1 – flower primordium, the beginning of petal differentiation, anther initial formation; *2* – petal development and anther differentiation, gynoecium does not initiate yet; *3a, b, c* – anthers during the first division of the archesporial cell; *4* – differentiation of wall layers in abaxial microsporangia; *5* – wall formation in adaxial microsporangia, increasing of sporogenous cells number and finishing of wall formation in abaxial microsporangia; *6* – abaxial microsporangium with microsporocytes at the stage of formed anther wall. *an* – anther, *co* – connective, *e l* – epidermal layer, *en* – endothecium, *f p* – flower primordium, *m l* – middle layer, *msc* – microsporocyte, *p c* – parietal cell, *pe* – petal, *p l* – parietal layer, *s* – stamen, *s c* – sporogenous cell, *st* – stigma, *t* – tapetum, *v b* – vascular bundle. Scale bars – 50 μm (*1, 2a,b, 3a,b*); 10 μm (*3c, 6*); 20 μm (*4, 5*).

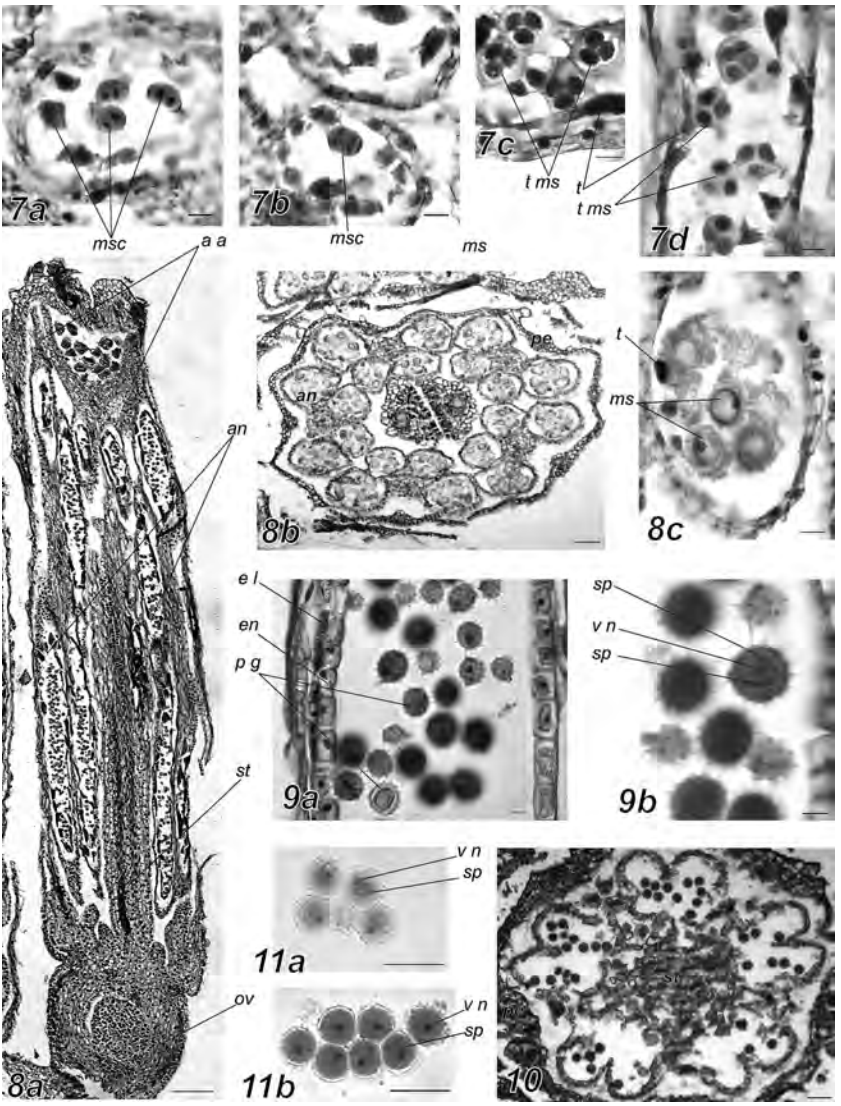

Figure 2. Microsporogenesis, pollen formation and anther development in *Helianthus ciliaris* and *Helianthus maximiliani*.

1a, b, c, d – successive stages of meiosis; *2a, b, c* – microspores after meiosis, their vacuolization and formation of exine sculpture; *3a, b* – anther locule with pollen grains, some of which are sterile, the anther wall is 2-layered, longitudinal sections; 3-celled pollen grains (*b*); *4* – transverse section of tubular flower with anthers at the stage of mature pollen, thecae of adjacent anthers look like united; *5a,b* – mature pollen grains with vegetative nucleus and sperm cells. *Helianthus ciliaris*: *1c*, *4, 5b; Helianthus maximiliani*: *1a,b,d, 2a,b,c, 3a,b, 5a*.

a a – anther appendage, *an* – anther, *e l* – epidermal layer, *en* – endothecium, *ms* – microspore, *msc* – microsporocyte, *ov* – ovary, *p g* – pollen grain, *sp* – sperm cell, *st* – stigma, *t* – tapetum, *t ms* – tetrad of microspores, *v n* – vegetative nucleus.

Scale bars – 50 μm (*2b, 4, 5a,b*); 10 μm (*1a,b,c,d, 2c, 3a,b*); 100 μm (*2a*).

ing microspore vacuolization, too. As a rule, tapetum degenerates entirely before the stage of 2-celled pollen grains. But in some anthers of *H. ciliaris* the tapetum remains were observed as dark conglomerations even at this stage. In such case, pollen grains had thickened wall.

The wall of mature anther consists of two layers, the epidermis and endothecium. Fibrous thickenings form in endothecium cells. In both species they become evident at the stage of 2-celled pollen grains. Sometimes it happens before meiosis completion in all microspores in the locule. The endothecium becomes thicker, than the epidermis by this time.

Starting with the formation of the 3-layered anther wall and the onset of microsporogenesis, the abaxial microsporangia of adjacent stamens touch by their epidermises and form the anther tube. The adaxial sporangia of neighboring stamens occasionally stick together. Sometimes the abaxial microsporangia of one stamen are in contact with their adaxial counterparts of the neighboring one. Postgenital accretion of stamens in one form or another was observed in both species (Fig. 2 *2b*).

Anthers dehisce by longitudinal slits before flower opening. The walls between the microsprangia of thecae break down simultaneously by this time. The edges of the adjacent anther slits come in touch due to their close location and anther aggregation. It is discernible in the transverse sections and looks like joining of the thecae of adjacent anthers in both species. It manifests mostly at the middle level of flower, where anthers dispose very tightly (Fig. 2 *4*). The upper parts of anthers are narrower, they are situated more loosely, and the slits of the anthers contact in a lesser degree.

In both species, anther opening was noted at the stage of immature 2-celled pollen grains.

The anthers and anther appendages form a canal to release pollen into it. The style pushes pollen through the anther tube. It results in accumulation of pollen as a small clump on the top of stamen (anther) tube in the flower of *Helianthus*.

Microsporogenesis is of simultaneous type (Fig. 2 *1a–c*). The process of cytokinesis is accompanied by callose wall formation between the microspores within the tetrad. Usually the tetrads of microspores are tetrahedral, rarely isobilateral. Meiosis is accompanied by spacing of microsporocytes. In *H. ciliaris*, they are densely packed and form a tissue before (Fig. *6*) and in the beginning of the meiosis. In *H. maximiliani*, microsporocytes begin to diverge from each other already at the onset of meiosis. Microspore tetrads of both species are free, widely spaced in locule (Fig. 2 *1d*).

Free microspores, and further pollen grains, differ in size and form.

For example, in *H. ciliaris*, malformed microspores were observed; cells with too thick walls, not characteristic of the current stage; intensely black-stained microspores and pollen grains, presumably, in destruction process; distorted cells; microspores and pollen grains of different size within the same locule.

In *H. maximiliani*, there are also observed pollen grains of different size within the same locule, differently stained ones and too large pollen grains with contorted content.

The characteristic sculpture of the exine forms gradually after microspore releasing from tetrads (Fig. 2 *2c, 3a,b*). Microspore cytoplasm becomes vacuolated, and the nucleus migrates towards the wall (Fig. 2 *2*c). The first mitotic division results in vegetative and generative cells. After that, vacuole reduces, and generative cell gradually moves away from the wall. Vegetative and generative cell nuclei are round-shaped. The nucleus of the vegetative cell is larger and stains less intensively.

The mitotic divisions inside the microspores take place asynchronously.

Mature pollen grains of both species are 3-celled, which is typical of sunflowers. Two small round sperm cells result from the generative cell division. They gradually become elongated (Fig. 2 *3b, 5a, b*). Sperm cells in mature pollen of *H. maximiliani* elongate so much that their length becomes more than pollen grain diameter, and they become curved (Fig. 2 *5a,b*).

References

Babro A.A., Voronova O.N. 2018. Development of male reproductive structures in *Helianthus ciliaris* and *H. tuberosus* (Asteraceae). *Bot. Zhurn*. **103**: 1093–1108. [In Russian]

Barykina R.P., Veselova T.D., Devyatov A.G., Dzhalilova H.H., Ilyina G.M., Chubatova N.V. 2000. *The basic principles of microtechnique in botany. A reference guide*. Moscow: Moscow Univ. Press. [In Russian]

Davis G.L. 1966. *Systematic embryology of the Angiosperms*. New York, London, Sydney: Wiley.

Kamelina O.P., Proskurina O.B., Zhinkina N.A. 1992. On the method of staining of embryological preparations. *Bot. Zhurn*. **77**: 93–96. [In Russian]

Schilling E.E., Heiser C.B. 1981. Infrageneric classification of *Helianthus* (Compositae). *Taxon* **30**: 393–403.

Voronova O.N., Babro A.A. 2018. Early stages of formation of female reproductive structures in *Helianthus ciliaris* and *H. tuberosus* (Asteraceae). *Bot. Zhurn.* **103**: 488–504. [In Russian]

Zhinkina N.A., Voronova O.N. 2000. On staining technique of embryological slides. *Bot. Zhurn*. **85**: 168–171. [In Russian]

PHARMACOGNOSTIC AND ANATOMICAL STUDIES OF THREE *JATROPHA* SPECIES FROM INDIA

Rani B. BHAGAT

Baburaoji Gholap College, Sangvi, Pune-27, India

rb_botany@rediffmail.com

Jatropha (Gk. – *jatros*: doctor, *trophe*: nutrition) with 172 species, referring to its medicinal use, belongs to the family Euphorbiaceae. *Jatropha* is worldwide

known for its significant economic importance. It is native to Central America and popularized in Africa and Asian countries due to its potential use as biofuel. It has an immense potential in traditional health care system of medicine. *Jatropha* species play a significant role in preventing infectious organisms. In this context, it is necessary to find out drug admixtures in market samples with the help of pharmacognostic and anatomical evaluation. Present research work deals with the evaluation of three *Jatropha* species, namely *J. gossypifolia*, *J. glandulifera* widely occurring throughout India and *J. nana* which is an ephemeral endemic and threatened species found in pune, Maharashtra. *Jatropha* species selected are reported for biofuel value and in traditional medicine for diarrhoea, dysentery, inflammation and pneumonia. The leaves and roots are investigated for its correct identity based on pharmacognostic and anatomical characters and by using marker compound. The powdered mature roots showed presence of starch grains in *J. glandulifera* and *J. nana* while these are absent in *J. gossypifolia*. In the secondary structure, a thick periderm formed by suber and phelloderm strata was detectable. Secondary xylem vessels are 1–4 cells in length with wider lumen in *J. glandulifera* and *J. nana* while these are 1–5 cells in length with narrow lumen in *J. gossypifolia*. Microscopic investigation of leaf powder showed the presence of calcium oxalate crystals in two species, *J. glandulifera* and *J. gossypifolia*, while these are absent in *J. nana*. In all three *Jatropha* species, stomata are paracytic and the leaves are amphistomatic. These species are also evaluated for stomatal number, stomatal index, vein-islet number and palisade ratio.

SEED DEVELOPMENT IN RANUNCULACEAE SPECIES AS MANIFESTATION OF ADAPTIVE POSSIBILITIES

Oksana G. BUTUZOVA

Komarov Botanical Institute of Russian Academy of Sciences,
Saint Petersburg, Russia
OButuzova@binran.ru

Most species of Ranunculaceae are characterized by the presence of underdeveloped embryo in the seed at dissemination. This phenomenon has been conserved in evolution in the most primitive gymnosperms and some angiosperms, and was an important step in establishing the period of seed dormancy, associated with adapting to experiencing adverse conditions, particularly in seasonal climates.

The embryo postdevelopment and seed germination are known to be a temperature dependent processes. They are rather often realized in the same species under the different temperature conditions, being connected with so-called physi-

ological mechanism of inhibiting (PhMI) of embryo development and germination. The period of seed formation is frequently very prolonged in this case, taking even 1–2 years before germination, and hereof is bound to certain seasons. So, the whole embryogenesis is vulnerable having to gain a combined reliable and plastic protection system to adapt to changing environments.

The present work is aimed to identify the characteristics of seed development and to detect their connection with the adaptive capabilities of some species of Ranunculaceae family, as well as with the morphogenetic pathways.

The phenomenon of embryo postdevelopment is most widely and variously represented in Ranunculaceae. A comparative study was carried out in three temperate species: *Pulsatilla vulgaris* Mill., *Helleborus niger* L., *Aconitum soongaricum* Stapf, which contrast by the degree of embryo differentiation at dissemination, the type of seed dormancy, life form, longevity of seed formation period before and after seed fall, ecological niche and habitats.

The forest European species *Pulsatilla vulgaris* is characterized by the early torpedo-shaped stage of embryo at dissemination and morphological type of seed dormancy *sensu* Nikolaeva (1999), the latter being caused only by underdeveloped embryo. The flowering continues from April to May, fruiting takes place in June.

Aconitum soongaricum is an endemics of Tien Shan Mountains, its embryo at dissemination is at the early torpedo-shaped stage, seed has morphophysiological type of dormancy, which is caused by the presence of underdeveloped embryo and physiological mechanism of germination inhibiting (PhMI). The flowering occurs in July–August, fruiting is in September.

The European mountain ephemeroid *Helleborus niger* has heart-shaped embryo in seed at dissemination, morphophysiological type of seed dormancy; its flowering proceeds from January to March, fruiting continues from May to June.

Optimal regimes of embryo postdevelopment and root emerging were experimentally revealed for each species. The seeds of *P. vulgaris* germinate within 17–23 days at 18–20 °C, *A. soongaricum* seeds germinate within 90–160 days at 0–10 °C and *H. niger* seeds germinate within 150–180 days at alternating temperatures (from 18–20 °C to 0–10 °C).

So, postdevelopment and germination take different periods of time against the background of varying degrees of embryo differentiation at dissemination and temperature conditions. The most differentiated embryo of *P. vulgaris* which forms in warm season takes the shortest period of time for embryo postdevelopment, the seeds germinating immediately thereafter. The mature seeds of *A. soongaricum* contain less differentiated embryo with well distinguishable organs. It develops under the lower temperatures, so the period of postdevelopment is longer. On the contrary, the embryo of *H. niger* at dissemination is at the heart-shaped stage, and the process of subsequent organogenesis proceeds under influence of low tempera-

ture, so it is the most prolonged, and the seeds require the alternation of warm and cold periods to germinate.

The phenomenon of embryo formation isolated from the maternal organism already imposes a number of features of seed development. Common traits of the formation of seeds with underdeveloped embryo were earlier revealed (Butuzova et al., 1997; Pozdova et al., 1998; Butuzova, 2014) as follows: the presence of specific endosperm cavity, in which the embryo grows; specific zonality of endosperm by cell structure and nutriments distribution; early accumulation of nutriments in embryo and endosperm cells; starch and protein as nutrients; the prolong function of the structures in micropylar and chalazal parts of the seed; high degree of histo- and organogenic differentiation of the embryo after completing postdevelopment.

However, all these traits are manifested and realized differently in the species investigated. So, the endosperm cavity around the embryo of *P. vulgaris* is filled with lyses products of the endosperm cells throughout the embryogenesis on the mother plant, whereas in *H. niger* it remains as if empty, having clear outlines formed by intact cell walls. The secondary endosperm cavity of *A. soongaricum* seed originates by combining the primary cavity around the embryo with the central vacuole, the latter remaining due to the arrested cell formation in the endosperm. This cavity prolongs from the micropylar end to the chalazal one.

Specific fan-shaped zonality of the cellular endosperm of *H. niger*, maintained up to dissemination, is worth being mentioned. Such a zonality was not observed in *P. vulgaris*. *P. vulgaris* is distinguished by the most active cells with the densest plasma and large nuclei displaced closer to the micropyle in endosperm central part. Endosperm zonality of *A. soongaricum* seeds is manifested by the straight cell rows which run perpendicular to the secondary endosperm cavity.

Nutriment accumulation and specialization of the integument cells differently correspond in time in species investigted. In *H. niger*, the nutriments in endosperm cells appear already at the proembryo stage and seed coat specialization begins at the globular stage of embryo. In *P. vulgaris*, both processes co-occur at the heart-shaped developmental stage. These processes are also synchronous in *A. soongaricum* but they take place at the early torpedo-shaped stage. The chalaza region structures and antipodes are longest to persist in *A. soongaricum*, they continue functioning up to the postdevelopment completion in disseminated seeds. In *P. vulgaris* seeds, the cells of postament and podium as well as antipodes stay active till the globular stage of embryogenesis and in *H. niger*, the cells of chalaza structures and antipodes derange and lyse already at the stage of early proembryo. The embryo of *A. soongaricum* is most advanced at the end of postdevelopment: it has the first leaf primordium and apparent bundles with developed protoxylem elements.

Besides many common features of seed formation, the species studied differ in pericarp with numerous starch grains in *P. vulgaris*, photosynthetizing perianth and heterospermy in *H. niger*, nutriment storing antipodes in *A. soongaricum* etc. The differences mentioned are believed to be associated with different pathways

of nutrient transportation and their change during the seed development on the maternal plant and after dissemination.

Photosynthetizing perianth in *H. niger*, earlier accumulation of nutrients in the endosperm, its specific fan-shaped zonality, ephemeral antipodes, clear boundaries of the endosperm cavity without cell lysis are all considered to be associated with switching from micropyle-sourced nutriment transport (before dissemination) into endosperm-sourced transport (at postdevelopment) and with economical consumption of substances throughout embryogenesis.

The pericarp with numerous starch grains in *P. vulgaris*, longer-functioning storage antipodes, lysis of endosperm cells adjacent to the endosperm cavity are believed to be associated with faster seed development without switching nutriment transport pathway.

Extremely long persistence and functioning of chalaza structures in *A. soongaricum* seems to be associated with the transition from apical nutriment supplying of the embryo to the basal one through podium, postament, antipodes and the secondary endosperm cavity.

The differences of seed formation in investigated ranunculaceous species are concluded to be related with their specific adaptations. There is firstly the extremely long period of embryogenesis, during which significant reorganizations of the seed structures and repartition of their functions can occur to ensure the normal seed development. Development of the embryo, endosperm and seed coat tightly correlates with the development of tissues of the perianth and gynoecium. Their development also correlates environmental changes.

The more complex and time-consuming are the processes of seed formation, dormancy breaking and germination, the more changeable they are. The phenomenon of embryo underdevelopment in seeds, though archaic and conservative is thought to have become sufficiently plastic during evolution. It seems to be adaptive in changing environments of seasonal climates. In addition, the phenomenon of underdeveloped embryo as a reproductive strategy enables the species to make seed bank for surviving and to avoid competition with more 'advanced' species.

References

Butuzova O.G., Titova G.E., Pozdova L.M. 1997. Peculiarities of seed development completed beyond maternal plant (the phenomenon of "underdeveloped embryo"). *Bull. Polish Acad. Sci*. **45**: 267–275.

Butuzova O.G. 2014. The problem of dormancy in seeds with underdeveloped embryo. *Proc. Intern. Sci. Conf. devoted to the 300th anniversary of Komarov Botanical Institute RAS.* Saint Petersburg. P. 40–43.

Nikolaeva M.G. 1999. Patterns of seed dormancy germination as related to plant phylogeny and geographical conditions of their habitat. *Plant Physiol*. **46**: 369–373.

Pozdova L.M., Butuzova O.G., Titova G.E. 1998. Embryo development in seeds with morphophysiological type of dormancy in *Aconitum soongaricum* (Ranunculaceae) as an example. *Bot. Zhurn*. **83**: 63–74.

THE IMPACT OF SHOOT APICAL MERISTEM SIZE ON THE STRUCTURE OF COMPOUND LEAF IN FASCIATED MUTANTS OF *PISUM SATIVUM*

Ekaterina A. BYKOVA*, *Vladimir V. CHOOB

Lomonosov Moscow State University, Moscow, Russia

katebykova.90@mail.ru

The rate of cell division in the central zone of shoot apical meristem depends on signaling cross talk between the rib-zone and upper layers of tunica. Any disturbance of this interaction leads to a change in the number of cells in the meristem. The phenomenon of significant intensification of cell division and consequent increasing of meristem size is called fasciation (Choob, Sinyushin, 2012). This process often occurs *via* the enrichment of stem cell pool in the central zone of the meristem.

During formation of any organ primordia, the meristem 'allocates' a certain number of cells, whose fate is rather strictly programmed. It is logical to assume that due to an increase of the cell number in the meristem, the 'allocated' cell pool can correlatively change, leading to modifications in organ morphology and arrangement.

In previous papers (Gourlay et al., 2000; Bykova et al., 2015) devoted to manifestations of fasciation in *P. sativum*, the 'allocated' portion of meristematic cells intended for the development of a single compound leaf (including its base and stipules) was designated as a blastozone. In the present study, we used seedlings of two fasciated mutant lines of pea: "Shtambovy" and "Rosacrone". Wild type plants of "Nemchinovskiy–766" variety served as control (isogenic to "Shtambovy").

Anatomical analysis of cells of the shoot apical meristem (SAM) of "Shtambovy" revealed ultrastructural features: irregular thickness of the cell walls and a large number of vesicles with electron dense loose inclusions, which were not characteristic of SAM of non-fasciated plants.

In fasciated mutants of pea, the number of leaflets and tendrils of the compound leaf did not change. These numbers increased gradually, depending on the node number, in the same manner as in wild type plants. The changes were only revealed in rachis and stipule number and arrangement. For example, instead of single rachis, two rachises per node are formed. This phenomenon is usually accompanied by development of the additional stipules from both sides of the new rachis. We also recorded incompletely divided stipules in between two rachises of the same node. However, in some cases, these rachises were not independent: we often found incompletely fused rachises. All these observations could be explained by gradual increasing of the blastozone size.

Thus, the complexity of leaf structure in certain node could be an indirect method of blastozone measurement. In order to obtain the direct data on the correlation between the changes in the compound leaf structure and the shoot meristem size, we carried out morphometric measurements of SAM in wild type and fasciated mutants.

The meristem size in the fasciated line "Rosacrone" increased gradually with the node number, significantly differing from the similar values in the wild type. Nevertheless, the differences between the wild type and another fasciated line "Shtambovy" cannot be unequivocally recognized. At the same time, the plants of "Shtambovy" exhibit a strong correlation between the maximal linear size of the meristem and the number of rachises per node. For example, when three rachises were located on one node, the average linear size of the meristem was 600 μm, if there was a single rachis on the node, the meristem linear size was approximately 170 μm. The difference is almost three-fold. We have not registered similar correlation in the other fasciated line "Rosacrone" probably because of late manifestation of fasciation in development (Bykova et al., 2015).

Consequently, as a final conclusion we note that the main impact of the linear meristem size on the compound leaf structure in pea involves mainly the increase of rachis and stipules number per node, rather than changes in leaflet and tendril number.

References

Bykova E.A., Labunskaya E.A., Choob V.V. 2015. Morphological changes in the structure of blastozones during fasciation of *Pisum sativum* L. and *Arabidopsis thaliana* (L.) Heynh. *Biol. Bull*. **42**: 179–185.

Choob V.V., Sinyushin A.A. 2012. Flower and shoot fasciation: from phenomenology to the construction of models of apical meristem transformations. *Russ. J. Plant Physiol.* **59**: 530–545.

Gourlay C.W., Hofer J.M.I., Ellis T.H.N. 2000. Pea compound leaf architecture is regulated by interactions among the genes *UNIFOLIATA*, *COCHLEATA*, *AFILA*, and *TENDRIL-LESS*. *Plant Cell* **12**: 1279–1294.

HETEROTOPIC EVOLUTION OF FLORAL NECTARIES IN APOCYNACEAE

Natalie CAPELLI*, *Diego DEMARCO

University of São Paulo, São Paulo, Brazil

na.capelli@gmail.com

Nectaries can occur in all parts of the flower and produce many types of sugary exudates, named nectar, which is one of the most important floral resources

produced by plants pollinated by animals (Fahn, 1979). In general terms, nectaries may be constituted by epidermis and/or parenchyma which may or may not be vascularized (Fahn, 2000; Pacini et al., 2003).

Among the families with floral nectaries, Apocynaceae are highlighted by having them in different positions and with different structures and strategies for the release and storage of nectar (Demarco, 2017; Monteiro, Demarco, 2017), being a good model for the study of the evolution of this gland in relation to the diversification of the family.

In Rauvolfioideae and Apocynoideae, the nectary may be present or absent. When present, in some species it forms a basal ring around the ovary, often lobed in the apical portion (Woodson, Moore, 1938; Rao, Ganguli, 1963; Galetto, 1997; Endress, Bruyns, 2000; Gomes et al., 2008; Morokawa et al*.,* 2015). Anatomically, these nectaries are usually composed of a nectariferous parenchyma that releases the nectar through stomata (Woodson, Moore, 1938; Walker, 1975; Simões et al., 2007). However, in some genera, such as *Aspidosperma*, *Himatanthus*, *Nerium* and *Plumeria*, the nectary has become inconspicuous or non-functional (Woodson, Moore, 1938; Haber, 1984; Herrera, 1991; Lin, Bernardello, 1999).

In Asclepiadoideae, the nectariferous tissue occurs primarily in the inter-staminal region of the filament tube (Galil, Zeroni, 1965; Christ, Schnepf, 1985; Kunze, 1991, 1995, 1997; Kunze, Liede, 1991; Endress, 1994; Endress, Bruyns, 2000; Vieira, Shepherd, 2002; Demarco, 2017; Monteiro, Demarco, 2017) and may present the nectar in the stigmatic chamber or in the corona or at the base of the corolla next to the gynostegium (Kunze, 1991; Demarco, 2017; Monteiro, Demarco, 2017). In this case, the nectary is composed only by one epidermis or by epidermis and one to four layers of parenchyma (Galil, Zeroni, 1965; Schnepf, Christ, 1980; Valente, 1984, 1995; Valente, Silva, 1984; Christ, Schnepf, 1985; Kunze, 1991, 1995, 1999; Kunze, Liede, 1991; Vieira, Shepherd, 2002; Valente, Costa, 2005; Demarco, 2017; Monteiro, Demarco, 2017). In addition, some genera of Asclepiadoideae have nectaries in the corona. Kunze (1999) observed three nectariferous regions in *Gonolobus*: stigmatic chamber, base of the filament tube and external portion of the ring formed by the corona, and Demarco (2017) and Monteiro & Demarco (2017) found nectariferous tissue in the staminal corona of *Blepharodon* and *Peplonia*, besides the staminal and inter-staminal corona of *Matelea.* The presence of nectaries in the corona seems to be a characteristic of Asclepiadoideae.

Considering the diversity of nectary positions in Apocynaceae associated with its great morphological and functional variation, this work aimed to analyze the structure, position and origin of the nectaries of Apocynaceae, with a focus on their heterotopic evolution. For this study, we used flowers of species belonging to the five subfamilies. These flowers were collected in the herbarium of the State University of Campinas (UEC) and the Municipal Botanical Museum of Curitiba (MBM). The herbarium specimens were rehydrated (Smith, Smith, 1942) embed-

ded in methacrylate (Meira, Martins, 2003) and serially sectioned in a rotary microtome. Some flowers were also dissected and analyzed using scanning electron microscopy.

The nectaries of the most basal subfamily, Rauvolfioideae, are originated by gynoecium. These nectaries protrude from the ovary, forming a ring or distinct lobes. Some species have inconspicuous nectaries with no projection of the ovarian tissues, being composed of few cells at the ovary base, near the receptacle. This morphological diversity is also observed anatomically. The secretory tissues of the nectaries are constituted by only epidermis, epidermis and parenchyma, or only parenchyma. In Apocynoideae, nectaries usually form a ring around the ovary or lateral projections partially fused to the ovary. These nectaries in some species are supplied by many vascular bundles or phloem strands, which allows to investigate their origin through analysis of the floral vasculature. Although morphologically some nectaries of Apocynoideae seem independent of the ovary, the vasculature demonstrate their origin from the gynoecium. Anatomically, the nectaries of this subfamily are similar to those of Rauvolfioideae, composed of secretory epidermis and parenchyma or only parenchyma.

In the most derived subfamily, Asclepiadoideae, nectaries are present in the androecium, in the inter-staminal region of the filament tube. In addition, there was a reduction of the secretory tissues in these nectaries, being composed of only epidermis in almost all members of the subfamily. Nectariferous parenchyma was rarely found in few species. Conversely, some genera have additional nectaries (secondary nectaries) in the corona, mainly in staminal position. These results show that there was some heterotopic alteration of these glands during the evolution of the flowers in the family. This higher number of nectary types may reflect new strategies of pollination which is related to the higher diversification of these flowers within the family.

The work was supported by FAPESP, grant No. 2018/09200-6.

References

Christ P., Schnepf E. 1985. The nectaries of *Cynanchum vincetoxicum* (Asclepiadaceae). *Isr. J. Bot*. **34**: 79–90.

Demarco D. 2017. Floral glands in asclepiads: structure, diversity and evolution. *Acta Bot. Bras*. **31**: 477–502

Endress M.E., Bruyns P.V. 2000. A revised classification of the Apocynaceae s. l. *Bot. Rev*. **66**: 1–56.

Endress P.K. 1994. Floral structure and evolution of primitive angiosperms: recent advances. *Plant Syst. Evol*. **192**: 79–97.

Fahn A. 1979. *Secretory tissues in plants.* London: Academic Press.

Fahn A. 2000. Structure and function of secretory cells. *Adv. Bot. Res*. **31**: 37–75.

Galetto L. 1997. Flower structure and nectar chemical composition in three Argentine Apocynaceae. *Flora* **192**: 197–207.

Galil J., Zeroni M. 1965. Nectar system of *Asclepias curassavica*. *Bot. Gaz*. **126**: 144–148.

Gomes S.M., Kinoshita L.S., Castro M.M. 2008. Hemisincarpia e nectário apendicular enfocadaos através de ontogênese floral em *Mandevilla velame* (A. St.-Hil.) Pichon, Apocynoideae. *Rev. Bras. Bot.* **31**: 81–93.

Haber W.A. 1984. Pollination by deceit in a mass-flowering tropical tree *Plumeria rubra* L. (Apocynaceae). *Biotropica* **16**: 269–275.

Herrera J. 1991. The reproductive biology of a riparian Mediterranean shrub, *Nerium oleander* L. (Apocynaceae). *Bot. J. Linn. Soc*. **106**: 147–172.

Kunze H. 1991. Structure and function in asclepiad pollination. *Plant. Syst. Evol*. **176**: 227–253.

Kunze H. 1995. Floral morphology of some *Gonolobeae* (Asclepiadaceae). *Bot. Jahrb. Syst*. **117**: 211–238.

Kunze H. 1997. Corona and nectar system in Asclepiadinae (Asclepiadaceae). *Flora* **192**: 175–183.

Kunze H. 1999. Pollination ecology in two species of *Gonolobus* (Asclepiadaceae). *Flora* **194**: 309–316.

Kunze H., Liede S. 1991. Observations on pollination in *Sarcostemma* (Asclepiadaceae). *Plant Syst. Evol*. **178**: 95–105.

Lin S., Bernardello G. 1999. Flower structure and reproductive biology in *Aspidosperma quebracho-blanco* (Apocynaceae), a tree pollinated by deceit. *Int. J. Plant Sci*. **160**: 869–878.

Meira R.M.S.A., Martins F.M. 2003. Inclusão de material herborizado em metacrilato para estudos de anatomia vegetal. *Rev. Árvore*. **27**: 109–112.

Monteiro M., Demarco D. 2017. Corona development and floral nectaries in Asclepiadeae (Asclepiadoideae, Apocynaceae). *Acta Bot. Bras*. **31**: 420–432.

Morokawa R., Mayer J.L.S, Simões A.O., Kinoshita L.S. 2015. Floral development of *Condylocarpon isthmicum* (Apocynaceae). *Botany* **93**: 769–781.

Pacini E., Nepi M., Vesprini J.L. 2003. Nectar biodiversity: a short review. *Plant Syst. Evol*. **238**: 7–21.

Rao V.S., Ganguli A. 1963. Studies in the floral anatomy of the Apocynaceae. *J. Indian Bot. Soc*. **42**: 419–435.

Schnept E., Christ P. 1980. Unusual transfer cells in the epithelium of the nectaries of *Asclepias curassavica* L. *Protoplasma* **105**: 135–148.

Simões A.O, Livshultz T., Conti E., Endress M. 2007. Phylogeny and systematics of the Rauvolfioideae (Apocynaceae) based on molecular and morphological evidence. *Ann. Mo. Bot. Gard*. **94**: 268–297.

Smith F.H., Smith E.C. 1942. Anatomy of the inferior ovary of *Darbya*. *Am. J. Bot*. **29**: 464–471.

Valente M.C. 1984. *Ditassa eximia* Decne (Asclepiadaceae). *Anatomia vegetal. Atas da Sociedade Botânica do Brasil*. **2**: 53–59.

Valente M.C. 1995. *Matelea maritima* subsp. *ganglinosa* (Vell.) Font. – Anatomia e vascularização floral (Asclepiadaceae). *Arq. Jard. Bot. Rio de Janeiro*. **33**: 75–98.

Valente M.C., Costa C.G. 2005. Estudo anatômico da flor de *Marsdenia loniceroides* E. Fournier (Asclepiadoideae – Apocynaceae). *Rodriguésia* **56**: 51–66.

Valente M.C., Silva N.M.F. 1984. Anatomia floral de *Barjonia erecta* (Vell.) Schum. (Asclepiadaceae). *Rodriguésia* **36**: 95–106.

Vieira M.F., Shepherd G.J. 2002. *Oxypetalum banksii* subsp. *banksii*: a taxon of Asclepiadaceae with an extragynoecial compitum. *Plant Syst. Evol*. **233**: 199–206.

Walker D.B. 1975. Postgenital carpel fusion in *Catharanthus roseus* (Apocynaceae): I. Light and scanning electron microscopic study of gynoecial ontogeny. *Am. J. Bot*. **62**: 457–467.

Woodson R.E., Moore J.A. 1938. The vascular anatomy and comparative morphology of Apocynaceae flowers. *Bull. Torrey Bot. Club*. **65:** 135–166.

POSITIONAL CONTROL OF PLANT TISSUE DIFFERENTIATION

Vladimir V. CHOOB

Lomonosov Moscow State University, Moscow, Russia
choob_v@mail.ru

Plant tissue differentiation in ontogeny follows precise spatial patterns. The procambial strand position is tightly associated with subsequent leaf and stem venation. Vascular bundles exhibit their polarity by formation of phloem and xylem in the proper spatial and temporal mode. Leaf trichomes and guard cells display visible proximal order with prohibition of new trichome or stomata formation in close neighborhood to each other. All these examples demonstrate that plant cells should differentiate according to various positional signals, emitting by singular cells or cell groups.

The term of positional information was invented by Lewis Wolpert (1969), who was attempted to solve the problem of differentiation of identical cells in concordance with their position. His famous model of French flag postulates the existence of some source of positional signal (morphogen). The morphogen concentration should decrease as it diffuses through the field of cells. Several threshold levels of morphogen concentration define the developmental fate of every cell, thus depending on the positional signal.

Differentiation of phloem and xylem from procambial strand could be well-circumscribed by the French flag model. The cells of the presumptive protophloem excrete a small peptide of CLE-family (TDIF), which plays the role of the positional signal. The concentration of TDIF decreases with the distance from the protophloem pole. Non-differentiated procambial cells expose the membrane receptor PXY, specifically binding to CLE-peptide (Fisher, Turner, 2007). The high level of CLE-peptide TDIF causes phloem differentiation, medium level of TDIF leads to cambial cell formation, whereas low level / absence of TDIF induces xylem development (Etchells, Turner, 2010). Thus mutations in *TDIF* or *PXY* drive toward xylem overproduction and defects in phloem differentiation, while the hyper-expression of *TDIF* has the opposite effect of massive phloem development.

Extracellular position signals in the form of small cysteine-rich peptides are used in stomata patterning. In *Arabidopsis* the meristemoid cells synthesize EPIDERMAL PATTERNING FACTORS 1 and 2 (EPF1, EPF2), inhibiting new meristemoid formation in close proximity to the existing ones. As a consequence of dysfunction of this positional signaling system, multiple clustered stomata develop in mutants *too many mouth,* encoding the subunit of the membrane EPF-receptor

complex, whereas the EPF1/2 overproduction is accompanied in low stomata density (Zoulias et al., 2018).

Positional signals may be distributed within plant cells through plasmodesmata. The establishment of radial patterning in root requires the interplay of central cylinder and cortical cell signals. In *Arabidopsis,* transcription factor SHORT ROOT (SHR) is transferred from pericycle cell lineage to the presumptive endodermis, where it induces expression of transcription factor SCARECROW (SCR). Mutual effect of SHR and SCR drives the cells to endodermal differentiation. Rapid cessation of positional signal toward cortex parenchyma cells occur due to block of transfer from endodermal lineage to cortex parenchyma *via* plasmodesmata (Helariutta et al., 2000). The mutation in *SCR* gene causes complete loss of endodermis in roots and starch sheath layer in shoots. These observations render the role of SCR in radial patterning both in roots and shoots (Wysocka-Diller et al., 2000). Recently, the involvement of SHR–SCR system of positional signaling, exploiting the same principles of plasmodesmatal transfer, was postulated for mesophyll–bundle sheath differentiation during the establishment of Kranz-anatomy in C_4 leaves (Slewinski et al., 2012; Fouracre et al., 2014).

All the listed examples suggest the important role of positional information in plant tissue differentiation, despite the diversity of the underlying molecular mechanisms. Therefore, the positional signaling orchestrates the proper spatial organization of plant tissues, necessary to fulfill their physiological functions.

References

Etchells J.P., Turner S.R. 2010. The PXY–CLE41 receptor ligand pair defines a multifunctional pathway that controls the rate and orientation of vascular cell division. *Development* **137**: 767–774.

Fisher K., Turner S.R. 2007. PXY, a receptor-like kinase essential for maintaining polarity during plant vascular-tissue development. *Curr. Biol*. **17:** 1061–1066.

Fouracre J.P., Ando S., Langdale J.A. 2014. Cracking the kranz enigma with systems biology. *J. Exp. Bot*. **65:** 3327–3339.

Helariutta Y., Fukaki H., Wysocka-Diller J., Nakajima K., Jung J., Sena G., Hauser M.T., Benfey P.N. 2000. The *SHORT-ROOT* gene controls radial patterning of the *Arabidopsis* root through radial signaling. *Cell* **101:** 555–567.

Slewinski T.L., Anderson A.A., Zhang C., Turgeon R. 2012. Scarecrow plays a role in establishing kranz anatomy in maize leaves. *Plant Cell Physiol.* **53:** 2030–2037.

Wolpert L. 1969. Positional information and the spatial pattern of cellular differentiation. *J. Theor. Biol.* **25:** 1–47.

Wysocka-Diller J.W., Helariutta Y., Fukaki H., Malamy J.E., Benfey P.N. 2000. Molecular analysis of SCARECROW function reveals a radial patterning mechanism common to root and shoot. *Development* **127:** 595–603.

Zoulias N., Harrison E.L., Casson S.A., Gray J.E. 2018. Molecular control of stomatal development. *Biochem. J*. **475:** 441–454.

LEAF VASCULATURE IN THREE SPECIES OF *CAPUTIA* B. NORD. ET PELSER (ASTERACEAE; SENECIONEAE)

Nikita N. CHUKAVIN*, *Rodion E. LEBEDEV*, *Constantin D. PAVLOV*, *Alexander C. TIMONIN

Lomonosov Moscow State University, Moscow, Russia
chukavinnik@gmail.com

Vasculature seems to be the most diverse constituent of the leaf, which vaguely correlates with leaf morphology (Klucking, 1995; Pole, 1991; etc.). The vasculature is specifically diverse in succulent leaves as it is usually 3-dimensional and shows differently arranged bundles and conducting tissues therein (Timonin, Ozerova, 1993; Ogura et al., 2018).

Leaf succulent species of species-poor genus *Caputia* radically differ from each other in their leaves, the latter varying from the flat obovate to linear to 2-types terete ones. The leaves of these species have anatomically been unexplored so far and their vasculature patterns have remained unknown. To fill this gap we anatomized leaf vasculature in *C. medley-woodii* (Hutch.) B. Nord. et Pelser, *C. pyramidata* (DC.) B. Nord. et Pelser and *C. tomentosa* (Haw.) B. Nord. et Pelser, which have flat obovate, terete cylindrical and terete fusiform leaves, respectively.

Leaves and shoots of the species concerned were collected from the live plants grown in the greenhouse of Tsitsin Main Botanical Garden of Russian Academy of Sciences and fixed and stored in 70% ethanol.

Serial transverse hand-razor sections were processed with 0.5% alcoholic Phloroglucinol and concentrated hydrochloric acid, and embedded in glycerin on slides according to Barykina et al. (2004). The preparations were analyzed under the light microscope. The obtained information was protocoled in the form of drawings, schemes and graphs.

Caputia medley-woodii has thick subpetiolate obovate externodromous *sensu* Pole (1991) leaves (fig. 1A). The petiole is adaxially flattened and abaxially convex.

Petiole vasculature of *C. medley-woodii* includes five principal bundles (fig. 1C), the median (M) and two pairs of lateral ones (L1 and L2). M and L1s regularly branch off minor bundles, which branch further on and anastomose each other forming plexus (fig. 1D). Anastomoses prevail over branching out minor bundles in the distal half of the leaf (fig. 2). The minor bundles are in a plane somewhat displaced towards the adaxial side in relation to the principal bundles (fig. 1D). The number of the minor bundles is highly labile and varies with the lamina width. They gradually integrate toward the leaf tip to fuse with the bundle M by its very tip (fig. 1B).

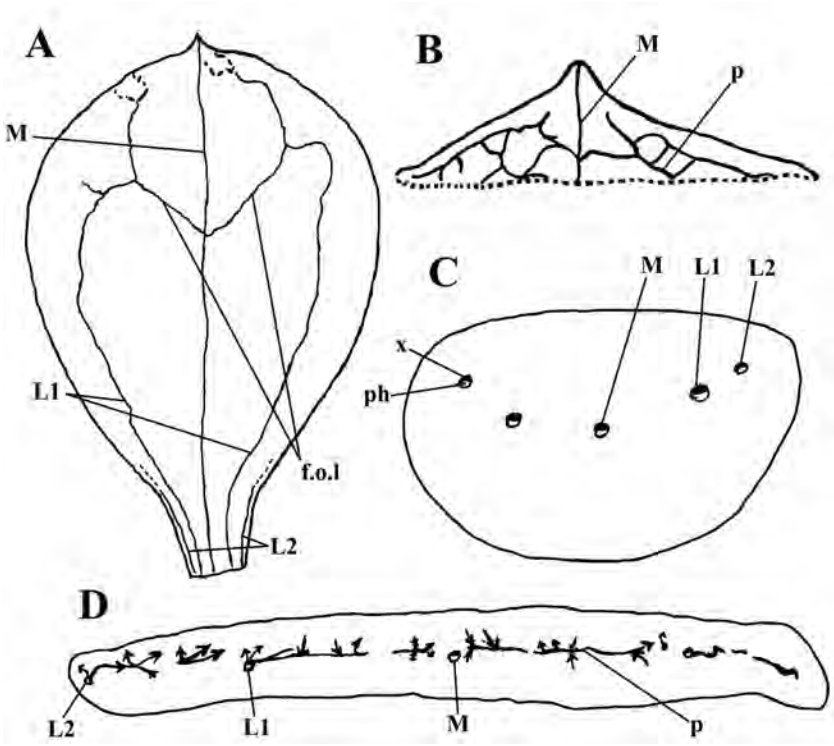

Fig. 1. Leaf vasculature of *C. medley-woodii.* A – venation pattern; B – leaf tip; C – petiole cross-section; D – lamina cross-section.
f.o.l – first order lateral bundle; *L1* – first lateral bundle; *L2* – second lateral bundle; *M* – median bundle; *p* – vascular plexus; *ph* – phloem; *x* – xylem.

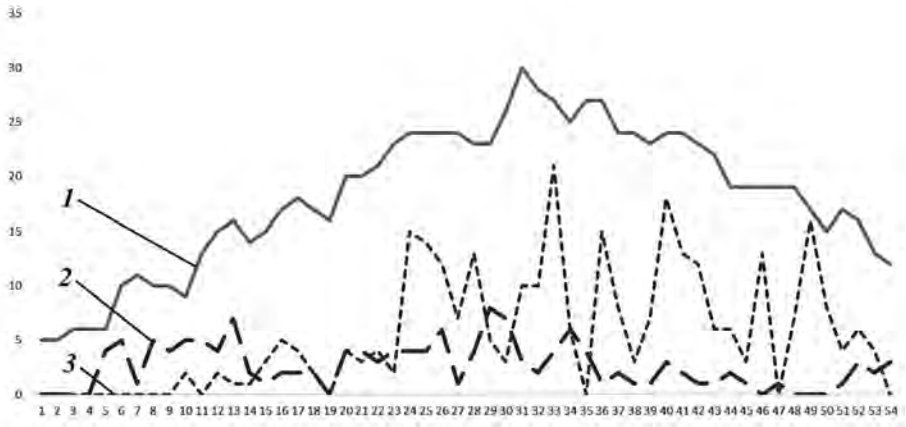

Fig. 2. Number of bundles in leaf of *C. medley-woodii.*
1 – total number; *2* – branching number; *3* – anastomose number.
Axis X – number of section; Axis Y – number.

The bundle M is observable to the very tip of the leaf where it terminates blindly (fig. 1B). It gives rise to a pair of the first order principal lateral bundles in the distal third of lamina (fig. 1A). These bundles arc acropetally to disappear in the terminal plexus of minor bundles. Both L1s run nearly 3/4 lamina, where they arc acropetally and disappear too in the plexus bundles near the first order laterals. The L2s continue through the petiole and merge with lateral plexus of minor bundles in the petiole-lamina transition zone (fig. 1A).

Caputia tomentosa has thick leaves of two morphological types: subpetiolate oblanceolate and (terete) fusiform. The leaf base is acroscopically concave and basiscopically convex in both types (fig. 3D). The lamina of subpetiolate leaves is semicircular to cordate in cross section with slightly convex to furrowed acroscopic side (fig. 3C). The fusiform leaves are circular in cross section (fig. 3A); the acroscopic furrow is sometimes absent. The leaf tip is dorsoventrally flattened in both leaf types.

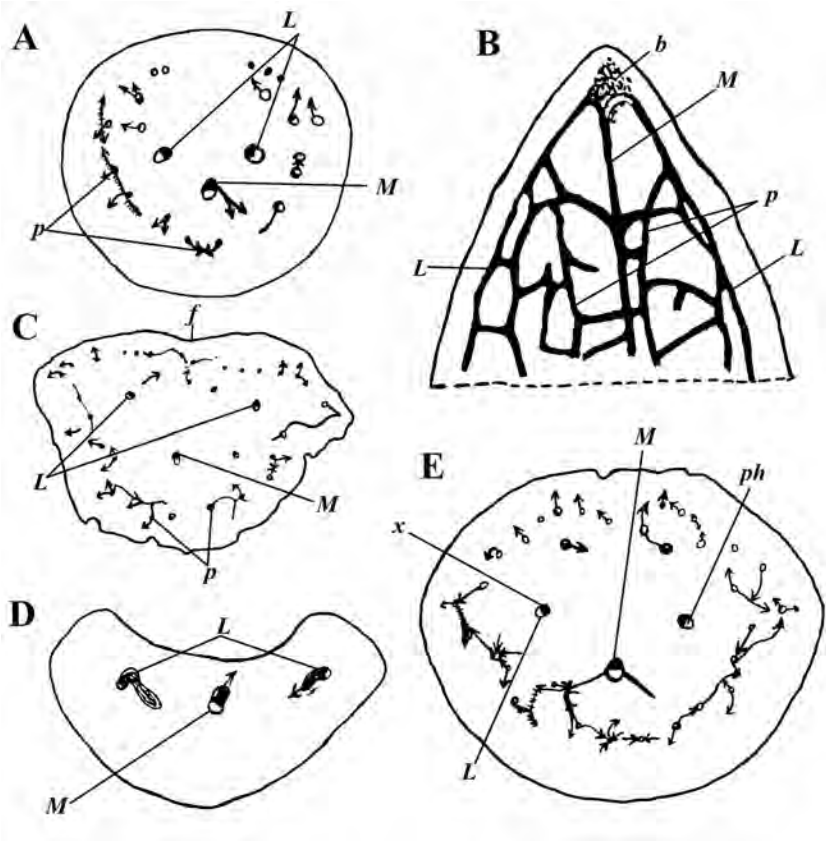

Fig. 3. Leaf vasculature of *C. tomentosa.* A, C–E – cross sections; B – surface view. A, E – terete leaf; B – leaf tip; C – oblanceolate leaf; D – petiole.
b – barrel tracheid body; *f* – furrow; *L* –lateral bundle; *M* – median bundle; *p* – vascular plexus; *ph* – phloem; *x* – xylem.

The leaf is supplied by three vascular bundles, the median (M) and two laterals (L). These bundles run through the leaf as its principal bundles up to the very tip where they merge into one bundle (fig. 3B). The xylem of these bundles faces to the acroscopic side and their phloem faces to the basiscopic side.

From the second quarter of the lamina, these bundles, especially the lateral ones, irregularly branch off smaller bundles. The derivatives of M mostly run to basiscopic side but some of them run laterally. Most of the derivatives of Ls run laterally. A few of them run acroscopically or basiscopically. Thus, three groups of peripheral bundles emerge.

Further, these groups distally unite to form acroscopically discontinuous and further on continuous circle. These bundles constitute a loose vascular plexus. Thus, the leaf vasculature consists of three inner principal bundles and peripheral vascular plexus. At the very tip, the bundles of the plexus unite with principal bundles (fig. 3B). The leaf vasculature is terminated by the body of barrel tracheids.

Caputia pyramidata has leaves with a very short basal part indistinctly delimited from a long terete distal part; the basal part is acroscopically concave and basiscopically convex; the distal part is acroscopically flat and basiscopically convex, with deep narrow basiscopic furrow except for its very tip. The basal part of vasculature consists of the median (M) and two lateral (L) bundles which are arranged in nearly one plane and have typically arranged tissues. These Ls bundles continue into the distal part as its 3 principal bundles. The M runs unchanged up to the leaf tip. The Ls shift acroscopically and turn exoscopic *sensu* Ogura et al. (2018). They fuse with the median one in the leaf tip. The lateral bundles irregularly give small branches which run mostly toward the acroscopic side to constitute peripheral bundle plexus (fig. 4C). However, some branches run toward the basiscopic side (fig. 4B). Resultantly, an ∩-shaped location of the peripheral bundles in cross-section acropetally turns into a Ω-shaped one (fig. 4D). Most peripheral bundles are exoscopic, but few of them show an unstable arrangement of their xylem and phloem. The peripheral bundles gradually fuse with each other and lateral bundles, the latter merging with their median counterpart in the leaf tip (fig. 4A).

The leaf of *C. medley-woodii* is undoubtedly bifacial as evidenced by its distinct margins and vasculature pattern, though the minor bundles are a little bit displaced adaxially. The oblanceolate leaves of *C. tomentosa* should also be considered bifacial due to clearly presented margins. Their vasculature is rather specific being differentiated into two subsystems of principal and peripheral bundles. The principal bundles are V-shaped in arrangement (fig. 3A, C, E). Their xylem is always oriented to the acroscopic side of the leaf and phloem is oriented to the basiscopic side of the leaf. This arrangement of the conductive tissues is typical of a bifacial leaf (Napp-Zinn, 1973). Peripheral bundles are arranged circularly. Most of them have xylem facing the acroscopic side of the leaf but a few have xylem oriented basiscopically. Thus, the arrangement of conductive tissues in peripheral bundles drastically differs from genuine unifacial leaf (Napp-Zinn, l.c.). Therefore,

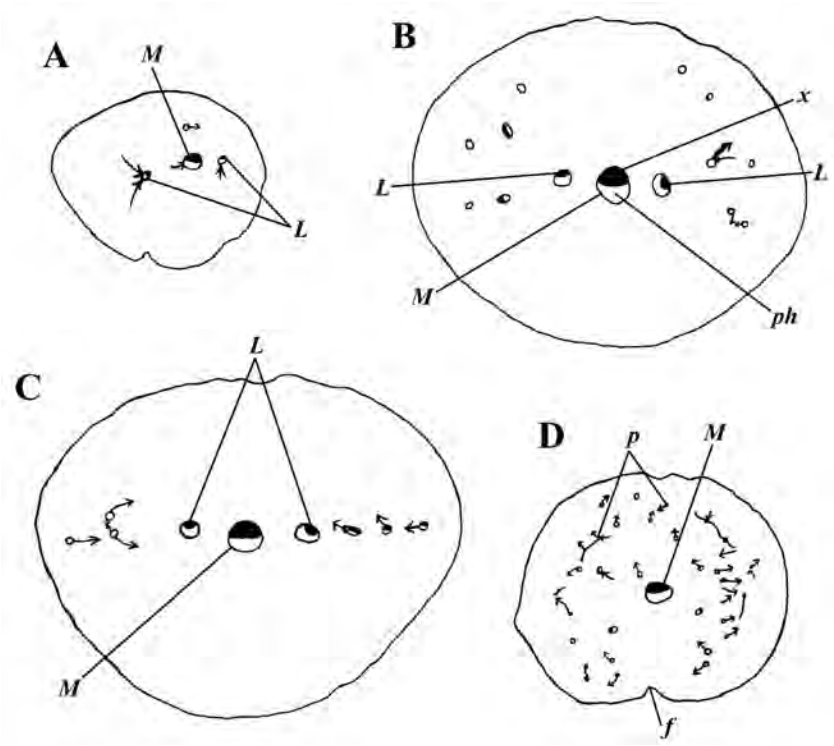

Fig. 4. Leaf cross sections of *C. pyramidata.* A – leaf tip; B – basal lamina; C – petiole; D – distal lamina.
f – furrow; *L* – lateral bundle; *M* – median bundle; *p* – vascular plexus; *ph* – phloem; *x* – xylem.

the anatomy of the oblanceolate leaf of *C. tomentosa* fits more the criteria of the bifacial leaf (Troll, 1939; Napp-Zinn, 1973).

The terete leaves differ from the above-mentioned leaves in their indiscernible margins. They look like unifacial leaves. Indeed, the terete leaves are usually unifacial or inverse unifacial (Troll, 1939; Napp-Zinn, 1973). Unifacial leaves have the abaxial side only, no primary margins and circularly arranged endoscopic bundles (Troll, l. c.; Napp-Zinn, l. c.). Inverse unifacial leaves have the adaxial side only, no primary margins and circularly arranged exoscopic bundles (Napp-Zinn, 1973). The vasculature of the terete leaves of *C. tomentosa* differs from these two types of leaves; it is similar to that of the bifacial oblanceolate leaves.

The leaves of *C. pyramidata* have a uniform surface throughout, indiscernible margins, but their vasculature includes three principal bundles with acroscopic xylem and basiscopic phloem and discontinuous circle of exoscopic peripheral bundles. The vasculature of these leaves is more similar to oblanceolate leaves than to both unifacial and inverse unifacial leaves.

The terete leaves of *C. tomentosa* and *C. pyramidata* are more similar to bifacial leaves in their vasculature, but they have uniform surface throughout and indiscernible margins. Thus, these leaves are neither typical unifacial nor typical inverse unifacial. They are not distinctly bifacial either. Therefore, these leaves are worth being considered *cryptic bifacial*.

Guédès (1979) considered terete leaves to be phyllodia. The terete leaves of both *Caputia* species consist of two radically different parts. There is only much shorter basal part that is nearly identical to the genuine petiole of *C. medley-woodii* in its form and vasculature. Therefore, there is this leaf part that we consider petiole of the terete leaves. Consequently, the much longer distal part is worth being considered leaf blade.

The leaf of *C. medley-woodii* seems to be the least altered. We recognized it close to the ancestral type. As is typical of the succulent leaves, their vasculature tends to become 3-dimensional as the minor veins are slightly displaced toward the adaxial side.

The oblanceolate leaves of *C. tomentosa* could have evolved from the ancestral ones via narrowing and thickening their laminas. The lamina thickening seems to have dramatically affected the leaf vasculature to have caused its differentiation into the inner principal bundles and peripheral bundles. The latter are likely to have displaced outward to form the vascular plexus near the lamina surface for efficient supplying the most active peripheral chlorenchyma. The adaxial thickening of the lamina should have prevailed, because the most peripheral bundles are above the principal ones. However, rather many peripheral bundles are below the principal ones thus indicating the abaxial thickening of the lamina. The principal bundles should have altered their original flat arrangement into the V-shaped one. We believe that this alteration could be caused by some previous folding of the lamina towards the adaxial side (fig. 5). The occasional furrow on the adaxial side of the oblanceolate leaves confirms this hypothesis.

Progressing narrowing and thickening of the lamina should have resulted in the loss of discernible margins and in the origin of the terete leaves. Such leaves are usually thought to be formed only by the “Rundungsmeristem” which maintains adaxial thickening of the leaf (Bünning, Gäumann, 1956). This is not the case of the terete leaves concerned, however.

The terete leaves of *C. tomentosa* have the same vascular pattern as the oblanceolate leaves. Therefore, arrested marginal growth, prevailing thickening and basiscopic thickening all must have been accompanied by some acroscopic folding of the lamina for the terete leaf to be evolved in this species (fig. 5B).

Flat arrangement of the principal bundles makes acroscopic folding of the lamina unlikely in evolving terete leaves of *C. pyramidata*. Such leaves could not be results of only “Rundungsmeristem” activity, because rather many their peripheral bundles are below the principal ones. Therefore, the basiscopic thickening should also have taken part in the origin of the terete leaves in this species. This thickening

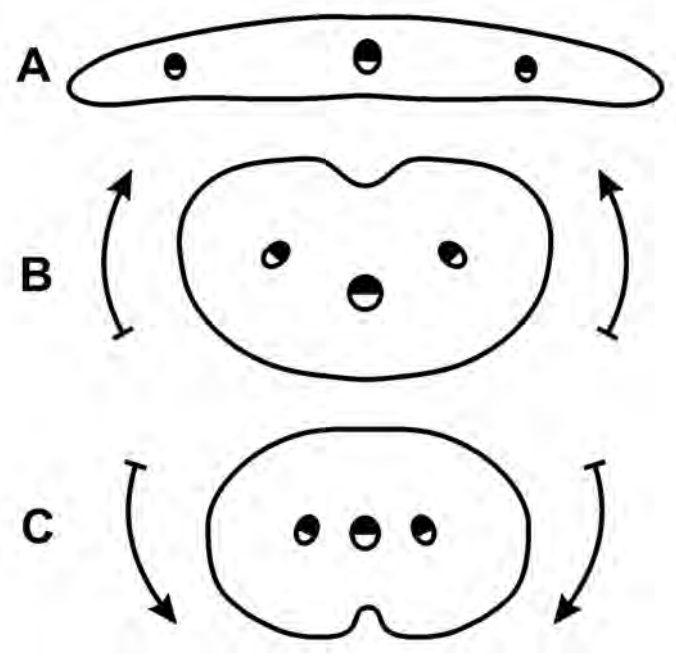

Fig. 5. Presumable evolution of leaves in *Caputia* genus.
A – *C. medley-woodii*; B – *C. tomentosa*; C – *C. pyramidata.*

must have differed from that in the above-mentioned species to form the abaxial furrow and Ω-shaped arrangement of the peripheral bundles. Both traits could have been resulted either from some basiscopic folding of the lamina (fig. 5C) or from the two separate submarginal sites of the basicsopic thickening.

Thus, *C. medley-woodii* seem to have retained the least altered or ancestral leaves of the genus *Caputia*. The terete leaves of *C. pyramidata* and *C. tomentosa* are of specific cryptic bifacial type. However, they differ in a set of traits and therefore represent two different evolutionary lines.

We are indebted to Dr. Ludmila Ozerova, Tsitsin Main Botanical Garden of Russian Academy of Sciences, Moscow, for providing material for our investigation.

References

Barykina R.P., Veselova T.D., Devyatov A.G., Dzhalilova Kh.Kh., Iljina G.M., Chubatova N.V. 2004. *Botanical microtechnics manual. Basics and methods*. Moscow: Moscow Univ. Press. [In Russian]

Bünning E., Gäumann E. 1956. Morphologie einschlieβlich Anatomie. *Fortschritte der Botanik*. **18**: 12–32.

Guédès M. 1979. *Morphology of seed-plants*. Vaduz: Cramer.

Klucking E. P. 1995. *Leaf venation patterns*. V. **7**. The classification of leaf venation patterns. Berlin; Stuttgart: J. Cramer.

Napp-Zinn K. 1973. Anatomie des Blattes. II. Blattanatomie der Angiospermen. A. Entwicklungsgeschichtliche und topographische Anatomie des Angiospermenblattes. 1. Lief. In: Zimmermann W., Carlquist S., Ozenda P., Wulff H.D. (Hrsg.): *Handbuch der Pflanzenanatomie*. Spezieller Teil. Bd. **8**. Teil 2A. Berlin; Stuttgart: Gebrüder Borntraeger.

Ogura A.S., Hernandes-Lopes J., Melo-de-Pinna G.F.A. 2018. A new anatomical interpretation for abaxialization in unifacial leaf blade of stone plants (Aizoaceae, Caryophyllales). *Braz. J. Bot*. **43**: 751–764.

Pole M. 1991. A modified terminology for angiosperm leaf architecture. *J. R. Soc. New Zeal*. **21**: 297–312.

Timonin A.C., Ozerova L.V. 1993. Structure, origin and evolution of the terete leaves in *Rowleyani* C. Jeffrey section of *Senecio* L. genus (Asteraceae). *Bul. Main Bot. Garden RAS*. **3**: 393–401. [In Russian]

Troll W. 1939. *Vergleichende Morphologie der höheren Pflanzen*. Bd. **1**. Teil 2. Berlin: Gebrüder Borntraeger.

EXPLOSIVE STYLE MOVEMENTS IN FABACEAE AND MARANTACEAE – STRUCTURAL DIVERSITY BEHIND A SIMILAR MECHANISM

***Regine CLAßEN-BOCKHOFF*, Matthias GRÖTEKE, Markus JEROMINEK, Elke PISCHTSCHAN**

Johannes Gutenberg-University, Mainz, Germany

classenb@uni-mainz.de

Explosive style movements mediating pollen transfer are rare among angiosperms. Well known examples are found in the families Fabaceae and Marantaceae. In both taxa, the style runs parallel to the floor of the flower and springs upwards. Though style function is rather similar, morphological and histological constructions differ considerably.

- In Fabaceae (e.g. *Ulex europaeus, Medicago falcata, Spartium junceum*), the style is hold under tension by the keel of the flower. Already in the bud, tension is set up by the jacketing keel. The style grows slightly curved upwards and becomes stiffened by sclerenchyma cells in the subepidermal layers. Only at the base of the lower style side, the sclerenchyma is lacking providing the style with an elastic tissue. When the pollinator opens the keel-wing construction, the stiff style springs forward by relaxing the elastic tissue. The androecial tube with the mature anthers follows the movement passively and the pollinator gets powdered with pollen.
- In Marantaceae, all species transfer pollen by an explosive style movement. This is always combined with secondary pollen presentation. Already in the bud, own pollen is deposited on the style head covered by the hooded

staminode. During the following growth, the style elongates faster than the staminode and tension is set up. The upper epidermis of the style is stretched and the style gets arched. When the pollinator touches the trigger appendage, tension is released and the style rolls inwards in a split of a second exchanging its own pollen with foreign pollen brought by the pollinator.

In both taxa, the movement is exclusively mechanical. The specific tissue construction facilitating pollen transfer is explained in detail. The comparison among the two unique style movements illustrates that even highly derived functional constructions can evolve in parallel and that there are more morpho-histological approaches than functional constraints.

WHAT IS SPECIFIC IN MONOCOT VASCULARISATION? NEW FINDINGS IN THE VEGETATIVE HISTOLOGY OF MARANTACAE

Regine CLAßEN-BOCKHOFF*, *Hansjörg KRÄHMER

Johannes Gutenberg-University, Mainz, Germany

classenb@uni-mainz.de

Differences in the organisation of the shoot apices in monocots and dicots have been known since decades, but obviously they are not completely understood. While vascular bundle formation (VBF) in dicots is sufficiently investigated, surprisingly little is known about VBF in monocots.

Traditionally it is assumed that VBF originates from procambial strands in dicots and from the mantle meristem (also called primary thickening meristem) in monocots. It is hypothesised that in monocots the procambial strands are either completely used or completely lost.

Comparative studies in nodal structures of dicots and monocots, particularly in Marantaceae, illustrate that VBF differs considerably among the lineages.

- In dicots, longitudinal ‘provascular strands’ (usually called procambial strands) remain meristematic, which go along with an early parenchymatisation of the nodal domain, a gradual VBF and the ability of cambial secondary thickening. They also cause the ring-like arrangement of the vascular bundles and the connection with the leaf traces in a common vascular system.
- In monocots, horizontal ‘provascular domains’ persist in the nodal areas, associated with a late differentiation of the nodes and an abrupt change in cell arrangement between the ‘chaotic’ pattern in the nodal domain and the collateral pattern in the internodes. Secondary growth is lacking,

but it is replaced in some monocot lineages by a secondary thickening meristem. The vascular bundles remain solitarily or get late into contact. Their arrangement follows the formation of the leaf traces during leaf development.

Bundle patterns in monocots are not uniform and even differ between closely related species. They have, however, so much in common that they can easily be distinguished from dicots.

TWO TYPES OF SECRETORY DUCTS WITH DISTINCT ORIGIN AND METABOLISM IN *KIELMEYERA* (CALOPHYLLACEAE: MALPIGHIALES)

Ellenhise R. COSTA*, *Diego DEMARCO

University of São Paulo, São Paulo, Brazil
ellenzinha27@gmail.com

Calophyllaceae is an important group in the Neotropics with many endemic and rare species. The family comprises 13 genera and 460 species, characterized by the presence of resin in all species. This resin is produced by secretory ducts which may be located in all organs mainly adjacent to the vascular system (Metcalfe, Chalk, 1950). In spite of their wide distribution in Calophyllaceae, the secretory ducts presented in the family are little known anatomically and, still, there are many doubts in the interpretation of the anatomy of those secretory structures as well as the substances secreted by them. In our study, we aimed to understand 1) How do the secretory ducts develop? 2) And which is the chemical composition of the secretion exuded by the ducts? For this investigation, we selected *Kielmeyera appariciana* as a model species, since *Kielmeyera* is one of the largest genera within Calophyllaceae with about 50 species among which *K. coriacea* Mart. et Zucc. and *K. rubriflora* Cambess are well-known for studies of the chemical nature of leaf and stem extracts of these species that are used in folk medicine as anti-inflammatory, anti-oxidant and even against cancer cell lines (Alves et al., 2000; Pinheiro et al., 2003; Mesquita et al., 2011; Jorge, 2014).

For the developmental study, shoot apices and samples of stem in secondary growth of *K. appariciana* were fixed in Karnovsky's fixative for 24 hours (Karnovsky, 1965), embedded in Paraplast and sectioned in a rotary microtome. For the identification of the main chemical classes of the duct secretions, fresh samples of stems in primary and secondary growth were sectioned in a freezing microtome at –25 °C. The sections were submitted to histochemical tests for lipids (Cain, 1947; Pearse, 1985), phenolic compounds (Johansen, 1940; Baerheim-

Svendsen, Verpoorte, 1983), polysaccharides (Gregory, Baas, 1989; Jensen, 1962; Pizzolato, 1977) and proteins (Fisher, 1968). All tests were conducted according to appropriate staining protocols.

Our results reveal that *K. appariciana* has primary ducts in the cortex and pith of the stem and near the vascular bundles of the leaf. Each duct originates from a single cell of the ground meristem which has thin walls, dense cytoplasm and prominent nucleus. Successive divisions of this initial cell form a rosette of meristematic cells. Then, the rosette cells move apart and form the duct lumen which will become larger during the secretory phase simultaneously to the release of secretion into the lumen.

Additionally, *K. appariciana* also has ducts in the secondary phloem of the stem but the secondary ducts are originated from a group of cells derived from the vascular cambium. There is a delay in the beginning of secondary ducts formation. Initially, the cambium produces many layers of cells before starts to originating ducts which may be found in stems with 7.0 mm of diameter at minimum. Then, the ducts are formed in a stratified pattern by the cambium.

The differences between primary and secondary ducts are not restricted to the origin. Histochemical tests detected the presence of various compounds, including lipids, terpenoids, phenolic compounds, polysaccharides and proteins in the secretion of the primary ducts, whilst the secondary ducts produce only polysaccharides. This is the first report of two types of ducts distinguished by origin and secretory metabolism in the same plant that leads to new questions on the relationship between the developmental nature and the secretory activity in plant glands. Although the secretory ducts differ in their developmental modes, both ducts are likely schizogenous.

Joel & Fahn (1980) have listed the main structural features that indicate lysogenic lumen formation, as the disorganized appearance of the cytoplasm of epithelial cells and the presence of wall debris inside the lumen. The epithelial cells of *K. appariciana* were intact and with no sign of lysis, indicating that the lumen was originated only by the separation of cells. According to Metcalfe & Chalk (1950), the secretory ducts in Calophyllaceae are schizogenous but new studies are needed to confirm this report.

The presence of two types of ducts in *K. appariciana* represents an apomorphic character of *Kielmeyera* which may be related to the diversification of the genus. While the primary resin ducts protect the young stems and leaves against herbivores, the secondary ones, aid in water absorption, retention and/or translocation from xylem to phloem in the tree after the developing wood has avoided the feeding of many herbivores (Fahn, 1979; Gibson, Nobel, 1986; Meyberg, 1998). Chemical analyses of leaf and stem extracts of *K. coriacea* detected the presence of xanthones, triterpenes and biphenyl as their main constituents (Audi et al., 2002; Cotez et al., 1998). Several studies have shown that the resin produced by ducts hinders herbivory. The most attacked organ by herbivores is usually the leaf (Aoyama,

Labinas, 2012), consequently, this organ tends to produce more defensive compounds when compared to other less predated organs. This trend was confirmed in our study. Primary ducts of *K. appariciana* produce phenolic compounds, which are substances closely related to defence against herbivores (Buchanan et al., 2001), but these compounds are absent in the secondary ducts. Further studies should be performed to better understand the evolutionary and ecological implications of the diversity of secretory ducts found in this study for the group.

The work was supported by FAPESP, grant No. 2017/15085-2.

References

Alves T.M.A., Silva A.F., Brandão M., Grandi S.M., Smânia E.F., Smânia J.R.A., Zani C.L. 2000. Biological screening of Brazilian medicinal plants. *Mem. Inst. Oswaldo Cruz*. **95**: 367–373.

Aoyama M.E., Labinas M.A. 2012. Características estruturais das plantas contra herbivoria por insetos. *Enciclop. Biosf.* **8**: 365–386.

Audi E.A., Otobone F., Martins J.V.C., Cortez D.A.G. 2002. Preliminary evaluation of *Kielmeyera coriácea* leaves extract on the central nervous system. *Fitoterapia* **73**: 517–519.

Cain A.J. 1947. The use of Nile Blue in the examination of lipids. *Q. J. Microsc. Sci.* **88**: 383–392.

Baerheim-Svendsen A., Verpoorte R. 1983. *Chromatorgraphy of alkaloids. Part A. Thin-layer chromatography.* Amsterdam; Oxford; New York: Elsevier Scientific Publ.

Buchanan B.B., Gruissem W., Jones R.L. 2001. *Biochemistry & molecular biology of plants.* Rockville: American Society of Plant Physiologists.

Cortez D.A.G., Benício A.A.F., Celso V. N., Benedito P.D.F., Andrew M., Kurt H. 2002. Antibacterial activity of a biphenyl and xanthones from *Kielmeyera coriácea. Pharm. Bio.* **40**: 485–489.

Fahn A. 1979. *Secretory tissues in plants*. London: Academic Press.

Fisher D.B 1968. Protein staining of ribboned epon sections for light microscopy. *Histochemie* **16**: 92–96.

Furr M., Mahlberg P.G. 1981. Histochemical analyses of laticifers and glandular trichomes in *Cannabis sativa*. *J. Nat. Prod*. **44**: 153–159.

Gibson A.C., Nobel P.S. 1986. *The Cactus Primer*. Cambridge: Harvard University Press.

Gregory M., Baas P. 2013. A survey of mucilage cells in vegetative organs of the dicotyledons. *Isr. J. Bot*. **38**: 125–174.

Jensen W.A. 1962. *Botanical histochemistry. Principles and practices*. San Francisco: Freeman.

Joel D.M., Fahn A. 1980. Ultrastructure of the resin ducts of *Mangifera indica* L. (Anacardiaceae). I. Differentiation and senescence of the shoot ducts. *Ann. Bot*. **46**: 225–233.

Johansen D.A. 1940. *Plant microtechnique.* New York: McGraw-Hill.

Jorge R. 2014. Calophyllaceae. In: Martinelli G., Messina T., Santos Filho L. (eds.): *O livro vermelho da flora do Brasil: plantas raras do Cerrado*. Rio de Janeiro: Andrea Jakobson: Instituto de Pesquisas Jardim Botânico do Rio de Janeiro: CNCFlora. P. 80–81.

Karnovsky M.J. 1965. A formaldehyde-glutaraldehyde fixative of high osmolality for use in electron microscopy. *J. Cell Biol*. **27**: 137–138.

Metcalfe C R., Chalk L. 1950. *Anatomy of the dicotyledons*. Oxford: Clarendon Press.

Mesquita M.L., Araújo R.M., Bezerra D.P., Filho R.B., Paula J.E., Silveira E.R., Pessoa C., Moraes M.O., Lotufo L.V.C., Espindola L.S. 2011. Cytotoxicity of δ-tocotrienols from *Kielmeyera coriacea* against cancer cell lines. *Bioorg. Med. Chem*. **19**: 623–630.

Meyberg M. 1988. Cytochemistry and ultrastructure of the mucilage secreting trichomes of *Nymphoides peltata* (Menyanthaceae). *Ann. Bot*. **62**: 537–547.

Pearse A.G.E. 1985. *Histochemistry: theoretical and applied*. Edinburgh: C. Livingstone.

Pinheiro L., Cortez D.A.G., Vidotti G.J., Young M.C.M.E., Ferreira A.G. 2003. Estudo fitoquímico e avaliação da atividade moluscicida da *Kielmeyera variabilis* Mart. (Clusiaceae). *Quim. Nova* **26**: 157–160.

Pizzolato T.D. 1977. Staining of *Tilia* mucilages with Mayer's tannic acid–ferric chloride. *Bull. Torrey Bot. Club*. **104**: 277–279.

STRUCTURAL, FUNCTIONAL AND DEVELOPMENTAL ASPECTS OF COMPARATIVE FLORAL ANATOMY IN ANGIOSPERMS: A CASE STUDY OF ANNONACEAE

Thierry DEROIN

Muséum National d'Histoire Naturelle, Paris, France
thierry.deroin@mnhn.fr

The Magnoliales order (AGP IV, 2016) consists of ca. 3050 species in 125 genera, in which 80% are Annonaceæ. Although several floral peculiarities (double-corolla, outer and inner staminodes, gynoecial arrangement) were yet recognized as theoretically significant during the nineteenth century (Dunal, 1817; Baillon, 1869), comparative morphological studies became feasible in this large and mostly tropical family only in the middle of the last century, with the improvements in availability of living material, in histological techniques and publishing of large monographical and floristical works (especially with the seminal researches of R.E. Fries, gathered in his work of 1959). In spite of our still patchy knowledge of the annonaceous flower at the present time, only based on ca. 25 genera, mostly African, some prospects may be drawn from its diversity, which have a certain weight for understanding the evolutionary trends in angiosperms.

Except for the gynoecium, tissues are well-differentiated from anthesis. Floral receptacle is remarkable by its complex vasculature most often exhibiting a trimerous whorled arrangement, and a more or less spread bundles longitudinal fusion in different patterns of cortical vascular system (CVS), according to pollination processes. CVS is lacking in the basal genera (e.g. *Anaxagorea*), only perianthal in some others (e.g. *Meiocarpidium*, *Piptostigma, Pseudartabotrys* – Deroin, Bidault, 2017), including stamen bundles in derived genera (*Annona*, *Asimina*), becoming irregular in reduced flowers (*Deeringothamnus* – Deroin, Norman, 2016). Vasculature appears however more variable inside each whorl (*Ambavia* – Deroin, Le Thomas, 1989). Pedicel histology yields some interesting features which may be put in a quantitative frame (bundles number / pedicel diameter). Petals play a major role during the pollination, by their changing conformation and the occurrence of nutritious tissues and food bodies, whose

variety is just suspected (Gottsberger et al., 1998; Gottsberger, Webber, 2018) and needs thorough cytological studies. The androecium is strictly trimerous, stamen histology showing a diplophyllous pattern, sometimes visible in the vasculature (*Cananga*, *Xylopia*). Angiosperm carpel was defined in the Annonaceae family first (Dunal, 1817), and its gynoecium exhibits actually a wide range of patterns from apocarpy to syncarpy, in ovule numbers and supply, as well as in stigmatic plates in close link with pollination and fruit set. Paracarpy is realized in *Isolona* and *Monodora*, with a carpel polymorphism hidden in a morphogenetical unit (Deroin, 1997), and is strikingly near pseudosyncarpy recognized in *Annona*, as suggested by molecular studies (Couvreur et al., 2008).

As a whole, the floral diagram of Annonaceae appears much more plastic than those of Magnoliaceae or winteroids, as recognized in the Malagasy genus *Fenerivia* (Deroin, 2007), and recently interpreted in a homeotic frame (Saunders, 2010). This major feature expresses the evolutionary dynamism of the family, which might be further analysed by comparative carpological studies**.**

Comparative anatomy based classically on seriate sections remains thus an effective tool for inspiring and supporting morphogenetical interpretations, and even for calibrating the results from computed tomography.

References

AGP IV. 2016. An update of the Angiosperm Phylogeny Group classification for the orders and families of flowering plants: APG IV. *Bot. J. Linn. Soc.* **181**: 1–20.

Baillon H. 1869. *Histoire des Plantes*. T. **1**. Paris: Hachette.

Couvreur T.L.P., Richardson J.E., Sosef M.S.M., Erkens R.H.J., Chatrou L.W. 2008. Evolution of syncarpy and other morphological characters in African Annonaceae: A posterior mapping approach. *Molec. Phyl. Evol.* **47**: 302–318.

Deroin T. 1997. Confirmation and origin of the paracarpy in Annonaceae. *Candollea* **52**: 45–58.

Deroin T. 2007. Floral vascular pattern of the endemic Malagasy genus *Fenerivia* (Annonaceae). *Adansonia*, sér. 3, **29**: 7–12.

Deroin T., Bidault E. 2017. Floral anatomy of *Pseudartabotrys* Pellegrin (Annonaceæ), a monospecific genus endemic to Gabon. *Adansonia*, sér. 3. **39**: 111–123.

Deroin T., Le Thomas A. 1989. Sur la systématique et les potentialités évolutives des Annonacées: cas d'*Ambavia gerrardii* (Baillon) Le Thomas, espèce endémique de Madagascar. *C. R. Acad. Sci.*, Paris **309**, Sér. III: 647–652.

Deroin T., Norman E. 2016. Notes on the floral anatomy of *Deeringothamnus* Small (Annonaceae): cortical vascular systems in a chaotic pattern. *Modern Phytomorph.* **9**: 3–12.

Dunal M.F. 1817. *Monographie de la famille des Anonacées.* Paris: Treuttel & Würtz.

Fries R.E. 1959. Annonaceae. In: Engler A., Prantl K.A. (Hrsg.): *Die natürlichen Pflanzenfamilien.* 2. Aufl. Berlin: Duncker & Humblot. Bd. **17a**. Abt. II. P. 1–171.

Gottsberger G., Webber A.C. 2018. Nutritious tissues in petals of Annonaceae and its function in pollination by scarab beetles. *Acta Bot. Brasil.* **32**: 279–286.

Gottsberger G., Webber A.C., Hildenbrand M. 1998. Nutritious tissues in flowers of Annonaceae. *Annonaceae Newsl.* **12**: 25–26.

Saunders R.M.K. 2010. Floral evolution in the Annonaceae: hypotheses of homeotic mutations and functional convergence. *Biol. Rev.* **85**: 571–591.

ECOLOGICAL ANATOMY OF TWO HOMOSPOROUS FERNS *LEPISORUS THUNBERGIANUS* (KAULF.) CHING AND *LEMMAPHYLLUM MICROPHYLLUM* C. PRESL.

Nina M. DERZHAVINA

Turgenev Orel State University, Orel, Russia
d-nm@mail.ru

Many ferns of the family Polypodiaceae are intriguing for their adaptations to special epiphytic and epilitic environments. The drought stress they regularly face has caused specific relations between their photosynthetic traits and morpho-anatomical characters (Nishida, Hanba, 2017). These relations are still not sufficiently explored because the most ferns were dealt with anatomically for their diagnostics (Nayar, 1964; Khare, 1965; Srivastava, 1967; Yu, Lin, 1997). The present investigation of sporophytes of *Lepisorus thunbergianus* and *Lemmaphyllum microphyllum* was aimed to reveal the general characteristics and trends of their adapting at different organization levels.

The two fern sporophytes were collected in the island of Miyajima (Tokyo Prefecture, Japan) in open habitats, on trunks of *Cycas* sp., *Pinus densiflora* Siebold et Zucc. and *Castanopsis* sp. (*Lepisorus thunbergianus* Kaulf. (Ching) and on stone banks of forest creek (*Lemmaphyllum microphyllum* C. Presl.).

Their photosynthetic apparatus was analyzed according to Mokronossov (1978) at structural levels of fronds, mesophyll cells and plastid apparatus. Siams Mesoplant laboratory complex of analysis of morphology and structure of plant photosynthetic apparatus (Department of Plant Physiology, Ural State University, Ekaterinburg) was used for investigation. Biomorphological characteristics of the species studied were determined according to Serebryakov (1962), Serebryakova (1980) and Shorina (1994).

Middle-aged sporophytes of these ferns are dorsiventral evergreen herbaceous perennial hemicryptophytes, short-rhizomatous in *Lepisorus thunbergianus* and erosulate long-rhizomatous in *Lemmaphyllum microphyllum*. Fronds are double-rowed on the dorsal side of the rhizomes. *Lepisorus thunbergianus* has monomorphic trophosporophylls, whereas *L. microphyllum* has both trophosporophylls and trophophylls.

Xero-, meso-, hygro-, helio- and sciomorphic traits differently combined were revealed at various organization levels in both species investigated.

Usually combined xeromorphic and heliomorphic traits at the organism level: nanism, reduced frond area, coriaceous fronds, evergreen phenorhythmotype, dense indumentum of trichomes and scales (both species); ability of fronds to roll up by means of sclerenchyma strands, trend to poikilohydry (*L. thunbergianus*).

Xeromorphic and heliomorphic traits at the tissue level: rather thick frond laminas, dorsiventral mesophyll, abscission layer, cuticle, dense network of veins (both species); hypodermis and vessels (*L. microphyllum*).

Xeromorphic and heliomorphic traits at the level of cells and plastid apparatus: pycnomorphic structure (densely packed numerous small cells per frond area unit, high values of specific surface frond density, high total surface area of the external chloroplast membrane per frond area unit – *L. thunbergianus*); parastrophic position of chloroplasts, rather high volume and number of chloroplasts (both species); small epidermal cells (*L. microphyllum*).

Sciomorphic traits: hypostomaty, relatively small number of stomata per frond area unit, sinuous epidermal cell walls, protuberances of spongy mesophyll cells, high chloroplast volume (both species); minimal cell surface to cell volume ratio (*L. microphyllum*).

Mesomorphic traits: differentiation of the mesophyll onto palisade and spongy tissue (both species); large cells, relatively high cell volume, cellular chloroplast volume and total area of the external cell membranes per frond area unit (*L. microphyllum*).

Hygromorphous traits: hydathodes, facultative bryophily (both species).

The obtained data allow us to nest the studied ferns among following ecological groups. *Lemmaphyllum microphyllum* and *L. thunbergianus* are versatile in the light environment of the biotope and can therefore be named shade-tolerant plants. *Lepisorus thunbergianus* has both mesomorphic and xeromorphic traits, the latter being more numerous than in *L. microphyllum*. Therefore, the former fern might be considered xeromesophyte, while the latter one might be considered mesophyte with the xeromorphic character syndrome.

Moreover, ecological valence of both species in respect to environmental humidity is rather wide. They are able to resist both water shortage due to their xeromorphic traits and water excess by eliminating extra water with their hydathodes. Therefore, they are concluded to be hydrolabile plants. *Lemmaphyllum microphyllum* is a homoiohydric plant. *Lepisorus thunbergianus* is intermediate between the homoiohydric and poikilohydric ferns, because it is able to resist short-term dehydration of its fronds.

Apparently, the optimal adaptive strategy of *L. microphyllum* must have been enhancing water retention in its cells and tissues, whereas those of *L. thunbergianus* must have been evolving of reversible dehydration of its tissues.

References

Khare P. 1965. On the morphology and anatomy of two species of *Lepisorus* (J. Smith) Ching: *L. thunbergianus* (Kaulf) Ching, and *L. excavatus* (Bory) Ching. *Can. J. Bot.* **43**: 1583–1588.

Mokronossov A.T. 1978. Mesostructure and functional activity of photosynthetic apparatus. In: Mokronossov A.T. (ed.): *Mesostructure and functional activity of photosynthetic apparatus*. Sverdlovsk: Ural State Univ. Publ. P. 5–30. [In Russian]

Nayar B.K. 1964. *Lemmaphyllum*. Ferns of India – XIV. *Bull. Nat. Bot. Gard*. **106**: 1–15.

Nishida K., Hanba Y.T. 2017. Photosynthetic response of four fern species from different habitats to drought stress: relationship between morpho-anatomical and physiological traits. *Photosynthetica* **55**: 689–697.

Serebryakov I.G. 1962. *Ecological plant morphology*. Moscow: Vysshaya Shkola Publ. [In Russian]

Serebryakova T.I. 1980. Once more to the term "life form" in plants. *Bull. Mosc. Soc. Natur. (Biol.)* **85**: 75–86.

Shorina N.I. 1994. *Ecological morphology and population biology of the members of the subclass Polypodiidae*. Dissert.

Srivastava P. 1967. Morphological and anatomical studies on *Lepisorus subrostratus* (Hook.) C. Chr., *L. macrosphaerus* (Bak.) Ching, and *L. kashyapii* (Mehra) Mehra. *Can. J. Bot*. **45**: 259–265.

Yu S.-l., Lin Y.-x. 1997. Comparative anatomy on the stipes and rhizomes of the fern genus *Lepisorus. Bull. Bot. Res*. **17**: 60–64.

FRUIT ANATOMY IN THE GENUS *ATRAPHAXIS* L. (POLYGONACEAE, POLYGONEAE)

Andrey G. DEVYATOV, Olga V. YURTSEVA

Lomonosov Moscow State University, Moscow, Russia
olgayurtseva@yandex.ru

The genus *Atraphaxis* L. comprises ca. 35 species distributed across North-Eastern Africa and Eurasia, ranging from the South-Eastern Europe to the Eastern Siberia, China and Mongolia (Pavlov, 1936; Rechinger, Schiman-Cheika, 1968; Lovelius, 1979; Gubanov, 1996; Bao, Grabovskaya-Borodina, 2003).

The anatomy of fruits was studied in six species of *Atraphaxis* (Ronse De Craene et al., 2000). In this study, we aimed to investigate fruit anatomy in a wider range of species and to compare the anatomical features with the positions of species in the plastid phylogeny of *Atraphaxis* resulted from ML and BI analyses applied for 3-plastid loci/65 tips matrix (Yurtseva et al., 2016). We used 31 specimens of 19 species of the genus *Atraphaxis* representing all sections: *Atraphaxis*, *Tragopyrum* (M. Bieb.) Meisn., and *Physopyrum* (Popov) Lovelius (Lovelius, 1979), as well as most subclades recovered with the plastid phylogeny. The study was conducted on the material taken from Herbaria: ALTB, FRU, IRKU, KUZ, LE, MHA, MW, NS. For anatomical study, mature fruits softened in alcohol:glycerol:water (1:1:1) were cut in sections 10–20 μm thick and either stained with 0.1% cresyl violet or processed with 0.1% phloroglucinol and concentrated HCl. Fruit structure was studied in the middle part of sides and at ribs. The cross and paradermal sections, as well as optical sections of the exocarp cells were studied with the microscope Carl Zeiss Axioplan 2 (Zeiss, Germany) using the camera Axiocam-MR and program AxioVision LE 64 free edition.

Fruits of *Atraphaxis* are mostly ellipsoidal-pyriform, with three equal sides, a short stipe and a long beak. The members of *Atraphaxis* section *Atraphaxis* have lenticular fruits with two broadly elliptical or ovoid sides.

The pericarp includes 6–7 layers of cells in sides and 10–12 ones in ribs: one-layered exocarp, several layers of parenchymatous cells of mesocarp and 1–2-layered endocarp. The mesocarp includes 4–5 layers of chlorenchyma at sides and 8–10 layers at ribs. Small vascular bundles running along the ribs consist of a few phloem and xylem elements with annular and helical thickenings. Two outer layers of the mesocarp are a little bit larger isodiametric cells which contain suberin in the walls and plastids in the protoplasts. The inner layers of the mesocarp and 1–2 layers of the endocarp are obliterated in the mature fruits.

The ovule is bitegmic, with each integument of two cell layers. The outer layer of the outer integument is preserved in the seed coat and consists of large cells, the inner layer of the outer integument and both layers of the inner one are obliterated. Perisperm consists of a layer of alive cells with dense content. The endosperm cells contain simple and compound starch grains; the outer one-cell-thick layer contains aleurone grains. The embryo has two cotyledons and a radicle located along one of the ribs of the trigonous or lenticular seed.

The exocarp cells are the most taxonomically informative and have the maximum diagnostic value. In the cross section, the exocarp cells are square, rectangular, or elongated-rectangular, 20–130 μm in height. The cells are shorter at sides and higher at ribs. The anticlinal walls are either almost straight or regularly and prominently undulating across the height, especially intensively near the surface. Shape and size of cell lumen partly depends on cell wall thickening, which is usually limited to the outer periclinal wall (OPW) and anticlinal walls. The anticlinal walls become gradually thicker from the base to the outer surface of the exocarp cell. This thickening leads to a 1) broadly rectangular lumen, 2) trapezoid lumen gradually narrowed towards the periphery, 3) lumen broaden at base and suddenly narrowed to the periphery, 4) triangular or low-domed lumen.

The outer periclinal walls are usually strongly thickened and permeated with narrow channels 2.0–3.0 μm in diam. departing from the lumen and directed towards the periphery. The channels are simple or dendritically branched out ones, twice and rarely thrice. They go through the thickened OPW to the smooth surface, or enter small semispherical tubercles present on the surface of the OPW (*A. atraphaxiformis, A. tortuosa, A. toktogulica*). In any case, the channels end blindly and never get to the surface and open outwards. In addition, transverse horizontal channels departing from the lumen are present in the species with undulating anticlinal walls and reach the middle lamellae.

In the paradermal section, the shape of exocarp cells changes at different levels. In the surface view, the cells have undulating anticlinal walls either across the height, or near the outer surface and near the base; in the middle of the height the exocarp cells may be polygonal with straight thickened anticlinal walls and rounded narrow lumen, sometimes slightly compressed. The lobes of adjacent exocarp cells interdigitate, providing firm connection of the cells. The anticlinal walls may be straight in the cross section, but sinuate in the surface view.

As a result, the lumen is broad and fits the sinuate outline of the exocarp cell at the base; it is narrow and rounded with some horizontal channels in the middle part. Near the surface the lumen is branched once or twice (rarely thrice) and form narrow channels directed to the lobes.

In mature fruits, the walls of exocarp cells are layered, thick and colorless, later lignified; in some cases colored yellow, brown or purple-black, as well as the protoplasts of the cells due to presence of phlobafene. The surface of the OPW is covered with a cuticle 1.0–1.5 (6) μm thick and epicuticular wax.

Exocarp structure of *Atraphaxis* species was compared with the positions of species in the plastid phylogenetic tree (Yurtseva et al., 2016). Although the structure of exocarp cells is rather variable in the genus *Atraphaxis*, it does not confirm the division of the genus into three sections. *Atraphaxis replicata* and *A. canescens* from the section *Atraphaxis* have the exocarp cells very similar to those of *A. frutescens* and *A. virgata* from the section *Tragopyrum*. *Atraphaxis teretifolia* from the section *Physopyrum* shares the exocarp structure with *A. pungens, A. grubovii, A. kuvaevii, A. selengensis* from the section *Tragopyrum*, although *A. teretifolia* has a much thicker cuticle.

The species of *Atraphaxis* differ in the height of exocarp cells, and these differences are partially consistent with the positions of taxa in the plastid phylogeny of the genus. We divided the species into three artificial groups: with tall, medium and short exocarp cells.

Atraphaxis ariana, A. alaica have the highest exocarp cells (70–130 μm) with sinuate anticlinal walls in the cross section. These species occupy basal positions in the clade *Atraphaxis* (Yurtseva et al., 2016). The highly supported subclade uniting *A. seravschanica, A. pyrifolia, A. muschketowi* from the Pamir and Tien Shan and *A. laetevires* from Dzhungar Alatoo also departs early in plastid topology. The other subclade unites *A. atraphaxiformis* from Tien Shan and *A. kopetdaghensis* from the Kopet Dagh. The exocarp structure of these species can be considered as a primary state for the genus. In the cross section, the exocarp cells have vast lumens gradually narrowed to the periphery, and strongly thickened and undulating anticlinal walls.

The species, which occupy more distal positions in the clade *Atraphaxis*, have the exocarp cell of medium (40–70 μm) height, with the lumens sharply or gradually narrowed to the periphery and divided into narrow channels in the thickened OPWs. The anticlinal walls of exocarp cells are strongly thickened and straight in the cross section. This group combines *A. teretifolia* from the section *Physopyrum*, the subclade of *A. frutescens* and *A. virgata, A. pungens, A. grubovii, A. kuvaevii*, all forming separate subclades, and the subclade of *A. davurica* and *A. selengensis*.

The members of the section *Atraphaxis* (*A. replicata* and *A. canescens*) form a subclade that departs late in the plastid phylogeny of the genus. They have the shortest exocarp cells 25–40 μm in height with triangular or low-domed lumen, straight anticlinal walls in the cross section, but sinuate in the paradermal section.

The differences in height and structure of exocarp cells can be explained by constraints of their morphological-anatomical constitution and adaptations to specific climatic conditions that affect flowering and fruiting time.

The species which occupy basal positions in the plastid phylogeny of *Atraphaxis,* have tall exocarp cells with strongly thickened and slightly lignified anticlinal walls, undulating in the cross section. They grow in Montane Regions of Central Asia with semi-arid climate with sufficient precipitation in April–May, but the lack or scarce precipitation in summer (Kottek et al., 2006). These species finish fruiting in May, rarely in June, which allows them to avoid the effects of drought on unripe fruits and preserve the structure of the exocarp, presumably the initial one for *Atraphaxis*.

The species which occupy distal positions in the plastid phylogeny of *Atraphaxis*, possess short exocarp cells with trapezoid to triangular lumens, narrowed to the peripheral into a vertical channel, which is branched in the thick OPWs. They have strongly lignified walls, the anticlinal walls being straight in the cross section. These species grow in steppe zone with hot summer continental climate. Short exocarp cells with low lumen and early lignified walls seem to appear as a result of drought influence during summer, when the seeds ripen.

The diversity of exocarp cells found in *Atraphaxis* is comparable to the diversity observed in Polygonaceae. The species of *Atraphaxis* demonstrate almost all variants of exocarp structure which were detected in the tribes Persicarieae, Polygoneae, and Rumiceae (Fedotova, 1991; Ronse De Craene et al., 2000). The obvious cell height reduction in the process of diversification in the genus *Atraphaxis* and settling in flat steppe and semi-desert communities from mountainous areas does not agree with the hypothetical scheme proposed by Ronse De Craene et al. (2000). Although the species which occupy different positions in plastid phylogeny of *Atraphaxis* strongly differ in the exocarp structure, the species which occupy similar climatic regions and habitats demonstrate much similarity in the structure of exocarp cells, pointing to the influence of environment on the exocarp structure.

This work was supported by Goverment order for the Lomonosov Moscow State University (project No. AAAA-A16-116021660045-2).

References

Bao B., Grabovskaya-Borodina A.E. 2003. *Atraphaxis* L. In: Wu Z.Y., Raven P.H., Hong D.Y. (eds.): *Flora of China*. Beijing: Science Press; St. Louis: Missouri Bot. Gard. Press. V. **5**. P. 328–332.

Gubanov I.A. 1996. *Conspectus of Flora of Outer Mongolia: vascular plants*. Moscow: Valang. [In Russian]

Kottek M., Grieser J., Beck C., Rudolf B., Rubel F. 2006. World map of the Köppen – Geiger climate classification updated. *Meteorol. Z.* **15**: 259–263.

Lovelius O.L. 1979. Synopsis generis *Atraphaxis* L. (Polygonaceae). *Nov. Syst. Pl. Vasc*. **15**: 114–128. [In Russian]

Pavlov N.V. 1936. *Atraphaxis* L. In: Komarov V.L. (ed.): *Flora URSS*. Moscow; Leningrad: USSR Academy of Sciences Publ. V. **5**. P. 501–527. [In Russian]

Rechinger K.H., Schiman-Czeika M. 1968. Polygonaceae. In: Rechinger K.H. (ed.): *Flora Iranica*. Graz: Academishe Druck- und Verlagsanstalt. V. **56**. P. 1–88.

Ronse De Craene L.P., Hong S.P., Smets E. 2000. Systematic significance of fruit morphology and anatomy in tribes Persicarieae and Polygoneae (Polygonaceae). *Bot. J. Linn. Soc*. **134**: 301–337.

Fedotova T.A. 1991. Polygonaceae. In: Takhtajan A. (ed.): *Anatomia seminum comparativa.* Leningrad: Nauka. V. **3**. Dycotyledones. Caryophyllidae – Dilleniidae. P. 83–94. [In Russian]

Yurtseva O.V., Kuznetsova O.I., Mavrodiev E.V. 2016. A broadly sampled 3-loci plastid phylogeny of *Atraphaxis* (Polygoneae, Polygonoideae, Polygonaceae) reveals new taxa: I. *Atraphaxis kamelinii* spec. nov. from Mongolia. *Phytotaxa* **268**: 001–024.

LEAF ANATOMY OF *IRIS ALBERTI* REGEL IN DIFFERENT ECOLOGICAL CONDITIONS IN UZBEKISTAN

Guljan M. DUSCHANOVA*, *Nargiza K. RAKHIMOVA

Russanov Tashkent Botanical Garden, Institute of Botany of the Academy of Sciences, Tashkent, Uzbekistan

guljon.duschanova@mail.ru

The genus *Iris* L. of more than 200 species is the most polymorphic one in the family Iridaceae (Tzvelev, 1982). Many plants of this family produce essential oils, some of them synthesize alkaloids. The species of the genus *Iris* are among the most ancient and popular ornamental cultures.

The aim of our research is to study leaf anatomy of *I. alberti* Regel in two localities with different environmental conditions. The material was collected in early June 2017 in natural habitats in Chatkal mountain range, nearby Kumushkan village and in the late June 2017 in the Russanov Tashkent Botanical Garden (Institute of Botany, Academy of Sciences of the Republic of Uzbekistan). Chatkal Range is a mountain range located in the Western Tien-Shan, limited from the northwest of the Fergana Valley. It has a length of about 200 km, a height of more than 3000 meters, and is located on the territory of the Tashkent region of Uzbekistan. Tashkent Botanical Garden is geographically located in the northeastern part of Tashkent, at an altitude of 473.3 meters above sea level. The climate is sharply continental. The average annual precipitation during the study period was 337 mm, the average annual temperature was 13.8 °C. Precipitation falls mainly in the autumn–winter and spring periods; soil is cultural-irrigated gray soil or irrigated sierozem.

The leaf epidermis was studied in paradermal and cross sections of the bifacial part of the leaf. In the paradermal section, the outlines of epidermal cells can be attributed to a straight type (Aneli, 1975). Epidermal cells belong to the rhomopod vascular wall type of a straight-line clan, which consists of a combination of straight

wall and diamond-shaped wall cells. Introduced plants have 80.6 ± 0.9 epidermal cells per 1 mm^2, the wild plants have 38.5 ± 0.31 ones per 1 mm^2. In both growing conditions, the shape of stomatal cells (from the surface) is oval (40.5 ± 0.34 μm in length, 30.5 ± 0.8 μm in width in natural growing conditions; 51.8 ± 0.6 μm in length, 43.8 ± 0.4 μm in width in the conditions of introduction), the stomata is of lentil-equilateral thickened type (Aneli, 1975), viz. two identical semi-lunar cells located symmetrically. On the frontal plane, the thickened stomatal ridges are almost uniform. The stomatal aperture is spindle-shaped. In *I. alberti* that grows under the conditions of introduction, the stomata are the most abundant (55.9 ± 0.7 per 1 mm^2), in the plants growing under natural conditions, they are less numerous (26.6 ± 0.2 per 1 mm^2). The stomata are more sunken in plants growing under the conditions of introduction (15.6 ± 0.2 μm) than in plants growing under natural environments (13.6 ± 0.09 μm) (Figure, Table).

The leaf mesophyll is dorsiventral *sensu* Vasilevskaya & Butnik (1981) and Butnik et al. (2015) or axiroid *sensu* Carolin et al. (1975).

Table. Quantitative characters of leaf of *I. alberti* in two different environmental conditions

Character (n = 30)	Chatkal mountain range, Tashkent region	Tashkent Botanical Garden
Epidermis:		
cell height, μm	27.3 ± 0.2	42.2 ± 0.5
outer wall thickness, μm	6.8 ± 0.06	6.3 ± 0.07
number per 1 mm^2	38.5 ± 0.31	80.6 ± 0.9
Stoma:		
length, μm	40.5 ± 0.34	51.8 ± 0.6
width, μm	30.5 ± 0.8	43.8 ± 0.4
sunken stomata depth, μm	13.6 ± 0.09	15.6 ± 0.2
number per 1 mm^2	26.6 ± 0.2	55.9 ± 0.7
Spongy parenchyma:		
cell diameter, μm	51.5 ± 0.53	40.6 ± 0.50
number of rows	4–5	5–6
Water-storage parenchyma:		
thickness, μm	328.6 ± 3.44	533.3 ± 6.9
cell diameter, μm	156.4 ± 1.37	94.3 ± 0.92
number of rows	2–3	5–6
Vessels:		
vessel diameter, μm	18.2 ± 0.3	15.6 ± 0.2
number of vessels per a bundle	5–6	7–8

Note: There are values underlined in which the natural and cultivated plants significantly differ.

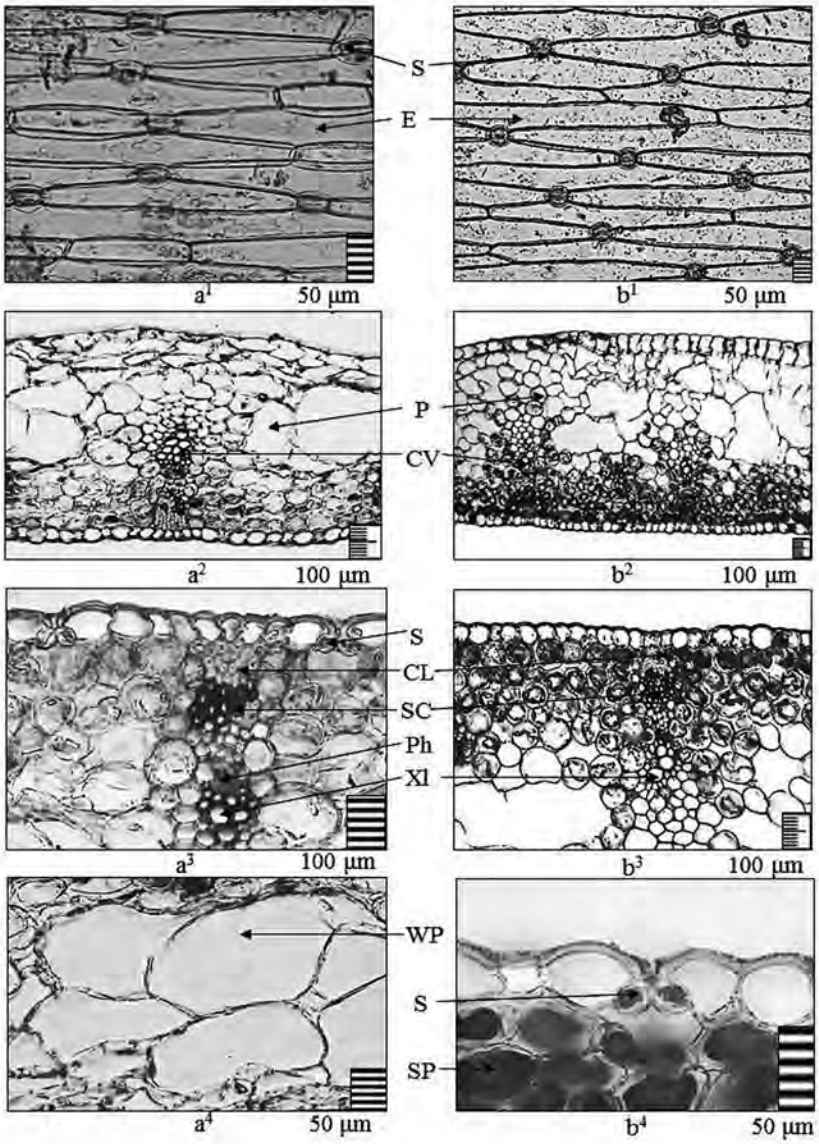

Figure. Anatomical structure of the leaf epidermis and mesophyll of natural (a1 – a5) and cultivated (b1 – b5) plants. a^1, b^1 – epidermis; a^2, b^2 – mesophyll; a^3, b^3 – mesophyll (detail) and vascular bundle; a^4 – water-storage parenchyma; b^4 – sunken stoma and chlorophyll-bearing palisade parenchyma.

WP – water-storage parenchyma, SP – spongy parenchyma, CL – collenchyma, Xl – xylem, P – parenchyma, CB – vascular bundle, S – stoma, Ph – phloem, E – epidermis.

In cross section, both epidermises consist of one layer of round-oval cells. The lower epidermal cells are the largest (42.2 ± 0.5 μm in height) under the conditions of introduction, small (27.3 ± 0.2 μm) in natural habitats. The thin outer wall of the epidermis was observed in both habitat conditions (6.3 ± 0.07 and 6.8 ± 0.06 μm, respectively). The spongy parenchyma consists of 4–6 rows of large and small, rounded cells. Larger spongy parenchyma cells were observed in plants growing under natural conditions (spongy cell diameter 51.5 ± 0.53 μm), small ones in introduced plants (spongy cell diameter 40.6 ± 0.5 μm). Vascular bundles are closed, collateral, numerous, consisting of phloem and xylem, with 5–8 large and small (15.6 ± 0.2 to 18.2 ± 0.3 μm in diam.) vessels per bundle. Water-storage parenchyma consists of 2–6 rows of large and small cells (Figure, Table).

Thick water-storage parenchyma was noted in the introduced plants (533.3 ± 6.9 μm), the thin one in naturally growing plants (328.6 ± 3.44 μm). The water-storage cells are 156.4 ± 1.37 μm in diameter in naturally growing plants vs. 94.3 ± 0.9 μm in diameter in cultivated plants (Figure, Table).

The following characteristics were recognized to be of diagnostic importance: pavement epidermal cells of rhombopodistoral wall type of a rectilinear clan; oval stomata, lentil-like-thickened type of stomata; anomocytic stomata; dorsiventral leaf mesophyll; chlorophyllous spongy parenchyma; collateral vascular bundles.

The following anatomical traits are considered xeromorphic: small, numerous pavement epidermal cells, small spongy and water-storage cells; multi-layered spongy and water-storage parenchyma; numerous sunken stomata; small and numerous vessels in vascular bundles. These traits prevail in the plants growing in the natural habitats.

Larger thin-walled epidermal cells, larger spongy and water-storage cells, low stomatal density, less multi-layered spongy and water-storage parenchyma, large and few vessels in vascular bundles are thought to be mesomorphic features. These features predominate in introduced plants.

References

Tzvelev N.N. 1982. Semeistvo irisovye (Iridaceae). In: Takhtajan A.L. (ed.): *Zhizn' rastenij*. Moscow: Prosveschenie Publ. V. **6.** P. 180–194. [In Russian]

Aneli N.A. 1975. *Atlas of leaf epidermis*. Tbilisi: Metsniereba. [In Russian]

Vasilevskaya V.K., Butnik A.A. 1981. Types of anatomical structure of dicotyledonous leaf (on the methods of the anatomical descriptions). *Bot. Zhurn.* **66**: 992–1001. [In Russian]

Butnik A.A., Tursynbaeva G.S., Duschanova G.M. 2015. *Mesophyll leaf of dicotyledonous plants* (*educational-methodical manual*). Tashkent: Nizami Tashkent Univ. Publ.

Carolin R.C., Jacobs S.W., Vesk M. 1975. Leaf structure in Chenopodiaceae. *Bot. Jahrb. Syst.* **95**: 226–255.

BEYOND POROSITY: 3D LEAF INTERCELLULAR AIRSPACE TRAITS THAT IMPACT MESOPHYLL CONDUCTANCE IN C_3 AND CAM BROMELIACEAE

***J. Mason EARLES*[1], *Guillaume THÉROUX-RANCOURT*[2], *Matthew E. GILBERT*[3], *Danny THOLEN*[2], *Andrew McELRONE*[3], *Craig BRODERSEN*[1]**

[1] Yale University, New Haven, USA
[2] University of Natural Resources and Life Sciences, Vienna, Austria
[3] University of California, Davis, USA
guillaume.theroux-rancourt@boku.ac.at

The leaf intercellular airspace (IAS) is generally considered to have a high conductance to CO_2 diffusion relative to the liquid phase. Yet, while previous studies accounted for leaf-level variation in porosity and mesophyll thickness, they omit inherently 3D IAS traits that potentially influence IAS conductance (g_{IAS}): tortuosity, diffusive path lengthening, and IAS connectivity. We theoretically re-evaluated the standard equation for g_{IAS} by incorporating tortuosity, diffusive path lengthening, and IAS connectivity (Earles et al., 2018). Then, we measured and spatially mapped these geometric IAS traits using X-ray microCT imaging and a novel computational approach within a broad range of species, from ferns to angiosperms, as well as within a family with diverse leaf architecture, the Bromeliaceae, including species with the CAM and C3 photosynthesis syndromes. We found substantial variation in porosity, tortuosity, lateral diffusivity, and IAS connectivity across our dataset and especially in Bromeliaceae leaves, predicting significantly lower g_{IAS} in CAM versus C_3 plants due to a coordinated decline in these traits. On the other hand, ferns generally compensate for low stomatal density and high diffusive path lengthening by building porous thin leaves, thus maximizing g_{IAS}. Moreover, we observed high spatial heterogeneity in these IAS geometric traits throughout the mesophyll, especially within CAM leaves. In conclusion, we argue that IAS traits beyond porosity influence g_{IAS} and that the impact of the IAS on mesophyll conductance should be carefully considered with respect to leaf anatomy, including stomatal distribution. Imaging tools such as X-ray microCT and novel 3D image processing techniques provide a platform for future investigation.

References

Earles J.M., Théroux-Rancourt G., Roddy A.B., Gilbert M.E., McElrone A.J., Brodersen C.R. 2018. Beyond porosity: 3D leaf intercellular airspace traits that impact mesophyll conductance. *Plant Physiol.* **178**: 148–162.

WHAT IS A UNIFACIAL LEAF?

Roland K. EBERWEIN

Regional Museum of Carinthia / Carinthian Botanic Center, Klagenfurt, Austria
roland.eberwein@landesmuseum.ktn.gv.at

Unifaciality is a phenomenon which had been discussed very controversially during the last decades. Chained to aspects of distinguishing leaf and axis of plants (e.g. Sattler, 1971), specification of polarity (e.g. Gleissberg et al., 2000) and regulation of symmetry (e.g. Yamaguchi et al., 2012), unifaciality plays a crucial role in many questions concerning the interpretation of the body plan of plants.

Crüger (1851) and De Candolle (1868) started the discussion on the status of leaves as distinct organs, leading to Arber's 'partial shoot theory of the leaf' (1950), Sattlers 'continuum morphology' (1971) and Rutishauser's 'fuzzy morphology' (Rutishauser, 1995) as examples. These concepts are linked with the question of unifaciality of leaves. This phenomenon was discussed in a greater extent by Čelakovský (1903) for the first time. Later on, Troll and others tried to define unifacial leaves on an anatomical basis (for refs. see Eberwein, 1995), but they failed to give a watertight definition (see Roth, 1954 and Troll & Meyer's reply 1955; Platonova et al., 2016). Nevertheless, unifaciality was, and still is used for interpretation of many monocot leaves (Rudall, Buzgo, 2002; Yamaguchi, Tsukaya, 2007), especially *Iris, Juncus* and *Acorus*-leaves (Kaplan, 1970a, 1975; Yamaguchi, Tsukaya, 2010; Yamaguchi et al., 2010), hypo- and epipeltation (Baum, 1952; Troll, 1932), three-dimensional rachis-leaves and mediane pinnae (Troll, 1935; Kaplan, 1970b; Eberwein, 1995), rounded succulent leaves (Timonin, Ozerova, 1993; Timonin et al., 2006; Ozerova, Timonin, 2009; Fedotov et al., 2016), precursor tips (Troll, 1955), ascidiate leaves (Roth, 1953), carpels (Endress, 2015), etc.

According to Hagemann's (1970) theory of angiospermous leaves and his correction of the anatomically based 'Randmeristem (marginal meristem)' to a morphologically defined 'blastozone' (Hagemann, Gleissberg, 1996), unifaciality turns out as solely morphological character. Applying this leaf-definition, unifaciality is impossible for complete leaves without dissolving the leaf-axis border. To prevent misunderstandings, other definitions should not be used without a clear definition.

Due to the importance of unifaciality, this phenomenon became object of many studies using modern molecular methods (e.g. Tsukaya, 2006, 2010; Yamaguchi, Tsukaya, 2007, 2010; Nicotra et al., 2011; Yamaguchi et al., 2012). Their results should encourage further studies leading to new interpretations not only of the leaf-axis complex but also of three-dimensional leaves, blastozones, peltations, the historical theory of 'programme shift' (incl. the phenomena 'snap effect' and 'snap mix', see Eberwein, 1995) and to include exceptional leaf development, like the possibility of an alternative pathway of peltation in *Rhopalocnemis phalloides*, Balanophoraceae (Eberwein, 2003), unusual developmental patterns like

Podostemaceae (Rutishauser, 1995) as well as flower development, resulting in a new understanding of the plant body-plan.

References

Arber A. 1950. *The natural philosophy of plant form*. Cambridge: University Press.

Baum H. 1952. Normale und inverse Unifazialität an den Laubblättern von *Codiaeum variegatum*. *Oester. Bot. Z.* **95**: 421–451.

Čelakovský L.J. 1903. O listech monofaciálních. *Rozpr. České Akad. Císaře Františka Josefa Vědy, Tř. 2, Vědy Math. Přír. 12 Číslo.* **8**: 1–40.

Crüger H. 1851. Über Axe und Blatt. *Bot. Zeit.* **14**: 545–565.

De Candolle A.C.P. 1868. Théorie de la feulle. *Arch. Sci. Phys. Nat.* Sér. 2. **32**: 32–64 Figs. I, II.

Eberwein R.K. 1995. *Bau und Ontogenese unkonventioneller Blätter des Typs 'unifaziale Phyllome' und deren Beitrag zur Theorie des Spermatophytenblattes*. Dissertation: RWTH Aachen.

Eberwein R.K. 2003. *Rhopalocnemis phalloides* (Balanophoraceae) – an alternative pathway to peltate structures. In: Novikov V.S., Timonin A.K., Shcherbakov A.V. (eds): XI *International Plant Phylogeny Symposium. Abstracts. (Moscow, 28–31 January 2003).* Moscow: BCC-Press. P. 118–119.

Endress P.K. 2015. Patterns of angiospermy development before carpel sealing across living angiosperms: diversity, and morphological and systematic aspects. *Bot. J. Linn. Soc.* **178**: 556–591.

Fedotov A.P., Ozerova L.V., Timonin A.C. 2016. Leaf development in *Curio articulatus* (L. f.) P.V. Heath (Asteraceae – Senecioneae). *Wulfenia* **23**: 135–146.

Gleissberg S., Kim M., Jernstedt J., Sinha N. 2000. The regulation of dorsiventral symmetry in plants. In: Kato M. (ed.): *The biology of biodiversity*. Tokyo: Springer. P. 223–241.

Hagemann W. 1970. Studien zur Entwicklungsgeschichte der Angiospermenblätter. *Bot. Jahrb. Syst.* **90**: 297–413.

Hagemann W., Gleissberg S. 1996. Organogenetic capacity of leaves: the significance of marginal blastozones in angiosperms. *Plant Syst. Evol.* **199**: 121–152.

Kaplan D.R. 1970a. Comparative foliar histogenesis in *Acorus calamus* and its bearing on the phyllode theory of monocotyledonous leaves. *Am. J. Bot.* **57**: 331–361.

Kaplan D.R. 1970b. Comparative development and morphological interpretation of "rachisleaves" in Umbelliferae. *Bot. J. Linn. Soc.* **63** (Suppl. 1): 101–125.

Kaplan D.R. 1975. Comparative developmental evaluation of the morphology of unifacial leaves in the monocotyledons. *Bot. Jahrb. Syst.* **95**: 1–105.

Nicotra A.B., Leigh A., Boyce C.K., Jones C.S., Niklas K.J., Royer D.L., Tsukaya H. 2011. The evolution and functional significance of leaf shape in the angiosperms. *Funct. Plant Biol.* **38**: 535–552.

Ozerova L.V., Timonin A.C. 2009. On the evidence of subunifacial and unifacial leaves: developmental studies in leaf-succulent *Senecio* L. species (Asteraceae). *Wulfenia* **16**: 61–77.

Platonova A.G., Remizowa M.V., Briggs B.G., von Mering S., Lock I.E., Sokoloff D.D. 2016. Vegetative morphology and anatomy of *Maundia* (Maundiaceae: Alismatales) and patterns of peripheral bundle orientation in angiosperm leaves with three-dimensional venation. *Bot. J. Linn. Soc.* **182**: 757–790.

Roth I. 1953. Zur Entwicklungsgeschichte und Histogenese der Schlauchblätter von *Nepenthes*. *Planta* **42**: 177–208.

Roth I. 1954. Beziehungen zwischen der Histogenese des Blattes und seiner äußeren Gestaltung. *Ber. Deutsch. Bot. Ges.* **67**: 10–11.

Rudall P.J., Buzgo M. 2002. Evolutionary history of the monocot leaf. In: Cronk Q.C.B., Bateman R.M., Hawkins J.A. (eds.): *Developmental genetics and plant evolution*. London: Garland Science. P. 431–458.

Rutishauser R. 1995. Developmental patterns of leaves in Podostemaceae compared with more typical flowering plants – saltational evolution and fuzzy morphology. *Can. J. Bot.* **73**: 1305–1317.

Sattler R. 1971. Ein neues Spross-Modell. *Ber. Deutsch. Bot. Ges.* **84**: 139.

Timonin A.C., Ozerova L.V. 1993. Structure, origin and evolution of the terete leaves in *Rowleyani* C. Jeffrey section of *Senecio* L. genus (Asteraceae). *Biol. Bull.* **3**: 393–401. [In Russian]

Timonin A.C., Ozerova L.V., Remizowa M.V. 2006. Development of unifacial leaves in *Senecio* L. s. lat. (Asteraceae). *Wulfenia* **13**: 217–227.

Troll W. 1932. Morphologie der schildförmigen Blätter. *Planta* 17: 153–314.

Troll W. 1935. Vergleichende Morphologie der Fiederblätter. *Nova Acta Leop.* **2**/4: 325–455.

Troll W. 1955. Über den morphologischen Wert der sogenannten Vorläuferspitze von Monocotylenblättern. *Beitr. Biol. Pfl.* **31**: 525–558.

Troll W., Meyer H.J. 1955. Entwicklungsgeschichtliche Untersuchungen über das Zustandekommen unifazialer Blattstiele. *Planta* **46**: 286–360.

Tsukaya H. 2006. Mechanism of leaf-shape determination. *Ann. Rev. Plant Biol.* **57:** 477–496.

Tsukaya H. 2010. Leaf development and evolution. *J. Plant Res.* **123**: 3–6.

Yamaguchi T., Nukazuka A., Tsukaya H. 2012. Leaf adaxial-abaxial polarity specification and lamina outgrowth: evolution and development. *Plant Cell Physiol.* **53**: 1180–1194.

Yamaguchi T., Tsukaya H. 2007. Evo-devo of leaf shape control with a special emphasis on unifacial leaves in monocots. *Korean J. Plant Taxon.* **37**: 351–361.

Yamaguchi T., Tsukaya H. 2010. Evolutionary and developmental studies of unifacial leaves in monocots: *Juncus* as a model system. *J. Plant Res.* **123:** 35–41.

Yamaguchi T., Yano S., Tsukaya H. 2010. Genetic framework for flattened leaf blade formation in unifacial leaves of *Juncus prismatocarpus*. *Plant Cell.* **22:** 2141–2155.

SYNCARPY IN RANUNCULACEAE: AN ANCESTRAL OR DERIVED CONDITION?

Elena S. EL[1]***, Florian JABBOUR***[2]***, Dmitry D. SOKOLOFF***[1]

[1] Lomonosov Moscow State University, Moscow, Russia
[2] Museum National d'Histoire Naturelle, Paris, France
interossi@gmail.com

Apocarpy is commonly viewed as a 'primitive' condition in angiosperms and syncarpy as a derived condition. Traditionally, it was considered that reversals from syncarpy to apocarpy were rare in course of the angiosperm evolution. Subsequent development of angiosperm phylogenetics challenged this view and suggested multiple occurrences of secondarily derived apocarpy, including that of such well-known eudicot families as Rosaceae and Leguminosae. Even within these more complex views on gynoecium evolution, the basal eudicot family Ranunculaceae (Ranunculales) remained one of the most convincing examples of the 'primitive apocarpy'. Recent studies, however, at least questioned the idea that the free-carpellate condition of *Ranunculus* is directly inherited from that of the ancestral angiosperm flower. The carpels are free in most species of Ranunculaceae, but there are some well-known exceptions such as *Nigella* where the carpels are congenitally

united throughout the length of the stigma, however, without producing a functional compitum. Our anatomical investigations demonstrated the presence of congenital intercarpellary fusion in the very short basal-most portion of gynoecia of some other Ranunculaceae, such as some species of *Aconitum*, *Delphinium*, *Staphisagria*, *Aquilegia*. At least in *Aconitum lasiostomum* and *A. lycoctonum*, the gynoecium has a very short synascidiate zone, then a very short unilocular symplicate zone followed by the long asymplicate zone. However, we documented the absence of syncarpy in some other species of *Aconitum*. Basally united carpels are known in bicarpellate gynoecia of *Glaucidium*, an early-divergent member of the family. Clearly, the evolutionary history of syncarpy must be complex in Ranunculaceae. More detailed studies of gynoecium anatomy are required before formal analyses of trait evolution. The studies should be focused on members of Ranunculaceae with five or less carpels in gynoecia, because this condition is likely plesiomorphic in the family and because carpel fusion is problematic due to architectural constraints in the derived multicarpellate gynoecia such as those of *Ranunculus* and *Anemone*. Outgroup comparison with the sister group, Berberidaceae, is not trivial, because the gynoecium of Berberidaceae has been interpreted as either monomerous (then the character of intercarpellary fusion inapplicable) or pseudomonomerous.

The work of ESE and DDS is supported by Russian Foundation for Basic Research (project No. 18-04-00797).

DECIPHERING CONTROVERSIAL ISSUES OF LAND PLANT MORPHOLOGICAL EVOLUTION: INFERENCES FROM A STUDY OF CELLULAR AND MOLECULAR ASPECTS OF THE SHOOT APICAL MERISTEM FUNCTIONING IN NON-MODEL SPECIES

***Anastasiia I. EVKAIKINA*[1], *Ekaterina A. KLIMOVA*[1,2], *Elena V. TYUTEREVA*[1], *Ksenia S. DOBRYAKOVA*[1], *Catarina RYDIN*[3], *Lidija BERKE*[4], *Estelle PROUX-WÉRA*[3], *Katharina PAWLOWSKI*[3], *Olga V. VOITSEKHOVSKAJA*[1], *Marina A. ROMANOVA*[2]**

[1] Komarov Botanical Institute of Russian Academy of Sciences, Saint Petersburg, Russia
[2] Saint Petersburg State University, Saint Petersburg, Russia
[3] Stockholm University, Stockholm, Sweden
[4] Wageningen University, Wageningen, The Netherlands
marinaromanova@mail.ru

The shoot apical meristem (SAM) – an organized self-perpetuating pool of proliferating cells on the shoot tip combines two most important functions in plant morphogenesis: indeterminate growth and production of the lateral organs. Therefore,

inferring its function in plants from divergent taxa might shed light on controversial issues of morphological evolution. More than 250 years of SAM research resulted in description of its structural diversity in land plants, classification of the structural types, and revealed that there is no obvious correlation between the SAM type and shoot morphology (Tooke, Battey, 2003; Romanova et al., 2010; Evkaikina et al., 2017). SAMs of so-called monoplex type (single apical initial, AI) are found in some heterosporous lycophytes (Selaginellales) with so-called microphylls (simple, usually small leaves with single leaf trace and no leaf gap in the stele) and most monilophytes (ferns and horsetails *sensu lato*) with megaphylls (compound leaves with complex leaf traces and leaf gaps in the nodes). Simplex SAM (several AIs in the surface layer) is characteristic of other homosporous and heterosporous lycophytes with microphylls and most gymnosperms with megaphylls. Duplex SAM type (multiple AIs located in several layers, where L1 and L2 initials divide exclusively anticlinally) is present in gnetophytes and all angiosperms. On the other hand, in all SAM types, it is possible to distinguish the central zone (CZ) composed by larger, more vacuolated and slower dividing cells and the peripheral zone (PZ) of smaller, less vacuolated and more intensively proliferating cells. This phenomenon allowed considering this compartmentalization as the essential SAM attribute, while number of AIs and their division pattern – as the taxonomic character (Friedman et al., 2004). Yet another viewpoint states that the number of AIs in the SAM is determined by the ability to form post-cytokinetic plasmodesmata (PD) where the only possible type in plants unable to produce secondary PD is the monoplex SAM (Cooke et al., 1996; Evkaikina et al., 2017).

To infer structural and functional organization of the SAM in evolutionary context it is essential to decipher molecular mechanisms of its regulation. For model angiosperms these studies confirmed compartmentalization of duplex SAM into the CZ and PZ and revealed the heterogeneity within the CZ, specified by differential expression of genes encoding a suite of transcription factors (TFs). Homeodomain TFs KNOX class I and WUS are the key regulators maintaining SAM cells in an undifferentiated state, while the switch to the leaf development program is controlled by ARP, YABBY and HD-Zip class III TFs (Gaillochet et al., 2015). ‘Meristem-specific’ and ‘leaf-specific’ TFs act as antagonists. Consequently, their expression is confined to the mutually exclusive domains. Most of these TFs act non-cell-autonomously and KNOX class I TFs are shown to gain functional competence only after selective acropetal transport through secondary PD between L3, L2 and L1 layers. Key role in this selective transport is attributed to specific amino acid residues (R30 and L53) within the homeodomain (Kim et al., 2003; Chen et al., 2014).

Although progress made in study of SAM regulators in phylogenetic context is far more modest, *WOX* (*WUSCHEL*-like Homeobox)*, KNOX, HD-Zip III* and *APR* homologs have been revealed in lycophytes and monilophytes with monoplex SAM and gymnosperms with simplex SAM (excepting ARP) (Floyd, Bowman,

2007; Frank et al., 2015; Harrison et al., 2005; Nardmann, Werr, 2013; Sano et al., 2005). *KNOX* class I homologs are expressed in SAMs of lycophytes, monilophytes and gymnosperms suggesting common mechanism of indeterminacy regulation, although in monoplex SAM transcripts are usually excluded from the single AI. However the KNOX / ARP interactions are not antagonistic both in lycophytes and monilophytes: in *Selaginella kraussiana* KNOX and ARP transcripts co-localize in the SAM while in *Osmunda regalis* – in leaf primordia. Expression of *HD-Zip III* homologs in both lycophytes and monilophytes marks SAM, leaf and sporangia primordia (Vasco et al., 2016).

However yet there are no data about regulation in the simplex SAM of lycophytes; data about potential homologs of "leaf-specific" TFs in gymnosperms are controversial. To fill this gap we have carried out a pioneer study of the molecular aspects of the simplex type SAM functioning in lycophytes and gymnosperms.

Sequencing and analysis of the shoot apices transcriptomes of *Huperzia selago* (Lycopodiales) and *Isoëtes lacustris* (Isoëtales) has shown that both lycophytes have homologs of *KNOX* genes from class I and class II, as well as potential *WOX* homologs. Independent duplication of KNOX I class genes in homosporous and heterosporous lycophytes has allowed us to hypothesize that KNOX class I proteins in Lycopodiales with simplex SAM and secondary PD, could have evolved capacity for intercellular transport. However it turned out that none of lycophyte KNOX proteins had domains responsible for intercellular transport. Expression of potential homologs of genes encoding ARP TFs have not been revealed in transcriptomes of both lycophytes. The fact that *YABBY* homologs were absent from the only sequenced genome of the non-seed plant, *Selaginella moellendorfii*, led to a viewpoint that these TFs are unique to seed plants (Floyd, Bowman, 2007). However in *H. selago* transcriptome we were able to identify expression of the gene encoding *YABBY* homolog, *HsYABBY* – the first homolog for non-seed plants (Evkaikina et al., 2017). Nevertheless, subsequent search for other *YABBY* homologs in transcriptome of *I. lacustris* and other lycophytes from OneKP database (www.onekp.com) gave no results, making *HsYABBY* unique for spore plants. Phylogenetic analysis showed that the *HsYABBY* gene is sister to *YABBY* genes of other plants, and that *YABBY* genes probably originated from a common ancestor of all land plants.

The fact, that transcripts of *ARP* homologs were absent from *H. selago* transcriptome as well as from genomes of *Physcomitrella patens* (Banks et al., 2011) and *Picea abies* (Nystedt et al., 2013) has lead us to the hypothesis that these TFs might not be involved in regulation of organogenesis in simplex SAM. To test this hypothesis we have searched for ARP homologs in different gymnosperm genome databases. This search has revealed a potential *Picea abies ARP* homolog *(PaARP)* in http://congenie.org database and has shown that *ARP*-independent regulation of organogenesis cannot be considered as a common feature of simplex SAM.

Visualization of *KNOX* homolog *HBK1* and *ARP* homolog *PaARP* by *in situ* RNA hybridization showed partial overlap of their expression patterns: genes en-

coding both TFs co-localized in SAM and young leaf primordia indicating a non-antogonistic KNOX/ARP interaction in gymnosperms. Unlike angiosperms, where *ARP* expression marks the adaxial domain of the growing leaf, *PaARP* was uniformly transcribed throughout the leaf primordium, suggesting that probably is not an adaxiality factor.

HsYABBY expression in *H. selago* has also showed a significant difference with angiosperms. While in angiosperms *YABBY* genes are never expressed in the SAM, and their ectopic expression leads to its disappearance, transcription of *HsYABBY* marked the SAM (except for the apical initials), leaf and sporangia primordia. On later stages of leaf development *HsYABBY* transcription was confined to the surface cells of its abaxial and adaxial sides (the protoderm), while in seed plants *YABBY* expression is confined to the abaxial domain of the leaf, controlling its histogenesis.

Thus, both *H. selago* and *P. abies* are characterized by expression of the homologs of "leaf" TFs *YABBY* (in *H. selago*) and *ARP* (in *P. abies*) in the SAM, which is different from angiosperms. This data suggest that the regulation of microphyll and megaphyll origin in simplex SAM have more common features as compared to regulation of megaphyll origin in the simplex (spruce) and duplex (angiosperms) SAMs.

These data confirm the viewpoint that despite common partition into CZ and PZ, different SAM types do have functional differences (Romanova et al., 2010). In the monoplex SAM both microphylls of lycophytes and megaphylls of monilophytes initiate through origin of the single LAC (leaf apical cell) resulting from formative division of one of the surface cells, that is in the CZ of the SAM, not PZ as in two other structural types. In simplex SAM both lycophyte microphylls and gymnosperm megaphylls originate through proliferation of a group of PZ cells. Thus both cellular and molecular aspects of leaf origin seem to be correlated with the SAM structural type, but not with the leaf type (mirophyll or megaphyll).

This work was supported by RFBR (project No. 17-04-00837) and the Komarov Botanical Institute institutional research project No. AAAA-A17-117051810115-1.

References

Banks J.A. et al. 2011. *Selaginella* genome identifies genetic changes associated with the evolution of vascular plants. *Science* **332**: 960–963.

Chen H., Jackson D., Kim J.-Y. 2014. Identification of evolutionarily conserved amino acid residues in homeodomain of KNOX proteins for intercellular trafficking. *Plant Signal Behav.* **9**: e28355.

Cooke T.D., Tilney M., Tilney L. 1996. Plasmodesmatal networks in apical meristems and mature structures: geometric evidence for both primary and secondary formation of plasmodesmata. In: Smallwood M., Knox J.P., Bowles D.J. (eds.): *Membranes: specialized functions in plants*. Cambridge: BIOS Sci. Publ. P. 471–488.

Evkaikina A.I., Berke L., Romanova M.A., Proux-Wéra E., Ivanova A.N., Rydin C., Pawlowski K., Voitsekhovskaja O.V. 2017. The *Huperzia selago* shoot tip transcriptome sheds new light on the evolution of leaves. *Genome Biol. Evol*. **9**: 2444–2460.

Floyd S., Bowman J.L. 2007. The ancestral developmental tool kit of land plants. *Int. J. Plant Sci*. **168**: 1–35.

Frank M. H., Edwards M.B., Schultz E.R., McKain M.R., Fei Z., Sørensen I., Rose J.K., Scanlon M.J. 2015. Dissecting the molecular signatures of apical cell-type shoot meristems from two ancient land plant lineages. *New Phytol.* **207**: 893–904.

Friedman W.E., Moore R.C., Purugganan M.D. 2004. The evolution of plant development. *Am. J. Bot.* **91**: 1726–1741.

Gaillochet C., Daum G., Lohmann J.U. 2015. O cell, where art thou? The mechanisms of shoot meristem patterning. *Cur. Opin. Plant Biol.* **23**: 91–97.

Harrison C.J., Corley S.B., Moylan E.C., Alexander D.L., Scotland R.W., Langdale J.A. 2005. Independent recruitment of a conserved developmental mechanism during leaf evolution. *Nature* **434**: 509–514.

Kim J.-Y., Yuan Z., Jackson D. 2003. Developmental regulation and significance of KNOX protein trafficking in *Arabidopsis*. *Development* **130**: 4351–4362.

Nardmann J., Werr W. 2013. Symplesiomorphies in the WUSCHEL clade suggest that the last common ancestor of seed plants contained at least four independent stem cell niches. *New Phytol.* **199**: 1081–1092.

Nystedt B. et al. 2013. The Norway spruce genome sequence and conifer genome evolution. *Nature* **497**: 579–584.

Romanova M. A., Naumenko A.N., Evkaikina A.I. 2010. Special features of apical morphogenesis in various taxa of seedless plants. *Vestnik St.-Petersburg State Univ.* Ser. 3. **3**: 29–36. [In Russian]

Sano R., Juárez C.M., Hass B., Sakakibara K., Ito M., Banks J.A., Hasebe M. 2005. KNOX homeobox genes potentially have similar function in both diploid unicellular and multicellular meristems, but not in haploid meristems. *Evol. Dev.* **7**: 69–78.

Tooke F., Battey N. 2003. Models of shoot apical meristem function. *New Phytol*. **159**: 37–52.

Vasco A., Smalls T.L., Graham S.W., Cooper E.D., Wong G.K., Stevenson D.W., Moran R.C., Ambrose B.A. 2016. Challenging the paradigms of leaf evolution: Class III HD-Zips in ferns and lycophytes. *New Phytol.* **212**: 745–758.

GENETIC AND EPIGENETIC BASES OF LEAF DEVELOPMENT

Tatiana A. EZHOVA, Evgenia V. KUPRIYANOVA

Lomonosov Moscow State University, Moscow, Russia

ekupriyanova@gmail.com

Plant species display an intriguing variety of leaf shapes and sizes. The molecular genetic mechanisms underlying the diversification of leaf shape have been revealed in several species, primarily in the model plant *Arabidopsis thaliana* (L.) Heynh. It was demonstrated, that class-1 *KNOX* genes promote proliferation and indeterminacy of stem cells in the shoot apical meristem; their epigenetic silencing in leaf primordium is indispensable for acquisition of cell determinacy during simple leaf development (Hay, Tsiantis, 2010). The maintaining of established cell

identity in developing leaf is based on epigenetic mechanisms, which are recruited to their target genes by AS1–AS2 protein complex. This complex initiates stable epigenetic silencing of class-1 *KNOX* genes and the genes of abaxial identity in adaxial leaf domain thus ensuring simple leaf development with normal dorsoventral polarity.

AS1–AS2 complex recruits the Polycomb Repressive Complex 2 (PRC2) to *KNOX* genes to establish the somatically heritable repressed chromatin state required for leaf development (Lodha et al., 2013). In addition, AS1 and AS2 can cooperate with histone deacetylase HDA6 in regulating chromatin state of the *KNOX* genes (Luo et al., 2012). Moreover, AS1–AS2 complex controls dorsoventral polarization via a PRC2-dependent mechanism and a non-Polycomb-mediated, but still potentially epigenetic, mechanism of repression of abaxial determinant genes in adaxial leaf side (Ueno et al., 2007; Iwasaki et al., 2013; Husbands et al., 2015). AS1–AS2 complex is also required for maintaining levels of CG methylation in the coding region of some abaxial identity genes (Iwasaki et al., 2013).

These epigenetic changes (DNA methylation and histone modifications) provide stable maintaining of early cell patterning of leaf primordium, which is *a sine qua non* prerequisite for normal leaf development. Because epigenetic mechanisms are able to induce heritable changes in gene expression, they have been proposed to play an important role in environmentally induced developmental plasticity (Sultan, 2017; Ecker et al., 2018). Indeed, in some species or under certain special environmental conditions, epigenetic memory may be impaired or reset. The removing of the epigenetic marks accompanied by altered gene expression patterns can be caused by mutations, ambient conditions and even by pathogens (Nakayama et al., 2014; Paponova et al., 2018). The resetting of epigenetic chromatin states can lead to heterophylly and cause leaf morphological diversity in close related species or even inside one species (developmental variation between biomorphs).

Developmental plasticity is a characteristic feature of plants, which seems to be related to the existence of specific genes in plants that can regulate the level of stability / lability of epigenetic modifications depending on environmental conditions and the physiological state of the plants. The natural and artificial selection of mutations in these regulatory genes can lead to the emergence of new forms and varieties of cultivated plants, species of wild plants, which demonstrate genetically determined changes in leaf development associated with loss of cellular memory at a certain stage of organ development.

The impressive examples of such species are the species of the genus *Curio* P.V. Heath. The fruitful research, carried out at the Department of Higher Plants of Moscow State University, demonstrated that some of these species are characterized by genetically determined differences in the degree and time of loss of dorsoventral polarity of the leaf primordia and the development of subunifacial or unifacial leaves (Ozerova, Timonin, 2009; Fedotov et al., 2016). The search for

the genes responsible for these ontogenetic reversions is the important challenge for future research.

It is easier to search for new regulatory genes on *Arabidopsis thaliana*, a model plant with a compact and sequenced genome. In our collection of *A. thaliana* mutants there is a mutant, which is characterized by loss of cellular memory during leaf development, formation of outgrowths and buds on the leaves, as well as impaired leaf polarization. This unique phenotype is caused by mutations of two genes that interact synergistically with the *AS1–AS2* genes. Our efforts are aimed at finding these genes in the *A. thaliana* genome.

This work was supported by the Russian Foundation for Basic Research (project No. 19-04-00149_a).

References

Ecker S., Pancaldi V., Valencia A., Beck S., Paul D.S. 2018. Epigenetic and transcriptional variability shape phenotypic plasticity. *BioEssays* **40**: 1–11.

Fedotov A.P., Ozerova L.V., Timonin A.C. 2016. Leaf development in *Curio articulatus* (L.f.) P.V. Heath (Asteraceae–Senecioneae). *Wulfenia* **23**: 135–146.

Hay A., Tsiantis M. 2010. KNOX genes: versatile regulators of plant development and diversity. *Development* **137**: 3153–3165.

Husbands A.Y., Benkovics A.H., Nogueira F.T.S., Lodha M., Timmermans M.C.P. 2015. The ASYMMETRIC LEAVES complex employs multiple modes of regulation to affect adaxial-abaxial patterning and leaf complexity. *Plant Cell* **27**: 3321–3335.

Iwasaki M., Takahashi H., Iwakawa H., Nakagawa A., Ishikawa T., Tanaka H., Matsumura Y., Pekker I., Eshed Y., Vial-Pradel S., Ito T., Watanabe Y., Ueno Y., Fukazawa H., Kojima S., Machida Y., Machida C. 2013. Dual regulation of ETTIN (ARF3) gene expression by AS1–AS2, which maintains the DNA methylation level, is involved in stabilization of leaf adaxial–abaxial partitioning in *Arabidopsis*. *Development* **140**: 1958–1969.

Lodha M., Marco C.F., Timmermans M.C. 2013. The ASYMMETRIC LEAVES complex maintains repression of KNOX homeobox genes via direct recruitment of polycomb-repressive complex2. *Genes & Dev*. **27**: 596–601.

Luo M., Yu C.W., Chen F.F., Zhao L., Tian G., Liu X., Cui Y., Yang J.Y., Wu K. 2012. Histone deacetylase HDA6 is functionally associated with AS1 in repression of KNOX genes in *Arabidopsis*. *PLoS Genetics* **8**: e1003114.

Nakayama H., Nakayama N., Seiki S., Kojima M., Sakakibara H., Sinha N., et al. 2014. Regulation of the KNOX–GA Gene module induces heterophyllic alteration in North American lake cress. *Plant Cell* **26**: 4733–4748.

Ozerova L.V., Timonin A.C. 2009. On the evidence of subunifacial and unifacial leaves: developmental studies in leaf-succulent *Senecio* L. species (Asteraceae). *Wulfenia* **16**: 61–77.

Paponova S.S., Chetverikov P.E., Pautov A.A., Yakovleva O.V., Zukoff S.N., Vishnyakov A.E., et al. 2018. Gall mite *Fragariocoptes setiger* (Eriophyoidea) changes leaf developmental program and regulates gene expression in the leaf tissues of *Fragaria viridis* (Rosaceae). *Ann. Appl. Biol.* **172**: 33–46.

Sultan S.E. 2017. Developmental plasticity: re-conceiving the genotype. *Interface Focus.* **7**: 20170009.

Ueno Y., Ishikawa T., Watanabe K., Terakura S., Iwakawa H., Okada K., Machida C., Machida Y. 2007. Histonedeacetylases and ASYMMETRIC LEAVES2 are involved in the establishment of polarity in leaves of *Arabidopsis*. *Plant Cell* **19**: 445–457.

LEAF AND NODAL ANATOMY OF *SENECIO KLEINIIFORMIS* SUESS. (ASTERACEAE) AND ITS PRESUMABLE PARENT SPECIES

Alexey P. FEDOTOV[1], ***Alexander C. TIMONIN***[2]

[1] Institute for Information Transmission Problems (Kharkevich Institute), Russian Academy of Sciences, Moscow, Russia
[2] Lomonosov Moscow State University, Moscow, Russia
Alex-f96@yandex.ru

The species-rich genus *Senecio* in its traditional circumscription is not monophyletic, the groups segregated from it being nested among other members of the tribe Senecioneae (Pelser et al., 2007). Rather many senecios are hard to be classified due to their hybrid origin. The leaf anatomy was shown to bring additional data for elucidating relationships of such groups, especially of succulent ones (Cicuzza et al., 2017).

Senecio kleiniiformis must have been an occasional culture-generated species. Rowley (1994, 2002) considered it a hybrid between *S. articulatus* (Haw.) Sch. Bip. and *S. talinoides* ssp. *cylindricus* (A. Berger) G.D. Rowley, or *S. ficoides* Sch. Bip., or *S. repens* (L.) H. Jacobsen, all species being thought nowadays members of *Curio* alliance (Ozerova et al., 2017). However, ITS sequencing shows closer relationship between *S. kleiniiformis* and *S. tropaeolifolius* than with *S. articulatus* (Malenkova et al., 2014).

The present investigation aims to study leaf and stem anatomy of *S. kleiniiformis* and its presumable parent species *S. articulatus* and *S. tropaeolifolius* to elucidate its origin.

The plant material was obtained from the Tsitsin Main Botanical Garden of Russian Academy of Science. According to standard protocols (Barykina et al. 2004), it was dissected by hand-razor, some sections were processed with Phloroglucinol and HCl, others were stained with Toluidine Blue. The sections were examined under light microscope Nikon eclipse Ci equipped with digital camera Nikon digital sight DS-Vi1.

Senecio kleiniiformis is a leaf succulent with long-petiolate ascidiate leaves. The leaf blade has a conical tip and usually two lateral teeth. The lower leaves of the annual shoot have flattened, rounded cochleariform blades with small teeth. The upper leaves have scaphoid leaf blades some of them develop additional teeth on one or both sides. The leaves of transitional form are in between.

The petiole is cordate in the cross-section. Unilayered epidermis is underlain with one layer of hypodermis; 3- or 4-layered homogeneous chlorenchyma is present under them. It is disrupted by a small band of water-storage tissue at the base of the petiole on its acroscopic side. The median (M) and 6 lateral (L1; L2; L3 on each side) collateral vascular bundles enter the petiole and are endoscopic and circularly arranged nearly throughout the petiole. Number of

the petiolar bundles increases up to 25 in the distalmost petiole part due to branching of L2s and L3s. Some bundles are accompanied by outer schizogenous ducts.

The leaf blade is hypostomatous with a subepidermal water-storage hypodermis (4–6 layers on the adaxial side and one layer on abaxial side) and 5–6 layers of chlorenchyma slightly differentiated in spongy and palisade tissues. Larger M, L1s, L2s and many their smaller derivatives are discernible in the chlorenchyma. Most of them are accompanied by the underlain schizogenous ducts.

Small L3-derivative (lateral vein) runs along the whole leaf blade margin. The midrib and L1 branch rarely and usually run directly to the leaf tip. One of the L1s branches once into 2 equal bundles. One of them goes to the leaf tip, another one innervates the lateral tooth. The L2 usually goes to the lateral tooth, where it merges with the lateral vein and with the L1 branch, if present. If there are more than 2 laterals teeth, both L2s branches equally at the base of the leaf blade. One of derivatives goes to the proximal teeth, while another goes to the distal one. Additional huge L2-derivate bundle (L2') also branches off in the petiole and goes to the proximal tooth.

The stem of *S. kleiniiformis* is covered with a unilayered epidermis. The cortex consists of two layers of circumferential collenchyma, 2–3 layers of chlorenchyma and inner parenchyma and no endodermis. 20–25 collateral vascular bundles of the typical eustele are accompanied by outer schizogenous ducts. The pith consists of isodiametric parenchyma cells. Nodes are 3-lacunar. Lateral leaf traces emerge from the stele at some distance from the median one and branch two times.

Senecio articulatus is a stem succulent with articulate stems and three-lobed leaves with a large middle lobe and smaller lateral ones oriented perpendicular to the middle lobe. Each lobe has a conic tip and sometimes bears 1 or 2 lateral teeth (more frequently on the middle lobe).

The petiole is cordate in the cross section. It is covered with a single layer of epidermis underlain by one-layered water-storage hypodermis. Few-layered homogenous chlorenchyma is under the hypodermis. It is penetrated by collateral vascular bundles which are arranged V-shaped and have an endoscopic xylem. They are accompanied by outer schizogenous ducts. The chlorenchyma is discontinuous throughout the petiole at its acroscopic side. The water-storage parenchyma occupies the central part of the petiole. Three vascular bundles enter the petiole from the node. Lateral bundles branch once therein; five vascular bundles resultantly enter the leaf blade.

The leaf blade is hypostomatous. The water-storage hypodermis is few-layered under the adaxial epidermis and 1-layered under the abaxial epidermis. The adaxial hypodermis gradually continues into the chlorenchyma slightly differentiated into the spongy and palisade tissues. It encloses collateral vascular bundles. The schizogenous ducts are absent in the leaf blade.

Senecio articulatus has a submarginal vein in the leaf blade. Midrib usually runs directly to the tip of the middle lobe, branches twice and gives two large de-

rivatives, which run the same way. One of L1s branches more frequently. The L1 runs to the tip of lateral lobe, while several big derivates innervate the base of the main lobe. Sometimes they also can innervate lateral teeth on one side of the main lobe. Derivatives of the L2s innervate the base of the leaf blade.

The stem of the *S. articulatus* is covered with a unilayered epidermis. The cortex consists of two layers of circumferential collenchyma with thickened periclinal cell walls, multilayered photosynthetic parenchyma and no endodermis. The typical eustele has many collateral vascular bundles accompanied with outer schizogenous ducts. The pith consists of roundish parenchyma cells. The nodes are 3-lacunar. The lateral leaf traces emerge from the stele at some distance from the median leaf trace.

Senecio tropaeolifolius is a liana bearing peltate leaves. The polygonal leaf blade has a cuneate undercut of variable depth in its basiscopic part and short leaf tip hardly discernible from numerous principal marginal teeth. Shorter additional teeth are sometimes present between these main teeth.

The petiole is circular in cross section with unilayered epidermis underlain by one layer of tangentially flattened hypodermal cells. Homogeneous chlorenchyma is under these cells. It continues inwards into the inner water-storage tissue. The chlorenchyma is discontinuous on the acroscopic side of the petiole where the water-storage paranchyma adjoins the hypodermis. Three collateral vascular bundles with acroscopic xylem enter the petiole from the node. The lateral bundles branch twice, thus 7 vascular bundles result to supply the leaf blade. Schizogenous ducts are absent.

The amphistomatous leaf blade has neither a hypodermis nor schizogenous ducts. The chlorenchyma adjoins the both epidermises. It is differentiated into spongy and palisade tissues. Collateral vascular bundles are between these tissues. There is a marginal vein that runs along the leaf margin. The midrib branches seldom to innervate the leaf tip and the nearest principal teeth. L1s and their branches innervate next 1–3 principal teeth on both sides of the leaf blade. The L3 derivatives innervate the most basiscopic tooth. The other principal teeth are innervated by derivatives of L2s.

The stem is covered with 1-layered epidermis. The cortex consists of an outer layer of collenchyma and inner photosynthetic parenchyma. The chloroplast number in its cells decreases inwards. There is no endoderm in the cortex. The stem vasculature is typical eustele. Cortical sclerenchyma strands are opposite the biggest vascular bundles of the stele. Pith consists of large parenchyma cells. Schizogenous ducts are absent. Nodes are 3-lacunar; lateral leaf traces run out of the stele close to the median one.

Our data on stem anatomy confirm the hypothesis that *S. articulatus* is one of the parent species of *S. kleiniiformis*. Both species have stems with many vascular bundles, the lateral leaf traces emerge from the stele rather distantly from the median leaf trace and run some distance around the stele to enter the petiole.

Additionally, there are also schizogenous ducts in front of most vascular bundles. Both species are lack of sclerenchyma in their shoots.

The leaf blade anatomy is very similar in *S. kleiniiformis* and *S. articulatus*. Both leaves are hypostomatous, of the same bauplan with 1-layered hypodermis on the abaxial side and multilayered hypodermis of larger cells on the adaxial side and with slightly different palisade and spongy chlorenchyma. The leaf blade structure of *S. kleiniiformis* could be derived from that of *S. articulatus* by means of hyperplasia of the leaf blade. The schizogenous ducts are absent in both hypothetical parent species of *S. kleiniiformis*, so these structures could be inherited from the other parent species to be revealed. In contrast, the leaf blades of *S. tropaeolifolious* are amphistomatous and have no hypodermis.

The leaf of *S. kleiiniiformis* would have evolved *via* leaf blade reduction irrespective of whether this species has originated from *S. articulatus* or *S. tropaeolifolius*. However, patterns of the leaf vasculature show that a transition from the leaf of *S. tropaeolifolius* to the leaf of *S. kleiiniformis* would be easier than transition from the leaf of *S. articulatus* to that of *S. kleiiniformis*. To get the *S. kleiniiformis* leaf blade, the leaf of *S. tropaeolifolius* would have reduced the number of lateral teeth, whereas the leaf of *S. articulatus* would completely have lost its lateral lobes. But the former one has 7 principal vascular bundles quite identifiable with the 7 principal vascular bundles of the *S. kleiniiformis* leaf, while the leaf of *S. articulatus* has only 5 principal vascular bundles entering the leaf blade. Therefore, an additional pair of principal vascular bundles must have appeared between the midrib and L1s, because the L1s would still innervate reduced lateral lobes transformed into lateral teeth of *S. kleiniiformis*.

The data obtained are thus controversial. Further studies are necessary for resolving the problem of parent species of *S. kleiniiformis*.

References

Barykina R.P., Veselova T.D., Devyatov A.G., Dzhalilova Kh.Kh., Iljina G.M., Chubatova N.V. 2004. *Handbook on botanical microtechniques. Principles and methods*. Moscow: Moscow Univ. Publ. [In Russian]

Cicuzza D., Staheli D.S., Nyffeler R., Eggli U. 2017. Morphology and anatomy support a reclassification of the African succulent taxa of *Senecio* s. l. (Asteraceae: Senecioneae). *Haseltonia* **23**: 11–26.

Malenkova E.D., Ozerova L.V., Schanzer I.A., Timonin A.C. 2014. Re-consideration on *Senecio oxyriifolius* DC. and *S. tropaeolifolius* MacOwan ex F. Muell. (Asteraceae: Senecioneae). *Wulfenia* **21**: 111–118.

Ozerova L.V., Schanzer I.A., Timonin A.C. 2017. *Curio* alliance (Asteraceae: Senecioneae) revisited. *Wulfenia* **24**: 29–52.

Pelser P.B., Nordenstam B., Kadereit J.W., Watson L.E. 2007. An ITS phylogeny of tribe Senecioneae (Asteraceae) and a new delimitation of *Senecio* L. *Taxon* **56**: 1077–1104.

Rowley G.D. 1994. *Succulent Compositae*: *A Grower's guide to the succulent species of* Senecio & Othonna. Mill Valley: Strawberry Press.

Rowley G.D. 2002. *Senecio*. In: Eggli U. (ed.): *Illustrated handbook of succulent plants*: *Dicotyledons*. Berlin: Springer. P. 29–43.

LEAF TRICHOMES, TEETH AND GLANDS OF SOME *POPULUS* SPECIES (SALICACEAE)

Tatiana A. FEODOROVA

Lomonosov Moscow State University, Moscow, Russia
torreya@mail.ru

Leaf trichomes, teeth and glands are widely used as important diagnostic and taxonomic characteristics in plant systematics. Ma et al. (2016) studied genes related to trichome development in *Populus pruinosa* Schrek. and *P. euphratica* Oliv. and location of trichomes on leaves, stems, petioles and seed coat by SEM.

The 'salicoid teeth' of leaves are set with "a dark, but not opaque, nondeciduous spherical callosity fused to the tooth apex" (Hickey, Wolfe, 1975, cit. by Wilkinson, 2007). Another definition of the 'salicoid teeth' was given by Nandi et al. (1998): "leaf teeth showing a proximally rounded hyaline gland with a concave gland body in herbarium samples". Differences between the teeth as observed in dry and fresh material can be the source of confusion when using this term. Wilkinson (2007) specified the meaning of this concept, and now 'the salicoid tooth' "seems to be a projection at the apex of the leaf tooth, the outermost layer of which is composed of radially elongate, palisade-like cells which are subtended by several layers of parenchyma cells This structure is of variable morphology and is supplied by one to three veins, mainly composed of xylem elements". However, the author considers that this definition has to be reconsidered after an anatomical investigation of the 'salicoid teeth' and glands in more genera and species of Salicaceae and Flacourtiaceae, as well as glands and 'salicoid teeth' in species of other families.

It is impossible to say that the 'salicoid teeth' of *Populus* and *Salix* were deprived of the attention of researchers. The first description of the function of these structures as producing resin was made by Hanstein (1868) on the example of *Populus*. The secretory function of the salicoid teeth was described for *P. balsamifera* L. and *P. laurifolia* Ledeb. by Reinke (1876). Tschirch (1906, cit. by Fehér, 1923) described secretion in *P. alba* L., *P. balsamifera*, *P. canadensis* Moench. (or *P. deltoides* Marshall), *P. canescens* (Ait.) Smith, *P. nigra* L., *P. tremula* L. and also described teeth. Trelease (1881) reported about release of 'nectar' by the teeth which he called extrafloral nectaries, of *P. balsamifera*, *P. candicans* Aiton, *P. grandidentata* Michx., *P. monilifer* Ait., *P. tremuloides* Michx. and *P. tremula*, but he did not report about resin. He considered that the nectar was secreted by the elongated epidermal cells of gland of teeth tips. He even described the nectar accumulation process leading to stretching and possible destruction of the cuticle. However, secretion of resin, not the nectar is of everyday occurrence in the majority of *Populus* species studied by Trelease. Edelstein (1902) described allocations of salicoid teeth of *P. laurifolia* and called the area in which they occurred the hydathode without epitema (Wilkinson, 1979). He also mentioned similar hyda-

thodes in *P. balsamifera* and *P. tremula* and was the first to assume that hydathodes appear near gland. Lippman (1925) believed that the resinous secretion comes from the tips of the teeth. According to Curtis & Lersten (1974), the first leaves of *P. deltoides* have trichomes and are deprived of secretory epidermis. There is a bigger vascular bundle which terminates in a tooth. Later these authors claimed that the leaves in the end of the summer and in the early autumn have several hydathodes over the end of the external bundle from which there is presumably an exudation. Thus, the function of hydathode is transpiration, but it is a nonspecific type of hydathodes which can also secrete nectar under certain conditions. Curtis & Lersten (1974) could not find sieve elements and companion cells in the bundle, but found cells, which could be interpreted as phloem parenchyma or perhaps a procambium stretching out beyond the limits of the xylem elements in teeth glands. The 'salicoid teeth' seem to be capable of excreting more than one substance. The gland tips of the teeth secrete the resin; the cells under the tips secrete the nectar from a specific type of hydathodes. Wilson et al. (1991) confirmed "that teeth in section have the top part (adaxial) with hydathodes complete with an epithema of deeply lobed cells with air large spaces between lobes, xylem elements below, and stoma in the epidermis" in *P. balsamifera*. It has been proven that the secret from the basal leaf glands of eight *Populus* species and two hybrids gave positive glucose reactions (Pemberton, 1992). Hickey & Wolfe (1975) believed that the 'salicoid teeth' of *Populus* presumably have a common origin with *Idesia* teeth of Flacourtiaceae. 'The salicoid teeth' of *Populus* species were not anatomically described by these authors.

The research of Wilkinson (2007), concerning 'the salicoid teeth' of three Salicaceae taxa (*P. ciliata* Wall., *P. trichocarpa* Torr. et A. Gray, *Salix lasiolepis* Benth.) and six Flacourtiaceae taxa, revealed the progressing development from glands of a simple structure to glands of a more complex structure in Flacourtiaceae and morphology and anatomy complication trend of Salicaceae species. Apparently, there is a transition from glands of a simple structure in Flacourtiaceae taxa to morphologically and anatomically more complex gland types of Salicaceae. The marginal glands of Flacourticaceae have common region of secretory, palisade-like cells with one to three vascular veins. Probably, there is a wide range from rather simple to more complex glands, for example, some types of *Salix*, *Populus* and, especially, *Dovyalis hebecarpa* (Gardner) Warb. A limited number of the studied species of *Salix* and *Populus* have globular or subglobular glandular part of tooth. The main features of tooth structure are strongly developed tracheal elements, although they do not enter the colleter gland of *D. hebecarpa*. Well developed xylem is characteristic of hydathodes, while well developed phloem testifies about the extrafloral nectaries. The existence of quite a large number of stomata on the adaxial surface of some teeth of a leaf of *Oncoba spinosa* Forssk., with smaller number of stomata in *P. trichocarpa* and *S. lasiolepis*, and a large number of the tracheal elements supplying leaf teeth, especially in *O. spinosa* and some spe-

cies of *Populus* demonstrate the hydathodic function and palisade-like cells maintain secretor function. Wilkinson also assumed that more taxa of Salicaceae and Flacourtiaceae families investigated would present a continual range from simple to more difficult structures and that the palisade-like secretory cells are common for all considered taxa.

Studying of leaf morphology of *P. deltoides* clones from all regions of the distribution area showed that the first leaves of northern clones have few basal glands per a leaf, if any, whereas the southern clones have four or more basal glands per a leaf (Marcet, 1961). Such conclusions, however, are the result of a small number of observations. It is possible that the timing for collecting the leaves was wrong. The leaves of the southern clones were unfurled earlier than the northern clones and therefore were at later stage of development already with several basal glands. The hypothesis of Marcet (1961) has to be reconsidered with these reasoning.

Thus, one of the aims of our research of the 'salicoid teeth' is the observations of the development of 'salicoid teeth' and basal glands at different ontogenetic stages of leaf development, because trichomes and gland parts of teeth can necrose or disappear early. Another objective was to investigate the distribution of trichomes on the seedling leaves and trichomes types, the morphological and anatomic structure of 'salicoid teeth' and basal glands of *P. nigra*, *P. deltoides* and *P. ×canadensis* for diagnostics, systematics and identification of their evolutionary directions.

Morphological and light and scanning electronic microscopy methods were used for the study of leaf teeth in ontogenesis, basal glands and pubescens features and trichomes types of *P. nigra* and possible hybrid *P. ×canadensis*. All plant material was obtained from Volga-Akhtubinskaya floodplain (Volgograd region), during 2018 year summer season. *Populus deltoides* was grown in the greenhouse of Russian State Agrarian University.

We studied leaves of *P. nigra* of several ontogenetic stages. The adaxial surface of a young leaf with a diameter about 1 cm has seldom smooth short acicular trichomes of 50–100 μm long and 5 μm thick and long acicular trichomes 200–300 μm long. The abaxial surface of veins, leaf basis and petiole has trichomes more often. Salicoid teeth consist of glandular roundish spherical or hemispherical and extended apical part, subapical contraction and basis. Glandular part is represented by palisade-like epidermal cells which secrete resin. The glandular part carries trichomes of different forms and lengths. Later, trichomes are reduced and therefore have not been noticed by researchers earlier. Possibly, these trichomes increase surface for transpiration and transpiration induced increasing of apoplastic solutes in palisade-like cells for resin secretion. Later the palisade-like cells are lignified and reduced. Subapical contraction is presented by the elongate cells. The basis of teeth covered with epidermal cells and one or two stomata as relictual, which is similar to *Idesia polycarpa* adaxial hydathode (Belin-Depoux, 1989). She considered that nectary and hydathode are relictual and that "the foliar glandularization is considered as more recent than hydatherous elements from phylogeneti-

cal point of view" (Belin-Depoux, 1982). Possibly, specific unspecialized type of hydathode may act as nectar in specific conditions (Curtis, Lersten, 1974). *Populus nigra* has one vascular bundle per teeth. The spiral and pitted elements of the xylem terminate in tips. Venation is eukamptodromous. The verge is between 'salicoid teeth' of the leaf. The verge is several rows of cells without chloroplasts which perform mechanical function. Some samples have basal glands or glands on the petioles, but it is not clearly, whether these are samples of *P. nigra* species or his hybrid with *P. deltoides*. It is generally accepted that no glands or nectaries are at leaf base or on the petiole of *P. nigra*.

The adaxial surface of *P. deltoides* leaves is covered with sparse smooth short acicular trichomes 50–100 μm long and 5 μm thick. The abaxial surface of veins, basis of leaf and petiole have trichomes more often. Glandular part of 'salicoid teeth' has different forms and is represented by palisade-like epidermal cells which secrete resin. The glandular part carries trichomes of different forms and length. Subapical contraction is presented by the elongate cells. The basal part of "salicoid teeth" and verge of leaf are covered by acicular trichomes. A bundle ends near the base of the tooth and includes spiral elements of xylem. Two large glands are at the leaf base or at the petiole (Ipatova et al., 2018).

The adaxial and abaxial surfaces of *P. ×canadensis* leaves are covered by sparse smooth short acicular trichomes 50–100 μm long and 5 μm thick. The veins and leaf petiole have trichomes more often. The glandular part of 'salicoid teeth' is triangular or spherical and is represented by palisade-like epidermal cells, which secrete resin. Later the palisade-like cells are lignified and reduced. A bundle ends near the base of the tooth and includes spiral elements of the xylem. The verge is between "salicoid teeth" of leaf. The border is several rows of cells without chloroplasts which perform mechanical function. Two large glands can be at the leaf base or at the petiole.

Thus, it is possible to formulate a whole range of morphological and anatomical discriminating features of the leaf: the shape of teeth in the glandular part, the number of teeth bundles, stomata density on the abaxial surface, trichome types and their distribution on the leaf.

References

Belin-Depoux M. 1982. Aspects histologiques des glandes foliares de l'*Idesia polycarpa* Maxim. (Flacourtiaceae). *Rev. Gen. Bot*. **89**: 11–120.

Belin-Depoux M. 1989. Des hydathodes aux nectaires foliares chez les plantes tropicales. *Bull. Soc. Bot. France*. **136**: 151–168.

Curtis J.D., Lersten N.R. 1974. Morphology, seasonal variation, and function of resin glands on buds and leaves of *Populus deltoides* (Salicaceae). *Am. J. Bot*. **61**: 835–845.

Edelstein W. 1902. Zur Kenntnis der Hydathoden an den Blättern der Holzgewächse. *Bull. Acad. Imper. Sci. St. Petersbourg*. **17**: 59–64.

Fehér D. 1923. Über die Abscheidung von Harzbalsam auf den jungen Trieben unserer einheimischen *Populus*-Arten. *Beih. Bot. Centralbl*. **39**: 81–103.

Hanstein J. 1868. Über die Organe der Harz- und Schleim-Absonderung in der Laubknospen. *Bot. Zeit*. **26**: 697–713, 721–736, 745–761, 769–787.

Hickey L.J., Wolfe J.A. 1975. The bases of angiosperm phylogeny: vegetative morphology. *Ann. Mo. Bot. Gard*. **62**: 538–589.

Ipatova D.A. 2018. *Design of species-specific DNA marker based on non-transcribed spacer (NTS) of 5S ribosomal nuclear DNA of* Populus nigra *L. (Salicaceae Mirb.) and its use for systematics and phylogenetics*. Degree Thesis in Biology, Bachelor's Level / Supervisors: Feodorova T.A., Alexandrov O.S. Moscow.

Lippman N.E. 1925. Ueber das Vorkommen der verschiedenen Arten der Guttation und einige physiologische und ökologische Beziehungen. *Bot. Arch.* **11**: 361–464.

Ma J., He X., Bai X., Niu Z., Duan B., Chen N., Shao X., Wan D. 2016. Genome-wide survey reveals transcriptional differences underlying the contrasting trichome phenotypes of two sister desert poplars. *Genes* **7**: 1–17.

Marcet E. 1961. Über die geographische Variabilitait blatt-morphologischer Merkmale bei *Populus deltoides* Bartr. *Silvae Genet*. **10**: 161–177.

Nandi O.I., Chase M.W., Endress P.K. 1998. A combined cladistic analysis of angiosperms using *rbc*L and non-molecular data sets. *Ann. Mo. Bot. Gard*. **85**: 137–212.

Pemberton R.W. 1992. Fossil extrafloral nectaries, evidence for the ant-guard antiherbivore defence in an Oligocene *Populus*. *Am. J. Bot*. **79**: 1242–1246.

Reinke J. 1876. Beiräge zur Anatomie der an Laubblättern, besonders an den Zähnen derselbem vorkommenden Secretions-organe. *Jahrb. Wiss. Bot*. **10**: 119–178.

Trelease W. 1881. The foliar nectar glands of *Populus*. *Bot. Gaz*. **6**: 284–290.

Wilkinson H.P. 2007. Leaf teeth in certain Salicaceae and 'Flacourtiaceae'. *Bot. J. Linn. Soc*. **155**: 241–256.

Wilson T.P., Canny M.J., McCully M.E. 1991. Leaf teeth, transpiration and the retrieval of apoplastic solutes in balsam poplar. *Physiol. Plant*. **83**: 225–232.

MALE FLOWER ANATOMY IN DITHECAL RESTIIDS (POALES): STRUCTURE AND COMPARISON WITH MONOTHECAL SPECIES OF RESTIONACEAE

Constantin I. FOMICHEV [1], ***Barbara G. BRIGGS*** [2], ***Terry D. MACFARLANE*** [3], ***Dmitry D. SOKOLOFF*** [1]

[1] Lomonosov Moscow State University, Moscow, Russia
[2] National Herbarium of New South Wales, Sydney, Australia
[3] Western Australian Herbarium, Perth, Australia

constantin.fomichev@gmail.com

One of the pollination modes among families in the order Poales is wind-pollination. It is common for such widespread groups as Poaceae, Cyperaceae and Typhaceae as well as for the members of the restiid clade (Restionaceae *sensu* APG IV) occurring mostly in Australia and South Africa. Hieronymus (1889) recognized

two groups of Restionaceae: Diplantherae and Haplantherae according to the occurrence of dithecal tetrasporangiate versus monothecal bisporangiate anthers. According to molecular phylogenetic data (Briggs et al., 2010, 2014), the restiid clade consists of two well-supported subclades, one comprising genera with dithecal anthers (Anarthriaceae *sensu* Briggs et al., 2014) and the other those with monothecal anthers (Restionaceae *sensu* Briggs et al., 2014). The group with dithecal anthers includes three species-poor genera restricted to SW Western Australia, *Anarthria*, *Lyginia* and *Hopkinsia*, whereas the monothecal group holds the vast majority of restiid species and genera. All shared non-molecular features of the dithecal clade are either symplesiomorphies (like the anther structure) or belong to characters that are quite homoplastic in Poales. According to molecular phylogenetic data, *Hopkinsia* and *Lyginia* are well-supported as a clade sister to *Anarthria* (Briggs et al., 2010, 2014). A detailed study of female flowers of dithecal restiids revealed that *Hopkinsia* and *Lyginia* possess ovules with length not exceeding the width and the micropyle oriented towards the dorsal side of the carpel, which is probably a synapomorphy, however, no potential synapomorphy of the whole dithecal clade was found (Fomichev et al., 2019). On the other hand, it is still possible that some apomorphic features shared by *Anarthria*, *Lyginia* and *Hopkinsia* could be among characters of the male flowers, which have been poorly studied as yet.

In dithecal restiids, the androecium is represented by three stamens located on the radii of the inner tepals; in other words, the outer whorl stamens are missing, which is consistent with the data on the monothecal Restionaceae (Eichler, 1875; Hieronymus, 1889; Dahlgren et al., 1985; Kircher, 1986; Linder et al., 1998). According to the literature (Dahlgren et al., 1985; Linder et al., 1998; Ronse De Craene et al., 2002), there is a pistillode in male flowers of monothecal Restionaceae. We studied in detail flowers of *Eurychorda complanata* as a representative of monothecal Restionaceae. *Eurychorda*, a montypic genus with dimerous flowers, is the basal branch of subfamily Leptocarpoideae in phylograms based on molecular data (Briggs et al., 2014). According to our data, male and female flowers develop in the same way up to the stage of thecal differentiation in the stamens and the formation of the asymplicate zone of the gynoecium (which appears developmentally after the symplicate and synascidiate zones). The gynoecium development stops at this stage in the male flower, and the pistillode is represented by two fused carpels, a pronounced floral center and rudiments of the ovules. In the center of the male flowers of *Anarthria*, there is a small undifferentiated bulge, which is interpreted here as a rudiment of the gynoecium. The pistillode is absent in the flowers of *Lyginia*, where the filaments are fused into a column. We found no signs of postgenital fusion at any developmental stages in male flower of *Lyginia*, which means that the column is formed as a result of congenital fusion. The fusion of stamens with each other to form a central column is possible only in unisexual flowers without rudiments of the gynoecium (Endress, 1994), which is the case in *Lyginia*. According to our data, there are also no signs

of a gynoecium in the male flowers of *Hopkinsia*. The absence of a pistillode is documented in the male flowers of *Aphelia* (centrolepid clade of the monothecal restiids), but the centrolepid clade is characterized by a complete reorganization of the flower groundplan (Sokoloff et al., 2009, 2015).

All three genera of dithecal restiids are characterized by a principally similar pattern of male flower vascularization. The pedicel is vascularized by three bundles located on the radii of the outer tepals. Each bundle undergoes a trifurcation producing two lateral bundles spreading tangentially and a median bundle strongly deflecting in the radial direction to supply an outer whorl tepal. The lateral bundles unite on the radii of the inner whorl tepals, then in each case produce radially a branch supplying the inner tepal, split once again tangentially and finally unite in the radii of the inner tepals to produce stamen bundles. The pattern of tepal vascularization is similar in male and female flowers of the same species, except for *Lyginia* where the tepals of the female flowers possess several vascular bundles (Fomichev et al., 2019). The vascular system of the column of *Lyginia* is formed by three bundles located on the radii of the inner tepals, in the same way as the androecium vasculature is arranged in the two genera of dithecal Restionaceae with free filaments (*Anarthria* and *Hopkinsia*). The pistillode in the male flower of *Anarthria* is unvascularized. In dimerous flower of *Eurychorda* two bundles located in the radii of the outer tepals supply the reduced gynoecium.

The anther wall of all studied genera of dithecal Restionaceae consists of four layers (i.e., the epidermis, the endothecium differentiated as a fibrous layer, the middle layer and the tapetum), which is consistent with the data on the histology of the anther wall in monothecal Restionaceae (Naumova, 1990). As in many monothecal Restionaceae, tannins are deposited in the protoplasts of the cells of the anther epidermis. This is more pronounced in *Lyginia*. This genus is also characterized by more abundant deposits of tannins in the tepals than in other studied members of Restionaceae.

Dahlgren & Clifford (1982) noted the spiral type of the endothecial thickenings in *Hypolaena* and the girdle type in *Anarthria*. Manning & Linder (1990) examined the characteristics of thickening in the anther wall in nine families of Poales including monothecal Restionaceae and three dithecal genera. According to their data, the basic condition of the endothecial thickening in monothecal Restionaceae is a helix, only *Leptocarpus canus* possesses U-shaped thickenings. In *Hopkinsia*, a simple helix becomes doubled, whereas *Anarthria* and *Lyginia* are characterized by annular and pseudoannular types (which correspond the girdle type mentioned above), although the basic condition is helical in these two genera (Manning, Linder, 1990). The same types are also shared within Poales with the centrolepid clade and some grasses (*Arundinaria*, *Bambusa*, *Leersia*, *Olyra*).

Our data show characteristic spiral thickenings of the endothecium in all three genera of Restionaceae with two thecae. The middle layer is obliterated in the early stages of development of pollen grains apparently in all studied dithecal

restiids. Tapetum of all studied genera of dithecal restiids is formed by large cells, rectangular in cross-section, which begin to degrade at the later stages of pollen grains development. Probably *Anarthria*, *Lyginia* and *Hopkinsia* possess a secretory tapetum, which is consistent with data of other authors for Restionaceae with one theca (Kircher, 1986; Naumova, 1990).

Our data, in general, indicate a stable state of the anther wall characters among all Restionaceae, and a fundamentally similar arrangement of the vascular system in male flowers of *Anarthria*, *Lyginia* and *Hopkinsia*. Differences in vasculature between studied genera of monothecal Restionaceae and *Eurychorda* are mainly associated with the differences in flower merism. Pistillode absence in male flowers of *Hopkinsia* and *Lyginia* can be considered as a potential synapomorphy, however, Kircher (1986) mentioned the presence of a strongly reduced gynoecium in the male flowers of *Apodasmia similis* (Edgar) B.G. Briggs et L.A.S. Johnson (monothecal clade of Restionaceae) and there are still no data for many other monothecal Restionaceae, so it is still possible that the character is homoplastic among restiids. In general, with much increased level of knowledge, there seems to be a very poor non-molecular support for the clade of dithecal restiids.

The work of CIF and DDS is supported by Russian Science Foundation (project No. 14-14-00250).

References

Briggs B.G., Marchant A.D., Perkins A.J. 2010. Phylogeny and features in Restionaceae, Centrolepidaceae and Anarthriaceae (restiid clade of Poales). In: Seberg O., Petersen G., Barfod A.S., Davis J.I. (eds.): *Diversity, phylogeny and evolution in the monocotyledons*. Aarhus: Aarhus Univ. Press. P. 357–388.

Briggs B.G., Marchant A.D., Perkins A.J. 2014. Phylogeny of the restiid clade (Poales) and implications for the classification of Anarthriaceae, Centrolepidaceae and Australian Restionaceae. *Taxon* **63**: 24–46.

Dahlgren R.M.T., Clifford H.T. 1982. *The monocotyledons. A comparative study*. London: Academic Press.

Dahlgren R.M.T., Clifford H.T., Yeo P.F. 1985. *The families of the monocotyledons*. Berlin: Springer.

Eichler A.W. 1875. *Blütendiagramme*. T. **1**. Leipzig: W. Engelmann.

Endress P.K. 1994. *Diversity and evolutionary biology of tropical flowers*. Cambridge: Cambridge Univ. Press.

Fomichev C.I., Briggs B.G., Macfarlane T.D., Sokoloff D.D. 2019. Structure and development of female flowers in early-diverging restiids, *Anarthria*, *Lyginia* and *Hopkinsia* (Restionaceae s.l.): further evidence of multiple pathways of gynoecium reduction in wind-pollinated lineages of Poales. *Bot. J. Linn.* Soc. **190**: 117–150.

Hieronymus G. 1889. Restionaceae. In: Engler A., Prantl K. (Hrsg.): *Die natürlichen Pflanzenfamilien*. Leipzig: Engelmann. Bd. **2**A. Abt. 4. S. 3–10.

Kircher P. 1986. Untersuchungen zur Blüten- und Infloreszenzmorphologie, Embryologie und Systematik der Restionaceen im Vergleich mit Gramineen und verwandten Familien. *Diss. Bot.* **94**: 1–219.

Linder H.P., Briggs B.G., Johnson L.A.S. 1998. Restionaceae. In: Kubitzki K. (ed.): *The families and genera of vascular plants*. Berlin: Springer. V. **3**. P. 425–445.

Manning J.C., Linder H.P. 1990. Cladistic analysis of patterns of endothecial thickenings in the Poales/Restionales. *Am. J. Bot.* **77**: 196–210.

Naumova T.N. 1990. The family Restionaceae. In: Batygina T.B., Yakovlev M.S. (eds.): *Comparative embryology of flowering plants. Monocotyledons. Butomaceae–Lemnaceae*. Leningrad: Nauka. P. 210–212. [in Russian].

Ronse De Craene L.P., Linder H.P., Smets E.F. 2002. Ontogeny and evolution of the flowers of South African Restionaceae with special emphasis on the gynoecium. *Plant Syst. Evol*. **231**: 225–258.

Sokoloff D.D., Remizova M.V., Linder H.P., Rudall P.J. 2009. Morphology and development of the gynoecium in Centrolepidaceae: The most remarkable range of variation in Poales. *Am. J. Bot.* **96**: 1925–1940.

Sokoloff D.D., Remizowa M.V., Barrett M.D., Conran J.G., Rudall P.J. 2015. Morphological diversity and evolution of Centrolepidaceae (Poales), a species-poor clade with diverse body plans and developmental patterns. *Am. J. Bot.* **102**: 1–31.

FRUIT ANATOMY IN THE CORE *ELATOSTEMA* CLADE OF *ELATOSTEMA* (URTICACEAE) AND ITS TAXONOMIC SIGNIFICANCE FOR A NEW CLASSIFICATION

***Long-Fei FU*[1], *Alexandra K. MONRO*[2], *Fang WEN*[1], *Zi-Bing XIN*[1], *Yi-Gang WEI*[1]**

[1] Guangxi Institute of Botany of Guangxi Zhuang Autonomous Region and Chinese Academy of Sciences, Guilin, China
[2] Royal Botanic Gardens, Kew, Great Britain
longfeifu@126.com

Elatostema J.R. Forst. et G. Forst. is one of the largest genera in Urticaceae, which consists of ca. 500 species. Recent research on delimitation *Elatostema* s.l. and closely related genera recovered a monophyletic *Elatostema sensu auct.* that included *Pellionia* but excluded *Elatostematoides* and *Procris*. Within this delimitation, *Elatostema* comprises four well-supported clades: core *Elatostema*, *Pellionia*, *Weddellia* and African *Elatostema*, for which morphological characters were also evaluated. The robust molecular phylogeny did not match the morphological evidence within each clade, especially the most species-rich clade, i.e., core *Elatostema*. We examined fruit (achene) micromorphology to seek additional morphological characters and evidence to evaluate the relationships among species within the core *Elatostema* clade. Phylogenetic analyses of core *Elatostema* clade and outgroups were performed using Bayesian inference (BI) and maximum likelihood (ML) based on the combined dataset of ITS, *psb*A-*trn*H and *psb*M-*trn*D. We also examined achene micromorphology of 50 species of core *Elatostema* clade by scanning electron microscopy (SEM). The phylogenetic tree showed that karst and

non-karst species divided into two strongly supported clades. We found length-width ratio of achene and achene length to be significant characters to distinguish the karst and non-karst clades. Achene colour (brown, white, black, and purple) and surface (smooth, ribbed, tuberculate, puncticulate, and winged) provided characters useful for distinguishing species. However, these characters have little systematic significance because of multiple occurrences in each clade (i.e., high level of homoplasy). Therefore, a new classification of core *Elatostema* clade is proposed and supported mainly by the characters of length-width ratio of achene and achene length.

SYSTEMATIC VALUE OF THE ANATOMY OF THE FERTILE PINNAE IN THE FERN FAMILY BLECHNACEAE (POLYPODIOPSIDA): CRITICISM OF SOME CRITICAL CHARACTERS

***Jose María GABRIEL y GALÁN*, Maria VICENT, Carmen PRADA, Sonia MOLINO, Rubén VÁZQUEZ, Andrea SERAL**

Universidad Complutense de Madrid, Madrid, Spain
jmgabrie@ucm.es

Blechnaceae is an important leptosporangiate fern family, with about 250 species in 25 genera. An important number of species have dimorphic fronds, i.e. present a highly differentiated morphology between sterile leaves (trophophylls) and fertile leaves (sporophylls): the sterile pinnae are much wider than fertile pinnae, which are heavily contracted, without green tissue when adult. The rest of species and genera are monomorphic, with all the leaves built as trophosporophylls, or subdimorphic, with slight differentiation between trophophylls and sporophylls. Besides that, the typical blechnoid fern is constantly described in floras and taxonomic treatments as having costal cenosori (some genera have discrete sori, as *Woodwardia* or *Doodia*), and protected by indusia (a flat, membranous, one-cell thick outgrowth) that open toward the costa (*Stenochlaena* is exindusiate).

In the context of a systematic review of the family Blechnaceae, focusing primarily on the generic level, we decided to incorporate information on anatomical traits, due to the following reasons: first, anatomy has shown a high taxonomic potential in other groups of plants; second, we noticed that some old anatomists contributed intriguing observations about the fertile structures of ferns, that has been overlooked by posterior pteridologists. The aim of this work is to present the results of an anatomical survey of the fertile pinnae of the Blechnaceae genera. Our results lead us to question some of the basic assumptions about the organization of the fertile pinnae in the Blechnaceae.

First: we detected that most of the dimorphic genera (for example, the species-rich *Parablechnum*, *Lomariocycas* and *Lomaridium*) present an indusial structure that is completely different from a typical indusium. This is what we call 'complex indusium', which consists on 'lamina'-like structures with complex anatomy, protruding from flat, contracted pinnae. The position of the margin with respect to the vascular bundles is specific. The anatomy of these structures constantly shows cell differentiation between adaxial and abaxial surfaces, and stomata have been detected in some species. In some cases in which the 'indusium' is heavily enrolled (*Spicantopsis*, *Salpichlaena*) there is also a cell differentiation from base to apex, fact which could be related to the curvature and break to liberate the spores.

Second: in *Austroblechnum*, one of the largest genera in the family, the fertile fronds have strongly revolved pinnae, whose margins are very much displaced with respect to the costa. These pinnae can bear a laminar, typical indusium but small, vestigial and non-functional, so with little or none contribution to the protective function. All this fits, in our opinion, in what pteridologists call pseudoindusium, which has never been documented in this family.

Third: we registered the presence of extended receptacles in several genera (*Parablechnum, Cranfillia, Lomaridium, Lomaria, Austroblechnum*). Sometimes, the sporangia appear even isolated from the abaxial epidermis without clear association to veins. In addition, we have detected undoubtedly diplodesmic veins in some genera (*Cranfillia*). As these two traits (sporangia isolated and diplodesmic venation) are typical of acrostichoid ferns, the presence of acrostichoid species in the Blechnaceae should be fully accepted.

In conclusion, we report here for the Blechnaceae three organizational patterns (complex indusial structures, pseudoindusia and acrostichoid sporangia), based on anatomical observations, which are unknown or have been overlooked and neglected by recent pteridology. We therefore conclude that there is need to carefully look to anatomical characters to properly re-define the Blechnaceae.

STRUCTURE AND DEVELPOMENT OF WINGED STEM IN *GREWIA CAFFRA* (MALVACEAE): A NEW TYPE OF CAMBIAL VARIANT WITHIN THE PLANT ORDER MALVALES

Gugu GAMA*, *Alexei OSKOLSKI

University of Johannesburg, Johannesburg, South Africa
gugumbalenhlegamar@gmail.com

Grewia L. is a genus of plant family Malvaceae comprising about 300 species which are widely distributed in Africa, Asia and Australia (Bayer, Kubitzki, 2003),

with 24 species in South Africa (Plants of southern Africa: an online checklist, 2003). All *Grewia* species have alternate leaves in distichous phyllotaxis. Most species of this genus are shrubs and small trees, but at least two species (*G. caffra* Meisn. and *G. flavescens* Juss.) are climbers having the stems with four prominent wings (Kuntze, 1891; Kotina et al., 2017). We studied the structure of juvenile and mature stems of *G. caffra* to clarify the anatomical background of the wing formation. Young stems of this species have no wings showing the suite of anatomical traits which is characteristic of Malvaceae (including abundant mucilage cavities in bark). On later stage, the cambial activity ceases in four zones along the stem: two zones of cessation are located along two orthostichies, and other two zones are at the right angle to them. Between these zones, the cambium continues to produce both secondary phloem and wood. As a result, four wings are formed at the angle 45° to the plane of orthostichies. Thus, the stem of *G. caffra* shows cambial variant with irregular activity of single cambium. Similar cambial variants have been reported in climbing species belonging to several plant families, but none of them shows the zones of normal bifacial cambial activity with the zones of its cessation. This condition may be considered as a new type of cambial variants. This is the first report of the cambial variant for the plant of the order Malvales.

References

Bayer C., Kubitzki K. 2003. Malvaceae. In: Kubitzki K. (ed.): *The families and genera of vascular plants*. Berlin: Springer. V. **5**. P. 225–311.

Kotina E.L., Oskolski A.A., Tilney P.M., Van Wyk B.-E. 2017. Bark anatomy of *Adansonia digitata* (Malvaceae). *Adansonia*. Sér. 3. **39**: 31–40.

Kuntze G. 1891. Beiträge zur vergleichenden Anatomie der Malvaceen. *Bot. Centralbl.* **45**: 161–32.

Plants of Southern Africa: an online checklist (2003–onwards). http://posa.sanbi.org/searchspp.

MULTILOCATION VARIATION OF FIBER LENGTH IN TISSUE CULTURE RAISED PLANTATION WOOD *POPULUS DELTOIDES* BATR. EX MARSH, CLONE L-34

***Pallavi GAUTAM*, P.K. PANDE**

Forest Research Institute, Dehradun, India

pallavi.gautam82@gmail.com

The experiment was conducted to study multilocation variation of fiber length in tissue culture raised plantation wood *Populus deltoides* of clone L-34 selected from three different locations. Five ramets from each location were selected randomly to cover the multilocation variations of fiber length. ANOVA showed that

multilocation variations were significant for fiber length. Vertical and radial variations for height were significant for fiber length, whereas directional variations in different ramets were non-significant. Significant multilocation variations indicate that environment may have impact on the dimensions of wood elements.

ANATOMICAL TRAITS OF *AMPHORICARPOS NEUMAYERIANUS* – ENDEMIC AND RELICT SPECIES OF COMPOSITAE

***Milan GAVRILOVIĆ*[1], *Dragana RANČIĆ*[1], *Núria GARCIA-JACAS*[2], *Alfonso SUSANNA*[2], *Zora DAJIĆ-STEVANOVIĆ*[1], *Petar D. MARIN*[1], *Pedja JANAČKOVIĆ*[1]**

[1] University of Belgrade, Belgrade, Serbia
[2] Botanic Institute of Barcelona, Barcelona, Spain
mgavrilovic@bio.bg.ac.rs

The genus *Amphoricarpos* comprises heterocarpic perennial mountain chasmophytic plants from the eastern Mediterranean (the Balkans, Anatolia and the Caucasus) of complex taxonomy (Susanna, Garcia-Jacas, 2009). There are three taxa distributed on the Balkan Peninsula: *A. neumayerianus* (Vis.) Greuter, *A. autariatus* Blečić et Mayer ssp. *autariatus* Blečić et Mayer and *A. autariatus* Blečić et Mayer ssp. *bertisceus* Blečić et Mayer (Blečić, Mayer, 1967; Greuter, 2003). Some authors have suggested that all Balkan *Amphoricarpos* should be treated as a single species, *A. neumayerianus* (Caković et al., 2015). In this work, anatomical investigations of vegetative organs of *A. neumayerianus* s. str., a Tertiary relict from Mt. Orjen (Montenegro), endemic for the Dinaric Alps, were conducted. The aim of this study was to investigate anatomy and to find possible new valid taxonomic characters. Microscopic slides were prepared following the standard histological procedures (Ruzin, 1999). In young root cross section, tetrarch radial vascular bundle is observed, while typical secondary tissues occur in the older root cross-section with well developed exodermis on its surface. In the rhizome cross section, the secondary tissues are noticed, with well developed periderm on its surface and parenchyma cortex below. In the central cylinder, a well developed xylem is noticed, which is interrupted by wide parenchyma rays. The pith, composed of very large parenchyma cells, is found in the central region. The upper stem cross section is characterized by more or less polygonal outline with one-layered epidermis, and by a well developed cortex of one cell thick layers of collenchyma and parenchyma, below. Medullary collateral vascular bundles are arranged in a circle, while a few cortical vascular bundles are also noticed. The leaf blade is amphis-

tomatous, dorsiventral. One vascular bundle, or one large and two small vascular bundles are in the heart-shaped main vein, with a surrounding parenchyma sheath which extended to both epidermises. Densely distributed, curly, non-glandular trichomes as well as biseriate glandular trichomes are present on the upper stem, as well as on both leaf sides, but much more so on the abaxial one. Observations examined here could be useful in resolving relationships of *A. neumayerianus* and close related taxa within the *Amphoricarpos* – a small but very complex genus from taxonomic and phylogenetic points of view.

References

Blečić V., Mayer E. 1967. Die europäischen Sippen der Gattung *Amphoricarpos* Visiani. *Phyton* **12**: 150–8.

Caković D., Stešević D., Schönswetter P., Frajman B. 2015. How many taxa? Spatiotemporal evolution and taxonomy of *Amphoricarpos* (Asteraceae, Carduoideae) on the Balkan Peninsula. *Org. Divers. Evol*. **15**: 429–45.

Greuter W. 2003. The Euro+Med treatment of Cardueae (Compositae): generic concepts and required new names. *Willdenowia* **33**: 49–61.

Ruzin S.E. 1999. *Plant microtechnique and microscopy*. Oxford; New York: Oxford Univ. Press.

Susanna A., Garcia-Jacas N. 2009. Cardueae (Carduoideae). In: Funk V.A., Susanna A., Stuessy T.F., Bayer R.J. (eds.): *Systematics, evolution and biogeography of Compositae*. Vienna: IAPT. P. 293–313.

3D RECONSTRUCTION OF SCLERENCHYMA ARRANGEMENT IN LEAF BLADES OF *FESTUCA VALESIACA* GAUD. AND *FESTUCA BECKERI* (HACK.) TRAUTV., GRAMINEAE JUSS.

Eugeniya V. GOREMYKINA*, *Anastasiya A. RYABYSHEVA

Volgograd State University, Volgograd, Russia
goremykina.eugenia@gmail.com

Leaf-blade anatomical characteristics are considered important traits for identifying grasses. Traditionally, cross sections in the middle part of a leaf blade have been used for such purposes (Ellis, 1976; Alexeev, 1980; Dube, Morisset, 1987; Stace et al., 1992; Ramesar-Fortner et al., 1995; Hosseini et al., 2013; Leandro et al., 2016; Martínez-Sagarra et al., 2017), but there is still a lack of knowledge regarding the spatial distribution of tissue throughout the leaf blade. At the present time, it is not clear whether the anatomical structure is the same in different cross sections of the leaf blade. If the middle of the leaf blade cannot be determined

(e.g. when analysing leaf fragments), the information gathered from the middle part of the leaf blade may turn out to be useless. Analysis of the spatial distribution of tissues along the entire leaf blade enables to comprehend data obtained from the two-dimensional cross section at the middle of the blade.

This study was undertaken to reveal the three-dimensional arrangement of tissues, mainly sclerenchyma, inside the entire leaf blades of the narrow-leaved fescues *Festuca valesiaca* Gaud. and *Festuca beckeri* (Hack.) Trautv. Taxonomic treatments and identifications of narrow-leaved fescues are difficult due to visual similarity between species (Hosseini et al., 2013; Martínez-Sagarra et al., 2017). Anatomical features are important for their classification and recognition (Alexeev, 1980). The arrangement of the sclerenchyma in the middle part of the leaf blade is considered to be the most useful feature (Martínez-Sagarra et al., 2017), however, it is known to vary in some fescues (Dube, Morisset, 1987; Stace et al., 1992; Ramesar-Fortner et al., 1995). Our work was aimed to construct 3D models of sclerenchyma from serial sections of the leaf blades. We also attempted to find out the quantitative patterns of the distribution of sclerenchyma through the leaf blade length in *F. beckeri* and *F. valesiaca*.

The material was collected in 2013–2014 in the steppe plant communities of the Volgograd region. The tillers were fixed in 95% ethanol. Three leaf blades were taken from each of five plant samples in both species. Before sectioning, the long leaf blades of *F. beckeri* were divided into 10 equal parts from the blade/sheath junction to the tip, the shorter leaf blades of *F. valesiaca* were divided into 5 equal parts. The free-hand cross sections were made at the boundaries of the marked parts, the distance between adjacent sections was 2–3 cm in both fescues. Photographs were taken with a ToupCam 9.0 MP digital camera and Mikmed-5 light microscope. Based on the resulting photos, schemes were designed and measurements were performed and statistically processed in Photoshop CC and STATISTICA10, respectively. 3D models of the sclerenchyma were made in Blender 2.79.

At the level of the blade/sheath junction the leaf blades of both species are folded, smooth on the abaxial surface, ribbed on the adaxial surface. Lignified sclerenchyma is commonly distributed under the lower epidermis and at the edges of the leaf blades. Vascular bundles are surrounded by lignified sheaths. At the lowest sections, the two fescues mainly differ in the number of vascular bundles (9–13 in *F. beckeri* and 5 in *F. valesiaca*) and in the outline of the sclerenchyma masses. The sclerenchyma of *F. beckeri* is arranged in a continuous layer. The layer is slightly thickened under the midrib and in the margins of the blade. The sclerenchyma of *F. valesiaca* is arranged in three thick strands (two in the margins and one under the midrib) connected with thin layers of fibers. The thin layers are continuous or have a few small gaps.

The number of vascular bundles of *F. valesiaca* is constant along the majority of the following sections but may decrease to 3–4 at the last section. The number of vascular bundles of *F. beckeri* decreases at the sections in the upper

half of the leaf blade and reduces to 6–9 in the last section. The arrangement of sclerenchyma varies along the leaf blades, quantitative changes is similar in both fescues. The mean cross-sectional areas of sclerenchyma increase from 62 962 μm^2 to 94 066 μm^2 in *F. beckeri* and from 49 077 μm^2 to 65 477 μm^2 in *F. valesiaca* between the first (the lowest) and the second sections. Significant differences between the mean values are confirmed by t-test at p-value << 0.05 in both species. The areas of sclerenchyma gradually decrease in successive sections to 23 682 μm^2 in *F. beckeri* and to 4816 μm^2 in *F. valesiaca* at the tips of the blades. Negative correlations between the areas of sclerenchyma and the distance from the basal parts of blades are confirmed by the Spearman's rank correlation test: the correlation coefficients are -0.9 (*F. valesiaca*) and -0.8 (*F. beckeri)* at p-value < 0.05 for both species above the second level of section.

The changes in the amount of sclerenchyma along the leaf blade differently affect the outlines of sections of this tissue in the species. Almost a uniform layer of the subepidermal sclerenchyma of *F. beckeri* becomes slightly thicker in the basal part and gets thinner in the remaining part of the blade, but the outline of the tissue does not change significantly over the length of the blade. There are no noticeable changes in the pattern of the sclerenchyma in cross sections a few centimeters up or down from the central part of leaf blade (Fig. A–C).

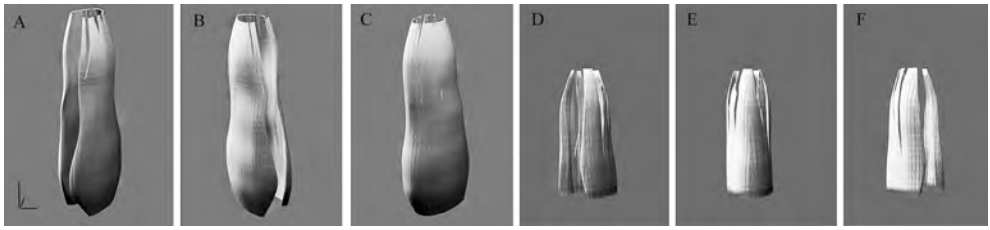

Figure. 3D reconstruction of sclerenchyma in the leaf blades of *F. beckeri* (A–C) and *F. valesiaca* (D–F). Image heights reduced 100 times than their widths to fit the figure frame.
Vertical scale bar – 20 mm, horizontal scale bar – 0.1 mm.

The uneven sclerenchyma layer of *F. valesiaca* changes its shape with changing amount of mechanical tissue. Increasing of this tissue is often accompanied either by gap closure or by gap appearance in the thin bands of fibers connecting massive strands of fibers, but there are sometimes no noticeable changes in the sclerenchyma layer. Decreasing of the mechanical tissue results in the appearance and widening of new breaks in the thin bands, whilst the former continuous uneven layer gradually splits into separate strands. Accordingly, the sclerenchyma arrangements can vary greatly in leaf cross sections that are a few centimeters apart in both directions from the middle part of the leaf blade (Fig. D–C).

Variability of the sclerenchyma arrangements along the leaf blade should be considered when using 2D sections of the leaf for plant diagnostics.

References

Alexeev E.B. 1980. *Ovsyanitsy Kavkaza (Caucasian Fescus).* Moscow: Moscow Univ. Press. [In Russian]

Dube M., Morisset P. 1987. Morphological and leaf anatomical variation in *Festuca rubra* sensu lato (Poaceae) from eastern Quebec. *Can. J. Bot.* **65**: 1065–1077.

Ellis R.P. 1976. A procedure for standardizing comparative leaf blade anatomy in the Poaceae. I. The leaf blade as viewed in transverse section. *Bothalia* **12**: 65–109.

Hosseini S.Z., Rahiminejad M.R., Saeidi H. 2013. Leaf anatomical structure of Iranian narrow-leaved species of the genus *Festuca* L. (Poaceae, Poeae). *Iran. J. Bot.* **10**: 86–93.

Leandro T.D., Shirasuna R.T., Filgueiras T.S., Scatena V.L. 2016. The utility of Bambusoideae (Poaceae, Poales) leaf blade anatomy for identification and systematics. *Braz. J. Biol.* **76**: 708–717.

Martínez-Sagarra G., Abad P., Devesa J. 2017. Study of the leaf anatomy in cross-section in the Iberian species of *Festuca* L. (Poaceae) and its systematic significance. *PhytoKeys* **83**: 43–74.

Ramesar-Fortner N.S., Aiken S.G., Dengler N.G. 1995. Phenotypic plasticity in leaves of four species of arctic *Festuca* (Poaceae). *Can. J. Bot.* **73**: 1810–1823.

Stace C.A., Al-Bermani A.K.K.A., Wilkinson M.J. 1992. The distinction between the *Festuca ovina* L. and *Festuca rubra* L. aggregates in the British Isles. *Watsonia* **19**: 107–112.

PRELIMINARY DATA ON STOMATAL DENSITY DISTRIBUTION IN LEAVES OF *GINKGO BILOBA* L.

***Elizaveta M. GUNKO*[1], *Eugeny V. KARASEV*[2], *Maja V. NILOVA*[1]**

[1] Lomonosov Moscow State University, Moscow, Russia

[2] Kazan Federal University, Kazan, Russia

lizaveta_gunko@mail.ru

The relationship of atmospheric CO_2 concentration with leaf stomatal density and stomatal index is repeatedly revealed on experiments with recent plants and analysis of fossil data (Beerling et al., 1998; Chen et al., 2001; Royer, 2001, 2003; Sun et al., 2018). However, fossil samples are often fragmentary. In this regard, it is very important to understand the possible limits of variation of stomatal density and stomatal index throughout the leaf surface. *Ginkgo biloba* is a model object for identifying these patterns in modern and fossil material (Retallack, 2001; Quan et al., 2009; Barclay, Wing, 2016). The aim of this investigation is to quantify changes in stomatal density (SD) on the surface of the *G. biloba* leaf.

The leaves of *G. biloba* were collected in the greenhouse of the Tsitsin Main Botanical Garden RAS and herbarized. The epidermis was sampled from the entire abaxial surface of the lamina (Fig. 1a), as *G. biloba* leaf is hypostomatous. The leaf margin was cut off on the width of 0.2 mm for easier separation

of epidermis after maceration. Leaf was macerated in the 5% alkali solution at 70–80 °C for 7–10 minutes, thoroughly purified from alkali to separate the entire abaxial epidermis thereafter. The epidermal plates were stained with 2% aqueous Safranin and embedded in glycerin-gelatin. A transparent film with a printed coordinate grid was used instead of a cover glass to obtain the coordinates of the field of observation. Stomata were counted under Nikon Eclipse Ci microscope and photographed with Nikon DS-Vi1 camera. The coordinate grid used to measure was created in the program Inkscape (https://inkscape.org). Our method of measuring stomatal density over the entire leaf area using a transparent grid can be used for any leaves with a flat leaf blade. We made a stomata distribution map and calculated the main statistics for different parts of the lamina. Such stomatal density maps have been constructed for a number of angiosperms (Poole et al., 1996, 2000; Weyers, Lawson, 1997; Lawson et al., 2002). All data analysis and plotting were performed with RStudio data analysis software (RStudio Team, 2015).

The area of the studied leaf was about 2100 mm^2. The measurements were taken from 247 fields of observation. The area of one field of observation for the calculation of stomata was 1 mm^2.

The stomatal density (SD) over the entire surface of the leaf varies from 26 to 55 per 1 mm^2, the average is 41.2 ± 5.7 per 1 mm^2. These values of SD are less than SD of the leaves obtained from other regions. For example, SD of the *Ginkgo biloba* leaves from China varies between 75–95 per 1 mm^2 (Sun et al., 2003). We believe that the lower SD values are related to the shade conditions or other growing conditions.

The coefficient of SD variation over the entire surface of the leaf is 13.8%. We calculated the area of the same SD values using the constructed map of stomata distribution. As a result, SD from 35 to 40 per 1 mm^2 occupies almost 80% of the lamina area, SD about 45 per 1 mm^2 takes about 10% of the area and SD less than 30 per 1 mm^2 and more than 50 per 1 mm^2 takes remaining 10% of the lamina area.

We distinguished the basal (lower), middle and upper parts of the lamina (fig. 1A). The SD average values are 41.4 ± 4.7, 40.3 ± 8.6, 40.3 ± 4.8 in the lower, middle and upper parts, respectively. The SD variation coefficient is 10–11% in the upper and middle parts and 20% in the lower part. The greater SD variability in the lower part is probably related to the greater thickness of the veins at the base of the leaf. On the contrary, the stomatal density is shown to increase generally from the leaf base to its tip in angiosperms (Salisbury, 1928; Zacchini et al., 1997; Royer, 2001).

The results of SD measurements in different parts of the leaf show that there are no statistically significant differences in SD values between different parts of the leaf (fig. 1B).

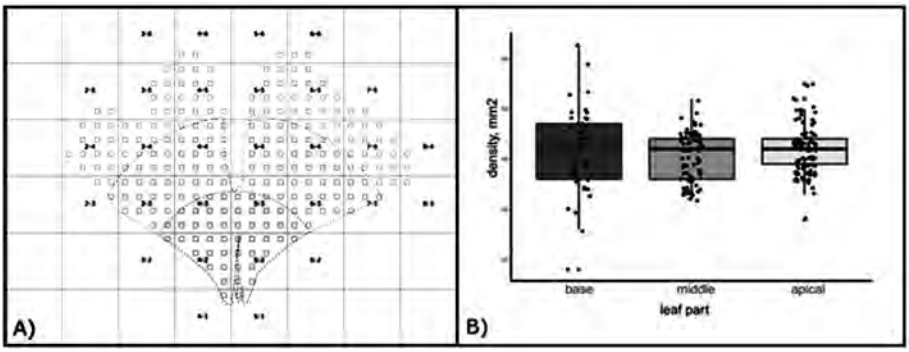

Figure. Stomatal density in different parts of the lamina.

The study was supported by the scientific program No. AAAA-A16-116021660045-2 of the Department of Higher Plants, Lomonosov Moscow State University.

References

Barclay R.S., Wing S.L. 2016. Improving the *Ginkgo* CO_2 barometer: implications for the early Cenozoic atmosphere. *Earth Planetary Sci. Lett.* **439**: 158–171.

Beerling D.J., McElwain J.C., Osborne C.P. 1998. Stomatal responses of the 'living fossil' *Ginkgo biloba* L. to changes in atmospheric CO_2 concentrations. *J. Exp. Bot.* **49**: 1603–1607.

Chen L.-Q., Li C.-S., Chaloner W.G., Beerling D.J., Sun Q.-G., Collinson M.E., Mitchell P.L. 2001. Assessing the potential for the stomatal characters of extant and fossil *Ginkgo* leaves to signal atmospheric CO_2 change. *Am. J. Bot.* **88**: 1309–1315.

Lawson T., Craigon J., Black C.R., Colls J.J., Landon G., Weyers J.D.B. 2002. Impact of elevated CO_2 and O_3 on gas exchange parameters and epidermal characteristics in potato (*Solanum tuberosum* L.). *J. Exp. Bot*. **53**: 737–746.

Poole I., Lawson T., Weyers J.D.B., Raven J.A. 2000. Effect of elevated CO_2 on the stomatal distribution and leaf physiology of *Alnus glutinosa*. *New Phytol*. **145**: 511–521.

Poole I., Weyers J.D.B., Lawson T., Raven J.A. 1996. Variations in stomatal density and index: Implications for palaeoclimatic reconstructions. *Plant Cell Environ*. **19**: 705–712.

Quan C., Sun C.-L., Sun Y., Sun G. 2009. High resolution estimates of paleo-CO_2 levels through the Campanian (Late Cretaceous) based on *Ginkgo* cuticles. *Cret. Res.* **30**: 424–428.

Retallack G.J. 2001. A 300-million-year record of atmospheric carbon dioxide from fossil plant cuticles. *Nature* **411**: 287–290.

Royer D.L. 2001. Stomatal density and stomatal index as indicators of paleoatmospheric CO_2 concentration. *Rev. Palaeobot. Palynol*. **114**: 1–28.

Royer D.L. 2003. Estimating latest cretaceous and tertiary atmospheric CO_2 from stomatal indices. In: Wing S.L. (ed.): *Causes and consequences of globally warm climates in the early paleogene*. Boulder: Geological Society of America. V. **369**. Special paper. P. 79–93.

RStudio Team. 2015. RStudio: Integrated Development for R. RStudio, Inc., Boston, MA. http://www/rstudio.com (accessed: 15 July 2016).

Salisbury E.J. 1928. On the causes and ecological significance of stomatal frequency, with special reference to the woodland flora. *Philos. Trans. R. Soc. London.* Ser. B. **216**: 1–65.

Sun B., Dilcher D.L., Beerling D.J., Zhang C., Yan D., Kowalski E. 2003. Variation in *Ginkgo biloba* L. leaf characters across a climatic gradient in China. *Proc. Natl. Acad. Sci. USA*. **100**: 7141–7146.

Weyers J.D.B., Lawson T. 1997. Heterogeneity in stomatal characteristics. *Adv. Bot. Res.* **26**: 317–352.

Zacchini M., Morini S., Vitagliano C. 1997. Effect of photoperiod on some stomatal characteristics of *in vitro* cultured fruit tree shoots. *Plant Cell, Tissue Organ Cult.* **49**: 195–200.

MUMMIFIED FOSSIL OF *KETELEERIOXYLON* FROM THE LATE PLIOCENE OF MAOMING BASIN, SOUTH CHINA, AND ITS PHYTOGEOGRAPHICAL AND PALEOECOLOGICAL IMPLICATIONS

Lu-Liang HUANG[1,2]***, Jian-Hua JIN***[1]***, Alexei A. OSKOLSKI***[2,3,4]

[1] Sun Yat-sen University, Guangzhou, China
[2] Nanjing Institute of Geology and Palaeontology CAS, Nanjing, China
[3] University of Johannesburg, Johannesburg, South Africa
[4] Komarov Botanical Institute RAS, Saint Petersburg, Russia

lssjjh@mail.sysu.edu.cn

In this paper, a new species *Keteleerioxylon maomingense* is described on the basis of mummified fossil wood from the late Pliocene Huangniuling Formation of the Maoming Basin, South China. Detailed anatomical study of well-preserved fossil wood confirms its close affinity to the extant conifer genus *Keteleeria* comprising three species distributed in central, southern, and southeastern China, northern Laos and in Vietnam. *Keteleerioxylon maomingense* is the most ancient fossil evidence of the occurrence of a taxa closely related to *Keteleeria* within the modern distribution area of this genus. This finding strongly suggests that the ancestors of extant *Keteleeria* ranged much further south in the late Pliocene than has been indicated by previous fossil records. Unlike more ancient fossil woods known from the Youganwo Formation of Maoming Basin (*Chadronoxylon maomingensis* and *Myrtineoxylon maomingensis*), *K. maomingense* has distinct growth rings confirming a progressive increase in rainfall seasonality in southern China from the middle to late Pliocene. The analysis of growth-rings in the fossil wood in comparison with those of modern *Keteleeria davidiana* suggests that in the late Pliocene of Maoming Basin there was humid subtropical monsoon climate with less pronounced rainfall seasonality than that seen in modern northeastern Vietnam.

This work was supported by the National Natural Science Foundation of China (Grant Nos. 41572011, 41210001, 41661134049); the grant of Natural Environment Research Council (No. NE/P013805/1); the joint Project of the National Natural

Science Foundation of China and the Russian Foundation for Basic Research (Grant Nos. 41811530082, 18-55-53015); the National Research Foundation of South Africa (Incentive Grant No. 109531); State Key Laboratory of Palaeobiology and Stratigraphy (Nanjing Institute of Geology and Palaeontology, CAS) (No. 173101); and the Scientific Research Fund, Hongda Zhang, Sun Yat-sen University. We thank the University of Johannesburg and the Komarov Botanical Institute (institutional research Project No. 01201456545) for financial support for A.A.O.

DOES MOSS PERISTOME ALWAYS HAVE A PERISTOMIAL FORMULA?

Michael S. IGNATOV[1,2]***, Ulyana N. SPIRINA***[2,3]***, Maria A. KOLESNIKOVA***[4]***, Svetlana V. POLEVOVA***[1]***, Elena A. IGNATOVA***[1]

[1] Lomonosov Moscow State University, Moscow, Russia
[2] Tsitsin Main Botanical Garden of Russian Academy of Sciences, Moscow, Russia
[3] Tver State University, Tver, Russia
[4] Moscow Institute of Physics and Technology, Dolgoprudny, Russia
misha_ignatov@list.ru

The study of peristome development in *Buxbaumia* revealed its strongly deviated pathway (Ignatov et al., 2018). The fundamental square patterning, characteristic of moss peristome formation, is lacking in *Buxbaumia*, except for occasional presence in the epidermal layer. Cells of the peristomial layers are not arranged in columns, but rather in a cone, and the number of cells forming the peristome is progressively increasing downwards due to additional and irregular anticlinal divisions in the peristomial layers. Naturally, such structure lacks any fixed number of cells in peristomial layers, as was noted by Philibert (1888), although subsequent authors tried to apply some fixed formula to the perstome of *Buxbaumia* (e.g. Edwards, 1979, 1984). The absence of cell columns in sporophyte of *Buxbaumia*, unlike in other mosses, and the progressive increase in the number of cells in peristomial layers makes any calculations of cells in the peristomial layers approximate, uncertain, and essentially senseless, obscuring the absence of homology.

References

Edwards S.R. 1979. Taxonomic implications of cell patterns in haplolepideous moss peristomes. In: Clarke G.C.S., Duckett J.G. (eds.): *Bryophyte systematics*. London: Academic Press. P. 317–346.

Edwards S.R. 1984. Homologies and inter-relations of moss peristomes. In: Schuster R.M. (ed.): *New manual of bryology*. Nichinan: Hattori Bot. Labor. V. **2**. P. 658–695.

Ignatov M.S., Spirina U.N., Kolesnikova M.A., Volosnova L.F., Polevova S.V., Ignatova E.A. 2018. *Buxbaumia*: a moss peristome without a peristomial formula. *Arctoa* **27**: 172–202.
Philibert H. 1888. De l'importance du péristome pour les affinités naturelles des mousses. *Rev. Bryol.* **15**: 6–12, 24–28, 37–44, 50–60, 65–69.

HOW TO DEFINE THE PRIMARY PERISTOME LAYER IN MOSSES?

***Elena A. IGNATOVA*[1], *Ulyana N. SPIRINA*[2,3], *Maria A. KOLESNIKOVA*[4], *Michael S. IGNATOV*[1,2]**

[1] Lomonosov Moscow State University, Moscow, Russia
[2] Tsitsin Main Botanical Garden of Russian Academy of Sciences, Moscow, Russia
[3] Tver State University, Tver, Russia
[4] Moscow Institute of Physics and Technology, Dolgoprudny, Russia
misha_ignatov@list.ru

Most moss species possess an arthrodontous peristome, formed of two rings of tooth-like elements. These elements are formed from three layers of cells, usually partly decomposed, with periclinal cell walls retained and fused, so the outer cell walls of the inner peristomial layer (IPL) appear adjoined with the inner cell walls of the middle layer, called primary peristomial layer (PPL), and the outer cell walls of the latter join with inner cell walls of the outer peristomial layer (OPL). These three layers were named by Blomquist & Robertson (1941), and PPL was considered as the most important layer by the following reasons: "The primary peristomial layer is composed of 16 cells which divide **no further**. They **enlarge rapidly and their inside walls soon become distinctly convex**. This is, therefore, the **first peristomial layer to appear conspicuously different** from the other layers. For this reason and because, as will be shown later, the **number of cells of which it is composed determines the number of teeth**, it seems desirable to designate this layer as the primary peristomial layer".

This definition was in perfect agreement with the peristome of *Aulacomnium*, which was studied by Blomquist & Robertson, and with other peristomes (about 15) studied for their development since then (Shaw et al., 1987, 1989a,b; Schwartz, 1994; etc.). However, subsequent studies revealed that peristomes of some other moss groups do not fit all of these criteria. Especially sound is the case of *Encalypta*, where almost none of the above mentioned criteria works. The IPL in *Encalypta* is notably thicker than in other mosses, so its cells do not divide up to the late stages of its development, maintaining peristomial formula 4:2:2. Probably by this reason, cells in other amphithecial layers are aligned by their anticlinal cell walls. Such

cell arrangement allows outstanding diversity of peristome types in *Encalypta*, so some authors, e.g. Fleischer (1900) and Edwards (1984) recognized Encalyptales as a special group, the Heterolepidae, as ranging in peristome type from diplo- to haplolepideous. The substitution of role of different layers in moss peristome development is discussed by Ignatov et al. (2018). Although any changes in terminology of IPL:PPL:OPL are not recommended, the function of them may somewhat shift in some evolutionary lineages of mosses.

References

Blomquist H.L., Robertson L.L. 1941. The development of the peristome in *Aulacomnium heterostichum*. *Bull. Torrey Bot. Club.* **65**: 569–584.

Edwards S.R. 1984. Homologies and inter-relations of moss peristomes. In: Schuster R.M. (ed.): *New manual of bryology*. Nichinan: Hattori Bot. Labor. V. **2**. P. 658–695.

Fleischer M. 1900. *Die Musci der Flora von Buitenzorg zugleich Laubmoosflora von Java mit Berücksichtigung aller Familien und Gattungen der gesamten Laubmooswelt.* Bd. **1**. Leiden: E.J. Brill.

Ignatov M.S., Spirina U.N., Kolesnikova M.A., Ashikhmina D.A., Ignatova E.A., Polevova S.V. 2018. Peristome development pattern in *Encalypta* poses a problem: what is the primary peristomial layer in mosses? *Arctoa* **27**: 1–17.

Shaw A.J., Anderson L.E., Mishler B.D. 1987. Peristome development in mosses in relation to systematics and evolution I. *Diphyscium foliosum* (Diphysciaceae). *Mem. New York Bot. Gard*. **45**: 55–70.

Shaw A.J., Anderson L.E., Mishler B.D. 1989a. Peristome development in mosses in relation to systematics and evolution III. *Funaria hygrometrica*, *Bryum pseudocapillare*, and *B. bicolor*. *Syst. Bot.* **14**: 24–36.

Shaw A.J., Anderson L.E., Mishler B.D. 1989b. Peristome development in mosses in relation to systematics and evolution IV. Haplolepideae: Ditrichaceae and Dicranaceae. *Bryologist* **92**: 314–323.

Schwartz O.M. 1994. The development of the peristome-forming layers in the Funariaceae. *Int. J. Plant Sci.* **155**: 640–657.

LEAF ANATOMY OF SOME EASTERN EUROPEAN OROBANCHACEAE SPECIES

Natalia A. IONINA, Svetlana E. PETROVA

Lomonosov Moscow State University, Moscow, Russia
petrovasveta@list.ru

The problem of parasitism in the plant kingdom has long attracted attention of researchers (Kuijt, 1969; Terekhin, 1977). The family Orobanchaceae is an excellent model taxon, since its species show the complete trophic spectrum from non-parasitic autotrophs to obligate holoparasites (Joel et al., 2013). Since the leaf is the most en-

vironment-depended organ of a plant, its inner structure should reflect the ecological specificity of this unusual group of plants. We conducted a comparative microstructural analysis of members of main Eastern European Orobanchaceae genera with an attempt to link the leaf anatomical features with the peculiarity of the lifestyle and functioning of parasitic and hemiparasitic plants. We present the results of our morphological and anatomical analyses of the leaf blades in 15 species of the Orobanchaceae.

In photosynthesizing hemiparasites (*Bartsia alpina*, *Castilleja lapponica*, *Euphrasia frigida*, *E. pectinata*, *Melampyrum nemorosum*, *M. sylvaticum*, *Odontites vulgaris*, *Rhinanthus minor*, *Pedicularis lapponica* and *P. sceptrum-carolinum*), the leaf blade is similar to that of the many mesophytic autotrophic plants. Foliage leaves of all studied hemiparasites are chlorophyll-bearing, pubescent, with anomocytic stomata and sinuous anticlinal walls of the epidermal cells. But they differ in some features. So, it can be distinguished: dorsoventral amphistomatic (*B. alpina*, *E. frigida*, *E. pectinata*, *M. nemorosum*, *O. vulgaris*, *P. palustris*, *Rh. minor*) and hypostomatic (*M. sylvaticum*, *P. kaufmanii*, *P. lapponica*, *P. sceptrum-carolinum*), and also isolateral amphistomatic (*C. lapponica*) leaf blades. The structure of the midrib is similar in all studied hemiparasitic plants: more or less protruding from the abaxial side; collenchima-like subepidermal cells; single massive vascular bundle with the xylem prevailing over the phloem.

Holoparasitic *Lathraea squamaria*, *Orobanche alba* and *O. hederae* have chlorophyll-free scales on flowering stems instead of normal leaves. In studied holoparasites such scales are pubescent, homogeneous, not differentiated into palisade and spongy mesophyll, of isodiametric cells. In both *Orobanche* species they are hypostomatic, with anomocytic stomata, with straight or weakly sinuous anticlinal walls of the epidermal cells; in *L. squamaria* they are without stomata, with sinuous anticlinal walls of the epidermal cells. The midrib is usually located in the most thickened part of the mesophyll in the studied parasites. In *Orobanche* and *L. squamaria*, the midrib has single vascular bundle immersed in the mesophyll; the xylem and phloem have been revealed therein, though the phloem was reported to be absent in *L. squamaria* (Kaplan, Inceoglu, 2003).

The quantitative data obtained are equivocal. The leaf blade is very thick in *C. lapponcia* (the thickest one, 431–731 μm), *E. frigida*, *P. lapponica*, *P. palustris*, *Rh. minor*, thick in *P. sceptrum-carolinum*, *M. nemorosum*, *M. sylvaticum*, *E. pectinata* and moderate thick in *B. alpina*, *O. vulgaris*, *P. kaufmanii* (the thinnest one, 174–186 μm). Thickness of the palisade and spongy mesophyll varies in the species concerned. Thin palisade mesophyll (44–78 μm) was noted in dorsoventral leaf blades of *O. vulgaris* and *P. kaufmanii*, the thickest one (332 μm) was revealed in *E. frigida*. The palisade ratio varies from 14–39% in *E. pectinata* up to 89% in *P. palustris*. The palisade ratio is 40% to 60% in most studied species to indicate their heliomorphic structure.

The size of the epidermal cells was estimated by the number of cells per 1 mm^2. The smallest value of this parameter is found in holoparasites of *Orobanche*

(the largest cells) and the highest one in the mountain tundra plant *P. lapponica* (the smallest cells). The epidermal cell density is rather high in the steppe species *P. kaufmanii*. The smaller epidermal cells indicate a greater xeromorphic nature of such plants.

One of the most prominent features of Orobanchaceae is the structure and variety of trichomes. We have identified 14 trichome types on the leaves of studied species (Fig.). We classified trichomes into glandular and nonglandular types. Nonglandular trichomes are quite common. They are present in five of the nine genera studied. The types I and II are noted in two genera – *Castilleja* and *Bartsia*. Only type I was found in the studied species of *Euphrasia*, *Melampyrum* and *Orobanche*. The glandular trichomes of types IV and VII are the most common, they were found on the leaves of *Bartsia*, *Euphrasia*, *Melampyrum*, *Odontites*, *Rhinanthus*, *Lathraea*. Trichomes of types V and VI are the most widely spread, each of them is found on the leaves of species of 2–3 genera (*Bartsia, Castilleja, Euphrasia, Melampyrum, Rhinanthus, Lathraea*). Trichomes of type III were found only in the genus *Euphrasia*. Trichomes of types IX–XIV are found only in one studied genus. So, trichomes of the IX type are observed only in *Pedicularis kaufmanii*, X – in *Odontites,* XI – in *Castilleja*, XII – in *Orobanche*, XIII and XIV – in *Lathraea*. The trichomes recognized here were also reported in other species of the same genera (Metcalfe, Chalk, 1950; Neumann et al., 1997; Kaplan, Inceoglu, 2003). Some of the trichome types are linked by intermediate morphological types. The diversity of trichomes may be higher on reproductive organs; in this paper we do not consider it.

The trichomes were repeatedly shown to play a key role in providing the hemiparasitic and parasitic lifestyle of Orobanchaceae, because some glandular hairs function as hydathodes (Groom, 1897; Govie et al., 1968; Světlíková et al., 2015) actively secreting water. There are the sessile glandular hairs (Types VI–IX) that are hydathodes, but hairs with a thin flattened single-celled stalk and a large head (Types III–V) could also be the hydathodes. *Orobanche* holoparasites contrasts with *Lathrea* as they have no trichome hydathodes. The scales of *Lathraea* are more similar to the leaves of hemiparasitic species, that confirming origin of this genus from photosynthetizing representatives of Rhinanthoideae.

Glandular long-stalked trichomes could maintain other functions (Hassan, El-Awadi, 2009). Different functions of glandular trichomes can be concluded from their distribution on the leaf blade.

The trichome number as well as trichome/stomata ratio should correlate with the degree of parasitism and biology of specific species. The hemiparasitic plants are known to highly transpire to extract intensively the water from their hosts. However, most of species presently studied (with the exception of *O. vulgaris* and *E. pectinata*) have low stomata density, but the total number of water-releasing structures (stomata and trichome hydathodes combined) is rather high.

In sum, the structure of typical heliomesophytes is a characteristic feature of the leaves of most phototrophic hemiparasites, the forest species *M. sylvaticum*

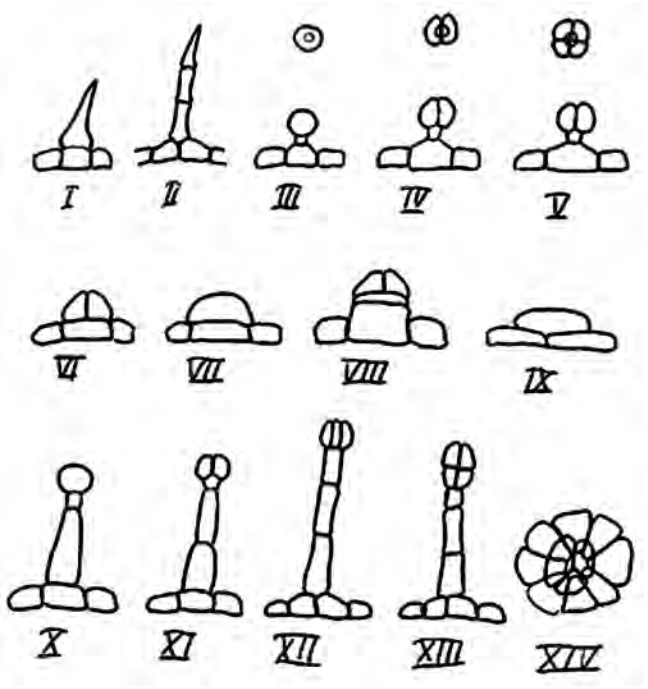

Figure. The variety of trichomes.

being a helioscyophilic mesophyte. The prevailing mesomorphism can probably be a result of leveling the influence of environmental factors such as moisture and soil richness of nitrogen, due to a stable water supply from the host. However, in some species, there are types of leaf blades deviating from this complex of traits, and there is often a discrepancy in the ecological condition (*C. lapponica*).

One of the most prominent features of the studied group of plants is the structure and variety of trichomes. The types of trichomes and their combination probably can be important for the systematics and diagnostics of the subfamily Rhinanthoideae. The diagnostic feature of different species is also the surface ornamentation of the hairs.

In annuals and biennials with unspecialized root system, we found high density of stomata and in general water-secreting structures, which provide a continuous flow of water from the host. It can be assumed, that the annual hemiparasites have a significantly higher intensity of processes, since their main task is to get the maximum amount of resources here and now for successful setting of fruits and seeds, after which they die off, and the further viability of the hosts is not important for them. At the same time, the vitality of the hosts is more essential for long-living perennials, because they often have to interact with them for longer time. This is only a working hypothesis, since any such correlations can be established only with a large number of measurements and taking into account many other factors (the position of the leaves, their area and number, ecological conditions of development, etc.).

In some hemiparasites, the number of glandular trichomes-hydathodes exceeds the number of stomata, this raises a problem why it is so and which structures work more efficiently? In *L. squamaria*, living mostly underground, the stomata are absent, and the glandular cryptotrichomes provide the continuity of the water flow with the dissolved substances absorbed from the host.

References

Govier R., Brown J.G.S., Pate J.S. 1968. Hemiparasitic nutrition in angiosperms II. Root haustoria and leaf glands of *Odontites verna* (Bell.) Dum. and their relevance to the abstraction of solutes from the host. *New Phytol*. **67**: 963–972.

Groom P.L. 1897. On the leaves of *Lathraea squamaria* and of some allied Scrophulariaceae. *Ann. Bot*. **11**: 385–398.

Hassan E.A., El-Awadi M.E. 2009. Study on the trichomes of the parasitic weed broomrape: morphology and histochemistry. *Gen. Appl. Plant. Physiol*. **35**: 13–21.

Joel D., Gressel J., Musselman L. 2013. *Parasitic Orobanchaceae. Parasitic mechanisms and control strategies*. Heidelberg: Springer.

Kaplan A., Inceoglu O. 2003. Leaf anatomy and morphology of 14 species belonging to the Turkish Rhinantheae (Scrophulariaceae) tribe. *Isr. J. Plant Sci*. **51**: 297–305.

Kuijt J. 1969. *The biology of parasitic flowering plants*. Berkeley: University of California Press.

Metkalfe C.R., Chalk L. 1950. *Anatomy of the Dicotyledons*. V. **2**. Oxford: Clarendon Press.

Neumann U., Paré J., Raynal-Roques A., Sallé G., Weber H.C. 1997. Characteristic trichomes and indumentum specialization in African and European parasitic Scrophulariaceae. *Bot. Acta*. **111**: 150–158.

Světliková P., Hájek T., Těšitel J. 2015. Hydathode trichomes actively secreting water from leaves play a key role in the physiology and evolution of root-parasitic rhinanthoid Orobanchaceae. *Ann. Bot*. **116:** 61.

Terekhin E.S. 1977. *Parasitic flowering plants: the evolution of ontogenesis and lifestyle*. Leningrad: Nauka. [In Russian]

CAN THE HIGHLY SPECIALIZED SPHAGNOID AREOLATION PATTERN BE HOMOPLASIOUS?

***Oleg V. IVANOV*[1], *Elena V. MASLOVA*[2], *Michael S. IGNATOV*[3]**

[1] Lebedev Insititute of Physics of Russian Academy of Sciences, Moscow, Russia

[2] Belgorod State University, Belgorod, Russia

[3] Lomonosov Moscow State University, Moscow, Russia

misha_ignatov@list.ru

Sphagnum mosses are well-known by leaf areolation pattern very different from any other mosses. Their cell dimorphism formation was in general

studied by Schimper (1858). Later Schnepf (1973) described it in great details. The earliest cell divisions in the leaf of *Sphagnum* do not differ from those of other mosses, but already since the stage when *Sphagnum* leaf consists of ca. 30 cells, its median lamina cells undergo two unequal divisions cutting off two smaller and narrower cells, which later transform into chlorocysts, while the remaining larger part of the "mother cell" develops into hyalocyst. Sphagnalean areolation pattern looks so specific that it is difficult to admit that it can originate more than once.

Protosphagnalean mosses constitute the largest group of extinct mosses of still uncertain affinity. Having general morphology of Bryopsida, some of them have leaves with an areolation pattern similar to that of modern *Sphagnum*. Therefore, Neuburg (1960) concluded that protospagnalean mosses are the ancestral group of modern *Sphagnum*, which more or less agrees with the evidence from age of fossils of these two groups.

However, studies of the early stages of leaf development of protosphagnalean mosses (Maslova et al., 2012) revealed that in this group the sphagnalean areolation pattern develops as a result of equal cell divisions taking place in a specific order followed by subsequent uneven cell growth. The protosphagnalean pathway of the sphagnalean areolation pattern development leads to considerably greater variation in the leaf structure of Protosphagnales than in modern sphagnalean mosses. Therefore, Ivanov et al. (2018) concluded that protosphagnalean mosses had a unique ability to switch the development of leaf areolation between the pathway unique to *Sphagnum* and another one common to all other mosses. This developmental polyvariancy hinders attempts to classify these mosses, as characters previously considered to be significant for generic level taxonomy can be shown to co-occur in one individual leaf. New understanding of the ontogeny has allowed us to re-evaluate the systematic significance of such diagnostic characters in these Palaeozoic plants, showing that their similarity to *Sphagnum* is less substantial.

References

Ivanov O.V., Maslova E.V., Ignatov M.S. 2018. Development of the sphagnoid areolation pattern in leaves of Palaeozoic protosphagnalean mosses. *Ann. Bot.* **122**: 915–925.

Maslova E.V., Mosseichik Y.V., Ignatiev I.A., Ivanov O.V., Ignatov M.S. 2012. On the leaf development in Palaeozoic mosses of the order Protosphagnales. *Arctoa* **21**: 241–264.

Neuburg M.F. 1960. Listostebel'nye mkhi iz permskih otlozhenii Angaridy. (Mosses from the Permian Angaraland.) *Trudy Geologicheskogo Instituta Akademii Nauk SSSR*. **19**: 1–104. [In Russian]

Schimper W.P. 1858. *Versuch einer Entwicklungsgeschichte der Torfmoose (Sphagnum) und einer Monographie in der Europa verkommenden Arten dieser Gattung.* Stuttgart: Schweitzerbart's Verlagshandlung.

Schnepf E. 1973. Mikrotubulus-Anordnung und Umordnung, Wandbildung und Zellmorphogenese in jungen *Sphagnum*-Blättchen. *Protoplasma* **78**: 145–173.

DIVERSITY OF FOLIAR TRICHOMES AND THEIR SYSTEMATIC RELEVANCE IN THE GENUS *CLEOME* (CLEOMACEAE)

Alexandra N. IVANOVA[1]***, Nuria K. KOTEYEVA***[1]***,***
Maria S. TARASOVA[2]***, Elena V. VOZNESENSKAYA***[1]

[1] Komarov Botanical Institute of Russian Academy of Sciences, Saint Petersburg, Russia
[2] Saint Petersburg State University, Saint Petersburg, Russia
alyx@bk.ru

Traditionally, the main structural characters used in *Cleome* systematics were morphology of seeds and pollen as well as flower structure, including stamen number (Hall et al., 2002; Sanches-Acebo, 2005). Trichome morphology and distribution are known to be reliable taxon specific traits and can be used in systematics and phylogenetics (Fahn, 2000; Spring, 2000). However, structural features of glandular trichomes are seldom considered as diagnostic traits because their frequency and secret composition can be affected by environmental conditions.

The objectives of our investigation were to study characters of glandular trichomes in *Cleome* in relation to systematics and to suggest the main trends of glandular trichome evolution within *Cleome* genus.

Trichome distribution, morphology, anatomy and ultrastructure were studied in 31 species using light, scanning and transmission electron microscopy. Obtained data were compared to phylogenetic trees of the genus (Feodorova et al., 2010).

Cleome includes about 170 species. The aerial parts of most of them are more or less pubescent. Four types of glandular trichomes according their morphology and anatomy were recognized in *Cleome*. I. Small uniseriate thichomes of 4–5 cells with unicellular glandular head. II. Trichomes of 4–8 cell series (both in the stalk and in the head) with stalk of middle size (*C. africana, C. viscosa, C. violacea*), long (*C. monophylla*, *C. viridiflora* and *C. hassleriana*) or without a stalk (C. *angustifolia*); this type prevails in *Cleome.* III. Trichomes with multiseriate stalks and multicellular heads (*C. droserifolia, C. paradoxa*). IV. Middle-sized trichomes with 4–6-seriate stalks and specifically structured head that can be spherical (*C. paradoxa*), ellipsoid (*C. gynandra*) or conical (*C. foliosa, C. paxii*). The comparison of trichome structure and distribution with phylogenetic trees and biogeography reconstructions (Feodorova et al., 2010) led us to combine clades in groups to reveale some trends in trichome evolution in *Cleome* genus.

The CENTRAL ASIAN / NORTH AFRICAN GROUP includes species of basal clades. Trichomes are uniformly distributed over leaves, petioles and stem. Three types of trichomes were found in the species of this group: type II in *C. africana,* C. *khorossanica*, types I and II in *C. violacea* and species of *Polanisia* clade, types I, II, III in *C. droserifolia* and C. *quinquenervia.* The uniform distri-

bution of trichomes was decided to be a primitive pattern of trichome distribution in *Cleome*. Long (up to 1 cm) trichomes of the type III with flattened head were found only in this group, similar trichomes were found in *Matthiola* belonging to Brassicaceae (Abdel Khalik, 2005; Beilstein et al., 2006), that is closely related to Cleomaceae.

Species of the NORTH AMERICAN GROUP are lack of glandular trichomes at all in contrast to other *Cleome: C. isomeris* has short non-glandular trichomes, *C. lutea* bears long hairs on its leaves and petioles. The North American group differs greatly from the other groups by some characters beside trichome structure (Iltis, Cochrane, 2007).

In the NORTH AFRICAN GROUP, *C. angustifolia* and *C. paradoxa* have glabrous leaves, but singular trichomes were found on their stems and petioles: small stalkless type II trichomes in *C. angustifolia* and large trichomes of type III with massive multiseriate stalk and globose head. So, the structurally different glandular trichomes demonstrate the similar distribution in the North African group.

In the SOUTH AFRICAN / AUSTRALIAN GROUP a set of trichome types differs between plant organs. Non-glandular hairs occur in some species besides the glandular trichomes. Glandular trichomes of type IV are common. They are localized preferentially on the stems, petioles, flower stalks; on the leaf blades they are obligatory over the veins. In the most species, all parts of plants in this group are pubescent. The specific character in this group is the densely pubescent style.

Glandular trichomes of two types usually occur simultaneously on the aerial parts of PAN AMERICAN GROUP species. They are I and II types in *C. spinosa* and closely related *C. hassleriana;* II type with very long stalks and IV type with globose head alongside with nonglandular hairs in *C. viridiflora*.

Typification of glandular trichomes based on their morphology and anatomy provided some insights into trichome evolution in *Cleome* genus. Study of trichome type distribution showed that 4–8-seriate trichomes (type II) occur in most species, alone or accompanied by other types. Prevailing of type II trichomes and uniform trichome distribution over leaves and stems in species of basal clades was decided to be the primitive pattern of pubescence in *Cleome* genus. It was stated that trichomes evolved as protrusions of single epidermal cell (Inamdar, Patel, 1973), however structural reduction may have taken place in sister species. The stems, petioles and flower stalks needs the extra protection against herbivores. They are the sites where new trichome types arise in the pubescent species (type IV trichomes in the South African / Australian group) or retain in almost glabrous species (North African group).

The ultrastructure of the glandular trichomes was studied in order to find some taxonomically important characters. The presence of chloroplasts in all trichome types of all studied species instead of leucoplasts that usually occur in secretory cells is one of the main features of *Cleome*. Exceptions are the upper head cells of type II trichomes in *C. viscosa*, type III trichomes of *C. droserifolia* and C. *para-*

doxa that contain leucoplasts and are thought to produce some terpenoids according to histochemical tests (*C. viscosa*) and development of large subcuticular space (*C. droserifolia* and C. *paradoxa*). Chloroplasts in head cells are very large, with invaginations and long protrusions. Structure of chloroplasts changes gradually from the head to the stalk of trichome: their shape is more regular and their grana contain more thylakoids from the upper to the lower cells of trichome. In the lowest stalk cells chloroplasts are identical to that in epidermal cells. Absence of barrier cells under secretory heads and gradual changing of ultrastructure lengthwise the trichome are characteristic of all studied trichome types in *Cleome* as well as in the closely related species *Polanisia dodecandra.* No differences or characters were found to be specific for group of species.

In order to find new relevant traits of trichome distribution, the seedlings of *Cleome* plants were studied using light and transmission electron microscopy. Trichomes of 4–6 series and 4–6 layers similar to that of *C. angustifolia* were found on cotyledons and hypocotyls of *C. africana, C. violacea, C. viscosa, C. gynandra, C. angustifolia* (outgroups and early-diverging clades, according to Feodorova et al., 2010, Fig. 1A) and not found in *C. monophylla*, *C. hasslerиana, C. hirta, C. ornitopodioides* (later-diverging clades, Feodorova et al., 2010, Fig. 1B). This fact seems to be nonrandom but its interpretation is embarrassing because characters of seedling trichomes were never analyzed in literature in relation to phylogeny. More data are necessary to make a suggestion about relevance of this trait.

In conclusion, typification of trichomes based on both morphology and anatomy provided some insights into trichome evolution in *Cleome* genus. The four main types of glandular trichomes were identified in *Cleome*. The arrangement of glandular trichomes is thought to be more characteristic for the species than trichome structural type. The uniform distribution of type II glandular trichomes over the whole plant body can be considered as primitive in *Cleome*. Types of glandular trichomes in *Cleome* are different in morphology but similar in ultrastructure of secretory and stalk cells. The presence of chloroplasts in secretory cells distinguishes Cleomaceae from many other families bearing glandular trichomes on the aerial parts of plants. Trichome distribution as well as morphology and anatomy of glandular trichomes are evident diagnostic traits in *Cleome* and could be used as significant characters in systematics and phylogeny of the genus.

References

Abdel Khalik K. 2005. Morphological studies on trichomes of Brassicaceae in Egypt and taxonomic significance. *Acta Bot. Croat.* **64**: 57–73.

Beilstein M.A., Al-Shehbaz I.A., Kellogg E.A. 2006. Brassicaceae phylogeny and trichome evolution. *Am. J. Bot.* **93**: 607–619.

Fahn A. 2000. Structure and function of secretory cells. In: Hallahan D.L., Gray J.C. (eds.): *Plant trichomes. Advances in botanical research incorporating advances in plant pathology*. New York: Academic Press. V. **31**. P. 37–75.

Feodorova T.A., Voznesenskaya E.V., Edwards G.E., Roalson E.H. 2010. Biogeographic patterns of diversification and the origins of C_4 in *Cleome* (Cleomaceae). *Syst. Bot.* **35**: 811–826.

Hall J.C., Sytsma K.J., Iltis H.H. 2002. Phylogeny of Capparaceae and Brassicaceae based on chloroplast sequence data. *Am. J. Bot.* **89**: 1826–1842.

Iltis H.H., Cochrane N.S. 2007. Studies in the Cleomaceae V: A new genus and ten new combinations for the flora of North America. *Novon* **17**: 447–451.

Inamdar J.A., Patel R.C. 1973. Structure, ontogeny and classification of trichomes in some Polemoniales. *Feddes Repert.* **83**: 473–488.

Sanchez-Acebo L. 2005. A phylogenetic study of the New World *Cleome* (Brassicaceae–Cleomoideae). *Ann. Mo. Bot. Gard.* **92**: 179–201.

Spring O. 2000. Chemotaxonomy based on metabolites from glandular trichomes. *Adv. Bot. Res.* **31**: 153–174.

ANATOMY OF *ARTEMISIA UMBELLIFORMIS* SSP. *ERIANTHA* (ASTERACEAE)

Pedja JANAČKOVIĆ [1], ***Milan GAVRILOVIĆ*** [1], ***Dragana RANČIĆ*** [1], ***Danijela STEŠEVIĆ*** [2], ***Zora DAJIĆ-STEVANOVIĆ*** [1], ***Petar D. MARIN*** [1]

[1] University of Belgrade, Belgrade, Serbia
[2] University of Montenegro, Podgorica, Montenegro
pjanackovic@bio.bg.ac.rs

Genus *Artemisia* L. (Anthemideae, Asteraceae) comprises more than 500 taxa (Vallès, Garnatje, 2005) with unresolved taxonomic and phylogenetic relationships (Hayat et al., 2009). *Artemisia umbelliformis* Lam. ssp. *eriantha* (Ten.) Vallès-Xirau et Oliva Brañas is a Central European alpine glacial relict, which inhabits rocks of the alpine regions of the Pyrenees, Alps, Apennines, as well as of mountains of the Balkan Peninsula and of Carpathians (Stevanović, 2011). In Montenegro, *A. umbelliformis* ssp. *eriantha* is distributed in the high mountain region of Mts. Durmitor, Komovi and Prokletije (Stevanović, 2011). In this work, anatomical investigations of vegetative organs of individuals of this species wild-growing at Mt. Durmitor were conducted. The aim of this study was to investigate general anatomy and particular anatomical features which are in relation with production of specialized metabolites, as well as to find possible new valid taxonomic characters. Microscopic slides were prepared following the standard histological procedures (Ruzin, 1999). In young roots, a triarch radial vascular bundle is observed, while typical secondary tissues occur in the older root cross-sections with well developed exodermis on its surface. Also, rhizome has secondary tissues, with periderm on its surface and parenchyma cortex below. In the central cylinder, a well developed xylem is noticed, while pith, composed of large parenchyma cells, is in the central region. The upper stem cross section

is characterized by more or less polygonal shape with one-layered epidermis, and well developed cortex, made up of one cell thick layers of collenchyma and parenchyma cells below. Collateral vascular bundles are arranged in a circle. Leaf cross section has oblong-linear shape, with well developed cuticle and the isolateral palisade structure. The leaf blade is amphistomatous and large stomatal chambers are noticed. Secretory canals are present in the root cortex parenchyma (endodermal secretory canals) and rhizome cortical parenchyma (also near to the endodermis). The stem and leaves are covered with non-glandular T-shaped and glandular biseriate trichomes. All of the obtained data contribute to anatomy of the genus *Artemisia*, and may be considered as possible valid taxonomic characters which could be helpful in better identification of the species. These findings may be valuable guideline in the future taxonomical, anatomical, micromorphological and phytochemical investigations of this and related species.

References

Hayat M.Q., Ashraf M., Khan M.A., Yasmin G., Shaheen N., Jabeen S. 2009. Diversity of foliar trichomes and their systematic implications in the genus *Artemisia* (Asteraceae). *Int. J. Agric. Biol*. **11**: 542–546.

Ruzin S.E. 1999. *Plant microtechnique and microscopy.* Oxford, New York: Oxford Univ. Press.

Stevanović V. 2011. *Artemisia eriantha*. IUCN Red List of Threatened Species, IUCN.

Vallès J., Garnatje T. 2005. *Artemisia* and its allies: genome organization and evolution and their biosystematic, taxonomic and phylogenetic implications in the Artemisiinae and related subtribes (Asteraceae, Anthemideae). In: Sharma A. (ed.): *Plant genome: biodiversity and evolution*. 1. *Phanerogams*. Enfield: Science Publ. Part B. P. 255–285.

MORPHO-ANATOMICAL CHARACTERISTICS OF LEAF ROSETTES IN *DRACAENA DRACO* L. – A STEP TOWARDS UNDERSTANDING WATER ACQUISITION STRATEGY OF DRAGON TREES

Joanna JURA-MORAWIEC*, *J. MARCINKIEWICZ

Botanical Garden – Centre for Biological Diversity Conservation in Powsin, Polish Academy of Sciences, Warsaw, Poland

j.jura-morawiec@obpan.pl; janozimek@gmail.com

Dracaena draco L. (Asparagaceae) is an arborescent monocot that belongs to the dragon tree group (Marrero et al., 1998). It is a vulnerable species native to the Canary Islands, Madeira, Cape Verde Islands and Morocco. Recent experimental studies demonstrated that *D. draco* can bypass soil water deficit by fog water uptake through the leaves that grow in rosettes at the tips of the branches (Nadezhdina,

Nadezhdin, 2017). The aim of this study was to determine the features of foliage of *D. draco* that enable to collect and store the water. The structure–function relationships at the level of the leaf rosette and along the axis of an individual leaf have been analyzed with dragon trees from the Jardín Botánico Canario "Viera y Clavijo" on Gran Canaria and the PAS Botanical Garden – CBDC in Powsin. Flexibility of leaves within rosettes and the length to width ratio favor the function of water absorption. Variation in e.g. leaf indumentum, distribution of parenchyma and location of a red resin 'dragon's blood' indicates functional specialization along the leaf length in relation to water absorption and storage. Water absorption takes place mainly in the area of leaf blade, while its storage mostly occurs in the parenchyma of the leaf base.

Field observations and plant material collection at the Jardín Botánico Canario "Viera y Clavijo" on Gran Canaria were possible thanks to the financial support of the National Science Centre, Poland 2017/01/X/NZ8/00533 (J.J-M).

References

Marrero A., Almeida R.S., Gonzalez-Martin M. 1998. A new species of the wild dragon tree, *Dracaena* (Dracaenaceae) from Gran Canaria and its taxonomic and biogeographic implications. *Bot. J. Linn. Soc.* **128**: 291–314.

Nadezhdina N., Nadezhdin V. 2017. Are *Dracaena* nebulophytes able to drink atmospheric water? *Environ. Exp. Bot.* **139**: 57–66.

ANATOMICAL AND MICROMORPHOLOGICAL CHARACTERS AND THEIR APPLICATION IN TAXONOMY OF INULEAE TAXA (ASTERACEAE)

Dunja S. KARANOVIĆ [1]***, Lana N. ZORIĆ*** [1]***,***
Bojan K. ZLATKOVIĆ [2]***, Jadranka Ž. LUKOVIĆ*** [1]

[1] University of Novy Sad, Novy Sad, Serbia
[2] University of Nyš, Nyš, Serbia
dunja.karanovic@dbe.uns.ac.rs

Comparative analyses of anatomical and micro-morphological characteristics of leaf and stem have been carried out on 17 Inuleae taxa, from several genera (*Inula*, *Pulicaria*, *Dittrichia*, *Limbarda*), using light and scanning electron microscopy. Taxa analysed in this study were previously located in different sections within *Inula*, and later some of them were segregated into separate genera. The delimitation of the genera within Inuleae tribe is controversial and has been the subject of a significant number of studies. The objective of the present communication was

to conduct comparative micro-morphological and anatomical analysis of vegetative organs of analysed taxa in order to estimate their systematic value, as well as, to define characters that would be useful in taxonomic delimitation. Obtained data were statistically processed by various numerical analysis methods usually used in taxonomic research. Result revealed that anatomical and micro-morphological characteristics of the leaf and stem are important for separating individual taxa, but their grouping did not follow the actual classification. The characters of the epidermis, presence of different trichome types and their distribution on vegetative organs, proved to be of the highest significance for differentiation of congeneric Inuleae taxa.

FLOWER STRUCTURE AND DEVELOPMENT IN *PENNANTIA CORYMBOSA* (PENNANTIACEAE)

Polina V. KARPUNINA[1]***, Kerry FORD***[2]***, Maxim S. NURALIEV***[1]***,***
Alexei A. OSKOLSKI[3,4]***, Dmitry D. SOKOLOFF***[1]

[1] Lomonosov Moscow State University, Moscow, Russia
[2] Landcare Research, Lincoln, New Zealand
[3] University of Johannesburg, Johannesburg, South Africa
[4] Komarov Botanical Institute, Saint Petersburg, Russia
p.karpunina@yandex.ru

Distinguishing types of gynoecium, in particular clarifying the differences between monomerous and pseudomonomerous gynoecia, is a classical problem of homology assessment in angiosperms. Although the distinction between these two conditions is highly important for analyses of floral evolution, as in many other cases in biology, there is no single method to distinguish between true monomery and the most derived cases of pseudomonomery. A monomerous gynoecium consists of a single carpel, whereas in a pseudomonomerous gynoecium, certain traces of reduced sterile carpel(s) can also be found. Recognition of these traces, which can be expressed in various degrees, is usually hampered by congenital nature of intercarpellary fusion. The asterid order Apiales is an interesting group to study different cases of carpel fusion and reduction. This order includes seven families comprising species with a range of carpel numbers, from highly polymerous gynoecia to pseudomonomerous and monomerous ones.

A monomerous gynoecium is characteristic only of some species of *Polyscias* (Araliaceae), where this condition gained at least four times (Karpunina et al., 2016). As the family Araliaceae is characterized by high degree of variation of flower merism, it is not surprising that monomery has evolved ‘simply’ as an extreme condition of variation of carpel number in a syncarpous gynoecium. Some

members of Araliaceae show totally unstable carpel orientation in monomerous and polymerous gynoecia. Unlike that, stable groundplan and orientation of the flower are characteristic of the closely related family Apiaceae. Most of the Apiaceae species have a gynoecium containing two carpels, but there are some species with a pseudomonomerous gynoecium, in which only one carpel is fertile and the second one is sterile. These species differ in the degree of sterile carpel reduction. At the same time, their gynoecium always occupies a median position in the flower and the positions of the fertile and sterile carpels are stable at the species level.

Pseudomonomerous gynoecia are characteristic of all representatives of the basal grade of Apiales, which comprises Torricelliaceae, Pennantiaceae and Griseliniaceae. These families possess tricarpellate gynoecia with only one fertile carpel.

According to published data, species of the monogeneric family Griseliniaceae have three styles and a unilocular ovary with four vascular bundles, two of which belong to the fertile carpel, and the other two are apparently dorsal bundles of the two sterile carpels (Philipson, 1967; Plunkett et al., 2004). The significance of that family for understanding flower evolution in the order Apiales cannot be underestimated, however only limited published data are available.

In the family Torricelliaceae, flower anatomy and development are studied in detail in the genus *Melanophylla* (Sokoloff et al., 2018). The gynoecium of *Melanophylla* has two small sterile locules on either side of a large fertile locule, each carpel has a style and a stigma.

We studied flower anatomy and development of *Pennantia corymbosa* (Pennantiaceae). The family includes one genus and four species native to New Zealand and North Eastern Australia. According to molecular phylogenetic data, Pennantiaceae are sister to the rest of the order Apiales. In the literature for this family it is noted that the trilete ovary form and the occurrence of three short styles are the evidence of the presence of three carpels (Gardner, de Lange, 2002). While Gardner & de Lange (2002) did not observe the locules of sterile carpels, Plunkett et al. (2004) reported two abortive locules adjacent to the single, fully developed one in *Pennantia*. However, Potgieter (2018) descibes the ovary as unilocular. Our work is the first study of flower development and the first detailed study of gynoecium anatomy, including vasculature of a member of Pennantiaceae. The information obtained in this work will be important for understanding gynoecium evolution in the basal grade and the whole order Apiales.

The New Zealand *P. corymbosa* is a small dioecious tree. The flowers have a double perianth. There are five sepals united in a short calyx tube, which remains at the fruit. Normally, there are five white petals, but there are flowers with four or six petals. The androecium of the male flowers is of five stamens with long filaments. As in the case of petals there are some flowers with four or six stamens. There is a small unvascularized dome-shaped structure in the centre of the male flower that might be interpreted as a highly reduced gynoecium. Female flowers possess vari-

ously developed staminodia. The gynoecium has a superior ovary, which is a rare condition in Apiales. In the development of the female flowers, three U-shaped carpels appear almost simultaneously, after the appearance of the fourth stamen, but before the fifth stamen. Already in the early developmental stages, two large carpels and a smaller one can be distinguished. This difference in size persists also at anthesis and the fruiting stage; it is manifested in the different size of the stigmas. The symmetry plane of the gynoecium is located in the median position with respect to the flower-subtending bract and the small carpel can occupy either an abaxial or an adaxial position. This feature distinguishes *Pennantia* from the case of *Melanophylla*, where the gynoecium is located in the transversal plane of the flower (Sokoloff et al., 2018).

The gynoecium of *P. corymbosa* differs from that of *Melanophylla* also in the absence of the two sterile locules that is convincingly confirmed by our observations. The ovary of *P. corymbosa* has a single locule. We interpret the ovule as a synascidiate zone of the gynoecium with locules of the two sterile carpels completely reduced and infer that the ovule of the fertile carpel is attached in the cross-zone. Sometimes, there are two ovules per fertile carpel: one fertile and another sterile, which is smaller than the fertile ovule. From the area of the ovule attachment, a large conducting bundle proceeds downwards in the ovary wall. This bundle innervates the ovule(s) and has two lateral branches extending upwards to the stigmas of two large carpels. The symplicate zone has a trilete shape and contains about nine vascular bundles. There are two large stigmas and a small one, each on a short style. Gynoecium morphology and vasculature indicates that the ovary locule is formed by the carpel bearing the small stigma. Thus the fertile carpel has a stigma that is smaller than those of the sterile carpels. The large bundle supplying the ovule can be interpreted as a synventral bundle shared by all three carpels. There are also three bundles in the corners of the ovary locule, which can be interpreted as dorsal bundles of the three carpels.

To summarize, the pseudomonomerous and tricarpellate nature of the gynoecium of *P. corymbosa* is convincingly confirmed by our results. This gynoecium shows a stable median orientation in the flower whereas the adaxial or abaxial position of the fertile carpel is variable. The stigmatic dimorphism is noteworthy, as the carpel with the small stigma is fertile and forms the ovary locule. A similar pattern of carpel dimorphism in three-carpellate gynoecia has been recently documented in some Malpighiaceae (Malpighiales) (Aliscioni et al., 2019).

References

Aliscioni S.S., Gotelli M., Torretta J.P. 2019. Gynoecium with carpel dimorphism in *Tricomaria usillo*, comparison with other genera of the *Carolus* clade (Malpighiaceae). *Protoplasma* **256**: 1133–1144.

Gardner R.O., de Lange P.J. 2002. Revision of *Pennantia* (Icacinaceae), a small isolated genus of Southern Hemisphere trees. *J. R. Soc. New Zeal*. **32**: 669–695.

Karpunina P.V., Oskolski A.A., Nuraliev M.S., Lowry P.P., Degtjareva G.V., Samigullin T.H., Valiejo-Roman C.M., Sokoloff D.D. 2016. Gradual vs. abrupt reduction of carpels in syncarpous gynoecia: A case study from *Polyscias* subg. *Arthrophyllum* (Araliaceae: Apiales). *Am. J. Bot*. **103**: 2028–2057.

Philipson W.R. 1967. *Griselinia* Forst. fil. – anomaly or link? *New Zealand J. Bot.* **5**: 134–165.

Plunkett G.M., Chandler G.T., Lowry II P.P., Pinney S.M., Sprenkle T.S. 2004. Recent advances in understanding Apiales and a revised classification. *South Afr. J. Bot*. **70**: 371–381.

Potgieter M.J. 2018. Pennantiaceae. In: Kubitzki K. (ed.): *The families and genera of vascular plants*. Springer Nature Switzerland AG. V. **15**. P. 533–538.

Sokoloff D.D., Karpunina P.V., Nuraliev M.S., Oskolski A.A. 2018. Flower structure and development in *Melanophylla* (Torricelliaceae: Apiales): Lability in direction of corolla contortion and orientation of pseudomonomerous gynoecium in a campanulid eudicot. *Bot. J. Linn. Soc*. **187**: 247–271.

FROST AND TREES: ARE RING-POROUS SPECIES MORE SENSITIVE?

Bulat F. KHASANOV

Institute of Ecology and Evolution RAS, Moscow, Russia
bulatfk@gmail.com

Wood anatomy was shaped as a tool exploring realm of plant taxonomy and evolution and focused on comparison of wood structure of various taxa. Dendrochronology, which can also be designated as tree-ring science, looks for variations in tree-ring traits inside a tree believing they might be of ecological meaning. The greater part of dendrochronological studies analyzes tree-ring variations of quantitative character including tree-ring width, wood density, vessel or tracheid lumen diameter, cell wall thickness etc. Measurements of quantitative anatomical traits have been considerably facilitated with introduction of new computer tools of image analysis and constitute fast growing area of tree-ring science.

Yet from its very beginning, dendrochronology examines qualitative modifications of tree-rings represented by specific structures developing under environmental stress and gradually acquires information related to various habitats and species. These macro- or microscopically visible traits can be further divided into physiological and traumatic modifications according to the cause of their formation. The former develop under environmental stress factors affecting root system or canopy, thus altering cambium hormonal status. Disturbances occurred either below or above ground result in formation of structures described in dendrochronological literature as flood rings, light rings and intra-annual density fluctuations (IADFs). Features designated as reaction/tension wood and missing rings can also be classified under this heading (see a detailed review in Schweingruber, 2007).

Traumatic features result from direct damage of cambial cells located in a certain part of the tree bole. For example, scars of various shapes can be formed after exposure to fire, impacts of stones or ice, wounds inflicted by animals etc. Count of such features in specimens sampled for dendrochronological studies can result in reconstruction of past wildfires, landslides, snow avalanches etc. (see a detailed review in Stoffel et al., 2010). Cambium cells and/or cells of cambial zone can also be affected by extreme frost events, which disrupt normal process of wood differentiation and leave specific marks in tree-rings known as frost rings. Extreme frost events can occur during winter as well as in the beginning and in the end of growth period. In all cases they are consequences of essentially the same meteorological phenomenon, advection of the extremely cold Arctic air mass into temperate regions. Fortunately, location of the specific anatomical feature inside tree-ring allows for the exact timing of the weather anomaly.

Frost rings were reported for various tree species from different regions. This study reviews these previously published findings as well as presents new observations in oak (*Quercus robur*) and ash (*Fraxinus excelsior*) trees from the Central Russia. In order to place these diverse examples into comprehensive narrative, frost ring occurrences will be treated according to the timing of frost and observations from Europe will be alternating with that of North America.

In winter, drop of air temperature below physiologically significant threshold causes formation of anatomically distinct features in ring-porous species (Khasanov, 2013). These severe winter rings were so far reported only from the European part of Russia (see review of related publications in Khasanov, 2013) with the one exception: they were also noticed in the 15th century wooden panels from England (Tapper et al., 1978). However, these panels were later identified as originating from Baltic countries (Wazny, 2002). Similar anatomical deviations were detected by Schweingruber (2007) in Switzerland in subtropical *Acacia dealbata* after a winter temperature drop below the freezing point. However, such features were not reported for other diffuse-porous trees or conifers.

While severe winter rings are characteristic of ring-porous species, diffuse-porous trees and conifers appear to be more frost-tolerant. This difference originates from physiological traits particular to the former. The differentiation of wood of ring-porous species begins at the time of a bud break with the development of wide earlywood vessels (Larson, 1994). Simultaneous formation of wide vessels and new leaves is related to physical restrictions: probability of vessel embolism during freeze/thaw cycles depends upon the vessel diameter (Sperry, Sullivan 1992). As a result, no wide vessels remain in a functional state after winter and ring-porous trees have to form a new layer of earlywood (Zimmermann, 1983). In order to meet physiological demands connected with described peculiarities of ring-porous wood, their cambial zone has some special features. Predecessors

of wide vessels are already formed in the previous autumn (Frankenstein et al., 2005). The drop of winter temperature below some critical point, which cells of cambial zone can withstand, damages them and prevents their development into vessel elements in the spring.

Other examples of frost rings occurrence can be found in Southern plains of the USA (Stahle, 1990) and in Germany (Land, 2013). In both cases frost rings were found in oaks (*Q. alba* and *Q. stellata* in the USA; *Q. robur* and *Q. petraea* in Germany) and were formed after cold spells in the beginning of the growth period. These cold spells occurred in March and April, respectively. Late frosts in May affect oak and ash trees in the European part of Russia (Kucherov, 2012; present study). Cold spells occurring still later (end of May – beginning of June) leave their signature in the wood of conifers in boreal and subarctic forests in Canada and Russia (Payette et al., 2010; Gurskaya, 2014). Impact of the cold spells in the end of growth period was detected in bristlecone pines (*Pinus aristata*) in California and Colorado (LaMarche, Hirschboeck, 1984; Brunstein, 1996).

Moving northward one can clearly see that the date of spring cold spell, which affects trees, gradually advances from March in Southern plains of the USA to June in boreal and subarctic forests. Obviously, this trend reflects delay of cambium initiation progressing from South to North. Much more interesting is a comparison of the long frost ring chronologies from different regions. Severe winter rings were observed in the European part of Russia throughout XIX and XX centuries, their occurrences more or less evenly distributed inside this time interval. The same pattern is characteristic of frost ring chronologies from Southern plains of the USA and Germany, where cold spells occurred in March and April, respectively. However, the last frost ring in the Central Russia was formed in 1876, though oak and ash trees faithfully recorded extreme frosts in May in previous years.

Two conditions are mandatory for extreme frosts: initial low temperatures in the Arctic and atmospheric blocking process, which promote advection in southward direction. We hypothesize that extremely cold air masses have been occasionally formed in the Arctic in winter and early spring during the last 200 years. However, changes in the atmospheric circulation, which mark transition from the Little Ice Age to modern period, ameliorated temperature conditions in high latitudes in late spring and summer. Since the end of XIX century, no air mass sufficiently cold to produce frost rings in oak and ash trees was formed in the Arctic in May or later.

Two groups of facts appear to be in contradiction with this statement. First, frost rings were observed in XX century in oak trees from Zilair plateau (Kucherov, 2012). As this area is in close proximity to Ural Mountains, their formation may conceivably be the result of specific meteorological conditions differing from that of Eastern European plains and associated with influence of mountains. Second,

conifers in boreal and subarctic forests of Canada and Russia are also recording cold spells in XX century. However, comparison of threshold values needed for frost rings formation in various species shows that conifers suffer from the relatively mild frosts slightly below 0 °C (Payette et al., 2010; Gurskaya, 2014). Yet they are susceptible to frosts damages only in the first 20–30 years of their lives. On the contrary, frost rings are formed in oaks after much more pronounced temperature drops, the threshold value were assessed as –5 °C (Stahle, 1990; Kucherov, 2012; Land, 2013). At the same time, oak and ash trees remain susceptible to frosts longer than conifers, though dependence of frost rings occurrence upon a tree age is characteristic of all studied species (Stahle, 1990; Payette et al., 2010; Khasanov, 2013; Gurskaya, 2014).

It is seen that frost tolerance of diffuse-porous species and conifers cannot be unambiguously claimed superior to that of ring-porous trees. Species of each type of wood organization have their own advantages and disadvantages. Yet study of frost rings occurrences in various species from different regions reveals previously unknown details of climate history.

The study was financially supported by RFBR (project No. 19-04-00632).

References

Brunstein F.C. 1996. Climatic significance of the bristlecone pine latewood frost-ring record at Almagre Mountain, Colorado, U.S.A. *Arctic and Alpine Res*. **28**: 65–76.

Frankenstein C., Eckstein D., Schmitt U. 2005. The onset of cambium activity – a matter of agreement? *Dendrochronologia* **23**: 57–62.

Gurskaya M.A. 2014. Temperature conditions of the formation of frost damages in conifer trees in the high latitudes of Western Siberia. *Biol. Bull*. **41**: 187–196.

Khasanov B.F. 2013. Severe winter rings of oak trees (*Quercus robur* L.) from Central European Russia. *Intern. J. Biometeorol*. **57**: 835–843.

Kucherov S.E. 2012. Reconstruction of abnormal weather events on Southeast border of the area of common oak on the basis of the analysis of tree-rings structure. *Izv. Samarskogo nauch. centra RAS*. **14**: 1481–1484. [In Russian]

LaMarche V.C., Jr., Hirschboeck K.K. 1984. Frost rings in trees as records of major volcanic eruptions. *Nature* **307**: 121–126.

Land A. 2013. *Holzanatomische Veränderungen als Reaktion auf extreme Umweltereignisse in rezenten und subfossilen Eichen Süddeutschlands und deren Verifizierung im Experiment*. Dissertation. University of Hohenheim.

Larson P.R. 1994. The vascular cambium: development and structure. In: Timell T.E. (ed.): *Springer series in wood science*. Berlin, Heidelberg, New York: Springer-Verlag.

Payette S., Delwaide A., Simard M. 2010. Frost ring chronologies as dendroclimatic proxies of boreal environments. *Geophys. Res. Lett*. **37**: L02711.

Tapper M., Fletcher J., Walker F.S. 1978. Abnormal small earlywood vessels in oak as chronological indicators: their relation to arrested heartwood formation (included sapwood) after cold winters. In: Fletcher J. (ed.): *Dendrochronology in Europe*. British Archaeological Reports International Series. **51**: 339–342.

Schweingruber F.H. 2007. *Wood structure and environment*. Berlin, Heidelberg, New York: Springer-Verlag.

Sperry J.S., Sullivan J.E.M. 1992. Xylem embolism in response to freeze-thaw cycles and water stress in ring-porous, diffuse-porous, and conifer species. *Plant Physiol*. **100**: 605–613.

Stahle D.W. 1990. *The tree-ring record of false spring in the southcentral USA*. PhD Dissertation. Tempe: Arizona State University.

Stoffel M., Bollschweiler M., Butler D.R., Luckman B.H. (eds.): 2010. *Tree rings and natural hazards. A state-of-art*. Dordrecht: Springer.

Wazny T. 2002. Baltic timber in Western Europe – an exiting dendrochronological question. *Dendrochronologia* **20**: 313–320.

Zimmermann M.H. 1983. Xylem structure and the ascent of sap. In: Timell T.E. (ed.): *Springer series in wood science*. Berlin, Heidelberg, New York, Tokyo: Springer-Verlag.

FRUIT ANATOMICAL CHARACTERS IN THE TAXONOMY OF THE UMBELLIFERAE

Euvgeny V. KLJUYKOV, Ekaterina A. ZAKHAROVA, Tatiana A. OSTROUMOVA

Lomonosov Moscow State University, Moscow, Russia
eazakhar@yandex.ru

Carpological characters have long been used in systematics of the Umbelliferae. The external morphological characters of fruits were mainly used for elaborating classification systems at an early stage of scientific systematics of the Umbelliferae as the most available to researchers. The characters of the internal structure of the fruit were less used. The following anatomical characters were mainly used: the outline of mericarp cross-section, the number of secretory ducts in pericarp and form of the endosperm (Hoffmann, 1814; Koch, 1824; De Candolle, 1830; Taush, 1834). Drude (1897–98), Calestani (1905) and Koso-Poljansky (1916) extensively used anatomical characters of fruits in their original systems of the Umbelliferae. Rompel (1895) drew attention to the presence of calcium oxalate crystals in the pericarp and endosperm and used this character in taxonomy. Koso-Poljansky (1914) was one of the first scientists to show the importance of mechanical tissues of fruits for the identification of the Umbelliferae. The internal structure of fruits was subsequently used in taxonomy of individual taxa (Pervukhina, 1947, 1950; Tamamshian, 1945; Tseng, 1967; Leute, 1969; etc.). An atlas of the anatomy of the fruits of the Umbelliferae of Czechoslovakia (Klan, 1947) should be noted, which includes detailed anatomical descriptions of the fruits and figures of their cross-sections. There are many figures of transverse sections and detailed anatomical drawings in the regional treatments of the Umbelliferae of the Far East (Gorovoy, 1966) and Russia (Pimenov, Ostroumova, 2012). The current complex studies of different groups of the Umbelliferae necessarily contain carpological data, including anatomical

ones (Winter et al., 2008; van Wyk et al., 2013; Kljuykov et al., 2018; etc.). We are working on the standardization of terminology for morphological-anatomical descriptions of the umbelliferous plants. The lists of terms of taxonomically important morphological-anatomical characters have been published elsewhere (Kljuykov et al., 2004; Pimenov, Ostroumova, 2014).

The material for anatomical studies had been obtained from the herbaria and collected in nature.

Fruit anatomy was examined under a light microscope. The fruits were kept in equal parts of glycerin, ethyl alcohol, and water for three days and hand-razored in the middle of mericarps. The sections were stained with aqueous Basic Fuchsin or processed successively with phloroglycinol and hydrochloric acid for lignifications test and then mounted in glycerol.

We refined taxonomically important anatomical characters of fruit and character states as follows.

1. Mericarp outline in transverse section: 1. strongly compressed dorsally (Fig. B); 2. slightly compressed dorsally; 3. not compressed (Fig. A, C, D). This character is rather constant and characterizes some taxa. For example, flattened fruits are found in almost all taxa of the tribe Tordylieae.

2. Exocarp cell size: 1. small (less than 30 μm); 2. large (more than 30 μm). Mericarps are covered by single-layered or more rare a two-layered exocarp. Large exocarp cells are found in some genera (*Aulacospermum* Ledeb., *Elaeosticta* Fenzl, *Ostericum* Hoffm., *Pleurospermum* Hoffm., *Taeniopetalum* Vis.). This character can be used for distinguishing these genera.

3. Commissure width; 1. narrow, exocarp almost reaches carpophore (Fig. A); 2. intermediate; 3. broad, exocarp terminates near the edges of marginal ribs (Fig. B–D). All species of a genus usually have the same commissure width. There are a few genera whose species have either narrow or wide mericarp commissure (*Angelica* L., *Seseli* L.). Some genera have species with either broad or medium mericarp commissure (*Carum* L., *Elwendia* Boiss.).

4. Mesocarp (main tissue): 1. not lignified parenchyma cells remained in mature fruit; 2. not lignified parenchyma cells largely destroyed in mature fruits; 3. mostly lignified parenchyma cells with pitted walls (Fig. D); 4. lignified parenchyma cells with pitted walls at the base of ribs; 5. lignified parenchyma cells with pitted walls fill whole ribs; 6. lignified parenchyma cells with pitted walls in only marginal ribs (Fig. B–C); 7. mesocarp with sclerenchyma cell group; 8. mesocarp with a continuous layer of sclerenchyma. All species within the genus often have the same mesocarp (*Bupleurum* L., *Angelica*, *Heracleum* L.). This character can vary within some genera (*Seseli*).

5. Hypendocarp (inner fibrous mesocarp): 1. present, continuous (Fig. B); 2. present, discontinuous; 3. obsolete. Most genera have obsolete hypendocarp. All taxa of the tribe Tordylieae and *Ferula* L. have distinct hypendocarp.

6. Vasculature: 1. compact; 2. vascular elements diffuse, not forming bundles. Most genera have single compact bundle in each primary rib (Fig. A–C). All species of the genus *Prangos* Lindl. have diffuse vascular elements (Fig. D).

7. Vascular bundle arrangement: 1. in primary rib bases; 2. in middle part of primary ribs; 3. in distal part of primary ribs. Rib vascular bundles are mostly in the base of the ribs, sometimes in the middle part (tribe Tordylieae) (Fig. B) and rarely in the distal part of the ribs (*Conioselinum* Hoffm., *Cenolophium* W.D.J. Koch, *Crithmum* L.).

8. Rib secretory ducts: 1. small, present in all ribs; 2. large, present in all ribs (*Trinia* Hoffm., *Eryngium* L., *Rumia* Hoffm.) (Fig. C); 3. small, present in some ribs only. Rib secretory ducts are outside of the bundles.

9. Vittae (= secretory ducts, excluding those in the rib) arrangement: 1. obsolete in mature fruits (Fig. C); 2. vallecular and commissural (Fig. A, B); 3. only vallecular; 4. only commissural; 5. cyclic in inner layer of mesocarp (Fig. D); 6. diffuse. There are vallecular and commissural vittae, sometimes vittae are arranged cyclically in the inner layer of the mesocarp (*Berula* Hoffm., *Bilacunaria* Pimemov et V.N. Tikhom., *Crithmum*, *Smyrnium* L., etc.) or scattered throughout the mesocarp (*Prangos*) (Fig. D).

10. Number of vallecular vittae: 1. solitary; 2. 2–4 per a furrow; 3. numerous.

11. Number of commissural vittae: 1. two; 2. 3–6; 3. numerous. Number of vallecular and commissural vittae can be variable in different species in the genus.

12. Crystals in pericarp: 1. obsolete; 2. diffuse in mesocarp and on commissural side (Fig. C); 3. only on commissural side; 4. in exocarp. Calcium oxalate crystals are present in cells of different pericarp tissues, as well as in endosperm in a number of species (species of the subfamily Saniculoideae, *Bilacunaria*, *Chaerophyllum* L., *Scandix* L.).

13. Endocarp: 1. not lignified; 2. somewhat lignified.

14. Endocarp cells form: 1. compressed, obscure; 2. highly elongated tangentially; 3. square or rectangular. Endocarp usually consists of cells tangentially elongated. In some species, the endocarp have these slightly lignified cells, endocarp cells are often compressed and invisible in transverse section of the mature fruits.

15. Endosperm (commissural side): 1. flat, slightly convex or slightly concave (Fig. A–C); 2. broad and shallow grooved; 3. broad and deeply grooved; 4. narrow, deep grooved; 5. mushroom-like grooved (Fig. D). The form of the commissural side of endosperm is comparatively constant but it rarely varies within genus, for example in the genus *Elaeosticta*.

16. Number of cotyledons: 1. two cotyledons; 2. single cotyledon. The majority of the Umbelliferae have embryos with two cotyledons. A single cotyledon is found in 14 genera (in all species or only in some of them).

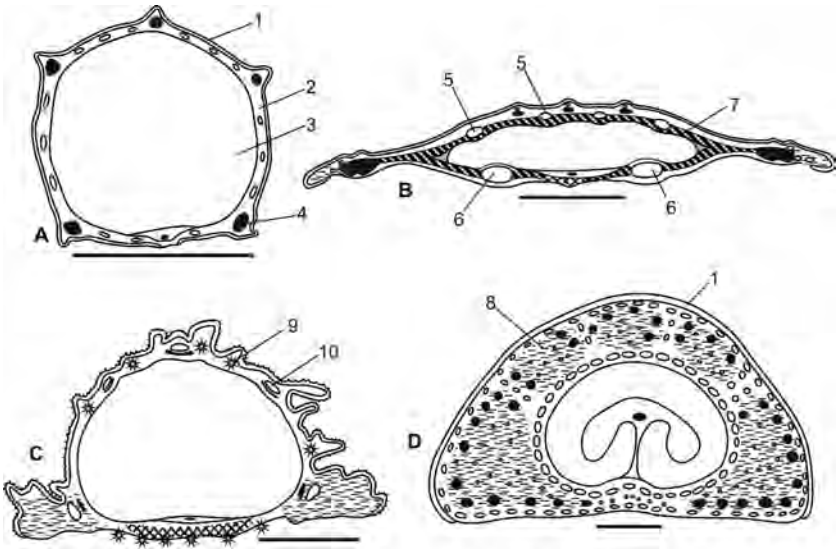

Figure. Schematic transects of mericarps. A – *Bupleurum falcatum* L.; B – *Heracleum sphondylium* L.; C – *Eryngium planum* L.; D – *Prangos odontalgica* (Pall.) Herrnst. et Heyn.
1 – exocarp, 2 – mesocarp, not lignified parenchyma cells, 3 – endosperm, 4 – vascular bundle, 5 – vallecular vittae, 6 – commissural vittae, 7 – hypendocarp, 8 – lignified parenchyma cells with pitted walls, 9 – crystals, 10 – rib secretory ducts. Scale bar – 1 mm.

Anatomical characters of fruit are important for the critical revision of umbelliferous taxa of every rank. They are often constant within genera and can characterize individual genera or group of closely related genera. However, the same anatomical character can occur in distant taxa.

References

Calestani V. 1905. Contributo alla sistematica delle Ombellifere d'Europa. *Webbia* **1**: 89–280.

De Candolle A.P. 1830. Umbelliferae. In: De Candolle A.P. (ed.): *Prodromus systematis naturalis regni vegetabilis*. Paris: Treuttel & Würtz. T. **4**. P. 55–250.

Drude O. 1897–1898. Umbelliferae. In: Engler A., Prantl K. (Hrsg.): *Die natürlichen Pflanzenfamilien*. Leipzig: Wilhelm Engelmann. Bd. **3**. Abt. 8. S. 49–192.

Gorovoy P.G. 1966. *Umbelliferae of Primorye and Amur River region*. Moscow: Nauka. [In Russian]

Hoffmann G.F. 1814. *Genera Plantarum Umbelliferarum*. Mosquae: N.S. Vsevolozskianis.

Klan Z. 1947. *Srovnavaci anatomie plody rostlin okolicnatych oblasti republicy Ceskoslovenske (anatomicky klic).* Praha: Nakladem Ceske Akademie Ved a Umeni.

Kljuykov E.V., Liu M., Ostroumova T.A., Pimenov M.G., Tilney P.M., van Wyk B.E. 2004. Towards a standardised terminology for taxonomically important morphological characters in the Umbelliferae. *S. Afr. J. Bot.* **70**: 488–496.

Kljuykov E.V., Liu M., Ostroumova T.A., Zakharova E.A., Ukrainskaja U.A., Petrova S.E. 2018. *Atlas of fruits of the Umbelliferae distributed across the European part of Russia*. Moscow: Torius. [In Russian]

Koch W.D.J. 1824. Generum tribuumque Umbelliferarum nova disposition. *Nova Acta Phys.-Med. Acad. Caes. Leop.-Carol. Nat. Cur.* **12**: 55–156.

Koso-Poljansky B.M. 1914. On the phylogeny of the Umbelliferae of Caucasus. *Trudy Tiflissk. Bot. Sada.* **16**: 172–229. [In Russian]

Koso-Poljansky B.M. 1916. Sciadophytorum systematis lineamenta. *Bull. Soc. Imp. Natur. Moscou.* **29**: 93–221.

Leute G.-H. 1969. Untersuchungen über den Verwandtschaftskreis der Gattung *Ligusticum* L. (Umbelliferae). 1. Teil. *Ann. Naturhist. Mus. Wien* **73**: 55–98.

Pervukhina N.V. 1947. Materials for the study of fruits of the Umbelliferae. *Sovetsk. Bot.* **15**: 27–31. [In Russian]

Pervukhina N.V. 1950. On the phylogenetic significance of some characters of the structure of the fruit of the Umbelliferae. *Trudy Bot. Inst. Akad. Nauk S.S.S.R.* **4**: 82–119. [In Russian]

Pimenov M.G., Ostroumova T.A. 2012. *Umbelliferae of Russia*. Moscow: KMK Scientific Press Ltd. [In Russia]

Pimenov M.G., Ostroumova T. A. 2014. Carpological characters in the Umbelliferae. In: Lotova L.I., Timonin A.C. (eds.): *Kaden's memorial book*. Moscow: MAKS Press. P. 158–172. [In Russian]

Rompel J. 1895. Krystalle von Calciumoxalat in der Fruchtwand der Umbelliferen und ihre Verwerthung für die Systematik. *Sitzungsber. Kaiserl. Akad. Wiss., Wien. Math.-Naturwiss. Cl.* Abt.1. **104**: 417–474.

Tamamshian S.G. 1945. About the value of some diagnostic characters of the Umbelliferae. *Sovetsk. Bot.* **13**: 3–11. [In Russian]

Taush I.F. 1834. Das System der Doldengewächse. *Flora*. **17**: 337–348.

Tseng C.C. 1967. Anatomical studies of flower and fruit in the Hydrocotyloideae (Umbelliferae). *Univ. Calif. Publ. Bot*. **42**: 1–79.

van Wyk B.-E., Tilney P.M., Magee A. 2013. *African Apiaceae. A synopsis of the Apiaceae / Umbelliferae of Sub-Saharan Africa and Madagascar*. Pretoria: Briza Academic Books.

Winter P.J.D., Magee A.R., Phephu N., Tilney P.M., Downie S.R., van Wyk B.-E. 2008. A new generic classification for African peucedanoid species (Apiaceae). *Taxon* **57**: 347–364.

CELL TO CELL CHANNELS IN *DIOSPYOS KAKI* THUNB. (EBENACEAE) ENDOSPERM ARE TRUE PLASMODESMATA!

Nicolay N. KOLACHEVSKI, Anton S. BEER

Lomonosov Moscow State University, Moscow, Russia

asbeer@yandex.ru

Endosperm cells of *Diospyros kaki* Thunb are a well known educational object in which we can observe cell to cell channels using common light microscopy. Traditionally, these structures are interpreted as plasmodesmata. A set of them penetrate the thick primary cell wall. But in many cases these structures resemble pores rather than plasmodesmata with pore channels being up to 0.2–0.4 μm in diameter and apparently possess pore membranes. These structures were found at

the beginning of the 20th century, before the electron microscopy was appeared. Despite of wide popularity of *D. kaki* as an educational object it still has not been studied using electron microscopy. We have studied *D. kaki* endosperm cell wall channels using transmission electron microscopy with osmium tetroxyde and ruthenium red contrasting, scanning electron microscopy with critical point drying and freeze drying, and using light microscopy with various histochemical reactions to compare with electron microscopy results. We found that *D. kaki* cell wall channels are true plasmodesmata with desmotubules and spoke proteins. Their structure is stable along the entire length and in the region of the middle lamella in particular. Unusually, the plasmosmata are 90–130 nm in diameter, but become narrower (30–50 nm) in the inner layer of cell wall. The endosperm cell wall has an uncommon structure among the angiosperm cell walls, with thin outer layer (which resembles a primary cell wall in the common parenchyma cells), very wide lamellate layer with storage polysaccharides, and inner thin layer with abundance of cross-linking glycans.

DIFFERENCES OF EMBRYOGENESIS IN THE TRIBE MALAXIDEAE (ORCHIDACEAE)

Galina L. KOLOMEITSEVA, Alexander V. BABOSHA, Andrey S. RYABCHENKO

Tsitsin Main Botanical Garden of Russian Academy of Science, Moscow, Russia
marchellos@yandex.ru

Orchids are characterized by myriads of small seeds with underdeveloped or absent endosperm and eliminated root and shoot apex of the embryo resulted from reduction of some embryogeny stages. Studying of embryogeny dynamics helps to determine the degree of seed maturity at different stages of embryogenesis and to get closer to solving practical problems of long-term storage and artificial germinating of orchid seeds *in vitro*.

Tribe Malaxideae (subfamily Epidendroideae) of 13 genera is considered to be close embryologically to the most typical (plesiomorphic) Cypripedioid-type (Clements, 1999). However, variable embryological traits were reported in members of this tribe. For instance, the suspensor varies from 1 to 6 cells in a number of species (Veyret, 1974; Sood, 1992) whereas it is absent in *Liparis viridiflora* (Rao, Rao, 1983). Embryogeny of *Dienia ophrydis* (J. Köenig) Seidenf. and *L. parviflora* (Blume) Lindl. was investigated to contribute to the embryology of Malaxideae.

Dienia ophrydis is a member of small genus of 19 terrestrial (rarely epiphytic) orchid species. More than 35 synonyms have been in use for this species since its description in 1791.

Liparis parviflora (Blume) Lindl. (subgenus *Cestichis*, section *Blepharoglossum* Schltr.) is a small sympodial terrestrial or epiphytic orchid from the mountain forests of South and Southeast Asia. It was described as *Malaxis parviflora* Blume in 1830, and 8 its synonyms are known so far.

The ranges of these species overlap in Thailand, Vietnam and Indonesia, but range of *D. ophrydis* is much wider.

Dienia ophrydis can be up to 100% self-pollinating in nature and average 68% self-pollinating in the greenhouse of Tsitsin Main Botanical Garden RAS, Moscow. Self-pollination results from the spontaneous dropping of the anther to move the pollinium over the edge of the rostellum. The self-pollination in *L. parviflora* does not exceed 30% in the greenhouse because it results from dissolution of part of the rostellum which takes place in only some flowers.

Both species have anatropic, bitegmal, medionucellular ovules, nucellus of a single layer of the epidermis, bipolar monosporic *Polygonum* type embryo sac.

Absent double fertilization is the most striking feature of the fertilization in most orchids from the subfamily Epidendroideae. Moreover, the polar nuclei often do not fuse and the diploid central nucleus of the embryo sac does not originate.

The first division of the zygote. In both species, the zygote divides periclinally, resulting in a 2-celled formation, whose apical (chalazal) cell *ca* generates the proper embryo, and the basal (micropilar) one *cb* gives rise to the suspensor. The *ca* is larger than the highly vacuolated *cb* in *D. ophrydis*, the two are almost equal-sized in *L. parviflora*. The epidermis of the nucellus is preserved, although its cells are severely deformed at this stage. The so-called 'petassum' viz. pollen tube remnant in the micropylar part of the embryo sac is clearly visible. It gives blue fluorescence with calcofluor and yellow-brown fluorescence with berberine. Similar blue fluorescence is also observed in the cell walls of the pollen tube stained with calcofluor.

3-celled embryo. Cells *cc* and *cd* derived from the *ca* constitute the 2-celled proembryo. Its *cc* constructively and functionally replaces the *ca*, and *cd* replaces the *cb* (Shamrov, 1997). The indices are assigned to the embryo tiers, taking into account this conditional removal of the true *cb* cell from the embryogenesis scheme while the designation of the non-dividing *cb* fits that in Souèges (1939) and Johansen (1950). The scheme of the 3-celled embryo is resultantly *cc* + *cd* + *cb*. Several relatively small vacuoles are formed in the suspensor of *D. ophrydis* whereas 1–2 large vacuoles occupy more than half of the *cb* cell in *L. parviflora*.

4-celled and 5-celled embryo. The *cd* cell periclinally divides into *m* and *ci* to result in a linear tetrad *cc* + *m* + *ci* + *cb*.

In *D. ophrydis*, only *m* and *cc* cells divide further on, while *cb* and *ci* cells do not divide throughout the embryogenesis. Five-celled embryo develops either by means of longitudinal division of *cc*, or by means of longitudinal division of *m*. After the second longitudinal division of both cells of *cc* tier, the quadrant formula can be written as *q* + *m* + *ci* + *cb*. The suspensor highly increases to deform

sometimes the nucellus. The vacuoles in the suspensor are especially numerous and voluminous at this stage. The suspensor of 4-celled embryo of *D. ophrydis* expands in its distal part and becomes thinner at its base to form a fitting. The *cb* cell nucleus is usually in the extended part and is surrounded by large vacuoles. Large vacuoles were sometimes visible in the very fitting (Kolomeitseva et al., 2017). The nucellus remains at this stage, its epidermal cells and their nuclei are flattened. A thin membrane, the mantle, becomes visible around the suspensor of *D. ophrydis* at the stage of 5-celled embryo. It is 0.6–0.9 μm thick and increases up to 3–4 μm thick with the embryo progress. The mantle surrounds only the suspensor but does not extend to the embryo. The outer layer of the mantle could consist of polysaccharides with phenol residues attached to them because it shows blue autofluorescence. The blue fluorophore is arranged in 0.6 to 1.3 μm point bunches, which make the mantle surface granular.

In *L. parviflora*, there are revealed typical and abbreviated modes of the cell division. The 5-celled embryo mostly forms by transverse division of the *ci* cell to form *n* and *n'* cells. The formula of such an embryo is resultantly *cc* + *m* + *n* + + *n'*+ *cb*. Longitudinal division of the apical *cc* cell very rarely takes place to make the embryo formula *cc* + *m* + *ci* + *cb*. The suspensor has no fitting at the base of the *cb* cell. The nucellus remains only at the base of the chalasal part of embryo sac, whose cell wall is still quite visible. Nuclei of the epidermal cells of nucellus are much flattened. Fragments of synergids and endosperm gradually disappear after the 5- to 7-celled embryo has formed.

Stages of quadrants and octants. In *D. ophrydis*, the cells of the *q* and *m* tiers continue to divide, giving rise to octant tiers. The *cb* suspensor cell and the basal cell *ci* never divide. Embryogeny of this species thus sharply contrasts to that of *Liparis pulverulenta* (Veyret, 1974), *Malaxis acuminata* (Sood, Rao, 1986), *Malaxis saprophyta* (Sood, 1992) of the same tribe Malaxideae: the cell *ci* is part of the embryo *per se*, but it is functionally closely connected with the suspensor it adjoins. This cell gradually develops huge vacuoles as large as those in the suspensor. It probably receives nutrients from the suspensor and distributes them into the cells of the embryo. The *cb* fitting begins elongating already at the stage of a 4- to 5-celled embryo. The *cb* fitting and *ci* cell elongate and form a kind of hose-like structure with the embryo progresses. The cell(s) of the tier *m* divide several times longitudinally, while those of the tier *q* divide transversely to form the tiers of octants *l* and *l'*. The resulting formula of the embryo becomes *l* + *l'* + *m* + *ci* + *cb*. The micropylar half of the cell wall of the embryo sac and the cells of the internal integument are destroyed at this stage. Therefore, the suspensor and then also the embryo are directly surrounded by the outer integument.

In *L. parviflora*, the second longitudinal division of each of the two cells of the *cc* layer and the transverse division of the *ci* cell result in the quadrant *q* + *m* + *n* + *n'* + *cb*. The median cells *n* and *n'* and their nuclei are strongly flattened. The suspensor shape is probably determined by the limited volume of

the embryo sac at the initial stages of development. It is between the embryo and the micropylar part of the embryo sac, irregular rounded flat and undivided into lobes. The suspensor emerges into the sub-integumentary space after destructing the embryo sac membrane. The petassum disappears at the same time. The suspensor divides into 3 elongated equally thick blades. Some of them protrude from the integuments, while others run downward to the chalazal end of the ovule under the integuments. The length of the suspensor blades exceeds the embryo length. They seem to gather nutrients from the cells of the inner layer of the outer integument. The inner integument almost completely destroys at the 10–15-celled embryo stage.

Table. Comparison of embryogeny of *Dienia ophrydis* and *Liparis parviflora*.

Stage of embryogenesis	*Dienia ophrydis*	*Liparis parviflora*
2-celled embryo	*cb* cell larger than *ca* cell	*ca* and *cb* cells of the same size
3-celled embryo	*cc* + *cd* + *cb* *cb* cell contains more than 10 small vacuoles	*cc* + *cd* + *cb* *cb* cell contains 1–2 large vacuoles
4–5-celled embryo	*cc* + *m* + *ci* + *cb* the fitting is in the tetrad stage	*cc* + *m* + *n* + *n'* + *cb* *cc* + *m* + *ci* + *cb* fitting is not pronounced
Quadrant stage	*q* + *m* + *ci* + *cb* rounded suspensor	*q* + *m* + *ci* + *cb* *q* + *m* + *n* + *n'* + *cb* lobe-shaped of suspensor
Octant stage	*l* + *l'* + *m* + *ci* + *cb*	*l* + *l'* + *m* + *n* + *n'* + *cb*

Thus, *D. ophrydis* and *L. parviflora* are similar in the absence of *cb* cell division and the presence of a unicellular suspensor with a fitting and mantle (Table) contrary to the previously studied species of the tribe Malaxideae (Veyret, 1974; Rao, Rao, 1983; Sood, 1992). Nevertheless, the two investigated species differ in the absence of *ci* cell division in *D. ophrydis* and its division in *L. parviflora*. The structure of the suspensor is another marked difference between these species. The mantle of *D. ophrydis* is thick and dense to make the distal part of its suspensor to remain subglobose throughout its existence. The mantle of *L. parviflora* is thinner to allow the suspensor to become lobed and partly protrude from the inner integument. Thus, the diversity of embryonic development in the Malaxideae is worth being further investigated.

The present investigation was carried out in accordance to Institutional research project No. 118021490111-5 at the Unique Scientific Installation “The Fund Greenhouse”.

References

Clements M.A. 1999. Embryology. In: Pridgeon A.M., Cribb J.C., Chase M.W., Rasmussen F.N. (eds.): *Genera Orchidacearum*. New York: Oxford University Press. V. 1. General Introduction, Apostasioideae, Cypripedioideae. P. 38–58.

Johansen D.A. 1950. *Plant embryology: embryogeny of the Spermatophyta*. Waltham: Chronica Botanica Co.

Kolomeitseva G.L., Ryabchenko A.S., Babosha A.V. 2017. Features of the embryonic development of *Dienia ophrydis* (Orchidaceae). *Cell Tissue Biol*. **11**: P. 314–323.

Rao P.R.M., Rao K.M. 1983. Embryology of *Liparis virdiflora*. *Acta Bot. Indica* **11**: 228–234.

Shamrov I.I. 1997. Principles of classification of types of embryogenesis. In: Batygina T.B. (ed.): *Embryology of Flowering Plants. Terminology and Concepts*. St. Petersburg: Mir i Semia-93. V. **2**. P. 493–508.

Sood S.K. 1992. Embryology of *Malaxis saprophyta*, with comments on the systematic position of *Malaxis* (Orchidaceae). *Plant Syst. Evol*. **179**: 95–105.

Sood S.K., Rao P.R.M. 1986. Gametophytes, embryogeny and pericarp of *Microstylis wallichii* Lindl. (Orchidaceae). *Bot. Mag*. **99**: 351–359.

Souèges R. 1939. Exposés d'embryologie et de morphologie végétales. X. Embryogénie et classification. Deuxième fascicule: essai d'un système embryogénique (Partie générale). *Act. Sci. Industr*. 1–85.

Veyret Y. 1974. Development of the embryo and the young seedling stages of orchids. In: Withner C.L. (ed.): *The orchids: scientific studies*. New York: John Wiley & Sons. P. 223–265.

MORPHOLOGY, ANATOMY AND FUNCTION OF CONTRACTILE ROOTS OF *GLADIOLUS GRANDIFLORUS* CV. EUROVISION CORMEL PLANTS

Irit KONSENS[1], ***Dov KOLLER***[2], ***Meira ZIV***[1]

[1] The Hebrew University of Jerusalem, Rehovot, Israel
[2] Deceased
irit.konsens@mail.huij.ac.il

The development, anatomy and function of contractile roots was studied in *Gladiolus grandiflorus* cv. Eurovision cormel plants grown under long day photoperiod (16 hrs) at 27/17 °C day/night temperature.

A gladiolus plant developing from a cormel produces 2–3 sheath-leaves without lamina, 1–2 foliage leaves with a lamina, and a daughter cormel at the base. Only 3–4 contractile roots develop on the daughter cormel base; their contraction pulls the daughter cormel into the soil. In gladiolus, the contractile roots are produced sequentially (not simultaneously), each contractile root developing in coordination with the previous one in the sequence. As contractile root elongates, its thick upper part swells, then contracts and thus buries the daughter cormel deeper in the soil.

A new contractile root develops and begins to contract only when its predecessor has completed its contraction. The phenomenon can be described as a 'relay race' among contractile roots, when each root in its turn causes additional deepening of the daughter cormel.

The swelling of the basal part of the contractile root and its subsequent contraction progresses acropetally from the more mature part of the contractile root towards its tip. The contracting zone is about 1 cm long and is limited to the basal part of the contractile root. As the contract zone of such a length deepens the daughter cormel by 1 cm, its original length can be concluded to be about 2 cm and the contraction rate is about 50%. The cumulative length of contractile zones per plant was linearly related to the number of contractile roots and the depth of the daughter cormel (regression coefficient is about 1). The thin lower part of the contractile root branches out below the contracted zone and anchors the root in the soil.

The anatomy of the contractile zones was studied in order to understand the contraction machinery of contractile roots. During root contraction, the cells of the middle and inner cortical parenchyma undergo changes in shape and size. These changes begin at the periphery of the middle cortex and progress towards the vascular cylinder. These processes continue from the beginning of the contractile root thickening until their complete contraction.

Each cell undergoes a gradual change in size. Each cell expands radially and tangentially causing the thickening of the root basal part. During the radial expansion, cells of the middle cortical parenchyma contract by 30–50% and their volume increases. Thus, the change in cell shape is associated with its active growth. There are therefore these tissues that take the active part in root contraction. Subsequently, the cell gradually collapses radially. The previously expanded cell walls fold, bend, and eventually collapse so that their tangential longitudinal walls become appressed. This collapse progresses centripetally from the periphery of the middle cortex. The cells become crushed when interior active cortex cells expand radially and shorten. Cell crushing begins when the thickened part of the contractile root is still smooth, in the periphery of the active middle cortex parenchyma. The collapse proceeds inwards to the inner cortex when the root contracts.

The parenchyma cells of the passive outer cortex collapse at a later stage, when the contractile root is mature and has completed its contraction. The active cortical tissues shorten, but adjoining outer tissues (rhizodermis, exodermis and outer cortical parenchyma) do not shorten. Therefore, they become folded and appear wrinkled.

The present study provides information about contractile roots in cormel plants, which is very limited to the best of our knowledge.

WOODY PLANTS IN THE ENVIRONMENTS OF ACTIVE VOLCANOES OF SAKHALIN AND KURIL ISLANDS: STRUCTURAL CHANGES OF BARK TISSUES

Anna V. KOPANINA

Institute Marine Geology and Geophysics of Far Eastern Branch
of Russian Academy of Sciences, Vladivostok, Russia
anna_kopanina@gmail.com

Volcanoes are broadly distributed around the world. Volcanic activity has profoundly been disrupting biomes and causing the adaptations of plants to harsh conditions since the earliest days of life. Information about the volcanic influence on plants structure is rare and incomplete. We have studied the bark tissues of woody plants of various life forms – liana (*Toxicodendron orientale*, Anacardiaceae), shrub (*Spiraea beauverdiana*, Rosaceae) and tree (*Betula ermanii*, Betulaceae) growing around active volcanoes of the South Kuril Islands and compared them with the same species growing under normal conditions on Sakhalin.

Detailed descriptions of bark were done for all studied samples. Classical anatomical methods were used to make sections and their analysing. Bark tissues were described according to current guidelines on bark anatomy of woody plants by Angyalossy et al. (2016). The bark samples from young branches of the 1 year-old to mature stems (up to 15 years-old in *Toxicodendron orientale*; 30 years-old in *Spiraea beauverdiana*; up to 55–60 years-old in *Betula ermanii*) were studied in detail. Statistical analysis was performed according to Minko (2004) using Microsoft Excel 2016 statistical analysis tools.

In *Spiraea beauverdiana,* structural deviations from normal growth and zones of non-specific anomalous structure were revealed at all ages. These zones alternate in the stem with areas of 'common structure'. The anomaly is caused by disturbances in the activity of phellogen and cambium. There is the periderm that is most severely affected in 3–5 years-old stems. The proportion of zones with anomalous secondary phloem increases in the stem with age. The phloem wedges clearly visible in cross sections form in these zones due to significant dilatation and sclerification of the phloem parenchyma. In the underground stem of *Spiraea beauverdiana* (13–15 years-old), there are the aggregate phloem rays up to 25–35 cells wide. Since 25 years-old, anomalies in the stem are represented only in the secondary phloem, while they are completely absent in the periderm. The anomalies formed in the secondary phloem are similar with the stem pitting.

The structural adaptations of *Toxicodendron oriental*e to extreme conditions near gas-hydrothermal springs are mainly related to the conducting phloem. Comparative analysis of the functional features of this tissue shows the following important trends: 1) increase of diameter and length of the sieve tubes in ontogenesis; 2) decrease of

diameter and increase of length of the sieve tubes under extreme conditions; 3) diffuse arrangement of sieve tubes in the conducting phloem in mature plants and also 4) significant amount of the uniseriate rays. These features can be considered as pedomorphosis of the secondary phloem. *Toxicodendron orientale* has stem structure similar to tropical lianas from Bignoniaceae (Angyalossy et al., 2012; Pace et al., 2015).

The response of *Betula ermanii* to the environmental factors of the gashydrothermal springs is different in young stems and in trunk. The bark in the trunk is wider under extreme environments due to the non-conducting phloem which accumulates 25–30% more in the trunk near the gashydrothermal springs. Cortex dilates with approximately the same rate in different environmental conditions, but its width is less near the gashydrothermal springs. The conducting phloem clearly reacts to extreme environments. Its width is bigger in these environments than in normal conditions. The shape of definitive secondary phloem sieve tubes changes. They become more rounded: the radial diameter is larger and the tangential diameter is smaller. At the same time, the radial diameter increases faster under extreme conditions, while the tangential one increases slower. The diameter of juvenile sieve tubes is normally 2–3 times smaller than sieve tubes of the trunk and 4–5 times smaller under extreme environments, respectively. The length of the sieve tube increases. The sclereid groups in the rays are formed already in 1 year-old bark (normally since 2 years-old) near the gashydrothermal springs. The size and specific area of sclereid groups is 50–70% larger. The dependence of the number of calcium oxalate crystals in the cortex and nonconducting phloem on the environmental conditions is not obvious from the available data. This indicator is very different from one age to another.

Combination of high temperatures in the rooting range, hot steam saturated with sulfur oxides, scattered sunlight and high concentrations of rare earth elements and heavy metals in the soil near the gashydrothermal springs was revealed to cause a disorder in the activity of the phellogen and cambium. Unstable functioning of the meristems leads to the formation of anomalous tissues in the bark and structural changes in the phloem.

The study was carried out with support from RBFR (No. 15-04-04774) and in the framework of the state order to the Institute of Marine Geology and Geophysics, Far Eastern Branch RAS.

References

Angyalossy V., Angelesb G., Pace, M.R., Limaa A.C., Dias-Lemed C.L., Lohmanna L.G., Madero-Vegab C. 2012. An overview on the anatomy, development and evolution of the vascular system of lianas. *Plant Ecol. Div*. **5:** 167–182.

Angyalossy V., Pace M.R., Evert R.F., Marcati C.R., Oskolski A.A., Terrazas T., Kotina E., Lens F., Mazzoni-Viveiros S.C., Angeles G., Machado S.R., Crivellaro A., Rao K.S., Junikka L., Nikolaeva N., Baas P. 2016. IAWA list of microscopic bark features. *IAWA J*. **37**: 517–615.

Minko A.A. 2004. *Statistical analysis in MS Excel*. Moscow: Williams Publ. [In Russian]

Pace M.R., Alcantara S., Lohmann L.G., Angyalossy V. 2015. Secondary phloem diversity and evolution in Bignonieae (Bignoniaceae). *Ann. Bot.* **116**: 333–358.

STRUCTURE AND FORMATION OF BARK TISSUES OF *BETULA ERMANII* (BETULACEAE) IN ONTOGENESIS

Anna V. KOPANINA

Institute of Marine Geology and Geophysics of Far Eastern Branch
of Russian Academy of Science, Vladivostok, Russia
anna.kopanina@gmail.com

Betula ermanii Cham. (stone birch) is one of the key tree species in the vast territory of the Far East, including the islands. It forms individual forest zone and actively participates in mixed deciduous and dark coniferous forests, as well as in various shrub communities at the latitudinal and altitudinal limits of its distribution. Within its range, the stone birch varies from large tree with an umbrella-shaped canopy to small multi-stemmed tree and shrub. We tried to reveal features of the bark structure as a multifunctional tissue complex which allow this species to grow in extreme coastal environments of the Sea of Okhotsk. In order to carry out such ecological assessments, it is necessary to study the formation of *Betula ermanii* bark tissues in environments typical of the species. At present, there is very little data in the literature on the structure of the *Betula ermanii* bark (Talalueva, 1985; Taipale et al., 1994; Yeremin, Kopanina, 2012). Our research is the first study of *Betula ermanii* bark formation from the initial development stages of the stem to the old-age states of the trunk.

Samples were collected in fir–stone birch shrub–forbs forest, the typical habitat of *B. ermanii,* on the slopes of Susunai Ridge, south Sakhalin Island. The stone birch is there a tree up to 12–14 m high, with a trunk diameter of 16–22 m, 55–80 years old. The bark of 1, 2, 5, 10, 27–30, 55–60 years old stems was sampled on October 18, 2015. The bark of annual stem was also sampled on 28.05. – 23.11.2018 from the plants cultivated in the Dendrology Park of the Institute of Marine Geology and Geophysics FEB RAS. In each habitat, the bark was sampled from three model trees. To scrutinize the dynamics of bark formation, the annual stems were taken 2 weeks after the growth season beginning and then every 2 weeks throughout the summer and then 1–2 times per month before the first winter dormancy.

Stem samples were fixed in 96% ethyl alcohol according to Barykina et al. (2004) and then analyzed using the equipment of the Laboratory for Plant Ecology and Geoecology, IMGG FEB RAS. Transverse, radial and tangential 10–25 μm thick sections of the stems were made with a sliding microtome Microm HM 430c with a fast freezing unit (Thermo Scientific, USA). The sections were stained regressively using Safranin and Nile Blue, washed up and dehydrated in ethyl alcohol series of increasing concentrations and cleared with carbol xylene and xylene (Barykina et al., 2004) and mounted in synthetic media. The bark samples were also macerated according to Wang et al. (2011) to reveal the structure of conducting

elements of the phloem. Histochemical reactions were used to determine chemical of the crystals in the bark tissues (Barykina et al., 2004).

Section images were processed with ZEN 2 lite software under light microscope Axio Scope.A1, CarlZeiss for measuring and photography. Bark tissue was described according to current guidelines on bark anatomy of woody plants by the International Association of Wood Anatomists – IAWA (Angyalossy et al., 2016).

We analyzed 37 characters of bark tissues of each model tree and of each age state. The dataset for each character of each model tree, for each age-specific state comprised at least 32 measurements. Data from three model trees were averaged and assembled. The sample mean and its confidence interval (for 95% probability) were estimated for each character. Statistical analysis was performed according to Minko (2004) using Microsoft Excel 2016 statistical analysis tools.

Three weeks old stem has completely differentiated unilayered epidermis with rare stomata and unicellular simple hairs 594.39 ± 36.70 μm long and multicellular peltate glands 117.56 ± 9.23 μm in height and 338.01 ± 33.31 μm in diameter. The glands are thus larger than those indicated by Taipale et al. (1994) (150–250 μm). The epidermis remains functioning during all summer, until phellem suberinization.

The first **phellogen** initiates in the subepidermal layer of the cortex collenchymatous parenchyma in a month after beginning of the vegetation. During the first month, it produces phellem with 0.75 ± 0.04 μm thick cells walls. From the early August and to the end of the growing season, the phellogen produces the phellem with 1.27 ± 0.08 μm thick cell walls. Thus, the two-layered phellem is formed by the end of the growing season.

The cortex consists of angular collenchyma-like parenchyma and inner aerenchyma-like parenchyma. The collenchyma-like parenchyma is 4–5 layers by the end of the first month of the growing season. Solitary nearly spherical druses and prismatic crystals of calcium oxalate are deposited in the cortical cells.

The **primary phloem** consists of the protophloem fibers, sieve tubes, companion cells and parenchyma cells. The compact groups of 25–40 fibers are square or roundish cap-shaped in cross-section. The fibers are polygonal to square in cross-section, 813.65 ± 62.22 μm long. They develop the secondary walls by 3rd or 4th week of the growing season. The crystals are deposited in the fibers, but they were not detected in the end of the growing season. The fiber groups are separated by 1–2 cells of the parenchyma and sclereids in the end of the growing season. Sclereids vary in shape, have distinctively pitted walls and contain crystals. The sieve tubes are solitary and in small groups of 2–6. The sieve-tube elements have only simple transverse or slightly oblique sieve plates.

The **secondary phloem** differentiates since 3rd week of the growing season. It consists of sieve tubes, companion cells, axial parenchyma and rays. From the very beginning, the calcium oxalate druses are present in the ray and axial paren-

chyma cells next to the cambium. This feature is maintained throughout the life of the tree. The sieve tubes are solitary and in small groups of 2–3, irregularly arranged. The sieve-tube elements are 142.74 ± 11.96 μm in length and associated with 3 to 5 companion cells. The sieve tubes can be classified into 2 groups. The first group includes the ultra-narrow 2–5 μm wide sieve tubes which have transverse or slightly oblique simple sieve plates and rounded irregularly arranged sieve areas on their side walls. The second group includes much wider sieve tubes (radial diameter 4.08 ± 0.19 μm, tangential diameter 10.60 ± 0.43 μm) which have inclined simple sieve plates and scalariform round or oval sieve areas on their side walls.

The bark structure changes with plant aging as follows. The first periderm persists for a long time, until formation of the subsequent periderms at the base of the 50–55 years old trunk. Arrangement of the subsequent periderms is reticulate. Each phellem has alternating bands of thin-walled and thick-walled phellem cells due to thin-walled phellem forms at the beginning of the growing season and thick-walled one develops in the second half of the growing season. It is structurally similar with the phellem of *Betula maximowicziana* (Shibui, Sano, 2018). The phelloderm is thin (1–3 cell layers). The phelloderm cells are parenchymatous. The filling tissue of lenticels is stratified (heterogeneous).

The **axial phloem parenchyma** is exclusively diffuse in the young stems, but it becomes diffuse and diffuse-in-aggregates since 10 years old. Short discontinuous tangential aggregates of this parenchyma are scattered in the conducting phloem. The parenchyma strands consist of 6–8 cells; their lengths 2 times increase linearly up to 801.89 ± 73.00 μm with trunk aging.

The **phloem rays** are undulated in the conducting phloem and wavy in the nonconducting one. The rays are 1 to 3 (4 or 5) cells wide, the ratio of the multiseriate rays increasing with trunk age. The ray cells are square and procumbent, the latter prevaling. The specific phloem ray number sharply drops in 1–5 years old trunk to become 1.5–2 times less in the 25–30 years old trunks. The rays are irregularly sclerified in the nonconducting phloem; some of them dilate.

The **conducting phloem** becomes wider in aging trunk to stabilize after 30 years old. The sieve tubes are arranged in tangential bands of 8–12 in perennial trunk. The shape and size of the sieve-tube elements change with trunk age. Their radial diameter increases 3.5–4 times up to 19.75 ± 1.27 μm in 27–30 years old trunk; their tangential diameter increases 2.5–3 times up to 38.59 ± 2.27 μm. The length of the sieve-tube elements also increases more than 3 times to 261.59 ± 26.84 μm in the 55–60 years old trunk. Only sieve-tube elements with compound sieve plates are produced since 2 years old. The sieve plates of later produced sieve-tube elements become longer and more oblique. The sieve plates in trunk phloem are scalariform and reticulate. The sieve areas on the side walls are scalariform and reticulate. The shape of the sieve areas is oval, rounded-triangular and rounded-square. Five to seven companion cells are associated with the sieve-tube element.

In the **nonconducting phloem** of the perennial stem, there are active processes of dilation and sclerification of the axial parenchyma and rays. The inner nonconducting phloem is stratified due to collapsing of tangentially clustered sieve tubes and axial parenchyma dilation; this stratified structure is lost in the outer zone due to sclerification of the phloem constutuents. Sclereids start forming already since 2 years old in some multiseriate rays. Rare groups of sclereids develop in the nonconducting phloem since 5 years old. In the bark, which is 17–18 years old or more, the main part of the nonconducting phloem consists of sclereid clusters. The size of sclereid clusters reaches 0.5–1 mm. Companion cells in nonconducting phloem are transformed into elongated sclereids. Similar sclerification of companion cells in nonconducting phloem was previously described, for example, for *Tilia americana* (Evert, 1963). In the trunk, the crystals are mainly located on the periphery of the nonconducting phloem. The specific number of crystals in the bark varies from one age to another; it can both decrease and increase.

The trunk bark of *Betula ermanii* is characterized by specific age changing to acquire definitive structure by the 25–30 years old. However, different bark constituents acquire definitive structure at different ages. The phellem becomes layered by the end of the first year. Regular arrangement of the sieve tubes and axial parenchyma appear at 5 years old. Definitive type of the sieve plates is established since 2 years old, whereas the shape and size of sieve-tube elements continue changing over the years.

The study was carried out with support from RBFR (No. 15-04-04774) and within state order to the Institute of Marine Geology and Geophysics Far Eastern Branch of the Russian Academy of Sciences.

References

Angyalossy V., Pace M.R., Evert R.F., Marcati C.R., Oskolski A.A., Terrazas T., Kotina E., Lens F., Mazzoni-Viveiros S.C., Angeles G., Machado S.R., Crivellaro A., Rao K.S., Junikka L., Nikolaeva N., Baas P. 2016. IAWA list of microscopic bark features. *IAWA J*. **37**: 517–615.

Barykina R.P., Veselova T.D., Devyatov A.G., Dzhalilova Kh.Kh., Iljina G.M., Chubatova N.V. 2004. *Mannual on botanical microtechnique. Basic principles and methods*. Moscow: Moscow Univ. Publ. [In Russian]

Evert R.F. 1963. Sclerified companion cells in *Tilia americana*. *Bot. Gaz.* **124**: 262–264.

Minko A.A. 2004. *Statistical analysis in MS Excel*. Moscow: Williams Publ. [In Russian]

Shibui H., Sano Y. 2018. Structure and formation of phellem of *Betula maximowicziana*. *IAWA J*. **39**: 18–36.

Talalueva L.V. 1985. Features of the anatomical structure of the stem bark of some species of the genus *Betula* (Betulaceae). *Bot. Zhurn.* **70**: 490–495. [In Russian]

Taipale H.T., Hirmilil L., Rousi M., Lapinjoki S.P. 1994. Histological and chemical comparison of triterpene and phenolic deterrent contents of juvenile shoots of *Betula* species. *Trees* **8**: 232–236.

Wang G., Shi S., Wang J.W., Yu Y., Cao S.P., Cheng H. 2011. Tensile properties of four types of individual cellulosic fibers. *Wood Fiber Sci*. **43**: 353–364.

Yeremin V.M., Kopanina A.V. 2012. *Atlas of the bark anatomy of trees, shrubs and lianas of Sakhalin and Kuril islands*. Brest: Poligrafika. [In Russian]

COMPARATIVE CHARACTERISTICS OF THE GLANDULAR TRICHOMES IN FOUR SPECIES OF *ARNICA* (ASTERACEAE): LOCALIZATION, MORPHOLOGY, ULTRASTRUCTURE AND HISTOCHEMICAL ANALYSIS

Olga V. KOSTINA*, *Lyudmila E. MURAVNIK

Komarov Botanical Institute of Russian Academy of Science, Saint Petersburg, Russia
olga.kostina@list.ru

The presence of the glandular trichomes (GTs) on reproductive and vegetative organs is a typical feature of Asteraceae (Metcalfe, Chalk, 1950). Nevertheless, information on the distribution of the GTs, their morphology, anatomy, and chemical composition of secretory products is rather limited (Ciccarelli et al., 2007). The secretory structures of plants are known to perform an important function of synthesis of secondary metabolites (Göpfert et al., 2005; Bombo et al., 2015).

The surface of the aerial organs in *Arnica* species is covered with different types of trichomes (Iljin, 1961), the character of which has not established up to date. *Arnica* plants have long been used in folk medicine as a strong antiseptic drug (Bone, Mills, 2013). The therapeutic effect of this plant has been proven to be due to some secondary metabolites, including phenolic compounds, terpenoids and sesquiterpene lactones.

The objectives of this work were 1) to study the GTs in four *Arnica* species, growing in the Leningrad region; 2) to obtain the detailed characteristics of their localization, morphology and anatomy; 3) to carry out a comparative histochemical analysis of the GTs located on the various organs; 4) to identify the main classes of chemical compounds that are synthesized by the secretory trichomes.

Three types of the GTs were found in four *Arnica* species. They start to function already during growth in the bud. GTs of the 1st type are situated on all aerial organs. In different parts of the plant, they differ in size, shape and number of cells. GTs of the 2nd type were found on the peduncle and phyllaries in *A. foliosa* and *A. longifolia*. GTs of the 3rd type are on the peduncle, phyllaries, as well as on the stem leaves of *A. montana* and *A. chamissonis*.

GTs of the 1st type are mainly cylindrical (fig. 1a). This structure is most typical of Asteraceae plants (Ciccarelli et al., 2007; Amrehn et al., 2014; Bombo et al., 2015). GTs of the 2nd type form a pronounced round two-celled head and a stalk of 4–6 cell pairs (fig. 1b). In GTs of the 1st and 2nd types, a subcuticular cavity is formed over the terminal cells (fig. 1a, b, *arrows*). The same structure is described in many species of the family (Nikolakaki, Christodoulakis, 2004; Ciccarelli et al., 2007). GTs of the 3rd type have a large, rounded two-layered head consisting of four cells and long stalk with eight to ten cell layers (fig. 1c). They are met in *A. montana* and *A. chamissonis*. Unlike first two types, the subcuticular cavity is absent in the GTs of the 3rd type.

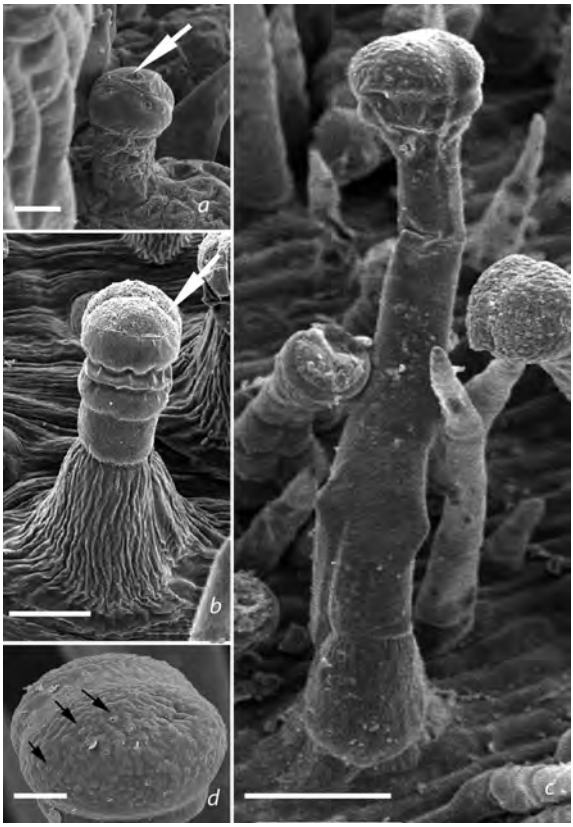

Fig. 1. The glandular trichomes of three types in *Arnica* species, SEM.
(*a*) – GTs of the 1st type, adaxial side of the *A. foliosa* leaf;
(*b*) – GTs of the 2nd type located on the *A. longifolia* peduncle;
(*c*) – GTs of the 3rd type located on the *A. montana* peduncle;
(*d*) – GTs of the 3rd type, trichome head with the pores (arrows), *A. chamissonis*.
Scale bars – 10 μm (*a, d*), 20 μm (*b*), 50 μm (c).

The presence of various primary and secondary metabolites in the GTs was shown in many representatives of Asteraceae family (Bombo et al., 2015; Amrehn et al., 2016; Muravnik et al., 2016, 2019). We used fluorescence microscopy and histochemical tests to identify various classes of the chemical compounds. During the experiments, differences in the degree of fluorescence, localization of colored cells, and intensity of color were found. In GTs of the 1st and 2nd type, the terminal cells and subcuticular cavity were colored most intensively. In GTs of the 3rd type, coloration was detected both in the head and in four upper pairs of the stalk cells.

Qualitative histochemical reactions revealed presence of pectin (with Safranin), neutral lipids (with Sudan III), fatty acids (with Nile Blue), polyphenols (with Toluidine Blue or Ferric Chloride), terpenoids (with NADI), and sesquiterpene lactones (with concentrated HCl) in the GTs. The localization of phenols was demonstrated with using of autofluorescence as well as fluorescent markers (Natural

Reagent or Wilson reagent). Despite having the same classes of substances, there are some differences between the three types of the GTs. The phenols were found in larger quantity in the GTs of the 1st and 2nd types. The intensity of the sesquiterpene lactone coloration was higher in the GTs of the 3rd type. Among all GTs of the 1st type only trichomes located in the base of the corolla tube do not demonstrate reaction on sesquiterpene lactones.

The main ultrastructural components of the terminal cells in the GTs of all types include a network of smooth endoplasmic reticulum with transparent or gray contents, cisterns of rough endoplasmic reticulum, and moderately active Golgi apparatus that produces the small secretory and coated vesicles. In addition, there are small leucoplasts of the various form including cup-shaped invaginations. In the GTs of the 1st and 3rd types leucoplasts contain dark inclusions (fig. 2a), which are larger in the GTs of 3rd type (fig. 2d), whereas in the GTs of the 2nd type inclusions are less evident. The reticular sheaths envelop the leucoplasts. Chloroplasts appear in the lower cells. These organelles are present in all stalk cells; the sizes of chloroplasts increase to the base of the GT. A lot of small vacuoles are situated in the cytoplasm. In the GTs of the 1st and especially of the 3rd types they often contain osmiophilic inclusions and myelin-like structures (fig. 2b, e). In the GTs of

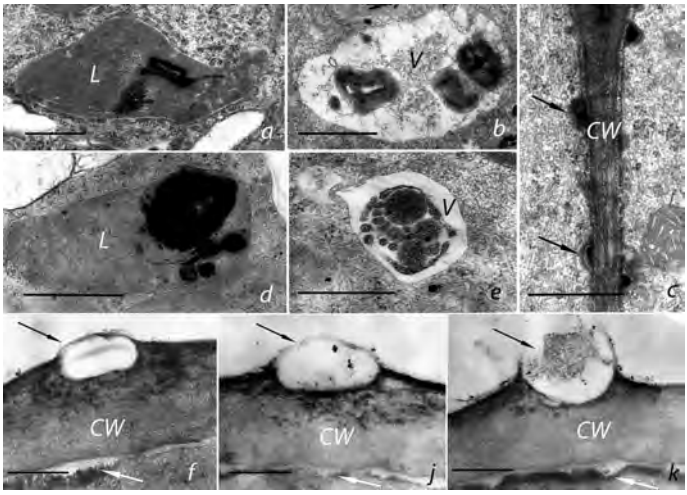

Fig. 2. Comparative ultrastructural characteristics
of the main differences between the GTs of three types.
(*a*) – Leucoplast in the GT of the 1st type in *A. foliosa*, lamellae contain the black inclusions;
(*b*) – vacuole in the cell of the second layer in GT of the 2nd type in *A. longifolia*;
(*c*) – anticline wall between two apical cells in GT of the 1st type in *A. montana*,
periplasmic space is filled with the dark secret (*arrows*);
(d) – leucoplast in the trichome of the 3rd type in *A. chamissonis* with large osmiophilic inclusions;
(e) – vacuole in the apical cells of GT of the 3rd type in *A. montana*;
(f–k) – formation of micro-cavities on the outer walls of the upper layer of GT
of the 3nd type in *A. montana*, periplasmic space (*white arrows*).
CW – cell wall; *L* – leucoplast; *V* – vacuole.
Bars – 0.5 μm (*a, f–k*), 1 μm (*b–c*).

the 2nd type the vacuoles are often transparent or have flocculent sediment. A similar ultrastructure of secretory cells producing phenols, terpenes and sesquiterpene lactones has been described in *Tussilago farfara* (Muravnik et al., 2016) and in three *Doronicum* species (Muravnik et al., 2019).

The periplasmic space is narrow; it is filled with osmiophilic substances in the GTs of the 1st and 2nd types (fig. 2c, *arrows*). The secretion accumulated in the subcuticular cavity is carried out on the trichome surface by mechanical rupture of a cuticle (fig. 1a, b, *arrows*). This method of accumulation of the secretory products is characteristic of glandular hairs of other Asteraceae species (Bombo et al., 2015; Amrehn et al., 2016). In the GTs of the 3rd type, a periplasmic space has the mixed grey and black grained contents (fig. 2f–k, *white arrows*). As opposed to the GTs of the 1st and 2nd types, many small subcuticular cavities are formed in the GTs of the 3rd type. The cuticle becomes thinner during accumulation of secretion and eventually ruptures throwing the contents outside (fig. 2f–k, *black arrows*). Examination of the trichome surface under the scanning electron microscope indicates that it holds the numerous pores. For the first time, the same small pores were found in the trichomes of very young leaves in one of Asteraceae species, *Inula viscosa* (Werker, Fahn, 1981). The formation of the separate cavities, which are later ruptured, is described in GTs of *Scutellaria galericulata* (Lamiaceae – Giuliani, Bini, 2008).

Three types of the GTs in *Arnica* species have obvious differences in the ultrastructural characteristics, which testify in favor of differences in the chemical composition of their secretion. GTs located on diverse organs differ in their functional activity. GTs of the 1st type produce polysaccharides and thereby provide the sliding to the growing young shoot. In addition, the shiny secretory drops reflect direct sunlight and protect the growing organ from drying out. GTs of the 1st and 2nd types synthesize the chemicals of the same composition. While GTs of the 1st type begin to function later than the GTs of the 2nd type, their secretory period becomes longer. GTs of the 3rd type located on the peduncle probably perform protective function obstructing eating of flowers by insects and playing the role of an antibacterial and fungicide barrier. Trichomes located at the base of the corolla tube likely synthesize volatile substances to attract pollinators.

References

Amrehn E., Aschenbrenner A.-K., Heller A., Spring O. 2016. Localization of sesquiterpene lactone biosynthesis in cells of capitate glandular trichomes of *Helianthus annuus* (Asteraceae). *Protoplasma* **253**: 447–455.

Amrehn E., Heller A., Spring O. 2014. Capitate glandular trichomes of *Helianthus annuus* (Asteraceae): Ultrastructure and cytological development. *Protoplasma* **251**: 161–167.

Bombo A.B., Appezzato-da-Glória B., Aschenbrenner A.K., Spring O. 2015. Capitate glandular trichomes in *Aldama discolor* (Heliantheae – Asteraceae): morphology, metabolite profile and sesquiterpene biosynthesis. *Plant Biol*. **18**: 455–462.

Bone K., Mills S.Y. 2013. *Principles and practice of phytotherapy*. 2nd ed. London: Elsevier Health Sciences.

Ciccarelli D., Garbari F., Pagni A. 2007. Glandular hairs of the ovary: a helpful character for Asteroideae (Asteraceae) taxonomy? *Ann. Bot. Fenn.* **44**: 1–7.

Iljin M.M. 1961. Genus *Arnica*. In: Shishkin B.K., Bobrov E.G. (eds.): *Flora of the URSS*. Moscow, Leningrad: USSR Acad. Sci. Publ. V.**26.** P.655–665. [In Russian]

Giuliani C., Bini L. M. 2008. Insight into the structure and chemistry of glandular trichomes of Labiatae, with emphasis on subfamily Lamioideae. *Plant Syst. Evol.* **276**: 199–208.

Göpfert J.C., Heil N., Conrad J., Spring O. 2005. Cytological development and sesquiterpene lactone secretion in capitate glandular trichomes of sunflower. *Plant Biol.* **7**: 148–155.

Metcalfe C.R., Chalk L. 1950. *Anatomy of the dicotyledons*. 2nd ed. Oxford: Clarendon Press.

Muravnik L.E., Kostina O.V., Mosina A.A. 2019. Glandular trichomes of the leaves in three *Doronicum* species (Senecioneae, Asteraceae): morphology, histochemistry, and ultrastructure. *Planta* DOI: https://doi.org/10/1007/s00709-018-01342-2

Muravnik L.E., Kostina O.V., Shavarda A.L. 2016. Glandular trichomes of *Tussilago farfara* (Senecioneae, Asteraceae). *Planta* **244**: 737–752.

Nikolakaki A., Christodoulakis N. 2004. Leaf structure and cytochemical investigation of secretory tissues in *Inula viscosa*. *Bot. J. Linn. Soc*. **144**: 437–448.

Werker E., Fahn A. 1981. Secretory hairs of *Inula viscosa* (L.) Ait. – development, ultrastructure and secretion. *Bot. Gaz.* **142**: 461–476.

SALT TOLERANCE MECHANISMS IN GRASSES WITH SALT EXCRETION

Nuria K. KOTEYEVA[1]***, Elena V. VOZNESENSKAYA***[1]***, Gerald E. EDWARDS***[2]

[1] Komarov Botanical Institute RAS, Saint Petersburg, Russia
[2] Washington State University, Pullman, USA
knouria@mail.ru

About 6% of land area affected by soil salinization that creates serious problems for world agriculture. Improving of salt tolerance in crops is a global challenge for the nearest future. Salt tolerance is a genetically and physiologically complex trait that causes the difficulties in breeding and genetic manipulations in salt-tolerant crops. For engineering the salt tolerance traits in crop, it is crucial to clarify the genetic and specific physiological backgrounds in different plant lineages. Among grasses, about 200 halophyte species were identified with over 70 different independent origins of salt tolerance (Bromham, 2015). About 30 grass species developed effective salt excretion system with one of them, *Oryza (= Porteresia) coarctata*, being close relative to cultivated rice.

The focus of our study was the comparison of salt tolerance mechanisms in grasses with salt excretion evolved in different grass lineages. *Oryza coarctata* is a wild rice species which has high tolerance to salt with traits which are of interest for improving tolerance of rice growing under saline conditions. *Spartina anglica* is a serious invasive species in natural saltmarsh ecosystems, and *Urochondra setulosa*, native to north-eastern Africa and southwestern Asia, grows in coastal sand dunes, salt marshes and

estuaries. The leaf anatomy and ultrastructure of salt glands, pattern of salt excretion, features of gas exchange, accumulation of key photosynthetic enzymes, maintenance of water content, Na^+ and K^+ accumulation, and osmolality along with levels of some osmolytes and betaine aldehyde dehydrogenase expression, were compared in the three species grown without salt, with 200 mM NaCl, and with 200 mM KCl.

Measurements of gas exchange showed that photosynthesis had not been affected by salt treatments. Stomatal conductance decreased under the salt treatments reducing water loss by transpiration with increasing of water use efficiency (WUE). Despite differences in the type of photosynthesis (*S. anglica* and *U. setulosa* are C_4 while *O. coarctata* is a C_3 plant), the three species have a similar leaf anatomy; the adaxial side has distinctive ridges while the abaxial side is flat in *S. anglica* and *O. coarctata* and undulated in *U. setulosa*. All species have salt glands with distinctive difference in their distribution, excretion rates, anatomy and ultrastructure. *S. anglica* and *U. setulosa* have bicellular glands with basal and cap cells, however, *O. coarctata* has unicellular glands. In contrast to a previous report, our results show that the multiple unicellular trichomes in *O. coarctata* are not responsible for salt secretion. All three species accumulate compatible solutes with increasing osmolality but they differ in osmolyte composition and amount.

In summary, *O. coarctata, S. anglica* and *U. setulosa* show high tolerance to salt based on function of photosynthesis, maintenance of leaf water content, synthesis of compatible solutes, and capacity for salt excretion from leaves; but, they have distinct differences in the salt excretion system and accumulation of osmolytes. In three species from different grass lineages, salt tolerance was evolved using similar principle reactions (increase of WUE, accumulation of osmolytes and establishment of salt excreting system) with variable mechanisms of their realization.

References

Bromham L. 2015. Macroevolutionary patterns of salt tolerance in angiosperms. *Ann. Bot*. **115**: 333–341.

MODES OF BARK DILATATION: FUNCTIONAL AND ECOLOGICAL IMPLICATIONS

Ekaterina L. KOTINA[1]***, Alexei A. OSKOLSKI***[1,2]

[1] Komarov Botanical Institute of Russian Academy of Sciences, Saint Petersburg, Russia
[2] University of Johannesburg, Johannesburg, South Africa
elkotina@gmail.com

Dilatation can be defined as transformations of bark in the course of increase in its circumference. Although these processes affect all components of bark, the

diversity of their modes is relatively well-studied only in secondary phloem and, in lesser degree, in cortex (e.g. Evert, 2006; Angyalossy et al., 2016). Dilatational changes of epidermis and periderm remain, however, underexplored. To survey diversity of the dilatation modes, we examined both the macroscopic appearance and anatomical structure of bark on different developmental stages in more than 100 species from 27 angiosperm families.

Tangential stretching of parenchyma cells and/or their anticlinal divisions are the most common ways of dilatation in cortex and secondary phloem. In some taxa as Araliaceae and Fabaceae, these processes occur also in the long-persisting epidermis. Tangential strands of 2–4 cells formed by anticlinal division of epidermal cells are found, for instance, in *Cyclopia galioides* (Fabaceae) and *Plerandra gabriellae* (Araliaceae). In cortex, the formation of schizogenous or rhexigenous intercellular spaces is also common (we observed it in some Apiaceae, Araliaceae, Rosaceae, Rutaceae and some other groups).

In the secondary phloem of most studied species, dilatation is commonly associated with anticlinal divisions of ray cells leading to formation of tangential strands of up to 10 cells, or with tangential stretching of both ray cells and axial parenchyma cells. The presence of dilatation meristem in rays has been reported in some Malvaceae including *Adansonia digitata* (Kotina et al., 2017b). Occasionally, dilatation of secondary phloem is effected by anticlinal divisions of axial parenchyma cells, as we observed it in *Cliffortia* and *Leucosidea* of Rosaceae (Kotina et al., 2017a).

Rough outer surface of mature bark with deep cracks and fissures is usually associated with presence of rhytidome. The rhytidome formation occurs by the successive development of periderms with the isolated tissues (cortex, secondary phloem) in between. These barks have furrowed, scaly or shaggy appearance found in some *Acer* (Sapindaceae), *Cussonia, Schefflera* and *Polyscias* (Araliaceae), *Prunus* (Rosaceae), *Quercus* (Fagaceae), *Tilia* (Malvaceae) and in other trees. Although this mechanism is commonly mentioned in textbooks, it cannot be used to explain the persistence of smooth bark surface stretched in the course of dilatation.

These smooth barks occur in many tree species, e.g. in *Betula* (Betulaceae), *Commiphora* (Burseraceae), *Heteromorpha* (Apiaceae), *Adansonia* (Malvaceae). They do not form a rhytidome, but usually they have a single periderm with prominent phelloderm gradually transformed into pseudocortex. The latter term was proposed by Whitmore (1962a, b) to denote a parenchymatous layer of mixed origin (derived from parenchyma of primary cortex, secondary phloem and periderm) underlying periderm in bark of some Dipterocarpaceae, but it was not used by other researchers. Our observations strongly suggest, however, that a pseudocortex occur in many taxa with smooth bark. Apparently, this layer provides cohesiveness of dilated bark, i.e. its ability to stretch without splitting and rupturing. This function of pseudocortex is also confirmed by the presence of numerous meristematic zones in this layer in mature bark of *Adansonia digitata* (Kotina et al., 2017b).

Smooth barks commonly have greenish subsurface due to the presence of chloroplasts in phelloderm and pseudocortex. Their single periderm with thin translucent phellem is favorable for stem photosynthesis, which would unlikely be possible in bark covered by rhytidome. Stem photosynthesis is considered as an adaptation of deciduous plants to survival in seasonally cold or dry climate (Pearson, Lawrence, 1958; Kotina et al., 2012). This process is significant for the energy balance of the stem, as well as a means of reducing losses attributable to respiration (Foote, Schaedle, 1976).

References

Angyalossy V., Pace M.R., Evert R.F., Marcati C.R., Oskolski A.A., Terrazas T., Kotina E., Lens F., Mazzoni-Viveiros S.C., Angeles G., Machado S.R., Crivellaro A., Rao K.S., Junikka L., Nikolaeva N., Baas P. 2016. IAWA list of microscopic bark features. *IAWA J.* **37**: 517–615.

Evert R.F. 2006. *Esau's Plant anatomy: meristems, cells, and tissues of the plant body – their structure, function, and development.* 3rd ed. Hoboken: John Wiley & Sons.

Foote K.C., Schaedle M. 1976. Physiological characteristics of photosynthesis and respiration in stem of *Populus tremuloides* Michx. *Plant Physiol*. **58**: 91–94.

Kotina E.L., Oskolski A.A., Tilney P.M., van Wyk B.-E. 2017a. Bark and wood anatomy of *Leucosidea* and *Cliffortia* (Sanguisorbeae, Rosaceae). *IAWA J.* **38**: 13–28.

Kotina E.L., Oskolski A.A., Tilney P.M., van Wyk B.-E. 2017b. Bark anatomy of *Adansonia digitata* (Malvaceae). *Adansonia*. Sér. 3. **39**: 31–40.

Kotina E.L., van Wyk B.-E., Tilney P.M., Oskolski A.A. 2012. The systematic significance of bark structure in Southern African genera of tribe Heteromorpheae (Apiaceae). *Bot. J. Linn. Soc*. **169**: 677–691.

Pearson L.C., Lawrence D.B. 1958. Photosynthesis in aspen bark. *Am. J. Bot.* **45**: 383–387.

Whitmore T.C. 1962a. Studies in systematic bark morphology. I. Bark morphology in Dipterocarpacae. *New Phytol.* **61**:191–207.

Whitmore T.C. 1962b. Studies in systematic bark morphology: II. General features of bark construction in Dipterocarpacae. *New Phytol.* **61**: 208–220.

VASCULAR BUNDLE MODIFICATIONS IN NODES OF SELECTED AFRICAN MARANTACEAE SPECIES

Hansjörg KRÄHMER, Regine CLAßEN-BOCKHOFF

Johannes Gutenberg-University, Mainz, Germany

classenb@uni-mainz.de

Vascular bundles in fully developed internodes of climbing African Marantaceae representatives are arranged in characteristic patterns. Bundles of *Haumania, Hypselodelphys* and *Trachyphrynium* species form rings with specific bundle types. One of these rings contains inverted bundles in the genus *Haumania* only (Tomlinson, 1969). This inversion can also be observed at the bases of inflores-

cence branches. Within nodes of African Marantaceae, vascular bundles are heavily augmented. This phenomenon can also be observed within species of the Poaceae family (Kraehmer, 2017, 2019). Also, bundles change directions within nodes. The bundle inversion in *Haumania* species is suspended within nodes and in short shoots. The number of inverted bundles within vegetative stems continuously decreases from the basis to the stem tip. One conclusion of our investigations is that cells in nodes of many monocot species keep their ability to divide and differentiate. As interfaces between leaves and stems, they show very special features.

References

Kraehmer H. 2017. On vascular bundle modifications in nodes and internodes of selected grass species. *Sci. Agric. Bohem*. **48**: 112–121.

Kraehmer H., ed. 2019. *Grasses: Crops, competitors and ornamentals*. Chichester: Wiley-Blackwell, in preparation.

Tomlinson P.B. 1969. Commelinales–Zingiberales. In: Metcalfe C.R. (ed.): *Anatomy of the monocotyledons*. Oxford: Clarendon Press. Vol. 3.

A REVIEW OF EXTRAFLORAL NECTARIES IN PAPILIONOID LEGUMES

Tatiana E. KRAMINA

Lomonosov Moscow State University, Moscow, Russia

tkramina@yandex.ru

Extrafloral nectaries (EFNs) are a common plant-defence trait widespread in vascular plants. EFNs are plant glands secreting nectar and located outside the flower. Weber & Keeler (2013) analyzed records of EFNs published over the last 135 years. EFNs have been reported in 3941 species representing 745 genera and 108 families, about 1–2% of vascular plant species and 21% of families. Foliar nectaries are known in four of 36 fern families, but unknown in gymnosperms. EFNs have not been found yet in early angiosperms and magnoliids. They occur in monocotyledons, but most EFNs are found within eudicots, especially in rosids. Phylogenetic analyses revealed the repeated gain and loss of EFNs across plant clades, especially in more derived dicot families, and imply that EFNs are found in a minimum of 457 independent lineages. The number of unreported cases of EFNs may be comparable to the number of species already reported (Weber, Keeler, 2013). Weber & Keeler (2013) formulated several hypotheses concerning the evolution of EFN such as “EFNs are tropical adaptations”, “EFNs evolve in response to resource availability”, “EFNs are more likely to evolve in vines” that need additional testing.

Biogeographic distribution. EFN-bearing plants occur in a wide range of habitats, mainly in tropics and subtropics, less often in temperate regions. EFNs from desert and other arid land plants are insufficiently studied (Marazzi et al., 2013).

Location on plant. Almost any above-ground plant part can bear EFNs, from vegetative parts such as leaves and stipules, to parts of the inflorescences, and even the outer floral organs not directly involved in pollination (Marazzi et al., 2013). EFN location in Fabales includes leaves, petioles, stipules, stems, pedicels, peduncles or stems of inflorescence, as well as sepals/calyx/perianth/tepals/floral bracts/cataphylls; EFNs located on the last group of organs are sometimes termed 'extrasoral', not 'extrafloral' (Marazzi et al., 2013). EFNs may vary in abundance and distribution on a plant during ontogeny (Marazzi et al., 2013).

Function. EFNs are not directly related to pollination. Ants are their main visitors. The benefits of plants that may be caused by the EFN related activity of ants and other small arthropods are: reducing leaf herbivory and twig destruction, increasing fruit and seed production, reducing of ant visitation to floral nectaries, thereby enhancing the pollination success and reducing seed predation (Bentley, 1977; Koptur, 1979; Guimarães Jr. et al., 2006).

Methods of detection and analysis. The majority of EFN studies include morphological and anatomical analyses; some studies also involve analysis of ultrastructure using SEM and TEM. Additionally, histochemical detection of reducing sugars using Fehling's reagent, measurement of nectar concentration with sugar hand-held refractometers (Díaz-Catelazo et al., 2005) and paper (Davis et al., 1988) or thin-layer chromatography (Paiva, 2009) were applied.

Morphology. EFNs can vary from simple glandular trichomes and cryptic non-structural or structural secretory tissue enclosed within EFN-bearing plant parts, to prominent, complex vascularized or non-vascularized glands on the surface of the EFN-bearing organ (Marazzi et al., 2013). Melo et al. (2010) distinguish two categories of EFNs: 1) substitutive nectaries, which are common structures (e.g., stipules, floral pedicels), that have evolved to function like EFNs; 2) non-substitutive EFNs which are glandular structures that have developed specifically to be EFNs. Substitutive EFNs may indicate a recent evolutionary acquisition (Melo et al., 2010).

Anatomy. In anatomically specialized EFNs, three kinds of tissues can be recognized: the epidermis, the nectary parenchyma, and the subnectary parenchyma (including the vascular bundles branching off from the leaf vasculature). In some EFN-bearing legumes, an additional fourth structure of one or two layers of cells can be observed between the nectary and the subnectary parenchyma (Melo et al., 2010; Marazzi et al., 2013).

TEM ultrastructure of EFNs was studied in several Papilionoideae species, e.g. *Vicia faba* (Davis et al., 1988) and *Erythrina speciosa* (Paiva, 2009). Some similarities in structure of nectaries and patterns of nectar secretion were found

between floral nectaries and EFNs: secretory epidermal cells of structural nectaries possess cell wall ingrowth and developed membrane system (endoplasmic reticulum (ER), dictyosomes, vacuoles); head cells of secretory trichomes have large nuclei, dense cytoplasm with dictyosomes, ER, mitochondria (MT), plastids (PL), and ribosomes (RS); in vascularized nectaries sieve elements and companion cells play significant role in nectar secretion mechanism; cell wall ingrowth was observed in phloem companion cells; both apoplastic and symplastic pathways may be included in nectar secretion. Alternative theories have been proposed to explain nectar secretion mechanism that can be applied to EFNs, i.e. granulocrine theory (Davis et al., 1988; Paiva, 2009) and pressure-driven mass flow mechanism (Vassilyev, 2010).

The legume family (Fabaceae) is known for its diverse interactions with ants and stands out among other plant families, with 30% of the EFN-bearing species (Marazzi et al., 2013).

EFNs in Papilionoideae. EFNs are more common for Caesalpinioideae (incl. Mimosoideae) (EFNs found in 89 of 148 genera) and less common for Papilionoideae, however found in 50 of 503 genera (Marazzi, oral talk on 7ILC, 2018). EFNs in Papilionoideae vary in structure; they can be substitutive or non-substitutive. Several examples of EFNs described in various tribes of Papilionoideae, taken from literature, are presented below. Tribal position of species is given according to Lewis et al. (2005). EFNs are mainly distributed within tribes Vicieae, Phaseoleae, Crotalarieae.

Tribe Vicieae (= Fabeae). In *Vicia faba* EFNs are brown spots on abaxial surface of each stipule (Bhattacharyya, Maheshwari, 1970; Davis et al., 1988; Heneidak, Hasan, 2007). They consist of densely gathered clavate glandular hairs and unicellular hairs, aggregated in shallow depression. Glandular hairs are capitate trichomes consisting of four-celled secretory head, one stalk cell and a basal cell. Both xylem and phloem are present in the stipule beneath the extrafloral nectary (Davis et al., 1988). Similar EFNs were described for *Vicia narbonensis, V. peregrina, V. sativa, V. angustifolia, V. sepium* and *V. grandiflora.* In *Vicia* subgenus *Vicilla* (*V. ervilia, V. montana*), EFNs are absent (Heneidak, Hasan, 2007). In *V. angustifolia*, nectaries were also located on calyx surface.

Tribe Phaseoleae. EFNs are found in *Calopogonium, Canavalia, Erythrina, Galactia, Macroptilium, Phaseolus, Rhynchosia, Vigna* (Bhattacharyya, Maheshwari, 1970; Díaz-Castelazo et al., 2005; Kost, Heil, 2005; Paiva, 2009; Melo et al., 2010; Gonzalez, Marazzi, 2018). The majority of recorded species are from tropical regions.

EFNs located on leaf parts (stipules, stipels, rachis, leaf surfaces) were described in *M. atropurpureum, P. lunatus, E. velutina, Rhynchosia* species. In *M. atropurpureum* and *Rhynchosia* these EFNs are represented by capitate trichomes.

EFNs developing in inflorescences on the nodes, floral pedicels or from aborted floral buds were recorded in *V. candida, V. peduncularis*, *M. prostratum*, *M. atropurpureum, G. latisiliqua, Canavalia rosea, E. velutina.* Anatomical structure of EFNs shaped as swollen scars on abscission site of aborted floral buds: secretory epidermis absent, the central abscission region is modified for nectar secretion and consists of several layers (cell remains of aborted bud, nectary and subnectary parenchyma), vascularized by one or two vascular bundles (Gonzalez, Marazzi, 2018). Substitutive EFNs of *E. velutina* located on leaf rachis and floral pedicels, comprised of a uniseriate epidermis, parenchyma cells, starch storage cavities and vascular bundles randomly arranged in the parenchyma. Exudation occurs through glandular trichomes which are grouped in the EFN secretory region (Melo et al., 2010).

Erythrina speciosa possesses pericarpal nectaries (PNs). PN is represented by a single hyaline trichome that consists of a basal cell, stalk cell(s) and a small secretory multicellular head. The apical stalk cell shows inner periclinal and anticlinal walls impregnated by lipids and lignin and has dense cytoplasm with abundance of MTs and ER. The secretory cells show large nuclei and dense cytoplasm, which predominantly has dictyosomes, rough ER, plastids, MTs and free RS. At the secretory stage, the periplasmic space is prominent and contains secretion residues (Paiva, 2009).

Tribe Crotalarieae. In a pantropical weed *Crotalaria pallida,* EFNs are located in the racemes, at the base of each flower or pod (Guimarães Jr. et al., 2006). In *Crotalaria incana,* EFNs are scars of fallen stipules and aborted buds as well as unicellular trichomes with secretory basal cell (Díaz-Castelazo et al., 2005).

Other tribes. EFNs were also reported in members of tribes Galegeae, Trifolieae, Dalbergieae, Genisteae and Loteae (Bhattacharyya, Maheshwari, 1970), however without detailed description. Extrafloral glands are common in *Lotus* and related genera, sometimes they are treated as EFNs (Magne et al., 2018), but their structure and secreted substances are unknown. EFNs are apparently absent in tribes Swartzieae, Sophoreae, Podalyrieae (Bhattacharyya, Maheshwari, 1970).

The study is supported by grant No 19-04-00883a from the Russian Foundation of Fundamental Research.

References

Bentley B.L. 1977. Extrafloral nectaries and protection by pugnacious bodyguards. *Ann. Rev. Ecol., Evol. Syst*. **8**: 407–427.

Bhattacharyya B., Maheshwari J.K. 1970. Studies on extrafloral nectaries of the Leguminales. I. Papilionaceae, with a discussion on the systematics of the Leguminales. *Proc. Indian Acad. Sci*. **37B**: 11–30.

Davis A.R., Peterson R.L., Shuel R.W. 1988. Vasculature and ultrasculpture of the floral and stipular nectaries of *Vicia faba* (Leguminosae). *Can. J. Bot*. **66**: 1435–1448.

Díaz-Castelazo C., Rico-Gray V., Ortega F., Angeles G. 2005. Morphological and secretory characterization of extrafloral nectaries in plants of Coastal Veracruz, Mexico. *Ann. Bot*. **96**: 1175–1189.

Gonzalez A.M., Marazzi B. 2018. Extrafloral nectaries in Fabaceae: filling gaps in structural and anatomical diversity in the family. *Bot. J. Linn. Soc*. **187**: 26–45.

Guimarães Jr. P.R., Raimundo R.L.G., Bottcher C., Silva R.R., Trigo J.R. 2006. Extrafloral nectaries as a deterrent mechanism against seed predators in the chemically protected weed *Crotalaria pallida* (Leguminosae). *Aust. Ecol*. **31**: 776–782.

Heneidak S., Hasan A.E. 2007. Morphological and anatomical studies of floral and extrafloral nectaries in some *Vicia* taxa (Fabaceae). *Int. J. Bot*. **3**: 329–341.

Koptur S. 1979. Facultative mutualism between weedy vetches bearing extrafloral nectaries and weedy ants in California. *Am. J. Bot*. **66**: 1016–1020.

Kost C., Heil M. 2005. Increased availability of extrafloral nectar reduces herbivory in Lima bean plants (*Phaseolus lunatus*, Fabaceae). *Basic Appl. Ecol*. **6**: 237–248.

Lewis G., Schrire B., Mackinder B., Lock M. (Eds.) 2005. *Legumes of the World*. Kew: Royal Botanic Gardens.

Magne K., George J., Tornero A.B., Broquet B., Madueño F., Andersen S.U., Ratet P. 2018. *Lotus japonicus* NOOT-BOP-COCH-LIKE1 is essential for nodule, nectary leaf and flower development. *Plant J*. **94**: 880–894.

Marazzi B., Bronstein J.L., Koptur S. 2013. The diversity, ecology and evolution of extrafloral nectaries: current perspectives and future challenges. *Ann. Bot*. **111**: 1243–1250.

Melo Y., Machado S.R., Alves M. 2010. Anatomy of extrafloral nectaries in Fabaceae from dry-seasonal forest in Brazil. *Bot. J. Linn. Soc*. **163**: 87–98.

Paiva E.A.S. 2009. Ultrastructure and post-floral secretion of the pericarpial nectaries of *Erythrina speciosa* (Fabaceae). *Ann. Bot*. **104**: 937–944.

Vassilyev A.E. 2010. On the mechanisms of nectar secretion: revisited. *Ann. Bot*. **105**: 349–354.

Weber M.G., Keeler K.H. 2013. The phylogenetic distribution of extrafloral nectaries in plants. *Ann. Bot*. **111**: 1251-1261.

PERICARP ANATOMY IN SOME SPECIES OF THE TRIBE SILENEAE DC. (CARYOPHYLLACEAE, *VISCARIA* GROUP)

Tatyana I. KRAVTSOVA[1]**, *Yana V. BOLOTOVA***[2]

[1] Komarov Botanical Institute of Russian Academy of Sciences, Saint Petersburg, Russia
[2] Amur Branch of the Botanical Garden-Institute, FEB RAS, Blagoveshchensk, Russia
TKravtsova@binran.ru

Molecular phylogenetic studies of the tribe Sileneae using different molecular markers of nuclear and chloroplast origin, starting with the work of Oxelman & Lidén (1995), revealed the following clades: basal clades *Agrostemma*, *Eudianthe*, *Petrocoptis*, the *Viscaria* group, the *Lychnis* group, and the terminal one, the largest *Silene* group, including two subclades. *Viscaria* group included initially four

morphologically distinct small genera: *Atocion* Adans., *Ixoca* Raf. (= *Heliosperma* (Reichb.) Reichb.), *Minjaevia* Tzvel. and *Viscaria* Bernh. Later, the position of *Ixoca* within the group was shown to be erroneous (Fraiman, Oxelman 2007; Mikhaylova, 2016; etc.). The close relationships of the genera in *Viscaria* clade is very doubtful in the opinion of many botanists, sister relationships between *Atocion* and *Viscaria* is one of the unexpected results obtained by Oxelman & Lidén (1995). This result can be considered as an example of glaring contradictions between morphology and molecular phylogeny, which are not uncommon in modern botany. There is a significant variation within the *Viscaria* group in several carpological characters used in Sileneae taxonomy to distinguish genera: carpel and capsule teeth number; septa presence or absence; septicidal or loculicidal dehiscence. According to many authors (for instance, Schishkin, 1936; Chowdhuri, 1957), the genera *Atocion* and *Minjaevia* are included into *Silene* s. l., in the sections *Compactae* (Boiss.) Schischk. and *Nanosilene* Otth (or *Rupifraga* Otth), respectively, while *Viscaria* sometimes is considered to be related to *Lychnis*.

The anatomical structure of fruits in the species constituting the *Viscaria* group, as well as in the whole tribe Sileneae, is presently insufficiently studied, mainly only in the teeth area (Weberbauer, 1898; Guttenberg, 1971). The aim of our study was to examine the pericarp structure in species included in *Viscaria* group (*A. armeria*, *M. rupestris*, *V. vulgaris*) and in two *Ixoca* species (*I. arcana*, *I. carpatica*) to consider the taxonomic significance of pericarp characteristics. The accepted taxonomy of the group corresponds to the classification of Tzvelev (2001).

Mature fruits (capsules) of 15 specimens from LE, KW, Botanical Museum BIN RAS, and those collected in nature were studied using light microscope (AxioImager A1 Carl Zeiss) and SEM (Jeol JSM-6390LA). Sections of the pericarp were prepared using freezing microtome. Histochemical reactions for lignin, cutin, silica were carried out with phloroglucinol and sulfuric acid, Sudan IV, hydrofluoric acid.

The observations show that the pericarp is composed by small number of cell layers. It has a common structural plan and is differentiated into exo-, meso-, and endocarp, the outer sclerenchymatous part is mainly two-layered. The mesocarp, developing from the mesophyll, includes the outer sclerenchymatous and the inner parenchymatous zones. Indistinctly visible membranous, structureless endocarp consists of compressed cells of inner epidermis with slightly thickened outer tangential walls.

Several pericarp regions were comparatively observed: usually thickened teeth region, a region of large-celled exocarp beneath the teeth, a middle small-celled region. In the capsule teeth, the exocarp sclereids are radially elongated in most genera, with the strongly U-thickened walls. The thickenings of the radial walls have the form of transversal (in relation to fruit) strands. Mesocarp sclereids, located in 1–2 layers, are large and longitudinally elongated; they are radially elongated at

the ends of teeth. Beneath the teeth, the pericarp is thinner; its cell altitude and cell wall thickness gradually decrease towards the capsule base. In the capsule middle, the outer mesocarp zone is represented by lignified parenchyma.

The exocarp sclereids differ in shape, orientation, shape of the cell wall thickenings between species. Their three main types were distinguished beneath the teeth:

1) in *Atocion* and *Minjaevia,* large, 30–60 μm in height, forming a palisade layer, columnar or cuboid, in *A. armeria,* mushroom-shaped with convex outer wall, in *M. rupestris,* with poorly convex outer wall, in section weakly expressed lenticular to horseshoe. They considerably exceed the height of the mesocarp sclereids, with outer tangential and radial walls impregnated with silica.

2) in *Viscaria,* small, 20–40 μm in height, not forming a palisade layer, for the most part low columnar or cuboid, less than or equal to the height of mesocarp sclereids, with poorly convex outer tangential wall, poorly expressed lenticular to horseshoe or arcuate in section, apparently not impregnated with silica.

3) in *Ixoca,* low, 15–30 μm in height, longitudinally elongated, from polygonal to linear, fiber- or bone-like, less than or equal to the height of the mesocarp sclereids.

The mesocarp sclereids are either mostly prosenchymatous, longitudinally elongated (*Atocion*, *Minjaevia*, *Ixoca*), or broader, both prosenchymatous and broadly oval, the same height as in the exocarp (*Viscaria*).

The results obtained show that despite the differences in the capsule morphology and pattern of its opening in *Atocion* and *Minjaevia* on the one hand, and in *Viscaria* on the other, there are many similar features in their pericarp anatomy and micromorphology which support the close relationship of these taxa: colliculate primary exocarp sculpture; thin few-layered pericarp; two-layered sclerenchyma both on the capsule top and in the middle; small structural differences between different parts of the fruit, related mainly to cell height and cell walls thickness; the outer mesocarp layer, represented in the capsule middle by lignified parenchyma. Two sclereid layers in the teeth region distinguish this group from most of Sileneae having multicellular teeth.

The greatest similarity in the pericarp structure, as in the capsule morphology, is found between *Atocion armeria* and *Minjaevia rupestris*. Both have a large-celled region in the exocarp beneath the teeth; the exocarp sclereids exceed considerably the mesocarp sclereids in height and have a larger lumen. Silica locality in exocarp outer cell walls is however different in two species. The mushroom-shaped exocarp sclereids are recognized to be a distinctive character of *Atocion armeria*. *Minjaevia rupestris* (= *Silene rupestris*) was included recently (Fraiman et al., 2013) in the genus *Atocion* as *A. rupestre* (L.) Oxelman, that is consistent with our findings.

Structural differences and the different chemical composition of the pericarp mark out *Viscaria vulgaris* in the group studied. The lack of palisade layer, not im-

pregnated with silica cell walls of the exocarp, and weak differentiation of pericarp sclerenchyma into two different cell layers determine less advanced pericarp structure in *Viscaria* in comparison with *Atocion* and *Minjaevia*. The distinctive features also include the abrupt transition from the large-cellular pericarp in teeth region to small-cellular pericarp beneath, the absence of the large-celled pericarp region beneath the teeth. The presence of the third, discontinuous inner lignified layer in the teeth can be a sign of teeth transitional (to *Silene*) structure in *Viscaria*.

It should be noted that for arctic-alpine species *Minjaevia rupestris*, unlike other species studied, a prominent infraspecific variation of both exocarp micromorphology and anatomical structure is characteristic. The exocarp surface sculpture may be a colliculate, reticulate-colliculate, reticulate or intermediate; the exocarp sclereids also differ in the form of wall thickenings between specimens.

Our results confirm the lack of close relationships between *Ixoca* and the genera of the *Viscaria* group. The genus is peculiar in the striate and reticulate-striate exocarp micromorphology, and the structure of exocarp sclereids which are longitudinally elongated, often osteosclereids and fiber-like sclereids having secondary thickenings of longitudinal radial walls. It differs from other species in similar form and orientation of the sclereids in both sclerenchyma layers. The capsule teeth also have a specific structure: though the sclerenchyma is two-layered (a common feature for other genera of the *Viscaria* group), the exocarp sclereids are tangentially (not radially) elongated, they have weaker wall thickenings. Such a teeth structure, according to Weberbauer (1898), is also found in *Petrocoptis* and members of certain genera (*Arenaria*, *Moehringia*) of the tribe Alsineae.

The investigation was carried out using equipment of Core Centre "Cell and Molecular Technology in the Plant Science" at the Komarov Botanical Institute (St. Petersburg). The authors appreciate the curators of Herbaria LE, KW and Botanical Museum LE, from which the material was received, L.A. Kartseva for technical assistance in SEM studies. The project was supported by the Russian Foundation for Basic Research (grant No. 16-34-50028 mol_nr).

References

Chowdhuri P.K. 1957. Studies in the genus *Silene*. *Notes R. Bot. Gard. Edinburgh*. **22**: 221–278.

Frajman B., Oxelman B. 2007. Reticulate phylogenetics and phytogeographical structure of *Heliosperma* (Sileneae, Caryophyllaceae) inferred from chloroplast and nuclear DNA sequences. *Mol. Phyl. Evol.* **43**: 140–155.

Frajman B., Thollesson M., Oxelman B. 2013. Taxonomic revision of *Atocion* and *Viscaria* (Sileneae, Caryophyllaceae). *Bot. J. Linn. Soc.* **173**: 194–210.

Guttenberg H. von. 1971. Bewegungsgewebe und Perzeptionsorgane. In: Zimmermann W., Carlquist S., Ozenda P., Wulff H.D. (Hrsg.): *Handbuch der Pflanzenanatomie*. 2. Aufl. Berlin; Stuttgart: Gebrüder Borntraeger. Bd. **5**. T. 5. S. 1–332.

Mikhailova Yu.V. 2016. Taxonomic position and phylogeography of the arctic-alpine species *Silene acaulis* (L.) Jacq. (Caryophyllaceae). Ph. D. Thesis. St. Petersburg. [In Russian]

Oxelman B., Lidén M. 1995. Generic boundaries in the tribe *Sileneae* as inferred from nuclear rDNA sequences. *Taxon* **44**: 525–542.

Schishkin B.K. 1936. Caryophyllaceae, Lychnideae. In: Komarov V.L. (ed.): *Flora of the USSR*. Moscow, Leningrad: Acad. Sci. USSR. V. **6**. P. 573–730. [In Russian]

Tzvelev N.N. 2001. On genera of the tribe Sileneae DC. (Caryophyllaceae) in Eastern Europe. *Nov. Syst. Pl. Vasc.* **33**: 90–113. [In Russian]

Weberbauer A. 1898. Beiträge zur Anatomie der Kapselfrüchte. *Bot. Centralbl.* **73**: 54–59, 97–105, 135–142, 161–168, 193–202, 250–257, 296–302.

ANATOMICAL STUDIES IN LIVERWORTS AND HORNWORTS FROM NORTHERN WESTERN GHATS OF INDIA

Rajendra A. LAVATE[1]***, Vinod B. SHIMPALE***[2]***, Sachin M. PATIL***[3]

[1] Raje Ramrao Mahavidhyalaya, Jath, India
[2] The New College, Kolhapur, India
[3] The Maharaja Sayajirao University of Baroda, Vadodara, India
bryoraj@gmail.com

Liverworts and hornworts are small terrestrial plants that occur closely packed together in mats or cushions and found in all habitats and climatic conditions except marine environment. Usually they are most common in rainy and humid areas. However, they give a preference for microclimate niches such as moist shaded ground, moist rocks, bogs, rock crevices, barks and the vicinity of small shady springs. Taxonomic studies of liverworts and hornworts have undergone incredible innovations, many new species and records have been reported during the last few decades from worldwide. In India there have been few comprehensive taxonomic works on liverworts and hornworts *viz*., Kashyap (1929, 1932), Srivastava & Udar (1975), Asthana & Srivastava (1991), Bapana & Kachroo (2000a,b), Singh (2002), Nair et al. (2005), Chaudhary et al. (2006, 2008), Singh & Nath (2007), Singh & Singh (2009), Dey & Singh (2012), Daniels & Daniel (2013), Sandhya Rani et al. (2014).

The liverworts and hornworts with large and distinctive thalli are identified often quickly and with more confidently than the smaller forms. But it is a difficult task for amateurs to identify the deceive patches of liverworts and hornworts in the field because most of the gametophytic thalli are looking alike.

Gametophytes and sporophytes of liverworts and hornworts are playing an important role in their identification and classification. Both fresh as well as dried sporophytic plant specimens greatly assist identification and classification. The expert bryologists can identify many bryophytes at both genus and species level after casual examinations by using hand lenses, dissecting or compound microscopes. For the identification and classification of thalloid liverworts, shape of the

gametophyte, the internal anatomy and cell contents in the thalloid species and the position of the sex organs and their protective structures as well as anatomical features of the sporophytes' seta, ornamentation of sporangial jackets and spores and structure of elaters are important. While for the identification and classification of leafy liverworts, these same external and internal features, in addition to leaf arrangement and the shape, cellular detail, size, colour, number, distribution and chemical composition of oil bodies and the position and branching patterns of rhizoids are also important. Again, for the identification and classification of hornworts, both the thallus structure especially the anatomy and cell contents as well as the sporophyte (containing the sporangial wall, the spores and their ornamentation, and sterile cells intermixed with spores) and the structure of the sterile cylinder (if present) in the sporangium are important.

The present investigation deals with the study of anatomical details of vegetative and reproductive structures of 42 liverworts and hornworts from the Northern Western Ghats of India especially from Kolhapur District. Among these taxa 32 species belonging to 15 genera and 11 families are liverworts while 10 species belonging to 4 genera and 2 families are hornworts.

References

Asthana A.K., Srivastava S.C. 1991. Indian hornworts (A taxonomic study). *Bryophyt. Bibliot.* **42**: 1–158.

Bapana K.R., Kachroo P. 2000a. *Hepaticology in India*. I. Delhi: Himanshu Publ.

Bapana K.R., Kachroo P. 2000b. *Hepaticology in India*. II. Delhi: Himanshu Publ.

Chaudhary B.L., Sharma T.P., Sanadhya C. 2006. *Bryophyte flora of Gujarat (India).* Udaipur: Himanshu Publications.

Chaudhary B.L., Sharma T.P., Bhagora F.S. 2008. *Bryophyte flora of North Konkan, Maharashtra (India).* Udaipur, New Delhi: Himanshu Publ.

Daniels A.E.D., Daniel P. 2013. *The bryoflora of the Southernmost Western Ghats, India.* Dehra Dun: Bishen Singh Mahendra Pal Singh.

Dey M., Singh D.K. 2012. *Epihyllous liverworts of Eastern Himalaya*. Kolkata: Bot. Sur. of India.

Kashyap S.R. 1929. *Liverworts of the Western Himalayas and the Panjab Plain I*. Lahore: Univ. Punjab.

Kashyap S.R. 1932. *Liverworts of the Western Himalayas and the Panjab Plain II*. Lahore: Univ. Punjab.

Nair M.C., Rajesh K.P., Madhusoodanan P.V. 2005. *Bryophytes of Wayanad in Western Ghats.* Kozhikode: Malabar Natural History Society.

Sandhya Rani S., Sowghandika M., Nagesh K.S., Susheela B., Pullaiah T. 2014. *Bryophytes of Andhra Pradesh*. Dehradun: Bishen Singh Mahendra Pal Singh.

Singh A. P., Nath V. 2007. *Hepaticae of Khasi and Jaintia Hills: Eastern Himalayas.* Dehradun: Bishen Singh Mahandrapal Singh.

Singh D.K. 2002. *Notothylaceae of India and Nepal. (A morpho-taxonomic revision).* Dehra Dun: Bishan Singh Mahendra Pal Singh.

Singh S.K., Singh D.K. 2009. *Hepaticae and Anthocerotae of Great Himalayan National Park and its environs (HP), India.* Kolkata: BSI.

Srivastava S.C., Udar R. 1975. Taxonomy of Indian Metageriaceae: a monograph. *New Bot.* **2**: 1–57.

HOMOLOGY AND FUNCTIONS OF INNER STAMINODES IN THE BEETLE-POLLINATED FLOWERS OF *ANAXAGOREA JAVANICA*

Bingxin LI*, *Fengxia XU

South China Botanical Garden of Chinese Academy of Sciences, Guangzhou, China

libingxin14@scbg.ac.cn

The Annonaceae is a pantropical family comprising 107 genera and about 2400 species, which is the most species-rich group of the Magnoliales and belongs to the largest families of the basal angiosperms (APG IV, 2016; Guo et al., 2017). In Annonaceae, outer staminodes were found in *Popowia* (Decraene, Smets, 1990), *Uvaria* (Van Heusden, 1992), *Xylopia*, *Orophea* (Keßler, 1988) and *Pseuduvaria* (Su et al., 2008); while the inner staminodes were only reported in *Anaxagorea* (Maas, Westra, 1985) and *Xylopia* (Van Heusden, 1992). The only one genus in Anaxagoreoideae, *Anaxagorea*, has been supported as the basic genus of Annonaceae (Doyle, Le Thomas, 1994, 1996; Sauquet et al., 2003). Studies combining morphological and molecular analysis suggest that some characters in *Anaxagorea*, as the sister to the rest of the Annonaceae, e.g. flaky stamens, monad pollen, and inner staminodes are primitive and homologous features associated with species in Eupomatiaceae, Degeneriaceae and Himantandraceae (Scharaschkin, Doyle 2005, 2006). The presence of the inner staminodes may be plesiomorphy within Magnoliales with a loss in Annonaceae, except for in *Anaxagorea* and *Xylopia* (Doyle, Endress, 2010, 2011). Therefore, the study of morphology and pollination function of the inner staminodes in *Anaxagorea* is significant to understanding the evolution of floral structure and pollination ecology in Annonaceae. In order to elucidate the pollination function of the inner staminodes, we documented floral phenology and visitors, and contrastively analyzed the content of exudates in inner staminodes and stigma of *Anaxagorea javanica* at pistillate and staminate phase, respectively. The floral vascularization and the anatomy and histochemical tests of the inner staminodes, stamens and carpels are compared to explain the homology of the inner staminodes.

Bisexual flowers of *A. javanica* are protogynous. At the pistillate phase, these inner staminodes are bent toward the tepals away from the pistils at a right angle, such that beetles penetrating the pollination chamber are canalized towards the region of the carpels with receptive stigmas. At the staminate phase, these staminodes incline towards the carpels, sometimes growing a bit and becoming longer and then they even partly cover the stigmas, making the way free for the beetles to penetrate further down into the region of the stamens. Through this mechanism, these inner staminodes act as a physical barrier preventing autogamy.

Fig. 1. Floral phenology of *A. javanica* during anthesis.
a – petals of *A. javanica* slightly opened. b – nitidulid beetles visited on petals at pistillate phase.
c – inner staminodes bent towards the stamens away from pistils at pistillate phase.
d – flower of *A. javanica* at interim phase.
e – inner staminodes commence to move to bent toward pistils at interim phase.
f – flower of *A. javanica* at the beginning of staminate phase.
g – petals widely opened at the end of staminate phase.
Inside the flower, there are several *Colopterus* spp. (Nitidulidae) dusted with pollen.
h – inner staminodes curved over the stigmas at staminate phase.
i – petals, stamens and inner staminodes begin to abscise from the receptacles.
C – carpel, S – stamen, St – staminode.

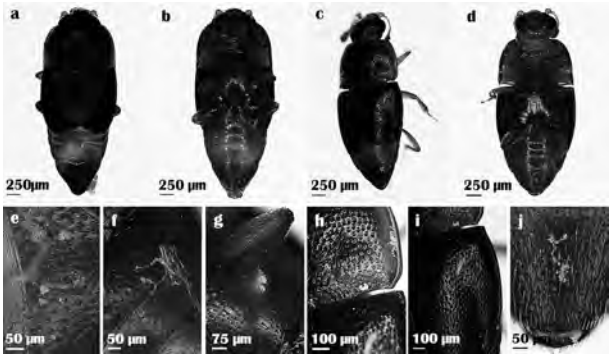

Fig. 2. Microphotographs of the two putative and most important pollinators.
a, b, e–g – *Colopterus* spp. (Nitidulidae). a – dorsal view. b – ventral view.
e–g – detail of pollen stick on the abdomen and legs of *Colopterus* spp. c, d,
h–j – *Epuraea* spp. (Nitidulidae). c – dorsal view. d – ventral view.
h–j – detail of pollen stick on the abdomen and legs of *Epuraea* spp.

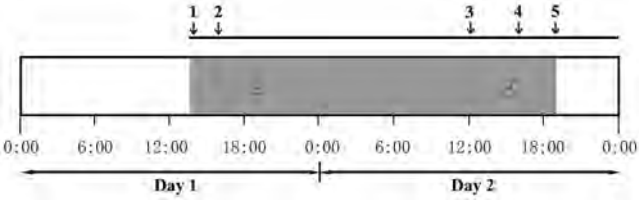

Fig. 3. Timing of anthesis of both morphs of *A. javanica* (Annonaceae):
1 – flowers spreading their petals. 2 – initiation of scent production.
3 – initiation of staminate stage. 4 – arrival of pollinators.
5 – end of the staminate stage.

The sections of flowers of *A. javanica* indicate that the vasculature of the inner staminodes is derived from the basal traces of the free stamen bundles, and then the bundles from inner staminodes fused with middle bundles of the carpels.

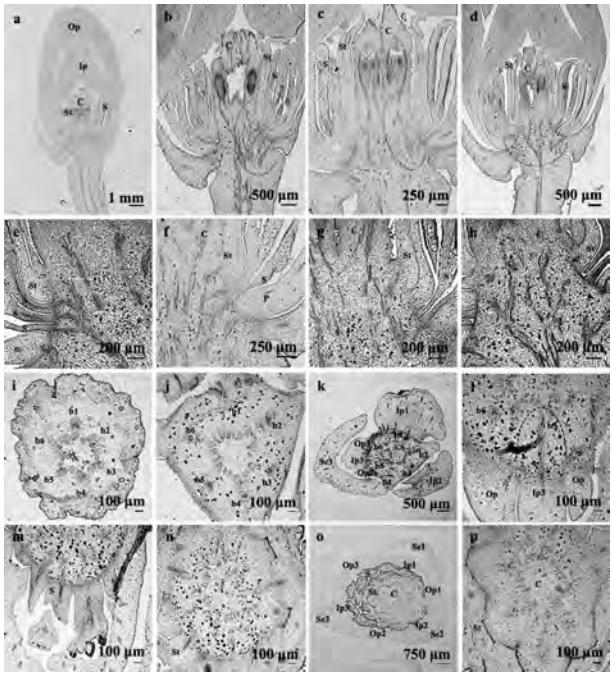

Fig. 4. The floral vasculature of *A. javanica*.
a–h – longitudinal microtome sections of *A. javanica*. a – whole floral vasculature.
b–d – vasculature of stamens, staminodes and carpels. e–h – details of the origin
of vascular bundles, showing the stamens and staminodes of common origin.
i–p – consecutive transverse sections of the floral vasculature from base to apex.
i – section through pedicel, showing stele.
j – base of receptacle, showing six groups of vascular bundles.
k, l – position where the inner petals are connected to receptacle, showing median bundles.
m–p – vasculature of stamen, staminodes, and carpels not fused
with the perianth cortical vascular system.
B – bundle, C – carpel, Ip – inner petal, Op – outer petal,
S – stamen, Se – sepal, St – staminode.

Therefore, the inner staminodes were suggested to have originated from the stamens. The long and narrow inner staminodes lack thecae, which is different with the laminar fertile stamens. The cross-section of the inner staminode is sub-rotund and consists of epidermis, cortex and one large vascular bundle located in central region, which is very similar to that of the filament of the fertile stamens. The structure of glandular hairs is different between those on the inner staminodes and stigmas: the distal part of the inner staminodes is densely covered with long uniseriate glandular hairs; while the stigmas are densely covered by filamentous and glandular hairs. The content of the exudates in the inner staminodes and stigmas is similar (Table); both contain proteins and lipids, without starches. Therefore, we speculated that the glandular secretion in the inner staminodes might be homologous with the stigmatic exudate, and the inner staminodes are transitional structures that grade between the stamens and pistils.

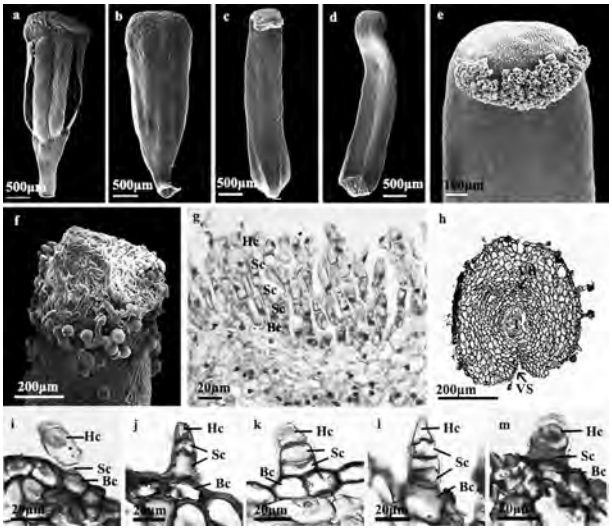

Fig. 5. Floral structures
under scanning electron microscope and light microscope.
a – stamen from dorsal side. b – stamen from ventral side. c – staminode from dorsal side.
d – staminode from ventral side. e – apical part of the inner staminode densely
covered by long uniseriate glandular hairs.
f – cylindrical stigma densely covered by filamentous and glandular hairs.
g – longitudinal microtome section of the apical part of inner staminode,
glandular hairs contain one basal cell, one to three stalk cells and one head cell.
h – cross-section of the stigma. i–l – capitate trichomes with 1 or 2 basal cells,
1–3 stalk cells and 1 head cell.
m – peltate trichomes with 1 basal cell, 1 stalk cell and multicellular head.
Bc – basal cell, Hc – head cell, I – infillings, Sc – stalk cell,
VB – vascular bundle, VS – ventral suture.

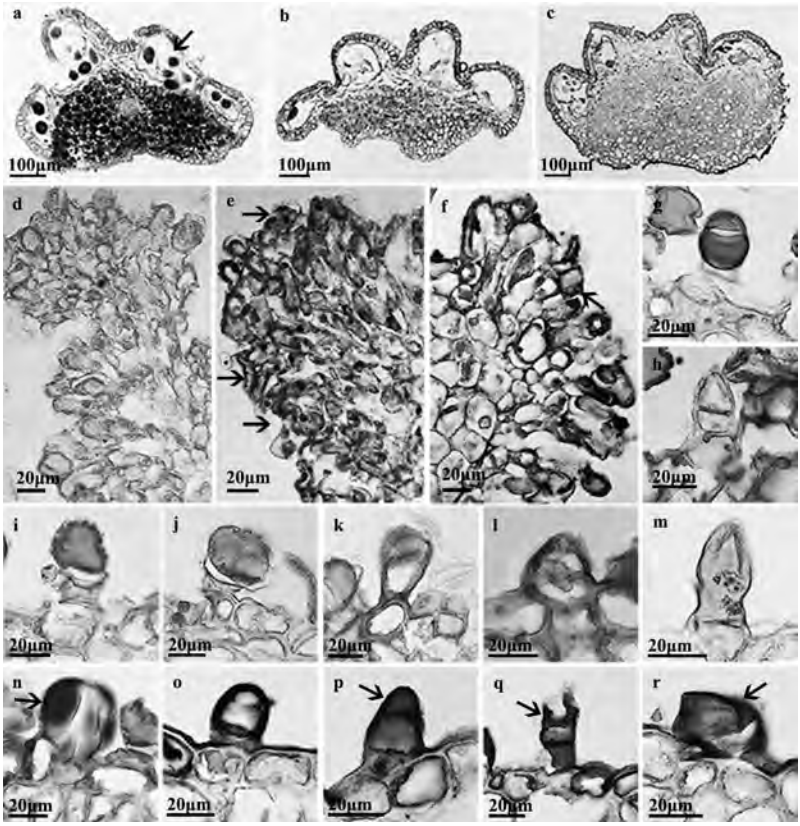

Fig. 6. Histochemical examination of stamens, staminodes, and stigma glandular hairs under light microscope.
a – stamens stained by iodine-potassium iodide showed large amounts of starch (*arrow*).
b – stamens stained by mercury bromophenol blue showed little protein.
c – pollen wall stained by Sudan black showed total lipids.
d – glandular hairs of staminodes were negative to iodine-potassium iodide.
e – glandular hair on staminode top stained by mercury bromophenol blue showed rich proteins (arrows).
f – glandular hair on staminodes stained by Sudan black showed small amounts of total lipids (*arrow*).
g–j – capitate glandular hairs on stigma were negative to iodine-potassium iodide.
k–m – capitate trichomes were negative to mercury bromophenol blue.
n – peltate trichome head stained by mercury bromophenol blue showed rich proteins (*arrow*). o–r – subcuticular space of capitate trichomes and peltate trichomes stained by Sudan black showed total lipids (*arrows*).

Table 1. Amino acid (AA) composition of the stigmatic exudate of inner staminodes and stigmas

Amino acid	Pistillate phase (μg/g)		Staminate phase (μg/g)	
Essential AAs	Inner staminodes	Stigmas	Inner staminodes	Stigmas
Threonine	440	34.5	91	186.3
Leucine	182.5	119.5	138.5	102.8
Histidine	111	23	48	10.3
Isoleucine	811	9	105	77.8
Valine	148.5	35	106.5	33.3
Phenylalanine	99.5	51	70	26.2
Methionine	142	341	20	2.2
Arginine	46.5	104	119	10.7
Lysine	79.5	48	81.5	37.7
Non-essential AAs				
Alanine	902.5	542	946.5	48
Serine	711	271	360	246.2
Tyrosine	493	109	306	203.3
Urea	173	61.5	40	316.8
Glutamic acid	330	131	55	90.83
γ-aminobutyric acid	403.5	220	175	148
Asparagine	1549	85.5	244.5	87.3
Phosphoserine	67.5	76.5	165.5	135
Aspartic acid	205	60.5	150	77.3
Glycine	41.5	11.5	27	8.7
α-aminobutyric acid	45.5	1	4.5	1.7
Cystine	93	4	5	10.8
β-aminoisobutyric acid	11.5	13.5	6.5	35.5
β-alanine	5.5	23.5	4.5	27.3
Ornithine	10.5	76	126.5	80.5
Taurine	58	21	19	7.5
Phosphorus ethanolamine	80	121	69	20.8
α-Amino-adipic acid	77	161.5	7	4.3
Citrulline	10	52.5	5	0.2
3-methyhistidine	164.5	28.5	1	26.7
1-methyhistidine	25.5	104	2.5	
Carnosine hydroxyproline	59	518.5	13	56.8
Proline		136		40
Total AAs	7576.5	3594.5	3512.5	2161.1

Either total amino acids or essential amino acids in these exudates of the inner staminodes are much higher than in the stigma at pistillate phase (Table). It indicates that the abundant proteins of the exudates of the inner staminodies can be related to the energy needs for nitrogen of flower visitors, and reduce the depletion of stigma mucus by pollinators at pistillate phase. There is obviously reducing of the total amino acids content in the inner staminodes during anthesis, and the change of total amino acid content is adaptive and correspond to nitidulid beetle activities, which crawl from the region of the carpels at pistillate stage down to the dehisced stamens at staminate stage.

Our study demonstrated that the inner staminodes are transitional structures that grade between the stamens and pistils, and function as physical barrier preventing autogamy and providing nutrient-rich food source for pollinators in *A. javanica*.

References

APG IV. 2016. An update of the Angiosperm phylogeny group classification for the orders and families of flowering plants: APG IV. *Bot. J. Linn. Soc.* **181**: 1–20.

Decraene L.P.R., Smets E. 1990. The floral development of *Popowia whitei* (Annonaceae). *Nord. J. Bot.* **10**: 411–420.

Doyle J.A., Endress P.K. 2010. Integrating Early Cretaceous fossils into the phylogeny of living angiosperms: Magnoliidae and eudicots. *J. Syst. Evol.* **48**: 1–35.

Doyle J.A., Endress P.K. 2011. Tracing the evolutionary diversification of the flower in basal angiosperms. In: Ronse De Craene L.P., Wanntorp L. (eds.): *The rediscovery of floral morphology in phylogenetics*. Cambridge: Cambridge Univ. Press. Systematics Association Special Volume Series **80**: 85–117.

Doyle J.A., Le Thomas A. 1994. Cladistic analysis and pollen evolution in Annonaceae. *Acta. Bot. Gallica* **141**: 149–170.

Doyle J.A., Le Thomas A. 1996. Phylogenetic analysis and character evolution in Annonaceae. *Bull. Mus. Natn. Hist. Nat. Sect. B. Adansonia* **18**: 279–334.

Guo X., Tang C.C., Thomas D.C., Couvreur T.L.P., Saunders R.M.K. 2017. A mega-phylogeny of the Annonaceae: taxonomic placement of five enigmatic genera and support for a new tribe, Phoenicantheae. *Sci. Rep.* **7**: 7323.

Keßler P.J.A. 1988. Revision der Gattung *Orophea* Blume (Annonaceae). *Blumea* **33**: 1–80.

Maas P.J.M., Westra L.Y.T. 1985. Studies in Annonaceae. II. A monograph of the genus *Anaxagorea* A. St. Hil. Part 2. *Bot. Jahrb. Syst.* **105**: 145–204.

Sauquet H., Doyle J.A., Scharaschkin T., Borsch T., Hilu K.W., Chatrou L.W., Le Thomas A. 2003. Phylogenetic analysis of Magnoliales and Myristicaceae based on multiple data sets: implications for character evolution. *Bot. J. Linn. Soc.* **142**: 125–186.

Scharaschkin T., Doyle J.A. 2005. Phylogeny and historical biogeography of *Anaxagorea* (Annonaceae) using morphology and non-coding chloroplast sequence data. *Syst. Bot.* **30**: 712–735.

Scharaschkin T., Doyle J.A. 2006. Character evolution in *Anaxagorea* (Annonaceae). *Am. J. Bot.* **93**: 36–54.

Su Y.C., Smith G.J., Saunders R.M.K. 2008. Phylogeny of the basal angiosperm genus *Pseuduvaria* (Annonaceae) inferred from five chloroplast DNA regions, with interpretation of morphological character evolution. *Mol. Phyl. Evol.* **48**: 188–206.

Van Heusden E. 1992. Flowers of Annonaceae: morphology, classification, and evolution. *Blumea* **7**: 1–218.

FLOWER AND FRUIT MORPHOLOGY AND ANATOMY OF THE AUSTRALIAN SPECIES OF *TRIGLOCHIN* (JUNCAGINACEAE)

Ingrid E. LOCK[1], ***Terry D. MACFARLANE***[2], ***Dmitry D. SOKOLOFF***[1]

[1] Lomonosov Moscow State University, Moscow, Russia
[2] Western Australian Herbarium, Perth, Australia

lock.ingrid@gmail.com

One of the centres of *Triglochin* species diversity is in Australia (Aston, 2011; von Mering, Kadereit, 2015). Fruit morphology plays a key role in systematics of the genus, but data on comparative fruit anatomy and on the correlations between the flower and fruit morphology are insufficient, especially for the Australian species. We present new data on flowers and fruits of some Australian species of *Triglochin* (*T. isingiana, T. mucronata, T. minutissima, T. longicarpa*). Like most other Australian species of the genus these are short-lived, sometimes small-sized annuals.

The studied species have many-flowered closed spikes (more than 20 flowers per inflorescence in *T. longicarpa*) or few-flowered closed racemes (two to five flowers in *T. isingiana*; about seven flowers in *T. minutissima* and usually ten to twelve flowers in *T. mucronata*). The flowers are ebracteate and spirally arranged. The terminal flower is polysymmetric. The lateral flowers are monosymmetric. Upper lateral flowers are developmentally retarded relative to the terminal flower. Primordia of lateral flowers are larger than that of the terminal flower. The gynoecium of *Triglochin* is quite peculiar: the carpels are arranged in two trimerous whorls and united *via* the floral centre only (Igersheim et al., 2001; Remizowa et al., 2010). In all studied species (as in most other species of the genus), the outer whorl carpels are sterile. The sterile carpels are of the same length as the fertile ones and possess a well-developed dorsal vascular bundle, but no ventral bundle. Each fertile carpel has a dorsal bundle extending up to the stigma and a ventral bundle supplying the ovule. The ventral bundle is absent above the level of the ovule attachment.

In *T. isingiana*, the terminal flower has a complete set of organs characteristic of the 'typical' flowers of *Triglochin* (the same as for example in the Northern Hemisphere *T. palustris*): six tepals in two whorls, six stamens in two whorls and six carpels. The lateral flowers have three tepals of the outer whorl, a well-developed abaxial stamen, two rudimentary stamens of the outer whorl and six carpels. We do not have enough developmental data on this species.

In *T. longicarpa* and *T. minutissima*, the terminal flower has three tepals of the outer whorl, three well developed stamens on the tepal radii and six carpels. Developmental data show initiation of the inner whorl tepals and inner whorl stamens as small primordia. They are then arrested in development and incon-

spicuous in the anthetic flower. The lateral flowers possess an abaxial tepal, an abaxial stamen and six carpels. Developmental data show initiation of two other outer whorl tepals and two other outer whorl stamens that are then arrested in development.

In *T. mucronata*, the terminal flower has three large tepals of the outer whorl, three small tepals of the inner whorl, three well-developed stamens of the outer whorl and six carpels. Lateral flowers have a large abaxial tepal and two medium-sized tepals in the outer whorl, three equal small tepals of the inner whorl, three well-developed stamens of the outer whorl and six carpels. Developmental data show occasional initiation of the inner whorl stamens (then arrested in development).

In fruits, the floral centre consists of lignified cells (*T. minutissima, T. longicarpa*) or remains parenchymatic (*T. mucronata* and *T. isingiana*). The endocarp is always of lignified cells in contrast to some African species (Lock et al., 2011). The anatomy of fruits in studied species resembles that of the widely distributed perennial species *T. striata* (Lock et al., 2011). Shared features are the lignification of the floral centre and the endocarp. However, the cavity of a fruiting carpel is trifid in cross-section in *T. striata* and rounded in the studied annual Australian species.

The work of IEL and DDS is supported by the Russian Science Foundation (project No 14-14-00250, fruit anatomy) and the Russian Foundation for Basic Research (project No 18-04-00797, flower development).

References

Aston H.I. 2011. Juncaginaceae. In: *Flora of Australia*. Melbourne: CSIRO Publ. V. **39**. Alismatales to Arales. P. 53–84.

Igersheim A., Buzgo M., Endress P.K. 2001. Gynoecium diversity and systematics in basal monocots. *Bot. J. Linn. Soc*. **136**: 1–65.

Lock I.E., Remizowa M.V., von Mering S., Köcke A.V., Sokoloff D.D. 2011. Flower and fruit anatomy in African *Triglochin* (Juncaginaceae: Alismatales). In: Demidov A.S. (ed.): Carpology and reproductive biology of higher plants: Proceedings of Russian natl. conf. with int. participants dedicated to the memory of Prof. A.P. Mekikian (October, 18th–19th, 2011, Moscow). Moscow: Astra-Polygraphia. P. 144–145.

Remizowa M.V., Sokoloff D.D., Rudall P.J. 2010. Evolutionary history of the monocot flower. *Ann. Mo. Bot. Gard*. **97**: 617–645.

von Mering S., Kadereit J.W. 2015. Phylogeny, biogeography and evolution of *Triglochin* L. (Juncaginaceae) – morphological diversification is linked to habitat shifts rather than to genetic diversification. *Mol. Phyl. Evol*. **83**: 200–212.

DISPLAYING OF THE PECULIARITIES OF ECOLOGICAL CONDITIONS IN THE ANATOMICAL STRUCTURE OF THE GROUND ORGANS OF HIGH-MOUNTAIN SPECIES OF THE GENERA *MINUARTIA* L. AND *EREMOGONE* FENZL. (CARYOPHYLLACEAE)

Nadezhda V. LYUBEZNOVA

Lomonosov Moscow State University, Moscow, Russia
nvlubeznova@gmail.com

In the alpine belt of the north-western Caucasus, four endemic species of the genus *Minuartia* L. inhabit a relatively small area. All of them are common in different communities and each has a number of specific adaptations for dwelling in them. *Minuartia aizoides* (Boiss.) Bornm., *M. imbricata* (M. Bieb.) Woronow and *M. circassica* (Albov) Woronow ex Grossh. are included in section *Spectabiles* (Fenzl) Hayek (Zernov, 2006). The ITS and ETS studies of nuclear ribosomal DNA show *M. aizoides* to be close to *M. imbricata* and *M. circassica* to be close to *M. biflora* (L.) Schinz et Thell. (Moore, Kadereit, 2013). *Minuartia oreina* (Mattf.) Schischkin was not covered in that work. A set of closely related species including *Eremogone saxatilis* (L.) Ikonn. from European Russia form a clade sister to high mountain *E. lychnidea* (M. Bieb.) Rupr. as evidenced by ITS (comprising ITS1, 5.8S rDNA, ITS2) of nuclear ribosomal (nr) DNA and the plastid rps16 intron (Sadeghian et al., 2015). In the anatomical structure, it is possible to trace what ecological orientation were in the ancestral species and how their properties helped the descendants to adapt to the new conditions.

Observations and collection of material for anatomical studies were carried out in 2006–2008 in the alpine belt of the Malaya Hatipara ridge, in the Teberda State Biosphere Reserve (Karachaevo-Cherkessian Republic of Russia), at 2800 m above sea level.

Communities the species were collected are arranged along a snow accumulation gradient: 0–30 cm – alpine lichen tundra with 4.5–5.5 months long growing season (*M. circassica*, *E. lychnidea*), 30–150 cm – alpine grasslands with 3.5–4.5 months long growing season (*M. oreina*), 3–6 m – alpine snowbeds with 2–2.5 months long growing season (*M. aizoides*), 3 m and more – the northern snowbeds rocks with 2.5–3 months long growing season (*M. imbricata*). These alpine communities vary in soils, character of moisture, and species composition.

In addition to Caucasian species, *E. saxatilis* was collected in the Ryazan region in 2017 in dry pine forests on sandy soils.

The material for anatomical analysis was fixed in a mixture of ethyl alcohol, glycerol and water (1:1:1). The anatomical structure was studied using

Axiopian 2 imaging microscope with the Axoivision 15.0 program. The reaction of Phloroglucinol and concentrated hydrochloric acid was used for detecting lignin.

The leaves of all *Minuartia* have thick cuticle. There are two-celled trichomes on the leaf margin in all studied species of *Minuartia.*

The leaves of *M. circassica* are up to 11 mm long, 1 mm wide, up to 0.5 mm thick, amphistomatous, isolateral. The cells of the abaxial epidermis are almost regularly rectangular in outline; the number of stomata is about 53 per 1 mm^2. The cells of the adaxial epidermis are also rectangular in outline with more sinuous walls; the number of stomata is about 100 per 1 mm^2 throughout the lamina. The palisade chlorenchyma consists of cells oval in outline (Fig. 3). It is 2-layered on the adaxial side (1-layered above the midrib) and 1-layered on the abaxial one (discontinuous under the midrib). Spongy chlorenchyma of five layers of densely packed cells is located between the veins. The leaf has three veins. The xylem is adjacent to the upper rounded cord of sclerenchyma fibers; the lower semilunar cord of sclerenchyma fibers accompanies the veins (Fig. 3).

Minuartia oreina has isolateral leaves smaller than those of M. *circassica*. The cells of the abaxial epidermis are almost square in outline; the number of stomata is about 40 per 1 mm^2. The cells of the adaxial epidermis are also square with more sinuous walls; the number of small stomata is about 100 per 1 mm^2 (Table). The palisade chlorenchyma of short cells is 2-layered on both sides (Fig. 1). Spongy chlorenchyma consists of three layers of densely packed cells located between the veins. The leaf has three veins each accompanied by two strands of sclerenchyma fibers.

Isolateral epistomatous leaves of M. *aizoides* are of the same size as those of M. *oreina*. In the middle of the lamina, there are 11 veins, which are interconnected and merge into one in the tip. Seven largest veins, including the midrib, have two strands of sclerenchyma fibers which run above and below the vascular bundle, respectively (Fig. 2). The palisade chlorenchyma of oval cells is 2-layered on the adaxial side and 1-layered on the abaxial one. Spongy chlorenchyma of 9 layers of densely packed cells is between the veins. The epidermis cells are rectangular with weakly sinuous walls. The stomata number is 310 per 1 mm^2.

Isolateral epistomatous leaves of *M. imbricata* are up to 5 mm long, 1 mm wide, up to 0.1 mm thick. The three veins are small, only the midrib is accompanied by two strands of the sclerenchyma fibers (Fig. 7). The palisade chlorenchyma of oval cells is 1-layered on both adaxial and abaxial sides. The spongy chlorenchyma is loose, only 3–4-layered, located between the veins. The adaxial epidermis cells are rounded in outline with strongly sinuous walls. The stomata are small, their density is about 180 per 1 mm^2. The cells of the abaxial epidermis are rectangular in outline with slightly sinuous walls.

Leaves of *Eremogone* are isolateral, triangular in cross section. There are translucent ‘wings’ at the base consisting of two cell layers (the adaxial and abaxial epidermises), which have lignified walls (Fig. 6). The pavement epidermal cells of *E. lychnidea* are rectangular, on the abaxial side with slightly sinuous walls.

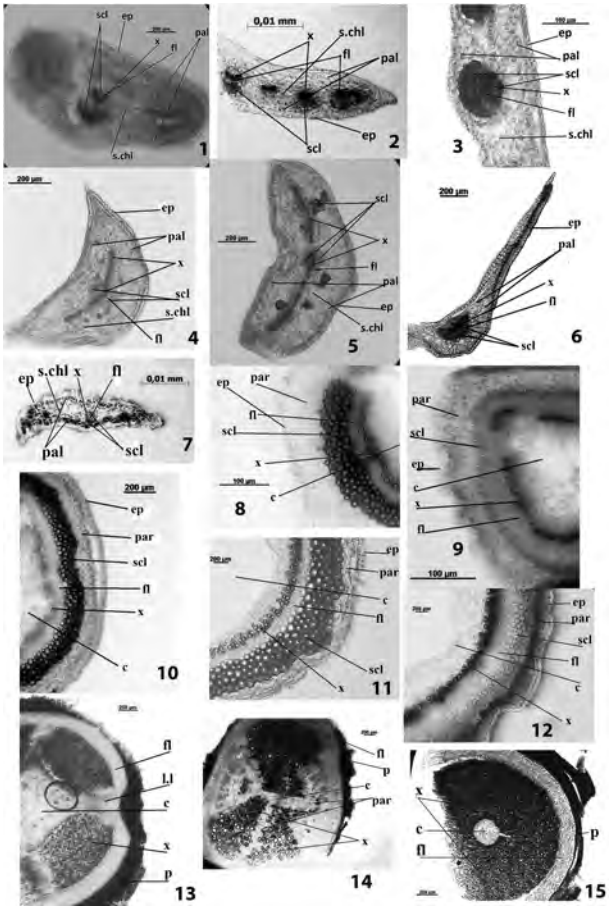

Fig. *Minuartia circassica*:
3 – leaf, 10 – stem, 15 – rhizome; *M. oreina*: 1 – leaf, 8 – stem; *M. aizoides:* 2 – leaf, 9 – stem;
M. imbricate: leaf – 7; *Eremogone lychnidea*: leaf – 4,6, stem – 11, rhizome – 13;
E. saxatilis: – 5 leaf, stem – 12, rhizome – 14.
ep – epidermis, x – xylem, fl – floem, scl – sclerenchyma, pal – palisade chlorenchyma,
s.chl – spongy chlorenchyma, c – pith, par – parenchyma, p – periderm.

Stomata density on the adaxial surface of leaf averages 210 per 1 mm^2. The number of stomata in *E. saxatilis* averages 150 per 1 mm^2 on the adaxial surface of leaf and 75 per 1 mm^2 on the abaxial surface. The leaf of *E. lychnidea* is isolateral, the palisade chlorenchyma is 2-layered on the adaxial side and 1-layered on the abaxial one. *E. saxatilis* has 1-layered palisade chlorenchyma on the adaxial side and 2-layered on the abaxial side. Spongy chlorenchyma is 4-layered of densely packed cells in *E. lychnidea* and 6-layered of loose cells in *E. saxatilis*.

Eremogone lychnidea leaves have one bundle with two strands of sclerenchyma fibers (Fig. 4), *E. saxatilis* leaves have 3 bundles. In the middle of the leaf, xylem forms an arc in cross-section (Fig. 5).

Minuartia circassica and *M. oreina* have inflorescences 5–6 cm long with 3–5 flowers. The cortex of the stem consists of 4–5 layers of oval chlorenchyma cells adjacent to the epidermis. Pericyclic fibers are located in a ring of 5–6 layers of cells; they have thick lignified walls, the thickest being in the cells in the outer ring (Fig. 8, 10). Xylem forms a continuous cylinder of 2–3 layers of cells in *M. circassica* (Fig. 10) and 1–2 layers of cells in *M. oreina*, phloem is of 4–5 layers of cells (Fig. 8). There is a parenchymatous pith with a large rhexi-lysigenous cavity.

Minuartia aizoides and *M. imbricata* have inflorescence up to 1 cm long with one, rarely two flowers. The cortex of the stem consists of 6–7 layers of oval chlorenchyma cells adjacent to the epidermis; the sclerenchyma tissue is 2–3 layered, of cells with slightly thickened walls (Fig. 9).

The stems of *Eremogone* inflorescence have a cortex with two layers of oval chlorenchyma cells. The ring of the sclerenchyma consists of 5–6 layers of cells with thick lignified walls in *E. lychnidea* (Fig. 11). The ring of the sclerenchyma of *E. saxatilis* consists of 3 lays (Fig. 12) and their cell walls are thinner than cell walls in *E. lychnidea*. Thin xylem forms a continuous cylinder of 1–4 layers of cells in *E. lychnidea* and 1–3 layers of cells in *E. saxatilis*, phloem is 3–4 layers of cells (Fig. 11, 12). There is pith with the large rhexi-lysigenous cavity.

All studied species of the genus *Minuartia* have the same structure of rhizomes (Fig. 15), which can probably be considered their systematic specifics. There is a small round pith of round cells. The secondary xylem forms a ring; there are no rays in it. The phellem consistis of 15–20 layers of tabular cells. Its outer layers burst and fall into large chunks (Fig. 15). The diameter of the rhizome is species-specific in *Minuartia* – 3 mm in plants with shortened shoots, 1 mm in plants with elongated shoots. There is pith with large densely packed cells. The secondary xylem forms a cylinder with 4 narrow rays of parenchyma cells in *E. lychnidea* (Fig. 13). The secondary xylem has 4 wide rays of parenchyma cells in *E. saxatilis* (Fig. 14). The periderm consists of 10 layers of tabular cells.

We believe that the ancestors of these species were xeromorphic plants from brightly lit habitats, as evidenced by the leaf with isolateral palisade chlorenchyma and bundles with two strands of sclerenchyma fibers. The spongy chlorenchyma is tightly packed with almost no intercellular spaces, with the exception of *M. imbricata*. The location of the stomata only or mainly on the adaxial surface of the leaf indicates that plants in drought conditions were able to fold leaves like modern *Eremogone* or fold a rosette like extant *Minuartia*. The isolateral palisade chlorenchyma allowed photosynthesis to continue in conditions of draining winds. The species of long-snow habitats (*M. aizoides*) has a xeromorphic structure of leaf. *Minuartia imbricata* occurring in the poor, shadow, protected from the prevailing wind community has leaves with friable spongy mesophyll. Contrary to the forest *E. saxatilis*, the leaves of highland *E. lychnidea* have one vein, stomata only on the adaxial surface of the leaf blade and lignified wings of the sheath.

In all species studied, the mechanical support of the inflorescence is performed by a ring of sclerenchyma in the pericycle, not by the xylem. The ring of mechanical tissues is weakened in species from long-snow communities, due to the smaller size of the inflorescence and number of flowers. Despite the three times greater number of flowers and 1.5–2 times greater length of the inflorescence in *E. saxatilis*, there is a thinner xylem and a much weaker ring of mechanical tissues.

The work was performed under the theme No. AAAA-A16-116021660105-3.

References

Moore A.J., Kadereit J.W. 2013. The evolution of substrate differentiation in *Minuartia* series *Laricifoliae* (Caryophyllaceae) in the European Alps: in situ origin or repeated colonization? *Am. J. Bot.* **100**: 2412–2425.

Sadeghian S., Zarre S., Rabeler R.K., Heubl G. 2015. Molecular phylogenetic analysis of *Arenaria* (Caryophyllaceae: tribe Arenarieae) and its allies inferred from nuclear DNA internal transcribed spacer and plastid DNA *rps*16 sequences. *Bot. J. Linn. Soc.* **178**: 648–669.

Zernov A.S. 2006. *Flora of the North-Western Caucasus*. Moscow: KMK. [In Russian]

MORPHO-ANATOMICAL FEATURES OF FLORAL NECTARIES OF *STACHYS ANNUA* (L.) L. (LAMIACEAE)

***Marina MAČUKANOVIĆ-JOCIĆ*, Dragana RANČIĆ, Maja TERZIĆ**

University of Belgrade, Belgrade, Serbia

marmajo@agrif.bg.ac.rs

Stachys annua (L.) L. (annual hedgenettle) is a herbaceous plant native to Europe and Western Asia, but introduced elsewhere. In Serbia, it is common in woodland edges and meadows up to 1,500 m altitude, cultivated fields, wastelands and within urban areas. It is a very important as melliferous plant as it has a long flowering period (June–October) offering *plenty* of nectar for *insect pollinators* including *honeybees*. White or pale yellow flowers are in whorls of 2–6 only. Receptacular four-lobed floral nectary is located at the ovary base in the form of an asymmetrical ring-like structure, with the anterior lobe longer than the others (Nicolson et al., 2007).

Morpho-anatomical features of *S. annua* floral nectaries were studied using light brightfield and fluorescence microscopy and scanning electron microscopy. For light microscopy the receptacles with the ovaries were fixed in FAA and post-fixed in 70% ethanol, dehydrated through a graded series of ethanol and then xylol before embedding in paraffin wax. After sectioning by sliding microtome, both transversal and longitudinal sections were stained with Alcian blue and Safranin (Ruzin, 1999). To examine the cuticle and xylem, freshly sectioned material was

observed for autofluorescence using epifluorescence microscope (LEICA DMLS, filter I3: BP 450–490 nm). For micromorphological investigation, the receptacle bearing the ovary was studied on fresh material without prior preparation procedure using scanning electron microscope (JEOL JSM 35).

Nectary structure is characterized by three main histological components: a uniseriate epidermis, subepidermal secretory tissue and vascular tissue. Epidermis is covered with a very thin continuous cuticle showing typical autofluorescence, and contains modified stomata involved in the nectar exudation process. Beneath the epidermis, there is a multilayered specialized nectary parenchyma of small isodiametric cells with densely staining cytoplasm. Subnectary parenchyma consists of larger cels, more loosely packed. Vascular bundles supplying the nectary consist of both phloem and xylem, but their terminal branches seem to be of only phloem elements.

References

Nicolson S.W., Nepi M., Pacini E. 2007. *Nectaries and nectar*. Dordrecht: Springer Netherlands.
Ruzin S.E. 1999. *Plant microtechnique and microscopy*. Oxford, New York: Oxford Univ. Press.

REPRODUCTIVE MORPHOLOGY AND ANATOMY OF "BASAL" EUDICOTS IN THE CRETACEOUS AND PALEOGENE

Steven R. MANCHESTER
University of Florida, Gainesville, USA
steven@flmnh.ufl.edu

Fossil flowers, fruits and seeds provide insights to patterns of stasis and change in pollination and seed dispersal mechanisms of extant families of early-divergent eudicot families including Platanaceae, Nelumbonaceae, Sabiaceae, and Trochodendraceae. Platanaceous inflorescences from the Albian and later stages of the Cretaceous resemble those of extant *Platanus* in being globose capitula composed of numerous florets; however, they have better developed perianth, and a more constant number of gynoecia per floret (usually fixed at five, contrasting with highly reduced perianth and the variable number of gynoecia per floret in modern *Platanus*). These features, along with smaller size of pollen grains suggest that insect pollination, rather than wind pollination, prevailed in the early history of this family.

The fruits borne by Cretaceous Platanaceae lack the prominent basal tuft of dispersal hairs seen in extant *Platanus*, and apparently were less specialized for wind

dispersal than extant species. At least one lineage with well-developed perianth and lacking disperal hairs on the achenes persisted to the late Eocene (*Macginicarpa*; Manchester, 1986), but fruits corresponding morphologically with those of modern *Platanus*, with well developed dispersal hairs, are also known by the Paleocene.

Nelumbonaceae, although paired closely with Platanaceae based on molecular phylogenetic investigations, is highly distinctive in its aquatic adaptations, and we do not have any fossil evidence directly linking these families. The diagnostic "shower head" fruiting structures of *Nelumbo*, consisting of numerous ellipsoidal fruits half-embedded in a wide receptacle, are known from Paleogene and Late Cretaceous sites, the oldest being from the Campanian–Maastrichtian, of Argentina (Gandolfo, Cuneo, 2005). These, and associated foliage match the configuration of fruits in the modern genus, *Nelumbo* – exemplifying long-term morphological stasis.

Fruits of Sabiaceae are known in the fossil record from at least the Maastrichtian of the late Cretaceous (Bodor et al., 2012) with some earlier reports in need of verification. The most prominent extant genus of this family, *Meliosma*, is represented by anatomically preserved fruits from the Paleocene (Crane et al., 1990) and Eocene (Reid, Chandler, 1933; Manchester, 1994), while fruits of *Sabia* have been identified based on casts and molds of fruits, but without detailed documentation of anatomy (Manchester, 1994). Endocarp morphology and anatomy of the Paleocene *Meliosma* fruits coincides closely with those of the modern subgenus *Kingsporoughia*, while the species known from the Eocene coincide mainly with the modern Paleotropical members of subgenus *Meliosma*. The fossil record indicates a constancy of drupe-like fruits in this family, suggesting dispersal by birds and/or mammals in the past, as today.

The fossil record of Trochodendraceae includes Paleogene and Neogene fruits of the two living genera, *Trochodendron* (Chelebaeva, Chigaeva, 1988; Manchester et al., 2018a, b) and *Tetracentron* (Manchester, Chen, 2006; Grímsson et al., 2008) plus some extinct genera in the Paleogene and Maastrichtian. Infructescences and capsular fruits of *Trochodendron* from the Paleocene and Eocene of western North America coincide with the extant genus in the number and position of styles, the presence of prominent stamen filament scars persisting on the receptacle of the fruit, substylar nectaries, and a lack of prominent perianth (Manchester et al., 2018b) – features indicating they are nearly identical to the single living species.

Although infructescences and fruits identical to modern *Tetracentron* are known from the Miocene (Manchester, Chen, 2006; Grímsson et al., 2008), they have not been identified unequivocally from the Paleogene. However, the extinct genus *Pentacentron*, from the Eocene of western North America (Manchester et al., 2018b) resembles *Tetracentron* in its spike-like inflorescences, capsular fruits, and styles that persist distally on the fruits. It consistently has five carpels rather than four, and differs from both extant genera, because the styles curve inward, toward the center of the fruit, rather than being recurved outward. *Pentacentron* is found

in shales associated with leaves identified as *Tetracentron*, leaving open the question whether *Pentacentron* bore *Tetracentron*-like leaves, or perhaps that extant *Tetracentron* was actually present, but that we failed to find its fruits (Manchester et al., 2018b). Extinct *Concavistylon*, from the Eocene and Miocene of western North America (Manchester et al., 2018a, b), and recently identified as well from the Paleocene of Wyoming, bore shortly pedicellate fruits on long racemes.

Concavistylon fruits are apically dehiscent capsules like those of *Trochodendron*, *Tetracentron* and *Pentacentron,* but *Concavistylon* fruits bear a prominent perianth scar, unlike extant *Trochodendron*, and the styles curve inward, as in *Pentacentron*, rather than outward as in the two modern genera. An elliptical nectary pad is situated beneath each style in all of these genera, indicating that the same mode of insect pollination has persisted since at least the Paleocene. The more prominent perianth scar in *Concavistylon* hints at an additional means of attracting pollinators, but we have not recovered any of the fossils at flowering stage.

Another extinct genus, *Nordenskioeldia*, known from the Maastrichtian and Paleocene across the Northern Hemisphere (Crane et al., 1991; Wang et al., 2009) and from the Miocene in Pacific Northwestern North America (Manchester et al., 1991), has been proposed as an extinct member of Trochodendraceae (Kryshtofovich, 1956; Crane et al., 1991), although this assignment has been challenged (Doweld, 1998). The similarities with Trochodendraceae include abiotically dispersed fruits of multiple carpels united in a radial configuration borne on elongate spikes, winged seeds and apparently vesselless wood. The persistent styles face outward, as in the two extant genera, but they do not migrate so far distally during fruit development. Nectaries are apparently lacking and the fruits disperse schizocarpically, unlike the extant genera of Trochodendraceae. More characters are needed for reconsidering the phylogenetic position of *Nordenskioeldia*.

Although diagnostic pollen was found adhering to the styles of Miocene *Tetracentron* fruits, we have not yet found pollen on the persistent styles of *Nordenskioeldia* fruits. These examples indicate that a range of abiotic and biotic pollen and seed dipsersal strategies were established in early divergent Eudicots by the early Paleogene and that some, but perhaps not all, of the mechanisms found in the modern genera were established during the Cretaceous.

References

Bodor E.R., Baranyi V., Heřmanová Z. 2012. The earliest Sabiaceae fruit remains of Hungary. *Hantkeniana* **7**: 11–18.

Chelebaeva A.L., Chigaeva G.B. 1988. The genus *Trochodendron* (Trochodendraceae) in the Miocene of Kamchatka. *Bot. Zhurn.***73**: 315–318. [In Russian]

Crane P.R., Manchester S.R., Dilcher D.L. 1990. A preliminary survey of fossil leaves and well-preserved reproductive structures from the Sentinel Butte Formation (Paleocene) near Almont, North Dakota. *Fieldiana Geol.* **1418**: 1–63.

Crane P.R., Manchester S.R., Dilcher D.L. 1991. Reproductive and vegetative structure of *Nordenskioldia* (Trochodendraceae), a vesselless dicotyledon from the Early Tertiary of the Northern Hemisphere. *Am. J. Bot.* **78**: 1311–1334.

Doweld A.B. 1998. Carpology, seed anatomy and taxonomic relationships of *Tetracentron* (Tetracentraceae) and *Trochodendron* (Trochodendraceae). *Ann. Bot.* **82**: 413–443.

Gandolfo M., Cuneo R.N. 2005. Fossil Nelumbonaceae from the La Colonia Formation (Campanian–Maastrichtian, Upper Cretaceous), Chubut, Patagonia, Argentina. *Rev. Palaeobot. Palynol.* **133**: 169–178.

Grímsson F., Denk T., Zetter R. 2008. Pollen, fruits, and leaves of *Tetracentron* (Trochodendraceae) from the Cainozoic of Iceland and western North America and their palaeobiogeographic implications. *Grana* **47**: 1–14.

Kryshtofovich A.N. 1956. *Oligocene flora of Mount Ashutus in Kazakstan*. Moscow: Nauka. [In Russian]

Manchester S.R. 1986. Vegetative and reproductive morphology of an extinct plane tree (Platanaceae) from the Eocene of western North America. *Bot. Gaz*. **147**: 200–226.

Manchester S.R. 1994. Fruits and seeds of the Middle Eocene Nut Beds flora, Clarno Formation, Oregon. *Palaeontogr. Amer.* **58**: 1–205.

Manchester S.R., Chen I. 2006. *Tetracentron* fruits from the Miocene of western North America. *Int. J. Plant Sci*. **167**: 601–605.

Manchester S.R., Crane P.R., Dilcher D. L. 1991a. *Nordenskioldia* and *Trochodendron* (Trochodendraceae) from the Miocene of northwestern North America. *Bot. Gaz*. **152**: 357–368.

Manchester S.R., Pigg K.B., DeVore M. L. 2018a. Trochodendraceous fruits and foliage in the Miocene of western North America. *Fossil Imprint* **74**: 45–54.

Manchester S.R., Pigg K.B, Kvaček Z., DeVore M.L., Dillhoff R.M. 2018b. Newly recognized diversity in Trochodendraceae from the Eocene of western North America. *Int. J. Plant Sci*. **179**: 663–676.

Reid E.M., Chandler M.E.J. 1933. *The London Clay flora*. London: British Museum (Natural History).

Wang Y.-H., Ferguson D. K., Feng G.-P., Wang Y.-F., Zhilin S.G., Li C.-S., Popova-Tselenkova S., Yang J., Ablaev A.G. 2009. The phytogeography of the extinct angiosperm *Nordenskioeldia* (Trochodendraceae) and its response to climate changes. *Palaeogeog., Palaeoclim., Palaeoecol.* **280**: 183–192.

TO THE ANATOMY OF THE LATENT ROOT SYSTEM WITHIN EMBRYO OF SOME DICOTYLEDONOUS ANNUAL PLANTS

Michael V. MARKOV

Moscow Pedagogical State University, Moscow, Russia
markovsmail@gmail.com

In a lot of papers dealing with root system investigation, we find an opinion that lateral roots initiation and development are post-embryogenetic events. Lateral roots arise post-embryonically from differentiated tissue, the pericycle (Verstraeten et al., 2014). Nevertheless, in the valuable textbook by Mauseth (2016: 243–244) we can read: “the epicotyl [of the embryo. – *M.M.*] may bear a few small leaves,

and the radicle often contains several primordia for lateral roots in its pericycle". Everybody would expect at least several examples supporting this statement, but there were no examples there. In some other publications one can read about two different groups of plants one of which forms lateral roots right from the apical root meristem even before the elongation zone whereas the second can initiate lateral roots only behind the elongation zone.

In almost all plant species from different families, the lateral root primordia initiate behind the elongation zone (Lloret, Casero, 2002). However, in cucurbits and few other species such as *Fagopyrum esculentum* (O'Dell, Foard, 1969), *Ipomoea purpurea*, *Pistia stratiotes* and *Eichhornia crassipes* (Ilina et al., 2018), lateral root primordia initiate and start developing in the apical meristem of the parental root. The special term 'latent embryonic root system' was assumed to designate these cases (Dubrovskii, 1974).

The role of the collet in apical initiation of the lateral roots is of importance (Compton, 1912; Parsons, 2009). The collet (= collar) is a morphologically distinguished basal zone of the hypocotyl, occurring in both monocotyledonous and dicotyledonous seedlings (Tillich, 2007). It can be recognized by its ability to give rise to collar rhizoids, and often it is prominently swollen, thus increasing the rhizoid-bearing surface. We added elsewhere *Impatiens noli-tangere* to the first group because its radicle stops developing at early stage as the collet; it even does not emerge from the germinating seed (Markov et al., 2013). Some good examples of lateral root primordium formation in the embryo primary roots of the dormant seeds of *Echinocistis lobata* and *Cucumis sativus* are shown in figs. 1–4.

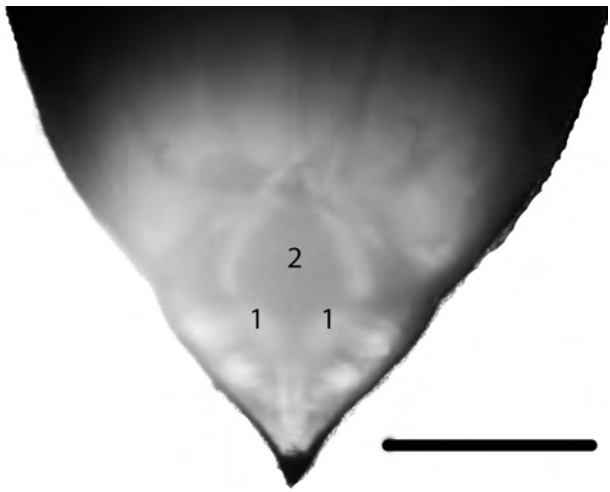

Fig. 1. Longitudinal section of the lower part of *Echinocystis lobata* seed embryo with primordia of lateral roots (1) and collet (2).
Scale bar – 0.5 cm.

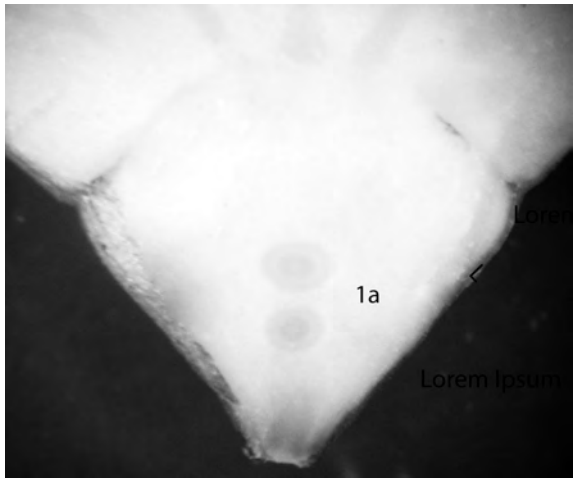

Fig. 2. The same as in Fig. 1,
but two lateral root primordia cross-sectioned (1a).

Fig. 3. Collet of *Impatiens noli-tangere* emerging from the testa with anthocyan-colored primordia of lateral roots.

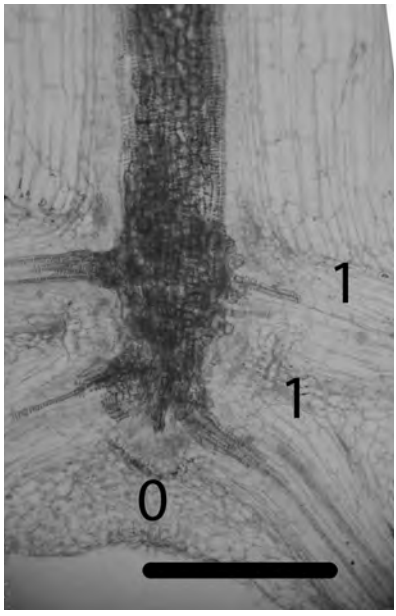

Fig. 4. Longitudinal section of the collet of *Impatiens noli-tangere* with lateral roots (1) and radicle which has stoped growing (0).
Scale bar – 0.5 mm.

In longitudinally sectioned lower part of embryos with collet region (2), the primordia of lateral roots are visible (1) near the radicle trace (0) without any growth markers. Germinating *Impatiens noli-tangere* seed shows a collet with a red antocyanic markers of lateral roots. In the cross section of the collet one of these lateral roots is just opposite to the primary xylem of the radial bundle thus confirming it is a genuine lateral root, not adventitious one.

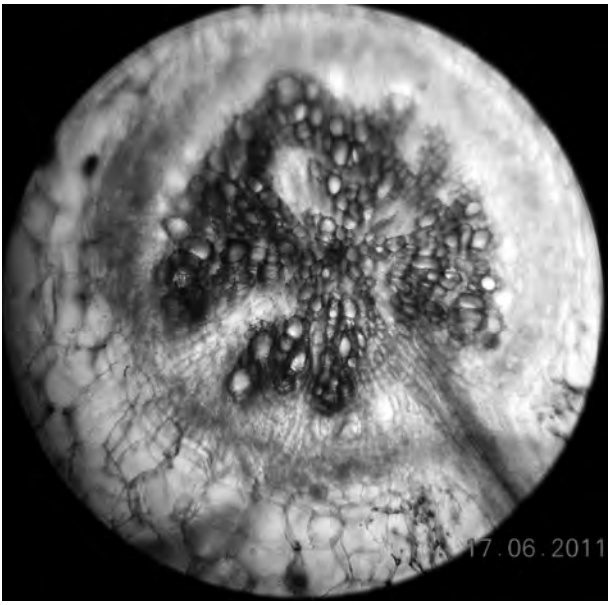

Fig. 5. Cross section of the collet of *Impatiens noli-tangere* with the lateral root located just opposite the primary xylem.

The biological importance of early root branching during the embryogenesis could be attributed to lianoid growth habitus of cucurbits and tendency to conditional epiphytism of *Impatiens noli-tangere*. Development of the lateral root primorida in the embryo enables plants to form root system from the very beginning of germination which can be advantageous for climbing plants of the flood plain forest (*Echinocystis*) and for occasional epiphyte (*Impatiens*) which can grow in tree hollows and on the soil extracted by roots of windfall trees. The most fertile surface layer of soil (rich with nutrients) becomes resultantly accessible for both plants.

References

Compton R.H. 1912. Theories of the anatomical transition from root to stem. *New Phytol*. **11**: 13–25.

Dubrovskii I.G. 1987. Latent embryonic root system in cucumber. *Bot. Zhurn*. **72**: 171–176. [In Russian]

Ilina E.L., Kiryushkin A.S., Semenova V.A., Demchenko N.P., Pawlowski K., Demchenko K.N. 2018. Lateral root initiation and formation within the parental root meristem of *Cucurbita pepo*: is auxin a key player? *Ann. Bot.* **121**: 1–16.

Lloret P.G., Casero P.J. 2002. Lateral root initiation. In: Waisel Y., Eshel A., Kafkafi U. (eds.): *Plant roots – the hidden half*. 3rd ed. New York: Marcel Dekker, Inc. P. 127–156.

Markov M.V., Yusufova V.Z., Tlyashev I. 2013. The lateral root primordia in the seed embryo of some Dicotyledonous annual plants. *Electronic journal Vestnik MGOU* / www.evestnik-mgou.ru. **3**: 1–12. [In Russian]

Mauseth J.D. 2016. *Botany: an introduction to plant biology*. 6th ed. Burlington: Jones and Bartlett Learning.

O'Dell D.H., Foard D.E. 1969. Presence of lateral root primordia in the radicle of buckwheat embryos. *Bull. Torrey Bot. Club* **96**: 1–3.

Parsons R.F. 2009. Hypocotyl hairs: an historical perspective. *Aust. J. Bot*. **57**: 106–108.

Tillich H.J. 2007. Seedling diversity and the homologies of seedling organs in the order Poales (Monocotyledons). *Ann. Bot*. **100**: 1–17.

Verstraeten I., Sébastien S., Geelen D. 2014. Hypocotyl adventitious root organogenesis differs from lateral root development. *Front. Plant Sci., Plant Gen. Genomics*. **5**: 1–13.

LATICIFERS IN SAPINDACEAE: STRUCTURE, DISTRIBUTION AND PHYLOGENETIC IMPORTANCE

***Maria Camila MEDINA*, Erika PRADO, Pedro DIAS, Pedro ACEVEDO-RODRÍGUEZ, Diego DEMARCO**

University of São Paulo, São Paulo, Brazil

camiliny@usp.br

Laticifers have a wide distribution in the plant kingdom and are present in 36 families without close evolutionary relationships (Lewinsohn, 1991; Judd et al., 2007). The presence of these structures in some groups indicates their great taxonomic importance (Simpson, 2010). However, comparative systematic studies of laticifers are scarce and the possible meaning of phylogenetic variations in the degree of specialization has not yet been revealed.

The chemical composition of latex has also a potential application as an aid in the delimitation of taxa and in the interpretation of the evolutionary history of a group (Rudall, 1987). This is the case of Sapindales, a large and diverse order that has some representatives, which exude a white secretion, usually interpreted as latex. Within Sapindales the presence of latex has been observed only in Sapindaceae, considered an uncommon character present in some species (APG, 2016).

Laticifers are poorly known among Sapindaceae species. They have only been cited in few works, without a description of its structure, ontogeny and histochemistry, which is of great importance to classify and distinguish them from idioblast cells.

There are few reports of latex in Paullinieae (Sapindoideae) (Ferraz, Costa, 1985; Weckerle, Rutishauser, 2005; da Cunha et al., 2017). In Hippocastanoideae, the presence of latex was also reported for some species of *Acer* and *Dipteronia* (Benedict, 1961; Amini et al., 2008), without further confirmation. Another factor that causes doubts on the description of laticifers in this family is the fact that there are few anatomical works using representatives of this group, and for most of them, the secretory cells have been described as idioblasts, a secretory structure abundant in all Sapindales. Considering the co-occurrence of these two secretory structures, only a histochemical analysis can distinguish them undoubtedly, once the difference between a secretory idioblast and a laticifer sometimes resides only in the nature of their secretion (Fahn, 1979).

Considering that the presence of laticifers, their type and the latex composition have taxonomic and systematic importance for many groups (Demarco et al., 2013), a comprehensive investigation of Sapindaceae was necessary to evaluate the occurrence of laticifers in their genera.

This work aimed to verify the presence of laticifers in 64 species belonging to 21 genera of Sapindaceae, and to analyze their anatomical characteristics, latex composition and evolution within the family.

For this, samples of young stem were obtained from herbarium specimens, rehydrated and embedded in methacrylate according to the usual techniques in plant anatomy (Smith, Smith, 1942; Meira, Martins, 2003). For histochemical analyses, fresh and fixed material was sectioned using a sliding microtome and the sections were submitted to different treatments for detection of the main chemical classes of compounds that constitute the latices. For ontogenetic analysis, fresh or Paraplast-embedded (Johansen, 1940) shoots apices were used.

To test hypotheses of laticifer evolution, we performed a character optimization under a ML using Mesquite v3.04 (Maddison, Maddison, 2017). Each genus was identified as a unit to construct a character matrix, which was made only with the presence or absence of laticifers. This was based on the phylogeny of Buerki et al. (2009) and Acevedo-Rodríguez et al. (2017).

The presence of articulated non-anastomosing laticifers was confirmed for 15 genera from two subfamilies, being described for the first time in most genera. Laticifers differ from idioblasts on the cell diameter, shape, color, distribution, and aspect of secretion. Laticifers are observed early in the developing shoot apex when the tissues are still in the meristematic phase. Laticifers of the family are originated from ground meristem and procambium and grow through addition of new laticiferous cells to the apex of the tubular structure.

The diameter of the laticifers can vary depending on the taxonomic group to which they belong. The widest laticifers are observed in the *Melicoccus* group, and the narrowest ones in the tribe Athyaneae. In general, laticifers in this family are small, short and narrow in comparison with those from other families, and perhaps for this reason, they remained unrecognized for a long time.

The histochemical tests allowed the observation of lipids (mainly terpens), carbohydrates, proteins, alkaloids, and phenolic compounds in the latex. Callose and suberin also occur in the laticifer walls of some species, helping in the interpretation of the infratribal relationships.

Presence or absence of laticifers is an informative character and can be used to help in taxonomic resolution and establishment of evolutionary relationships within Sapindaceae. Our results revealed that the polyphyletic genus *Cardiospermum* varies in relation to the occurrence of laticifers. While *Cardiospermum s.str.* is non-latescent, species of *Cardiospermum* which are closer to *Serjania* and *Urvillea,* undoubtedly have laticifers.

Optimizing our data on the phylogeny of Sapindaceae (Buerki et al., 2009; Acevedo-Rodríquez et al., 2017), we inferred that the ancestor of Sapindaceae probably did not possess laticifers, and this character state emerged multiple times in different lineages of Sapindaceae with secondary losses occurring in some groups.

References

Acevedo-Rodríquez P., Wurdack K.J., Ferrucci V.S., Johnson P., Dias P., Coelho R.G., Somner V.G., Steinmann V.W., Zimmer E.A., Strong M.T. 2017. Generic relationships and classificaion of tribe Paullinieae (Sapindaceae) with a new concept of supertribe Paullinioidae. *Syst. Bot*. **42**: 96–114.

Amini T., Zare H., Assadi M. 2008. *Acer mazandaranicum* (Aceraceae), a new species from Northern Iran. *Iran. J. Bot*. **14**: 81–86.

APG. 2016. An update of the Angiosperm Phylogeny Group classification for the orders and families of flowering plants: APG IV. *Bot. J. Linn. Soc*. **181**: 1–20.

Benedict A.H. 1961. The floral anatomy of *Dipteronia*. *Am. J. Bot*. **48**: 918–924.

Buerki S., Forest F., Acevedo-Rodríguez P., Callmander M.W., Nylander J.A.A., Harrington M., Sanmartín I., Küpfer P., Alvarez N. 2009. Plastid and nuclear DNA markers reveal intricate relationships at subfamilial and tribal levels in the soapberry family (Sapindaceae). *Mol. Phyl. Evol*. **51**: 238–258.

da Cunha N.I.L., Martins F.M., Somner G.V., Tamaio N. 2017. Secretory structures in stems of five lianas of Paullinieae (Sapindaceae): morphology and histochemistry. *Flora* **235**: 29–40.

Demarco D., Castro M. De M., Ascensão L. 2013. Two laticifer systems in *Sapium haematospermum*–new records for Euphorbiaceae. *Botany* 91: 545–554.

Fahn A. 1979. *Secretory tissues in plants*. London: Academic Press.

Ferraz C.L. de A., Costa C.G. 1985. *Paullinia carpopodea* Camb. (Sapindaceae). Anatomia foliar. *Rodriguésia* **37**: 79–90.

Johansen D.A. 1940. *Plant microtechnique*. New York: McGraw-Hill.

Judd W.S., Campbell C.S., Kellogg E.A., Stevens P.F. 2002. *Plant systematics: a phylogenetic approach*. Sunderland: Sinauer Associates.

Lewinsohn T.M. 1991. The geographical distribution of plant latex. *Chemoecology* **2**: 64–68.

Maddison W.P., Maddison D.R. 2017. *Mesquite: A modular system for evolutionary analysis*. http://mesquiteproject.org.

Meira R.M.S.A., Martins F.M. 2003. Inclusão de material herborizado em metacrilato para estudos de anatomia vegetal. *Rev. Árvore*. **27**: 109–112.

Rudall P.J. 1987. Laticifers in Euphorbiaceae – a conspectus. *Bot. J. Linn. Soc*. **94**: 143–163.

Simpson M.G. 2010. *Plant systematics*. San Diego: Elsevier.

Smith F.H., Smith E.C. 1942. Anatomy of the inferior ovary of *Darbya*. *Am. J. Bot.* **29**: 464–471.
Weckerle C.S., Rutishauser R. 2005. Gynoecium, fruit and seed structure of Paullinieae (Sapindaceae). *Bot. J. Linn. Soc*. **147**: 159–189.

ONTOGENETIC BASIS OF LEAF DIVERSITY AMONG SAPINDALES: PSEUDOSTIPULE, METASTIPULE AND ABORTED LEAFLETS

Gladys F.A. MELO-de-PINNA*, *Mariana RAPOZO*, *Charles BARROS*, *Marcelo DEVECCHI*, *José R. PIRANI

University of São Paulo, São Paulo, Brazil
gfmpinna@usp.br

Sapindales includes 9 families and about 6,000 species, an outstanding group among the rosids eudicotyledons by high morphological diversity and economic importance (Muellner et al., 2003; APG, 2016; Muellner-Riehl et al., 2016). The presence of pinnate leaves without stipules is a putative synapomorphy for the order (Gadek et al., 1996), although other leaf types occur, mainly palmate (bifoliolate, trifoliolate and unifoliolate) and simple leaves (Kubitzki, 2011). Within Sapindales, the clade formed by Rutaceae, Meliaceae and Simaroubaceae represents an important group for studies of leaf development, since they encompass varied examples of leaf morphologies.

In Rutaceae, the unifoliolate leaves have been interpreted as simple leaves endowed with a joint between the petiole and the leaf (Claßen-Bockhoff, 2001; Bell, Bryan, 2008), or as special composite leaves resulting from a reduction in the number of leaflets, which is evidenced by a joint or swelling at the base of the blade (Kubitzki et al., 2011). In the latter work, even though the authors highlight this difference between unifoliolate and simple leaves, they propose to treat all genera with single or unifoliolate leaves as having unifoliolate leaves.

Our studies have shown that in Rutaceae the development of the leaflets of the species of *Metrodorea* is spatially limited by the presence of stipules located in the leaf base, leading to the formation of unifoliolate compound leaves (Cruz et al., 2015). In other taxa, as *Esenbeckia pilocarpoides* (an essentially trifoliolate species) there is no stipules similar to *Metrodorea*, but aborted leaflets occur leading to the formation of leaves with two or one leaflets (unifoliolate compound leaves). Contrasting, the unifoliolate leaves of *Simaba obovata* (Simaroubaceae) show no morphological evidence of aborted leaflets, while in some shoots scattered trifoliate leaves are found. Another example of variation of leaf development occurs in some Simaroubaceae with pinnate leaves, as *Homalolepis intermedia*. Leaves in this species bear 5–7 leaflets, but those more distant from the stem apical meristem are provided with strongly reduced basal leaflets.

Besides the wide diversity of foliar types related to leaf division (simple or compound leaves), observed in Sapindales as previously mentioned, there are several questions that remain open regarding to the origin and development of stipules (Cruz et al., 2015). Although the occurrence of these modifications of the leaf base is absent in most Sapindales (Weberling, Leenhouts, 1966), Nooteboom (1960) described the presence of deciduous stipules in the genus *Picrasma*. In another species of the family Simaroubaceae, *Ailanthus altissima*, Schiller (1903) cited the occurrence of pseudostipules, due to the large number of leaflet pairs per leaf. For Weberling & Leenhouts (1966) *Picrasma*, *Ailanthus* and *Harrisonia* have no true stipules. In *Metrodorea* (Rutaceae), which present opposite phyllotaxy, Cruz et al. (2015) showed that such a structure, previously defined as a sheath, is in fact a pair of connate stipules originating from primordia at the base of the leaf.

According to Sinnott & Bailey (1914), the stipules were considered as accessory leaves, independent organs; as products of the base of the foliar primordia; as pairs of lateral leaflets of a trifoliolate leaf; as incomplete axillary ligaments, or even as a reduced leaf sheaths. According to Weberling & Leenhouts (1966), structures called true stipules are derived from the base of the leaf, developing in the early stages of foliar ontogenesis, even before the top of the leaf. Structures denominated as *pseudostipules* are derived from the upper region of the leaf, which do not present as constant character in related groups, appear in only a few leaves and have late development in ontogeny; and structures considered as *metastipules* are lateral appendages of the base of the leaf, that share all the morphological features with the true stipules, but they are systematically isolated. However, the lack of ontogenetic data that demonstrate the nature of these structures in Sapindales suggests the need for a study focusing on questions such as: may stipules represent a pair of leaflets that develop differently, i.e. is the primordium of stipule homologous to the primordium of leaflet? Also, are there anatomical differences in the development of structures described as *pseudostipule* and *metastipule*? Our results show that in *Ailanthus altissima* (Simaroubaceae), the structures described as pseudostipules are true stipules (glandular stipules) whose morphology is very similar to the stipules found in some *Passiflora* species, such as *Passiflora foetida* (Passifloraceae, Malpighiales). In *Picrasma crenata* (Simaroubaceae) the stipules present an initial development similar to the leaflets, but there is no marginal meristem activity, that is, there is no medio-lateral growth resulting in a flattened structure like the leaflets. A similar situation was observed in *Trichilia pseudostipularis* (Meliaceae), where the structures described as reduced basal leaflets present limited marginal activity when compared to the more distal leaflets. This pair of basal leaflets protects the axillary bud, similar to the situation observed in stipules of several other species in varied eudicot families.

In summary, our results have led us to consider the hypothesis that stipules in Sapindales (and perhaps in several other groups) are a pair of leaflets that develop differently, that is, the stipule primordium is homologous to a leaflet primordium. Therefore, this particular ability to originate different morphology from leaf pri-

mordium, as stipules, reduced or aborted leaflets, makes Simaroubaceae, Rutaceae and Meliaceae a key group for further leaf development studies.

The work of GMdP was supported by Brazilian Foundation (FAPESP) grant No. 2015/15158-4.

References

APG. 2016. An update of the Angiosperm Phylogeny Group classification for the orders and families of flowering plants: APG IV. *Bot. J. Linn. Soc.* **181**: 1–20.

Bell A.D., Bryan A. 2008. *Plant form: an illustrated guide to flowering plant morphology*. Portland, London: Timber Press.

Claßen-Bockhoff R. 2001. Plant morphology: the historic concepts of Wilhelm Troll, Walter Zimmermann and Agnes Arber. *Ann. Bot.* **88**: 1153–1172.

Cruz R., Duarte M., Pirani J.R., Melo-de-Pinna G.F.A. 2015. Development of leaves and shoot apex protection in *Metrodorea* and related species (Rutaceae). *Bot. J. Linn. Soc.* **178**: 267–282.

Gadek P.A., Fernando E.S., Quinn C.J., Hoot S.B., Terrazas T., Sheahan M.C., Chase M.W. 1996. Sapindales: molecular delimitation and infraordinal groups. *Am. J. Bot.* **83**: 802–811.

Kubitzki K. 2011. *Families and genera of vascular plants.* V. **10**. *Flowering plants. Eudicots. Sapindales, Cucurbitales, Myrtaceae*. New York: Springer-Verlag.

Kubitzki K., Kallunki J.A., Duretto M., Wilson P.W. 2011. Rutaceae. In: Kubitzki K. (ed.): *The families and genera of vascular plants*. Heidelberg: Springer. V. **10**. P. 276–356.

Muellner A.N., Samuel R,, Johnson S.A., Cheek M., Pennington T.D., Chase M.W. 2003. Molecular phylogenetics of Meliaceae (Sapindales) based on nuclear and plastid DNA sequences. *Am. J. Bot.* **90**: 471–480.

Muellner-Riehl A.N., Weeks A., Clayton J.W., Buerki S., Nauheimer L., Chiang Y., Cody S., Pell S.K. 2016. Molecular phylogenetics and molecular clock dating of Sapindales based on plastid *rbc*L, *atp*B and *trn*L-*trn*F DNA sequences. *Taxon* **65**: 1019–1036.

Nooteboom H. P. 1960. Simaroubaceae. In: *Flora Malesiana-Series. 1, Spermatophyta.* V. **6.1**: 193–226.

Schiller J. 1903. Untersuchungen über Stipularbildungen. *Sitzungsber. K. Akad. Wiss. Wien. (Math. Naturw. Kl.)* **112**: 793–819.

Sinnott E.W., Bailey I.W. 1914. Investigations on the phylogeny of the angiosperms. 3. Nodal anatomy and the morphology of stipules. *Am. J. Bot.* **9**: 441–453.

Weberling F., Leenhouts P.W.1966. Systematisch-morphologische Studien an Terebinthales-Familien [Burseraceae, Simaroubaceae, Meliaceae, Anacardiaceae, Sapindaceae]. *Abh. Akad. Wiss. Mainz, Math.-naturwiss.* **10**: 497–584.

STYLOPODIUM IN CYPERACEAE (POALES): A POTENTIAL KEY INNOVATION IN THE DIVERSIFICATION OF SOME CYPEROIDEAE

Mariana Maciel MONTEIRO[1]***, Aline ORIANI***[2]***, Diego DEMARCO***[1]

[1] University of São Paulo, São Paulo, Brazil
[2] Universidade Estadual Paulista (UNESP), Rio Claro – SP, Brazi
Marimonteiro199@gmail.com

The family Cyperaceae has a cosmopolitan geographical distribution with highest diversity on the Neotropics and comprises ca. 100 genera and ca. 5700 spe-

cies (Goetghebeur, 1998; Govaerts et al., 2007), most of them occurring in savanna marshes and wetland vegetation (Govaerts et al., 2007). Cyperaceae is monophyletic and divided into two subfamilies: Mapanioideae with ca. 130 species, and Cyperoideae with the massive majority of the species diversity (Hinchliff, Roalson, 2013). Cyperoideae possess flowers with a typical bauplan with essentially two trimerous perianth whorls, one whorl of stamens and a trimerous gynoecium (Vrijdaghs et al., 2009). Reduction and modifications of floral organs is common leading to a highly variable floral morphology found in the subfamily (Vrijdaghs et al., 2009).

Cyperoideae present a great diversity of genera, being *Rhynchospora* Vahl., *Bulbostylis* Kunth, *Fimbristylis* Vahl, and *Eleocharis* R.Br. one of the most species-rich genera and with cosmopolitan distribution (Goetghebeur, 1998; Simpson et al., 2007; Muasya et al., 2008). Curiously, these genera share a noticeable reproductive feature: a thickening at the base of style, known as stylopodium, also present in other genera such as *Fuirena* Rottb. and *Abildgaardia* Vahl. However, these cited genera do not belong to the same clade (Hinchliff, Roalson, 2013).

The stylopodium is taxonomically informative specially to distinguish species and subsections of *Rhynchospora* (Strong, 2006). This structure may remain on the top of the fruit in some genera (persistent), as well as detach with the rest of the style (deciduous). Its functional role to species fitness and reproduction is poorly understood, been related as a region where competition and selection of pollen tubes take place (Reutemann et al., 2012), a structure that may be related to pollination mechanisms (Monteiro et al., 2017), fruit dispersal (Vrijdaghs et al., 2009), or seed imbibitions attributed to the cells with helical wall thickenings (tracheids) (Gonzalez, López, 2010).

In order to understand the morphological diversity of the stylopodium, as well as establish homologies among the genera in which the stylopodium occurs, it is essential to understand the morphology and ontogeny of this structure. Moreover, the application of phylogenetic analysis to evaluate the evolution of some traits has shown to be of great importance to establish a correlation between a trait and the diversification of non-correlated clades, indicating the presence of key innovations that may have an important role in the diversification rates (Rolland et al., 2012).

Within this context and considering the potential role of the stylopodium in species fitness and reproduction, we analyzed comparatively the stylopodium of species of the most species-rich genera in Brazilian Cerrado (Alves et al., 2009): *Rhynchospora albiceps, Fimbristylis autumnalis, Eleocharis filiculmis*, and *Bulbostylis hirtella*, to test the hypothesis that the stylopodium presents the same origin among these different genera and whether its anatomical structure evidences its potential role in the water uptake for seedling germination. Such aims were addressed by an integrative approach of anatomy and ontogeny to 1) identify any type of tissue or cell that potentially indicate a strategy to water

uptake and 2) to establish whether the stylopodium has the same origin in all species studied, indicating its relevance to the adaptation of Cyperaceae to dry and warm environments.

For the anatomical study, inflorescences with flowers and fruits at different developmental stages were fixed in FAA (formaldehyde, glacial acetic acid, 50% ethanol, 1:1:18 v/v) (Johansen, 1940) and stored in 70% ethanol. Then the material was dehydrated in a tert-butyl alcohol series and embedded in Paraplast. The embedded materials were sectioned at 13–15 μm on a rotary microtome, stained with Astra Blue and Safranin and mounted on slides with Permount. Photomicrographs were obtained using an image-capturing device coupled to a microscope Leica DMLB, using the software Scan System Images (IM50). For the ontogenetic study of the stylopodium, flowers and fruits at different developmental stages were dissected in 70% alcohol under a stereomicroscope, dehydrated through an ethanol series, critical-point dried, coated with gold and examined in a 1.5 Supra 55VP SEM.

The anatomy of the stylopodium in all studied species showed the presence of tracheids scattered throughout the style base. The presence of scattered tracheids in a structure that remains in the mature fruit (except for *Fimbristylis*) suggests that this structure plays an important role in improving the entrance of water after the fruit dispersion, as also reported for Bulbostylis (Gonzalez, López, 2010). Helical tracheoidal cells were also reported for orchid seeds as part of the mechanism of water uptake (Prutsch et al., 2000). Such structures have an important role in the seed germination in dry and hot environments, as the Brazilian savannas where these genera are widely distributed. Even for species where the stylopodium does not remain in the fruit, as in *Fimbristylis*, tracheids were also observed and may contribute in the water transference during the maturation of the fruit, since the stylopodium only detaches from the fruit when it is completely mature.

The stylopodium shows different shapes in the mature fruit among the studied species, however in the ontogenetic analysis they showed to share the same developmental pattern. In all of the studied species, the stylopodium is initiated at the pre-anthesis stage as a thickening of the style base. Although the stylopodium has the same ontogenetic origin in all species, when analyzed in a phylogenetic context this structure is probably homoplastic in Cyperaceae, since it most likely arose several times during the evolution of the family.

Considering the diversification of Cyperaceae clades, the major radiation occurred during the transition from the Paleocene to the Eocene, when the climate was changing to be drier (Escudero, Hipp, 2013). While some clades became restricted to tropical wet environments, others inhabit from tropical to temperate zones, as the species-rich clades Sclerieae, Rhynchosporeae, Cariceae, Eleocharideae, Abilgaardieae, and Cypereae (Escudero, Hipp, 2013). Many factors are cited as key-innovations for the diversification of such clades, for instance: the evolution of C_4 photosynthetic pathways and wind pollination (Linder, Rudall,

2005; Givnish et al., 2010). Since all the clades above cited present genera with stylopodium, except for Cariceae and Cypereae, we believe that the acquisition of such structure should be investigated as a possible key-innovation, together with physiological changes, that contributed to the high diversification rate of these clades.

References

Alves M., Araújo A.C., Prata A.P., Vitta F., Hefler S., Trevisan R., Gil A.S.B., Martins S., Thomas W. 2009. Diversity of Cyperaceae in Brazil. *Rodriguésia* **60**: 771–782.

Escudero M, Hipp A. 2013. Shifts in diversification rates and clade ages explain species richness in higher-level sedges taxa (Cyperaceae). *Am. J. Bot.* **100**: 2403–2411.

Givnish T.J., Ames M., McNeal J.R., McKain M.R., Steele P.R., dePamphilis C.W., Graham S.W., Pires J.C., Stevenson D.W., Zomlefer W.B., Briggs B.G., Duvall M.R., Moore M.J., Heaney J.M., Soltis D.E., Soltis P.S., Thiele K., Leebens-Mack J.H. 2010. Assembling the tree of the monocotyledons: plastome sequence phylogeny and evolution of Poales. *Ann. Mo. Bot. Gard.* **97**: 584–616.

Goetghebeur P. 1998. Cyperaceae. In: Kubitzki K. (ed.): *The families and genera of vascular plants*. Berlin: Springer. V. **4**. P. 141–190.

Gonzalez A.M., López M.G. 2010. Development and morphology of the gynoecium and nutlet in two South-American *Bulbostylis* (Cyperaceae) species. *Flora* **205**: 211–220.

Govaerts R., Simpson D.A., Goetghebeur P., Wilson K.L., Egorova T., Bruhl J. 2007. *World checklist of Cyperaceae. Sedges*. Kew: Royal Botanic Gardens, Kew Publ.

Hinchliff C.E., Roalson E.H. 2013. Using supermatrices for phylogenetic inquiry: an example using the sedges. *Syst. Biol.* **62**: 205–219.

Johansen D.A. 1940. *Plant microtechnique*. New York: McGraw-Hill Book Company.

Linder H.P., Rudall P.J. 2005. Evolutionary history of Poales. *Annu. Rev. Ecol. Evol. Syst.* **36**: 107–124.

Monteiro M.M., Scatena V.L., Oriani A. 2017. Comparative floral anatomy of *Rhynchospora consanguinea* and *Rhynchospora pubera* (Cyperoideae, Cyperaceae). *Plant Syst. Evol.* **303**: 283–297.

Muasya A.M., Simpson D.A., Verboom G.A., Goetghebeur P., Naczi R.F.C., Chase M.W., Smets E. 2008. Phylogeny of Cyperaceae based on DNA sequence data: current progress and future prospects. *Bot. Rev.* **75**: 52–66.

Prutsch J., Schardt A., Schill R. 2000. Adaptations of an orchid seed to water uptake and storage. *Plant Syst. Evol.* **220**: 69–75.

Reutemann A., Lucero L., Guarise N., Vegetti A.C. 2012. Structure of the Cyperaceae inflorescence. *Bot. Rev.* **78**: 184–204.

Rolland J., Cadotte M.W., Davies J., Devictor V., Lavergne S., Mouquet N., Pavoine S., Rodrigues A., Thuiller W., Turcati L., Winter M., Zupan L., Jabot F., Morlon H. 2012. Using phylogenies in conservation: new perspectives. *Biol. Lett.* **8**: 692–694.

Simpson D.A., Muasya A.M., Alves M., Bruhl J.J., Dhooge S., Chase M.W., Furness C.A., Ghamkhar K., Goetghebeur P., Hodkinson T.R., Marchant A.D., Nieuborg R., Reznicek A.A., Roalson E.H., Smets E., Starr J.R., Thomas W.W., Wilson K.L., Zhang X. 2007. Phylogeny of Cyperaceae based on DNA sequence data: a new *rbc*L analysis. *Aliso* **23:** 72–83.

Strong M.T. 2006. Taxonomy and distribution of *Rhynchospora* (Cyperaceae) in the Guianas, South America. *Contr. U.S. Natl. Herb.* **53**: 1–225.

Vrijdaghs A., Muasya A.M., Goetghebeur P., Caris P., Nagels A., Smets E. 2009. A floral ontogenetic approach to homology questions within the Cyperoideae (Cyperaceae). *Bot. Rev.* **75**: 30–51.

STRUCTURAL AND FUNCTIONAL DIFFERENCES BETWEEN THE GLANDULAR TRICHOMES OF THE VEGETATIVE AND REPRODUCTIVE ORGANS

Lyudmila E. MURAVNIK[1], ***Olga V. KOSTINA***[1], ***Anna A. MOSINA***[1], ***Nina L. ZAPOROZHETS***[2]

[1] Komarov Botanical Institute of Russian Academy of Sciences, Saint Petersburg, Russia
[2] Herzen State Pedagogical University of Russia, Saint Petersburg, Russia
lemur50@mail.ru

The glandular trichomes (GTs) are able to synthesize various substances of the primary and secondary metabolism including hydrolytic enzymes, polysaccharides, terpenoids, phenolics, and alkaloids (Vassilyev, 1977; Fahn, 1979). Secretory products promote plant interaction with insects, fungi and bacteria. They can be used as a lubricant for developing young shoots (Thomas, 1991); they protect leaves from excessive ultraviolet radiation (Tattini et al., 2000) and attract pollinating insects (Lopes et al., 2002). Morphologically varied glands are known to be quite often on different organs of the same plant. For example, in number Lamiaceae species, the peltate and small capitate hairs are situated on the leaves and bracts, while the large capitate hairs present on their calyces (Giuliani, Maleci Bini, 2008). The short GTs are found on all organs in *Inula* species (Asteraceae), whereas the long ones are formed only on leaves and stems (Sulborska, 2013). The present work is aimed to determine whether there is a structural and functional difference between the GTs developed on the vegetative and reproductive organs of the same plant species.

There are two types of the GTs of cylindrical shape on the leaves of three *Doronicum* species (Senecioneae, Asteraceae) (Muravnik et al., 2019). In GTs of the 1st type, a head consists of two cells, while eight to ten cell tiers compose the stalk. GTs of the 2nd type have the same two-celled head and shorter stalk. Subcuticular cavity is developed in the heads of GTs of both types to accumulate secretion. Histochemical tests and fluorescent microscopy reveal acid polysaccharides, polyphenols, flavonoids and terpenoids in GT's heads of both types. Main ultrastructural features of GTs of the 1st type are proliferation of RER and activity of Golgi apparatus denoting the synthesis of enzymes and pectin. The ultrastructural characteristics of GTs of the 2nd type are advanced SER, diversiform leucoplasts with reticular sheaths and chloroplasts with peripheral plastid reticulum indicating the predominant synthesis of lipid components. Since GTs of the 1st type synthesize more acid polysaccharides than GTs of the 2nd type, they seem to protect the growing shoots from mechanical damage during germination. GTs of the 2nd type are able to defend the young leaves from pathogens and herbivores, because they mainly synthesize flavonoids and terpenoids.

The capitate GTs of the 3rd type of large head and long stalk develop on the peduncles and phyllaries. Head diameter usually exceeds the stalk diameter. Form of the head cells is specific for each *Doronicum* species. Histochemical tests and fluorescent microscopy show scant acid polysaccharides in the GTs, whereas phenolic and terpenoid substances are abundant and accumulated in the cytoplasm and cell wall. Contrary to the GTs of the 1st and 2nd types, the GTs of the 3rd type have no subcuticular cavity. Instead, the external walls of their head cells have a thickened cutinized layer with dense network of dendritic structures and interfibrillar lamellae. The network of dendrites is oriented perpendicular to the plasma membrane, while lamellae resemble a chain of transparent crystals, which lie parallel to it. Abundant SER and significantly developed leucoplasts are formed in the cytoplasm of the secretory cells. Therefore, we have assumed the main function of the GTs of the 3rd type is a secretion of volatile substances to attract insect pollinators.

Three types of GTs are formed on the aerial organs of some *Arnica* species (Heliantheae, Asteraceae). The GTs of the 1st type have a typical of family biseriate structure including a two-celled head and a short stalk of 4 to 5 cell tiers. These GTs are on the leaves, peduncles, phyllaries, and corolla tubes. GTs of the 2nd type consist of small head and a longer stalk; they are on the peduncle and phyllaries in *A. foliosa* Nutt. and *A. longifolia* D.C. Eaton. In *A. montana* L. and *A. chamissonis* Less., instead of GTs of the 2nd type there are GTs of the 3rd type that have 4 cells in the head and long stalk. While a subcuticular cavity is developed in the head of GTs of the 1st and 2nd types, a great number of micro pores in the cuticle are found in GTs of the 3rd type. Secretion is discharged through these micro pores. Phenolic substances, terpenoids and sesquiterpene lactones was detected in the subcuticular cavity as well as in cytoplasm of the GTs. Phenols and terpenoids were the basic secretion components of GTs of the 1st and 2nd types, but GTs of the 3rd type mostly contained sesquiterpene lactones. Tubular SER, leucoplasts with osmiophilic inclusions and chloroplasts are the main ultrastructural characteristics of GTs of the 1st and 2nd type. In the head cells of GTs of the 3rd type, SER is also a typical organelle; in addition, leucoplasts often form cup-shaped invaginations. We concluded from the structure of GTs of the 1st and 2nd types in *Arnica* that they function as protectors against herbivores and pathogens, just as similar trichomes in *Doronicum*. The same capitate trichomes as GTs of the 3rd type were found in *Majorana syriaca* (Werker et al., 1985). The scent emitted by trichomes through their cuticular micropores is believed to attract pollinating insects.

The surface of the leaves and flowers of *Millingtonia hortensis* L. f. (Bignoniaceae) is covered with the GTs of three types. The peltate trichomes are the most numerous on the leaves, peduncles, calyces, petals, and ovaries. These trichomes consist of 12- to 16-celled disk-shaped head and a single-celled stalk. The cells are arranged radially in the head. GTs of the second type are on the corolla tube;

they are capitate trichomes with 2- to 4-celled head on the wide multicellular stalk. GTs of the third type look as the immersed peltate trichomes; they develop only on the petals. Different secondary metabolites are contained in the GTs as evidenced by the series of histochemical reactions and fluorescent microscopy. Phenolic substances were predominantly identified in foliar GTs whereas terpenoids were more copious in the GTs of petals, corolla tubes and ovaries.

GTs of each type has specific ultrastructural features.

In the peltate trichomes of the ovary, an amorphous light-coloured secretion is accumulated between structural material of the primary cell wall and its cutinized layer. Dark drops of secretion are deposited in a periplasmic space. Large leucoplasts in the secretory cells contain dark inclusions. Reticular sheaths surround the plastid envelope. Vacuoles are transparent.

In the capitate GTs of the corolla tube, the subcuticular cavity is practically absent. The secretory cells have external wall with large cutinized layer with dendrites. Numerous vesicles are in periplasmic space thus indicating the exocytosis of secretion products. Abundant SER with grey contents occupies the peripheral cytoplasm; it often contacts with plasma membrane. Vacuoles result from swelling of the tubular SER; grey contents appear in them. Leucoplasts have plastoglobuli and lamellar network. If nectaries are absent in the flowers of some plants, the secretory trichomes around the ovary are known to produce the drops of sweet mucilage and attract insects for pollination (Lopes et al., 2002). Based on this, we consider the GTs of the reproductive organs in *M. hortensis* to be secretory structures which attract pollinators. We believe that the foliar GTs protect young vegetative shoots against small herbivorous animals and pathogens.

References

Fahn A. 1979. *Secretory tissues in plants*. London. New-York, San Francisco: Academic Press.

Giuliani C., Maleci Bini L. 2008. Insight into the structure and chemistry of glandular trichomes of Labiatae, with emphasis on subfamily Lamioideae. *Plant Syst. Evol.* **276**: 199–208.

Lopes A.V., Vogel S., Machado I.C. 2002. Secretory trichomes, a substitutive floral nectar source in *Lundia* DC. (Bignoniaceae), a genus lacking a functional disc. *Ann. Bot.* **90**: 169–174.

Muravnik L.E., Kostina O.V., Mosina A.A. 2019. Glandular trichomes of the leaves in three *Doronicum* species (Senecioneae, Asteraceae): morphology, histochemistry and ultrastructure. *Protoplasma* DOI: doi.org/10.1007/s00709-018-01342-2

Sulborska A. 2013. Structure and distribution of glandular and non-glandular trichomes on aboveground organs in *Inula helenium* L. (Asteraceae). *Acta Agrobot*. **66**: 25–34.

Tattini M., Gravano E., Pinelli P., Mulinacci N., Romani A. 2000. Flavonoids accumulate in leaves and glandular trichomes of *Phillyrea latifolia* exposed to excess solar radiation. *New Phytol.* **148**: 69–77.

Thomas V. 1991. Structural, functional and phylogenetic aspects of the colleter. *Ann. Bot.* **68**: 287–305.

Vassilyev A.E. 1977. *Functional morphology of plant secretory cells*. Leningrad: Nauka. [In Russian]

Werker E., Ravid U., Putievsky E. 1985. Structure of glandular hairs and identification of the main components of their secreted material in some species of the Labiatae. *Isr. J. Bot*. **34**: 31–45.

3-D MODELING OF THE INTERFIBER BODERED PIT OF *BETULA PENDULA* ROTH

Nadezhda N. NIKOLAEVA*, *Vitaliy V. VOROBIEV

Forest Research Institute of Karelian Research Center of Russian Academy of Sciences, Petrozavodsk, Russia

nnnikol@krc.karelia.ru

Combining light, transmission and scanning electron microscopies, scientists have got a wealth of information for understanding such processes as perforation plate development, tylose formation, the formation of reaction wood, septate fiber ultrastructure, etc. Modelling of real object of real size and simulating different processes are paramount in some investigations. Lens et al. (2011) showed a correlation between the pressure required to reduce hydraulic conductance by 50% and pit features in *Acer* species. Correlations were found between the pit chamber depth, the pit membrane thickness, the pit chamber diameter and the aperture fraction. Bordered pits are advantageous for combining large area of the pit membrane with minimal loss of strength of the discontinuous secondary cell wall. Quality, quantity and shape of pits could partly be responsible for the stiffness of the wood fiber. This research is intended to expand information about characteristics of the fiber for better understanding their complexity, adaptive potential and industrial usability.

The study was carried out on 30-years-old trees of silver birch (*Betula pendula* Roth). 0.5 × 0.5 × 0.5 cm specimens of wood were sampled from 10 trees and prepared according to the most common technique of the scanning electron microscopy (SEM) (Jansen et al., 2008, 2009). Observations were carried out using TESCAN Vega II LSH at the Center for Collective Usage of Scientific Equipment, Karelian Research Center of the Russian Academy of Sciences. Dimensions of bordered pits (Fig. 1) were obtained using a VideoTest-Morphology 5.0 software package (VideoTesT, Russia).

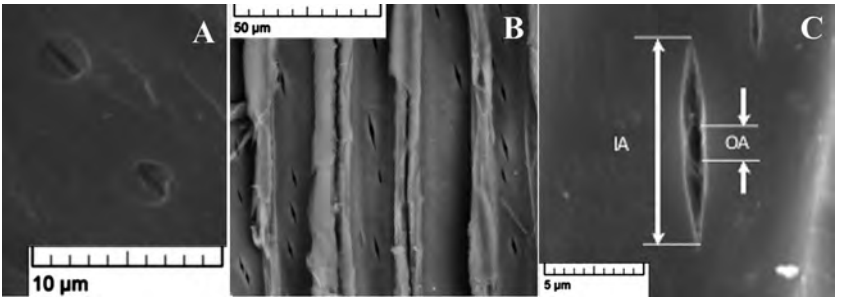

Fig. 1. Pits, SEM photographs.
A – a view from outside the fiber; B – tangential view from inside the fiber;
C – bordered pit with extended inner aperture.
IA – inner aperture, OA – outer aperture.

To construct 3D model of bordered pit, we used free medical software InVesalius which is usually used to generate virtual 3D reconstructions of structures on the base of their 2D images. After constructing 3D DICOM images, the software enables to generate STL (stereolithography) files. These files can be used for rapid prototyping. Among various tools, the InVesalius has advanced 3D visualization tools which use raycasting technique. It also has projection tools such as Maximum Intensity Projection (MaxIP or MIP), Minimum Intensity Projection (MinIP), Mean Intensity Projection (MeanIP), MIDA, Contour MaxIP and Contour MIDA.

We used additionally Free Online File Viewer (FOFV) from Autodesk. FOFV enables to combine project views, to construct axonometric projection of the object, to calibrate measurements and to share the project using URL. 3D-reconstruction is done by superposing 'slices', interpolating gaps between them and forming volume image of the object (Fig. 2). InVesalius has manual and semi-automatic segmentation tools based on threshold, region growing and watershed techniques. Linear and angular measurement tools in 2D and 3D. It also has volumetric measurement and surface area. Linear measurements are possible in three planes of object volume.

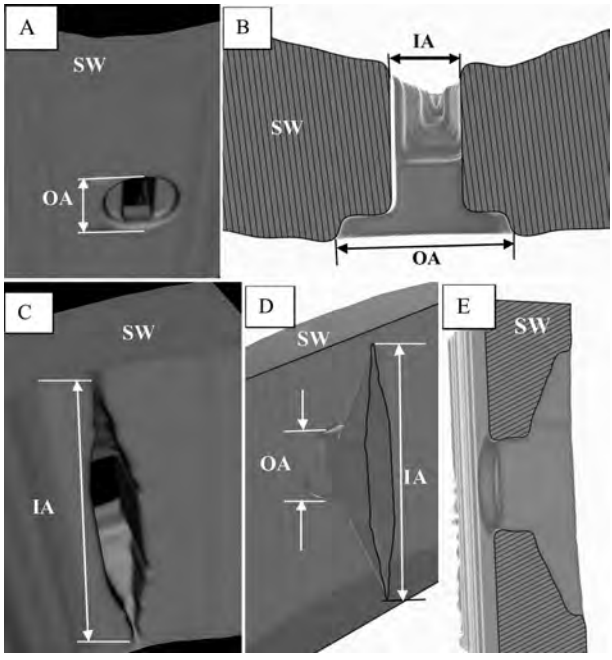

Fig. 2. 3D models of bodered interfiber pit of *B. pendula*.
A – view from outside the fiber; B – transverse view; C, D – view from inside the fiber; C–E – tangential longitudinal view; D – semitransparent view of the bodered pit from inside the fiber. IA – inner aperture, OA – outer aperture, SW – secondary wall.

The results provide a useful instrument for modelling and comprehension of pit geometry in various processes wood fibers are subjected to.

References

Lens F., Sperry J.S., Christman M.A., Choat B., Rabaey D., Jansen S. 2011. Testing hypotheses that link wood anatomy to cavitation resistance and hydraulic conductivity in the genus *Acer*. *New Phytol*. **190**: 709–723.

Jansen S., Choat B., Pletsers A. 2009. Morphological variation of intervessel pit membranes and implications to xylem function in angiosperms. *Am. J. Bot*. **96**: 409–419.

Jansen S., Pletsers A., Sano Y. 2008. The effect of preparation techniques on SEM-imaging of pit membranes. *IAWA J*. **29**: 161–178.

GIRDLING EFFECTS ON WOOD ELEMENTS DEFORMATION IN SILVER BIRCH

Nadezhda N. NIKOLAEVA*, *Vitaly V. VOROBIEV*, *Diana S. IVANOVA*, *Tatiana V. TARELKINA

Forest Research Institute of Karelian Research Center of Russian Academy of Sciences, Petrozavodsk, Russia

nnnikol@krc.karelia.ru

Double girdling (Daudet et al., 2005) is a valuable research tool to discern the tight coupling between water (xylem) and sugar and hormone (phloem) transport. Double girdling was applied to five 25 years-old *Betula pendula* Roth trees to manipulate the sugar and hormone (primarily the auxin) flow. The bark was completely mechanically cut off from the trunk at two height levels as follows. The bottom line of the first girdle ran at 110 cm above the ground. The bottom line of the second girdle was at 125 cm above the ground. Both cut strips of the bark were 5 cm wide. Unaffected bark 10 cm wide thus remained in between these girdles. Wood surface in the girdles was additionally scraped with a knife to prevent callus formation and resumption of assimilate transport. Three intact trees were used as a control.

Three zones were recognized in trunk of the double-girdled trees (Fig. 1): (1) the upper trunk zone (U) above the second girdle still receiving new assimilates from the leaves, (2) the bottom trunk zone (L) below the first girdle receiving only stored sugars from the roots, and (3) the middle trunk zone (M) 10 cm wide in between the girdles completely isolated from both crown and roots. The distorting effects of girdling on wood elements were investigated by analyzing the morphology of fibers and vessel elements. In October, 0.5 × 0.5 × 0.5 cm^3 wood samples were taken from each zone of each tree. These samples were split into 1 mm thick slivers in the radial direction to be macerated according to Wang et al. (2011). The qualitative parameters were evaluated visually, i.e. the comparative shape of the vessel elements, the appendices, perforation plates and fibers. At least 100 vessel

elements and fibers in each tree sample were measured. Part of the wood samples and permanent preparations were deposited and registered in the Abnormal Wood Collection of the Forest Research Institute of the Karelian Research Centre RAS.

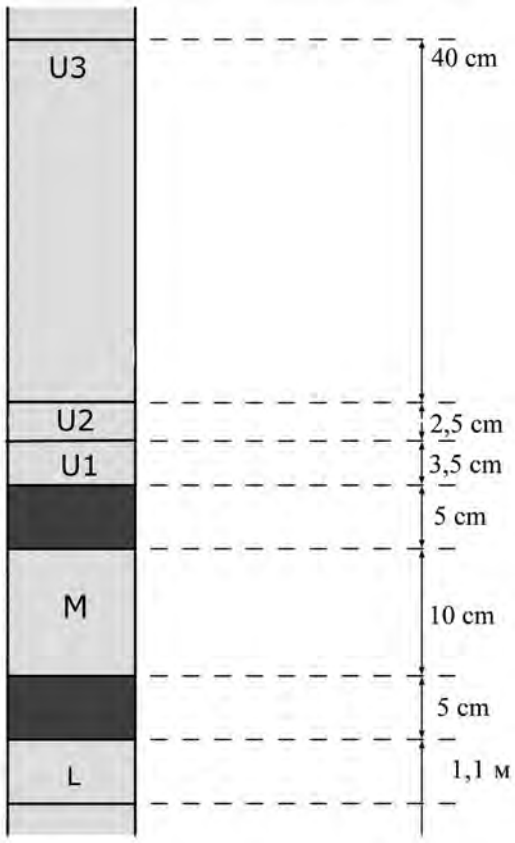

Fig. 1. The arrangement of zones within the plant.

Termination of the phloem transport while the xylem one being unaffected in the zone L, as well as termination of the phloem transport and substantially reduced xylem transport in the zone M completely arrest cambial activity in these two zones. Transverse sections of the zones L and M of girdled trees showed that cambium stopped functioning and died off immediately after girdling. Therefore, these zones were excluded from the consideration.

The U zone was subdivided into three subzones (Fig. 1): (1) U1 – 2.5 cm wide, 1 cm above the second girdle; (2) U2 – 2.5 cm wide, 3.5 cm above the second girdle; (3) U3 – 2.5 cm wide, 45 cm above the second girdle.

The xylem response to girdling depending on its distance from the girdle was evaluated by the zone-specific gradients of the fiber lengths and their deviations

from the spindle-like shape. The shortest and most deviated fibres were in the U1 subzone (Fig. 2A) whereas both length and shape of fibers and vessel elements were almost unaffected in the U3 subzone.

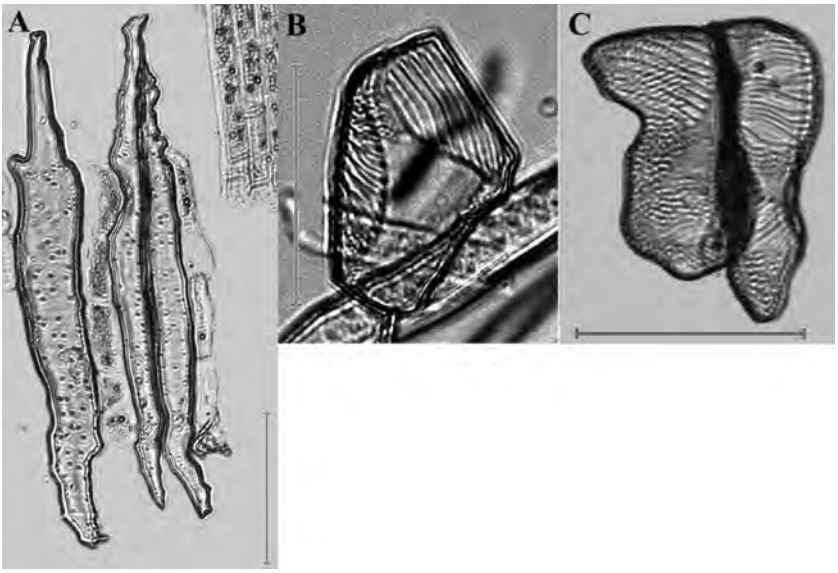

Fig. 2. Deformed xylem elements from the zone U1.
A – fibers; B, C – vessel elements. Bars – 100 μm.

According to Wodzicki (2001) the diameter of the fibers and thickness of their walls and the diameter of vessel elements are under tight genetic control in hardwoods, whereas fiber length is under moderate control. In our study, the fiber diameters insignificantly deviated from 25 μm in every zone of the experimental and control trees.

The fibers in subzones U1–U2 of the experimental trees are highly diverse in their ends up to being bifurcated to 2/3 of their lengths.

Our data confirm the previous results that mechanical damage induces the formation of narrower vessels in some hardwoods (Bauch et al., 1980; Kuroda, Shimaji, 1985; Kuroda, 1986; Lev-Yadun, Aloni, 1993). The vessel elements were also substantially deformed in the U1 subzone (Fig. 2B, C).

Interrupted phloem transport increased concentration of the sugars and hormones being maximal in the U1 subzone. The excess auxin and sucrose due to absence of their basipetal flow resulted in the development of deformed elongated fibers and vessel elements which are very similar to those in figured wood of Karelian birch (*Betula pendula* Roth var. *carelica* (Mercl.) Hämet-Ahti). We have previously showed that excess sucrose in the conducting phloem and the cambial zone can induce development of the figured wood in the latter tree (Novitskaya, 2008; Novitskaya, Kushnir, 2006; Novitskaya et al., 2016). The elevated glucose

resulted from sucrose cleavage promotes auxin conjugation, thus blocking the differentiation of vessels and fibers, and causes disruption of the regular arrangement of the wood constituents.

The fibers and vessel elements from the zones U1–U2 in the experimental trees were usually curved and sometimes bizarre-shaped. The fibers were shorter and wider, their widths often varied along their lengths. Vessel elements were narrow and shorter. The most deviated fibers and vessel elements were in the U1 subzone.

References

Bauch J., Shigo A.L., Starck M. 1980. Wound effects in the xylem of *Acer* and *Betula* species. *Holzforschung* **34**: 153–160.

Daudet F.A., Améglio T., Cochard H., Archilla O., Lacointe A. 2005. Experimental analysis of the role of water and carbon in tree stem diameter variations. *J. Exp. Bot.* 56: 135–144.

Kuroda K. 1986. Wound effects on cytodifferentiation in the secondary xylem of woody plants. *Wood Res.* **72**: 67–118.

Kuroda K., Shimaji K. 1985. Wound effects on cytodifferentiation in hardwood xylem. *IAWA Bull*. n.s. **6**: 107–118.

Lev-Yadun S., Aloni R. 1993. Effect of wounding on the relations between vascular rays and vessels in *Melia azedarach* L. *New Phytol*. **124**: 339–344.

Novitskaya L. L. 2008. *Karelian birch: mechanisms of growth and development of structural abnormalities*. Petrozavodsk: Verso. [In Russian]

Novitskaya L.L., Kushnir F.V. 2006. The role of sucrose in regulation of trunk tissue development in *Betula pendula* Roth. *J. Plant Growth Regulat*. **25**: 18–29.

Novitskaya L.L., Nikolaeva N.N., Galibina N.A., Tarelkina T.V., Semenova L.I. 2016. The greatest density of parenchyma inclusions in Karelian birch wood occurs at confluences of phloem flows. *Silva Fenn*. **50**: 1461.

Wang X., Shi S., Wang J., Yu Y., Cao S., Cheng H. 2011. Tensile properties of four types of individual cellulosic fibers. *Wood and Fiber Sci.* **43**: 353–364.

Wodzicki T. J. 2001. Natural factors affecting wood structure. *Wood Sci. Technol.* **35**: 5–26.

COLLECTION OF WOODS OF THE DEPARTMENT OF HIGHER PLANTS, LOMONOSOV MOSCOW STATE UNIVERSITY

Maja V. NILOVA*, *Vladimir R. FILIN

Lomonosov Moscow State University, Moscow, Russia

nilova_maja@mail.ru

The collection of woods was started with the work of Mikhail Ilyich Golenkin (1864–1941), the professor and Head of the Department of Higher Plants of Moscow State University. He traveled to Java, where he worked in the Buitenzorg (Bogor) Botanical Garden and brought back a rich collection of generative and vegetative

organs of tropical plants. Some of his samples are still used in teaching for demonstration. Unfortunately, the collection of wood has not been cataloged, and labels of many samples were gone.

The catalog of wood collection began to be created by V.R. Filin. In 1957 he studied fossil woods from Pleistocene and Holocene deposits of Great Lyakhovsky Island (New Siberian Islands). For comparison, it was necessary to have a reference collection of wood samples of plants widely distributed in Russia. He collected them first in the Moscow region and later during his trip to the Crimea, Eastern Siberia, the Polar Urals and Kamchatka. At his request, wood samples were also collected by staff members and students of the Department of Higher Plants and other institutions. Especially should be noted V.N. Tikhomirov, V.N. Vekhov, K.D. Volchansky, A.A. Korobkova and L.A. Tonkoshtan.

Wood collection of microtome slides of the most important tree species of the USSR, made at the factory for teaching aids was significantly enriched by G.B. Kedrov. He started with investigaton of wood anatomy of ash and later continued with wood samples of the other species including tropical ones. Wood samples of tropical species were gifted to him from the collection of Leningrad Forestry Academy by the leading xylotomist of that time, A.A. Yatsenko-Khmelevsky and his pupil, the Head of the Botanical Museum of Komarov Botanical Institute, E.S. Chavchavadze. Kedrov made microtome slides of wood of about 200 species.

Slides of the collection together with additionally prepared slides of new species were photographed and described in 2015–2018 within the framework of the RFBR project No 15-29-02508. Digital images of these wood slides formed a xylotomic block of an open information system on the anatomy and morphology of higher plants, which also includes the palynological and carpological collections. This open access information system represents a database-associated web-site (http://botany-collection.bio.msu.ru). The system was developed to consolidate and digitize large collections of the department to facilitate the work of experts in identification of pollen grains, spores, fruits, seeds and woods. These objects are often encountered in the analysis of plant material and are widely used for various reconstructions and expertises in paleobotany, archeology, criminology and museum work. The information system includes three blocks corresponding to three collections – “Wood” (wood anatomy collection), “Pollen” (palynological collection) and “Fruits and seeds” (carpological collection) – and has a joint interactive catalogue of all registered samples with a search function by the names of species, genera, families, and life forms. In addition, each collection has a separate catalogue with the function of search by various parameters.

In the block “Wood”, each sample is represented by 5–12 images of anatomical sections in transverse, radial, and tangential projections. The images are obtained using a light microscope at magnification 50×, 100×, and 400× and are accompanied by descriptions of key characters. Samples can be searched and sorted by

characters of wood structure. For gymnosperms, the search can be carried out by the presence or absence of resin canals in wood, type of tracheid pitting in radial walls and cross-field pitting. For angiosperms, the search is carried out by the presence or absence of vessels in the wood, distribution of vessels in the cross section (porosity), characteristics of the structure of the vessels (type of perforation plates, intervessel pitting) and rays (type, ray width, ray height, vessel-ray pitting).

To date, the collection includes more than 3000 wood samples collected in different regions of the world and cover > 800 plant species. In addition to dry wood samples, the collection includes material fixed in alcohol and permanent slides (transverse, radial, tangential sections) (about 500 species). The collection has electronic and paper catalogs. Samples of 400 species from 60 plant families are digitized and downloaded into information system, their images and descriptions are available online. Modern wood samples are accompanied by herbarium speciments.

Wood sampling and storing is supported by State Assignment of the Department of Higher plants, Lomonosov Moscow State University No. AAAA-A16-116021660045-2.

INTERNAL AND EXTERNAL STRUCTURE OF PLANTS: CONTRADICTORY HARMONY OF MODULAR ORGANIZATION

Alexander A. NOTOV

Tver State University, Tver, Russia

anotov@mail.ru

The complexity and heterobathmy of morphological and anatomical organization as well as the widespread parallelism make it difficult to reveal the ways of evolutionary transformations in higher plants (Lotova, 1989; etc.). Similar morphologies are realized in different taxa on the basis of distinct tissue architectures (Peters et al., 2000). The idea of a conjugate study of the internal and external structure of plants was repeatedly expressed (Hagemann, 1982, 1992). Despite this, anatomists and morphologists still generally work independently. The system analysis of the modular organization of plants is also relevant in order to give an assessment of the integrity and harmony of the organization (Beklemishev, 1964; Bertalanffy, 1969; etc.).

Beklemishev (1964) characterized the integral system qualities of living objects. His ideas match the ideas of philosophers and methodologists (Vinogray, 2011). Living beings should be considered according to (**A**) the level of the organization and the degree of the organization, (**B**) the complexity and hierarchical

structure of the organization, (**C**) the nature of the participation of internal non-living parts, (**D**) isolation of the organization, (**E**) the harmony of the organization (Beklemishev, 1964). These properties have been examined to varying degrees in plants and are of interest for botany.

A. The criteria of what should be considered as a high degree of the organization have been repeatedly discussed and are taken into account in the evolutionary theory (Severtsov, 1925; Iordansky, 2009). The degree of organization is one of the characteristics of the level of organization (Beklemishev, 1964). Zoological approaches to classifying the levels of organization deserve attention (Borisov et al., 1989; Mamkaev, 2008). In animals, there are three types of tissues which correspond with the main stages of their specialization: 1) primary; 2) metazoic; 3) specialized tissues of vertebrates with differentiated histogenetic units (Borisov et al., 1989). Mamkaev (2008) identified the following main phases (states) in the evolution of organ systems in unitary animals: 1) the diffuse phase (no specialized organs); 2) the dispersed phase (specialized units operate independently and are not morphologically related); 3) the coalition phase (organs function in a coordinated manner, forming a holistic apparatus); 4) the centralized phase (the central organ is distinguished in the integral apparatus). Variants of combinations of the leading integration subsystems (in animals, regulatory and transport subsystems) correspond to the main forms of constructive types.

Similar ideas can be developed in botany. The key function of integration in plants is performed by the transport and shaping subsystems. Both provide regulation at the organism level (Polevoi, 2001; Gamalei, 2004; Lucas et al., 2013). However, plants have only few degrees of the organization, which are less distinct than in animals. Even flowering plants do not reach the centralized phase of the organization of structural functional subsystems, although the structure of the transport system of seed plants corresponds to the coalition stage. Due to the specifics of the organization and structural evolution of plants, the principle of typification along the steps of organization can help to carry out a conjugate analysis of the stages of complication of the external and internal structure.

All morphologically separate ‘organs’ of plants are ‘external’ (Timonin, 2007). They are fundamentally different from the internal organs of animals, to which in the plants to some extent correspond “…tissue systems that permeate the whole body” (Shafranova, 2001). The paths of morphological and anatomical differentiation of plants are strategically multidirectional and to some extent independent. Morphology ‘provides’ the functional activity and efficiency of the interaction with the environment, and anatomy maintains the integrity of the plant organism.

There are two main directions of morphological differentiation. The first direction is associated with the separation of two subsystems (body parts) that interact with various components of the external environment (solid and gaseous or liquid media). Differentiation into axial and appendicular elements was achieved within the second direction. At the anatomical level, the formation and progressive com-

plication of the transport and shaping subsystems was of key importance. Secondary meristems along with the ability for secondary thickening and intercalary growth appeared because of differentiation of the shaping subsystem (Shafranova, 1981; Timonin, 2011).

The main directions of the transformation of the external structure of the body were carried out independently in different taxa on different structural bases. Specialization of axial and appendicular structures, as well as the structures contacting with the substrate, was carried out on the basis of syphone cells of plectenhymous and parenchymatous thalli, tissue talli, telomes and shoots in different groups of cladophytes and telophytes (Gollerbakh, 1977; Zmitrovich, 2006; Notov, 2016). The tendency to the differentiation of apical meristem appeared in all these series (Shafranova, 1981). However, only higher plants achieved the main stages of complication in tissue organization, especially in the transport subsystem (Tomescu, Groover, 2019). Due to the wide parallelism, a detailed analysis of the evolution of morphological and functional subsystems using the described approach can help to assess the conjugation of the key morphological and anatomical transformations.

B. The analysis of these properties in higher and especially flowering plants that have reached the maximum structural and functional differentiation and the complexity is important for understanding the mechanisms of the progressive evolution of modular plants. In contrast to unitary animals, the hierarchy of the structure in seed plants has a clear morphological expression. A complex system of plant structural units can include up to 12 subordinate levels (Gattsuk, 2008). The analysis of this system became the basis for the development of biomorphology and population-ontogenetic studies.

The hierarchy of cycles of structural evolution is well pronounced in higher plants due to the peculiarities of their modular organization. The main cycles of structural aggregation and integration led to the emergence of cladophytes and telophytes, to the emergence of a telomic, syntelomic and cladome organization (Zmitrovich, 2006; Notov, 2016). Separate structures and parts of axial (shoot) systems were transformed as a result of lower-level integration cycles. The further comprehensive study of these processes based on the concept of pseudocycles is necessary (Notov, 2016).

The concept of histion (modular) tissue structure is developed (Savostyanov, 2005). For plants, only the detection of more or less isolated multicellular units is reported. However, further studies in this direction are promising. For example, xylem vessels form separate clusters that act as functional units whose activity determines the flow paths of water (Park et al., 2015).

C. Living beings have the so-called non-living parts of different size classes in their bodies (Beklemishev, 1964). The level, scale and role of non-living parts in a plant body can be quite significant. The cell walls of dead cells form the mechanical framework and the basis of the xylem transport system. In woody plants, non-living components can form a large part of the body. *Pinus longaeva* is unique

in this respect, reaching a record age (up to 5 thousand years). Senile plants, with a huge array of dead body parts, almost do not have living elements (Zhmylev, 2006). Despite this, the plant retains its viability for a very long time. Body of seed plants often contains dying off or dead shoots and shoot complexes. Appropriate system analysis of apoptosis in plants is necessary (Dickman et al., 2017).

D. According to the concepts of morphogenetic isolation-openness *sensu* Beklemishev (1964) plants are of particular interest, as they have a widespread hybridization, apomixis, natural chimerism, and multicomponent symbiosis (Rinkevich, 2011; Notov, 2016).

E. Although the interest in the harmony of the organization of living beings arose long ago (Driesch, 1909; Beklemishev, 1964; etc.), this problem is still one of the least developed. Associated with the analysis of integrity and many integral characteristics of biosystems, this problem is of great importance for understanding the essential properties of an organization (Vinogray, 2011). According to Beklemishev (1964: 37) "…harmony of the organization is assessed by the degree of reciprocity or mutualism in the interrelationship of the vital units of the organism". In addition to the functional consistency of the parts and the whole, harmony implies the ability to maintain the integrity of the system with increasing tension of internal contradictions (Vinogray, 2011). The nature of the interrelation of structures of different levels, the high contingency of the processes of functioning and ontomorphogenesis, of course, indicate a high degree of harmony in the modular organization of higher plants. However, a number of phenomena are not consistent with the concept of harmony and need a philosophical understanding. They can be associated with specific models of plant ontogenesis, in which the loss of the integrity of the organism becomes the norm, the mechanisms leading to its death are activated, and the variant of prolonged existence in the 'half-dead' state is realized (Zhmylev, 2006). The phenomena are as follows: 1. Deterministic loss of physical and physiological integrity and 'potential immortality' in organisms that make up clones. 2. The state of 'chronic' senility with an extremely high percentage of dead body parts and a critically low number of living elements. 3. Monocarpics with deterministic quick aging and instant death.

Some examples of relatively low consistency of developmental programs are associated with homeotic structures that are very common in plants (Notov, 2015). Some types of polyvariancy of ontogenesis associated with the loss of different stages and the realization of alternative pathways of development also indicate a lack of coordination between the interrelationships of the parts and the whole.

Thus, the conjugate analysis of the internal and external structure of plants from the standpoint of a systematic approach can contribute to further development of structural and theoretical botany. It allows achieving a deeper understanding of the specifics of the modular organization of plants and ways of its progressive complication. It also helps to develop criteria for assessing the harmony and integrity of biological systems at the organism level.

References

Beklemishev V.N. 1964. On the general principles of the organization of life. *Byull. Moskovsk. Obshch. Isp. Prir. Otd. Biol.* **69**: 22–38. [In Russian]

Bertalanffy L. 1969. *General system theory. Foundation, development, application*. New York: George Brasiller.

Borisov I.N., Dunaev P.V., Bazhanov A.N. 1989. *Phylogenetic bases of animal tissue organization*. Novosibirsk: Nauka. [In Russian]

Dickman M., Williams B., Li Y., de Figueiredo P., Wolpert T. 2017. Reassessing apoptosis in plants. *Nat. Plants* **3**: 773–779.

Driesch H. 1909. *Philosophie des Organischen*. Leipzig: W. Engelmann.

Gamalei Y.V. 2004. *The transport system of vascular plants*. St. Petersburg: St. Petersburg Univ. Press. [In Russian]

Gattsuk L.E. 2008. Plant organism: experience of construction of a hierarchical system of its structural-biological units. In: Savinykh N.P., Bobrov Yu.A. (eds.): *Modern approaches to the description of the plant structure*. Kirov. P. 26–47. [In Russian]

Gollerbakh M.M. (ed.). 1977. *Life of plants.* V. **3**. Moscow: Prosveshchenie. [In Russian]

Hagemann W. 1982. Vergleichende Morphologie und Anatomie – Organismus und Zelle, ist eine Synthese möglich? *Ber. Dtsch. Bot. Ges.* **95**: 45–56.

Hagemann W. 1992. The relationship of anatomy to morphology in plants – a new theoretical perspective. *Int. J. Plant Sci.* **153**: 38–48.

Iordansky N.N. 2009. Factors of evolutionary progress. In: Grinin L.E., Korotaev A.V., Markov A.V. (eds.): *Evolution: cosmic, biological, social*. Moscow: LIBROKOM. P. 154–176. [In Russian]

Lotova L.I. 1989. Morphological and functional aspects of evolution of the conducting apparatus in higher plants. *Byull. Moskovsk. Obshch. Isp. Prir. Otd. Biol.* **94**: 92–102. [In Russian]

Lucas W., Groover A., Lichtenberger R., Furuta K., Yadav S.-R., Helariutta Y., He X.-Q., Fukuda H., Kang J., Brady S.M., Patrick J.W., Sperry J., Yoshida A., López-Millón A.-F., Grusak M.A., Kachroo P. 2013. The plant vascular system: evolution, development and functions. *J. Integr. Plant Biol.* **55**: 294–388.

Mamkaev Y.V. 2008. Influence of morphogenetic mechanisms on constructive characteristics of organisms. *Vestn. Tver. Gos. Univ. Ser. Biol. Ecol.* **9**: 139–147. [In Russian]

Notov A.A. 2015. Homeosis and evolution of modular organisms. *Paleontol. J.* **49**: 1681–1690.

Notov A.A. 2016. Pseudocyclical similarities and structural evolution of modular organisms. *Biol. Bull.* **43**: 226–234.

Park J., Kim H.K., Ryu J., Ahn S., Lee S.J., Hwang I. 2015. Functional water flow pathways and hydraulic regulation in the xylem network of *Arabidopsis. Plant Cell Physiol.* **56**: 520–531.

Peters W.S., Hagemann W., Tomos A.D. 2000. What makes plants different? Principles of extracellular matrix function in 'soft' plant tissues. *Comp. Biochem. Physiol.* **125**: 151–167.

Polevoi V.V. 2001. The physiology of plant integrity. *Rus. J. Plant Physiol.* **48**: 545–555. [In Russian]

Rinkevich B. 2011. Quo vadis chimerism? *Chimerism* **2**: 1–5.

Savostyanov G.A. 2005. *The base of structural histology. Spatial organization of epithelia.* St. Petersburg: Nauka. [In Russian]

Severtsov A.N. 1925. *The main directions of the evolutionary process*. Moscow: A.V. Dumnov & Co. [In Russian]

Shafranova L.M. 1981. Branching in plants: process and result. In: Veshchikova T.V., Gattsuk L.E., Serebrjakova T.I. (eds.): *Life forms: structure, spectra, and evolution*. Moscow: Nauka. P. 179–212. [In Russian]

Shafranova L.M. 2001. Homology problem in plant world: plant as an object of homologization. In: Oskolski A.A., Sokoloff D.D., Timonin A.C. (eds.): *Homologies in botany: experience and*

reflections. St. Petersburg: Saint-Petersburg Association of Scientists and Scholars. P. 30–38. [In Russian]

Timonin A.C. 2007. *Botany.* V. **3**. Higher plants. Moscow: Akademia Publ. [In Rusian]

Timonin A.C. 2011. *Anomalous secondary thickening in Centrosperms: specificity of the morphological and functional evolution of plants*. Moscow: KMK. [In Russian]

Tomescu A.M.F., Groover A.T. 2019. Mosaic modularity: an updated perspective and research agenda for the evolution of vascular cambial growth. *New Phytol.* https://doi.org/10.1111/nph.15640.

Vinogray E.G. 2011. Integrated systems categories as characteristics of holistic analysis of complex objects. *Sociol. Vestn.* **2**: 126–142. [In Russian]

Zhmylev P.Y. 2006. The evolution of plant life span: facts and hypotheses. *Zh. Obshch. Biol.* **67**: 107–119. [In Russian]

Zmitrovich I.V. 2006. Phytoepiphenomena and their ecomorphological nature. *Vestn. Ekol. Les. Landshaft*. **7**: 3–29. [In Russian]

THE USE OF THE CHARACTERS OF ANATOMICAL STRUCTURE IN THE SYSTEMATICS OF THE BLUEGRASSES (*POA* L.) OF THE SECTION *STENOPOA* DUMORT.

Marina V. OLONOVA

Tomsk State University, Tomsk, Russia

olonova@list.ru

Section *Stenopoa* Dumort. is one of the largest in the genus *Poa*. According to various estimates, in Siberia it contains from 10 to 20 species. The species of this group play an important phytocenotic role, often being dominants and edificators of plant communities in extratropical Eurasia. Evolution in the *Stenopoa* section is known to have followed the path of xerophilization, and now the species of the section occupy a variety of habitats, ranging from wetlands to dry stony steppes. All this makes the species of the section an extremely convenient object for studying the stages of evolution, but on the other hand, their tendency to hybridize enriches the genotype and leads to noticeable anatomical and morphological changes and blurr the boundaries between species. Indeed, it is necessary to search the anatomical structure in order to reveal the new characters, suitable for both taxon discrimination and non-molecular characterization of branches of the phylogenetic tree. The difficulty of the study of grasses, and, in particular, bluegrasses, lies in the fact that the structure of both vegetative and reproductive organs is extremely monotonous, and the number of characters used in systematics and the number of states of these characters are small. Meanwhile, anatomical data (mainly covering the leaf blade) are widely used in the system-

atics and diagnostics of grasses both in our country and abroad. In comparative anatomical studies of the genus *Poa* L., the main attention was paid to the study of cross sections of the leaf blade (Konstantinova, 1960; Poyarkova, 1966; Galkin, 1974; Probatova, 1974; and others); in Siberia these kind of researches are unlikely to have been conducted. For taxonomists, the qualitative characters that are the indicators of genetic relationship are of the greatest value (Davis, 1977). One of these signs is the type of sclerenchyma in the leaf blades. This feature is the key character in the systematics of xeromorphic species of *Festuca* L., and in the taxonomy of bluegrasses it is used to distinguish different species of *Poa* (Poyarkova, 1966; Galkin, 1974; Probatova, 1974).

The purpose of this work was to study opportunities of using of the pattern of sclerenchyma arrangement for systematics and diagnostics of the Siberian bluegrasses of the *Stenopoa* section.

The preparations were made according to generally accepted methods (Barykina et al., 2004).

When studying leaves on a cross section, the following features were taken into account: the type of middle and lateral veins according to Vucoloff (1929), which detect the distribution of sclerenchyma in the leaf, the shape of the keel. Vucoloff (1929) recognized six types of sclerenchyma arrangement around the vascular bundles taking into account the presence of the girders and strands and their different composition

In *P. nemoralis*, according to Galkina & Seredin (1973), the midrib is of I type only (girders from abaxial and adaxial sides). The study of Siberian materials (the most typical specimens of the species were selected with a short, not longer than 1 mm, ligule, pubescent rachilla and an uppermost node located in the upper half of the stem) showed that this type of midrib was found only in 18% of individuals out of 83. The midrib was type II (girders from one side and strands from another) in 27% of samples, and type III (strands from both sides) in 55% of samples. The amount of sclerenchyma strands also varied greatly. This supports the opinion of Tsvelev (2009) that *P. nemoralis* is replaced by a different species in Siberia.

Poa skvortzovii Probat. is a more xeromorphic species that replaces *P. nemoralis* in arid habitats in the east of the region. In this species, the midrib of type III already occurs much more often: in 78% cases. At the same time, type I was found in 11% of individuals and type II occur in 11% of samples.

Poa palustris is a very polymorphic and variable species occupying a wide variety of habitats (the most typical specimens of the species with long leaves and long ligule, glabrous rachilla and uppermost node located in the upper half of the stem were studied). Poyarkova (1966), Probatova (1974) and Galkin & Seredin (1973) indicated the midrib of type I for this species, whereas 130 (64%) Siberian plants of *P. palustris* had the midrib of type III. Type I and II were found in 7% and 29% of individuals, respectively.

Populations of bluegrasses, combining the characters of both *P. nemoralis* and *P. palustris* (attributed here to the hybridogenic complex *P. intricata* Wein) were also studied. They also have the midribs of the first three types, and, like in the previous species, the type does not depend on the habitat. However, in plants collected on stony slopes, the vast bundles of sclerenchyma can reach the midrib.

Poa urssulensis Trin. is an aggregate of presumably hybrid origin, which, according to Tzvelev (1976), occupies an intermediate position between *P. nemoralis*, *P. palustris* and *P. versicolor* Bess. On the territory of Siberia, it is represented by three species – genuine *P. urssulensis, P. krylovi*i Reverd. and *P. buriatica* (Olonova) Olonova.

The study of *P. urssulensis* s. str. (plants with a short, not more than 1.5 mm ligule, glabrous rachilla and an uppermost node located in the lower part of the middle third or in the upper part of the lower third of the stem) and *P. buriatica,* morphologically close to this species, showed that both the structure of the leaves and the location of the sclerenchyma are very diverse. There are plants with the midrib of I, II, III, V types, and the specific type, not mentioned by Vukolov (the midrib with an adjacent area of sclerenchyma) was found twice. Such veins have been described by Probatova (1974) in the species of *Arctopoa* Probat. Thus, the midrib of types III and II (47% and 40%, respectively) are dominated within *P. urssulensis* and *P. buriatica;* the individuals of types I (10%) and V (3%) are much less common. In some plants, the sclerenchyma girders are expressed so strongly that they form the thickenings above and below the lateral veins, which is why the leaves in the cross section are of a distinct shape.

Poa krylovii differs from the other species of the section in dominating of types I and II of the midrib, which account for 35% each, and only 30% of the individuals have the type III vein. In other words, type I of midrib is more common here than within mesomorphic *P. nemoralis* and *P. palustris*. Such a deviation from the general tendency of type III to dominate with increasing xeromorphy could be explained by the fact that, against the background of the general development of hybridization processes within the mesomorphic species, the anatomical structure of *P. krylovii* leaves remained closer to the ancestral form as a result of mosaic evolution. The majority of the Siberian samples of *P. nemoralis* and *P. palustris* have lost their characteristic arrangement of sclerenchyma strands as a result of hybridization and adaptive evolution.

Poa stepposa, P. botryoides, P. reverdattoi Roshev. and *P. argunensis* Roshev. are of more xeromorphic structure than *P. urssulensis*, and their leaves are narrower, enrolled, with bulges above the veins and in the most xeromorphic individuals with sulculus between them. In these species, type III of midrib, which is characteristic of the most xeromorphic species of the section, prevails (85%), and 15% have II type of midrib. Among the lateral veins type III prevails as well.

Poa attenuata is the most xeromorphic species of the section. Type III of midrib is common among this species. The number of lateral veins is reduced to 5 (7)

on each side. All sclerenchyma strands are well developed, the leaves often have grooves between the veins, which reduce the transpiration.

The next group of species – *P. glauca* Vahl., *P. altaica* Trin., and *P. litwinoviana* Ovcz. – is attributed to despecialized hybridogenous aggregate *P. glauca*. They have a wide variety of leaf blades, from mesomorphic (long, flat and soft) to xeromorphic (short, rolled and hard), their structure types are varied, ranging from having all the veins of type I to all veins of III type with well pronounced sclerenchyma cords, like the xeromorphic species of *Stenopoa.*

The obtained data show that in the species of the *Stenopoa* section, the proportion of individuals with type III vein increases with increasing xeromorphy of the species. All samples of the most xeromorphic species (*P. attenuata*) have III type of midrib. The only deviation from the general trend was observed in *P. krylovii*, in which type I of the midrib prevailed, and the proportion of individuals with this type exceeded that in mesomorphic *P. nemoralis* and *P. palustris*. A study of the Siberian representatives of *P. nemoralis* and *P. palustris* showed that, in contrast to European and Far Eastern individuals, the midrib of type III is more common among Siberian samples. This can obviously be explained by the wide development of hybridization processes in Siberia.

The anatomical structure of the leaf blade of Siberian *Stenopoa* is most stable in those species, in which the macromorphological features vary slightly. Accordingly, in species of large polymorphism the anatomical structure usually varies greatly as well. In some species, the type of the midrib in the cross section remains more or less constant, but studies of this trait at the population level have shown that in most cases only a certain, apparently, genetically determined tendency remains. The very same feature varies widely due to the widespread hybridization processes among the grasses. This is especially noticeable when comparing the variation of ancient low-chromosome species and young species of clearly hybrid origin.

Nevertheless, the type of the midrib seems to be hereditarily determined and practically does not depend on the growing conditions of the plant. Thus, although it cannot be used as a discriminator, it can be used to identify a possible relationship.

The research was supported by the RFBR grant No. 19-04-00973.

References

Barykina R.P., Veselova T.D., Devyatov A.G., Dzhalilova Kh.Kh., Iljina G.M., Chubatova N.V. 2004. *Handbook of botanical microtechnique. Basics and methods*. Moscow: Moscow Univ. Press. [In Russian]

Galkin M.A. 1974. To the use of anatomical studies in the diagnosis and taxonomy of plants on the example of bluegrass. *Actual issues of pharmacy. Stavropol*. **2**: 329–333.

Galkin M.A., Seredin R.M. 1973. On the microscopic structure of the bluegrass leaves of the Caucasus flora. *Scientific Report of High School. Biol. Sci*. **11**: 55–59. [In Russian]

Poyarkova E.N. 1966. Anatomical structure of the leaves of bluegrass flora of the Ukrainian SSR. *Bot. Zhurn*. **51**: 841–844. [In Russian]

Probatova N.S. 1974. On the new genus *Arctopoa* (Griseb.) Probat. (Poaceae). *Nov. Syst. Plant. Vasc*. **11**: 44–54. [In Russian]
Konstantinova A.G. 1960. Anatomical features of the wild species of bluegrasses (*Poa* L.) in Ukrainian flora. *Ukrain. Bot. Zurn.* **17**: 51–58. [In Russian]
Tzvelev N.N. 1976. *Grasses of the USSR*. Leningrad: Nauka. [In Russian]
Tzvelev N.N. 2009. The species of bluegrass (*Poa* L., Poaceae) sections *Stenopoa* Dumort. in Eastern Europe. *Nov. Syst. Plant. Vasc*. **41**: 18–53. [In Russian]
Davis J.A. 1977. Epidermal anatomy in *Puccinelia* (Poaceae). *Am. J. Bot*. **74**: 1744–1749.
Vucoloff V. 1929. Comparative anatomy of leaf-blade of *Poa* sp. grown in Czechoslovakia. *Sbornik Československé Akad. Zemědělskich. Věd* **4**: 417–452.

SECONDARY PHLOEM OF *AMBORELLA*: WHAT KINDS OF SIEVE ELEMENTS ARE THERE IN THE BASAL ANGIOSPERMS?

Alexei A. OSKOLSKI

University of Johannesburg, Johannesburg, South Africa
Komarov Botanical Institute RAS, Saint Petersburg, Russia
oskolski@yandex.ru

It is commonly supposed that sieve cells are characteristic for phloem of gymnosperms whereas sieve-tube members are confined to angiosperms. Mature sieve elements of both types are enucleate cells with sieve areas (clusters of pores with cytoplasmatic strands) on their walls; they also have symplastic connections to certain parenchyma cells. In contrast to sieve cells, however, the sieve-tube members are characterized by the presence of sieve plates (i.e. highly specialized sieve areas on end walls) and by their close association with ontogenetically related parenchyma cells termed as companion cells (e.g. Esau, 1939; Cheadle, Whitford, 1941; Behnke 1975; Evert, 1984). In addition to these traits, sieve-tube members can usually be distinguished also by the presence of P-protein, chromatolytic nuclear degeneration and relatively wide sieve pores derived from single plasmodesmata. Unlike them, gymnosperm sieve cells are characterized by pycnotic nuclear degeneration, absence of P-protein, formation of sieve areas from branched plasmodesmata with median cavities (Evert, 1984; Behnke, 1986).

Among flowering plants, the sieve elements without sieve plates have been reported only in *Austrobaileya* (Srivastava, 1970), the only genus of the family Austrobaileyaceae representing one of the basal angiosperm lineages. Although these sieve elements resemble sieve cells of gymnosperms, they show many characteristic features of angiosperm sieve-tube members, including their association with companion cells (Behnke, 1986). This combination of traits may be presumably considered as an intermediate form of sieve elements shedding light on the

origin of typical sieve-tube members in early evolution of flowering plants. If this condition is ancestral for flowering plants, we can expect to find it on other lineages of ANITA clade. To test this hypothesis, we studied the structure of secondary phloem elements in *Amborella* (Amborellaceae) belonging to the basalmost lineage of extant angiosperms.

Our light microscopic observations show that sieve elements of *Amborella* are formed by few transverse divisions of fusiform cambial derivatives. Sieve areas occur both on side walls and on transverse end walls of these cells. The latter ones show certain resemblance to simple sieve plates, but they cannot be distinguished by light microscopy from the sieve areas localized on side walls. The successive sieve elements that seemingly derived from different fusiform cambial derivatives are interconnected only with sieve areas on side walls. Thus, the sieve elements are arranged into short 'sieve strands' rather than into sieve-tubes. Companion cells closely associated with sieve elements occasionally occur. These cells are seemingly derived from common mother cells by their lateral anticlinal divisions. Besides them, the connections found between sieve elements and parenchyma cells formed by anticlinal divisions of ray cells.

Therefore, the sieve elements of *Amborella* resemble those in *Austrobaileya* differing from the latter mainly in the occurrence of sieve areas on transverse end walls. Our preliminary results suggest that the lack of sieve plates coupled with the presence of companion cells associated with sieve elements is an ancestral condition for angiosperms. This combination of gymnosperm and angiosperm features of sieve elements can expectedly be found in other basal lineages of angiosperms, i.e. in Nymphaeales and Austrobayleyales other than Austrobaileyaceae. Careful ultrastructural investigations of sieve elements in *Amborella* are required, however, to confirm or reject our suggestions.

This work was supported by the Russian Foundation for Basic Research [grant No. 18-04-00797a].

References

Behnke H.-D. 1975. Phloem tissue and sieve elements in algae, mosses and ferns. In: Aronoff S. et al. (eds.): *Phloem Transport*. New York, London: Plenum Press. P. 187–210.

Behnke H.-D. 1986. Sieve element characters and the systematic position of *Austrobaileya*, Austrobaileyaceae – with comments to the distinction and definition of sieve cells and sieve-tube members. *Plant Syst. Evol.* **152**: 101–121.

Cheadle V.I., Whitford N.B. 1941. Observations on the phloem in the Monocotyledoneae. I. The occurrence and phylogenetic specialization in structure of the sieve tubes in the metaphloem. *Am. J. Bot.* **28**: 623–627.

Esau K. 1939. Development and structure of the phloem tissue. *Bot. Rev.* **5:** 373–432.

Evert R.F. 1984. Comparative structure of phloem. In: White R.A., Dickison D.C. (eds.): *Contemporary problems in plant anatomy*. New York: Academic Press. P. 145–234.

Srivastava L.M. 1970. The secondary phloem of *Austrobaileya scandens*. *Can. J. Bot.* **48**: 341–359.

ANATOMICAL CHARACTERS OF FRUIT AND LEAF IN THE FAMILY UMBELLIFERAE, SUBFAMILY APIOIDEAE, AND THEIR EVOLUTION

Tatiana A. OSTROUMOVA

Lomonosov Moscow State University, Moscow, Russia

ostro_t_a@mail.ru

The fruit characters are widely used in the systematics of the family Umbelliferae, since the fruits are very diverse, and many characters of the fruit are constant within the species. A lot of material on the morphology and anatomy of the fruit has been accumulated.

The task of comparing species is simplified by the fact that the subfamily Apioideae is recognized as natural (i.e. monophyletic), the fruits have basically the same structure, and the homology of the fruit elements is beyond doubt. Flowers are semiepigynous, ovary consists of two carpels, in the ovary wall there are 10 vascular bundles: five for the calyx teeth and stamens, and five for the petals. In most species, the fruits split into two mericarps and a column; the wall of each mericarp contains 5 vascular bundles, each bundle corresponds to a rib of a certain shape. Strictly speaking, the ribs of the mericarps of one fruit are not entirely homologous: in one mericarpium, the median rib corresponds to the petal bundle while in the other, to the sepal+stamen bundle. Heteromericarpy is observed in a few species; in some cases, it is associated with the fact that the 'sepal ribs' are larger than the 'petal ribs'.

The external fruit morphology was described with varying degrees of detail for almost all umbelliferous species. To identify such important details of the pericarp structure as the composition of the tissues, the thickness and lignification of the cell walls, the distribution of small secretory ducts, and the boundary of the exocarpium (i.e. commissure width), the magnification of at least ×400 is necessary. High-quality descriptions of fruit anatomy with detailed drawings or photographs are known for 750–800 species. Most studies have been carried out on mature fruits. The study of the fruit development provides interesting material. For example, in some species, the secretory ducts in mature fruits are destroyed or crushed, but are well visible in young fruits.

We preliminarily reviewed fruit characters in the form of a database. There are both common and relatively rare character states which are unevenly distributed among the taxa. Such a rare character state as the long calyx teeth (longer than the stylopodia) are found in the genera *Astrantia*, *Chaetosciadium*, *Eryngium*, *Grammosciadium*, *Kailashia*, *Lagoecia*, *Ligusticopsis*, *Oenanthe*, and *Oreocome* that cannot be regarded as closely related. A similar pattern shows the campylospermy (endosperm with strongly revolute edges), which was considered of great importance in the 19th century. It is characteristic of the *Bilacunaria*, *Caucalis*,

Echinophora, *Heptaptera*, *Margotia*, *Prangos*, *Scandix*, *Smyrniopsis*, *Turgenia*, and others. Large epidermal cells (> 30 μm) are known in *Elaeosticta*, *Hymenidium*, *Ostericum*, *Pleurospermum*, *Taeniopetalum*, etc. Large secretory ducts under vascular bundles were found in the European genus *Oreoselinum* and the South African genus *Nanobubon*. Large rib ducts, which were considered an important feature in the subfamily Saniculoideae, were found in other umbelliferous groups in the genera *Dichoropetalum*, *Rumia*, *Saposhnikovia*, *Trinia*, *Xanthoselinum*, etc. The similarity in one or a few characters cannot be considered an indicator of close relationship between umbelliferous taxa.

We have repeatedly written that the fruit traits are of key importance to the systematics of Umbelliferae. We believe that serious taxonomic revision cannot be fulfilled without analyzing the fruit structure. However, the overestimation of carpological characters and the application of few traits for distinguishing genera have led to great difficulties. For example, more than 900 nomenclature combinations are known in the genus *Peucedanum*; many species with flat fruits, broad commissure, and weakly projecting dorsal ribs were included into this genus. More than 300 species name combinations have been published in the genus *Carum*, to which species with terete mericarps and equal low ribs were attributed. More than 300 combinations are known for species of the genus *Ligusticum* with more or less equal winged ribs. At present, most of these species are realized to be rather distantly related to the type species of these genera, and many combinations have become synonyms.

Several anatomical traits of the leaf are shown to be of great taxonomic importance, especially the internal structure of the petiole and the stomatal types. Petiole characters are useful for identifying species, especially their vegetative individuals in the field studies. The presence of vascular bundles in the center of the petiole, along with the ring of peripheral bundles, is the most constant character at the genus level. Two versus three to five epidermal cells around the stomata are the most important character for taxonomy.

We selected following anatomical features that are relatively rare in the concerned subfamily and constant in most of its genera (either subgenera or sections) studied: 1) stomata with two ajacent epidermal cells, 2) central bundles in petioles, 3) large exocarp cells, 4) campylospermy (revolute endosperm), 5) large rib secretory ducts, 6) large secretory ducts under the vascular bundles in the ribs, and 7) cyclic secretory ducts. All these characters are worth being considered taxonomically important. We traced their distribution within the two most well-known classifications of the family, viz. the system of Drude (1897–1898), based on morphological traits (Table 1), and the clades of Downie et al. (2010), based on the study of the ITS region of nuclear ribosomal DNA (Table 2). Most of the abovementioned character states, along with the usual ones, were found in several divisions of each of the systems in accordance with Vavilov's law of homologous series (Vavilov, 1922).

Table 1. Distribution of some character states in the tribes and subtribes of subfamily Apioideae. System of Drude (1897–1898) modified by Pimenov & Leonov (1993).

	1	2	4	3	5	6	7
Echinophoreae		+	+				
Scandiceae	+	+	+				+
Caucalideae	+	+	+				
Laserpitieae	+	+	+				
Coriandreae		+					
Smyrnieae		+	+	+			+
Apieae–Ap	+	+		+	+		+
Apieae–Foen	+	+		+			+
Angeliceae	+	+		+			+
Peucedaneae	+	+		+	+	+	+
Tordylieae	+	+		+			

Table 2. Distribution of some character states in the molecular clades of subfamily Apioideae as listed according to Downie et al. (2010).

	1	2	3	4	5	6	7
Acronema	+		+				+
Apieae	+						
Arcuatopterus					+		
Cachrys		+		+			+
Careae	+		+				
Komarovia		+		+			
Oenantheae							+
Opopanax		+		+			
Physospermopsis				+			
Pimpinelleae	+						+
Pleurospermeae			+				
Pyramidoptereae		+	+				+
Scandiceae F		+					
Scandiceae S	+	+		+			+
Scandiceae T				+			
Selineae	+	+	+	+	+	+	+
Smyrnieae				+			+
Tordylieae L						+	
Tordylieae T	+	+					

It is necessary to emphasize that the similarity of taxa in a few traits does not always mean the close relationship between them, but the differences should be taken into consideration as they could evidence the need to exclude a taxon from the higher taxon. The genus *Pimpinella* is characterized by stomata with 2 adjacent epidermal cells (diacytic and paracytic), but East Asian species *P. acuminata* and *P. purpurea* do not have diacytic stomata. Therefore, we had doubts about the validity of nesting these species in the genus *Pimpinella*. Zhou et al. (2008) do recently have shown that these species belong to the clade Physopermopsis, not Pimpinelleae.

The tables show that character state series are scattered throughout the subfamily. Many species seem to be able to form identical character sets, but these sets randomly realize in the subfamily concerned.

Plant microcloning somewhat confirms this idea conjecture. Phytohormones are widely used when culture is passed through callus or suspension to result in chromosomal aberrations. Rozhanskaya (2016) received many blooming and fruiting descendants of one *Onobrychis arenaria* individual. Various plants of the same clone had traits of stems, inflorescences, flowers and fruits that were characteristic of closely related species *O. viciifolia, O. transcaucasica*, and *O. sibirica*. Thus, the *Onobrychis arenaria* genotype is able to produce organs of alien specificity under certain conditions. Kunakh (2004) also reported that callus-passed plants can generate traits of other species of the same genus and that suspension-passed ones occasionally generate traits of other genera.

Another confirming example comes from zoology. Colonies of hydroid *Dynamena pumila* (Hydrozoa, Leptolida) resemble plants, so they are described with 'botanical' terms 'shoot', 'internode', 'stem', etc. Its shoots typically bear distichous opposite hydrants. Many abnormalities were revealed by Marfenin et al. (1995) among more than 300 000 investigated shoot segments. Some deviant segments were similar with the segments of other species: uniseriate hydrants are similar to those of the genus *Hydrallmania*, distichous alternate hydranths are similar to those of the genus *Abietinaria*, whorled (three-lane) hydrants simulate in detail the hydrants of *Sertularia tatarica*, and aberrant rotated plane of the internode is usual for *S. staurotheca*. Typical and deviate forms can coexist in a single colony.

Mosaic and combinatory distribution of the characters dealt with is observable in the subfamily Apioideae. Each character could be arranged in morphological series, even in continuous one. However, these series are hardly isomorphous to the trait evolution. Primitive-to-advanced graduating of the traits concerned seems unconvincing for the subfamily Apioideae. Construction of homologous series of traits is a more suitable method for describing the diversity of characters in this subfamily. Combinatory and repeating diversity hinders the distinguishing of genera in the family Umbelliferae.

References

Downie S.R., Spalik K., Katz-Downie D.S., Reduron J.-P. 2010. Major clades within Apiaceae subfamily Apioideae as inferred by phylogenetic analysis of nrDNA ITS sequences. *Plant Div. Evol.* **126**: 111–136.

Drude O. 1897–1898. Umbelliferae. In: Engler A., Prantl K. (Hrsg.): *Die natürlichen Pflanzenfamilien*. Leipzig: Engelmann. **3**(8). S. 63–250.

Kunakh V.A. 2004. The N.I. Vavilov's law of homologous series in plant somaclonal variation. In: *Genetics in 21th century: modern state and perspeciteves of development. 3d Congress of Vavilov society of geneticists and breeders (Moscow, June 6–12, 2004). Abstracts*. Moscow: Almatreid. **V. 1**. P. 73. [In Russian]

Marfenin N.N., Margulis R.J., Mayer E.M. 1995. Morphological variability of the colonial hydroid *Dunaliella pumila*, with classification of found morphotypes. *Proc. Zool. Institute St. Petersburg*. **261**: 71–89. [In Russian]

Pimenov M.G., Leonov M.V. 1993. *The genera of the Umbelliferae*. Kew: Royal Botanic Garden.

Rozhanskaya O.A., Shilova T.V., Gorshkova E.M. 2016. Variability of taxonomic characteristics in populations of regenerated plants and generative progenies of *Onobrychis arenaria* (Kit.) DC. In: *Problems of Botany of South Siberia and Mongolia. Proceedings of the 15th International Scientifc and Practical Conference (Barnaul, 23–26 May 2016)*. Barnaul: Altai Univ. Publ. P. 321–324. [In Russian]

Vavilov N.I. 1922. The law of homologous series in variation. *J. Genet*. **12**: 47–89.

Zhou J., Peng H., Downie S.R., Liu Z.-W., Gong X. 2008. A molecular phylogeny of Chinese Apiaceae subfamily Apioideae inferred from nuclear ribosomal DNA internal transcribed spacer sequences. *Taxon* **57**: 402–416.

MAMMILLARIAN REVERSION TO (QUASI)LEAFY ORGANIZATION: AN ANATOMICAL EXPLORATION

Lyudmila V. OZEROVA[1], ***Alexander C. TIMONIN***[2]

[1] Tsitsin Main Botanical Garden RAS, Moscow, Russia
[2] Lomonosov Moscow State University, Moscow, Russia
lyozerova@yandex.ru

Transformation of brachyblasts into areoles and substitution of trophophylls by assimilating cortex are principal and the most conspicuous trends of somatic evolution of cacti (Nyffeler, 2002; Edwards et al., 2005). The congenital fusion of the areole with the leaf base of its subtending leaf resulted in the tubercle (Troll, 1935) characteristic of the subfamily Cactoideae. The tubercles merged into ribs in vast majority of Cactoideae (Troll, 1935; Higgins, 1936), but re-appeared in some its lineages (Higgins, 1936).

The tubercles in *Mammillaria* alliance (tribe Cacteae s.ampl.) are thought to be regained (Higgins, 1936; Wallace, Gibson 2002; Hernández- Hernández et al., 2011). Such regained tubercles are believed to increase water-storage or/and as-

similating tissue (Troll, 1935) or to enhance regulation of the stem volume during dehydration–rehydration cycles (Mauseth, 2006). These tubercles are elongated in some mammillarians into leaf-like terete formations and up to triquetrous quasi-leaves in *Leuchtenbergia principis* Hook., so that the plant resembles co-inhabiting *Agave lophantha* Schiede (Troll, 1935; Mauseth, 2006).

The evolution from the typical shoot to typical cactus organization was repeatedly scrutinized morphologically, anatomically, histologically and physiologically (see Mauseth, 2006 for details). However, the mammillarian reversion to the (quasi) leafy organization seems to stay underexplored to date.

To fill this gap, we studied anatomically typical firm 5–6 mm long tubercles of *Mammillaria vetula* ssp. *gracilis* (Pfeiff.) D.R. Hunt, elongated flaccid 15–20 mm long tubercles of *M. decipiens* ssp. *albescens* (Tiegel) D.R. Hunt; longer terete flaccid 20–25 mm long quasi-leaves of *M. longimamma* DC. and the longest triquetrous firm 60–150 mm long quasi-leaves of *Leuchtenbergia principis* Hook. This series of species is in no way phyletic (Butterworth et al., 2002; Vásquez-Sánchez et al., 2013), but it could quite illustrate the tubercle to quasi-leaf transformations in the *Mammillaria* alliance. Genuine terete 4–13 cm long leaves of *Austrocylindropuntia subulata* (Muehl.) Bakeb. were used as a reference object.

The material was collected from living plants grown in the greenhouse of Tsitsin Main Botanical Garden of Russian Academy of Science, Moscow, and fixed in 70% alcohol. The formations under consideration were hand razor- or microtome-sectioned longitudinally or serially transversely. The sections were either successively processed with phloroglucinol and hydrochloric acid or stained with Carbolic Fuchsine and Delafield's Haematoxylin according to Barykina et al. (2004).

All tubercles and quasi-leaves studied are of the same structural type, though those of *L. principis* have a 2-layered hypodermis, which is absent in *Mammillaria* species. The palisade chlorenchyma occupies the outer part of the wide cortex. This tissue invariantly consists of oblique outward ascending rows of rather short palisade cells and long slightly tortuous intercellular spaces in between. The outer chlorenchyma is discontinuous under the terminal depression of the tubercle bearing clustered thorns. Large isodiametric cells with chloroplasts constitute the inner cortex parenchyma, the latter one being rather similar with the ray and medulla parenchyma of the narrower stele. A few small collateral stelar bundles terminate in the hydrocytic body which is under the tubercle terminal depression and consists of short wide 'wide-band' tracheids (Mauseth, 2006). The hydrocytic body is the bulkiest in the firm tubercles of *M. vetula*, where it runs about distal 1/3 tubercle length. The body is much lesser in *M. longimamma*. It is a thin lobed transverse plate in *M. decipiens* and *L. principis*.

The cortex has its specific conducting system of peripheral vascular plexus under the chlorenchyma. This plexus is connected with the stelar bundles in the base of the typical firm tubercle and with the terminal hydrocytic body of the latter.

The peripheral vascular plexus is supplemented by the sparse bundles branched off from the stelar ones along the stele in longer flaccid tubercles of *M. decipiens* and in quasi-leaves of *M. longimamma* and *L. principis*.

High decreasing of the hydrocytic body is the only notable alteration of the anatomical structure of the typical tubercle evolving to the quasi-leaf. The functional value of this formation evidently decreases to a minimum with the tubercle changing to the quasi-leaf. That is why the hydrocytic body seems to be unimportant for supplying the chlorenchyma, in spite of its direct connection with the peripheral vascular plexus.

Not only quasi-leaves but ordinary mammillarian tubercles are noteworthy to be anatomically similar with the genuine terete leaves of *A. subulata*. The two organ types similarly have the outer palisade chlorenchyma of oblique outward ascending rows of 4–6 short palisade cells, the inner parenchyma of larger isodiametric cells with chloroplasts, and the peripheral vascular plexus under the palisade chlorenchyma. Only the tubercle stele fundamentally differs from the leaf midvein in accordance to the different morphological essence of these organs.

Deep resemblance between the typical tubercle and the terete leaf means that the former one is structurally preconditioned to evolve into the leaf-like organ, without altering its anatomy.

The research was supported by the State Assignment of MBG RAS No. 118021490111-5 at the Unique Scientific Installation Fund Greenhouse.

References

Barykina R.P., Veselova T.D., Devjatov A.G., Dzhalilova Kh.Kh., Iljina G.M., Chubatova N.V. 2004. *Manual of botanical microtechnique. Principles and methods*. Moscow: Moscow Univ. Press. [In Russian]

Butterworth C.A., Cota-Sanchez J.H., Wallace R.S. 2002. Molecular systematic of tribe Cacteae (Cactaceae: Cactoideae): a phylogeny based on *rpl*16 introne sequence variation. *Syst. Bot*. **27**: 257–270.

Edwards E.J., Nyffeler R., Donoghue M.J. 2005. Basal cactus phylogeny: implications of *Pereskia* (Cactaceae) paraphyly for the transition to the cactus life form. *Am. J. Bot*. **92**: 1177–1188.

Hernández-Hernández T., Hernández H.M., De-Nova J.A., Puente P., Eguiarte L.E., Magallón S. 2011. Phylogenetic relationships and evolution of growth form in Cactaceae (Caryophyllales, Eudicotyledoneae). *Am. J. Bot*. **98**: 44–61.

Higgins V. 1936. Lines of evolution in cacti. *Cact. J*. **4**: 67–71.

Mauseth J.D. 2006. Structure–function relationships in highly modified shoots of Cactaceae. *Ann. Bot*. **98**: 901–926.

Nyffeler R. 2002. Phylogenetic relationships in the cactus family (Cactaceae) based on evidence from *trn*K/*mat*K and *trn*L-*trn*F sequences. *Am. J. Bot*. **89**: 312–326.

Troll W. 1935. *Vergleichende Morphologie der höheren Pflanzen*. Bd.**1**. Vegetationsorgane. Teil 1. Berlin: Gebrüder Borntraeger.

Vásquez-Sánchez M., Terrazas T., Arias S., Ochoterena H. 2013. Molecular phylogeny, origin and taxonomic implication of the tribe Cacteae (Cactaceae). *Syst. Biodiv*. **11**: 103–116.

Wallace R.S., Gibson A.C. 2002. Evolution and systematics. In: Nobel P.S. (ed.): *Cacti: Biology and uses*. Berkeley, Los Angeles: Univ. California Press. P. 1–21.

EVOLUTION OF PHYTOMELANIN IN ASTERACEAE: INSIGHTS FROM DEVELOPMENTAL ANATOMY

Arun K. PANDEY[1]***, Roshni Rajamohan MATHUR***[2]

[1] Mansarovar Global University, Bhopal, India
[2] University of Delhi, New Delhi, India

arunpandey79@gmail.com

Phytomelanin is a rigid, blackish brown, inert and amorphous layer which develops in the pericarp of Asteraceae members after fertilization and is secreted by the hypodermal layer of the ovary wall in the schizogenous space created after splitting of the hypodermis and fibre layer. Phytomelanin is deposited in those regions where the papillae are in contact with the hypodermis. These regions appear as pores. The pegs in Eupatorieae are formed due to greater space developed between the hypodermal cells along with the schizogenous space. Presence of striations has been a character of evolved tribes such as Bahieae, Madieae, Tageteae and some evolved subtribes of Heliantheae. The non-striate cypselae have larger pores as observed in Coreopsideae and Athroismeae. The tribe Athroismeae which forms a basal clade of the alliance has 3 subtribes of which the subtribes Anisopappinae and Centipedinae lack phytomelanin whereas it is present in the subtribe Athroisminae. Pegs are truncate projections characteristic of the tribe Eupatorieae. Presence of striations in the pericarp of cypselae is an apomorphic condition. The formation of phytomelanin in the cypselae may be a product which evolved due to environmental stress. The tribes with striated cypselae are distributed mainly in the temperate regions of the new world. The evolution of phytomelanin to counter the heat and cold stress in the derived groups within Asteraceae could be one of the reasons for the evolutionary success of the Heliantheae alliance. The cypselae of four genera in the Sipolisia group of Vernonieae show spotty phytomelanin in the pericarp. Phytomelanin is an important taxonomic character which has been used in the tribal and subtribal classification in the family Asteraceae. The occurrence of phytomelanin in the pericarp within the Heliantheae alliance has led to the conceptualization of an informal group (Phytomelanin Cypsela Clade) to include all the taxa with this ambiguous substance.

INFLUENCE OF STOMATAL RINGS ON MOVEMENTS OF GUARD CELLS

Anatoly A. PAUTOV[1], ***Svetlana M. BAUER***[1], ***Olga V. IVANOVA***[1], ***Elena G. KRYLOVA***[1], ***Olga V. YAKOVLEVA***[2], ***Yulia O. SAPACH***[1], ***Irina A. PAUTOVA***[2]

[1] Saint Petersburg State University, Saint Petersburg, Russia
[2] Komarov Botanical Institute of Russian Academy of Science, Saint Petersburg, Russia
a.pautov@spbu.ru

Cuticular folds have been described for nearly all above-ground surfaces of plants including their leaf epidermis (Koch et al., 2009). They are often present on the stomatal complex cells. The guard cells of some plants bear folds of cuticle, so called stomatal rings. These rings can be located either immediately on guard cell walls around the outer ledges (marginal stomatal rings), or on the outer ledges themselves (rings of ledges). Light, scanning, and transmission electron microscopy were used to study the stomata of the leaf epidermis in *Viburnum suspensum* Lindl. (Caprifoliaceae), *Lauro-cerasus officinalis* M. Roem. (Rosaceae), *Sarcococca humilis* Stapf (Buxaceae), *Artocarpus heterophyllus* Lam. (Moraceae), *Exbucklandia populnea* (R. Br. ex Griff.) R.W. Brown (Hamamelidaceae), *Carissa spectabilis* (Sond.) Pichon, *Acokanthera oblongifolia* (Hochst.) Codd and *Acokanthera oppsitifolia* (Lam.) Codd (Apocynaceae), which have stomatal rings. All plant material was collected in the Botanical gardens of St. Petersburg State University and Komarov Botanical Institute (St. Petersburg, Russia).

All studied species are represented by evergreen plants with dense or leathery leaves. Their mesophyll is differentiated into palisade and spongy tissues and the latter makes up the bulk of it. The leaves are hypostomatic. The stomatal complexes are anomocytic in *L. officinalis* and *A. heterophyllus*, mainly laterocytic in *V. suspensum* and *S. humilis*, mainly cyclocytic in *E. populnea*, *C. spectabilis, A. oblongifolia* and *A. oppositifolia.* The guard cells of all studied species are located on the subsidiary or neighbouring cells.

The stomata of *V. suspensum*, *L. officinalis*, *A. heterophyllus*, *S. humilis* have marginal stomatal rings. These rings are usually formed by cuticular folds and pectin-like material which fills the subcuticular space of the folds. The guard cell walls lying under marginal stomatal rings can be deformed. It was discovered that the marginal stomatal ring arises in the early stages of stoma development. After its arising, the ring stretches together with the growing stoma. The squeeze of stoma by ring can happen if the stretching of stomatal ring ceases before the stoma growth is completed. The stomata of *E. populnea*, *C. spectabilis, A. oblongifolia* and *A. oppositifolia* have rings of ledges. They are located on the hypertrophycally developed outer ledges. These rings are formed exclusively by the cuticle.

To elucidate the role of the rings, we have applied dynamic modelling using the finite-element method (FEM), also called finite element analysis (FEA) (Basov, 2005; Madenci, Guven, 2006). The data on the shape of the guard cells, uneven thickness of their walls, localization and the relative sizes of stomatal ledges and rings were exactly reproduced during model stomata construction. We have taken the approach to the studying of stomatal mechanics, according to which the wall material of the guard cells is isotropic, homogeneous and follows Hooke's law (Sharpe et al., 1987). The Poisson's ratio values of the cell walls are generally estimated to range from 0.45 to 0.5 (Fung, 1993; Braybrook, 2015). In our computations, it was assumed that the Poisson's ratio was 0.48. The turgor pressure was simulated by creating the load distributed on the inner surface of the guard cells.

The dynamic modelling has shown that the marginal stomatal rings are able to influence the movements of guard cells located on the subsidiary cells. The turgid guard cells which have no outer ledges and marginal stomatal rings bulge above the leaf surface. The wide opening pore between such guard cells moves in the same direction and rises above the leaf surface as well. The influence of marginal rings on stomatal movements depends on the mechanical characteristics of the rings, namely on their rigidity and squeezing of stoma by them. According to modelling results, the formation of rigid rings or rings squeezing stoma in addition to rigid ledges leads to deep sinking of the open pore below the leaf surface. The main movements in such stoma happen in central parts of the inner tangential walls of the guard cells.

It has already been shown that large outer ledges prevent wide opening of the stomatal pore and cause it to become sunk below the leaf surface. The more is the rigidity of the ledges, the narrower is the open pore and the deeper is its sinking into the epidermis (Pautov et al., 2017). Rings of ledges are ribs of rigidity. They rib the outer ledges. Like mechanical characteristics of marginal rings do, this property of ledges influence the stomatal pore position of the open stoma.

The studied plants belong to different taxonomic groups, grow in different environments and have different life forms. Judging by widespread occurrence, their leaf structure is adaptive to different environmental conditions. It resembles the leaf structure of evergreen sclerophyllous plants which are connected, according to Axelrod (1975), in their origin with subhumid tertiary laurophyllous forests. It is possible that the stomatal complexes with rings were typical of a part of the woody plants which grew in these forests. According to current concepts, the stomatal movements depend on turgor pressure in the guard cells, their shape and wall structure (Sharpe et al., 1987; Wilmer, Fricker, 1996). The present study has shown that stomatal rings are essential functional elements of the stomata of some extant plants. According to the results of modelling, they are able to influence the stomatal movements.

This study was supported by the Russian Foundation for Basic Research (grant No. 17-04-01213a to AAP). The study was carried out using laboratory facilities of the Research Resource Centres for molecular and cell technologies of St. Petersburg State University and Komarov Botanical Institute RAS.

References

Axelrod D.I. 1975. Evolution and biogeography of Madrean–Tethyan sclerophyll vegetation. *Ann. Mo. Bot. Gard*. **62**: 280–334.

Basov K.A. 2005. *ANSYS*: *User manual*. Moscow: DMK Press. [In Russian]

Braybrook S.A. 2015. Measuring the elasticity of plant cells with atomic force microscopy. In: Paluch E.K. (ed.): *Biophysical methods in cell biology*. San Diego: Academic Press. V. **125**. P. 237–254.

Fung Y.C. 1993. *Biomechanics: mechanical properties of living tissue*. New York: Springer Science + Business Media.

Koch K., Bhushan B., Barthlott W. 2009. Multifunctional surface structures of plants: an inspiration for biomimetics: invited review. *Prog. Mater. Sci.* **54**: 137–178.

Madenci E., Guven I. 2006. *The finite element method and applications in engineering using ANSYS*. New York: Springer Science + Business Media.

Pautov A., Bauer S., Ivanova O., Krylova E., Sapach Yu., Gussarova G. 2017. Role of the outer stomatal ledges in the mechanics of guard cell movements. *Trees* **31**: 125–135.

Sharpe P.J.H., Wu H., Spence R.D. 1987. Stomatal mechanics. In: Zeiger E., Farquhar G.D., Cowan R. (eds.): *Stomatal Function*. Stanford: Stanford Univ. Press. P. 91–114.

Wilmer C.M., Fricker M.D. 1996. *Stomata*. 2nd ed. London: Chapman & Hall.

MICROSTRUCTURE OF VEGETATIVE AND REPRODUCTIVE ORGANS OF TWO *CHENOPODIUM QUINOA* WILLD. VARIETIES GROWN IN SERBIA

***Ilinka PEĆINAR*[1], *Boris CZEKUS*[2], *Sladjana SAVIĆ*[2], *Steva LEVIĆ*[1], *Zorica JOVANOVIĆ*[1], *Radmila STIKIĆ*[1]**

[1] University of Belgrade, Belgrade-Zemun, Serbia
[2] Megatrend University, Belgrade, Serbia
ilinka@agrif.bg.ac.rs

Quinoa (*Chenopodium quinoa* Willd.) is an annual pseudo-cereal crop belonging to the Amaranthaceae family and originated from South America. The plant is currently in focus due to its high tolerance to drought or salinity (Jacobsen, 2017), as well as exceptional nutritional value of its fruits and plant vegetative parts (Gordillo-Bastidas et al., 2016). In Serbia, a country with the Southeastern European agro-climatic conditions, quinoa is not yet growing. Considering the quinoa in terms of the modern food industry, the examination of microstructure of two quinoa varieties (Puno and Titicaca) may be promising as well as increase the understanding of physiological and ecological behaviour of this crop in Serbia. The leaf, stem, root and fruit microstructure of two quinoa varieties were investigated. Slides for light microscopy were made according to Ruzin (1999). The microslides were examined with a light microscope Leica DM2000 equipped with

a digital camera (Leica DFC320). According to leaf microstructure, *C. quinoa* is amphistomatic species with heterofacial leaf structure. The polygonal shape of the stem transverse sections is common features for *Chenopodium* spp. (Bonzani et al., 2003). In the stem transverse section there are discernible the epidermis, cortex and central cylinder with conjoint open collateral vascular bundles arranged in three concentric rings arisen from successive rings of pericyclic cambium. In transverse section, the root has an angular shape, with periderm on the surface and a very thin cortical region, due to the development of anomalous secondary thickening arisen from a succession of cambia inside the central cylinder. In the fruit's longitudinal section, two-layered pericarp and the seed's compartments could be observed. In the quinoa seed, the embryo consists of a hypocotyl-radicle axis and two cotyledons surrounding the perisperm like a ring. Our study of quinoa microstructure together with additional microspectroscopic analysis are under investigation.

References

Bonzani N.E., Barboza G.E., Bugatti M.A., Ariza Espinar L. 2003. Morpho-histological studies in the aromatic species of *Chenopodium* from Argentina. *Fitoterapia* **74**: 207–222.

Gordillo-Bastidas E., Díaz-Rizzolo D.A., Roura E., Massanés T. 2016. Quinoa (*Chenopodium quinoa* Willd.), from nutritional value to potential health benefits: an integrative review. *J. Nutr. Food Sci.* **6**: 1–10.

Jacobsen S.E. 2017. The scope for adaptation of quinoa in Northern Latitudes of Europe. *J. Agron. Crop Sci.* **203**: 603–613.

Ruzin S.E. 1999. *Plant Microtechnique and Microscopy*. New York, Oxford: Oxford Univ. Press.

USING HISTOLOGICAL AND CYTOLOGICAL ANALYSIS FOR OBSERVATION OF FRUIT DEVELOPMENT IN TOMATO WILD TYPE AND ITS ABA MUTANT

Ilinka PEĆINAR[1]***, Dragana RANČIĆ***[1]***, Sofija PEKIĆ QUARRIE***[2]***, Nadia BERTIN***[3]***, Radmila STIKIĆ***[1]

[1] University of Belgrade, Belgrade-Zemun, Serbia
[2] State University of Novi Pazar, Novi Pazar, Serbia
[3] French National Institure for Agricultural Research, Avignon, France
ilinka@agrif.bg.ac.rs

Pericarp cell number and size determine the final fruit size. In this study, we investigated fruit development of two tomato genotypes, cv. Alisa Craig (wild type) and its ABA-deficient mutant flacca, characterized by less concentration of ABA in its vegetative and reproductive organs. Fruits of both genotypes were harvested at ten different developmental phases during the period from 3 days after anthesis (daa) to ripe fruit stage. We performed histological and cytological analysis of

fruit pericarp and prepared microslides for light microscopy according to standard paraffin procedure (Ruzin, 1999) or using a method of maceration by pectinase solution (Bertin et al., 2002). Pericarp sections were observed by Leica DMLS stereomicroscope and images were acquired by Leica DC300 digital camera. For cell size measurements public domain Image J software (Rasband, 1997–2009) were used. The analysis of cell size combined with the identification of pericarp cell layers allowed us to visualize the spatial distribution of cell sizes according to their position in the pericarp, indicated late cell division and cell expansion phases. The total number of pericarp cell increased up to 20 days after anthesis in wild type and in flacca, suggesting a similar period of cell division in both genotypes. However, final fruits were about three times smaller in flacca compared with wild type, which is related to the reduction in pericarp cell number and means cell size. It is known that ABA can directly influence cell division through its effect on cell cycle genes (Nitsch et al., 2012) and on stimulation of cell enlargement during tomato fruit growth as we noted in wild type, while an involved reduction in both processes, cell division and expansion. Comparing these two methods for analyzing tomato pericarp we can conclude that maceration by pectinase solution is faster and could serve for obtaining information about quantitative trait such as number of cell in whole fruit pericarp, while histological sections are more time consuming but it could give real view of cell size distribution and complete view of pericarp cell layers development from anthesis to ripe fruit stage.

References

Bertin N., Gautier H., Roche C. 2002. Number of cells in tomato fruit depending on fruit position and source-sink balance during plant development. *J. Plant Growth Regul.* **36**: 105–112.

Nitsch L., Kohlen W., Oplaat C., Charnikhova T., Cristescu S., Michieli P., Wolters-Arts M., Bouwmeester H., Mariani C., Vriezen W.H., Rieu I. 2012. ABA-deficiency results in reduced plant and fruit size in tomato. *J. Plant Physiol*. **169**: 878–883.

Rasband W.S. 1997–2009. *ImageJ*. U. S. National Institutes of Health, Bethesda, Maryland, USA. Available at: http://rsb.info.nih.gov/ij (accessed June 14, 2018).

Ruzin S.E. 1999. *Plant Microtechnique and Microscopy*. New York, Oxford: Oxford Univ. Press.

THE VARIABILITY OF CROSS-FIELD PIT MORPHOLOGY IN LIGNITIC FOSSIL CONIFEROUS WOOD

Anna G. PLATONOVA*, *Vladimir R. FILIN

Lomonosov Moscow State University, Moscow, Russia

platon-anna@yandex.ru

Since the work of Gothan (1905), the features of cross-field pit morphology and their distribution within cross-field are of great significance in the coniferous

wood identification. In the last list of the soft wood microscopic features proposed by IAWA (IAWA list.., 2004), six 'types of pitting' are distinguished, namely 'window-like' (fenestriform), pinoid, piceoid, cupressoid, taxodioid, and araucarioid. The types of pitting are also distinguished for radial tracheids (araucarioid, abietoid and mixed), and for pitting of tangential and terminal walls of ray parenchyma (abietoid and *Juniperus*-type). However, xylotomists often do not distinguish two terms – type of pits and type of pitting. They do not consider, that the word 'pit' is a concrete noun, and the word 'pitting' is an abstract noun; the term 'type of cross-field pit' characterizes the pit itself, but the term 'type of cross-field pitting' characterizes the cross-field, and the term 'type of cross-field' would be the synonym to it. We suppose that these terms should be considered as distinct features.

The cross-field pits are traditionally called a half-bordered pits, because they comprise of a pair of pits between longitudinal tracheid (bordered pit) and ray parenchyma cell (simple pit). The features of cross-field pit are established by the pit of the tracheid; the type of these pits is identified by the aperture width/ border width ratio (the width is determined in the widest part of pit), and the other characters (such as length of aperture) are used as additional features. We propose to distinguish only four types of cross-field pits: pinoid (with very narrow border and considerably wide aperture), taxodioid (the border is wider than in former case, but it is narrower than the aperture), cupressoid (the border and the aperture are of similar width), and piceoid (the aperture is very narrow, often slit-like, and the border is wide; the aperture often extended). Certainly, the differences between these types are conditional.

The types of cross-field pitting are proposed to be distinguished by size of pits, their number and distribution by Chavchavadze (1979), but she did not take into account the orientation of the pit aperture. Chavchavadze distinguished 15 types of cross-field pitting. But xylotomysts often distinguish the type of cross-field based on the predominant type of cross-field pits. Among six cross-field pitting types proposed by IAWA list (2004), four are named by the name of cross-field pit type, which we characterized above. Araucariod cross-field pitting, according to IAWA list, possesses pits of predominantly cupressoid type, the pits are numerous within a cross-field, arranged in alternating rows, and contiguous with flattened borders. The 'window-like' type of pitting can hardly be distinguished from the pinoid type according to IAWA description, and these two types differ to each other predominantly in the number of pits per cross-field: 1–2 in 'window like' and 1–6 (commonly 3 or more) in the pinoid type. The pits of the 'window-like' type are described as simple or apparently simple, and this type is reported for *Pinus sylvestris* L. and *Sciadopitys verticillata* Siebold et Zucc. However, in *P. sylvestris*, we observed the pits of the pinoid type (or sometimes taxodioid in latewood), but in *S. verticillata* the pits are very variable, but often of taxodioid or cupressoid types. The question about the types of cross-field pitting, certainly, requires the special discussion.

Traditionally, the wood anatomy was studied by light microscopy (LM), but at present, the scanning electron microscopy (SEM) becomes more and more popu-

lar. But the cross-field pits in radially split dried wood on the SEM micrographies considerably differ from the familiar for us LM illustrations. Using SEM, we may observe cross-field pits from the cavity of a parenchyma cell or from the cavity of a tracheid, the cell wall may be intact or partially delaminated. When the cross-field is viewed from the parenchyma cell, the pits are not visible, or they are noticeable as depressions or convexities with indistinct outlines. After the whole or partial delamination of the pit membrane and the wall of parenchyma cell, the aperture and the border of the cross-field pit becomes well visible. In the view from the tracheid, the pit aperture is well visible, but the border is often not visible, or it looks like a low elevation with indistinctly limited outlines. The inner layers of the tracheid cell wall often delaminate. We suppose that they relate to the S2 layer of the secondary wall, in which the layers of cellulose and xyloglucans are separated by the layers of hydrophilic pectins (Gorshkova, 2007). In delaminated tracheid wall, the "imprints" of both pit aperture and border on the surface of S1 layer are often well visible. Therefore, we are able to identify the type of cross-field pits by SEM, only when the cell wall is partially delaminated. Sometimes, however, the outer and inner aperture of a tracheid pit differ from each other in outlines, and the combination of different views (from intact and partially delaminated cell wall) is necessary for the exact pit structure establishment.

Investigation of lignitic wood is associated with additional difficulties in the identification of the cross-field pit type caused by structural changes happened in the fossilization process. We established it in the LM and SEM study of the lignitic wood from Middle Jurasssic of the Kursk region, Russia, identified as *Cupressinoxylon*, *Phyllocladoxylon* and *Protocedroxylon*. *Cupressinoxylon* sp. and *Protocedroxylon* sp. possess several separate small circular or elliptic pits per cross-field; in *Cupressinoxylon* sp. the number of pits per cross-field is usually 3–5 but may reach up to 8 or more in marginal ray cells, in *Protocedroxylon* sp., there are often 2–4 pits per cross-field. *Phyllocladoxylon* sp. possesses a large, more or less rectangular pit per cross-field.

The appearance of cross-field pits is considerably diverse in all three types of wood under LM, but the pits looking different not always belong to different types, and the variability may be caused by cell wall degradation. Such cases were revealed using SEM. For example, in some cross-field pits under LM the border and aperture are distinguished, but the aperture is encircled with dark narrow rim, which may be widened at the ends of the aperture. The width and outline of the aperture considerably vary in such pits, sometimes even in one pit in different optic sections. Under SEM, the tracheid wall of such pits is partially delaminated, but the thin 'neck' rises around the pit aperture. The edges of the 'neck' may collapse at the top or may widely split to form the various outlines. This 'neck' looks like to be formed from the more resistant part of the inner layers of tracheid wall, which surrounded the pit canal; this layer shows a stronger connection with the outermost layer of secondary wall of tracheid. This 'neck' corresponds with dark rim in LM.

The inner layers of the secondary wall of tracheids are often disrupted in fossil wood, especially in the tracheids with thick walls. Such degradation of the tracheid wall obviously leads to occurrence of some other changes of cross-field pits, such as the pits with 'tails'. Under LM, such pits possess a more or less distinct border and a wide or narrow aperture, which considerably exceeds the border as two sharpened 'tails'. SEM reveals that such 'tails' are formed as a result of spiral cracks in the inner layers of tracheid cell wall. Moreover, the part of the pit, which is light in LM, not always corresponds to the real aperture and may be caused by cracks in the pit membrane and wall of parenchyma cell.

Therefore, we conclude that the type of cross-field pits in lignitic wood of *Protocedroxylon* sp. and *Cupressinoxylon* sp. vary from taxodioid to cupressoid, in *Phyllocladoxylon* sp. it varies from pinoid to cupressoid. The type of cross-field pits may be used for systematic purposes only after a careful analysis of large number of pits from different parts of fossil wood sample, and only as an additional feature combined with other features.

We thank N.V. Gordenko and A.V. Broushkin for their help in the collection of the material on fossil wood (funded with RFBF grant No. 14-04-01412a). We are greatly indebted to the staff of the Laboratory of Electron Microscopy, Biological Faculty, Lomonosov Moscow State University, for their assistance and for providing SEM and TEM facilities. We are grateful to D.D. Sokoloff for critical reading and advices on the manuscript.

References

Chavchavadze E.S. 1979. *Wood of conifers*. Moscow, Leningrad: Nauka. [In Russian]

Gothan W. 1905. *Zur Anatomie lebender und fossiler Gymnospermen-Hölzer*. Berlin: König. Geol. Landesanstalt u. Bergakademie.

Gorshkova T.A. 2007. *Plant cell wall as dynamic system*. Moscow: Nauka. [In Russian]

IAWA list of microscopic features for softwood identification. 2004. *IAWA J.* **25**: 1–70.

MORPHO-ANATOMICAL INVESTIGATIONS OF EXTRAFLORAL NECTARIES OF APRICOT (*PRUNUS ARMENIACA* L., ROSACEAE)

Dragana RANČIĆ, Marina MAČUKANOVIĆ-JOCIĆ, Maja TERZIĆ, Radenko RADOŠEVIĆ

University of Belgrade, Belgrade, Serbia

rancicd@agrif.bg.ac.rs

Prunus armeniaca (apricot) is small to medium sized tree, extensively cultivated for its edible fruits in many countries, predominantly in temperate areas. It

blossoms in the early spring (from March to April) and is pollinated by insects. The leaves are ovate, with a rounded base, a pointed tip and a finely serrated margin, long red-purple petioles and visible extrafloral nectaries. The extrafloral nectar, serving as an attractant to some insect species, particularly ants, significantly reduces the infestation level and the leaf damage caused by small herbivores. The aim of the present paper is to provide morphological and anatomical description of extrafloral nectaries occurring on leaf parts of *Prunus armeniaca*.

Fresh samples of full developed leaves were micromorphologically examined by stereomicroscope (Nicon SMZ18). For light microscopy, the plant material was fixed in FAA and dehydrated with a graded ethanol series, infiltrated and embedded in paraffin, sectioned by sliding microtome (8–10 μm thick) and stained with Safranine and Alcian Blue (Ruzin, 1999). Observation and photographs were done using a light microscope (Leica DM2000) equipped with a digital camera (Leica DFC320) and image analyzing software (Leica IM1000).

The extrafloral nectaries in *P. armeniaca* occur at a few leaf positions: on both sides of the distal part of the petiole and at the base of the leaf blade at the top of the marginal teeth. The petiolar extrafloral nectaries are larger than the marginal ones. Glands are easily recognized, prominently elevated, red-colored, and oval or discoid with a central concavity. Regarding the anatomical structure, nectariferous tissue is composed of the two-layered secretory epidermis consisted of evidently elongated cells and a multilayered subepidermal parenchyma of densely packed cells irregular in shape and of different sizes, supplied by lateral veins derived from the leaf petiole.

References

Ruzin S.E. 1999. *Plant microtechnique and microscopy*. Oxford: Oxford Univ. Press.

GYNOECIUM STRUCTURE AND DEVELOPMENT IN CORE CARYOPHYLLALES: A MATTER OF PROPORTIONS

Louis RONSE DE CRAENE

Royal Botanic Garden, Edinburgh, Great Britain

lronsedecraene@rbge.org.uk

An overview of the development of the ovary in core Caryophyllales is presented in relation to the anatomical distribution of vascular bundles. Different evolutionary trends have affected the number of carpels, the formation of septa, and the number of ovules (Hofmann, 1994). The ancestral gynoecium was prob-

ably pentamerous and isomerous with the other floral whorls; ovules are clearly separated from the carpellary wall and inserted on the central axis of the flower.

Two major developmental events are responsible for the diversity in gynoecial forms in core Caryophyllales and are linked to the proportional development of carpellary (peripheral: P) tissue and the floral meristem (FM).

(1) Meristic change is caused by an expansion or reduction of the FM. An expansion linked with small carpels leads to polygyny; a reduction leads to lower carpel numbers. Reductions to a single carpel have occurred several times independently.

(2) Different ovary shapes can be recognized at mid-developmental stages and indicate the way ovaries evolve. With an equal development of P and FM, young ovaries take the shape of a *salt haker*; with extensive development of FM and delay of P, a *club-shaped* ovary is formed; with faster growth of P linked with intercalary growth and an arrested growth of FM, a (half-)inferior *cup-shaped* ovary develops. Different growth forms are linked with the development of septa and ovules. The club-shaped ovary is linked with a loss of septa and a reduction of the ovule number to one. The salt haker shape leads to ovaries with well developed septa and several ovules. The cup-shaped ovary leads to a shift of ovules away from the FM.

The vasculature of the ovary is highly conserved but is also reflected in the developmental differentiation of different types. It is demonstrated that subtle shifts in proportional growth lead to a high diversification of ovaries in core Caryophyllales and the establishment of predictable developmental trends.

References

Hofmann U. 1994. Flower morphology and ontogeny. In: Behnke H.-D., Mabry T.J. (eds.): *Caryophyllales. Evolution and systematics*. Berlin: Springer Verlag. P. 123–166.

ANATOMICAL DIAGNOSTIC CHARACTERS OF *ACHNATHERUM CONFUSUM* (LITV.) TZVELEV AND *ACHNATHERUM SIBIRICUM* (L.) KENG EX TZVELEV (POACEAE) IN THE FLORA OF ALTAI

***Daria D. RYZHAKOVA*[1], *Polina D. GUDKOVA*[1,2], *Marina V. OLONOVA*[1]**

[1] Tomsk State University, Tomsk, Russia
[2] Altai State University, Barnaul, Russia
pdgudkova2017@yandex.ru

The genus *Achnatherum* P. Beauv. currently includes approximately 56 species that are common in temperate and subtropical countries in North Africa, Eurasia

and North America. This genus is taxonomically difficult because its volume and volumes of its constituent species are still to be clarified (Wu, Phillips, 2006; Zhang et al., 2018; Nobis et al., 2019). The closely related species *A. confusum* (Litv.) Tzvelev and *A. sibiricum* (L.) Keng ex Tzvelev are hardly discernible and contradictory interpreted. Most researchers consider them as separate species (Tzvelev, 1977; Probatova, 1985; Lomonosova, 1990), but some still include *A. confusum* into *A. sibiricum* (Wu, Phillips, 2006). The main problem of the treatment of these species is the transgression of most their characters. The main objective of this research is to study the anatomical characters of species *A. confusum* and *A. sibiricum* in order to evaluate their diagnostic reliability and find new ones, suitable for using in systematics.

Approximately 70 samples of *A. confusum* and *A. sibiricum*, stored in the herbarium of the Altai State University (ALTB) and the Krylov Herbarium of the Tomsk State University (TK) were studied under stereomicroscope Nikon SMZ800N and 30 specimens were examined under the electron scanning microscope. Fragments of leaf blades of vegetative shoots, glumes and lemmas were selected for the study. Photographs of the micromorphological structure were taken with SNE-4500M (Korea). The terminology proposed by Metcalfe (1960), Clifford & Watson (1977) and Ellis (1979) was used for description.

The diagnostic value of the prickle location on the glume surface and the type of the leaf blade pubescence on both its sides, which were used earlier by many botanists (Litvinov, 1928; Tzvelev, 1976; Lomonosova, 1990; Wu, Phillips, 2006), was confirmed. Density of the hairs and prickles on the lemma surface was found to be a new valuable diagnostic character.

Achnatherum confusum has scabrous abaxial surface of the leaf blade, hairs and prickles on the adaxial surface (Fig. C, E). In *A. sibiricum*, the prickles on the abaxial surface are very sparse (10–40 in the field of view, ×100) to absent. On the adaxial surface, the prickles and hooks were observed, the hairs are very sparse (Fig. D, F). The location of the prickles on the glumes is the most important character for distinguishing these species: *A. confusum* (Fig. A) has scattered prickles throughout the glumes, whereas *A. sibiricum* (Fig. B) has the prickles, located only along the veins. *A. confusum* has fewer hairs on the lemma, approximately 5 in the field of view (×300) as well as small prickles and hooks (about 0.05 mm), scattered throughout the lemma, whereas *A. sibiricum* has 10–15 hairs in the field of view (at ×300). Prickles and hooks are absent or very rare.

Thus, *A. confusum* and *A. sibiricum* possess a combination of anatomical characters that allow us to recognize them as segregate species. In addition, these data are supported by the form of callus which is obtuse in *A. confusum* and acuminate in *A. sibiricum*. For this reason, we consider these taxa to be independent species.

We thank the Russian Foundation for Basic Research (RFBR), research projects Nos. 18-34-20112, 19-04-00973.

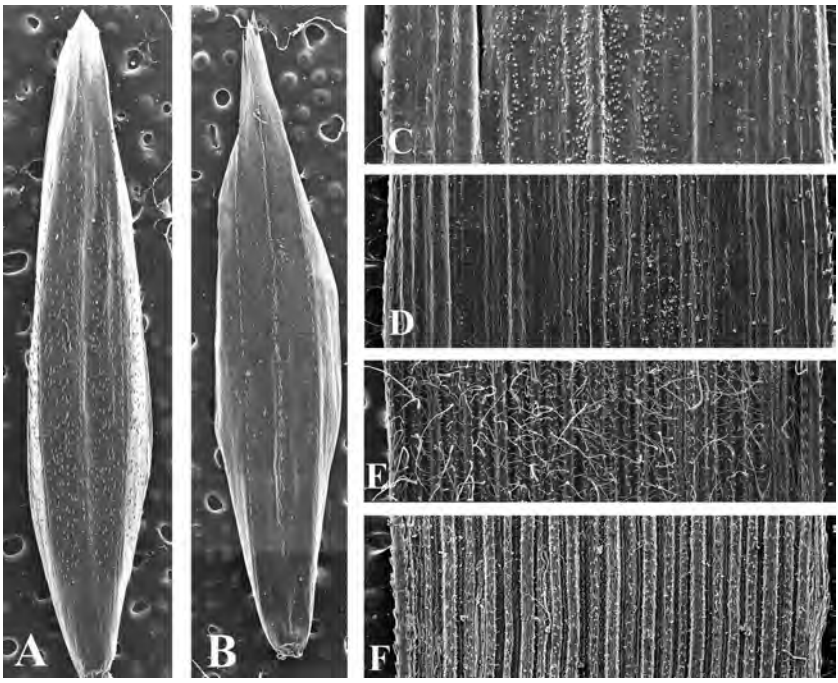

Figure. *Achnatherum confusum*:
A – glume; C – abaxial surface of the leaf blades; E – adaxial surface of the leaf blades.
A. sibiricum: B – glume; D – abaxial surface of the leaf blades;
F – adaxial surface of the leaf blades.

References

Clifford H.T., Watson L. 1977. *Identifing grasses: Data, methods and illustrating*. St. Lucia: Univ. Queensland Press.

Ellis R.P. 1979. A procedure for standardizing comparative leaf anatomy in the Poaceae. The epidermis as seen in surface view. *Bothalia* **12**: 641–671.

Litvinov D.I. 1928. Feather grass mixed under the name *Stipa sibirica* (L.) Lam. *Izvestiya Akademii nauk SSSR*. VII seriya. Otdeleniye fizikomatematicheskikh nauk. **1**: 49–64. [In Russian]

Lomonosova M.N. 1990. *Achnatherum* Beauv. In: Malyshev L.I. (ed.): *Flora of Siberia*. Novosibirsk: Nauka. V. **2**. P. 220–221. [In Russian]

Metcalfe C.R. 1960. *Anatomy of the Monocotyledons. I. Gramineae*. Oxford: Clarendon Press.

Nobis M., Gudkova P., Nowak A. 2019. *Neotrinia* gen. nov. and *Pennatherum* sect. nov. in *Achnatherum* (Poaceae: Stipeae). *Turczaninowia* **22**: 37–41. [In Russian]

Probatova N.S. 1985. Poaceae Barnhart. In: *Plantae vasculares Orientis Extremi Sovietici*. Leningrad: Nauka. V. **1**. P. 89–383. [In Russian]

Tzvelev N.N. 1976. *Grasses of USSR*. Moscow: Nauka. [In Russian]

Tzvelev N.N. 1977. About the origin and evolution of feather grasses. In: *Problems of ecology, geobotany, botanical geography and floristics*. Leningrad: Nauka. P. 139–150. [In Russian]

Wu Z.L., Phillips S.M. 2006. Tribe *Stipae*. In: Zhengyi W., Raven P.H., Deyuan H. (eds.): *Flora of China*. Beijing: Science Press; St. Louis: Mo. Bot. Gard. Press. V. **22**. P. 188–212.

Zhang Z.-Sh., Jiang Sh.-W., Chen W.-L. 2018. *Achnatherum pilosum* (Stipeae, Poaceae), a new species from Qinghai-Tibet Plateau. *Phytotaxa* **350**: 086–092.

ECOLOGICAL ANATOMY OF IBERIAN SAXICOLOUS SPLEENWORTS (ASPLENIACEAE, POLYPODIOPSIDA)

Andrea SERAL, Jose María GABRIEL y GALÁN, Antonio MURCIANO, Sonia MOLINO, Rubén VÁZQUEZ

Universidad Complutense de Madrid, Madrid, Spain

jmgabrie@ucm.es

Little is known about the ecological significance of anatomical traits in ferns. This is dramatically true for the saxicolous species, despite the high interest of this quite hostile habitat. In this work, we begin a first approach to the study of the ecological anatomy of several species of spleenworts (*Asplenium*), with the aim to find critical anatomical traits that could inform about the adaptive strategies of the saxicolous ferns. The Iberian Peninsula is an excellent geographical location where to carry on this type of studies, mainly due to the existence of two sharply different bioclimates: Mediterranean and Eurosiberian-Atlantic. The main differences between them are the existence of an arid period and an overall lesser rainfall in the former. Therefore, it is quite easy to test several bioclimatic hypotheses related to fern anatomy and adaptation to climatic hydric stress.

We chose two species: *Asplenium trichomanes* L. and *Asplenium ceterach* L., that are widespread in Western Europe, occurring frequently in areas under both Atlantic and Mediterranean macroclimates. Several fronds from several individuals from a number of different populations were sampled. Anatomical sections were done in petioles and pinnae, and we measured the following main anatomical characteristics: xyleme area, diameter of tracheids, total leaf thickness and cuticle thickness. Selected climatic variables are related to temperatures (min and max of hottest and coldest months) and rainfall. Statistical analyses were done to investigate explicative correlations of the climatic variables over the anatomical traits.

STAMINAL HAIRS: AN ADDITIONAL TAXONOMIC CHARACTER FOR IDENTIFICATION OF INDIAN IPOMOEAS (CONVOLVULACEAE)

***Vinod B. SHIMPALE*, Amrapali V. KATTEE**

The New College (affiliated to Shivaji University), Kolhapur, India
shimplae@yahoo.com

In the earlier systems of classification only external morphological characters (phenetic), especially those of flower characters were utilized for the classification. But during last 8–10 decades data from anatomy, embryology, palynology, cytology and more recently phytochemistry have been profitably utilized in taxonomic classification at various levels. The reproductive organs of the flower show high degree of conservation and hence they have been widely used in the classification of various taxa of flowering plants. Now a day, few anatomical characters of vegetative and floral parts have been immensely utilized to solve some of the taxonomic problems and also for the prediction of phylogenetic relationships.

The genus *Ipomoea* L. is a member of family Convolvulaceae and it is one of the dominant genera of the family. About 650 species of the genus *Ipomoea* are reported from the world and that are mainly distributed in tropical and warm temperate regions (Mabberley, 2017). In Indian flora, it is reported by about 55 taxa and mainly distributed in the peninsular India (Kattee et al., in press). During taxonomic revision of the genus *Ipomoea* for India, it was noted that the morphology of staminal hairs plays an immense significance in delimitation of species and can be used in identification and classification of different species and also plays significant role in the understanding the phylogeny of the genus. During present study authors have screened about 40 species of the genus for its staminal hairs and interestingly it was observed that this character is unique for each species and can be utilized as a taxonomic character.

During this investigation it was noted that the staminal hairs are composed of stalk and gland. On the shape of glands, these can be grouped into four types i.e. clavate, rounded, ogee and elongated. The species like *I. biflora*, *I. clarkei*, *I. dichroa*, *I. obscura*, *I. ochracea*, *I. pes-tigridis*, *I. salsettensis* and *I. tenuipes* have clavate glands; only two species like *I. acanthocarpa*, *I. carnea* possess rounded glands; the species like *I. batatas*, *I. laxiflora*, *I. triloba*, *I. littoralis* have ogee-shaped glands while elongated and pointed glands were observed in *I. aculeata*, *I. aquatica*, *I. marginata*, *I. staphylina*, *I. horsfallae*. Among all studied species the stamina hairs of *I. hederifolia* and *I. quamoclit* are very unique as the staminal hairs are much reduced. The exact role of staminal hairs is not known but these

hairs may secrete some chemicals which may attract the insects and these insects may protect the flowers from herbivores. Also, morphology of staminal hairs is first time utilized in the infrageneric classification of the genus *Ipomoea* that is proposed by Austin (1980) and few species which are not included in this classification are first time placed in the infrageneric classification. All the aspects respect with morphology of staminal hairs, their applications in the classification are discussed in present work.

References

Austin D.F. 1980. Additional comments on infrageneric taxa in *Ipomoea* (Convolvulaceae). *Taxon* **29**: 501–502.

Kattee A.V., Patil C.R., Shimpale V.B. Genus *Ipomoea* in India. *J. Threat. Taxa* (In press).

Mabberley D.J. 2017. *Mabberley's plant-book: a portable dictionary of plants, their classification and uses*. 4th ed. Cambridge: Cambridge Univ. Press.

ANATOMY AND MORPHOLOGY RESTRICT HYDRAULIC FUNCTION IN THREE *VITIS* ROOTSTOCKS

Ilana SHTEIN, Yair HAYAT, Sarel MUNITZ, Eran HARKABI, Michal AKERMAN, Elyashiv DRORI, Amnon SCHWARTZ, Yishai NETZER

Ariel University and Eastern R&D center, Ariel, Israel

ynetzer@gmail.com

Graft is a union between two species/cultivars, which produces a plant with new qualities. Though rootstocks have been extensively used for fruit tree propagation for at least 2000 years (Webster, 1995), their effects on scion physiology are still not fully understood. Over the years, several attempts of mechanistic explanations of this phenomenon were presented. Those can be roughly divided into three categories: 1. Hormonal effects (*Leucopersicum*: Albacete et al., 2009; *Gossypium*: Dong et al., 2008; *Vitis*: Skene, Antcliff, 1972), 2. Assimilate and nutrient movement (*Vitis*: Tardáquila et al., 1995; *Malus*: Jones, 1976) and 3. Water status (*Malus*: Cohen, Naor, 2002; *Olea*: Nardini et al., 2006; *Vitis*: Alsina et al., 2011). The overall picture is quite complex and the data are sometimes contradictory.

In red grapevine cultivation, grape yield quality rather than quantity is the important parameter, which depends chiefly on a drought stress development dur-

ing the growth season. Excessive water availability induces strong canopy growth, high yields and low quality grapes, while drought stress causes yield reduction and negatively affect the plant vitality (Bravdo, Hepner, 1987; Munitz et al., 2016a,b, 2018). In *Vitis* it is possible to generate rootstock/scion combinations that produce a desired drought stress effect crucial for high quality wine production, though the mechanisms for such interactions are complex and poorly understood. *Vitis vinifera* is the commonly grown *Vitis* species in the Old World, while in North America *Vitis riparia*, *Vitis labrusca* and *Vitis rotundifolia* are frequently used for grape and wine production. Cross-breeding among *V. berlandieri*, *V. riparia* and *V. rupestris* has produced several widely used rootstocks. Rootstocks are selected on the basis of their performances: soil types, water requirements, and disease susceptibility – while the scion is selected mainly on the basis of vigor and yield quantity and quality.

In the study reported here significant differences in water status and subsequently yield parameters were found in vines with the identical scion grafted on three different rootstocks in clay soil with relatively high water content (Shtein et al., 2017). In such a soil, it is difficult to achieve low water potentials and subsequently high quality grapes. The current study attempts to explain the differences in water status of different grafts by examining the underlying anatomical constraints. The research was done on vines with an identical scion (*Vitis vinifera* 'Cabernet Sauvignon') grafted on three different rootstocks: 1. Riparia Gloire (*Vitis riparia*), 2. Paulsen 1103 (*Vitis berlandieri* × *Vitis rupestris*) or 3. 420A (*V. berlandieri* × *V. riparia*). Physiological parameters were measured during the season. Functional anatomy of the rootstock and scion stems, roots and branches was assessed.

There was a significant difference in physiological responses, yield and grape quality between the grafts. Riparia Gloire grafts had the lowest water potentials and the highest quality grapes, as well as lower root, scion stem and branch specific hydraulic conductivity. Paulsen grafts had the best physiological performance.

The different rootstock stems had very diverse vessel size distributions, as they belong to different species/hybrids. On the other hand, scion vessel size distribution was very similar between grafts, all of them being 'Cabernet Sauvignon'. The different rootstock stem vessel diameters were different, while the scion vessel diameters were very similar. We analyzed both the average vessel diameter and separately large (over 100 μm) vessel diameter – as only the large vessels have a significant impact on hydraulic conductivity (Tyree, Ewers, 1991). Riparia Gloire rootstock stems had the widest vessel diameter and the widest large (> 100 μm) vessel diameter. Paulsen 1103 rootstock stems had the lowest maximal vessel diameter and fewer large vessels than the other rootstocks. Scion stems of all the grafts had similar vessel diameters. Similar trends could be seen in vessel size distribution frequencies. It is important to

note that all the stems (except Paulsen rootstocks) showed a bimodal vessel size distribution, with numerous small vessels and numerous large vessels, with a decrease in medium-sized vessel frequency. Such a bimodal distribution is typical of vines and climbing plants (Carlquist, 1985), and is thought to increase both conductivity and safety. Rootstock stems had a large variation in vessel size frequency. Paulsen 1103 rootstock stems had less very small vessels (under 60 μm) and less very large vessels (over 160 μm) than the other two rootstocks, and the vessel distribution did not show the classical bimodal curve. 420A and Riparia Gloire rootstock stems both showed a bimodal distribution, with Riparia Gloire having a larger percentage of both very small and very large vessels. Scion stem vessels were very similar in all the grafts, showing bimodal vessel distribution. Vessel distribution frequency in scions seemed most similar to 420A rootstocks. Vessel diameters in scion stems were larger than in the rootstock stems – vessels of over 280 μm were inexistent in rootstocks but comprised over 4% of the vessels in scions.

Similarly, in peach grafts the rootstocks had very little effect on scion vascular anatomy (Tombesi et al., 2010). The main anatomical difference in scion stems in different grafts was the annual growth ring area. In scions grafted on Riparia Gloire the annual growth rings were significantly narrower than in the other two grafts, causing a significantly lower specific hydraulic conductivity. The narrow annual ring size in scion stem was imposed by the morphological constraint of the stem size. In hydraulically inferior Riparia Gloire grafts the difference was disproportionally large, with a wide scion grafted on a very narrow rootstock, and Paulsen 1103 had the smoothest graft union. The narrow annual ring size in scion stem was imposed by the morphological constraint of the stem size. It seems that the hydraulic restriction point was basically the diameter difference between rootstock and scion stems. In order to adapt itself to growing on a narrow rootstock stem, the scion is forced to limit its stem size by narrowing the annual rings. Thus such simple morphological constraint causes more elaborate anatomical and physiological changes. Interestingly, Weber (1948) considered the graft union shape in *Citrus* as the definitive indicator of grafting success – while a smooth graft union was regarded as more successful.

Our results indicate that the ability to develop drought stress in *Vitis* grafts depends on rootstock-imposed physical restriction of hydraulic conductivity, similar to effects of dwarfing rootstocks. It seems that the restricting action of Riparia Gloire rootstock is akin to the mechanism of dwarfing rootstocks, which induce a lower hydraulic conductivity in the scion (Cohen, Naor, 2002; Tombesi et al., 2010). Similarly, narrow growth rings were found to be the most important anatomical factor in dwarf woody plants (Baas et al., 1984). Thus, the ability to develop drought stress in Riparia Gloire grafts was mostly due to narrow annual rings that limited the water flow capacity.

References

Albacete A., Martínez-Andújar C., Ghanem M.E., Acosta M., Sánchez-Bravo J., Asins M.J., Cuartero J., Lutts S., Dodd I.C., Pérez-Alfocea F. 2009. Rootstock-mediated changes in xylem ionic and hormonal status are correlated with delayed leaf senescence, and increased leaf area and crop productivity in salinized tomato. *Plant Cell Environ*. **32**: 928–938.

Alsina M.M., Smart D.R., Bauerle T., De Herralde F., Biel C., Stockert C., Negron C., Save R. 2011. Seasonal changes of whole root system conductance by a drought-tolerant grape root system. *J. Exp. Bot*. **62**: 99–109.

Baas P., Xinying Z., Chenglee L., Keming C., Yuefen D. 1984. Some effects of dwarf growth on wood structure. *IAWA J*. **5**: 45–63.

Bravdo B., Hepner Y. 1987. Water management and effect on fruit quality on grapevines. In: Lee T.F. (ed.): *Proceedings of the 6th Australian wine industry technical conference*. Adelaide: Australian Industrial Publications. P. 150–158.

Carlquist S. 1985. Observations on functional wood histology of vines and lianas: vessel dimorphism, tracheids, vasicentric tracheids, narrow vessels, and parenchyma. *Aliso* **11**: 139–157.

Cohen S., Naor A. 2002. The effect of three rootstocks on water use, canopy conductance and hydraulic parameters of apple trees and predicting canopy from hydraulic conductance. *Plant Cell Environ*. **25**: 17–28.

Dong H., Niu Y., Li W., Zhang D. 2008. Effects of cotton rootstock on endogenous cytokinins and abscisic acid in xylem sap and leaves in relation to leaf senescence. *J. Exp. Bot*. **59**: 1295–1304.

Jones O.P. 1976. Effect of dwarfing interstocks on xylem sap composition in apple trees: effect on nitrogen, potassium, phosphorus, calcium and magnesium content. *Ann. Bot*. **40**: 1231–1235.

Munitz S., Netzer Y., Schwartz A. 2016a. Sustained and regulated deficit irrigation of field-grown Merlot grapevines. *Austal. J. Grape Wine Res*. **23**: P. 87–948.

Munitz S., Netzer Y., Shtein I., Schwartz A. 2018. Water availability dynamics have long-term effects on mature stem structure in *Vitis vinifera*. *Am. J. Bot*. **105**: 1–10.

Munitz S., Schwartz A., Netzer Y. 2016b. Evaluation of seasonal water use and crop coefficients for 'Cabernet Sauvignon' grapevines as the base for skilled regulated deficit irrigation. *Acta Hortic*. **1115**: 33–40.

Nardini A., Gascó A., Raimondo F., Gortan E., Lo Gullo M.A., Caruso T., Salleo S. 2006. Is rootstock-induced dwarfing in olive an effect of reduced plant hydraulic efficiency? *Tree Physiol*. **26**: 1137–1144.

Skene K.G.M., Antcliff A.J. 1972. A comparative study of cytokinin levels in bleeding sap of *Vitis vinifera* (L.) and the two grapevine rootstocks, Salt Creek and 1613. *J. Exp. Bot*. **23**: 283–293.

Shtein I., Hayat Y., Munitz S., Harcavi E., Akerman M., Drori E., Schwartz A., Netzer Y. 2017. From structural constraints to hydraulic function in three *Vitis* rootstocks. *Trees*. **31**: 851–861.

Tardáquila J., Bertamini M., Giulivo C., Scienza A. 1995. Rootstock effect on growth, dry weight partitioning and mineral nutrient concentration of grapevine. *Acta Hortic*. **388**: 111–116.

Tombesi S., Johnson R.S., Day K.R., Dejong T.M. 2010. Relationships between xylem vessel characteristics, calculated axial hydraulic conductance and size-controlling capacity of peach rootstocks. *Ann. Bot*. **105**: 327–331.

Tyree M., Ewers F. 1991. The hydraulic architecture of trees and other woody plants. *New Phytol*. **119**: 345–360.

Webber H.J. 1948. Rootstocks: their character and reactions. In: Batchelor L.D., Webber H.J. (eds.). *The* Citrus *industry*. Berkeley: Univ. California Press. V. **2**. P. 69–168.

Webster A.D. 1995. Rootstock and interstock effects on deciduous fruit tree vigour, precocity, and yield productivity. *New Zeal. J. Crop Hortic. Sci*. **23**: 373–382.

SEED COAT ANATOMY IN TRIBE FABEAE (FABACEAE) AND ITS DEPENDENCE ON THE GENOME SIZE

Andrey A. SINJUSHIN[1], ***Yuliya S. TRIFONOVA***[2]

[1] Lomonosov Moscow State University, Moscow, Russia
[2] Public school 179, Moscow, Russia
asinjushin@mail.ru

Tribe Fabeae (= Vicieae) is one of few leguminous tribes distributed preferentially in temperate regions. It includes five genera (*Lathyrus*, *Vicia*, *Pisum*, *Lens*, and *Vavilovia*), and many of them have a high agricultural value. These are peas, lentils, faba beans, some cultivated species of vetches and vetchlings. Among its notable features, one may list a comparatively high amount of DNA in nucleus (C-value in terms of haploid genome size) (Bennett, Leitch, 2012). Tribe Fabeae includes members with the largest leguminous genomes, while polyploidy is rare in this group.

As discussed previously (Bennett, 1972), C-value has two effects which can hardly be avoided. These are (i) increase of cell sizes together with an increase of C-value and (ii) retardation of replication process and overall cell cycle caused by extra DNA. Thus, one may predict that increase of C-value can affect structure and functionality of all structures, which have single cell-dependent sizes. In plants, these are pollen grains and spores, stomata, epidermal cells and their derivatives (such as trichomes) etc. Our work aims at study of seed coat structure in tribe Fabeae, basing both on published and originally acquired data. Numerous papers are dedicated to the external ultrastructure of seed coat in Fabeae revealed by the scanning electron microscopy (SEM) (e.g., Abou-El-Enain et al., 2007). However, we focused on the anatomy of seed coat, which has been surveyed much less to date. Data from the available publications were extracted for analysis (Burlyaeva, Smekalova, 1987, 1988; Redkina, 1971; Redkina, Khoroshailov, 1974).

We studied seed coat anatomy of selected species of genera *Lathyrus* (14 species), *Pisum* (1 sp.) and *Vavilovia* (1 sp.). After mechanical scarification, seeds were soaked in water for three days. Sections were made with hand razor and visualized under light microscope. Measurements of exotesta (palisade layer) and hypoderm thickness were carried out on digital images. Data on C-values were acquired from the Plant DNA C-values Database (Bennett, Leitch, 2012) and estimated originally for few specimens *via* flow cytometry. The protocol for cytometry and details of C-value estimation are beyond the scope of a given report.

When comparing our results with those published previously, we found that absolute values of both parameters exceed ones in available descriptions of the same species (Burlyaeva, Smekalova, 1987, 1988). Although some intraspecific variation between seed samples is possible, some of these differences may refer to

differences in the preparation of material (such as dry *vs*. soaked seeds etc.). That is why we further avoided any statistical analyses on joint sample of original data together with the ones obtained from literature.

Surprisingly, no reliable correlation was found between C-value and thickness of either seed coat layer. The Spearman's rank correlation coefficient (applied here and elsewhere) comprised 0.300 for the link between C-value and epidermis thickness and 0.321 for C-value and hypoderm thickness ($p > 0.05$ in both cases). The only significant correlation was found between thicknesses of two seed coat layers ($r = 0.615$, $p < 0.05$).

Data from previously published papers (Burlyaeva, Smekalova, 1987, 1988; Redkina, 1971; Redkina, Khoroshailov, 1974) were also analyzed concerning relation between C-value and thickness of seed coat. At least one remarkable feature was found that in *Lathyrus* and *Vicia* the observed correlation is unequal. For epidermis layer, the correlation between thickness and C-value was insignificant ($p > 0.05$) both for *Lathyrus* ($r = 0.208$) and *Vicia* ($r = 0{,}352$). For hypoderm, the difference was more obvious: $r = 0.083$ ($p > 0.5$) in *Lathyrus* versus $r = 0.417$ ($p < 0.05$) in *Vicia*.

The overall weak correlation between studied parameters is unexpected and can be possibly explained by the peculiarities of cell differentiation. As indicated for the pavement cells of epidermis, they undergo few rounds of DNA replication resulting in their polyploidy (Melaragno et al., 1993). One may speculate that similar process occurs during seed coat development, so the unequal number of endoreplication rounds compensates the initial difference in DNA content. However, this hypothesis needs further investigation.

We may conclude that seed coat has a similar structure in all studied specimens with three distinct layers present, viz. epidermis (palisade layer also referred to as macrosclereids), hypoderm (osteosclereids) and parenchyma. Concerning the main premise of this study, we found no reliable correlation between thickness of seed coat layers and C-value, at least in *Lathyrus*. Representatives of *Vicia* seem more C-value-sensitive with respect to seed coat anatomy.

The work was partially supported by the Russian Foundation for Basic Research (project No. 18-34-00511).

References

Abou-El-Enain M.M., Loufty M.H.A., Shehata A.A. 2007. Seed surface characters and their systematic significance in the genus *Lathyrus* (Leguminosae, Papilionoideae, Vicieae). *Feddes Repert.* **118**: 269–285.

Bennett M.D. 1972. Nuclear DNA content and minimum generation time in herbaceous plants. *Proc. R. Soc. London. B. Biol. Sci*. **181**: 109–135.

Bennett M.D., Leitch I.J. 2012. Plant DNA C-values database. Release 6.0. Retrieved 28.02.2019 from: http://data.kew.org/cvalues

Burlyaeva M.O., Smekalova T.N. 1987. Anatomical features of seeds of some *Lathyrus* species and potential to use them in systematics. *Tr. Prikl. Bot., Gen. Sel.* **112**: 75–81. [In Russian]
Burlyaeva M.O., Smekalova T.N. 1988. Comparative anatomical characteristics of seed coat in vetchling of section *Cicercula*. *Tr. Prikl. Bot., Gen. Sel.* **117**: 94–105. [In Russian]
Melaragno J.E., Mehrotra B., Coleman A.W. 1993. Relationship between endopolyploidy and cell size in epidermal tissue of *Arabidopsis*. *Plant Cell* **5**: 1661–1668.
Redkina Z.V. 1971. Morphological and anatomical characterization of seeds of vetches. *Tr. Prikl. Bot., Gen. Sel.* **44**: 83–107. [In Russian]
Redkina Z.V., Khoroshailov N.G. 1974. Key to seeds of weed and field vetches of USSR. *Tr. Prikl. Bot., Gen. Sel.* **51**: 3–48. [In Russian]

HOW ANATOMY HELPS UNLOCK THE PLANT FOSSIL RECORD: EXAMPLES FROM MONOCOTS

Selena Y. SMITH
University of Michigan, Ann Arbor, USA
sysmith@umich.edu

Incorporating paleontological data into evolutionary, ecological, and biodiversity studies is becoming more and more important as we seek to understand how life influences and is influenced by tectonic and climatic factors over geological time (thousands to millions of years) scales. For plants, which are especially critical to consider because of their role as the primary producers in terrestrial ecosystems, there is much taxonomic value in anatomically preserved structures such as stems, fruits, and seeds. Having anatomy permits more detailed investigations into a fossil's identity and phylogenetic relationships. Because monocots are an economically and ecologically important group, we wish to maximize the information derived from their fossil occurrences. Anatomy has helped to resolve affinities of fruits and seeds, for example the widespread genus *Spirematospermum* from North America and Eurasia, and palm fruits from the Cretaceous of India. Phytoliths have been useful in reconstructing the role of monocots in the Paleogene and early Neogene of Montana, USA, demonstrating the persistence of 'tropical' taxa like spiral gingers and palms, and that grasses were present and thrived in disturbed environments long before they expanded to form the grassland ecosystems we are familiar with today. However, there is still much we don't know with the structure of monocots, which hinders our ability to accurately interpret fossils. This is of fundamental importance in understanding the changes in biodiversity over the Cretaceous and Cenozoic and how they relate to factors such as climate.

DIVERSITY AND EVOLUTION OF ARCHEGONIA AND EMBRYOS IN LAND PLANTS

Dmitri D. SOKOLOFF*, *Margarita V. REMIZOWA

Lomonosov Moscow State University, Moscow, Russia

sokoloff-v@yandex.ru

Although the presence of a multicellualar diploid generation (sporophyte) distinguishes land plants from the closest relatives, streptophyte algae, the sporophyte embryo and the matrotrophy are also among their key characters. There is no direct data on the origin of the land plant life cycle. Subsequent evolution of their embryos is also enigmatic in many respects, but highly important for understanding differences between major groups of embryophytes. The land plant zygote remains in the position of the egg cell, and positional information from surrounding structures is essential for patterning and orientation of the embryo. At least in bryophytes, pteridophytes and most gymnosperms, the egg cell appears in the archegonium, another land plant specific organ. It is reasonable to discuss the evolution of embryo along with the evolution of archegonium.

Both male and female sexual organs of land plant haploid generation (gametophyte), antheridia and archegonia, are multicellular and develop due to three-dimensional growth (with precisely regulated cell divisions in different planes), the latter being yet another land plant specific character. An archegonium always develops from a single initial cell. The main parts of the archegonium are the venter and the neck. The venter houses the egg cell and the ventral canal cell (these are always sister cells), and the neck usually encloses a row of the neck canal cells (all normally derived from the same initial cell). In hornworts and tracheophytes, the venter and sometimes the entire archegonium (e.g., in hornworts and gymnosperms) is congenitally united with surrounding tissue, so that it is sunken into the gametophyte body. Mosses and liverworts are the only land plants possessing fully exposed archegonia with free venter. This condition is traditionally viewed as ancestral (plesiomorphic) for land plants. However, apart from theoretical considerations and ‘common sense’ there is no support of this view. Female organs of streptophyte algae are fundamentally different from land plant archegonia and cannot be used for outgroup comparison. Recent phylogenetic data suggest that mosses and liverworts form a clade (called setaphytes), and with some land plant tree toplogies (e.g., hornworts basal), it is more parsimonious to consider the fully exposed archegonia as a derived condition.

There are clear differences between archegonia of extant bryophytes and tracheophytes (Renzaglia et al., 2000). In bryophytes, the archegonium (or the archegonium proper) development starts with three longitudinal divisions of an initial cell to form a central triangular axial cell surrounded by three peripheral cells. The peripheral cells form the walls of both neck and venter whereas the axial cell gives

rise to the neck canal cells, the ventral canal cell and the egg. With further divisions, the neck wall is composed by five or six rows of cells, at least in setaphytes. The neck wall is difficult to distinguish from surrounding gametophyte tissues in hornworts, because of their sunken archegonia. In extant tracheophytes, the first division of the epidermal initial cell is transversal. In pteridophytes (Renzaglia et al., 2000), the upper cell develops a neck wall, which invariantly has four rows of cells. The lower cell produces the neck canal cells, the ventral canal cell and the egg. Archegonium development in gymnosperms is essentially similar, though the neck canal cells are absent. In conifers and *Ephedra*, the basic structure of the neck includes single to many tiers of four cells as in pteridophytes, but tiers with more cells are occasionally found; two-celled necks are charactersitic of gynkgo, most cydads and a few conifers (Chamberlain, 1935; Zhang, Zheng, 2016). Recognizing an archegonium is problemetic in angiosperms (their synergids are likely the neck cell homologues) and impossible in *Gnetum* and *Welwitschia*, but there is no problem in homologization of the zygote polarity between all gymnosperms and angiosperms by its position relative to micropyle.

A common groundplan of all land plant archegonia can be found by considering the occurrence of so-called cover cells in most bryophytes (Campbell, 1895; though they are absent in *Haplomitrium*). Along with the egg and canal cells, the primary cover cell is yet another (the distal-most) product of the axial cell in the bryophyte archegonia. Typically, the primary cover cell undergoes and equal anticlinal division, followed by another anticlinal division in the perpendicular plane. As a result, a tier of four cover cells is formed that is most likely homologous to the neck of tracheophytes.

To simplify, there is a common developmental pattern across most land plant archegonia, but (1) the three initial unequal anticlinal divisions are absent (lost?) in tracheophytes and (2) the necks of setaphytes and tracheophytes are not homologous to each other. These facts may lead to a hypothesis that the fully sunken hornwort archegonia are similar (1) to the ancestral type of land plant archegonia or (2) to archegonia of a transitional form from bryophytes to tracheophytes. These hypotheses are sensitive to the rooting of land plant phylogeny. On the other hand, both hypotheses are problematic in the light of the data on archegonia of the Devonian fossils from Rhynie, which are the oldest known land plant fossils with documented life cycle. Their sporophytes dominated in life cycle and were polysporangiate, so that these taxa are commonly placed in a grade leading to the (core) tracheophyte clade (Kenrick, Crane, 1997; Kenrick, 2017). Gametophytes of the Rhynie plants described so far possessed archegonia with a sunken venter and a free massive neck that possessed tiers of 8 or more cells (Remy et al., 1993). Necks with so many cells per tier are known in a few extant conifers, but this could be a homoplastic similarity. If the currently accepted phylogenetic placent of the Rhynie fossils is correct, then the similarity between the bryophyte cover cells and the tracheophyte neck appeared in course of parallel evolution. One can imagine the origin of this

similarity through evolutionary fixation of early developmental stages with two successive equal anticlinal divisions of the uppermost cell of young archegonium. These ideas may provide indirect evidence on yet undescribed archegonium development of Rhynie plants. Another possibility is that the Rhynie plants belong to stem group of land plants and appeared before divergence of bryophytes and tracheophytes (see Remy et al., 1993), which agrees with the absence of unequivocal bryophytes in Rhynie and older fossils. If so, the four cells per tier at the archegonium apex should be a synapomorphy of all extant land plants.

A coenocyte developing from zygote is found in gymnosperms, a liverwort *Monoclea* and in *Paeonia* among angiosperms. All other land plants (and possibly sometimes *Monoclea*) possess *ab initio* cellular embryo. The first division of zygote can be longitudinal, oblique or more commonly transverse with respect to the axis of archegonium. The transverse division is often unequal and then the larger daughter cell is apparently always closer to the neck. The *occurrence* of unequal transverse division is homoplastic among the land plants, so the strong tendency for the arrangement of the larger and the smaller cell merits further attention. Even with the delayed cellularization in conifers, the larger cells are those closest to the neck. With the first embryo division being longitudinal in some hornworts, the second, transverse division cuts larger cells that are closer to the neck. The large upper cell(s) is (are) related to suspensor formation in tracheophytes and sporangium formation in bryophytes.

There is a homoplastic diversity of cell arrangement relative to the archegonium axis in four-celled embryos of land plants. Interestingly, there is an apparent constraint against the arrangement of all four cells in a tier derived from two successive longitudital divisions of zygote.

Embryo development is exoscopic (with sporangial or shoot pole at the side of the archegonium neck) in bryophytes and a few tracheophytes such as horsetails. It is endoscopic in most tracheophytes (Niklas, Kutschera, 2009). The endoscopic development creates a spatial constraint for further sporophyte development. Different ways of overcoming this constraint are known in various tracheophytes. In seed plants, emergence of the shoot apex often results from asymmetric intercalary growth of the cotyledon bases. Cotyledons are commonly viewed as a synapomorphy of the seed-plant lineage and as the first leaves of a seedling. It is possible that the program of intercalary growth in leaves first evolved in cotyledons and was subsequently recruited for foliage leaves in the seed-plant lineage (Sokoloff et al., 2015).

References

Campbell D.H. 1895. The origin of the sexual organs of the Pteridophyta. *Bot. Gaz*. **20**: 76–78.

Chamberlain C.J. 1935. *Gymnosperms. Structure and evolution*. Chicago: Univ. Chicago Press.

Kenrick P. 2017. Changing expressions: a hypothesis for the origin of the vascular plant life cycle. *Phil. Trans. R. Soc. London. B: Biol. Sci*. **373**: 20170149.

Kenrick P., Crane P.R. 1997. *The origin and early diversification of land plants: a cladistic study*. Washington: Smithsonian Institution.

Niklas K.J., Kutschera U. 2009. The evolutionary development of plant body plans. *Funct. Plant Biol*. **36**: 682–695.

Remy W., Gensel P.G., Hass H. 1993. The gametophyte generation of some early Devonian land plants. *Int. J. Plant Sci*. **154**: 35–58.

Renzaglia K.S., Duff R.J., Nickrent D.L., Garbary D.J. 2000. Vegetative and reproductive innovations of early land plants: implications for a unified phylogeny. *Phil. Trans. R. Soc. London. B.* **355**: 769–793.

Sokoloff D.D., Rudall P.J., Bateman R.M., Remizowa M.V. 2015. Functional aspects of the origin and subsequent evolution of cotyledons in seed plants. *Bot. Pacif*. **4**: 35–47.

Zhang M., Zheng C.-X. 2016. Archegonium and fertilization in Coniferopsida. *Trees* **30**: 75–86.

PHYTOLITHS IN THE EPIDERMIS OF GRASSES: MICROMORPHOLOGY AND MORPHOMETRY

***Marina Yu. SOLOMONOVA*[1], *Sergey D. KOTOV*[1], *Daria D. RYZHAKOVA*[2], *Polina D. GUDKOVA*[1,2], *Natalya Yu. SPERANSKAYA*[1]**

[1] Altai State University, Barnaul, Russia
[2] Tomsk State University, Tomsk, Russia
solomonova@edu.asu.ru

Phytolith analysis is a robust method for reconstruction of past ecosystems. Phytoliths are microscopic silica bodies in plant cells. In grasses, they are found in leaf epidermis. Phytolith morphometrics is used to discriminate between grass taxa. The form of some phytoliths is under genetical control and is thought to be of great taxonomic importance for Poaceae (Fredlun, Tieszen, 1994; Ball et al., 1996, 1999; Gudkova, Olonova, 2012; Neumann et al., 2017). However, the phytoliths are phenotypically changeable as influenced by varying environment.

20 species of grasses of the southern Western Siberia were studied to reveal phytolith morphotypes and their location. The form of the epidermal cells was compared with phytolith morphotypes extracted from these species. The form of leaf epidermis cells was studied under the scanning electron microscope. Phytoliths were examined in immersion oil under an Olympus optical microscope (×200–×400) to comprehend their 3D shapes under rotation. Phytolith morphotypes were documented by light microphotographs and permanent reference slides. When describing grass phytolith morphotypes we followed the classification system of Blinnikov (2005) and Solomonova et al. (2019) as modified from Mulholland (1989) and Fredlund & Tieszen (1994). We also used the Glossary for the International Code for Phytolith Nomenclature 1.0 (Madella et al., 2005).

The greatest variability is found in formation of silica bodies in trichomes and long cells of the epidermis. Not all species which have trichomes form lanceolate silica bodies. We assume that this fact is the confirmation of the ecologically caused silicification of some cells (trichomes, long cells). Silica bodies in short cells generally repeat their shape. However, some differences in shapes of the epidermal cells and phytoliths therein were found. For example, grass species with rounded short cells have not only conical rondel but also low trapezoid (pyramidal) rondel, and upper base of trapeziform polylobate is different from short cells of epidermis by degree of sinuosity. So we think that morphometry of these morphotypes is necessary to distinguish among the taxa by phytoliths.

Trapeziform polylobate has been studied in various populations of *Dactylis glomerata* in order to identify intraspecific variation. We used recommendations of the International Committee for Phytolith Morphometrics for morphometry application, criteria for data collection and publication, definitions for basic measurements (Ball et al., 2016).

The size of *Dactylis glomerata* polylobate phytoliths was measured by the following characteristics of the upper side: area, convex area; convex perimeter; length; width; fiber length (length of the phytolith along its medial axis); equivalent diameter, inscribed radius. The form of phytoliths was studied using the following design parameters: form factor; roundness; convexity; solidity; compactness; aspect ratio; elongation; curl.

The size and shape of *Dactylis glomerata* polylobate phytoliths were found to be intraspecific different. The strongest variation is observed in their length, fiber length, curl and elongation. The other descriptors are less variable. Perhaps further research will confirm their potential for taxonomy and as palaeoecological proxies.

References

Ball T., Gardner J.S., Brotherson J.D. 1996. Identifying phytoliths produced by the inflorescence bracts of three species of wheat (*Triticum monococcum* L., *T. dicoccum* Schrank., and *T. aestivum* L.) using computer-assisted image and statistical analyses. *J. Archaeol. Sci*. **23**: 619–632.

Ball T.B., Gardner J.S., Anderson N. 1999. Identifying inflorescence phytoliths from selected species of wheat (*Triticum monococcum, T. dicoccum, T. dicoccoides,* and *T. aestivum*) and barley (*Hordeum vulgare* and *H. spontaneum*). *Am. J. Bot*. **86**: 1615–1623.

Ball T.B., Davis A.L., Evett R.R., Ladwig J.L., Tromp M., Out W.A., Portillo M. 2016. Morphometric analysis of phytoliths: recommendations towards standardization from the International Committee for Phytolith Morphometrics. *J. Archaeol. Sci*. **68**: 106–111.

Blinnikov M.S. 2005. Phytoliths in plants and soils of the interior Pacific Northwest, USA. *Rev. Palaeobot. Palynol*. **135**: 71–98.

Fredlund G., Tieszen L.T. 1994. Modern phytolith assemblages from the North American Great Plains. *J. Biogeogr*. **21**: 321–335.

Gudkova P.D., Olonova M.V. 2012. Micromorphology of abaxial epidermis of Siberian *Stipa* L. leaf blades. *Tomsk State University Journal of Biology*. **3**: 33–45. [In Russian]

Madella M., Alexandre A., Ball T. 2005. International code for phytolith nomenclature 1.0. *Ann. Bot*. **96**: 253–260.

Mulholland S.C. 1989. Phytolith shape frequencies in North Dakota grasses: a comparison to general patterns. *J. Archaeol. Sci.* **16**: 489–511.

Neumann K., Fahmy A.G., Müller-Scheeßel N., Schmidt M. 2017. Taxonomic, ecological and palaeoecological significance of leaf phytoliths in West African grasses. *Quat. Intern*. **434**(B): 15–32.

Solomonova M.Y., Blinnikov M.S., Silantieva M.M., Speranskaya N.Y. 2019. Influence of moisture and temperature regimes on the phytolith assemblage composition of mountain ecosystems of the mid latitudes: a case study from the Altay Mountains // *Front. Ecol. Evol.* **7**. DOI: 10.3389/fevo.2019.00002

ONCE AGAIN ON MOSS PARAPHYLLIA

***Ulyana N. SPIRINA*[1,2], *Tatyana V. VORONKOVA*[1], *Michael S. IGNATOV*[1,3]**

[1] Tsitsin Main Botanical Garden RAS, Moscow, Russia
[2] Tver State University, Tver, Russia
[3] Lomonosov Moscow State University, Moscow, Russia
misha_ignatov@list.ru

Paraphyllia are the moss stem surface structures, which are important in pleurocarpous mosses systematics. Their characters are highly diagnostic for many genera and families. Paraphyllia are treated as adventive structures (appendages) of stem epidermis, in contrast to foliose or filamentose structures around branch primordia commonly referred to the pseudoparaphyllia. Our previous works suggested that it is better to treat pseudoparaphyllia simply as proximal branch leaves, as they have phyllotaxis, even if they are arranged at some distance from the compact 'bud' and divided, representing a special case called 'compound leaf' (Spirina, Ignatov, 2015; Ignatov, Spirina, 2012).

Bonnot (1967) overviewed possible homologies of paraphyllia, which were treated as appendages of stem epidermis, additional leaf-like structures, reduced leaves, trichomes, modified protonematal structures, but always without relation to the branch primordia. Although the main feature of paraphyllia (in traditional view) is that they are not concentrated around branch primordia, this is true only to a certain extent. Paraphyllia are more or less scattered, but they are sometimes obviously more numerous around branch primordia. Examples from different families support this statement. Therefore, the definition of paraphyllia by Akiyama & Nishimura (1993), who pointed on not-connection with branch primordia, is not always apparent. Ignatov & Hedenäs (2007) suggested an alternative interpretation of paraphyllia (some types of them) as of proximal branch leaves escaped from the branch primordium. Now we can add that sometimes they can be homologous not to the whole leaf, but also to parts of compound leaves, especially in such families as Neckeraceae (Spirina, Ignatov, 2015).

An example of *Leskea polycarpa* allows us to develop this point of view further on. Apical cells of branch primordia appear in the mother stem apical zone very early; such cells are big and numerous, but not all of them proceed to well developed branch primordia. Some of branch apical cells produce normally developed branches with leaves, some form only weakly developed primordium and stop development, and, ultimately, some 'branch apical cells' do not produce even merophytes of their typical arrangement around apical cell. Down the stem, such undeveloped 'primordia' appear to be hidden, almost totally, under the stem epidermis, and surrounded by smaller cells. The margins of such zones around hidden apical cells are flanked by leaf-like structures (paraphyllia?), sometimes with apparent phyllotaxis of branch leaves.

Some other mosses have similar paraphyllia phyllotaxis, e.g. *Cratoneuron*, *Haplocladium*, *Leptodon*, *Metaneckera* and *Thuidium*. Paraphyllia in the genus *Thuidium* are very dense on the main stem and primary branches, but they are few on the secondary branches, so the characteristic pattern of so-called paraphyllia arrangement in a way similar to *Leskea* and other pleurocarps is clearly seen.

It is interesting that the quantity of paraphyllia in all genera mentioned above increased after exogeneous abscisic acid (ABA) treatment *in vitro*. It was shown that ABA stimulates uplifting of cells both in paraphyllia and leaves (Spirina, Voronkova, 2017).

Although we refrain from the abandon the term paraphyllia, which is useful for descriptive purposes, the homology of paraphyllia with leaves seems apparent. Branch initials appear sometimes totally virtual, but still keep phyllotaxis around them. The raising of cells of stem epidermis, and sometimes continuing to develop into leaf-like structures is facilitated by exogenous ABA, providing a useful model object for morphogenetic observations.

References

Akiyama H., Nishimura N. 1993. Further studies of branch buds in mosses; "pseudoparaphyllia" and "scaly leaves". *J. Plant Res.* **106**: 101–108.

Bonnot E.-J. 1967. Sur la valeur et signification des paraphylles chez les Bryales. *Mém. Soc. Bot. France*. P. 236–248.

Ignatov M.S., Hedenäs L. 2007. Homologies of stem structures in pleurocarpous mosses, especially of pseudoparaphyllia and similar organs. In: Newton A.E., Tangery R. (eds.): *Pleurocarpous mosses: systematic and evolution*. Boca Raton: CRC Press. P. 269–286.

Ignatov M.S., Spirina U.N. 2012. Morphogenesis of proximal branch leaves in mosses. *Russ. J. Developm. Biol.* **43**: 148–156.

Spirina U.N., Ignatov M.S. 2015. Bilobed leaves in mosses? Structure and adaptive significance of proximal branch leaves in Lembophyllaceae. *Arctoa* **24**: 124–140.

Spirina U.N., Voronkova T.V. 2017. On homologies of paraphyllia and pseudoparaphyllia in mosses. In: Sokoloff D.D. et al. (eds.): *Taxonomy and evolutionary morphology of plants: Materials of the Conference dedicated to 85 anniversary of V.N. Tikhomirov (January 31 – February 3, 2017, Moscow)*. M.: MAKS Press. P. 371–373.

WOOD ANATOMY OF THE TRIBES PROTEAE AND LEUCADENDREAE (PROTEACEAE)

Anna V. STEPANOVA[1], ***Alexei A. OSKOLSKI***[1,2]

[1] Komarov Botanical Institute RAS, Saint Petersburg, Russia
[2] University of Johannesburg, Johannesburg, South Africa
AStepanova@bin.ran

Proteaceae is a relatively large family with 68 genera and more than 1000 woody species confined almost exclusively to Southern Hemisphere, with highest diversity and endemism in Australia and South Africa. This family was classified (Weston, Barker, 2006) into five subfamilies: Bellendenoideae and Persoonioideae belong to the basally diverged lineage whereas Symphionematoideae together with Proteoideae and Grevilleoideae comprise two large crown clades (Weston, 2014). Proteaceae is placed into the order Proteales that includes also the families Nelumbonaceae, Platanaceae and Sabiaceae (APG, 2016).

Wood anatomy of Proteaceae is less studied than that of Sabiaceae (Carlquist et al., 1993) and Platanaceae (e.g. Brush, 1917; Brazier, Franklin, 1961; Wheeler, 1995). Wood anatomical investigations of this family were focused mostly on the genera of subfamiles Persoonioideae and Grevilleoideae from Australia, New Zealand and South America (Chattaway, 1948; Mennega, 1966; Lanyon, 1979; Patel, 1992; InsideWood, 2004), while Proteoideae, the large subfamily centered in South Africa, remains underexplored. Among its genera, the wood anatomical information has been published to date only for the Malagasy genus *Dilobeia* (Lanyon, 1979) and few species of southern African genera *Protea*, *Leucadendron* and *Faurea* (Chattaway, 1948; Kromhout, 1975).

We studied the wood structure of 40 species of nearly all genera representing three lineages of the crown subclade of Proteoideae, i.e. the tribes Proteae (South African *Protea* and *Faurea*), Petrophileae (*Petrophile* from Western Australia and *Aulax* from South Africa), and Leucadendreae (*Leucadendron*, *Leucospermum*, *Serruria*, *Spatalla*, *Diastella*, *Paranomus* and *Mimetes* from South Africa, as well as *Adenanthos* and *Isopogon* from Western Australia).

The members of Proteoideae examined in the present study are rather uniform in their wood structure (which is also typical of many other genera of Proteaceae) and characterized by diffuse-porous wood, vessels with simple perforation plates, alternate minute to small intervessel pits, non-septate fibres, unilateral paratracheal axial parenchyma, and rays of two distinct sizes (1–2-seriate and > 5-seriate ones, up to 22-seriate rays in some *Protea* species). *Isopogon, Petrophile* and *Faurea* are distinctive from other genera in having helical thickenings on vessel walls. We did not found any wood traits that can be diagnostic for the tribes under study.

Bordered pits on fiber walls were found in all genera under study except for *Faurea*. This trait has also been reported in most genera of Persoonioideae, i.e. in

Garnieria, *Toronia*, *Persoonia* and *Placospermum* (Lanyon, 1979; Patel, 1992), but is not common in Grevilleoideae. Such distribution suggests that the occurrence of bordered pits on fiber walls is an ancestral condition for the family. Noteworthy, that this trait is confined to the plant from fynbos and kwongan, two sclerophyllous plant communities from Mediterranean-climate areas of South Africa and Western Australia, respectively. The presence of tracheids in secondary xylem is one of the characteristic of Californian chaparral, another type of sclerophyllous vegetation shaped by Mediterranean climate; this trait plays an important role in maintaining safety of water conductance in this seasonally dry environment (Carlquist, Hoekman, 1985; Pratt et al., 2015). These data suggest that the fibers with bordered pits (fiber-tracheids) in the fynbos and kwongan species of Proteaceae are also involved in water conductance and, therefore, linked to its safety.

This work was supported by the Russian Foundation for Basic Research (grant No. 19-04-00714a).

References

APG. 2016. An update of the Angiosperm Phylogeny Group classification for the orders and families of flowering plants: APG IV. *Bot. J. Linn. Soc.* **181**: 1–20.

Brazier J.D., Franklin G.L. 1961. Identification of hardwoods. A microscope key. *For. Prod. Res. Bull*. **46**: 1–96.

Brush W.D. 1917. Distinguishing characters of North American sycamores. *Bot. Gaz.* **64**: 480–496.

Carlquist S., Morrell P.L., Manchester S.R. 1993. Wood anatomy of the Sabiaceae. *Aliso* **13**: 521–549.

Carlquist S., Hoekman D.A. 1985. Ecological wood anatomy of the woody southern California flora. *IAWA Bull.* **6**: 319–347.

Chattaway M.M. 1948. The wood anatomy of the Proteaceae. *Aust. J. Biol. Sci.* **1**: 279–302.

InsideWood. 2004-onwards. Published on the Internet. http://insidewood.lib.ncsu.edu/search [20.03.2019].

Kromhout C.P. 1975. 'n Sleutel vir die mikroskopiese uitkenning van die vernaamste inheemse houtsoorte van Suid-Afrika. *Bull. Dep. For. South Africa*. **50**: 1–140.

Lanyon J.W. 1979. The wood anatomy of three Proteaceous timbers *Placospermum coriaceum*, *Dilobeia thouarsii* and *Garnieria spathulaefolia*. *IAWA Bull*. **2–3**: 27–33.

Mennega A.M.W. 1966. Wood anatomy of the genus *Euplassa* and its relation to other Proteaceae of the Guianas and Brazil. *Acta Bot. Neerl.* **15**: 117–129.

Patel R.N. 1992. Wood anatomy of the dicotyledons indigenous to New Zealand 22. Proteaceae. *New Zeal. J. Bot*. **30**: 415–428.

Pratt R.B., Percolla M.I., Jacobsen A.L. 2015. Integrative xylem analysis of chaparral shrubs. In: Hacke U.G. (ed.): *Functional and ecological xylem anatomy*. Heidelberg, New York, Dordrecht, London: Springer. P. 189–207.

Weston P.H. 2014. What has molecular systematics contributed to our knowledge of the plant family Proteaceae? In: Besse P. (ed.): *Molecular plant taxonomy. Methods in molecular biology (Methods and protocols)*. Totowa: Humana Press. V. **1115**. P. 365–397.

Weston P.H., Barker N.P. 2006. A new suprageneric classification of the Proteaceae, with an annotated checklist of genera. *Telopea* **11**: 314–344.

Wheeler E.A. 1995. Wood of *Platanus kerrii*. *IAWA J*. **16**: 127–132.

SPECIFIC STRUCTURAL FEATURES OF THE BARK IN ANNUAL STEMS OF *BETULA ERMANII* CHAM. EXPOSED TO HYDROTHERMAL GASES AND FLUIDS OF BARANSKY VOLCANO, ITURUP ISLAND

Anastasia I. TALSKIKH*, *Anna V. KOPANINA, Inna I. VLASOVA

Institute Marine Geology and Geophysics Far Eastern Branch RAS,
Vladivostok, Russia
anastasiya_talsk@mail.ri

The Kuril Islands is an area with high volcanic and post-volcanic activity, which is a key stress factor for plants growing in these landscapes. The vegetation forming in these settings is closely associated with the life strategies of individual plant species which are able to survive under such specific environmentals due to their properly changed vital processes (Manko, Sidelnikov, 1989). A noteworthy example of these plant is a Stone (Erman's) birch, *B. ermanii* Cham. (Betulaceae S.F. Gray), one of the main sylvic tree of coastal woods around the Sea of Okhotsk, which also inhabits volcanic landscapes.

Betula ermanii is a monoecious, deciduous, anemophilous tree of first, second or third size categories, or a large shrub. It can form pure or mixed forests in mountains and at foothills, as well as dwarf birch thickets (yernik) on seacoast and in high mountain areas. *Betula ermanii* features a wide norm of reaction and is highly adaptable to a variety of habitats (Kabanov, 1972). This study aimed to investigate the distinctive structural change of the bark tissues of annual stems of *B. ermanii* growing under extreme conditions at the active Baransky Volcano in Iturup Island (Kuril Islands).

Samples were collected in stone birch-bamboo forest on Starozavodskoye solfatara field on August 2, 2018 and in stone birch-larch-bamboo forest nearby hot springs around Golubye Ozera on July 31, 2018. Samples for reference were collected in typical of the species fir-stone birch shrub-forbs forest on Susunai Ridge, Sakhalin Island on October 18, 2015 and in Dendrology Park of the Institute of Marine Geology and Geophysics FEB RAS on August 13, 2018. The water of thermal fluids in Starozavodskoye solfatara field are of the sodium-calcium sulfate type, around 100 °C hot, siliceous, acidic (pH = 3.5). The prevalent gaseous emission is carbon dioxide (64%), another gases are nitrogen (28%), oxygen (6%), sulfurous gases (less than 2%). Golubye Ozera hot springs are two deep funnels filled with opalescent bluish water, fringed with bright dispersed sulfur rims. The water is of the sulfate-chloride type, ultra-acidic (pH = 1.2), up to 107.5 °C hot. The emission gases are nitrogen (31%); carbon dioxide (38%), oxygen (9%), methane and other hydrocarbons (0.05%) (Zharkov, 2014). Vegetation alongside the hot springs is represented by shrub mosaics and dwarf shrub communities. Several meters away, communities include *B. ermanii*.

In each habitat, annul shoots were sampled from three model 60–80-years-old trees with 14–22 cm trunk diameter. Stem samples were fixed in 96% ethyl alcohol according to Barykina et al. (2004) and then analyzed using the equipment of the Laboratory for Plant Ecology and Geoecology, IMGG FEB RAS. Transverse, radial and tangential 10–25 μm thick sections of the stems were made with a sliding microtome Microm HM 430c with a fast freezing unit (Thermo Scientific, USA). The sections were stained regressively using Safranin and Nile Blue, washed up in ethyl alcohol series of increasing concentrations, dehydrated and cleared with carbol xylene and xylene (Barykina et al., 2004) and mounted in synthetic mounting media. The bark samples were also macerated according to Wang et al. (2011) to reveal the structure of conducting elements of the phloem. Histochemical reactions were used to determine chemical of the crystals in the bark tissues (Barykina et al, 2004).

Tissues and cells at similar ontogenetic states were compared in extreme habitats and reference samples.

Section images were processed with ZEN 2 lite software under light microscope Axio Scope.A1, CarlZeiss for measuring and photography. Bark tissue was described according to current guidelines on bark anatomy of woody plants by the International Association of Wood Anatomists – IAWA (Angyalossy et al., 2016).

We analyzed 17 characters of bark tissues in transverse and longitudinal sections for each model tree. The dataset for each character of each model tree comprised at least 32 measurements. Data from three model trees were averaged and assembled in the Table. The sample mean and its confidence interval (for 95% probability) were estimated for each character. Statistical analysis was performed according to Minko (2004) using Microsoft Excel 2016 statistical analysis tools.

Our data complement those of Yeremin & Kopanina (2012) as they show bark structure in the second half of the growing season. The histological composition of the bark from the extreme environments was the same as that from the reference habitat. The epidermis, periderm, cortex (of collenchyma and ground parenchyma), protophloem fibers and sclereids, primary and secondary phloem succeed inward each other.

The site of the phellogen initiation and the phellem structure were similar in samples from both environments. The periderm in samples from Starozavodskoye solfatara field was 7% wider than that from Golubye Ozera because the phellogen produce more phellem layers (see Table), whereas the phelloderm of parenchyma cells remains typically 1-layed.

Table. Characters of bark tissues of *Betula ermanii* in various environmentals

Characters, units	Sakhalin Island		Iturup Island	
	Dendrology Park of the IMGG FEB RAS (typical habitats)	Susunai Ridge (typical habitats)	Baransky Volcano, Starozavodskoye solfatara field	Baransky Volcano, Golubye Ozera hot springs
Bark width, μm	384.50 ± 14.92	355.35 ± 6.88	366.31 ± 8.53	372.94 ± 11.19
Phellem width, μm	89.01 ± 2.63	88.79 ± 1.86	95.32 ± 2.94	90.55 ± 3.90
Number of phellem cells in the radial row	13.78 ± 0.42	16.22 ± 0.26	14.69 ± 0.31	14.16 ± 0.77
Radial diameter of phellem cells, μm	6.31 ± 0.58	5.84 ± 0.19	6.65 ± 0.48	6.55 ± 0.42
Tangential diameter of phellem cells, μm	18.32 ± 1.37	19.78 ± 0.67	23.48 ± 1.54	21.89 ± 1.66
Specific area of protophloem fibers and sclereids, %	22.99 ± 0.93	22.39 ± 0.48	23.50 ± 0.96	33.11 ± 1.04
Specific number of crystals in cortex and phloem parenchyma per mm^2		74.40 ± 2.68	20.42 ± 3.02	17.48 ± 2.80
Secondary phloem width, μm	43.99 ± 2.29	41.37 ± 1.24	51.14 ± 3.07	44.96 ± 2.75
Radial diameter of sieve tubes, μm	4.63 ± 0.36	4.08 ± 0.19	5.76 ± 0.53	6.47 ± 0.45
Tangential diameter of sieve tubes, μm	10.57 ± 0.90	10.60 ± 0.43	12.51 ± 0.98	14.16 ± 0.83
Sieve tube element length, μm	146.31 ± 7.96	149.05 ± 5.56	149.86 ± 10.19	154.58 ± 8.87
Total number of phloem rays per 1 mm	28.06 ± 0.69	27.11 ± 0.49	22.97 ± 0.55	23.91 ± 0.82
Number of uniseriate rays per 1 mm	26.47 ± 0.70	25.90 ± 0.50	22.56 ± 0.56	23.66 ± 0.85
Number of 2-seriate rays per 1 mm	1.16 ± 0.34	1.02 ± 0.15	0.38 ± 0.18	0.22 ± 0.15
Number of 3-seriate rays per 1 mm	0.41 ± 0.18	0.17 ± 0.08	0.03 ± 0.06	0.00 ± 0.00
Number of 4-seriate rays per 1 mm	0.03 ± 0.06	0.04 ± 0.04	0.00 ± 0.00	0.00 ± 0.00
Ray width in cell number	2.31 ± 0.28	2.05 ± 0.13	1.44 ± 0.20	1.22 ± 0.15

The collenchyma consists of 2–3 layers of round or oval cells. The cortical ground parenchyma consists of circular (isodiametric) cells and has well-developed network of intercellular spaces between them.

Calcium oxalate crystals are deposited in ground parenchyma cells in the cortex as well as in ray and axial parenchyma cells of the phloem. In the reference specimens the crystals aggregate in clusters. The specific number of crystals in samples from hydrothermal fields around Baransky Volcano is 73–76% lower than in the reference ones (Table).

Reference plants formed nearly continuous heterogeneous ring of primary mechanical tissues by the end of the growing season, which is occasionally interrupted by 1–2 parenchyma cells. The sclerenchyma specific area varies in plants from the extreme habitats. In samples from Starozavodskoye solfatara field, this area equals that of reference plants, whereas samples from around Golubye Ozera hot springs had 44% greater specific area of sclerenchyma compared to the control (Table).

Secondary phloem consists of sieve tubes and companion cells, axial and ray parenchyma. Diffusely located sieve tubes are tangentially elongated in the transverse section. Similarly to cortical parenchyma, axial and ray parenchyma cells of the phloem also have calcium oxalate crystals. The phloem rays are homo- and heterocellular, 1- to 3-seriate. Width of the secondary phloem in samples from Golubye Ozera surroundings remains unaffected, whereas in samples from Starozavodskoye solfatara field, this tissue is 16% wider. Similar widening of the secondary phloem was previously revealed in the annual twigs of *Toxicodendron orientale* Greene from the vicinity of Verkhnedoktorskiye hot springs of Mendeleev Volcano, Kunashir Island (Kopanina, 2016). The sieve tubes in samples from the two Baransky Volcano sampling sites were greater than in reference samples. They were 41% wider radially and 18% wider tangentially in samples from the solfatara field. The sieve tubes are 59% wider radially and 34% wider tangentially in samples from vicinity of the thermal lakes. The number of the uniseriate rays in the secondary phloem in samples from the extreme environments is reduced to result in total 12–15% reduction of the phloem ray number versus the norm.

No abnormal structures have been found in the bark.

Statistical analysis of the bark structural characters of samples affected by the hydrothermal gases and fluids of Baransky Volcano revealed similar decreasing of the specific number of crystals in cortex and phloem parenchyma cells, the sieve tube diameters, the total number of phloem rays and number of the uniseriate ones as compared with the reference samples. Other bark characters either remained unchanged or changes specifically in every habitat. Phellem width, number of phellem cells in the radial row, secondary phloem width were modified in samples from the Starozavodskoye solfatara field.

The extreme environments concerned mostly affect sieve tubes and ray parenchyma characters. Deposition of calcium oxalate crystals as indication of the metabolic rates also declines. Samples from Starozavodskoye solfatara field have thicker outer

tissues, whereas Golubye Ozera samples contain more sclerenchyma. The structural response of the bark of annual stems of *B. ermanii* to the extreme conditions around the hydrothermals is complex and multidirectional. These results are in agreement with the data previously obtained for other plant species (Kopanina et al., 2017).

The study was carried out with support from RBFR (grants Nos. 15-04-04774, 15-05-01768) and in accordance with the state order to the Institute of Marine Geology and Geophysics, Far Eastern Branch RAS.

References

Angyalossy V., Pace M.R., Evert R.F., Marcati C.R., Oskolski A.A., Terrazas T., Kotina E., Lens F., Mazzoni-Viveiros S.C., Angeles G., Machado S.R., Crivellaro A., Rao K.S., Junikka L., Nikolaeva N., Baas P. 2016. IAWA list of microscopic bark features. *IAWA J.* **37**: 517–615.

Barykina R.P., Veselova T.D., Devyatov A.G., Dzhalilova Kh.Kh., Iljina G.M., Chubatova N.V. 2004. *Mannual on botanical microtechnique. Basic principles and methods*. Moscow: Moscow Univ. Press. [In Russian]

Kabanov N.E. 1972. *Botanical-geographic and silvicultural aspects of Erman's birch forests*. Moscow: Nauka. [In Russian]

Kopanina A.V. 2016. Structural ecological and anatomical studies of woody plants in Sakhalin and Kurile islands. *Bull. Bot. Gard.-Inst. FEB RAS.* **15**: 36–38. [In Russian]

Kopanina A.V., Vlasova I.I., Vacerionova E.O. 2017. Structural adaptation of woody plants to volcanic landscapes of the Kuril Islands. *Vestnik Far Eastern Branch Russ. Acad. Sci.* **1**: 88–96. [In Russian]

Manko Yu.I., Sidelnikov A.N. 1989. *Influence of volcanism on vegetation*. Vladivostok: DVO AN SSSR. [In Russian]

Minko A.A. 2004. *Statistical analysis in MS Excel*. Moscow: Williams Publ. [In Russian]

Wang G., Shi S., Wang J.W., Yu Y., Cao S.P., Cheng H. 2011. Tensile properties of four types of individual cellulosic fibers. *Wood and Fiber Sci.* **43**: 353–364.

Yeremin V.M., Kopanina A.V. 2012. *Atlas of the bark anatomy of trees, shrubs and lianas of Sakhalin and Kuril islands*. Brest: Poligrafika. [In Russian]

Zharkov R.V. 2014. *Thermal springs of the Kuril Islands*. Vladivostok: Dalnauka. [In Russian]

ANATOMICAL STRUCTURE OF LEAVES IN SOME CULTIVATED REPRESENTATIVES OF THE GENUS *BEGONIA* L.

Anzhelika Yu. TEPTINA[1]***, Lolita V. REYN***[1]***, Marina B. ZAVYALOVA***[2]

[1] Ural Federal University, Ekaterinburg, Russia
[2] Institute Botanic Garden Ural Branch RAS, Ekaterinburg, Russia
ateptina@gmail.com

Begonia L. is one of the five largest genera of vascular plants (Hoover et al., 2004) comprising approximately 1,500 species, arranged in 66 sections (Ali, 2013;

Doorenbos et al., 1998). The genus has a pantropical distribution in humid regions of Central and South America, Asia, Africa, and Pacific Islands (Jacques, Mamede, 2005). Species of *Begonia* are valuable food and medicinal plants (Laferriere, 1992; Tebbitt, 2005) and are widely known as ornamentals.

Nowadays, more than 200 species of *Begonia* are cultivated (Tebbitt, 2005). They easily hybridize and about 10,000 hybrids of a variety of colors and leaf textures have been made (Neale et al., 2006). Many begonias are fast-growing plants producing a lot of seeds, to make them excellent candidates for genetic research. Morphological and anatomical features of species and cultivars of *Begonia* are extremely variable, but poorly known. A few anatomical data are available in the literature: Irmscher (1935) used anatomical features for classifying species into sections; Bailey (1949) and Fotsch (1933) used stem anatomy for arranging species into groups; Barkley & Hozid (1971) thoroughly investigated anatomy of leaves and stems in some species.

The aim of the present study is to discover the anatomical characters for identification of herbaceous species and cultivars of *Begonia* from sections *Gireoudia* (Klotzsch) A. DC. and *Gaerdtia* (Klotzsch) A. DC. The material was taken from greenhouse-grown specimens in the Botanical Garden of Urals Branch of Russian Academy of Sciences. Pieces of leaves were fixed in the Farmer's fixative (acetic acid : ethanol 1:3). Cross sections of leaf blades and petioles were made using a freezing microtome. Preparations were analyzed, and microphotographs were taken using microscope Leica DM 5000 (Leica Microsystems, Germany) with SINAGIS digital camera (Russia). Systematic position of *Begonia* species was considered in accordance with the World Checklist of Begoniaceae (Govaerts, 2019). Species of the section *Gireoudia* are distributed in Central America, while species of *Gaerdtia* section are distributed in the eastern Brazilian region.

Section *Gaerdtia* was represented by *B. maculata* Raddi and *B. albopicta* W. Bull in the present work (Table). Petioles are terete in a cross-section; the epidermis consists of a single layer of thick-walled cells, occasionally forming hairs. The stomata are dispersed. Two or three layers of tiny angular collenchyma cells are located under the epidermis. Further, 3–4 layers (in *B. maculata*) or 6–8 layers (in *B. albopicta*) of large parenchyma cells are located inside to the collenchyma layer (Fig. 1A) and adjoin circularly arranged vascular bundles. A number of parenchyma cells contain calcium oxalate crystals. The petioles have a peripheral vascularisation pattern with collateral endoscopic vascular bundles, where the phloem cells are oriented outwards and the xylem cells are oriented inwards. The central part of the petiole consists of large thin-walled cells (Fig. 2A), which contain numerous crystals of calcium oxalate (Fig. 3).

Table. Comparative anatomical features of *Begonia* species

Scientific name / Section	Collenchyma (petiole)	Parenchyma cells (petiole)	Vascular bundle (petiole)	Hypodermis (lamina)	Stomata (lamina)
Gaerdtia:					
B. albopicta	2–3 layers angularly thickened	6–8 layers	collateral	absent	single
B. maculata	2–3 layers angularly thickened	3–4 layers	collateral	absent	single
Gireoudia:					
B. bowerae	3 layers angularly thickened	3–4 layers	collateral	1 layer	from single to clusters of 2–3
B. heracleifolia	3–4 layers angularly thickened	4–5 layers	collateral, bicollateral	1–2 layers	from single to clusters of 2–4
B. manicata	3–4 layers angularly thickened	4–5 layers	collateral	1 layer	from single to clusters of 2–3
B. nelumbiifolia	4–5 layers angularly thickened	4–5 layers	collateral, medullar	1–2 layers	from single to clusters of 2
B. crassicaulis	4–5 layers angularly thickened	2–3 layers	collateral	1 layer	single

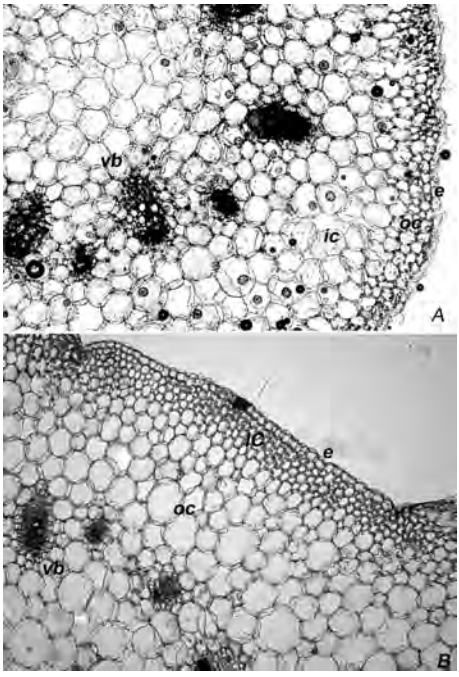

Fig. 1. Cross sections of the petiole, ×50.
A – *Begonia albopicta*, sect. *Gaerdtia*; B – *B. heracleifolia*, sect. *Gireoudia*.
e – epidermis, *ic* – inner cortex, *oc* – outer cortex, *vb* – vascular bundle.

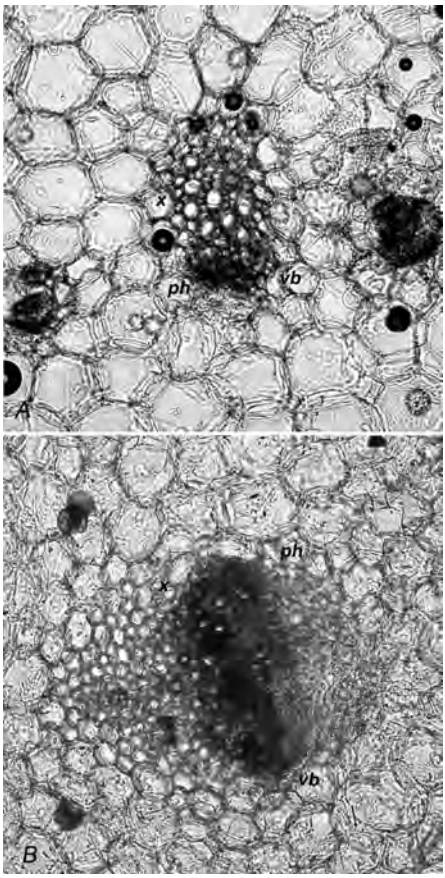

Fig. 2. Cross-sectioned vascular bundles of the petiole, ×100.
A – *Begonia albopicta*, sect. *Gaerdtia*; B – *B. heracleifolia*, sect. *Gireoudia*.
h – phloem, *vb* – vascular bundle, *x* – xylem.

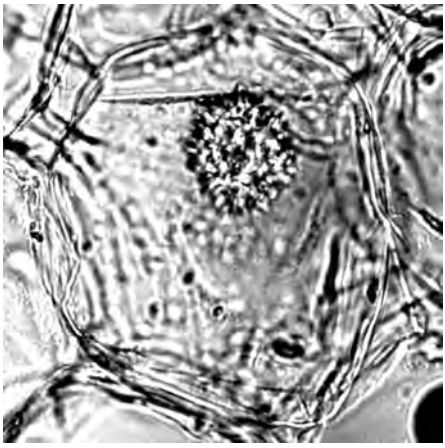

Fig. 3. Calcium oxalate druse in the cortex
of the petiole of *Begonia albopicta*, ×200.

The upper and lower epidermises of leaf blades consist of large flat cells of a regular form. The upper epidermis is thicker than the lower one (Fig. 4A). The stomata are evenly distributed in the lower epidermis. The characteristic feature of the studied representatives of *Gaerdtia* section is single, not clustered stomata. While *B. albopicta* has single stomata only, *B. maculata* occasionally has paired stomata. The mesophyll is differentiated into a palisade and a spongy tissue. Hypodermis is absent and cystoliths were not detected (Fig. 5A).

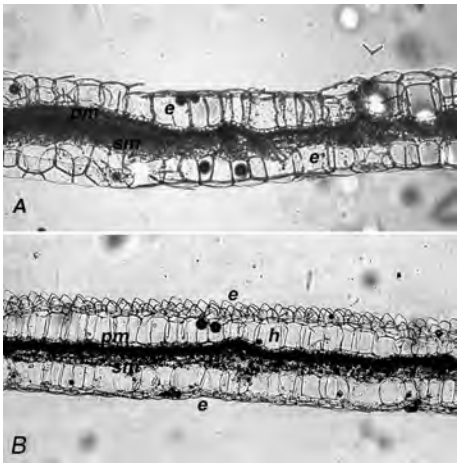

Fig. 4. Cross sections of the lamina, ×50.
A – *Begonia maculata*, sect. *Gaerdtia*; B – *B. heracleifolia*, sect. *Gireoudia*.
e – epidermis, *h* – hypodermis, *sm* – sponge mesophyll, *pm* – palisade mesophyll.

Section *Gireoudia* was represented by cultivars of *B. bowerae* Ziesenh., *B. heracleifolia* Schltdl. et Cham., *B. manicata* Brongn., *B. nelumbiifolia* Schltdl. et Cham. and *B. crassicaulis* Lindl. (Table). The anatomy of their leaves is similar to that of representatives of section *Gaerdtia*, but some distinctive features were revealed. The cells of petiole epidermis are regular in shape, and characteristically bulged outwards. Glandular hairs were found only on petioles of *B. crassicaulis*. There are 3 to 5 layers represented by small, angular collenchyma cells (Fig. 1B) under the epidermis. These cells have angular thickenings and contain chloroplasts. The large parenchyma cells of irregular shape, arranged in four to six layers, are present inward to the collenchyma and border with a ring of vascular bundles. The vascularisation pattern is similar to that of the previous section having collateral endoscopic vascular bundles (Fig. 2B). In addition to these bundles we noted medullar bundles in *B. nelumbiifolia*, which, according to Lee (1974), indicates the presence of succulent features in species of *Begonia*. The central part of the petiole is filled with large parenchyma cells. The crystals of calcium oxalate in the parenchyma cells of *Gireoudia* section species are relatively rare compared to species of the previous section (Fig. 3).

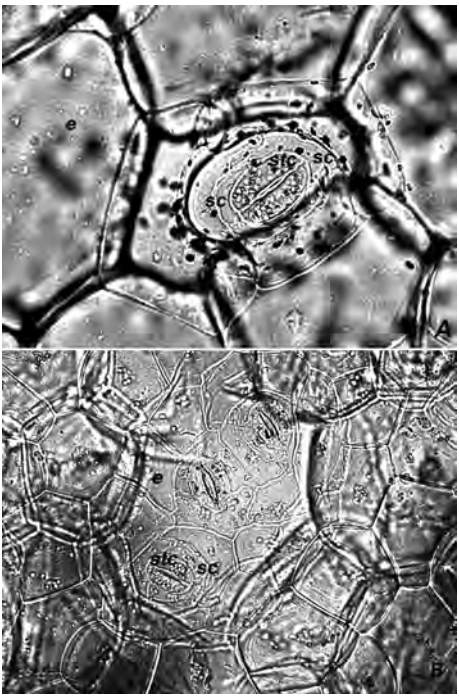

Fig. 5. Surface view of the lower epidermis.
A – *Begonia maculata*, sect. *Gaerdtia*, ×400; B – *B. heracleifolia*, sect. *Gireoudia*, ×200.
e – epidermal cell, *sc* – subsidiary cell, *stc* – guard cells.

The epidermis of leaf blades of *Gireoudia* is often formed by papillary cells. One or rarely two layers of very large thin-walled hypodermis cells are located under the upper and lower epidermis. Almost all studied representatives of *Gireoudia* section have a hypodermis on both sides of the leaf blades. The mesophyll is differentiated into a palisade and a spongy tissue (Fig. 4B). Stomata are normally arranged in clusters of 2 or 3, but single stomata rarely occur in *B. nelumbiifolia* and *B. bowerae* (Fig. 5B). A variable number of stomata (from single to groups of 4) was noted in *B. heracleifolia*.

References

Ali M.S. 2013. *Genetic architecture of species level differences in* Begonia *section* Gireoudia. Institute of Cell and Molecular Biology, School of Biological Sciences, University of Edinburgh. PhD thesis.

Bailey L.H. 1949. *Manual of cultivated plants*. New York: Macmillan Co.

Barkley F.A., Hozid B. 1971. Leaf anatomy of *Begonia*. *Begonian* **38**: 135–142.

Doorenbos J., Sosef M.S.M., de Wilde J.J.F.E. 1998. *The sections of* Begonia *including descriptions, key and species list. Studies in Begoniaceae VI*. Wageningen: Agricultural University.

Fotsch K.A. 1933. *Die Begonien*. Stuttgart: Ulmer.

Govaerts R. 2019. *World checklist of Begoniaceae. Facilitated by the Royal Botanic Gardens, Kew.* Published on the Internet http://wcsp.science.kew.org (accessed 1 March 2019).

Hoover W.S., Karegeannes C., Wiriadinata H., Hunter J.M. 2004. Notes on the geography of South-East Asian *Begonia* and species diversity in mountain forests. *Telopea* **10**: 749–764.

Irmscher E. 1935. Begoniaceae. In: Engler A., Prantl K. (Hrsg.): *Die natürlichen Pflanzenfamilien*. 2.Aufl. Leipzig: Wilhelm Engelmann. Bd. **21**: 548–588.

Jacques E.L., Mamede M.C.H. 2005. Notas nomenclaturais em *Begonia* L. (Begoniaceae). *Rev. Brasil. Bot.* **28**: 579–588.

Laferriere J.E. 1992. Begonias as food and medicine. (Notes on economical plants). *Econ. Bot.* **46**: 114–116.

Lee Y.S. 1974. A study of stem anatomy in Begonia L. *Phytologia* **27**: 464–489.

Neale S., Goodall-Copestake W., Kinder C.A. 2006. The evolution of diversity in *Begonia*. In: Teixeira da Silva J.A. (ed.): *Floriculture, ornamental and plant biotechnology: Advances and topical issues*. Isleworth: Global Science Books. V. **4**: 606–611.

Tebbitt M.C. 2005. *Begonias cultivation, identification, and natural history*. Portland: Timber Press.

LEAVES SPEAK VOLUMES: 3D LEAF ANATOMY AND THE DOMINANCE OF ANGIOSPERMS UNDER A LOW CO_2 WORLD

Guillaume THÉROUX-RANCOURT

University of Natural Resources and Life Sciences, Vienna, Austria

guillaume.theroux-rancourt@boku.ac.at

Plant leaves present a complex organization of tissues encompassing multiple leaf functions that are inherently 3D processes, like the diffusion of CO_2 in and water vapor out of the stomata. However, our understanding of the relationship between anatomy and leaf functions comes from a wealth of 2D cross sections, patiently embedded and imaged. Yet, imaging techniques such as high-resolution X-ray micro-computed tomography (microCT), used in plant biology for over a decade now, allow to image in 3D undisturbed plant samples and thus actually visualizing volumetric leaf anatomical traits that were previously estimated or conceptualized. Using microCT allowed us to measure anatomical traits related to the diffusion in the leaf airspace, such as geometric tortuosity, related to the organization of palisade and spongy mesophyll cells, path lengthening from the stomata, as well as the stomatal 'vapourshed', the airspace volume and adjacent cell surface most connected to a single stoma. More importantly, using a volume basis for mesophyll cell traits, like surface area of cells exposed to the airspace (SA_{mes}/V_{mes}), allow comparing leaves on a common ground, removing the bias introduced by leaf thickness and shape when expressing traits on a leaf area basis. This allowed us to compare leaves across the phylogeny and, as microCT allows visualizing stomata and veins on the same sample, investigate how leaf traits evolved in ferns, gymnosperms, and

angiosperms. Angiosperms and ferns have constructed leaves with more SA_{mes}/V_{mes} than gymnosperms, but angiosperms present the broadest range of values. Within all plant clades, higher SA_{mes}/V_{mes} is associated with smaller mesophyll cell diameter and in general with a higher photosynthetic capacity. By concomitantly improving vein and stomatal density with SA_{mes}/V_{mes}, angiosperms were able to explore a broad trait space of vein, stomatal, and mesophyll cell properties, and outperform ferns and gymnosperms that were confined to specific habitats due to anatomical limitations. Hence, the mesophyll surface area and cell diameter could be viewed as a link between the improvement of vein density and stomatal traits, which allowed angiosperms to conquer new habitats as atmospheric CO_2 declined since the end of the Cretaceous.

LEAVES SPEAK VOLUMES: DIFFERENCES IN 3D DIFFUSIONAL TRAITS BETWEEN SUN AND SHADE *VITIS* LEAVES REVEALED BY NON-INVASIVE microCT IMAGING

Guillaume THÉROUX-RANCOURT*, *Carlos HERRERA*, *Danny THOLEN

University of Natural Resources and Life Sciences Vienna, Austria

guillaume.theroux-rancourt@boku.ac.at

The diffusion of gases within leaves is inherently a 3D process, and leaf construction is considered to be optimized for diffusion under the specific growth environment under which the leaf developed. Yet there is limited empirical data linking actual leaf gas exchange to 3D and volumetric anatomical traits. Here, we provide one of the first characterizations of leaf anatomy using non-invasive high-resolution computed tomography (microCT) linked to gas-exchange measurements, allowing for the comparison of leaf-area-based to volumetric-based traits in *Vitis vinifera* cv. Cabernet Sauvignon, using shading as a way to modify leaf anatomy.

Shading decreased leaf thickness and the surface of mesophyll cells exposed to the intercellular airspace (SA_{mes}) per leaf area (SA_{mes}/A_{leaf}, commonly known as S_m), but had no effect on SA_{mes} per total mesophyll volume (SA_{mes}/V_{mes}), indicating that leaves tend to preserve the total amount of diffusive surface and volume of cell per single leaf. Light saturated photosynthesis per cell volume was not different between sun and shade leaves, and no relationship was observed between photosynthesis and SA_{mes}/V_{mes}, reemphasizing that diffusive surface is a conserved trait during leaf construction and allows for leaves to optimize CO_2 assimilation

under the condition they developed in. Yet, shade leaves build leaves with more volume of air connected to single stoma but with the same amount of cell surface, and thus have a lower diffusive surface per diffusive volume ratio, which could be limiting under high light condition but not under the conditions the shade leaves grown in.

Hence, 3D anatomy sheds new light on how shade leaves maximize light capture to optimize photosynthesis per cell volume, and thus potentially provide as much as sun exposed leaves.

REMOTE EVOLUTIONARY CONSTRAINT TO THE VASCULAR CAMBIUM

Alexander C. TIMONIN

Lomonosov Moscow State University, Moscow, Russia
timonin58@mail.ru

The vascular cambia have long been classified into nonstoried and storied ones according to the relative arrangement of the fusiform cambial initials (FCI), the basic constituents of this meristem (Larson, 1994). Characteristic arrangement of the FCIs in these cambia is usually attributed to different ways of the FCI multiplicative divisions therein (Larson, 1994; Iqbal, 1995). The difference of the FCI multiplicative divisions is the most notable, but all FCI divisions are different (Larson, 1994).

The FCI multiplicative divisions are longitudinal radial in the storied cambium to result in paired equal daughter FCIs which are as long as their mother FCI. The FCI multiplicative divisions are pseudotransverse (= oblique transverse) in the nonstoried cambium to give rise to paired daughter FCIs which are much shorter than their mother FCI. Therefore, both cells grow intrusively in length and form new primary pit fields without the phragmoplast machinery to become full-fledged FCIs. The FCI multiplicative divisions are highly redundant in the nonstoried cambia, and most generated FCIs are eliminated from the cambium in the shortest period of time (Larson, 1994; Włoch et al., 2009). The believable redundancy of the FCI multiplicative divisions in the storied cambia is still underexplored, but it seems to be insignificant (Larson, 1994) and the FCIs of this cambium do not expend resources to grow intrusively and to form new pit fields.

The FCI transformative divisions are pseudotransverse or longitudinal radial in the nonstoried cambia to result in short ray rudiment cell (Larson, 1994). Serial transverse divisions of the latter one and its derivatives (= 'segmentation') give rise

to the strand of the ray initials. The FCIs of the storied cambia directly function as the ray rudiment cells which start a set of transverse cell divisions to generate the strand of the ray initials.

The FCI additive divisions look alike in both cambia, but they differ in that the FCIs of the nonstoried cambia are much longer than their counterparts of the storied cambia. Therefore, the additive FCI divisions are more time- and resource-consuming in the nonstoried cambia. Furthermore, intracellular communication seems to be hampered in the longer cells.

Thereof, the nonstoried cambium functioning looks too complicated and expensive. This type of cambia has long been concluded to be more primitive (Iqbal, 1995), the conclusion being consistent with the character-mapping data. The nonstoried cambium is inherent in all soft-wooded plants and in most hard-wooded ones, whereas the storeid cambium is confined to more advanced dicotyledons.

However, the storied cambia are too narrowly distributed among the dicotyledons in comparison to other their advanced characters, though the cambium is an ancient inheritance of seed plants and it had much longer period of time to advance. Thence, cambium evolution is likely to have been highly constrained.

The evolutionary constraints are usually attributed nowadays to the lack of certain genes, or to gene pleiotropy, or to too numerous genes determining development of the character concerned (Hoffman 2014; Hansen, 2015). However, this is not the case. The FCIs of the nonstoried cambium are able to divide radially. Though these divisions are transformative (Larson, 1994), not multiplicative, they show that there is the machinery of FCI radial division and its determining genes in plants with the nonstoried cambium. That is why the evolutionary constraints of vascular cambium are unlikely to be gene-based. Schmalhausen's (1983) coordination concept seems to be more appropriate for seeking the constraint basics.

The structure of the vascular cambium matches its only function, *viz*. generating of efficient secondary conductive tissues. Therefore, the vascular cambium must have been evolving 'in coordination with' generated conductive tissues, mostly with the secondary wood, as it is a principal derivative of the cambium.

The vascular cambium arose in mid-Devonian Spermatophyta whose vesselless secondary wood functioned as water-conducting and supporting tissue combined. Both functions could be performed efficiently only if the tracheids are nonstoried and overlapped at certain degree (Kedrov, 2012). Nonstoried arrangement of the FCIs is the most efficient way to cause and maintain optimal overlapping of numerous tracheids, not the separate intrusive growing of the latter. The longer are the constituent tracheids, the more efficient is the vesselless wood. Optimal functioning of the vesselless wood causes the FCIs to be maximally long and properly overlapped. These attributes of the FCIs can only result from their pseudotransverse

multiplicative divisions followed by the intrusive growing of new arisen FCIs. The intrusive growing of the new FCIs inevitably unbalances preexisted overlapping of the contiguous FCIs. Enormous elimination of the arising FCIs seems to be a cost of restoring proper overlapping of the FCIs and their derivative tracheids. Anyway, the structure of the vesselless wood seems to constrain strongly vascular cambium advancing.

Most woody dicotyledons have gained the vessels, but they retain the tracheids in their woods to perform its supporting function or to perform its supporting function and to interconnect its vessels. Such tracheids maintain mostly lateral water conductance between the vessels, if any. However, their supporting functioning depends of their lengths and overlapping degree, thus preventing the FCIs from becoming much shorter and storey-arranged.

The origin of the directly interconnected vessels has preconditioned transformation of the (fiber) tracheids into the libriform fibers in the advanced secondary hard woods. The libriform fibers are able to grow intrusively to become much longer and overlapping than their mother FCIs. This ability makes unnecessary both considerable length of the FCIs and their nonstoried arrangement. The vascular cambium is resultantly able to change into the storied one. The origin of the direct interconnections of vessels in advanced woods is worth being considered to have removed the evolutionary constraint of the vascular cambium advancing.

The pseudotransverse multiplicative divisions of the FCIs do developmentally cause the nonstoried arrangement of these cells and their derivative tracheids in more primitive woods. Quite contrary, there is the nonstoried arrangement of the tracheids in both vesselles and hard secondary woods that evolutionarily maintains the nonstoried arrangement of the FCIs and pseudotransverse multiplicative divisions of the latter.

References

Hansen T.F. 2015. Evolutionary constraints. In: Losos J. (ed.): *Evolutionary biology – Oxford bibliographies*. DOI: 10.1093/obo/9780199941728-0061

Hoffman A. 2014. Evolutionary limits and constraints. In: Losos J.B. (ed.): *The Princeton Guide to evolution*. Princeton, Oxford: Princeton Univ. Press. P. 247–252.

Iqbal M. 1995. Structure and behaviour of vascular cambium and the mechanism and control of cambial growth. In: Iqbal M. (ed.): *The cambial derivatives* / Carlquist S., Cutler D.F., Fink S., Ozenda P., Roth I., Ziegler H. (eds.): Handbuch der Pflanzenanatomie. Berlin, Stuttgart: Gebrüder Borntraeger. Spez. Teil. Bd. 9. Teil 4. P. 1–67.

Kedrov G.B. 2012. Functioning wood. *Wulfenia* **19**: 57–95.

Larson P.R. 1994. *The vascular cambium: development and structure*. Berlin: Springer.

Schmalhausen I.I. 1983. *Paths and patterns of the evolutionary process*. Moscow: Nauka. [in Russian]

Włoch W., Jura-Morawiec J., Kojs P., Iqbal M., Krawczyszyn J. 2009. Does intrusive growth of fusiform initials really contribute to circumferential growth of vascular cambium? *Botany* **87**: 154–163.

SEASONAL GROWTH OF XYLEM OF *PINUS SYLVESTRIS* L. GROWING IN CONTRASTING HABITATS

Denis V. TISHIN*, *Nelly A. CHIZHIKOVA, Irina V. ZHURAVLEVA

Kazan Federal University, Kazan, Russia

dtishin@kpfu.ru

This project aims to assess the impact of climate and soil on the xylogenetic activity of pine growing under contrasting conditions at the southern border of the forest zone of the East European Plain. The objective of the work is to study the seasonal dynamics of radial growth of pine xylem cells in contrasting habitats of the Middle Volga region, Russia. The obtained data expand knowledge about possible changes in the productivity of pine trees and help to formulate a forecast of pine forest dynamics in response to climate change.

The studies were conducted at the territory of the Volga-Kama Reserve, Republic of Tatarstan, Russia (N 55.900879, E 48.82221). Two pine forest habitats were studied. These habitats differ in their opposing hydrothermal soil conditions, as a bog and a dry land.

Studies were conducted from May to October 2018. There were studied: microcores of tree-ring seasonal growth sampled by Trephor corer (Rossi et al., 2006); air temperature (at a height of 0.5, 2, and 10 m); temperature of soil (at a depth of 30 cm), temperature of trunks (at a height of 1.5 m on the north side of the trunk); sapflow (EMS51, Brno, Czech Republic). Parameters of forming annual rings were measured on thin transverse sections obtained using a GSL-1 microtome. The microslides were prepared by the procedure described in Gartner & Schweingruber (2013). The number and size of cells were evaluated using an image analysis system and the AxioVision 4.8.2 software package. Logistic model and the Gompertz model were chosen to analyze seasonal growth. Data processing, model building and statistical analysis was undertaken in R environment (R Core Team, 2012).

The age of the cored trees was 90–100 years. The habitats studied differed in the temperature regimes of air, soil and in the temperature of the wood. The bog is characterized by a wider range of fluctuations of the air, soil and wood temperatures, a more intense xylem sap flow in the afternoon hours, compared to the dry land.

The resulting number of tracheids per annual ring width is 6–7 in the bog and 14–15 in dry land habitat (Fig. 1). The dynamics of the seasonal growth of the wood layer showed a classic sigmoid shape (Fig. 2).

The first xylem cells start synchronously forming at both sites, on May 26, which corresponds to the sum effective temperatures 256 °C. The cell growth was culminated on June 15 in the bog, and on July 20 in dry land (Fig. 2). The length of seasonal growth period was 71 days in the bog, and 87 days in dry land. The cell growth in the bog finished on August 5 which is 16 days earlier than on dry

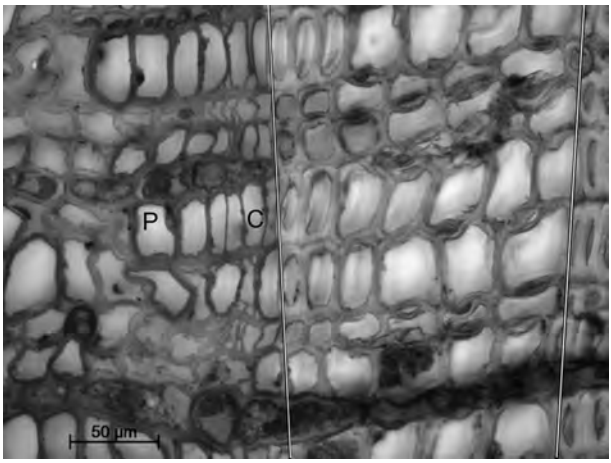

Fig. 1. Tracheids of annual ring formed in 2018.
Cross-section of microslide of tree #1 growing on a bog.
C – cambium, P – phloem.

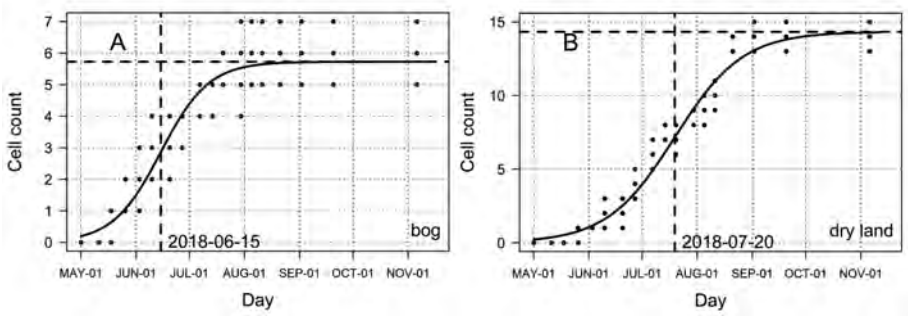

Fig. 2. Logistic model of increasing of xylem cells number in 2018.
A – bog habitat pines; B – dry land habitat pines.

land (August 21). The earlier stop of growth in the bog may be associated with a sharp rise of the air temperature and with a maximal drop of the groundwater level in early August.

The work was done with the financial support of the RFBR and the Government of the Republic of Tatarstan within the framework of the research project No. 18-44-160028.

References

Gartner H., Schweingruber F. 2013. *Microscopic preparation techniques for plant stem analysis*. Remagen: Kessel Publishing House.

Rossi S., Anfodillo T., Menardi R. 2006. Trephor: a new tool for sampling microcores from tree stems. *IAWA J.* **27**: 89–97.

R Core Team. 2017. *R: A language and environment for statistical computing*. Vienna: R Foundation for Statistical Computing. URL: http://www.R-project.org. [Computer program]

DID CONDUCTING TISSUES EVOLVE BY STERILIZATION OF SPOROGENOUS TISSUES?

Alesandru Mihail F. TOMESCU
Humboldt State University, Arcata, USA
mihai@humboldt.edu

Given the crucial role of conducting tissues in plant evolution and their importance in plant biology, their origin and evolution have seen surprisingly little scrutiny. Previous studies indicate that class III HD-ZIP genes (C3HDZ) are expressed in vascular tissue in all the tracheophytes tested and in sporogenous tissue in all the embryophytes (Floyd et al., 2006; Prigge, Clark, 2006; Vasco et al., 2016; Yip et al., 2016). These expression patterns suggest ancestral functions in sporangium or spore development for C3HDZs across the embryophytes, and in vascular tissue development, across the tracheophytes. Despite these two distinct ancestral functions, phylogenies of embryophyte C3HDZ genes indicate that the common ancestor of tracheophytes inherited a single C3HDZ from its bryophyte-grade precursors (Vasco et al., 2016), implying that this ancestral gene had roles in both reproductive and vascular development.

These data are relevant to questions on the origin of vascular tissues and the evolution of their developmental regulation. The Early Devonian euphyllophyte *Psilophyton*, one of the best characterized early tracheophytes (Banks et al., 1975; Noetinger et al., 2018), exhibits features relevant to these questions: conspicuous anatomical continuity between the tissues of sporangia and subtending vegetative axes, and direct contact between the vascular strand that enters the sporangium and the spore mass. The intimate association of these two specialized tissues suggests continuity of their precursor tissues, which entails shared identity and underlying regulation of these precursor tissues, thus, a certain degree of evolutionary-developmental relatedness of sporogenous and vascular tissues.

At the turn of the 20th century, F.O. Bower (1894, 1908) hypothesized that progressive sterilization was a central driver in the evolution of the complex vegetative organization of the sporophyte. In this context, the common regulatory and developmental origin of sporogenous and vascular tissues, which is suggested by genetic data and information from fossils, fits a scenario of vascular tissue evolution by sterilization of sporogenous tissue, which adds depth and specificity to Bower's progressive sterilization hypothesis: (1) an ancestral C3HDZ specifies pre-sporogenous identity, as part of radial tissue patterning, in the central region of the sporophyte; this region expands as a central strand, paralleling the evolution of sporophytes of larger sizes through delayed onset of reproductive development and meiosis, and extended vegetative growth; during differentiation of

the central strand, (2) delayed initiation of the regulatory program that completes reproductive development allows for (3) expression of an enhancer for vascular identity in the pre-sporogenous tissue in which sporogenous fate is repressed. A role for the ancestral tracheophyte C3HDZ in specifying pre-sporogenous tissue, at the origin of the pre-sporogenous-provascular pathway, could have originated in bryophytes: in mosses, C3HDZs are expressed in both sporangium and seta, as well as in gametophyte conducting tissues (Yip et al., 2016), and have demonstrated potential for the type of interaction with miR165/166 that regulates vascular development in tracheophytes (Floyd, Bowman, 2004; Hisanaga et al., 2014). This is also consistent with the apical growth hypothesis of sporophyte evolution (Tomescu et al., 2014), whereby a delayed onset of the reproductive developmental program allowed for apical growth leading to elongation and branching of the embryophyte sporophyte.

Testing the sterilization hypothesis entails finding putative mechanisms that could have (1) inhibited the reproductive program and (2) initiated vascular development in the precursor tissue specified by C3HDZs. Potential candidates can be identified based on current knowledge of the regulation of vascular development and of the transition to reproductive development. Putative inhibitors of the transition to the reproductive program include AGO-transposable element-siRNA interactions of the type documented by Hisanaga et al. (2014); KNOX 1-KNOX 2 mutually antagonistic interactions (e.g., Harrison, 2017); antagonists of PRC2 genes, which mediate the transition to the reproductive growth program (Tomescu et al., 2014); euAP2 genes (Floyd, Bowman, 2007); or cytokinin, known to induce vegetative axial elongation in the moss seta (Hisanaga et al., 2014). Putative promoters of provascular fate in the pre-sporogenous–provascular tissue include C3HDZ dosage regulation by miR165/166 and SHR, which specifies procambial identity and has been identified in all tracheophytes (Hisanaga et al., 2014).

All these putative developmental regulators and the entire sterilization hypothesis suggest multiple tests, including molecular genetic work, as well as detailed developmental studies, in seed-free tracheophytes and, especially, mosses that possess large sporophytes and well-developed conducting tissues in both the gametophytes and the sporophytes.

References

Banks H.P., Leclercq S., Hueber F.M. 1975. Anatomy and morphology of *Psilophyton dawsonii* sp. n. from the Late Lower Devonian of Quebec (Gaspe), and Ontario, Canada. *Palaeontogr. Am.* **8**: 75–127.

Bower F.O. 1894. Studies in the morphology of spore-producing members. Equisetineae and Lycopodineae. *Phil. Trans. R. Soc. London. B* **185**: 473–572.

Bower F.O. 1908. *Origin of a land flora*. London: Macmillan.

Floyd S.K., Bowman J.L. 2004. Ancient microRNA target sequences in plants. *Nature* **428**: 485–486.

Floyd S.K., Bowman J.L. 2007. The ancestral developmental tool kit of land plants. *Int. J. Plant Sci.* **168**: 1–35.

Floyd S.K., Zalewski C.S., Bowman J.L. 2006. Evolution of class III Homeodomain-leucine zipper genes in streptophytes. *Genetics* **173**: 373–388.

Harrison C.J. 2017. Development and genetics in the evolution of land plant body plans. *Phil. Trans. R. Soc. London. B* **372**: 20150490.

Hisanaga T., Miyashima S., Nakajima K. 2014. Small RNAs as positional signal for pattern formation. *Curr. Op. Plant Biol.* **21**: 37–42.

Noetinger S., Strayer S.L., Tomescu A.M.F. 2018. Spore wall ultrastructure and development in a basal euphyllophyte: *Psilophyton dawsonii* from the Lower Devonian of Quebec (Canada). *Am. J. Bot.* **105**: 1212–1223.

Prigge M.J., Clark S.E. 2006. Evolution of the class III HD-Zip gene family in land plants. *Evol. Dev.* **8**: 350–361.

Tomescu A.M.F., Wyatt S.E., Hasebe M., Rothwell G.W. 2014. Early evolution of the vascular plant body plan – the missing mechanisms. *Curr. Op. Plant Biol.* **17**: 126–136.

Vasco A., Smalls T.L., Graham S.W., Cooper E.D., Wong G.K.-S., Stevenson D.W., Moran R.C., Ambrose B.A. 2016. Challenging the paradigms of leaf evolution: class III HD-Zips in ferns and lycophytes. *New Phytol.* **212**: 745–758.

Yip H.K., Floyd S.K., Sakakibara K., Bowman J.L. 2016. Class III HD-Zip activity coordinates leaf development in *Physcomitrella patens*. *Dev. Biol.* **2016**: 14.

STRUCTURAL CHANGES IN THE BARK OF *SPIRAEA BEAUVERDIANA* (ROSACEAE) IN GOLOVNIN VOLCANO'S CALDERA (KUNASHIR ISLAND, SOUTH KURILES)

***Ekaterina O. VATSERIONOVA*, Anna V. KOPANINA, Inna I. VLASOVA**

Institute of Marine Geology and Geophysics,
Far Eastern Branch of Russian Academy of Sciences, Vladivostok, Russia
katya.vatserionova.85@mail.ru

This study is a continuation of our efforts to investigate the response of woody plants to the specific conditions of volcanic landscapes in the Kuril Islands. Our first results showed that the stem structure is the most significantly altered in solfatara fields, where the stress level of a majority of environmental factors is high (Kopanina, Yeremin, 2011; Kopanina, Vacerionova, 2015; Kopanina, 2016; Kopanina et al., 2017). In this paper we deal with the structural transformations of the stem of *Spiraea beauverdiana* Schneid. under the impact of the set of factors in solfatara fields of Golovnin volcano caldera. *Spiraea beauverdiana* is a shrub widespread in the Far East, Siberia, China and Japan.

Spiraea beauverdiana stems were sampled and fixed in 96% ethyl alcohol mixture for anatomical analysis according to Barykina et al. (2004). Samples

were collected as near as possible to gas vents of the Central Eastern (Tsentralnoe Vostochnoe) solfatara field of the Golovnin volcano caldera. All the gas vents and hot springs are situated along the shores of Lake Kipyashchee and underwater near the shore. Occasional *S. beauverdiana* specimens grow as compact shrubs not higher than 10–15 cm on volcano's rocky slope some 10–15 m away from the solfatara vents along the shore of the thermal lake Kipyashchee.

Analysis of the samples and computer processing of the images of stem microsections were performed under light microscope Axio Scope.A1, CarlZeiss using ZEN 2 lite software. 45 quantitative characters of bark tissues (aged 1 to 30 years) were analyzed. At least 30 measurements were taken for each character at each age. The sample mean and its confidence interval (at 95% confidence probability) were calculated for each character in each age group. Bark tissues were described based on the analytical approaches widely accepted in xylotomy and following current guidelines by the International Association of Wood Anatomists (IAWA) on bark anatomy of woody plants (Angyalossy et al., 2016).

By the end of the growing season, the bark of a 1-year-old stem is 122.8 ± 8.64 μm thick and comprises periderm, perivascular fibers, and phloem. All primary tissues (epidermis and cortex) outward the phellem are deformed, with only small fragments retained on the stem. The periderm in a 1-year-old stem is 28.5 ± 1.13 μm thick. The phellem is bilayered, homogenous, with cell walls thickened slightly and evenly. Cell lumina filled with dark substance. Radial cell rows distinct. Phellogen single-layered, phelloderm bilayered. Primary phloem is hardly discernible. Secondary phloem is 18.3 ± 0.80 μm thick. Sieve tubes in the cross-section vary in outlines, arranged in radial or tangential groups of 2 or 3, rarely solitary. Axial parenchyma diffuse. Rays uniseriate, up to 21 rays per 1 mm in the cross-section.

Stem diameter increases with age owing to annual increments of wood and bark. Bark thickness increases to 172.0 ± 6.18 μm in 2–3 years, but decreases again to 101.0 ± 3.96 μm at 4–5 years of age, apparently due to the epidermis and cortex being stripped off by the periderm formed underneath. The bark thickness triples by the age of 30 years, mainly owing to the expansion of the non-conducting phloem and periderm. Phellem thickness in a 1-year-old stem is 19.4 ± 0.66 μm, then it increases 5-fold in 13–15 years-old stems, and lose 65% its thickness by 30 years of age due to the shedding of outer layers. The same changes were observed also in phellem thickness: 28.5 ± 1.13 μm in a 1-year-old stem, 117.2 ± 9.40 μm in 13–15 years-old ones, 96.0 ± 5.26 μm at 30 years. However, the radial diameter of the phellem cells remains relatively stable throughout the ontogeny (6.8 ± 0.37 – 8.0 ± 0.58 μm), though the first layer of the phellem cells in 1-year-old stems are larger, 10.3 ± 0.58 μm. The tangential diameter of phellem cells increases with age (11.9 ± 1.14 μm at 1 year, 15.8 ± 1.03 μm at 30 years). Phellem thickness in abnormal periderm increases from 31.0 ± 1.05 μm (1 year) to 241.5 ± 13.62 μm (11–12 years) owing to a growing number of phellem cells per radial row.

By the age of 30, secondary phloem thickness increases 18-fold due to the non-conducting phloem: 18.3 ± 0.8 μm in 1-year-old vs. 303.0 ± 22.6 μm in 30-years-old stems. The total number of cells per radial row in the conducting phloem remains steady roughly until 10 years of age (4.2 ± 0.15 – 4.5 ± 0.29 cells). This parameters begins growing gradually since the age of 11 (5.5 ± 0.21 cell) to reach 8.0 ± 0.45 cells at 30 years. The number of sieve tubes per radial row is 2.7 ± 0.26 at 1 year, and doubles at the age of 25–30 years. Radial and tangential diameters of the sieve tubes also increase (4.2 ± 0.35 μm at 1 year, 6.5 ± 0.53 μm at 30 years and 7.0 ± 0.62 μm at 1 year, 9.0 ± 0.69 μm at 30 years, respectively). The total number of the phloem rays hardly changes with aging: 21.03 ± 0.70 per 1 mm at 1 year – 20.83 ± 1.09 rays per 1 mm at 30 years. The biseriate and triseriate rays appear at the age of 4–5 years.

30 years-old stem bark comprises the phloem and the periderm of the phellem, phellogen and phelloderm. The phellem is multilayered, homogenous; the phellem cells are tangentially elongated, with evenly thin cell walls and lumina filled with dark substance, its outer layers flake off. The phellogen is single-layered, the phelloderm is thin (1–3 cell layers). The secondary phloem comprises both the conducting and the non-conducting zones. Sieve tubes in the conducting phloem are rectangle-shaped and situated in radial rows. The axial parenchyma is diffuse. The 4-seriate rays which appear at the age of 30 years are markedly dilated in the non-conducting phloem. Some of them widen significantly, acquiring the shape of a triangle with the base towards the periphery. Phloem rays are uneven. Sclerification of rays absent or central ray cells sclerified. The sclerenchyma groups include fibers and fibrous sclereids. Fibers are tangentially elongated. Fibers and fibrous sclereids predominantly situated in the radial rows, and only few fibrous sclereids are very rare scattered.

The stems were found to contain areas of abnormal structure, where bark cell elements deviate from their typical growth and differentiation patterns, axial orientation and undergo sclerification and other transformations. Structurally abnormal areas occur locally in young stems, sometimes occupying up to 90% of the stem in the cross-section. Structural anomaly may affect both wood and bark, or be localized in only one tissue. The most frequent anomalies in 1-year-old stems are those of the periderm. The quantitative characteristics of the abnormal zone in the periderm are notably distinct in the cross-section from non-deformed stem tissues. The phellem in these areas is multilayered. Phellem cells are arranged irregularly, part of them forming straigth radial rows, while others deviate to form uneven rows. Part of the phellem becomes similar with the perennial bark phellem already in the first year of stem growth – flattened thin-walled cells arranged in radial rows. They have smaller dimensions than juvenile phellem cells. The shape of the cells in the cross-section varies from the typical square to polygonal or triangular. Abnormal phellem cells are thin-walled, but there are small groups of cells with notably thickened walls. The

phelloderm also deviates from its normal structure. It contains groups of small cells with thickened and sclerified walls. Some groups of its cells (3–5) are substantially larger than the others and are irregularly trapezoid or polygonal in the cross-section. Some cells, situated near sclerenchyma fibers, form brachysclereids. On the 2nd–3rd years of stem growth, the anomalies expand owing to high activity of the phellogen, which produces a thick periderm layer. The arrangement of cork cells may sometimes lose regularity. The sclerification process is initiated in the phelloderm.

Abnormal phloem occurs as limited areas where axial and ray parenchyma is represented by large sclerified cells and fibers. The tangential and radial dimensions of such cells are 2–3-fold larger than in normal tissue. Rays in such areas are heterocellular, dilated. Sieve tubes form under the pressure of the enlarged parenchyma there. Just a year later, these abnormal zones contain large solitary or clustered sclereids. The cross-section of areas with abnormal secondary phloem and secondary xylem show the cambium 'dips' into wood due to substantial dilatation and sclerification of the phloem parenchyma. The structure of bark and wood tissues in between the abnormal areas is not typical either. The cambium and phellogen in these areas 'repose or fading' (Kopanina et al., 2017; Vacerionova, Kopanina, 2016).

At the age of 11–12 years, the anomalies developing in the periderm get detached by phellogen initiation in deeper bark layers. As the stem grows, the anomalies affecting the deep-lying layers (secondary phloem and xylem) take the form of dips into wood. No anomalies are observed in the periderm at the age of 25–30 years.

The deviations from normal structure and anomalies detected in *S. beauverdiana* stems from the solfatara field of the Golovnin volcano caldera are noted for their specific structure. Cambium activity in abnormal zones is intermittent, resulting in uneven increment of secondary phloem and secondary xylem. It is therefore very hard to discern the boundaries of annual layers in the wood. The activity of stem axial meristems in solfatara fields is uneven: elevated in abnormal areas and inhibited in stem areas in between the anomalies.

The study was carried out with support from RFBR (initiative-based grant No. 15-04-04774) and within state order to the Institute of Marine Geology and Geophysics, Far East Branch Russian Academy of Sciences.

References

Angyalossy V., Pace M.R., Evert R.F., Marcati C.R., Oskolski A.A., Terrazas T., Kotina E., Lens F., Mazzoni-Viveiros S.C., Angeles G., Machado S.R., Crivellaro A., Rao K.S., Junikka L., Nikolaeva N., Baas P. 2016. IAWA list of microscopic bark features. *IAWA J.* **37**: 517–615.

Barykina R.P., Veselova T.D., Devyatov A.G., Dzhalilova Kh.Kh., Iljina G.M., Chubatova N.V. 2004. *Mannual on botanical microtechnique. Basic principles and methods*. Moscow: Moscow Univ. Press. [In Russian]

Kopanina A.V. 2016. Structural ecological and anatomical studies of woody plants in Sakhalin and Kurile Islands. *Bull. Bot. Gard.-Inst. FEB RAS.* **15**: 36–38. [In Russian]

Kopanina A.V., Vlasova I.I., Vacerionova E.O. 2017. Structural adaptation of woody plants to volcanic landscapes of the Kuril Islands. *Vestnik Far Eastern Branch Russ. Acad. Sci.* **1**: 88–96. [In Russian]

Kopanina A.V., Yeremin V.M. 2011. Structural features of the bark of some shrubs and dwarf-shrubs in the conditions of hydrothermal activity of volcano on the island of Kunashir (South Kuril Islands). In: Novitskaya L.L. (ed.): *Structural and functional deviations from normal growth and development of plants under the influence of environmental factors: Materials of international conference*. Petrozavodsk: Karelian Research Center RAS. P. 127–131.

Prozina M.N. 1960. *Botanical Microtechnique*. Moscow: Vyssh. Shkola Publ. [Iin Russian]

Kopanina A.V., Vacerionova E.O. 2015. The structural features of the annual *S. beauverdiana* stem under the influence of the gas-hydrotherm of Golovnin volcano (Kunashir Island, Kuril Islands). In: Levin B.W., Likhacheva O.N. (eds.): *Geodynamical Processes and Natural Hazards. Lessons of Neftegorsk: International scientific conference, Yuzhno-Sakhalinsk, May 26–30, 2015: Proceedings*. Vladivostok: Dalnauka. V. **2**. P. 379–382. [In Russian]

Vacerionova E.O., Kopanina A.V. 2016. Features of the structure of young stems of *Spiraea beauverdiana* in terms of the solfatar fields of Golovnin volcano caldera, Kunashir Island. *Bull. Bot. Gard.-Inst. FEB RAS.* **15**: 8–10. [In Russian]

STRUCTURE AND FUNCTION OF MULTIPLE ARCHESPORIUM IN *PAEONIA* SPECIES: WHY ONLY ONE EMBRYO SAC DEVELOPS IN THE OVULE?

Galina Yu. VINOGRADOVA*, *N.A. ZHINKINA

Komarov Botanical Institute of Russian Academy of Sciences, Saint Petersburg, Russia
vinogradova-galina@binran.ru

Differentiation of the female archesporium is one of the poorly understood questions in developmental biology of angiosperms.

The term ‘archesporium’ was suggested by Goebel (1880) to describe ‘initial cells of spore-formed tissue’ of earlier researchers, but he did not give their characteristics. As a result, the followers differently interpreted this term. Schnarf (1929) believed that the archesporium of angiosperms differentiated in the subdermal layer on the ovule top at the earliest developmental stage and that it could be one-celled or multi-celled, capable of dividing periclinally or not (he distinguished six types of archesporium on these criteria). The capability of periclinal division of the subdermal cells caused a wide terminological discussion. In this connection, Dahlgren (1928) suggested to distinguishing a ‘primary’ and ‘secondary’ (after parietal cells separation) archesporium. Sladkov & Grevtsova (1989) considered the archesporium as the cells producing spores only, regardless of their position under the epidermis or under the parietal tissue. Nikiticheva & Shamrov (1994)

think contrariwise that the archesporium includes subdermal cells of the central part of the primordium, which divide to form parietal and sporogenous cells (the archesporial cell transforms directly into sporogenous cell when a periclinal division is absent, although criteria of such transformation are hardly defined). Some authors compared the achesporium with a meristem, because all nucellus cells are uniform at the early developmental stage of some crassinucellate ovules, and sporogenous cells become visible within the nucellar tissue after several periclinal cell divisions in subdermal layer (Romanov, 1954; Lodkina, 1971). Solntseva (1965) believed that the term 'archesporium' was illegitimate for describing early stages of strawberry ovule development, because the central cells of the meristematic ovule primordium developed asynchronously resulting in a complex of cells on different development stages (megasporocytes, dyads, megaspore tetrads); the author identified this complex as 'reproductive tissue'.

Although the term 'archesporium' still remains unclarified, exploration of the regulation of cell differentiation in the ovule primordium and the signals controlling development of both sporophyte and gametophyte seems more actual nowadays.

Modern genetic and molecular data confirm a similarity of developmental processes in the ovule primordium and in the shoot apical meristem. Action of the gene *WUSCHEL* (*WUS*) is linked with genes *AINTEGUMENTA* (*ANT*), *BELL* (*BEL1*), *INNERNOOUTER* (*INO*) responsible for initiation of the integuments in *Arabidopsis* (Gross-Hardt et al., 2002; Sieber et al., 2004; Benchivenga et al., 2011); mutations *ant*, *bel1* and *ino* revealed developmental defects of both the integument and the gametophyte, suggesting a close relationship between the archesporium differentiation and integument initiation. Phytohormones participate in the ovule development, its cell proliferation and specification, the auxin and its PIN-FORMED (PIN) protein-mediated polar transport being the most studied (Benchivenga et al., 2011). In the ovule of *Arabidopsis*, PIN1 protein was detected at the earliest developmental stage and its locations suggest that auxin flows through the epidermal cells from funiculus toward the nucellus apex where its maximum concentration is revealed (Pagnussat et al., 2009). In a crassinucellate ovule, the PIN protein was found not only in the epidermis but in the inner cell layers surrounding a sporogenous cell except for the chalazal zone (Lora et al., 2017).

Data from immunocytochemistry confirm the meristematic characteristics of the ovule primordium cells. These data show the presence of some pectins, arabinogalactan and extensin in the cell wall of just differentiated archesporial cell located in the central position in the nucellus under several parietal layers. These substances are not visualized in the cell walls at the earlier stages of primordium development (Lora et al., 2017).

The multiple archesporium can differentiate and several cells acquire the sporogenous fate in some angiosperms with crassinucellate ovule. However, the

development of multiple archesporium remains a poorly studied problem. The genus *Paeonia* is characterized by the archespoium of this type and members of the genus provide a good model to study the question of its cell differentiation and specification.

In *Paeonia veitchii*, *P. mlokosewichii*, *P. peregrina*, *P. suffruticosa* the cells of the ovule primordium are uniform at the early stage. At this time, subdermal cells are divided periclinally and formed a parietal layer. Archesporial (sporogenous) cells become visible when 1–2 parietal layers formed above them and the inner integument has initiated. Sporogenous cells can also divide periclinally to result in a sporogenous complex of 10–16 cells similar in their size and morphology. This complex could be named multiple archesporium. During further development of the ovule, its lopsided growth is observed, which causes it to curve. This process is accompanied with an intensive growth of the inner integument and initiation of the outer integument. The periclinal divisions begin in the epidermis of the ovule apical part to form a nucellar cap. The nucellus is 2–3-layered in its lateral and basal parts.

When the inner integument elongates almost to the nucellus top, the archesporial cells transform to megasporocytes: they enlarge, their nuclei become bigger and can dislocate to the micropylar pole of cell, cell walls become thickened and the callose appears. These differentiation processes are asynchronous, the inner cells of the sporogenous complex outpace their peripheral counterparts. Therefore, 1–4 central cells enter the meiosis when the neighboring ones have just differentiated. It should be noted that the callose is found on the cell walls of only 1 (rarely 2–3) central megasporocyte of the complex. Perhaps, this feature determines a possibility of only one megasporocyte to develop further on to finish its meiosis and to result in a single megaspore tetrad and a single embryo sac.

The callose is known to be of importance for the megasporogenesis being an efficient filter for transport of different substances; it also participates in the isolation of the megasporocyte during the meiosis and development of functional megaspore (Rodkiewicz, 1970). However, we assume that the callose can also participate in the mechanism of 'lateral inhibition'. According to the hypothesis of lateral inhibition (Chevalier et al., 2011), all inner cells of the ovule primordium are archesporial and potentially capable to differentiate into the megasporocytes, but only one of them develops into the female gametophyte because emits signals to block sporogenous identity of adjacent nucellar cells. This hypothesis is based on the studies of genetic regulation of early ovule development in some plants. The genes *MULTIPLE ARCHESPORIAL CELL 1* (*MAC1*) in maize (Sheridan et al., 1996) and *MULTIPLE SPOROCYTE 1* (*MSP1*) in rice (Nonomura et al., 2003) were shown to activate signaling in the archesporial cell group, which inhibits most of them from differentiation into megasporocytes (mutation *mac1* and *msp1* are characterized by differentiation of multiple megaspore mother cells). Other molecular genetic mechanism of the regulation of the sporogenous cells differentiation are

signaling small RNAs associated with AGO9, the protein of ARGONAUTE family, which is found in subdermal layer (L1) of *Arabidopsis* ovule; failure of AGO9 leads to formation of supernumerary megasporocytes in nucellus (Olmedo-Monfil et al., 2010).

Based on these data, we suppose that cell(s) located in the central part of *Paeonia* ovule and advancing neighboring ones (that coordinates with callose deposition on its cell walls) emit(s) signals (perhaps small RNAs) when entering meiosis to inhibit further differentiation of its(their) adjacent cells. Only one (2–3 rarely) megaspore tetrad resultantly develops and one functional megaspore gives rise to one female gametophyte in the ovule. All other megasporocytes degenerate during ovule development to give room for growing embryo sac.

If suggested mechanisms really exist, what is the functional significance of multiple archesporium? Batygina (2014) proposed a concept of the system of organism reliability which is assumed by the existence of reserves (duplicated structures) in this system (such as the ovule). These reserves contain the morphogenetic potencies that are realized in case of death of the main structures. Sharing her views, we believe that the cells of the multiple archesporium in *Paeonia* are just such a reserve and if the main (central) megasporocyte is destructed, its peripheral cells can develop saving the reproductive potencial of the ovule.

References

Batygina T.B. 2014. *Biology of plant development. Life Symphony.* St. Petersburg: DEAN Press. [In Russian]

Benchivenga S., Colombo L., Masiero S. 2011. Cross talk between the sporophyte and the megagametophyte during ovule development. *Sex. Plant Reprod.* **24**: 113–121.

Chevalier É., Loubert-Hudon A., Zimmerman E.L., Matton D.P. 2011. Cell–cell communication and signaling pathways within the ovule: from its inception to fertilization. *New Phytol.* **192**: 13–28.

Dahlgren K.V.O. 1928. Hakenformige Leistenbildungen bei Synergiden. *Ber. Dtsch. Bot. Ges.* **46**: 434–443.

Goebel K. 1880. Beiträge zur vergleichenden Entwicklungsgeschichte der Sporangien. *Bot. Ztg*. **38**: 545–553.

Gross-Hardt R., Lenhard M., Laux T. 2002. WUSCHEL signaling functions in interregional communication during *Arabidopsis* ovule development. *Genes Dev.* **16**: 1129–1138.

Lodkina M.M. 1971. On the term «archesporium». In: Yakovlev M.P. et al. (eds.): *V All-Union session on the plant embryology*. Kishinev: Stiintsa. P. 101–102. [In Russian]

Lora J., Herrero M., Tucker M.R., Hormaza J.I. 2017. The transition from somatic to germline identity shows conserved and specialized features during angiosperm evolution. *New Phytol.* **216**: 495–509.

Nikiticheva Z.I., Shamrov I.I. 1994. Archesporium. In: Batygina T.B. (ed.): *Embryology of flowering plants. Terminology and concepts*. St. Petersburg: World and Family–95 Publ. V. **1**. P. 143–145.

Nonomura K., Miyoshi K., Eiguchi M., Suzuki T., Miyao A., Hirochika H., Kurata N. 2003. The *MSP1* gene is necessary to restrict the number of cells entering into male and female sporogenesis and to initiate anther wall formation in rice. *Plant Cell* **15**: 1728–1739.

Olmedo-Monfil V., Duran-Figueroa N., Arteaga-Vazquez M., Demesa-Arevalo E., Autran D., Grimanelli D., Slotkin R.K., Martienssen R.A., Vielle-Calzada J.P. 2010. Control of female gamete formation by a small RNA pathway in *Arabidopsis*. *Nature* **464**: 628–632.

Pagnussat G.C., Alandete-Saez M., Bowman J.L., Sundaresan V. 2009. Auxin-dependent patterning and gamete specification in the *Arabidopsis* female gametophyte. *Science* **324**:1684–1689.

Rodkiewicz B. 1970. Callose in cell walls during megasporogenesis in angiosperms. *Planta* **93**: 39–47.

Romanov I.D. 1954. Embryological study of cotton. I. Spore-formed cells development in the ovule. *Proc. Middle-Asian State Univ.* **53**: 3–58. [In Russian]

Schnarf K. 1929. *Embryologie der Angiospermen.* Berlin: Gebrüder Borntraeger.

Sheridan W.F., Avalkina N.A., Shamrov I.I., Batygina T.B., Golubovskaya I.N. 1996. The *mac1* gene: controlling the commitment to the meiotic pathway in maize. *Genetics* **142**: 1009–1020.

Sieber P., Gheyselink J., Gross-Hardt R., Laux T., Grossniklaus U., Schneitz K. 2004. Pattern formation during early ovule development in *Arabidopsis thaliana*. *Dev. Biol.* **273**: 321–324.

Sladkov A.N., Grevtsova N.A. 1989. On the formation of megasporanguim wall in angiosperms. *Byull. Moskovsk. Obshch. Isp. Prir. Otd. Biol.* **94**: 75–79. [In Russian]

Solntseva M.P. 1965. On the development of the multicellular archesporium in strawberry. In: Yakovlev M.P. (ed.): *Flower morphology and reproductive process of angiosperms*. Moscow; Leningrad: Nauka. P. 189–204. [In Russian]

STOMATAL CHARACTERISTICS OF SOME SPECIES OF *SOLIDAGO* L. (ASTERACEAE)

Yulia K. VINOGRADOVA

Tsitsin Main Botanical Garden of Russian Academy of Sciences,
Moscow, Russia
gbsad@mail.ru

The correlation between some micromorphological structures and the degree of plant adaptation to various ecological conditions in the secondary distribution range is proved for many species from various families: *Crataegus* spp. (Ganeva et al., 2009), *Amelanchier ovalis* Medic. (Ganeva, Uzunova, 2010), *Cornus* spp. (Klymenko, Klymenko, 2017), *Cydonia oblonga* Mill., *Pseudocydonia sinensis* (Thouin) C.K. Schneid. and *Chaenomeles japonica* (Thunb.) Lindl. ex Spach (Vinogradova et al., 2018).

The evaluation of the adaptive capacity of alien species is very important. It makes predictable their further expansion in the secondary distribution range. This is especially relevant for the genus *Solidago*, because several species of this genus have already 'escaped' from cultivation and started actively invading the natural communities. There are data only on the leaf structure of alien *S. canadensis* L., *S. gigantea* Ait. (= *S. serotinoides* Á. Löve et D. Löve) and *S. graminifolia* (L.) Salisb., as well as of the native *S. virgaurea* L. (Szymura, Wolsky, 2011;

Vinogradova, 2012). Data for other *Solidago* spp. concerned only macromorphology of these species (Weber, 2000). Our work is the first study of leaf anatomy for the most *Solidago* spp., growing in the Europe.

The purpose of this work is a comparative analysis of stomatal characteristics of cultivated *Solidago* species to assess the adaptive capabilities of these alien species.

The North American species of *Solidago* have been cultivated in European botanical gardens since the end of the XVII century. The most complete collection of this genus is represented in the oldest botanical garden of Europe – in Padua (Italy). The garden was established in 1545 by the decision of the Venetian Senate with the aim to growing 'medicinal herbs' for the Faculty of Medicine of the University of Padua. In 1997, it was included by UNESCO into the List of World Heritage Site as the 'prototype of all botanic gardens'. Alien *Solidago* species from the collection of the Padua botanical garden are the objects of the present study: *S. altissima* L.*, S. caesia* L., *S. canadensis, S. graminifolia, S. juncea* DC.*, S. latifolia* L.*, S. lepida* DC.*, S. rugosa* Mill.*, S. sempervirens* Michx.*, S. serotinoides*, and *S. uliginosa* Nutt. All these species naturally grow in North America and are established in Europe through an intentional introduction. Three of them (*S. altissima, S. canadensis* and *S. serotinoides*) are naturalized in Europe and invaded the natural phytocenoses. In recent years, *S. graminifolia* has actively been expanding its secondary distribution range. It is registered as an invasive plant in Poland and Belarus.

We collected leaves of each species at the beginning of June 2017. Three shoots of each species were selected for the analysis, and from each shoot three leaves were collected from the basal part of the stem (total 9 leaves per each species). The size of the leaf blades of the studied species decreases in the following order: *S. sempervirens* → *S. juncea* → *S. altissima* → *S. serotinoides* → *S. canadensis* → *S. rugosa* → *S. lepida* → *S. caesia* → *S. uliginosa* → *S. graminifolia*.

The method of lacquer replicas was used to study the characters of the stomatal complexes. The following micro-morphological characters were analyzed: the number of guard cells (n), the length of the polar axis of the stoma (l), the length of the equatorial diameter (d), the l/d ratio of the stomata, the stoma area ($s_{ellipse} = \pi(l/2)\cdot(d/2)$), the number of stomata in microscope field of view (n), the total transpiration area (= s·n). The relative transpiration area (relative transpiration index, I_{ot}) was calculated as the ratio of the total average transpiration area to the total area of the underside of the leaf blade, according the formula:

$$I_{ot} = \frac{\sum n\pi LD}{\sum S} 100\%.$$

Table. Quantitative characteristic of stomata in *Solidago* species

Taxon	Number of stomata (n)			Stoma area (s), μm²			Total area of all stomata (s·n), μm²
	min	max	$\bar{x} \pm S_x$	min	max	$\bar{x} \pm S_x$	$\bar{x}$
abaxial leaf surface							
S. altissima	5	7	6.2 ± 0.4	1877.7	4483.9	3175.3 ± 93.0	19687
S. juncea	4	6	4.6 ± 0.4	2336.2	3416.3	2881.7 ± 52.5	13256
S. serotinoides	3	6	4.6 ± 0.6	1884.0	3937.6	2531.4 ± 115.6	11644
S. sempervirens	2	3	2.4 ± 0.2	2904.5	4421.1	3768.3 ± 125.4	9044
S. lepida	4	8	6.4 ± 0.7	656.3	1846.3	1360.6 ± 49.3	8708
S. canadensis	3	6	4.6 ± 0.6	1243.4	2285.9	1664.0 ± 51.8	7654
S. graminifolia	4	6	5.6 ± 0.4	907.5	1727.0	1355.9 ± 41.0	7593
S. uliginosa	2	5	3.7 ± 0.5	1227.7	2747.5	1890.7 ± 79.1	6933
S. caesia	2	5	3.2 ± 0.4	791.3	2166.6	1670.7 ± 84.6	5290
S. rugosa	2	5	3.2 ± 0.5	483.6	1780.4	1004.0 ± 106.7	3213
adaxial leaf surface							
S. sempervirens	2	4	3.0 ± 0.4	2901.4	4396	3543.87 ± 86.4	10632
S. graminifolia	4	9	6.8 ± 0.9	904.3	1733.3	1382.2 ± 38.2	9399
S. juncea	2	4	3.4 ± 0.4	1808.6	3645.5	2681.9 ± 111.0	9119
S. lepida	4	9	6.0 ± 1.5	904.3	1805.5	1275.9 ± 52.0	7655
S. uliginosa	2	3	2.2 ± 0.2	1381.6	2210.6	1661.9 ± 70.1	3656
S. serotinoides	0	1	0.9 ± 0.5	1413.0	1752.1	1544.9 ± 104.9	1545
S. caesia	0	1	0.1 ± 0.3	1011.1	1570.0	1331.37 ± 166.4	133
S. altissima	None stoma was observed						
S. canadensis	None stoma was observed						
S. rugosa	None stoma was observed						

Note: min, max – minimal and maximal measured values; $\bar{x}$ – arithmetic mean; S_x – standard error of mean.

These seven characters were studied for both the upper and lower sides of the leave blade, and then their ratio was calculated. The stomatal complexes of 10 species are characterized by 21 quantitative traits. Morphology of the stomatal complexes was examined under the Keyence VHX-1000E digital microscope. The number of stomata in microscope field of view under ×1500 magnification was counted in 10 replicates. The size of stomata was calculated by measuring 50–100 stomata for each species.

Three species (*S. altissima, S. canadensis* and *S. rugosa*) have hypostomatous leaves; in other species, the leaves are amphistomatous. In most samples, the stomata are rounded: the l/d ratio is 1.2–1.4. Only in *S. serotinoides* on the upper side of the leaf blade, the stomata are elongated, and this ratio is 1.7.

Plants increase the total transpiration area by different methods. There are: 1) increasing of the size of stomata (*S. sempervirens, S. altissima, S. juncea*); 2) increasing of the number of stomata (*S. altissima*); 3) formation of amphistomatous leaves (*S. lepida, S. graminifolia*); 4) increasing of the leaf blade area, especially in rosette leaves (*S. sempervirens*, *S. juncea, S. uliginosa*); 5) increasing of the number of leaves per shoot (*S. lepida*); 6) increasing the number of shoots (*S. serotinoides, S. graminifolia*).

The size of the stomata is negatively correlated with their average number. For correct comparison of these species on their transpiration area, the relative transpiration index (I_{ot}) was calculated: the ratio of the average total transpiration area (the area of one stoma × number of stomata) to the total area of the abaxial leaf surface (in the field of the microscope view). According to this index I_{ot}, the studied species line up in the following order: *S. altissima* (50%), *S. juncea* (34%), *S. serotinoides* (29%), *S. sempervirens* (23%), *S. lepida* (22%), *S. canadensis* (19%), *S. graminifolia* (19%), *S. uliginosa* (18%), *S. caesia* (13%) and *S. rugosa* (8%). The relative transpiration area index is correlated quite well with the invasive activity of the studied taxa. *S. altissima* and *S. serotinoides*, which are widespread in the secondary distribution range, have the largest relative transpiration area (from 25 to 50%). *S. juncea*, which also has a high value of this indicator, starts invading the natural communities of Tver district. *Solidago sempervirens, S. lepida* and *S. uliginosa* have the index ranging from 15 to 25%. They are similar in this character with the invasive *S. canadensis* and *S. graminifolia*, they are able to adapt well to the environments of the Old World. Fortunately, they are less decorative and their presentation in the culture is not enough. This prevents (for now!) to the wide distribution of these species. *Solidago caesia* and *S. rugosa* are poorly adapted to the conditions of the new homeland ($I_{ot} < 15\%$), the latter also had short shoots with few leaves in the beds in the Padua Botanical Garden.

Thus, we can take into consideration the stomatal structure (in addition to other features) for predicting possible expansion of some alien species in their secondary distribution range. If an alien species has $I_{ot} > 25\%$, it is more likely to transform into an invasive taxon. Such species require stronger control measures of their dissemination.

The work was carried out in accordance with the Main Botanical Garden of Russian Academy of Sciences Research Project No. 118021490111-5 and partly supported by the Russian Foundation for Basic Research, grant No.18-04-00411.

References

Ganeva T., Uzunova K., Koleva D. 2009. Comparative leaf epidermis investigation in species of genus *Crataegus* L. (Rosaceae) from Bulgaria. *Feddes Repert.* **120**: 169–184.

Ganeva T., Uzunova K. 2010. Leaf epidermis structure in *Amelanchier ovalis* Medic. (Rosaceae). *Biotechnol. Eq.* **24**: 36–38.

Klymenko S., Klymenko O. 2017. Leaf anatomy of the members of *Cornaceae* family in conditions of the forest-steppe of Ukraine. *Ann. Romanian Soc. Cell Biol*. **21**: 28–39.

Szymura M., Wolsky K. 2011. Leaf epidermis traits as tools to identify *Solidago* L. taxa in Poland. *Acta Biol. Cracov*. Ser. Bot. **53**: 38–46.

Vinogradova Yu.K., Riabchenko A., Gorbunov Yu., Grygorieva O., Brindza J. 2018. Characteristic of stomata for *Cydonia oblonga* Mill., *Pseudocydonia sinensis* (Thouin) C.K. Schneid. and *Chaenomeles japonica* (Thunb.) Lindl. ex Spach species. *Ann. Romanian Soc. Cell Biol*. **22**: 18–25.

Vinogradova Yu.K. 2012. Biodiversity of *Solidago* L. taxa by micromorphological characters. In: *Biodiversity: problems of study and conservation. Proc. Internat. Sci. Conf. Tver*. P. 346–350. [In Russian]

Weber E. 2000. Biological flora of Central Europe: *Solidago altissima* L. *Flora* **195**: 123–134.

ROOT ANATOMY IN *ASPIDISTRA* (ASPARAGACEAE)

Nikolay A. VISLOBOKOV

Lomonosov Moscow State University, Moscow, Russia

n.vislobokov@gmail.com

Aspidistra is a genus of herbaceous rhizomatous monocot herbs inhabiting tropical forests of Southeast Asia. The genus currently comprises about 170 species with a few new species being described every year (Vislobokov et al., 2016, 2017, 2019). Species of *Aspidistra* show extremely high diversity of flower morphology. Features of flower are the most important for species recognition; however, many features of anatomy are still underexplored and are known in a few species only. This work is aimed to investigation of diversity and taxonomical significance of features of root anatomy in the genus *Aspidistra*.

The multilayered rhizodermis (velamen) was noted for genus *Aspidistra* as well as for order Asparagales in general (Mulay, Deshpande, 1959; Deshpande, 1960). The presence of velamen is typical of epiphytic plants (Lotova, 2007; Timonin, 2007), but it was also found in roots of some terrestrial plants (Mulay, Deshpande, 1959). Features of root anatomy may be taxonomically significant within the order Asparagales (Kauff et al., 2000).

Material for the present investigation was collected in nature as well as from plants cultivated in Botanical Garden München-Nymphenburg (Germany) and Tsitsin Main Botanical Garden of the Russian Academy of Sciences (Russia). The roots were fixed in 70% ethanol. Cross sections of the roots were made manually and stained with phloroglucinol in acid conditions (HCl). Root anatomy of 30 species of *Aspidistra* was investigated.

The roots of the investigated species of *Aspidistra* are covered with 1–4-layered velamen with persistent root hairs. The velamen is underlain by a single

layer of exodermis. Most species have 2–3-layered endodermis underlain by a single layer of pericycle cells (Fig. A, B). Sometimes, some cells of pericycle are with lignified walls.

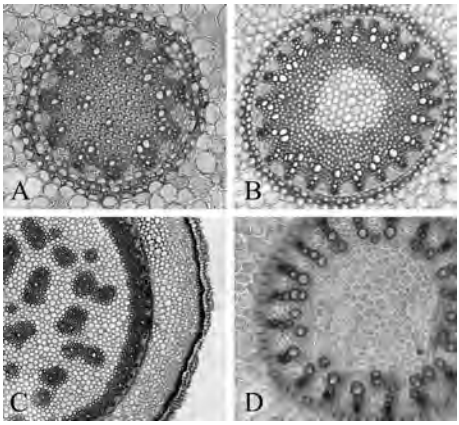

Figure. Root anatomy of *Aspidistra*:
central cylinder of root in *A. geastrum* (A), *A. lutea* (B),
A. locii (C) and *A. opaca* (D).

A few species (e.g. *A. atroviolacea*, *A. opaca*, *A. phanluongii*) have roots with only single distinguishable layer of the endodermis. However, central cylinder in root of each of these species shows low degree of lignification. The vascular bundle consists of separate arrays of lignified tissue of xylem (xylem parenchyma is not lignified) and has large central mass of parenchyma (Fig. D). The central cylinder of other species, which have multilayered endodermis, contains continuous massive of lignified tissue with small cylinder of parenchyma in the center (ring-like) or without parenchyma (round-like) (Fig. A, B). Probably, such differences of root anatomy are a result of higher or lower degree of general xeromorphism in different species and have no evolutionary significance.

Anatomy of central cylinder in *Aspidistra locii* is very different from all other investigated species. It looks the same as ring-like type described above but there are many separate additional vascular bundles in central part among parenchyma like in an atactostele (Fig. C). Such anatomical structure is unique among investigated species of *Aspidistra* and probably has a taxonomical significance. Notably, *A. locii* possesses very unusual flowers: the perianth has no lobes and looks like entire cupula-shaped structure with a little orifice at the top (Bogner, Arnautov, 2004). Also, flower vasculature of *A. locii* significantly differs from all other species of *Aspidistra* (Vislobokov, 2014).

The presence of multilayered rhizodermis (velamen) and endodermis, probably, is evolutionary significant character for Asparagales in general. However, the pattern of variation of other features of root anatomy (e.g. the volume of

sclerenchyma and parenchyma in central cylinder) probably corresponds to the degree of xeromorphism. Thus, the observed features developed convergently within Asparagales (Kauff et al., 2000; Li et al., 2003).

The study was funded by RFBR according to the research project No. 18-34-20135.

References

Bogner J., Arnautov N. 2004. *Aspidistra locii* (Convallariaceae), an unusual new species from Vietnam. *Willdenowia* **34**: 203–208.

Deshpande B.D. 1960. Velamen in terrestrial monocots. II. Ontogeny and morphology of velamen in the Amaryllidaceae with a discussion on the exodermis in Amaryllidaceae and the Liliaceae. *J. Indian Bot. Soc.* **39**: 593–600.

Kauff F., Rudall P.J., Conran J.G. 2000. Systematic root anatomy of Asparagales and other monocotyledons. *Plant Syst. Evol*. **223**: 139–154.

Li F., Tang S., Wang R., Li G. 2003. The anatomy study on nutritive organs of *Aspidistra* plants in China. *Guangxi Zhiwu* **24**: 239–242.

Lotova L.I. 2007. *Botany. Morphology and anatomy of higher plants*. Moscow: KomKniga.

Mulay B.N., Deshpande B.D. 1959. Velamen in terrestrial monocots. I. Ontogeny and morphology of velamen in the Liliaceae. *J. Indian Bot. Soc.* **38**: 383–390.

Timonin A.C. 2007. *Botany*. V. **3**. Higher plants. Moscow: Academia.

Vislobokov N.A. 2014. *Comparative morphology and reproductive biology of some Vietnamese species of genus* Aspidistra *(Asparagaceae s.l., Asparagales)*. PhD thesis.

Vislobokov N.A., Kuznetsov A.N., Kuznetsova S.P., Kuzmicheva E.A. 2019. *Aspidistra corniculata* (Asparagaceae, Nolinoideae), a new species from Vietnam. *Phytotaxa* **397**: 125–128.

Vislobokov N.A., Kuznetsov A.N., Kuznetsova S.P., Romanov M.S., Nuraliev M.S. 2017. *Aspidistra viridiflora* (Asparagaceae, Nolinoideae), a new species from Vietnam. *Phytotaxa* **313**: 203–209.

Vislobokov N.A., Nuraliev M.S., Kuznetsov A.N., Kuznetsova S.P. 2016. *Aspidistra globosa* (Asparagaceae, Nolinoideae), a new species with erect stem from southern Vietnam. *Phytotaxa* **282**: 46–52.

SPECIFIC MICROTECHNIQUES FOR BARK TISSUES OF WOODY PLANTS

Inna I. VLASOVA, Anna V. KOPANINA

Institute Marine Geology and Geophysics
Far Eastern Branch of Russian Academy of Sciences, Vladivostok, Russia
iiblasova@gmail.com

Preparation of woody plant samples for anatomical analysis of bark tissues is a pivotal process, on which the research result and its correct interpretation depend. A particularly challenging task is to collect and fix samples from poorly accessible locations in the Russian Far East under its extreme environmental conditions. The

samples fixed in the field must remain fit for manipulation for several months upon return from the expedition. Besides, the preparation for analysis of bark of woody plants of different ages growing under extreme environmental settings (fumarole fields, juvenile volcanic substrates, saline sea coasts) also requires a 'tailor-made' approach to techniques.

We describe the approaches and techniques specifically adjusted to the microscopic preparation of the bark – histologically and chemically complex object. Our procedures are based on the methods of microtechnique developed by Prozina (1960), Barykina et al. (2004), Wang et al. (2011).

The process of preparing a bark sample falls into several successive stages, each with its own specifics: sample collection and fixation in the field; storage of fixed samples; preparation of labware; preparation of reagents and stains; sample preparation for microtome sectioning; staining and mounting. We use maceration to enhance the anatomical details, and microchemical reactions to determine crystal qualities.

We either collect samples from three woody plant specimens or three entire individuals of low-growing plants depending on their growth-forms. The single specimen must often be dealt with due to extreme environments. The best quality microsections come from the samples collected in autumn, in the end of the growing season. This is the second half of September through October in Sakhalin, and October in the South Kurile Islands. Sampling during the summer entails difficulties at each stage. Slicing, staining, mounting on slides, moisture removal by filter paper cause thin sections to get foliated and fall apart. Even where thicker sections can be obtained, they provide little information due to poor differentiation of living tissues.

The specimens to be fixed are undamaged shoots of all ages or age classes in larger trees. Dwarf shrubs and prostrate plants are fixed as whole individuals or a partial clump. The time elapsed between sample collection and fixation must not exceed 1.5 days since living tissues die off. All samples are labeled at fixation. In the field, the samples prepared are placed in 2 to 10 liter plastic containers, which are tightened with thread seal tape along the rim, filled with 95% ethyl alcohol and securely closed. In the laboratory, stem samples are seasoned for at least two weeks in a mixture of 95% ethyl alcohol and glycerol (3:1).

High-quality microsections require pre-treatment of glassware, which is soaked in 0.5% solution of detergent or laundry soap, washed thoroughly in flowing water, and rinsed with distilled water. Glass slides are degreased with 1:1 mixture of ethanol and diethyl ether. At present, permanent slides are prepared using factory-degreased microscope slides and coverslips.

Tissue contrast is enhanced by the following reagents and stains: 0.5% Safranin; 0.5% Nile blue; 25%, 50%, 75%, 95% ethyl alcohol, carbol xylene, xylene; hydrochloric acid in alcohol, acetic acid in alcohol. Samples are prepared for microscopy using combined staining methods. We apply regressive staining (Prozina, 1960).

Safranin is prepared by dissolving 1 g dye in 100 ml 95% ethyl alcohol and then diluting to double volume with water: the result is 0.5% solution in 50% alcohol. Nile blue is prepared similarly.

To prepare 25% ethyl alcohol we take 26 ml of 96% alcohol, for 50% – 52 ml, for 75% – 78 ml, and add water to get 100 ml. Carbol xylene is prepared by dissolving 10–30 g phenol in 100 ml xylene. Alcohol mixture with hydrochloric and acetic acids is prepared by dissolving one drop of hydrochloric and 1–3 drops of acetic acid in 200 ml alcohol.

The stem age should be determined before bark sectioning. Young stem should be cross-sectioned with hand razor to count the number of wood annual rings in slides. After that, an area of the stem to be microtome-sectioned is chosen. The age of perennial stems and trunks is determined during fixation in the field by examining sawn sections under the stereoscope. It is not always possible to cut a small fragment bearing fully preserved bark, especially with periderm or outer bark, off a large chunk of a mature hardwood trunk (e.g., *Betula ermanii* Cham.). In this case, sections are made just of bark or a necessary fragment thereof. Sometimes, a small sample can be separated from the bole only after having macerated a fragment of the trunk. The size of stem or bark fragment for microtome sectioning should be 7 × 7 × 7 mm.

The samples are then processed with distilled water in weighting bottles for at least 12 hours to remove alcohol and glycerol, with the water replaced every 3 hours. The process was specially modified for Erman's (stone) birch, whose bark contains abundant scrlereid groups amid dilated phloem parenchyma as follows. Bark from the bole was macerated for up to 2.5–3 days, 15–20-years-old bark for 1–2 days and bark from young stems for up to 12 hours depending on the sample age and on the habitat conditions. Even one-year-old stems of dwarf shrubs need maceration of at least 1–1.5 days, if sampled from mud and magma volcanoes.

Stem or bark microsections 10–30 μm thick of pre-processed plant fragments are made with a sliding microtome Microm HM 430 with a freezing unit Microm KS 34 (Thermo Scientific). Sample hardness and age are taken into account when sectioning. Knife angles are adjusted for each individual sample, permitting quite thin, up to 5 μm, microsections to be made. Specimens finer than 7 × 7 × 7 μm can be sliced by removable blade cartridges inserted in a special sectioning device on the microtome; such blades are reusable, and the cutting angle of the knife should be decreased in this case. Hard tree trunk and large shrub bark samples containing large sclerified tissue areas (e.g., *Betula ermanii*, *B. platyphylla* Sukaczev) are sectioned with microtome knife made of high-duty tungsten carbide alloy at 10° tilt. The knife should be moistened with a wet brush at each run through the sample. The sections are brushed off the knife and placed in water-filled weighting bottles. The quality of the microsections needs to be checked in the process of sectioning by microscopic examination. Therefore, microsections should periodically be brushed off the knife directly onto the slide to be checked under the microscope.

The microsections are regressively stained with Safranin and Nile blue. The object is placed in a staining solution and kept therein until the section is fully stained. Next is the destaining procedure. 0.5% Safranin solution is added to the bottle containing the microsections and to soak for 30 sec. The samples are then washed out with the water until the water is no longer tinted pink. After that, the microsections immersed in aqueous solution are transferred to Petri dishes, where the most apt sections are selected and transferred to a microscope slide with a water drop using a preparation needle and dental spatula under a stereoscope or an illuminated stationary magnifying glass.

On-slide staining with Safranin is applied where sectioning is done by 'knife to slide' transfer. The period of exposure to dye is then reduced. Before applying the next dye, the slide is blotted dry by filter paper. Excess stain is then washed out with progressive concentrations of ethyl alcohol. Washing continues until the alcohol stops getting stained. Clearing can be improved by additional application of carbol xylene after exposure to 95% ethyl alcohol. The sections sometimes are insufficiently destained even after complete treatment with rising alcohol concentrations and carbol xylene. In this case, the sample should be very cautiously exposed to 95% alcohol with a minor addition of hydrochloric acid (one drop per 200 ml) to be instantly withdrawn and then washed with 95% alcohol and dehydrating solution. However, this method is only acceptable if detection of the oxalate crystals is unnecessary.

Destainig can also be done using acetic acid in alcohol. The sections thus processed should be dehydrated and cleared with carbol xylene, and residual moisture should be removed with xylene. The carbol xylene can sometimes deform the microsections if residual moisture has been removed too fast. The microsections should be immediately treated with pure xylene to avoid this artifact.

The microsections should then be embedded in a drop of mounting medium under coverslip. Each slide with differently oriented microsections should be labeled and analyzed under AxioScop A1 microscope (Zeiss) with ZEN 2 software after a fortnight.

To enhance visibility of the structure of conducting elements, the plant material needs to be macerated. The maceration technique follows Wang et al. (2011). Small bark or stem fragments are placed in weighting bottles in distilled water – glacial acetic – 33% hydrogen peroxide (4:5:1 v/v) mixture prepared directly before use. The bottles are kept tightly closed at 50 °C for 2.5–3 days for the bole of *Betula ermanii*, but this period of time should be extended for macerating bole samples from volcanic fumarole fields which contain large amounts of lignified and sclerified elements. Otherwise this period of time should be reduced to 1 day for annual stems of this species sampled from normal conditions, and to 2 days for those from aggressive environments (volcanic landscapes). Thus macerated specimens are washed out with distilled water until the smell of acetic acid is gone. To enhance separation of individual elements, the macerated material is crushed inside the bottle

by means of magnetic stirrer and centrifuge at 1000–1500 RPM. A small amount of Safranin should be added to preparations to contrast staining of the lignified elements. Only temporary preparations are available for analyzing, since the permanent ones are impossible to be done from the macerated bark elements.

Calcium oxalate crystals should be distinguished from other crystals occurring in the tissues by means of microchemistry methods described by Prozina (1960).

References

Barykina R.P., Veselova T.D., Deviatov A.G., Dzhalilova Kh.Kh., Iljina G.M., Chubatova N.V. 2004. *Manual on botanical microtechnique. Basic principles and methods*. Moscow: Moscow Univ. Press. [In Russian]

Prozina M.N. 1960. *Botanical microtechnique.* Moscow: Vysshaya Shkola. [In Russian]

Wang G., Shi S.Q., Wang J., Yu Y., Cao S., Cheng H. 2011. Tensile properties of four types of individual cellulosic fibers. *Wood & Fiber Sci*. **43**: 353–364.

STRUCTURAL BASES OF C_4 PHOTOSYNTHESIS

Elena V. VOZNESENSKAYA[1], ***Nuria K. KOTEYEVA***[1], ***Gerald E. EDWARDS***[2]

[1] Komarov Botanical Institute of Russian Academy of Sciences, Saint Petersburg, Russia
[2] Washington State University, Pullman, USA
elena-voz@mail.ru

The main feature of photosynthesis in all plants is the fixation of CO_2 into organic matter *via* Rubisco. A constraint on the process in terrestrial plants is in conditions where CO_2 becomes limiting due to high temperature, drought, or soil salinity. In response to CO_2 limitations, some plants evolved mechanisms to concentrate CO_2 around Rubisco through a C_4 cycle. This requires spatial separation of fixation of atmospheric CO_2 into C_4 acids, and the donation of CO_2 from C_4 acids *via* decarboxylases to Rubisco. For today, C_4 plants have been found in 19 families of terrestrial plants, with the largest number of species appearing in grasses, sedges and chenopods. For many years after the discovery of C_4 in terrestrial species, this was exclusively associated with Kranz anatomy. C_4 plants with this anatomy have two structurally and biochemically specialized photosynthetic cell types functioning coordinately in carbon assimilation. C_4 photosynthesis has evolved independently many times with great diversity in forms of Kranz anatomy and biochemistry of the C_4 cycle. Molecular phylogeny estimates that C_4 photosynthesis has been evolved independently at least 60 times between terrestrial plants, and the most of separate structural types show the independent origin of those branches in corresponding taxa. After the discovery of C_4 photosynthesis its functioning was exclusively associated with the presence of the specific structure of assimilating organs, so called

Kranz anatomy. In this case two steps of C_4 photosynthesis (fixation of CO_2 on PEPC and its transportation to Calvin cycle) take place in two different types of chlorenchyma cells (palisade parenchyma and chlorenchymatous bundle sheath cells) with specific distribution of photosynthetic enzymes between cells. Currently, 25 main structural types of Kranz anatomy are distinguished (9 types in grasses, 4 in sedges and 12 in dicots), with the main differences in the distribution of two characteristic chlorenchyma layers in relation to vascular bundles and other leaf tissues. Besides, tree biochemical subtypes were characterized among C_4 plants based on the main decarboxylating enzyme in bundle sheath cells (NADP-ME, NAD-ME, PEP-CK).

Besides well-known C_4 species with Kranz leaf anatomy, at the beginning of the 21st century, species having unique leaf structure were discovered in the family Chenopodiaceae. In these species, the entire C_4 photosynthesis occurs inside individual chlorenchyma cells *via* the formation of two spatially separated domains. In representatives of the monotypic genus *Borszczowia* two structural and biochemical domains are formed at the opposite ends of elongated chlorenchyma cells, while in species of another genus *Bienertia* they are confined to the peripheral cytoplasm and the central spherical cytoplasmic compartment surrounded by the vacuole and containing numerous chloroplasts and mitochondria. There is a strong enzyme compartmentation between two cytoplasmic domains inside one cell in single-celled variant of C_4, while in species with Kranz type of anatomy the sharing of biochemical functions exists between two separate cell types.

Despite high structural diversity in C_4 plants, there are only three ultrastructural subtypes differed in the degree of grana development in chloroplasts of bundle sheath and mesophyll cells and the structure of bundle sheath mitochondria. Structural differences have strong correlation with their affiliation to three biochemical subgroups of C_4 plants and can be used as diagnostic feature. Thus, in NADP-ME species, bundle sheath cells contain chloroplasts with reduced grana, while mesophyll cells have chloroplasts with well-developed grana. In contrast, in NAD-ME species grana reduction is observed in mesophyll chloroplasts with intensively developed grana in bundle sheath chloroplasts. This subtype is also characterized by the presence of numerous, specialized mitochondria in bundle sheath cells. The third biochemical subtype was found in grasses, with PEP-CK as a main decarboxylating enzyme and in species of this group, the degree of grana development in chloroplasts is nearly equal in both chlorenchyma cells. Species with single-celled C_4 photosynthesis belong to NAD-ME biochemical subtype and show the presence of chloroplast dimorphism, characteristic of this biochemical subtype with concentration of specific mitochondria in the part of the cell which is analogous to bundle sheath cells.

In general, C_4 photosynthesis represents an amazing mechanism allowing for plants to adapt to the desert and semi-desert environments. C_4 plants have higher photosynthetic rates and water use efficiency resulting in higher yields. The com-

prehensive study of plants with C_4 photosynthesis will allow to expanding our ideas about the possible ways of the establishment of the structural and functional diversity in photosynthetic types in close relation to ecological growing conditions. This will take us closer to the understanding of the C_4 pathway evolution, its regulation and development, and how it can be manipulated.

MULTI-SEASONAL VS. INTRA-SEASONAL STRUCTURAL CHANGES IN GRAPEVINE: A COMPLEX STRESS RESPONSE

***S. WOLBERG*[1,2], *Sarel MUNITZ*[1], *T. ROSENZWEIG*[2], *Yishai NETZER*[1], *Ilana SHTEIN*[1]**

[1] Eastern R&D Center, Ariel, Israel
[2] Ariel University, Ariel, Israel
ilanash@ariel.ac.il

Grapevine (*Vitis vinifera*) is an agriculturally and economically important crop, which serves as a model plant for ecophysiological responses to water stress (Lovisolo et al., 2010). The grapevine water status has fundamental implications on growth, yield and wine quality: while moderate water stress is needed in order to achieve premium wine quality, high stress is harmful and may cause permanent damage to the plants. Water availability influences the water status, among other things, by changing the hydraulic anatomy of the grapevine (Munitz et al., 2016, 2018). Hydraulic anatomy influences both water flow and the mechanical stability. Thus, wide xylem vessel diameter significantly increases the hydraulic conductivity, but also increases vessel vulnerability towards embolism and cavitation, and makes the vessels mechanically weaker (Shtein et al., 2011). In addition, in the structure-function context of plant-water relations, the cell wall architecture and composition is extremely important. The cell wall composition influences the cell growth, water adsorption and biomechanical properties of the plant (Marom et al., 2017; Shtein et al., 2017, 2018). Cell walls of plants are complex organs, comprised of load bearing cellulose microfibrils, embedded in a soft matrix of pectins, hemicelluloses and various glycoproteins. Each matrix component group is complex in its own right, and undergoes diverse further modifications. In current study, our first goal was to investigate the multi-annual influence of different water availability on the hydraulic anatomy of mature grapevines, and secondly to explore the effects of the intra-seasonal water availability on morphological changes, hydraulic anatomy and cell wall composition.

The research was conducted on a commercial vineyard planted with red wine grapevines (*Vitis vinifera* cv. 'Cabernet Sauvignon'), planted in 2008. Irrigation

treatments began in 2014, thus the plants have endured a multi-seasonal stress. Three irrigation treatments were investigated: 1) Non-stressed control: intensively irrigated grapevines grown in drainage lysimeters, with a surplus of water supply (irrigation every hour). 2) Mild water stress treatment: irrigation was initiated with the beginning of budbreak. 3) Severe water stress treatment: irrigation began only when the values of stem water potential reached 1.2 MPa. Throughout the growing seasons of 2016–2018, following vegetative and physiological parameters were measured: leaf area index (LAI), stem water potential and gas exchange. In addition, the parameters of stem xylem anatomy were measured. For the investigation of intra-seasonal dynamic stress, leaf petioles were sampled on three dates during the season, and were analyzed for morphology, hydraulic anatomy, histology and immunohistochemical investigation of pectic cell wall components. The leaf petioles, being a continuously produced organ, represent the recent status of the grapevine, while the multi-seasonally functional stem xylem represents the perennial, long-term status.

The non-stressed controls maintained an improved water status and vigorous canopy throughout the season, while in both the mild and severe stress treatments a steep decline of physiological parameters was already observed in the middle of the season. In the perennial parts of the plant (the stems) our findings indicate a reduction of hydraulic anatomical characteristics as a consequence of drought stress. Surprisingly, though the stem water potential at this point was not low, in petioles severe drought stress lead to diverse morphological and anatomical changes already at the beginning of the season. These changes included: shorter petioles, reduction of vessel diameter and increased vessel density, and various changes in the cell wall composition. The cell wall compositional changes indicated increased level of stiffened cell wall components (more lignin and increase in pectic homogalacturonans methyl-esterification). As the season progressed, similar changes occurred in all of the treatments regardless of water availability, likely as a response to the seasonal environmental changes. The seasonal changes in methyl-esterification of homogalacturonans are especially interesting, as they suggest that enzymatic activity takes part in grapevine stress response, and opens new questions about the mechanical, protective role of pectic homogalacturonans in particular and cell walls in general.

Apparently, hydraulic structural changes in the stem constitute the structural memory of the vine, and they influence the plant structure and function already at the beginning of the next season. However, intra-seasonally, the structure becomes independent of the water status. Temperature is a strong determinator of the plant structure (Shtein et al., 2011; Zait et al., 2018), and we assume it is the main intra-seasonal influencing factor in current study. This research is innovative as it demonstrates how perennial water stress influences mature field grown grapevines and indicates, for the first time, intra-seasonal trends of structural response. Future integration of the practical and theoretical aspects of current research may expose

additional water stress adaptations in grapevines, and may hopefully facilitate the development of cell wall constituents as indicators of water stress in real time in the vineyard.

References

Lovisolo C., Perrone I., Carra A., Ferrandino A., Flexas J., Medrano H., Schubert A. 2010. Drought-induced changes in development and function of grapevine (*Vitis* spp.) organs and in their hydraulic and non-hydraulic interactions at the whole-plant level: a physiological and molecular update. *Funct. Plant Biol*. **37**: 98–116.

Marom Z., Shtein I., Bar-On B. 2017. Stomatal opening: the role of cell-wall mechanical anisotropy and its analytical relations to the bio-composite characteristics. *Front. Plant Sci*. **8**: 2061.

Munitz S., Netzer Y., Schwartz A. 2016. Sustained and regulated deficit irrigation of field-grown Merlot grapevines. *Aust. J. Grape and Wine Res*. **23**: 1–8.

Munitz S., Netzer Y., Shtein I., Schwartz A. 2018. Water availability dynamics have long-term effects on mature stem structure in *Vitis vinifera*. *Am. J. Bot*. **105**: 1443–1452.

Shtein I., Bar-On B., Popper Z.A. 2018. Plant and algal structure: from cell walls to biomechanical function. *Physiol. Plant*. **164**: 56–66.

Shtein I., Meir S., Riov J., Philosoph-Hadas S. 2011. Interconnection of seasonal temperature, vascular traits, leaf anatomy and hydraulic performance in cut *Dodonaea* "Dana" branches. *Postharvest Biol. Technol*. **61**: 184–192.

Shtein I., Shelef Y., Marom Z., Zelinger E., Schwartz A., Popper Z.A., Bar-On B., Harpaz-Saad S. 2017. Stomatal cell wall composition and cellulose crystallinity: distinctive structural patterns are associated with different phylogenetic groups. *Ann. Bot*. **119**: 1021–1033.

Zait Y., Shtein I., Schwartz A. 2018. Long-term acclimation to drought, salinity and temperature in the thermophilic tree *Ziziphus spina-christi*: revealing different trade offs between mesophyll and stomatal conductance. *Tree Physiol*. DOI: 10.1093/treephys/tpy133

ANATOMY OF LEAVES AND SEED CONES OF *DACRYCARPUS* (ENDLICHER) DE LAUBENFELS (PODOCARPACEAE) FROM THE MIOCENE OF SOUTHERN CHINA

***Xin-Kai WU*[1], *Natalia V. GORDENKO*[2], *Tatiana M. KODRUL*[3], *Natalia E. ZAVIALOVA*[2], *Natalia P. MASLOVA*[2], *Xiao-Yan LIU*[1], *Cheng QUAN*[4], *Jian-Hua JIN*[1]**

[1] Sun Yat-sen University, Guangzhou, China
[2] Borissiak Paleontological Institute of Russian Academy of Sciences, Moscow, Russia
[3] Geological Institute of Russian Academy of Sciences, Moscow, Russia
[4] Chang'an University, Xi'an, China
kodrul@mail.ru

The genus *Dacrycarpus* (Endlicher) de Laubenfels (Podocarpaceae) with nine extant species is discontinuously distributed in tropical mountain rainfor-

ests of the southwestern Pacific region, ranging from New Zealand and Fiji to northern Myanmar and southernmost China, with the highest diversity in New Guinea (de Laubenfels, 1988; Eckenwalder, 2009; Farjon, 2010). However, fossil record indicates that *Dacrycarpus* was widely distributed in the Cenozoic floras of Australasia and Patagonia. The earliest *Dacrycarpus* megafossils so far found are from the Eocene of Chile, Argentina and Australia (Florin, 1940; Greenwood, 1987; Wells, Hill, 1989; Hill, Carpenter, 1991; Wilf, 2012). By the Oligocene, the distribution of *Dacrycarpus* was mainly limited to southeastern Australia and New Zealand (Cookson, Pike, 1953; Wells, Hill, 1989; Hill, Carpenter, 1991). The latest *Dacrycarpus* fossils are from the Miocene of Australia and New Zealand (Hill, Whang, 2000; Pole, 2007; Lewis, Drinnan, 2013). So far, however, no megafossil record has been reported from the Northern Hemisphere resulting in an incomplete understanding of the origin of the modern distribution pattern and phytogeographic history of *Dacrycarpus*.

The first Northern Hemisphere megafossils of *Dacrycarpus* represented by three-dimensionally preserved foliage, ovuliferous cones and pollen cones with *in-situ* pollen were obtained from the Miocene of the Guiping Basin, Guangxi Province, southern China. The typical features of these fossils are spirally inserted, decurrent on the axis, and dimorphic foliage leaves as well as the ovuliferous structures with a warty receptacle and a terminal seed cone containing one inverted ovule. An incompletely preserved pollen cone is subtended by a short stalk with a few bifacially flattened leaves. Microsporophylls are helically arranged, each bears two globular sporangia. Pollen grains have a prominent corpus and three sacci.

The new *Dacrycarpus* species possesses strongly dimorphic foliage leaves comprised of bifacially flattened 'adult' leaves on long shoots and bilaterally flattened 'juvenile' leaves on feather-like short shoots. The leaves on the short shoots generally show a complete transition from bifacial to bilateral, and the leaves on the fertile shoots often display intermediate stages of this transition. Bilaterally flattened leaves are distichous, falcate, straight to slightly apically incurved, and strongly keeled with a single prominently raised vein. The leaves are amphistomatic, with two longitudinal bands of stomata which run from the leaf base to the apex on each surface. Each band contains one to five rows of stomata (typically two or three). Stomatal axes are parallel to the midvein. Florin rings are prominent, sunken below the leaf surface. Stomatal complexes are paratetracytic, elliptical, with four to six subsidiary cells (mostly four). The leaf cross section is ellipsoidal to rhomboidal. The epidermis is covered by a cuticle. Hypodermis fibres are 3–5 μm in diameter. The vascular bundle is single, 30 μm wide. Tracheids of the vascular bundle possess scalariform and reticulate thickenings. A transfusion tissue is developed above the vascular bundle; it consists of reticulate transfusion tracheids up to 20 μm in diameter. A resin canal is up to 100 μm in diameter. Only a palisade mesophyll was occasionally observed in the bilateral leaves.

Bifacial leaves are small, scale-like, triangular to linear-lanceolate or sometimes slightly falcated, loosely to nearly appressed, strongly keeled, deployed on long shoots as well as at the base of short shoots and fertile structures. The leaf tip is incurved and the margin is entire. The leaves are amphistomatic; the stomata are confined to two more or less continuous bands on each surface, those of the adaxial surface are narrower and shorter than on the abaxial surface. The stomatal zone is one to four rows wide; the rows are parallel to the leaf longitudinal axis and separated typically by one to four epidermal cells. Florin rings are prominent. The stomata are paratetracytic, elliptical, and with four to six subsidiary cells (mostly four). Epidermal cells are longitudinally oriented, with granular periclinal walls and smooth anticlinal walls. Leaf cross-section is triangular to rhomboidal. The epidermis is covered by a cuticle. The hypodermis consists of fibers 3–5 μm in diameter. The vascular bundle is single, central, collateral, about 50–70 μm wide. Tracheids of the vascular bundle are with scalariform and reticulate thickenings. Transfusion tissue is developed above the vascular bundle and gradually replaces the tracheids of the vascular bundle laterally. Transfusion tissue consists of reticulate transfusion tracheids up to 30 μm in diameter. A large resin canal (60–90 μm in the diameter) is present below the vascular bundle. Mesophyll is distinctly dimorphic only at the leaf base (an abaxial palisade mesophyll and adaxial spongy mesophyll are present). More distally, only the palisade mesophyll is developed. Abundant epiphytic and endophytic micromycetes were found on the leaves of the new *Dacrycarpus* species.

The leaf anatomical features of the new fossil *Dacrycarpus* are similar to those of extant species but there are some differences. The hypodermis in *D. imbricatus* (Blume) de Laubenfels is also developed in all leaf morphotypes but it possesses stronger fibres (up to 20 μm in the diameter). Resin canals in *D. imbricatus* are smaller (up to 50 μm in the diameter). In bifacial leaves, the palisade tissue is developed only on their adaxial side; the spongy tissue is abaxial, whereas the leaves in the fossil species possess adaxial spongy tissue and abaxial palisade tissue. In bilateral leaves of *D. imbricatus* only the palisade tissue is developed, as in the fossil species. The fossil species differs from the extant *D. dacrydioides* (A. Rich.) de Laubenfels by possessing fibres in all types of leaves, whereas in *D. dacrydioides* the fibers are present only in the leaves of long shoots. Moreover, the adaxial palisade tissue in *D. dacrydioides* is developed only in the leaves of the short shoots (Dörken, Parsons, 2016), but in the new fossil species it occurs in all types of leaves.

Ovuliferous shoots arise from the leafy long shoots and are composed of involucral leaves, a podocarpium and a seed cone. The involucral leaves are spreading or clasping the basal half of the podocarpium. Warty, bumpy podocarpia are 2.3–4.1 mm long, composed of at least two expanded, fused leaves. The seed cones are terminal, oval-shaped, obovate and deployed singly or doubly on a podocarpium, consisting of an ovule, epimatium and fertile bract. The inverted ovule is surrounded

by the epimatium being partly fused with the fertile bract, forming a crest along one side of the epimatium that ends in a sideways beak. Computer tomography (CT) showed that the seed cone consists of nucellus remains and fertile bract fused to the epimatium, which in turn is fused to the seed coat (testa). The epimatium contains numerous resin canals filled by massive amber. The testa consists of a thick mesotesta layer and a thin endotesta layer. The exotesta is reduced, as previously shown for the *Dacrycarpus* seed cones by Melikian & Bobrov (2000).

Apparently, new fossil species represents the most complete and best-preserved megafossil remains of *Dacrycarpus* known to-date. Of all the extant species, this fossil species shows a close similarity in morphological and anatomical characters to *D. imbricatus*, the only species of *Dacrycarpus* presented today in China.

The research was supported by the National Natural Science Foundation of China (grants Nos. 41820104002, 41661134049, 41210001), the Russian Foundation for Basic Research (grant No. 19-04-00046, to N.V. Gordenko, N.P. Maslova, in part to T.M. Kodrul), and the State project No. 0135-2019-0044 (Geological Institute, RAS, to T.M. Kodrul).

References

Cookson I.C., Pike K.M. 1953. The Tertiary occurrence and distribution of *Podocarpus* (section *Dacrycarpus*) in Australia and Tasmania. *Aust. J. Bot.* **1**: 71–82.

de Laubenfels D.J. 1988. Coniferales. In: *Flora Malesiana. Series I.* **10**: 337–453.

Dörken V.M., Parsons R.F. 2016. Morpho-anatomical studies on the change in the foliage of two imbricate-leaved New Zealand podocarps: *Dacrycarpus dacrydioides* and *Dacrydium cupressinum. Plant Syst. Evol.* **302**: 41–54.

Eckenwalder J.E. 2009. *Conifers of the world: the complete reference*. Portland: Timber Press.

Farjon A. 2010. *A handbook of the world's conifers*. Leiden, Boston: Brill.

Florin R. 1940. The Tertiary conifers of south Chile and their phytogeographical significance. *K. Vet. Akad. Handl.* **19**: 1–107.

Greenwood D.R. 1987. Early Tertiary Podocarpaceae: megafossils from the Eocene Anglesea locality, Victoria, Australia. *Aust. J. Bot.* **35**: 111–133.

Hill R.S., Carpenter J. 1991. Evolution of *Acmopyle* and *Dacrycarpus* (Podocarpaceae) foliage as inferred from macrofossils in south-eastern Australia. *Aust. J. Bot.* **4**: 449–479.

Hill R.S., Whang S.S. 2000. *Dacrycarpus* (Podocarpaceae) macrofossils from Miocene sediments at Elands, eastern Australia. *Aust. J. Bot.* **13:** 395–408.

Lewis E.K., Drinnan A.N. 2013. The Miocene conifer flora of Balcombe Bay, Victoria, Australia. *Aust. Syst. Bot.* **26**: 145–155.

Melikian A.P., Bobrov A.V. 2000. Morphology of female reproductive structures and an attempt of construction of phylogenetic system of orders Podocarpales, Cephalotaxales and Taxales. *Bot. Zhurn.* **85**: 50–68. [In Russian]

Pole M.S. 2007. Conifer and cycad distribution in the Miocene of southern New Zealand. *Aust. Syst. Bot.* **55**: 143–164.

Wells P.M., Hill R.S. 1989. Fossil imbricate-leaved Podocarpaceae from Tertiary sediments in Tasmania. *Aust. Syst. Bot.* **2**: 387–423.

Wilf P. 2012. Rainforest conifers of Eocene Patagonia: Attached cones and foliage of the extant Southeast Asian and Australasian genus *Dacrycarpus* (Podocarpaceae). *Am. J. Bot.* **99**: 562–584.

FLORAL STRUCTURE OF *THISMIA* (THISMIACEAE, DIOSCOREALES) WITH EMPHASIS ON THE ASIAN SPECIES

Sophia V. YUDINA[1], ***Ekaterina A. SHEPELEVA***[1], ***Truong BA VUONG***[2], ***Anton S. BEER***[1], ***Maxim S. NURALIEV***[1,3]

[1] Lomonosov Moscow State University, Moscow, Russia
[2] Institute of Tropical Biology of Vietnam Academy of Science and Technology, Hochiminh City, Vietnam
[3] Joint Russian-Vietnamese Tropical Scientific and Technological Center, Hanoi, Vietnam

Yudina.Sophia@gmail.com

Thismia Griff is the largest genus of the family Thismiaceae, which belongs to the order Dioscoreales. It comprises more than 75 species, which mainly inhabit tropical regions of Asia and America; some species are found in subtropical and temperate areas.

Members of the genus *Thismia* are mycoheterotrophic achlorophyllous herbs with curious flower morphology and highly reduced vegetative structure. Flowers are mostly actinomorphic, characterized by hypanthium and perianth of six tepals in two whorls. The hypanthium orifice is covered by a special structure called annulus to form a closed chamber. Perianth elements are very diverse in their shape. In some species, the outer and inner tepals are free and sometimes terminate at the apex into the processes, while in the others the inner tepals fuse to form a mitre, which sometimes also bears appendages. Six stamens are hung up from the annulus and fuse postgenitally to form a tube. Ovary is inferior, unilocular, with three placentas alternating with styles.

We have compared the floral vasculature of five species of *Thismia*: *T. annamensis, T. aseroe* and *T. rodwayi* with free inner tepals, and *T. americana* and *T. mucronata* with inner tepals forming a mitre. Of them, *T. annamensis* and *T. mucronata* are studied here for the first time, while the data on the other three species were taken from the literature sources (Pfeiffer, 1914; Rao, 1969; Rübsamen, 1986). These five species belong to a monophyletic group that comprises all *Thismia* species except for the Neotropical ones (Shepeleva et al., in prep.). The phylogenetic position of *T. americana* remains questionable, as it has never been included into molecular phylogenetic analysis. However, it was shown that this species is most likely closely related to certain Asian and Australian *Thismia* species (Merckx, Smets, 2014).

We have found that all the analyzed species possess similar vasculature of gynoecium and hypanthium. The ovary has six vascular strands arranged in two rings of three. Bundles of the inner ring are opposite to placentas (and inner tepals) and bundles of the outer ring alternate with them, i.e., occupy the radii of the styles

(and outer tepals). Bundles of the inner ring send branches into placentas. At the level of the ovary top, bundles of the outer ring divide each into four branches: one median and two lateral bundles, which run upwards into the hypanthium, and one centripetal trace, which innervates the style.

Hypanthium thus receives 12 bundles from the ovary wall, of which three groups of three bundles of the outer ring alternate with three solitary bundles of the inner ring.

In *T. americana*, *T. annamensis*, *T. aseroe* and *T. rodwayi*, the median bundles of the outer ring and the inner ring bundles send radial branches towards flower centre at the top of the hypanthium (below the level of attachment of outer tepals) that become traces of stamens. These traces pass through the annulus and stamen filaments and run downwards into the anther connectives. In *T. mucronata*, bundles of the inner stamens appear in the same way, while bundles of the outer stamens do not branch off at this level and possess a different origin (see below).

Above the level of departure of the stamen traces, lateral bundles of the outer hypanthium ring (alternating with tepals) bifurcate tangentially to form branches that run upwards into the tepals (in *T. mucronata*, only some of them enter the tepals).

In *T. americana*, the median bundle of the outer ring and two adjacent branches of lateral bundles of the outer ring run upwards into the outer tepal where they merge with each other and form a united bundle. In *T. rodwayi*, the three traces of the outer tepal appear in the same way, and their further behavior is unknown. In *T. mucronata*, two adjacent branches of lateral bundles of the outer ring fuse with the median bundle of the outer ring in the hypanthium. The common bundle enters the annulus where it curves down and becomes a trace of an outer stamen. As a result, there are no traces in outer tepals of *T. mucronata*.

In *T. annamensis*, the outer tepals are innervated each by seven traces. Each branch of the lateral bundle of the outer hypanthium ring sends two branches of the next order in tangential plane, which results in the presence of three traces at each side of the median trace of the outer tepal (the branching occurs in the hypanthium, at the level below the attachment of the tepal). In a distal part of the outer tepal, three central bundles merge to form a unified bundle that runs into the apical process; the others end blindly. Finally, no information on tepal innervation in *T. aseroe* is currently available.

Inner tepals are innervated by bundles of the inner hypanthium ring (forming median tepal traces) and branches of the lateral bundles of the outer hypanthium ring (forming lateral tepal traces). In species with inner tepals forming a mitre (*T. americana*, *T. mucronata*), these three bundles merge within the tepal to form a unified bundle that runs upwards to the mitre apex. In *T. rodwayi*, the inner tepals are also innervated by three traces, and further behavior of these bundles is unknown.

In *T. annamensis* (with free tepals), the inner tepals are innervated by five traces. The bundle of the inner hypanthium ring forms a median tepal trace. At the

level below the attachment of the inner tepal, branches of the lateral bundles of the outer hypanthium ring bifurcate tangentially to form four lateral tepal traces at each side of the median tepal trace. In a distal part of the inner tepal, three central bundles merge to form a unified bundle that runs into the apical process; the others end blindly in the tepal blade.

We have found some variation in number of tepal traces in *T. annamensis*. One of the two analyzed flowers had three traces in the inner tepal and five traces in the outer tepal. We suppose that this difference is related to the stage of flower development, as the second flower was significantly younger and apparently underdeveloped.

As follows from our results, some features of the floral vasculature are rather constant in *Thismia*, while the others vary to some extent. Ovary, hypanthium and stamens of the studied species possess uniform vasculature. The number of tepal bundles shows considerable variation and probably correlates with the presence or absence of the mitre.

The study was supported by Russian Foundation for Basic Research (project No. 18-04-00619).

References

Merckx V.S.F.T., Smets E.F. 2014. *Thismia americana*, the 101st anniversary of a botanical mystery. *Int. J. Plant Sci.* **175**: 165–175.

Pfeiffer N.E. 1914. Morphology of *Thismia americana*. *Bot. Gaz*. **57**: 122–135.

Rao V.S. 1969. Certain salient features in the floral anatomy of *Burmannia*, *Gymnosiphon* and *Thismia*. *J. Indian Bot. Soc*. **48**: 22–29.

Rübsamen T. 1986. *Morphologische, embryologische und systematische Untersuchungen an Burmanniaceae und Corsiaceae (Mit Ausblick auf die Orchidaceae-Apostasioideae)*. Berlin: Cramer.

TAXONOMIC AND PHYLOGENETIC VALUE OF CARPOLOGICAL CHARACTERS IN *TORDYLIUM* (UMBELLIFERAE)

Ekaterina A. ZAKHAROVA, Tatiana A. OSTROUMOVA, Galina V. DEGTJAREVA, Michael G. PIMENOV

Lomonosov Moscow State University, Moscow, Russia
degavi@mail.ru

Modern research in the field of taxonomy and phylogeny of the Umbelliferae is characterized by wide usage of various methods, among which the most important are carpological and molecular ones. The most significant results of such

an integrated approach are given in the application to critical polymorphic taxa, especially at the genus level.

Tordylium L. is one of the moderately critical genera in the Umbelliferae and its taxonomy remains complicated. Many genera that were split from *Tordylium* in the past (e.g. *Ainsworthia* Boiss., *Hasselquistia* L., *Condylocarpus* Hoffm. and *Synelcosciadium* Boiss.), are now proposed to be congeneric with it (reviewed in Al-Eisawi, Jury, 1988; Doğru-Koca, 2016) that renders the genus more heterogeneous. In floristic treatments, the genus *Ainsworthia* is treated as independent (Alava, 1971, 1972; see also Pimenov, Leonov, 1993). Comprehensive studies that consider molecular markers are lacking for the genus. At present, the genus *Tordylium* s.l. encompasses about 20 species distributed in Europe, Asia and N. Africa. It is particularly diverse in Turkey, where 19 of the 20 species occur. All species of *Tordylium* are annual herbs preferring dry habitats. Nomenclatural type (lectotype) of *Tordylium* is *T. maximum* L.

In the last monograph of the genus (Al-Eisawi, Jury, 1988) based on detailed comparative studies of morphology and chromosome numbers, the authors suggested subdivision of *Tordylium* into subgenus *Tordylium* (sect. *Tordylium*) and subgenus *Ainsworthia* (with three sections – sect. *Condylocarpus*, sect. *Hasselquistia*, and sect. *Univittata*). This subgeneric classification of *Tordylium* is compatible with circumscription of its allied genera, and taxonomic significance of the most remarkable carpological features of *Tordylium* such as the occurrence of dimorphic fruits and the presence of numerous vittae in mesocarp were over-estimated in the past.

With the aim to resolve relationships of *Tordylium* s.l. we reassess in detail the carpological characters that are still important criteria in the taxonomy and identification of Umbelliferae (Pimenov, Ostroumova, 2014), and conduct analysis of nucleotide sequences of nuclear ribosomal DNA internal transcribed spacer (ITS) region.

According to our ITS sequence data (Fig. 1), *Tordylium* s.l. is not monophyletic. Its species are nested in three distinct highly supported clades: (1) majority of *Tordylium* species including *T. maximum*; (2) accessions of *T. apulum* L. placed within *Pastinaca* + *Heracleum* + *Leiotulus* clade; (3) accessions of *T. aegyptiacum* (L.) Lam. placed within a moderately supported *Semenovia* + *Tetrataenium* + *Heracleum* clade. The results suggest that *Synelcosciadium* and *Ainsworthia* are nested within *Tordylium*, confirming their current congeneric taxonomic treatment with *Tordylium*. *Hasselquistia* (*T. aegyptiacum*) and *Condylocarpus* (*T. apulum*) could be reinstated as separate monotypic genera. Within *Tordylium*, several clades are apparent, which are partially compatible with sectional subdivision of the genus, but are not consistent with subgeneric delimitation according to classification of Al-Eisawi & Jury (1988).

Our carpological study of 16 species of *Tordylium* has revealed that they are similar in many characters: low conical stylopodia, recurved styles, broad mericarp

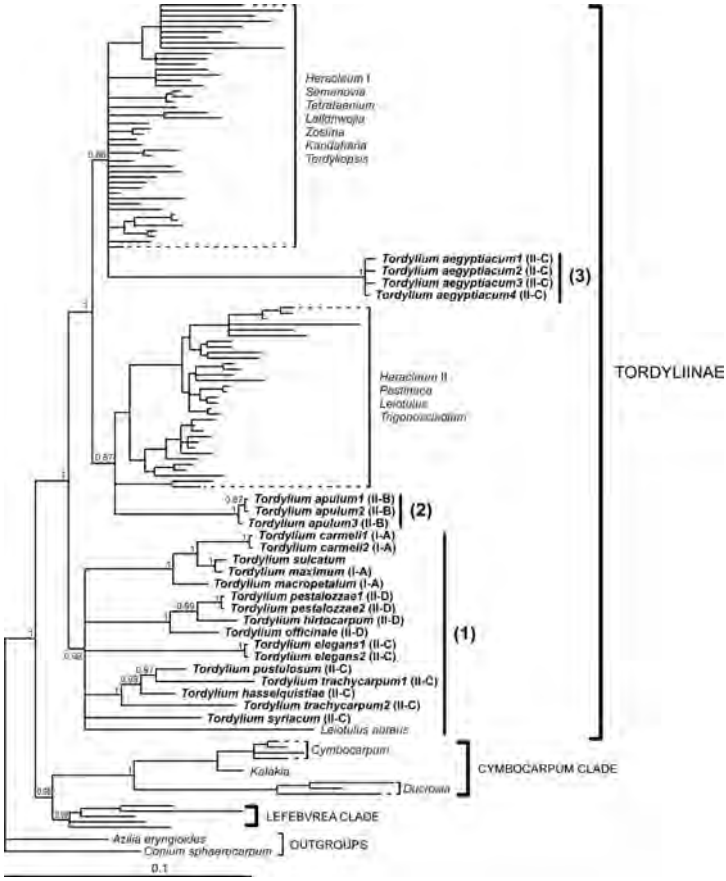

Fig. 1. Phylogenetic tree inferred from Bayesian analysis of ITS sequences from Umbelliferae tribe Tordylieae and outgroups. Only relationships with greater than 0.85 posterior probabilities are shown, other branches are collapsed. Species of *Tordylium* are shown in bold. Infrageneric classification established for the genus *Tordylium* by Al-Eisawi & Jury (1988) is given after species name as follows: I – subgenus *Tordylium*: A – section *Tordylium*; II – subgenus *Ainsworthia*: B – section *Condylocarpus*, C – section *Hasselquistia*, D – section *Univittata*.

commissure, dorsal (filiform) ribs different from marginal (winged) ribs, mesocarp consisting of unlignified parenchyma cells outside of marginal ribs and lignified parenchyma cells with pitted walls in the marginal ribs, hypendocarp (inner fibrous mesocarp), compact vascular bundles, compressed and obscure endocarp cells, and a flat endosperm on the commissure side (Fig. 2A–C). However, there are significant variations in fruit morphological and anatomical structure. In the most species, fruits are orbicular or elliptic in outline and strongly compressed dorsally. The majority of the studied species have fruits with prominent short calyx teeth. In *T. pustulosum* Boiss., *T. pestalozzae* Boiss., *T. hasselquistiae* DC., *T. trachycarpum* (Boiss.) Al-Eisawi et Jury calyx teeth are obsolete. The marginal ribs can be bulged (*T. apulum*,

T. cappadocicum Boiss., *T. hirtocarpum* Cand., *T. officinale* L., *T. pestalozzae*, *T. pustulosum*) or without bulges. The marginal ribs can be thickened only distally and thinner in their basal part (*T. apulum*, *T. cordatum* Poir., *T. lanatum* et al.) (Fig. 2A, B) or marginal ribs are thickened throughout (*T. cappadocicum*, *T. officinale*, *T. pestalozzae* etc.) (Fig. 2C). Rib secretory ducts are obsolete (the majority of the studied species) or small, present only in some ribs (*T. apulum*, *T. cappadocicum*, *T. hirtocarpum, T. maximum*, *T. syriacum* L.). Most species have fruits with long vallecular vittae, some species (*T. brachytaenium* Boiss. et Heldr., *T. pestalozzae*) have, however, short vallecular vittae located at the top of the mericarp. Fruits of *T. elegans* and *T. hasselquistiae* have the discontinuous central vallecular vittae. Most species have fruits with solitary vallecular vittae in each furrow and two commissural vittae (Fig. 2B). Only *T. apulum* have fruits with numerous vallecular and commissural vittae (Fig. 2A). The central vallecular vittae absents in *T. brachytaenium* and *T. pestalozzae* (Fig. 2C). *Tordylium* is remarkable in heterocarpy, observed in some its species (*T. elegans, T. lanatum, T. aegyptiacum*).

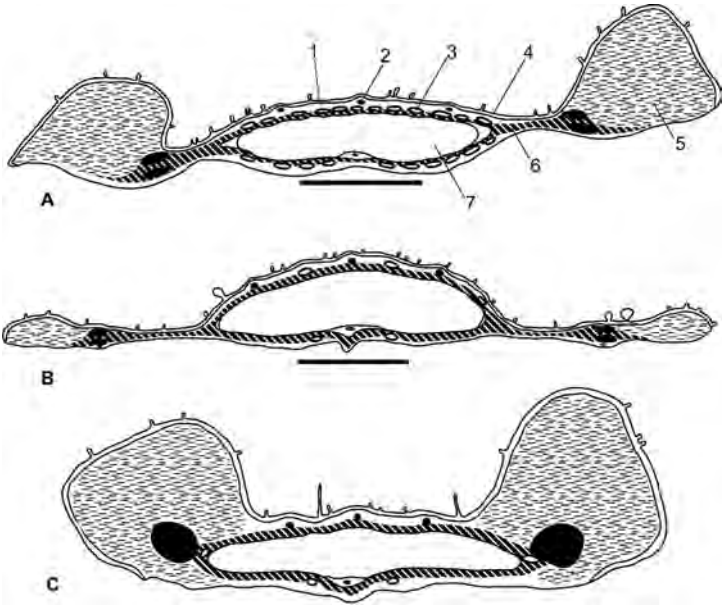

Fig. 2. Schematic transects of mericarps.
A – *Tordylium apulum*; B – *T. lanatum*; C – *T. pestalozzae*.
1 – mesocarp, unlignified parenchyma cells, 2 – vascular bundle, 3 – vittae,
4 – exocarp, 5 – lignified parenchyma cells with pitted walls,
6 – hypendocarp, 7 – endosperm.
Scale bar – 1 mm.

In *Tordylium* the majority of species have uniform strongly compressed dorsally bicarpellate fruits, whereas *T. elegans, T. lanatum* and *T. aegyptiacum* have

two types of fruits. Globose unicarpellate fruits consist of only one mericarp with marginal ribs rolled to the ventral side; the internal structure of such mericarps, however, does not differs in other characters from the standard anatomy. Although fruit dimorphism in some *Tordylium* species was noted in early studies, heterocarpy was not thought, from Boissier (1872) to Al-Eisawi & Jury (1988), to be of important taxonomic significance. Indded, the three species with heterocarpous fruits belong to different clades of the molecular tree obtained by us.

Fruit micromorphology shows different types of indumentum. *Tordylium carmeli* and *T. maximum* have strigose hairs (Fig. 3C), while other species have various vesicular hairs: small globose (*T. aegyptiacum* and *T. hirtocarpum,* Fig. 3A), large globose 50–70 μm in diam. (*T. brachytaenium*, *T. carmeli*, and *T. trachycarpum,* Fig. 3B), or both types of hairs (*T. apulum*, *T. hasselquistiae, T. lanatum, T. officinale, T. pestalozzae, T. pustulosum,* and *T. syriacum*), or elongated vesicular hairs (*T. elegans, T. hirtocarpum, T. officinale*, and *T. pestalozzae*). Non-vesicular ribbon-like hairs present on the fruit surface of *T. aegyptiacum, T. cappadocicum, T. elegans*, and *T. syriacum*; the fruits of *T. cappadocicum* are without any vesicular hairs. Strigose hairs are 400–700 μm long and have numerous conical projections on their surface. Small globose hairs are 20–40 μm in diam., large globose ones are 50–70 μm in diam., elongated vesiculose hairs are 100–500 μm long, and ribbon-like hairs are 250–400–700 μm long. Globose and elongated vesiculose hairs are often compressed and acquire different shapes – peltate, spoon-like etc.

Cell surface on the marginal rib is either flat (*T. aegyptiacum, T. brachytaenium, T. elegans, T. hasselquistiae, T. lanatum, T. maximum, T. officinale, T. pestalozzae, T. pustulosum, T. sulcatum, T. syriacum*, and *T. trachycarpum*), or all cells are domed and papillose (Fig. 3D: *T. aegyptiacum, T. apulum, T. hirtocarpum*, and *T. pestalozzae*), or bear conical projections (Fig. 3E: *T. cappadocicum, T. officinale*, and *T. pestalozzae*). On the marginal ribs of *T. pustulosum* there are depressions ca. 100 μm in diam. with a large dome that has rugulate-tuberculate surface and resembles large globose hair (Fig. 3F). Flat and globose fruits of heterocarpic species do not differ in other morphological traits.

The majority of fruit morphological and anatomical characters do not correlate with groups delineated in molecular ITS tree. Most of the traits exhibit considerable variation. It is possible to suppose that the occurrence of dimorphic fruits in *Tordylium*, as well as the presence of bulges at marginal mericarp ribs, the presence of calyx teeth, and the presence of thinner basal part of thickened marginal ribs evolved independently. The molecular data are consistent only with type of indumentum (strigose hairs in *T. maximum* and *T. carmeli*) and number of vittae (numerous vallecular and commissural vittae are characteristic only of *T. apulum*, which is recognized by some authors as distinct genus *Condylocarpus*).

The fruits of *Tordylium* and Umbelliferae in general exhibit an array of structural peculiarities that may facilitate mericarp dispersal. Winged fruits are generally regarded as adapted to transportation by wind (Theobald, 1971). Fruit appendages

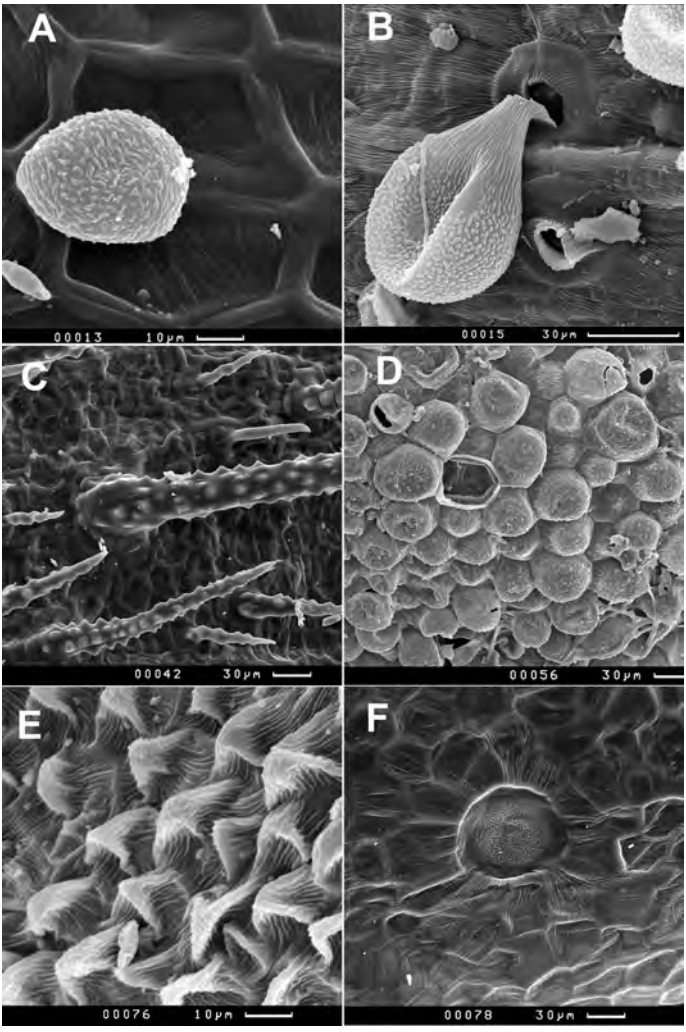

Fig. 3. Fruit micromorphology in *Tordylium*.
A – *T. lanatum*, small globose hair. B – *T. trachycarpum*, large globose hair with a ring at the base. C – *T. maximum*, strigose hairs with conical projections. D – *T. apulum*, dome-shaped cells of the marginal rib. E – *T. officinale*, conical projections on the exocarp cells of the marginal rib. F – *T. pustulosum*, large depression with a dome.

may be therefore a subject to strong selective pressure resulting in homoplasy. In general, despite the probable homoplasy, fruit morphology and anatomy together with molecular data can provide valuable characters to revise *Tordylium* systematics.

The work is supported by the Russian Foundation of Basic Research (grants Nos. 16-04-00525, 19-04-00370). We are greatly indebted to T.H. Samigullin for his help with molecular phylogenetic analysis.

References

Alava R. 1971. The genus *Ainsworthia* (Umbelliferae). *Notes R. Bot. Gard. Edinburgh* **31**: 109–118.

Alava R. 1972. *Tordylium* L., *Ainsworthia* Boiss. In: Davis P.H. (ed.): *Flora of Turkey and the East Aegean Islands*. Edinburgh: Edinburgh Univ. Press. V. **4**. P. 504–513.

Al-Eisawi D., Jury S.L. 1988. A taxonomic revision of the genus *Tordylium* L. (Apiaceae). *Bot. J. Linn. Soc.* **97**: 357–403.

Boissier E. 1872. Umbelliferae. In: *Flora Orientalis*. Geneva; Lyon: H. Georg. V. **2**. P. 819–1090. [In Latin]

Doğru-Koca A. 2016. Phylogeny of the genus *Tordylium* (Tordylineae, Apioideae, Apiaceae) inferred from morphological data. *Nordic J. Bot.* **34**: 111–119.

Pimenov M.G., Leonov M.V. 1993. *The genera of the Umbelliferae. A Nomenclator.* Kew: Royal Botanic Gardens.

Pimenov M.G., Ostroumova T.A. 2014. Carpological characters in the Umbelliferae systematics. In: Lotova L.I., Timonin A.C. (eds.): *Kaden's Memorial Book*. Moscow: MAKS Press. P. 158–172.

Theobald W.L. 1971. Comparative anatomical and developmental studies in the Umbelliferae. In: Heywood V.H. (ed.): *The biology and chemistry of the Umbelliferae*. London: Academic Press. P. 177–197.

FLORAL ONTOGENY OF *ILLICIUM LANCEOLATUM* (SCHISANDRACEAE), IMPLICATION OF THE ORIGIN OF CARPEL

Xin ZHANG

Northwest A&F University, Yangling, China
xin.zhang@nwsuaf.edu.cn

There are two competing hypotheses for the origin of flowers. The traditional hypothesis is phyllosporous origin which regards a conduplicate carpel as an ancestral form that is the result of longitudinal folding of a leaf bearing ovules along its margins. Alternatively, the carpel formation is the result of a fusion between an ovule-bearing branch and its subtending leaf-like structure; if true, the ovule would originally occur at the middle of the leaf-like structure. For the majority of the angiosperms, the carpel is a single leaf-like structure with the ovule developing later on the lamina. *Illicium* is a member of the Austrobaileyales, which are one of the three ANA lines that diverged before all other extant angiosperms. This genus with apocarpous gynoecium has various ancestral morphological characteristics in terms of carpel, ovule, and floral apex. Although various aspects of *Illicium* morphology have been previously investigated, many evolutionary characteristics remain unclear. A more detailed examination of the carpel, ovule, and floral apex of *Illicium* is needed. In this study, the development of carpel, ovule, and floral

apex of *I. lanceolatum* was studied using LM and SEM. The results showed that the ovule primordium originates at the point where the carpel touches the floral axis. Based on the comparison with other taxa, the evolutionary implication of a persistent floral apex is an apical meristem remnant of a shoot. So the carpel of *Illicium* is a leaf-like structure that encircles the ovule. This kind of carpel fits the hypothesis that the carpel is a fusion of two parts, ovule-bearing branch and its subtending leaf-like structure.

COMPARATIVE WOOD ANATOMY OF *ASTROPANAX* AND *NEOCUSSONIA*, TWO AFRO-MALAGASY LINEAGES OF ARALIACEAE

Dayana A. ZHERNOVA[1]***, Maja V. NILOVA***[1]***, Alexey A. OSKOLSKI***[2,3]

[1] Lomonosov Moscow State University, Moscow, Russia
[2] University of Johannesburg, Johannesburg, South Africa
[3] Komarov Botanical Institute of Russian Academy of Sciences, Saint Petersburg, Russia
daayana@ro.ru

The genera *Astropanax* Seem. and *Neocussonia* (Harms) Hutch. have recently been resurrected from two subclades within monophyletic group encompassing the African and Malagasy species of the large polyphyletic genus *Schefflera* J.R. Forst. et G. Forst. (Araliaceae). Species of both genera are trees with palmately compound or unifoliolate leaves, growing mostly in humid lowland and montane forests. *Astropanax* comprises 15 species, 11 of which occur in tropical and subtropical Africa, three in Madagascar and one in the Seychelles. *Neocussonia* includes 16 species, two in eastern and southern Africa and 14 in Madagascar. Molecular phylogenetic data suggest the African origin of both lineages with independent dispersals to Madagascar which can be followed in *Neocussonia* by a secondary dispersal back to Africa (Gostel et al., 2017; Lowry et al., 2017). The anatomy and morphology of the two genera are very poorly explored; the wood structure of only three *Astropanax* species has been studied to date (Oskolski, 1995). This study aims to survey the structural diversity of secondary xylem in *Astropanax* and *Neocussonia* with evolutionary and ecological implications.

We studied wood structure in 8 species of *Astropanax* and 11 species of *Neocussonia*. Both genera are similar to other Araliaceae in the presence of septate fibers, scanty paratracheal axial parenchyma as well as the occurrence of radial canals in few species of both genera. *Neocussonia* is distinctive, however, by predominantly (> 95%) to exclusively scalariform perforation plates, the occurrence of ones with numerous bars (> 11 bars, up to 63 bars in *N. rainaliorum*), and small

intervessel pits (3.3–5.7 μm in average vertical size). Unlike this genus, most *Astropanax* species (except for *A. volkensii*) have more numerous simple perforation plates (up to exclusively simple ones in *A. mannii* and in the *A. abyssinicus* sample from Cameroon), and the number of bars on scalariform ones does not exceed 11. Apart from that, the *Astropanax* species share larger intervessel pits (5.0–7.4 μm in average vertical size) as well as wider and fewer vessel lumina (5–37 per 1 mm^2) than the members of *Neocussonia* (20–67 vessels per 1 mm^2).

To assess the relationships between interspecific variation of wood traits and climatic parameters of ecological niches of the species under study, the coordinates of the species occurrences were retrieved from the Global Biodiversity Information Facility (GBIF). With this data set, the values of 19 bioclimatic variables representing the variation of temperature and precipitation were extracted from the WorldClim climate layers (Hijmans et al., 2005) for each occurrence using the Raster package (Hijmans, Etten, 2012) in R. We found that the interspecific variation of vessel diameter, percentage of solitary vessels, percentage of simple perforation plates and size of intervessel pits within *Astropanax* and *Neocussonia* show significant negative correlation with average temperature seasonality (BIO4). Actually, these correlations represent the traits variation along climatic gradient across the distributional range of two genera: wide and mostly solitary vessels with exclusively simple perforation plates and large intervessel pits found in tropical wet climate of the Gulf of Guinea region, whereas more narrow and grouped vessels mostly with scalariform perforation plates and small intervessel pits are predominant in southeastern Africa and Madagascar, the regions with subtropical seasonal climate. The tendences in variation of wood characters are consistent with global geographic trends of these traits (with exception of the intervessel pit size) as well as with their functional and adaptive value (Hargrave et al., 1994; Davis et al., 1999; Hacke et al., 2006; Wheeler et al., 2007; Lens et al., 2011, 2016; Zanne et al., 2014).

Neocussonia umbellifera from eastern Africa is distinctive from the Malagasy species of the genus by more numerous simple perforation plates (> 3%) and larger intervessel pits (> 5 μm in average vertical size). *Neocussonia bojeri* has the highest level of vessel grouping within the genus that is consistent with the adaptation of this species to the areas with prolonged dry periods (Lowry et al., 2017).

We did not find any significant differences in wood structure between *A. myrianthus* from Madagascar and *A. polysciadus* from continental Africa, two cryptic species that have long been classified as *Schefflera myriantha*. *Astropanax polysciadus* has recently been separated from the former species on the basis of evidence from geographic and molecular data despite a lack of morphological diagnostic characteristics (Gostel et al., 2017; Lowry et al., 2017). We studied, however, only one wood sample of each species; more representative sampling is required for comprehensive assessment of (dis-)similarities between *Astropanax myrianthus* and *Astropanax polysciadus.*

Two wood samples of *Astropanax abyssinicus* collected from different parts of disjunct distribution range of this species (Lowry et al., 2017) show remarkable difference in structure of perforation plates. While the wood from Burundi (J. Lewalle 2157) has mostly scalariform perforation plates (81%) with 1–6 bars, the sample from Cameroon (G. Mann 1161) has exclusively simple perforation plates. Such a sharp distinction in wood structure suggests that populations of *Astropanax abyssinicus* from Cameroon are not closely related to those from eastern Africa presumably representing another species. A molecular phylogenetic analysis is required to test this hypothesis.

This work was supported by the Russian Foundation for Basic Research (grant No. 19-04-00714a).

References

Davis S.D., Sperry J.S., Hacke U.G. 1999. The relationship between xylem conduit diameter and cavitation caused by freezing. *Am. J. Bot.* **86**: 1367–1372.

Gostel M.R., Plunkett G.M., Lowry P.P. II 2017. Straddling the Mozambique Channel: molecular evidence for two major clades of Afro-Malagasy *Schefflera* (Araliaceae) co-occurring in Africa and Madagascar. *Plant Ecol. Evol.* **150**: 87–108.

Hacke U.G., Sperry J.S., Wheeler J.K., Castro L. 2006. Scaling of angiosperm xylem structure with safety and efficiency. *Tree Physiol.* **26**: 689–701.

Hargrave K.R., Kolb K.J., Ewers F.W., Davis S.D. 1994. Conduit diameter and drought-induced embolism in *Salvia mellifera* Greene (Labiatae). *New Phytol.* **126**: 695–705.

Hijmans R.J., Cameron S.E., Parra J.L., Jones P.G., Jarvis A. 2005. Very high resolution interpolated climate surfaces for global land areas. *Int. J. Climatol.* **25**: 1965–1978.

Hijmans R.J., van Etten J. 2012. Raster: geographic analysis and modeling with raster data. *R package* version 1. P. 9–92.

Lens F., Sperry J.S., Christman M.A., Choat B., Rabaey D., Jansen S. 2011. Testing hypotheses that link wood anatomy to cavitation resistance and hydraulic conductivity in the genus *Acer*. *New Phytol.* **190**: 709–723.

Lens F., Vos R., Charrier G., van der Niet T., Merckx V., Baas P., Aguirre Gutierrez J., Jacobs B., Chacon Doria L., Smets E., Delzon S., Jansen S. 2016. Scalariform-to-simple transition in vessel perforation plates triggered by differences in climate during the evolution of Adoxaceae. *Ann. Bot.* **118**: 1043–1056.

Lowry P.P. II, Plunkett G.M., Gostel M.R., Frodin D.G. 2017. A synopsis of the Afro-Malagasy species previously included in *Schefflera* (Araliaceae): resurrection of the genera *Astropanax* and *Neocussonia*. *Candollea* **72**: 265–282.

Oskolski A.A. 1995. Wood anatomy of *Schefflera* and related taxa (Araliaceae). *IAWA J.* **16**: 159–190.

Wheeler E.A., Baas P., Rodgers S. 2007. Variations in dicot wood anatomy: a global analysis based on the Insidewood database. *IAWA J.* **28**: 229–258.

Zanne A.E., Tank D.C., Cornwell W.K., Eastman J.M., Smith S.A., FitzJohn R.G., McGlinn D.J., O'Meara B.C., Moles A.T., Reich P.B., Royer D.L., Soltis D.E., Stevens P.F., Westoby M., Wright I.J., Aarssen L., Bertin R.I., Calaminus A., Govaerts R., Hemmings F., Leishman M.R., Oleksyn J., Soltis P.S., Swenson N.G., Warman L., Beaulieu J.M. 2014. Three keys to the radiation of angiosperms into freezing environments. *Nature* **506**: 89–96.

STEREOLOGICAL METHOD IN ANATOMICAL RESEARCH OF CULTIVATED PLANT SPECIES

***Lana N. ZORIĆ*, Dunja S. KARANOVIĆ, Jadranka Z. LUKOVIĆ**

University of Novi Sad, Novi Sad, Serbia

lana.zoric@dbe.uns.ac.rs

Stereological method is used in botany for quantitative, three-dimensional evaluation of plant organ structure, by observation of two-dimensional sections. Compared to classical anatomical analysis, stereological method gives more precise information about the proportions of individual tissues in plant organs. It could be succesfully applied in agronomy, for quantification of histological structure, in estimation of volume densities of different tissues in plant organs of cultivated species.

Sampling procedures for simple and compound leaves, petioles and herbaceous stems of several cultivated species are explained. Uniform random sampling includes plant organs as a whole, with 5–7 sections per organ. Sampling procedures for compound leaves are explained. Data obtained using stereological method are applied in estimation of volume densities of tissues connected to digestibility and nutritional value of forage crops, volume densities of tissues that affect photosynthesis, tissue parameters connected to plant resistance, increased tolerance to drought, as well as yield components of different cultivated species, like industrial crops, grain forages, forage crops (Zorić et al., 2011, 2014, 2015; Luković et al., 2016). Distribution of tissues in plant organs, as well as changes in tissue proportions during plant maturation can also be traced using this method. Obtained data are useful for selection and breeding process of new varieties and genotypes of cultivated plant species.

References

Zorić L., Mikić A., Antanasović S., Karanović D., Cupina B., Luković J. 2015. Stem anatomy of annual legume intercropping components: white lupin (*Lupinus albus* L.), narbonne (*Vicia narbonensis* L.) and common (*Vicia sativa* L.) vetches. *Agricult. Food Sci.* **24**: 139–149.

Zorić L., Mikić A., Cupina B., Luković J., Krstić Dj., Antanasović S. 2014. Digestibility-related histological attributes of vegetative organs of barrel medic (*Medicago truncatula* Gaertn.) cultivars. *Zemdirbyste-Agriculture* **101**: 257–264.

Zorić L., Luković J., Matić-Kekić S., Merkulov Lj. 2011. Modified stereological method for analysis of compound leaves and an example of its application. *J. Biol. Systems* **19**: 617–627.

Luković J., Zorić L., Piperac J., Nagl N., Karanović D., Matić-Kekić S., Milić D. 2016. The analysis of petiole histological traits through an evaluation of water deficit tolerance of sugar beet genotypes. *Sugar Tech.* **18**: 160–167.

CONTENTS

Научное издание

АНАТОМИЯ РАСТЕНИЙ: ТРАДИЦИИ И ПЕРСПЕКТИВЫ

Материалы Международного симпозиума, посвященного 90-летию профессора Людмилы Ивановны Лотовой

16–22 сентября 2019 г.

В двух частях

Часть 1

МАТЕРИАЛЫ НА АНГЛИЙСКОМ ЯЗЫКЕ

Редакторы: А. К. Тимонин, Д. Д. Соколов

На обложке воспроизведены учебные таблицы вторичной флоэмы, изготовленные лично Л. И. Лотовой

Cover: L. I. Lotova's drawings

Подготовка оригинал-макета:
Издательство «МАКС Пресс»
Главный редактор: *Е. М. Бугачева*
Верстка: *В. Е. Иванов*
Корректор: *Е. А. Алтайская*
Обложка: *А. В. Кононова*

Подписано в печать 05.08.2019 г.
Формат 70x100 1/16. Усл.печ.л. 26,56. Тираж 250 экз. Изд. № 172.

Издательство ООО «МАКС Пресс»
Лицензия ИД N00510 от 01.12.99 г.
119992, ГСП-2, Москва, Ленинские горы,
МГУ им. М. В. Ломоносова, 2-й учебный корпус, 527 к.
Тел. 8(495) 939–3890/91. Тел./Факс 8(495) 939–3891.

Отпечатано в полном соответствии с качеством
предоставленных материалов в ООО «Фотоэксперт»
115201, г. Москва, ул. Котляковская, д.3, стр. 13.

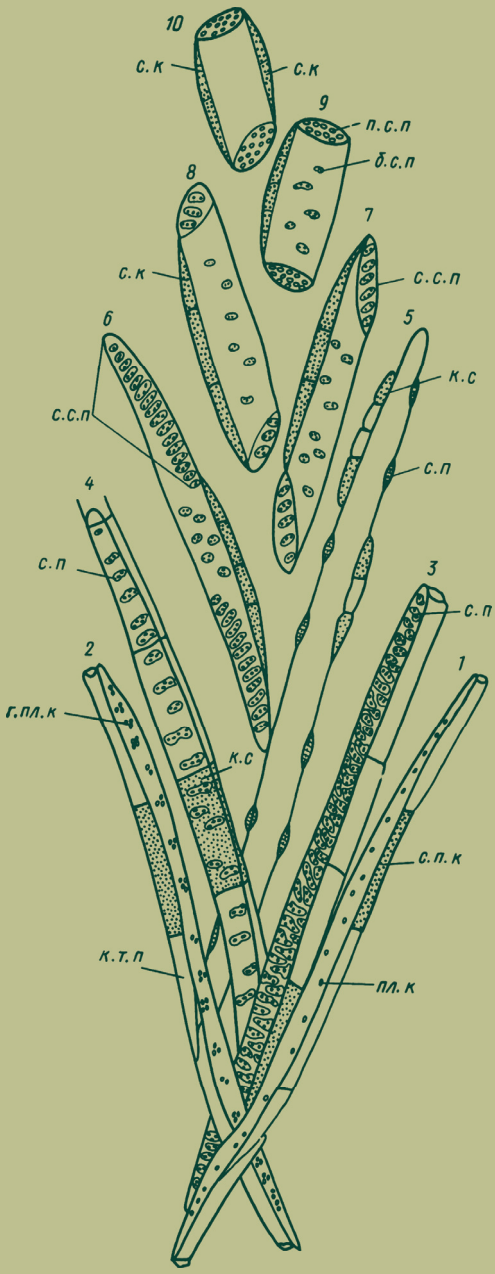
10
с. к
с. к
9
п. с. п
б. с. п
8
с. к
7
с. с. п
6
с. с. п
5
к. с
с. п
4
с. п
3
с. п
2
г. пл. к
к. с
1
с. п. к
к. т. п
пл. к

МАКС ПРЕСС